TESE DE DOUTORAMENTO

RHEOLOGICAL AND PHYSICO-CHEMICAL CHARACTERISTICS OF GLUTEN-FREE CHESTNUT FLOUR PRODUCTS WITH DRIED BROWN SEAWEED POWDERS

Asdo.: .....

Santiago Arufe Vilas

Programa de Doutoramento en Enxeñaría Química e Ambiental

Santiago de Compostela

2017

USC
UNIVERSIDADE
DE SANTIAGO
DE COMPOSTELA

AUTORIZACIÓN DOS DIRECTORES DA TESE

D. **Ramón Felipe Moreira Martínez** e D. **Jorge Sineiro Torres**, ámbolos dous Profesores Titulares do Departamento de Enxeñaría Química da Universidade de Santiago de Compostela, como Directores da Tese de Doutoramento titulada "*Rheological and physico-chemical characteristics of gluten-free chestnut flour products with dried brown seaweed powders*" presentada por D. **Santiago Arufe Vilas** alumno do Programa de Doutoramento en Enxeñaría Química e Ambiental.

Autorizan a presentación da tese indicada, considerando que reúne os requisitos esixidos no artigo 34 do regulamento de Estudos de Doutoramento, e que como Director da mesma non incurre nas causas de abstención establecidas na lei 40/2015.

Para que así conste aos efectos oportunos, expiden o presente informe en Santiago de Compostela, a de Xullo de 2017.

Asdo.: Asdo.:

Ramón Felipe Moreira Martínez Jorge Sineiro Torres

USC
UNIVERSIDADE
DE SANTIAGO
DE COMPOSTELA

Adicado ó meu
medio amigo

USC
UNIVERSIDADE
DE SANTIAGO
DE COMPOSTELA

Agradecementos

Esta Tese foi levada a cabo gracias ó apoio financieiro por parte do Ministerio de Economía y Competitividad de España e o Fondo Europeo de Desarrolo Regional (FEDER) a través do proxecto CTQ-2013-43616/P e parcialmente polo Ministerio de Economía e Innovación de España e o Fondo Europeo de Desarrolo Regional (FEDER) a través do proxecto CTQ 2010-15309/PPQ.

Tendo en conta que un traballo de catro anos conleva necesariamente pasar por momentos levadeiros e momentos máis duros gustaríame poder agradacer a tódolas persoas ou institucións que dun xeito ou doutro son donos dunha parte desta Tese:

- Ós meus directores de Tese **Ramón Moreira** (Moncho) e **Jorge Sineiro** (Xurxo) por levarme da man nestes catro anos, durante os cales axudaron á miña formación como investigador fomentando sempre un espírito crítico, axudándome na análise científica e poñendo á miña disposición todos os medios (humanos e materiais) dos que dispoñían para poder levar a cabo esta tese. Sentínme un privilexiado cando fun aceptado para formar parte do voso grupo de investigación, e sígome sentindo da mesma maneira case 5 anos despois.

- Ó profesor **Francisco Chenlo**, dende o primeiro día que recibín unha clase súa considereino un exemplo de profesionalidade no traballo, anos despois esa primeira impresión sigue completamente vixente. Gracias polo teu bo trato, por involucrarte e preocuparte polo meu traballo dun xeito desinteresado, por introducirme no apaixonante mundo da reoloxía, e como non, polas historias de galiñas e gráns de millo.

- Á **Universidade de Santiago de Compostela** e especialmente ó **Departamento de Enxeñaría Química** por poder realizar os meus estudos de doutoramento, axudarme a mellorar a miña formación docente a través das

prácticas de laboratorio e permitirme formar parte dunha institución con máis de 500 anos de historia.

- A **Portomuíños**® pola súa xenerosidade á hora de facilitarnos algunhas das algas empregadas para a realización da Tese.

- Ó **Grupo de Investación de Procesos de Separación e Equilibrio entre Fases** (GI-1616), pola súa xenerosidade á hora de permitirme o uso do seu equipo de DSC sen o cal unha parte importante desta Tese non podería terse levado a cabo. Especialmente gustaríame facer mención a **Iria** e **María** pola súa predisposición a axudarme sempre que o necesitei e polos momentos vividos xuntos.

- A **Jessica** polo dinamismo e o aire fresco que aportou ó laboratorio durante a súa estancia, e polo seus marabillosos xeles ;).

- Ós estudantes que ó longo destes catro anos pasaron polo laboratorio e aportaron o seu gran de area para que este traballo puidese saír á luz, **Patricia**, **Blanquita**, **Óscar** e **Uxía**.

- Ós estudantes de Máster (**Silvia**, **Adrián**, **Diego** e **Santi**), que se involucraron ó máximo nos seus respectivos traballos xerando un bo ambiente de traballo e colaborando tamén de xeito importante na realización desta Tese.

- A **Bea** e **Carolina**, compañeiras de laboratorio durante moito tempo, polas risas e polas cousas aprendidas durante estes catro anos.

- En especial a **Loly**, por ser a mellor compañeira cun doutorando agobiado pode ter e un referente no que fixarse para tratar de seguir mellorando no campo da investagación. Pola tranquilidade e os bos consellos que aporta no día a día no laboratorio.

- A **José Manuel** e **Diego**, polas comedelas, as estatísticas absurdas, os debates políticos, futbolísticos e ata os de hockey xeo (Fetisov!), en definitiva polos bos momentos pasados xuntos.

- **Guy Della Valle**, Animateur de l'équipe Matériaux, création & comportement (MC2), pour m'avoir accueilli au sein de l'Unité des Biopolymères Interactions Assemblages (BIA) de l'INRA Nantes, et pour me laisser travailler à ses côtés où j'ai beaucoup appris.

- Tous mes collègues, **Hubert**, **Kamal**, **Laurent**, **Anne-Laure**, **Jean-Eudes**, etc, pour l'accueil que j'ai reçu pendant mon séjour de Nantes en 2015 et pour m'avoir apporté leur aide dans mes expérimentations. Je ne peux pas oublier **Fabien** et **Arnaud** pour les bons moments passés au "fournil".

- A toda a tropa friki, **Antón**, **Arg** (Santi de novo), **Álvaro**, **Caba**, **Sando**, **Adrián**, **Lela** polos bos momentos pasados xuntos durante a carreira, durante o doutorado e polos que quedan por vir.

- A **Nancy**, **Rodri**, **Clara**, **Ale**, **Lidia**, **Inma** e demais familia coa comecei a miña pequena historia na Escola que agora toca ó seu fin.

- **Ós da casa**, por educarme na cultura do esforzo e a humildade e por tirar de min cando me fixo falta. A **Gea** e **Hera**, pola súa compañía durante o tramo final de escritura da Tese.

- A **Julie**, por aceptar as miñas decisións, por difíciles que sexan, por apoiarme en todo e polos bos momentos que nos quedan por vivir.

En xeral, a todos aqueles que dun xeito ou doutro participaron na miña vida durante estes últimos 4 anos e que contribuíron a que esta Tese se fixese realidade. **Graciñas** a todos!

Resumo

A Tese de Doutoramento Características reolóxicas e físico-químicas de productos libres de glute de fariña de castaña con pos de algas pardas secadas baséase nomeadamente no estudo do proceso de obtención de produtos sen glute con alto carácter antioxidante, aptos para a poboación celíaca, a partires de materias primas autóctonas de Galicia, castaña (*Castanea sativa Mill.*) e algas pardas con altos contidos en polifenois (*Ascophyllum nodosum*, *Bifurcaria bifurcata* e *Fucus vesiculosus*) co obxectivo de aumentar e diversificar o seu consumo. Os estudos realizados nesta Tese estiveron enfocados á determinación das condicións máis axeitadas no proceso de obtención de micronizados de alga (operacións unitarias de secado e moenda) cunha alta actividade antioxidante e un alto contido en polifenois e nos efectos da súa adición nas masas sen glute (amasado e enfornado) para obter un produto final apto, en base as súas propiedades físicoquímicas (cor, textura e actividade antioxidante).

Palabras Chave: castaña, alga parda, reoloxía, actividad antioxidante, galleta sen glute

Resumen

La Tesis Doctoral "*Características reológicas y físico-químicas de productos libres de gluten de harina de castaña con polvos de algas secadas*" se basa principalmente en el estudio del procese de obtención de productos sin gluten con alto carácter antioxidante, aptos para la población celíaca, a partir de materia primas autóctonas de Galicia, castaña (*Castanea sativa Mill.*) y algas pardas con altos contenidos en polifenoles (*Ascophyllum nodosum*, *Bifurcaia bifurcata* y *Fucus vesiculosus*) con el objetivo de aumentar y diversificar su consumo. Los estudios realizados en esta Tesis estuvieron enfocados a la determinación de las condiciones más adecuadas en el proceso de obtención de micronizados de alga (operaciones unitarias de secado y molienda) con una alta actividad antioxidante y un alto contido en polifenoles y en los efectos de su adición en las masas sin gluten (amasado y horneado) para obtener un producto final apto, en base a sus propiedades fisicoquímicas (color, textura y actividad antioxidante).

Palabras Clave: castaña, alga parda, reología, actividad antioxidante, galleta sin gluten

Abstract

The PhD Thesis "*Rheological and physico-chemical characteristics of gluten-free chestnut flour products products with dried brown seaweed powders*" is mainly based on the study of the process of obtaining gluten-free products with a high antioxidant character, suitable for the celiac population, from raw materials native from Galicia, chestnut (*Castanea sativa Mill.*) and brown seaweeds with high polyphenols content (*Ascophyllum nodosum*, *Bifurcaria bifurcata* and *Fucus vesiculosus*) in order to increase and diversify their consumption. The studies carried out in this Thesis were focused on the determination of the most adequate conditions in the process of obtaining seaweed powders (drying and milling operations) with high antioxidant activity and polyphenols content and on the effects of their addition in the gluten-free doughs (kneading and baking) to obtain a suitable final product based on its physicochemical properties (colour, texture and antioxidant activity).

Keywords: chestnut, brown seaweed, rheology, antioxidant activity, gluten-free cookie

USC
UNIVERSIDADE
DE SANTIAGO
DE COMPOSTELA

Contents

List of Figures

List of Tables

Abstract

This PhD Thesis is mainly based on the study of the process of obtaining gluten-free products with a high antioxidant character, suitable for the celiac population, from raw materials native from Galicia, chestnut (*Castanea sativa Mill.*) and brown seaweeds with high polyphenols content (*Ascophyllum nodosum*, *Bifurcaria bifurcata* and *Fucus vesiculosus*) in order to increase and diversify their consumption. The valuation of these raw materials through their transformation into new products is considered as socioeconomic interest for the rural and marine sectors.

The use of gluten-free raw materials to obtain bakery products is a challenge due to the technological difficulty in achieving good quality in terms of nutritional characteristics and consumer acceptance. For example, in the production of gluten-free bread the main problem is that the doughs obtained from gluten-free flours have a poor gas retention capacity due to the absence of this protein, which provides the necessary viscoelastic properties for doughs that allow a stable increase of its volume during the fermentation stage. In this way, in general, a final product is obtained with a low volume and with a crumbling texture. However, such problems are less pronounced in the manufacture of gluten-free cookies, since the necessary development of the gluten network is less important and the final texture of these products is mainly associated with the thermal processes of starch (and other minor components Measured) that occurs during baking rather than protein-starch interactions.

Thus, the type of bakery product chosen for the realization of this Thesis was gluten-free cookies using chestnut flour. In order to increase the antioxidant activity, different amounts (up to 9% flour basis, f.b.) of brown seaweed powders (*Ascophyllum nodosum*, *Bifurcaria bifurcata* and *Fucus vesiculosus*) were added to the flour previously processed and characterized. In addition, different gluten-free flours of Galician maize varieties (white (Rebordanes), yellow (Sarreaus) and purple (Meiro)) were studied for comparative studies.

The studies carried out in this Thesis were focused on the determination of the most suitable conditions in the process of obtaining brown seaweed powders (drying and milling operations) and the effects of its addition on the gluten-free doughs (kneading and baking) to obtain a final product suitable from a technological point of view. The adsorption and desorption isotherms of water of the three selected species of brown seaweeds were determined in a temperature range from 5 to 65°C at different water activities (0.09-0.91). The main objective of this study was to determine the end conditions of the drying process of seaweeds (desorption process) and the corresponding for its adequate storage (desorption/adsorption). The experimental data were modelled by Halsey model throughout all the range of water activities and by the BET model for activities smaller than 0.5. A new model is proposed for the estimation of the equilibrium moisture content for the adsorption and desorption of water as function of the water activity and temperature. The water sorption process was evaluated by thermodynamic models obtaining, for each one of the species, properties related to the energy phenomena of drying operation and product stability (differential and integral enthalpies and entropies). The monolayer moisture content, traditionally considered as the optimal for product storage, evaluated by the BET model was coincident with the moisture content of minimum integral entropy (0.10 kg water / kg dry weight (d.b.)) for *Ascophyllum nodosum* and 0.05 d.b. for *Bifurcaria bifurcata* and *Fucus vesiculosus*).

The drying of the selected seaweeds was carried out in a tray dryer using different temperatures (35, 50, 60 and 75°C) and load densities (from 1.5 (monolayer) to 15 kg·m^2 (deep-bed)). The aim of this study was to determine drying kinetics using these operating conditions and their influence on the properties of the dry products, mainly by means of scavenging capacity (DPPH) and composition (polyphenols and total carbohydrate content) of their aqueous extracts. The modelling of the constant and decreasing drying rate periods of drying allowed the determination of the individual coefficients of mass transfer in the external phase (air) and the effective water diffusivity inside the solid, respectively, using theoretical models. The diffusion coefficients determined considering cylindrical geometry and shrinkage of the sample during the drying varied with the drying temperature and also between species. *Ascophyllum nodosum* presented the highest values of diffusion coefficient (2.8 - 5.4·10^{-10} m^2·s^{-1}) and *Bifurcaria bifurcata* the lowest (1.2 - 2.0·10^{-10} m^2·s^{-1}). The dried seaweeds were milled to obtain powders and their size, colour, water retention and swelling capacity as well as their solubility in water were determined. The seaweed powders showed particle sizes similar to those of commercial additives. In all cases a decrease of the antioxidant activity and the total polyphenol content of aqueous extracts were observed with an increase of drying temperature. The extracts with the highest scavenging activity were obtained

from *Ascophyllum nodosum*. The seaweed powders selected to add to chestnut flour were those obtained from drying at 35°C.

The production of chestnut flour required different operations: dehulling, peeling, grinding, drying and milling. Particle size, damaged and total starch content of chestnut flours were determined and compared with other maize flours studied. Chestnut flour showed a smaller particle size (35.4 μm), total (51%) and damaged starch content (8%). Among the maize varieties, white showed the highest values of size (97.1 μm) and damaged starch (25%). Total starch for maize flours varied in a small range (60 - 75%).

Once the seaweed powders and the gluten-free flours were obtained, kneading experiments were carried out on flours and chestnut flours mixtures with algae contents of 3, 6 and 9% (f.b.), using the Mixolab® laboratory kneader in order to obtain mixing properties with water at a target consistency (1.1 Nm). Three different kneading protocols were used, two standard protocols: one mixing at 30°C for 30 min at 80 rpm and other where thermal processes in doughs were studied by heating from 30 to 90°C and subsequent cooling of doughs to 50°C during a constant kneading at 80 rpm and a proposed protocol where a thermal sweep was performed from 50 to 90°C in order to obtain pregelatinized doughs. This study indicated the need of guar gum addition at 2% (f.b.) to the chestnut flour in order to obtain gluten-free doughs with adequate characteristics. The addition of seaweeds increased the hydration of doughs and improved their mixing properties, increasing their stability and reducing their mechanical weakening and retrogradation. From the study of the different maize flours it was concluded that higher amounts of damaged starch causes a greater hydration of doughs.

The obtained doughs were rheologically characterized at 30°C through small amplitude oscillatory tests (SAOS) and of creep and recovery tests using plate-plate geometry. The SAOS tests showed elastic behaviour higher than the viscous in all studied doughs, as is common in the gluten-free dough. Chestnut flour doughs presented values of the viscoelastic modules higher than those of corn flour. The addition of seaweed powder to chestnut flour caused a decrease in the values of the viscoelastic modules due mainly to the higher hydration of doughs. The creep and recovery tests were in agreement with the SAOS, for example, stiffer doughs (higher elastic modulus) showed a lower deformation capacity. The maximum limit of seaweed addition that did not modify creep and recovery properties was 9% for *Ascophyllum nodosum* and *Fucus vesiculosus* and 6% for *Bifurcaria bifurcata*. On the other hand, it was observed that doughs obtained with the pregelatinization protocol had higher values of recovery deformation and, consequently, showed adequate properties for subsequent baking. The final baked product was elaborated from these doughs, with and without addition of seaweed.

The study of thermal transitions of biopolymers present in the dough, that take place during the cooking/baking processes of the bakery products, is very important to understand the processes involved in the formation of crumb and crust. These studies were carried out through two different techniques, Differential Scanning Calorimetry (DSC) and Dynamic Mechanic-Thermal Analysis (DMTA) in a temperature range from 30 to 180°C. The comparison of the results obtained by the two methods allowed to establish a novel determination protocol for all studied doughs of different thermal transitions associated with starch (granule swelling and gelatinization, G and M1 transitions), amylose-lipid complex fusion (transition M2) and amylose fusion (M3 transition) through the DMTA data. It was observed that higher hydration of flours caused a decrease in the temperatures of the beginning of gelatinization process. The effect of addition of seaweeds to chestnut flour caused a decrease in the temperature at which the starch granules break, without significantly modifying the other transitions. On the other hand, no thermal transitions were detected associated to the biopolymers of the seaweeds, which seems to indicate that they were not transferred to the dough matrix preventing the interactions with the other components present in the dough.

The effect of storage of chestnut flour at controlled conditions (4°C and vacuum packaging) was evaluated by analysing the physicochemical properties of flours and the thermal and kneading characteristics of the corresponding doughs. The results of the study indicated the possibility of storage of chestnut flour in the aforementioned conditions in a period of at least one year without modifying their properties. This period is considered acceptable from an industrial point of view, taking into account the annual periodicity of the chestnut harvesting.

The pregelatinized doughs obtained after kneading process were baked at 180°C for 25 min. The textural, antioxidant and colorimetric properties of the obtained cookies were determined in order to evaluate the effect of the seaweed addition. It was observed that an addition of seaweed higher than 6% significantly increased the hardness and Young's modulus of cookies. The green color and polyphenol content of cookies increased with the addition of seaweeds while the antioxidant properties, in general, were similar between chestnut and seaweed-enriched cookies, mainly due to formation of Maillard compounds during baking that overlaps the antioxidant effect of the added marine biocompounds.

Finally, the effect of *Fucus vesiculosus* powder addition to a wheat standard formulation for bread obtaining was determined. The addition of seaweed increased the viscosity of doughs and decreased the volume at the end of proofing resulting in breads with higher density and crumb hardness. From a technological point of view, seaweed powder can be added to wheat flour up to 4% (f.b.) without impairing the properties compared to a standard wheat bread.

Resumen Extenso

Esta Tesis Doctoral se basa principalmente en el estudio del procese de obtención de productos sin gluten con alto carácter antioxidante, aptos para la población celíaca, a partir de materia primas autóctonas de Galicia, castaña (*Castanea sativa Mill.*) y algas pardas con altos contenidos en polifenoles (*Ascophyllum nodosum*, *Bifurcaria bifurcata* y *Fucus vesiculosus*) con el objetivo de aumentar y diversificar su consumo. La valorización de estas materias primas mediante su transformación en nuevos productos se considera de interés socieconómico para los sectores rural y marino.

La enfermedad celíaca es una intolerancia crónica a las proteínas del gluten cuyo único tratamiento es el seguimiento de una estricta dieta libre e gluten durante toda la vida, ya que su ingesta provoca una lesión en la mucosa del intestino delgado, disminuyendo la absorción de los nutrientes, produciendo carencias nutricionales. Debido al aumento de pacientes celíacos, la demanda de productos alimentarios libres de gluten de alta calidad ha tenido un incremento considerable en los últimos años. Pese a ello, el uso de materias primas sin gluten para la obtención de productos de panificación es todavía un reto hoy en día debido a la dificultad tecnológica a la hora de alcanzar una buena calidad en términos de características nutricionales y de aceptación por parte del consumidor. Por ejemplo, en la producción de pan sin gluten el principal problema es que las masas obtenidas a partir de harinas sin gluten tienen una capacidad de retención de gas muy deficiente debido precisamente a la ausencia de esta proteína, la cual aporta las propiedades viscoelásticas adecuadas a las masas que permiten un aumento estable de su volumen durante la etapa de fermentación. De esta forma, en general se obtiene un producto final con un bajo volumen y con una textura desmigajada. Sin embargo, tales problemas son menos acusados en la fabricación de galletas sin gluten, dado que el desarrollo necesario de la red de gluten es menor y la textura final de esto productos está principalmente asociada a los procesos térmicos del almidón (y otros componentes en menor medida) que tiene lugar durante el horneado más que a las interacciones proteína-almidón.

Así, el tipo de producto de panificación escogido para la realización de esta Tesis fueron las galletas sin gluten empleando harina de castaña. Con el fin de aumentar la actividad antioxidante, se añadieron a la harina diferentes cantidades (hasta un 9 % en base harina, b.h.) de micronizados de algas pardas (*Ascophyllum nodosum*, *Bifurcaria bifurcata* y *Fucus vesiculosus*) previamente procesadas y caracterizadas. Adicionalmente, se estudiaron harinas sin gluten de diferentes variedades gallegas de maíz (blanco (Rebordanes), amarillo (Sarreaus) y morado

(Meiro)) para realizar estudios comparativos.

Los estudios realizados en esta Tesis estuvieron enfocados a la determinación de las condiciones más adecuadas en el proceso de obtención de micronizados de alga (operaciones unitarias de secado y molienda) y en los efectos de su adición en las masas sin gluten (amasado y horneado) para obtener un producto final apto desde el punto de visto tecnológico.

Se llevó a cabo la determinación de las isotermas de adsorción y desorción de agua en un rango de temperatura desde 5 hasta 65°C a diferentes actividades de agua (0,09 - 0,91) de las tres especies de algas pardas seleccionadas. El objetivo principal de este estudio fue la determinación de las condiciones de finalización de la etapa de secado de las algas (proceso de desorción) y las correspondientes para su correcto almacenamiento (desorción / adsorción). A altas actividades de agua, el alga más higroscópica fue el *Ascophyllum nodosum* sin diferencias significativas entre *Bifurcaria bifurcata* y *Fucus vesiculosus*. A bajas actividades de agua no se observaron diferencias entre las algas estudiadas. Las curvas obtenidas fueron en todos los casos, de acuerdo con la clasificación de Brunauer – Emmett - Teller (BET), de tipo II con una tendencia a tipo III con el aumento de temperatura. Los datos experimentales fueron modelados a través del modelo Halsey en todo el rango de actividades de agua y del modelo BET a actividades menores de 0,5. Se propone un modelo para la estimación de la humidad de equilibrio para la adsorción y desorción de agua en función, simultáneamente, de la actividad de agua y la temperatura. El proceso de sorción de agua fue evaluado mediante modelos termodinámicos obteniéndose, para cada una de las especies, propiedades relacionadas con los fenómenos energéticos de la operación de secado y de estabilidad del producto (entalpías y entropías diferenciales e integrales). La humedad de la monocapa, tradicionalmente considerada como óptima para el almacenamiento de un producto, evaluada mediante el modelo BET se verificó que coincide con la humedad de mínima entropía integral (0,10 kg agua ·(kg sólido seco)$^{-1}$ (b.s.) para *Ascophyllum nodosum* y 0,05 b.s. para *Bifurcaria bifurcata* y *Fucus vesiculosus*).

El estudio del secado de las algas seleccionadas se llevó a cabo en un secadero de bandejas empleando diferentes temperaturas (35, 50, 60 y 75°C) y densidades de carga (desde 1,5 (monocapa) a 15 kg · m−2 (lecho)) a una humedad relativa (30 %) y velocidad de aire (2 m·s^{-1}) constantes. El objetivo de este estudio fue determinar las cinéticas de secado empleando estas condiciones de operación y su influencia en las propiedades de los productos deshidratados, principalmente en la capacidad antirradicalaria (DPPH) y la composición (contenido en polifenoles y carbohidratos totales) de sus extractos acuosos. El estudio de las cinéticas de secado empleando una densidad de carga de 15 kg · m−2 indicó que

la temperatura óptima de secado basándose en la transferencia de materia es de 50°C para AN, 75°C para *Bifurcaria bifurcata* y 60°C para *Fucus vesiculosus*. La modelización de los periodos de velocidad de secado constante y decreciente de las cinéticas de secado en monocapa, permitió la determinación, respectivamente, de los coeficientes individuales de transferencia de materia en la fase externa (aire) y las difusividades efectivas de agua en el interior del sólido empleando modelos teóricos. Los coeficientes de transferencia de materia fueron similares para todas las algas en el secadero empleado (13.7 - 21.8·$^{-3}$ m·s^{-1}). Los coeficientes de difusión determinados considerando geometría cilíndrica y encogimiento de la muestra durante el secado variaron con la temperatura de secado y también se encontraron diferencias significativas entre especies. *Ascophyllum nodosum* presentó los mayores valores de coeficiente de difusión (2,8 - 5,4·10^{-10} m2·s^{-1}) seguido de *Fucus vesiculosus* (1,0 - 2,7·$^{-10}$ m2·s^{-1}) y *Bifurcaria bifurcata* (1,2 - 2,0·$^{-11}$ m2·s^{-1}).

El alga seca fue molida obteniéndose micronizados a los que se les determinó su tamaño, color y capacidad de retención de agua e hinchazón así como su solubilidad en agua. El tamaño de partícula de los micronizados dependió del tipo de alga. Por ejemplo, el diámetro medio de superficie fue mayor para los polvos de *Fucus vesiculosus* (133 - 147 μm) comparado con *Bifurcaria bifurcata* (106 - 126 μm) y *Ascophyllum nodosum* (77 - 108 μm) mientras que la distribución de tamaños de partícula fue bimodal para *Ascophyllum nodosum* y *Fucus vesiculosus* y unimodal para *Bifurcaria bifurcata*. Pese a las diferencias observadas, los valores obtenidos de tamaño de partícula estuvieron dentro del rango de tamaño típico de aditivos de harinas comerciales. La determinación de la capacidad de hinchazón y retención de agua indicó que *Bifurcaria bifurcata* posee valores más altos de estos parámetros comparado con *Ascophyllum nodosum* y *Fucus vesiculosus*, los cuales no mostraron diferencias significativas entre sí. El estudio del color de los polvos indicó una fuerte predominancia del color verde, además, se observó que el color de los polvos integrales puede ser estimado a través del color correspondiente a cada fracción de tamaño de partícula y su fracción en masa mediante una regla de mezcla siempre y cuando ninguna fracción de tamaño de partícula supere el 40 % en peso de la harina integral.

Para la obtención de extractos acuosos de los micronizados de algas se realizaron ensayos preliminares para el establecimiento de las condiciones de extracción óptimas que llevasen a un mayor contenido en polifenoles. Dichas condiciones fueron 4 min de tiempo de retención y 30 w / w de relación líquido / sólido. El alga cuyos extractos acuosos mostraron un mayor contenido en polifenoles ($\approx$ 3000 mg PHL ·(100 g polvo seco)$^{-1}$) y actividad antioxidante ($\approx$ 75 %) fue *Ascophyllum nodosum* seguido de *Bifurcaria bifurcata* y *Fucus vesiculosus*. En el caso del contenido en carbohidratos totales el mayor contenido

se observó en los extractos de *Fucus vesiculosus* y *Ascophyllum nodosum* ($\approx$ 6000 mg GL $\cdot$(100 g polvo seco)$^{-1}$). En todos los casos se observó un decrecimiento de la actividad antioxidante y el contenido en polifenoles totales de los extractos acuosos con un aumento de la temperatura de secado. Altas temperaturas durante el secado redujeron dramáticamente el contenido en polifenoles (hasta un 54 % a 75°C comparado con 35°C) y la actividad antioxidante de los extractos lo que indicó que la temperatura óptima de secado que resulta en los valores más elevados de estos parámetros son 35°C para *Bifurcaria bifurcata* y *Fucus vesiculosus* y $\leq$ 50°C para AN. Los micronizados seleccionados para añadir a la harina de castaña fueron los obtenidos tras el secado a más baja temperatura (35°C). El uso de temperaturas de secado por encima de 60°C decreció también el contenido en carbohidratos total para *Ascophyllum nodosum* y *Bifurcaria bifurcata*, mientras que este permaneció constante en el caso de *Fucus vesiculosus*. Finalmente, se observó una relación lineal entre el color verde los polvos de algas (parámetro colorimétrico a*) y la actividad antioxidante de los correspondientes extractos, cuando estos tiene una actividad antioxidante superior al 45 %.

La obtención de harina de castaña necesitó la realización de diferentes operaciones: descascarado, pelado, triturado, secado y molienda. El tamaño de partícula, el contenido de almidón dañado y total de la harina de castaña fueron determinados y comparados con otras harinas de maíz estudiadas. La harina de castaña mostró un menor tamaño de partícula (35,4 μm), contenido en almidón total (51 %) y dañado (8 %). Entre las variedades de maíz, el blanco mostró valores más altos de tamaño (97,1 μm) y almidón dañado (25 %). El almidón total para las harinas de maíz varió en un pequeño rango (60 – 75 %).

Una vez obtenidos los micronizados y las harinas sin gluten, se llevaron a cabo ensayos de amasado de las harinas y de las mezclas de harina de castaña con contenidos de alga del 3, 6 y 9 % (b.h.), empleando la amasadora de laboratorio Mixolab®, para obtener propiedades de mezcla con agua a una consistencia objetivo (1,1 Nm). Se emplearon tres protocolos de amasado diferentes, dos protocolos estandarizados: uno de mezcla a 30°C durante 30 min a 80 rpm y otro en donde se estudiaron los procesos térmicos en las masas mediante calentamiento desde 30 hasta 90°C y posterior enfriamiento de las masas hasta 50°C durante un amasado constante a 80 rpm y un protocolo propuesto en donde se realizó una rampa térmica desde 50 hasta 90°C con el objetivo de obtener masas pregelatinizadas. Las harinas de maíz mostraron diferentes absorciones de agua en función de la variedad de maíz. La harina maíz blanco necesitó mayor cantidad de agua (90 % b.h.) comparado con la de maíz morado (81 % b.h.) y amarillo (63 %) para obtener al torque deseado debido a su mayor contenido en almidón dañado. El aumento de tamaño de partícula en

la harina de maíz blanco provocó una disminución de la hidratación (≈ 49 % b.h.) y un considerable aumento en el tiempo de desarrollo y estabilidad de las masas. Este estudió indicó la necesidad de la adición de gomar guar á 2 % (b.h.) a la harina de castaña para obtener masas libres de gluten con características adecuadas. Su hidratación fue de en torno al 57 % (b.h.) La adición de micronizados de alga aumentó significativamente la hidratación de las masas (hasta el 71% b.h.) y mejoró sus propiedades, aumentando su estabilidad y reduciendo su debilitamiento mecánico y su retrogradación.

Las masas obtenidas fueron caracterizadas reológicamente a 30°C a través de ensayos oscilatorios de pequeña amplitud (SAOS, en inglés) y de ensayos de fluencia y recuperación empleando una geometría plato-plato. Los espectros mecánicos de las masas ensayadas mostraron que los módulos de almacenamiento (G') y pérdida (G'') aumentan con la frecuencia angular para cada uno de los sistemas estudiados en el rango de frecuencias angulares analizadas. Se observó además, un comportamiento elástico mayor que el viscoso en todas las masas, como es común en las masas de harina sin gluten. En el caso de las masas de maíz blanco, el aumento del tamaño de partícula de la harina provocó un aumento en los módulos viscoelásticos de las masas, mientras que para tamaños de partícula similares, los mayores valores de los módulos viscoelásticos se observaron en las masas de maíz amarillo sin diferencias significativas entre las de maíz morado y blanco. Las masas de harina de castaña presentaron valores de los módulos viscoelásticos más altos que las de harina de maíz. La adición de polvo de alga a la harina de castaña provocó un descenso en los valores de los módulos debido principalmente a la mayor hidratación de las masas. Los ensayos de fluencia y recuperación concordaron con los SAOS, por ejemplo, las masas más rígidas (mayor módulo elástico) mostraron una capacidad de deformación menor. El límite máximo de adición de alga que no modificó las propiedades de fluencia y recuperación fue del 9 % para *Ascophyllum nodosum* y *Fucus vesiculosus* y del 6 % para *Bifurcaria bifurcata*. Por otro lado, se observó que las masas obtenidas con el protocolo de pregelatinización presentaron valores más elevados de recuperación de la deformación y en consecuencia mostraron propiedades adecuadas para su posterior horneado. De esta forma, el producto final horneado fue elaborado a partir de estas masas, con y sin adición de algas.

El estudio de las transiciones térmicas de los biopolímeros presentes en la masa que tienen lugar durante los procesos de cocción / horneado de los productos de panificación es fundamental para conocer los procesos envueltos en la formación, en su caso, de la miga y la corteza. Estos estudios fueron llevados a cabo a través de dos técnicas diferentes, calorimetría diferencial de barrido (DSC, en inglés) y análisis dinámico mecánico térmico (DMTA, en inglés) en un rango de temperaturas desde 30 hasta 180°C. La comparación de los resultados obtenidos

por los dos métodos permitió establecer un novedoso protocolo de determinación para todas las masas estudiadas de diferentes transiciones térmicas asociada al almidón (hinchazón del gránulo y gelatinización, transiciones G y M1), fusión de complejos amilosa-lípido (transición M2) y fusión de la amilosa (transición M3) a través de los datos de DMTA. Se observó que una mayor hidratación de las harinas provocó un descenso en las temperaturas de inicio del proceso de gelatinización. El efecto de la adición de alga a la harina de castaña se traduzco en un descenso de la temperatura a la cual tiene lugar la rotura de los gránulos de almidón, no modificando significativamente las demás transiciones. Por otro lado, no se detectaron transiciones térmicas asociadas a los biopolímeros de las algas lo que parece indicar que no fueron transferidos a la matriz de la masa impidiendo las interacciones con los demás componentes en la misma.

Se realizó un estudio del efecto del almacenamiento en condiciones controladas (4°C y envase a vacío) de harina de castaña mediante el análisis de las propiedades fisicoquímicas y las características térmicas y de amasado de las correspondientes masas. Los resultados del estudio indicaron la posibilidad de almacenamiento de harina de castaña en las citadas condiciones en un período de como mínimo un año sin que sus propiedades se vean modificadas. Este período se considera suficiente desde el punto de vista industrial, teniendo en cuenta la periodicidad anual de la cosecha de castaña.

Las masas pregelatinizadas obtenidas tras el proceso de amasado fueron horneadas a 180°C durante 25 min. Las propiedades texturales, antioxidantes y colorimétricas de las galletas obtenidas fueron determinadas con el objetivo de la evaluación del efecto de la adición de alga. Además se determinaron dichas las mismas propiedades para las mezclas de harina de castaña y algas para evaluar el efecto del horneado. Se observó que el proceso de horneado aumentó significativamente el contenido en polifenoles (desde $\approx$ 100 hasta $\approx$ 700 mg PHL $\cdot$(100 g polvo seco)$^{-1}$) de las galletas y su actividad antioxidante (desde el 12 % hasta el 59 %). La adición de alga mayor al 6 % aumentó significativamente la dureza y el módulo de Young de las galletas. El color verde y el contenido en polifenoles de las galletas aumentó con la adición de alga mientras que las propiedades antioxidantes, en general, fueron semejantes entre las galletas de castaña y las enriquecidas con alga, debido principalmente a la formación de compuestos de Maillard durante el horneado que enmascaran el efecto antioxidante de los biocompuestos marinos añadidos.

Comparado con productos comerciales similares, el producto obtenido posee una alta capacidad antioxidante y altos valores de polifenoles, unos parámetros colorimétricos en el rango de los observados para otras galletas y unos valores de dureza que se sitúan en el límite superior de los observados en la literatura.

Por último, se realizó un estudio del efecto de la adición del micronizado de *Fucus vesiculosus* en una formulación estándar de trigo para la obtención de pan. El estudio del efecto de la inclusión de polvo de *Fucus vesiculosus* en harinas de trigo para obtención de pan indicó que dicha adición incrementa la viscosidad de las masas (desde 1,2·105 hasta 3,5·105 Pa·s a 0,025 s-1) y su estabilidad (≈ 20 %) y tiene un efecto negativo en la porosidad de la masa después de la fermentación (disminuyendo su valor desde 0,77 hasta 0,52). La determinación de las propiedades finales del pan (densidad del pan y dureza de la miga) indicó que el polvo de *Fucus vesiculosus* puede ser añadido a harina de trigo para la obtención de panes de trigo enriquecidos hasta un máximo de un 4 % b.h. sin modificar significativamente las propiedades finales del producto obtenido comparado con un pan de trigo standard.

Resumo Extenso

Esta Tese de Doutoramento baséase nomeadamente no estudo do proceso de obtención de produtos sen glute con alto carácter antioxidante, aptos para a poboación celíaca, a partires de materias primas autóctonas de Galicia, castaña (*Castanea sativa Mill.*) e algas pardas con altos contidos en polifenois (*Ascophyllum nodosum*, *Bifurcaria bifurcata* e *Fucus vesiculosus*) co obxectivo de aumentar e diversificar o seu consumo. A valorización destas materias primas mediante a súa transformación en novos produtos considérase de interese socioeconómico para os sectores rurais e mariños.

O uso de materias primas sen glute para a obtención de produtos de panificación é un reto debido á dificultade tecnolóxica á hora de acadar unha boa calidade en termos de características nutricionais e aceptación por parte do consumidor. Por exemplo, na produción de pan sen glute o principal problema atópase en que as masas obtidas a partires de fariñas sen glute teñen unha deficiente capacidade de retención de gas debido precisamente á ausencia desta proteína, a cal aporta as propiedades viscoelásticas axeitadas ás masas que permiten un aumento estable do seu volume durante a etapa de fermentación. Deste xeito, en xeral obtense un produto final cun baixo volume e cunha textura esmigallada. Porén, tales problemas son menos acusados na fabricación de galletas sen glute, dado que o necesario desenvolvemento da rede de glute é menor e a textura final destes produtos está principalmente asociada aos procesos térmicos do amidón (e doutros compoñentes en menor medida) que teñen lugar durante o enfornado máis que ás interaccións proteína-amidón.

Así, o tipo de produto de panificación escollido para a realización desta Tese foron as galletas sen glute empregando fariña de castaña. Co fin de aumentar a actividade antioxidante, engadíronse á fariña diferentes cantidades (ata 9% en base fariña, b.f.) de micronizados de algas pardas (*Ascophyllum nodosum*, *Bifurcaria bifurcata* e *Fucus vesiculosus*) previamente procesadas e caracterizadas. Adicionalmente, estudáronse fariñas sen glute de diferentes variedades galegas de millo (branco (Rebordanes), amarelo (Sarreaus) e morado (Meiro)) para realizar estudos comparativos.

Os estudos realizados nesta Tese estiveron enfocados á determinación das condicións máis axeitadas no proceso de obtención de micronizados de alga (operacións unitarias de secado e moenda) e nos efectos da súa adición nas masas sen glute (amasado e enfornado) para obter un produto final apto dende un punto de vista tecnolóxico. Levouse a cabo a determinación das isotermas de adsorción e desorción da auga nun rango de temperatura dende 5 ata 65ºC a diferentes actividades de auga (0,09 - 0,91) das tres especies de algas pardas

seleccionadas. O obxectivo principal deste estudo foi a determinación das condicións de finalización da etapa do secado das algas (proceso de desorción) e as correspondentes para o seu correcto almacenamento (desorción/adsorción). Os datos experimentais foron modelados a través do modelo Halsey en todo o rango de actividades de auga e do modelo BET a actividades menores de 0,5. Proponse un modelo para a estimación da humidade de equilibrio para a adsorción e desorción da auga en función, simultaneamente, da actividade de auga e a temperatura. O proceso de sorción da auga foi avaliado mediante modelos termodinámicos obténdose para cada unha das especies propiedades relacionadas cos fenómenos enerxéticos da operación de secado e de estabilidade do produto (entalpías e entropías diferenciais e integrais). A humidade da monocapa, tradicionalmente considerada como óptima para o almacenamento dun produto, avaliada mediante o modelo BET verificouse que coincide coa humidade de mínima entropía integral (0.10 kg auga/kg sólido seco (b.s.) para *Ascophyllum nodosum* e 0.05 b.s. para *Bifurcaria bifurcata* e *Fucus vesiculosus*).

O estudo do secado das algas seleccionadas levouse a cabo nun secadoiro de bandexas empregando diferentes temperaturas (35, 50, 60 e 75°C) e densidades de carga (dende 1,5 (monocapa) a 15 kg·m^2 (leito)). O obxectivo deste estudo foi determinar as cinéticas de secado empregando estas condicións de operación e a súa influencia nas propiedades dos produtos deshidratados, nomeadamente na capacidade antirradicalaria (DPPH) e composición (contido en polifenois e carbohidratos totais) dos seus extractos acuosos. A modelización dos períodos de velocidade de secado constante y decrecente permitiu a determinación, respectivamente, dos coeficientes individuais de transferencia de materia na fase externa (aire) e as difusividades efectivas da auga no interior do sólido empregando modelos teóricos. Os coeficientes de difusión determinados considerando xeometría cilíndrica e encollemento da mostra durante o secado variaron coa temperatura de secado e tamén se atoparon diferencias significativas entre especies. *Ascophyllum nodosum* presentou os maiores valores de coeficiente de difusión (2,8 - 5,4·10^{-10} m^2·s^{-1}) e *Bifurcaria bifurcata* os menores (1,2 - 2,0·10^{-10} m^2·s^{-1}). A alga secada foi moída obténdose micronizados aos que se lle determinou o seu tamaño, cor, capacidade de retención de auga e inchazón así como a súa solubilidade en auga. Os micronizados de alga mostraron tamaños de partícula semellantes aos dos aditivos comerciais. En tódolos casos observouse un decrecemento da actividade antioxidante e o contido en polifenois totais dos extractos acuosos cun aumento da temperatura de secado. Os extractos cunha actividade antirradicalaria máis alta foron os obtidos a partires de *Ascophyllum nodosum* e logo os de *Bifurcaria bifurcata*. Os micronizados seleccionados para engadir á fariña de castaña foron os obtidos tralo secado a máis baixa temperatura (35°C).

A obtención da fariña de castaña precisou da realización de diferentes operacións: descascado, pelado, triturado, secado e moenda. O tamaño de partícula, o contido de amidón danado e total da fariña de castaña foron determinados e comparados coas outras fariñas de millo estudadas. A fariña de castaña foi aquela cun menor tamaño de partícula (35,4 μm), contido en amidón total (51%) e danado (8%). Entre as variades de millo, o branco amosou valores máis altos de tamaño (97,1 μm) e amidón danado (25%). O amidón total para as fariñas de millo variou nun pequeno rango (60-75%).

Unha vez obtidos os micronizados e as fariñas sen glute, leváronse a cabo ensaios de amasado das fariñas e de mesturas de fariña de castaña con contidos de alga do 3, 6 e 9% (b.f.), empregando a amasadora de laboratorio Mixolab®, para obter propiedades de mestura coa auga cunha consistencia obxectivo (1,1 Nm). Empregáronse tres protocolos de amasado diferentes, dous protocolos estandarizados: un de mestura a 30°C durante 30 min a 80 rpm e outro onde se estudaron os procesos térmicos nas masas mediante quentamento dende 30 ata 90°C e posterior arrefriamento das masas ata 50°C durante un amasado constante a 80 rpm, e un protocolo proposto onde se realizou unha rampla térmica dende 50 a 90°C co obxectivo de obter masas prexelatinizadas. Este estudo indicou a necesidade da adición de goma guar ó 2% (b.f.) á fariña de castaña para obter masas libres de glute con características axeitadas. A adición da alga aumentou a hidratación das masas e mellorou as súas propiedades, aumentando a súa estabilidade e reducindo o seu enfraquecemento mecánico e a súa retrogradación. Do estudo das diferentes fariñas de millo concluíuse que maiores cantidades de amidón danado provocan unha maior hidratación das masas.

As masas obtidas foron caracterizadas reoloxicamente a 30°C a través de ensaios oscilatorios de pequena amplitude (SAOS, en inglés) e de ensaios de fluencia e recuperación empregando unha xeometría prato-prato. Os ensaios SAOS mostraron un comportamento elástico maior que o viscoso en tódalas masas, como é común nas masas de fariña sen glute. As masas de fariña de castaña presentaron valores dos módulos viscoelásticos máis altos que as de fariña de millo. A adición de po de alga á fariña de castaña provocou un descenso nos valores dos módulos debido principalmente á maior hidratación das masas. Os ensaios de fluencia e recuperación concordaron cos SAOS, por exemplo, as masas máis ríxidas (maior módulo elástico) mostraron unha capacidade de deformación menor. O límite máximo de adición de alga que non modificou as propiedades de fluencia e recuperación foi do 9% para *Ascophyllum nodosum* e *Fucus vesiculosus* e do 6% para *Bifurcaria bifurcata*. Por outra banda, observouse que as masas obtidas co protocolo de prexelatinización presentaron valores máis elevados de recuperación da deformación e en consecuencia mostraron propiedades axeitadas para o seu posterior enfornado. Deste xeito, o produto final enfornado foi elaborado a partires

destas masas sen e coa adición de algas.

O estudo das transicións térmicas dos biopolímeros presentes na masa que teñen lugar durante os procesos de cocción/enfornado dos produtos de panificación é fundamental para coñecer os procesos envolvidos na formación, no seu caso, do miolo e da codia. Estes estudos foron levados a cabo a través de dúas técnicas diferentes, calorimetría diferencial de barrido (DSC, en inglés) e análise dinámico mecánico térmico (DMTA, en inglés) nun rango de temperaturas dende 30 ata 180ºC. A comparación dos resultados obtidos por ámbolos dous métodos permitiu establecer un novidoso protocolo de determinación para tódalas masas estudadas de diferentes transicións térmicas asociadas ó amidón (inchazón do gránulo e xelatinización, transicións G e M1), fusión de complexos amilosa-lípido (transición M2) e fusión da amilosa (transición M3) a través dos datos de DMTA. Observouse que unha maior hidratación das fariñas provocou un descenso nas temperaturas de comezo do proceso de xelatinización. O efecto da adición da alga á fariña de castaña traduciuse nun descenso da temperatura á cal ten lugar a rotura dos gránulos de amidón, non modificando significativamente o resto das transicións. Por outra banda, non se detectaron transicións térmicas asociadas aos biopolímeros das algas o que parece indicar que non foron transferidos á matriz da masa impedindo as interaccións cos demais compoñentes da mesma.

Realizouse un estudo do efecto do almacenamento en condicións controladas (4ºC e envasadas a baleiro) da fariña de castaña mediante a análise das propiedades fisicoquímicas e as características térmicas e de amasado das correspondentes masas. Os resultados do estudo indicaron a posibilidade de almacenamento de fariña de castaña nas citadas condicións nun período de como mínimo un ano sen que as súas propiedades se vexan modificadas. Este período considérase suficiente dende o punto de vista industrial, tendo en conta a periodicidade anual da colleita de castaña.

As masas prexelatinizadas obtidas tralo proceso de amasado foron enfornadas a 180ºC durante 25 min. As propiedades texturais, antioxidantes e colorimétricas das galletas obtidas foron determinadas co obxectivo da avaliación do efecto da adición de alga. Observouse que unha adición de alga maior ó 6% aumentou significativamente a dureza e o módulo de Young das galletas. A cor verde e o contido en polifenois das galletas aumentou coa adición de alga mentres que as propiedades antioxidantes, en xeral, foron semellantes entre as galletas de castaña e as enriquecidas con alga, debido principalmente á formación de compostos de Maillard durante o enfornado que enmascaran o efecto antioxidante dos biocompostos mariños engadidos.

Por último, realizouse un estudo do efecto da adición de micronizado de *Fucus vesiculosus* nunha formulación estándar de trigo para a obtención de pan. Observouse que a adición da alga aumentou a viscosidade das masas e provocou un menor volume da mesma ó final da fermentación o que resultou nun pan cunha maior densidade e dureza do miolo. Os resultados indicaron que dende un punto de vista tecnolóxico pódese engadir ata un 4% (b.f.) de po desta alga á fariña de trigo sen que as propiedades dos pans enriquecidos presenten diferencias significativas cun pan de trigo estándar.

Chapter 1

Introduction

In this chapter basic information about different topics like coeliac disease, technological challenges that involves, the drying of seaweeds and the manufacture of gluten-free bakery product specifically with chestnut flour, the raw materials employed in this Thesis, is provide.

1.1 Generalities

Celiac disease is a permanent intolerance to gluten of wheat, barley, rye and probably oatmeal that occurs in genetically predisposed individuals, characterized by an inflammatory, immune-based, mucosal reaction of the small intestine that makes absorption of macro and micronutrients difficult. The estimated prevalence in Europeans and their offspring is 1% being more frequent in women in a 2:1 ratio (Borrelli *et al.*, 2010).

A significant percentage of patients (75%) are undiagnosed due to the fact that the celiac disease was exclusively related to its classic clinical presentation form for years (Mäki & Collin, 1997). However, the recognition of other atypical presentation forms, oligo and asymptomatic, combined with the greater and better use of the complementary tests available, has allowed to discover the existence of different types of celiac disease. These types are classified as:

- Symptomatic. The symptoms are very diverse but all patients show a genetic serology, histology and test compatible with celiac disease.

- Subclinical. There are no symptoms or signs, although the rest of the diagnostic tests are positive.

- Latent. They are patients who at a given moment, consuming gluten, have no symptoms and the intestinal mucosa is normal (Feighery, 1999). There are two variants:

  Type A. Patients were diagnosed with celiac disease in childhood and recovered completely after the onset of the gluten-free diet, remaining in a subclinical state with normal diet.

  Type B. In this case, on the occasion of a previous study, it is verified that the intestinal mucosa is normal, but later the patients develop the disease.

- Potential. Those people who never presented a biopsy compatible with the celiac disease but, like the previous groups, have a genetic predisposition. Although serology may be negative, there is an increase in the number of intraepithelial lymphocytes. The probability of developing an active celiac disease is 13% and a latent 50% celiac disease (Feighery, 1999).

The previously mentioned types of celiac disease are represented in the icerberg model, Figure 1.1, commonly employed to explain the prevalence of celiac disease.

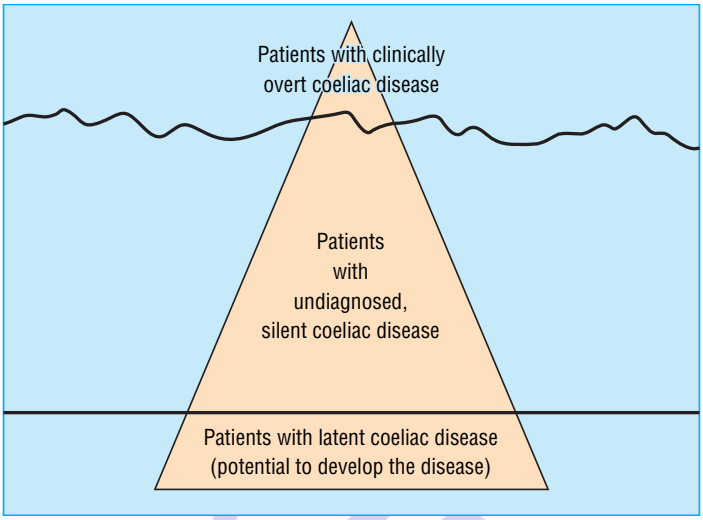

Figure 1.1. Iceberg of celiac disease (Feighery, 1999)

In the acquisition of celiac disease, there are three factors: gluten, genetic predisposition and environmental factors. Gluten produces an immune reaction in genetically predisposed individuals. Regarding genetic susceptibility, all celiac patients present the same type of HLA (humam leukocyte antigens), although not all of them with this gene develop the disease, so other genes may be involved in the onset of the disease. Environmental factors such as a too premature introduction of gluten in the diet may cause the onset of celiac disease (Murray, 1999).

The only effective treatment for celiac disease is a strict gluten-free diet during the patient's entire life. This causes a clinical and functional normalization, as well as the repair of the vellosity injury (Gallagher *et al.*, 2004). Celiac must base its diet on natural foods such as vegetables, meat, fish, eggs, fruits, and gluten-free cereals such as rice and corn or even others not as commonly consumed as chestnut. Foods prepared and/or packaged must be avoided, as far as possible, since it is more difficult to guarantee the absence of gluten in them. Digestion of small amounts of gluten, in a continuous way, can cause significant undesirable disorders.

Gluten is an amorphous protein that is found in the seed of many cereals (wheat, barley, rye, spelled, kamut, triticale and possibly oats) combined with starch. It represents 80% of wheat proteins and is composed of gliadin and

glutenin. It is responsible for the elasticity of the flour doughs that contain it, and gives the elastic and spongy consistency of breads and baked products. It can be obtained from wheat flour and other cereals, washing starch. The resulting product has a fibrous and adhesive texture similar to that of chewing gum. For this reason it is appreciated in feeding by its thickening power.

In recent years, interest in gluten-free products is on the rise. The chemical composition and nutritional properties of commonly used gluten-free flours, as well as an extensive discussion about their suitability for people suffering some of the three pathologies associated with gluten intake (i.e. gluten allergy, coeliac disease and gluten sensitivity) has been addressed on recent reviews (Rosell *et al.* (2014); Naqash *et al.* (2017)). These authors addressed that available gluten-free products lead to nutritional deficiencies in micronutrients, protein and dietary fibre and the absence of gluten is translated into the defects that appear in terms of quality attributes and consumer acceptance of final products. Technologically, the development of these products is complicated because the absence of gluten produces an impact on the characteristics of the crust and on the inside of the baking product, in its volume, porosity and other parameters of quality (Sivaramakrishnan *et al.*, 2004). Since the gluten-free products do not match gluten containing counterparts in terms of technological attributes and quality, it is a pre-requisite to adopt techniques ensuring their acceptability to the population consuming gluten-free. For this reason, many of the GF products that are on the market have a lower quality compared to the same products made with wheat. The replacement of gluten with other compounds in order to simulate its viscoelastic properties, presents a major technological challenge, as is an essential structure-building protein, contributing to the appearance and crumb structure of many baked products (Lazaridou *et al.*, 2007). For this reason, GF formulations used include the mixing of different GF flours and the incorporation of starches of different origin to wheat, such as corn, rice or potatoes, fibre, fats and hydrocolloids (Gambus *et al.*, 2001). Taking this into account, the research on possible alternatives that improve the nutritional and technological properties of existing products by their combination to other GF flours, like it could be chestnut flour, seems to be a very interesting starting point.

Non gluten containing sources frequently used include cereals (rice, maize and sorghum), minor cereals (fonio, teff, and millets) and pseudocereals (buckwheat, quinoa and amaranth) (Taylor *et al.*, 2014). Some varieties of oats are another cereals, which have recently been considered for inclusion in gluten-free products, although there is an ongoing debate concerning the presence or absence of proteins that could be toxic for coeliacs (Rosell *et al.*, 2014). Moreover, a wide range of non cereals (pulses as lentils, fruits as bananas, vegetables as potatos and nuts as chestnuts, among others) are also available for providing gluten-free flours,

even increasing the nutritional pattern of cereal products (Torres *et al.* (2013), Witczak *et al.* (2016)).

New different gluten-free baked products with health promoting components (fibre, antioxidants and/or minerals), the optimization of formulations, and the characterization of the final products in terms of technological aptitude, sensory acceptance and potential functional properties have acquired a lot of interest in the last few years (Giménez-Bastida *et al.*, 2015). Capriles *et al.* (2016) focused on the contemporary approaches that are used to increase nutrient and bioactive compound content of gluten-free bread, highlights the need to use nutrient dense alternative raw materials, nutritional and functional ingredients, and their combinations. However, enhancing the functional properties of gluten-free products by the incorporation of new ingredients on the formulations remains an important task for research and development, which is a concomitant challenge towards the improvement of technological and sensory properties.

In this sense, marine algae in general and specifically brown algae represent a suitable supplement and additive for food due to their high nutritional value and the health benefits they can provide. Moreover, in recent years there has been an increasing interest in natural antioxidants from different sources to replace synthetic additives in foods or nutraceuticals. Natural antioxidants not only have the capability to improve oxidative stability (preventing rancidity), but they can also provide a wide variety of additional health benefits. It is suggested that the addition of these compounds might enhance the body's defences against reactive oxygen species (ROS) related diseases (Wang *et al.*, 2012). Taking this into account, marine algae can play the role as source for natural antioxidants. Although they are exposed to light and oxygen, causing the formation of free radicals and other oxidizing agents, there is no presence of oxidative damage in the structural components of seaweeds and their stability to oxidation during storage. This suggests that their cells have protective antioxidative defence systems (Jiménez-Escrig *et al.*, 2001). There are two types of substances present in marine algae that are strongly related to the antioxidant activity: certain polysaccharides (fucoidans) (Hahn *et al.*, 2012) and polyphenols (phlorotannins) (Keyrouz *et al.*, 2011).

South Asian countries were the first to introduce seaweeds for their utilization for medicinal and food purposes. Conventionally, Western World has used marine algae for the production of colloids. Around 18 million tonnes of marine algae and other aquatic plants are harvested annually with an estimated value of around 4,000 million *e*. Even though, marine algae market is mainly limited to the obtaining of agar, carrageenan and alginates. Bioactive potential of these species is underexploited. Nowadays, many initiatives are being carried out in Europe

to exploit these marine valuable resources. Marine algae are abundant in Europe and have the potential to become an excellent source of bioactive compounds such as dietary fibre, omega-3 fatty acids, carotenoids, vitamins, and minerals (Kadam *et al.*, 2013). However, the main challenge would be to determine how the processing of this material (collection, extraction, drying and storage) affects these properties.

Taking into account the aforementioned relationship between celiac disease and gluten proteins and also the lack of diversity on gluten-free products in the actual market. This Thesis is mainly based on the suitability of development of new gluten-free products with antioxidant character, suitable for celiac population, from two autochthon raw materials of Galicia (chestnut and seaweed) with socio-economic interest to diversify their consumption. Moreover, some studies will be also carried out with other gluten-free starchy material such as maize. To achieve this goals, chestnut flours will be produced from chestnuts fruits after various stages of processing (dehulling, peeling, crushing, drying and milling) and doughs will be obtained by adding water and seaweed powders. The mixing, rheological and mechanical behaviour of doughs will be studied, with particular attention to the influence of thermal processes taking place in the baking step, to establish the dependence of rheological properties of doughs regarding the transformations of starch and presence of various seaweeds. Furthermore, the antioxidant properties of seaweeds added as well as that of the baked products will be evaluated.

1.2 Gluten-free starchy materials

As previously explained, the chosen starchy materials to carry out this Thesis were chestnut and maize due to the absence of gluten on their composition and their socio-economic interest for the Galician country.

1.2.1 Chestnut

Chestnut group belongs to the genus *Castanea* of a few species in the family *Fagaceae*. Major chestnut species include *Castanea crenata* in Japan, *Castanea mollissima* in China and Korea, and *Castanea sativa* mostly grown in Europe and South America (De Vasconcelos *et al.* (2010); FAOSTAT (2017)).

The European chestnut (*Castanea sativa* Mill.) probably had its origins in the eastern Mediterranean region over 90 million years ago in the middle Cretaceous, later spreading throughout Europe during the Cenozoic period (Adua, 1999).

In recent years, chestnuts have become more important in human health because of their nutritional qualities and potential beneficial health effect (Borges *et al.* (2007); Demirkesen *et al.* (2010)) and its unique flavour, eating quality, and nutritional composition (Zhu, 2016). Moreover, due to the absence of proteins like gluten on chestnut makes its derived products as chestnut flour a potential viable source to be used in the development of gluten-free products (O'Shea *et al.*, 2014). It has been reported to contain good nutritive properties such as vitamins E and B, iron, folate, essential fatty acids, and dietary fibre, nutritional components which gluten-free products are usually lacking (Sacchetti *et al.*, 2004).

1.2.1.1 Market

The world production of chestnut fruits is around 2.05 million tonnes per year. The highest percentage corresponds to Asia ($\approx$ 90%), followed by Europe ($\approx$6%) and América ($\approx$3.5%). The production is concentrated in very few countries. Among them, China ($\approx$ 82%), Bolivia ($\approx$ 3.5%) and Turkey ($\approx$ 3%). Spain is placed as 10^{th} country with 0.79% of worldwide production (FAOSTAT, 2017).

The European chestnut (*Castanea sativa* Mill.) is a traditional nut from Mediterranean countries and one of the most popular over the world. However, there is no data available that differences chestnut varieties which make difficult to know exactly the production of this chestnut variety. If it is considered that European chestnut production is mainly concentrated in the Mediterranean countries then Italy is the main producer with $\approx$ 52,000 tonnes/year (39% of total european production), followed by Greece ($\approx$ 30,000 tonnes/year), Portugal ($\approx$18,500 tonnes/year) and Spain ($\approx$ 16,000 tonnes/year) (FAOSTAT, 2017).

Based on these statistics it could be said that, although worldwide production of chestnut fruits increased in the past decade, the production of chestnut fruit in Europe is stationary since the past 20 years, Figure 1.2.

1.2.1.2 Morphology and Composition

From a botanical viewpoint, chestnut is a fruit with a starchy nut with cream-colored cotyledons (the seed, the edible part) covered with an astringent membrane called the pellicle (episperm). Brown peel wraps the nut which is protected by a spiny burr. When the fruit starts to ripe, the burr changes colour becoming yellow-brown and breaks in 2-4 lengthways lines releasing three nuts (Figure 1.3 (a)). Sometime the burr opens on the tree, more often the burr drops and opens on the ground due to the high humidity, releasing chestnuts (Ferrini, 1997).

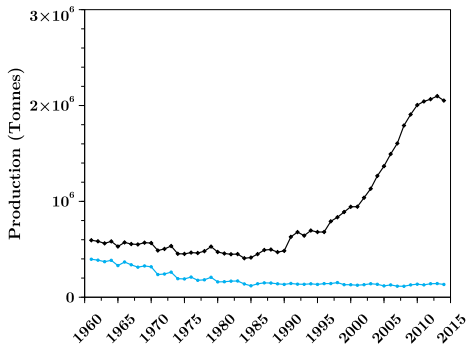

Figure 1.2. Production of chestnut fruit from 1960 to 2014. World (♦) and Europe (♦)

The chestnut fruit consist of distinct layers: external tegument or pericarp, internal tegument of episperm and seed. The external tegument presents elastic nature, more or less hairy or practically hailess. The internal tegument forms a thing film that penetrates the fissures of the cotyledons that covers, Figure 1.3 (b).

Chemical composition and health effects of raw and processed chestnuts of *Castanea sativa* have been reviewed previously (Korel & Balaban (2009); De Vasconcelos *et al.* (2010)). Chestnut is high in starch and sucrose contents and relatively low in protein and lipid. The fatty acids include oleic, linoleic, and palmitic acids with the majority being unsaturated (over 80%). Vitamins include vitamins E, C, and others. Chestnut is a good source of certain types of organic acids and polyphenols such as ellagic acid and also minerals (e.g. Mg and K) (Korel & Balaban (2009); De Vasconcelos *et al.* (2010); Braga *et al.* (2015)).

Figure 1.4 shows a typical composition of chestnut fruit (dry basis, d.b.): starch (50-68%), sugar (15-25%) mainly sucrose, protein (4-11%), fibre (4-23%), lipid (1-4%), minerals (1-2%) and ash (2-3%) (Miguelez *et al.*, 2004).

Functional components such as polyunsaturated fatty acids and phenolics make chestnut nutritionally appealing. For example, ellagitannins (castalagin and vescalagin) present in chestnut have potent antimicrobial, antitumor, and antimalarial properties (De Vasconcelos *et al.*, 2010).

It should be noted that the chemical composition of chestnuts is determined by genetics, environment, and their interactions (Künsch *et al.* (2001); Morrone *et al.* (2015)). The outcome of processing is also greatly dependent on the chestnut

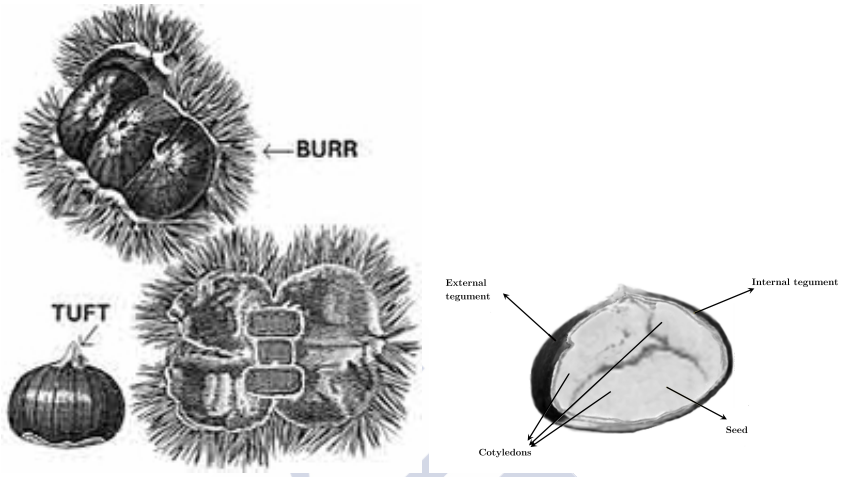

(a) (b)

Figure 1.3. Spiny burrs with chestnuts (a) and physical structure of chestnut fruit (b).

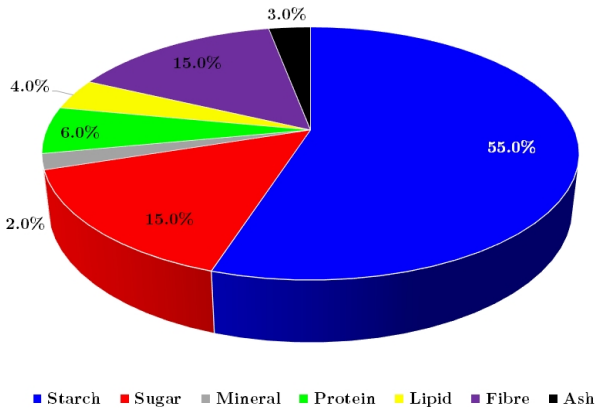

Figure 1.4. Average composition of chestnut.

variety. Chestnut is traditionally processed into flour in some European countries as an alternative to wheat flour due to its pleasant taste and unique texture of food products (Zhu, 2016).

Starch

Starch is the most abundant component in chestnut, suggesting that these fruits can be a good alternative to conventional starch resources, such as cereals and tubers. Chestnut starch is a glucose polymer composed by amylose and amylopectin in different proportion depending on the chestnut variety. Typically starch is 20–30% amylose but there are amylomaizes with more than 50% amylose while waxy maize produces almost pure amylopectin with less than 3% amylose (Correia & Beirao da Costa, 1999). Starch determines the physical properties and functionality of the chestnut, and these properties are greatly dependent on the amylose/amylopectin ratio. Amylopectin is the branched polymer, more abundant than the linear polymer (amylose). However, amylose has received more attention from the scientific community because it is considered an indicator of cooking quality (Fitzgerald, 2004).

Sugars

The sugars content can represent up to one-third of the total carbohydrates. Previous analysis revealed the presence of various mono- and disaccharides (glucose, fructose, sucrose and maltose) that are very important for the assessment of chestnut fruit commercial quality. Specifically, the sucrose content is between 90 and 99% of the total sugars depending on the chestnut fruit variety (citepDelaMontana2004; De Vasconcelos *et al.* (2010)). The energy value of chestnuts fruits, as in any other food sources, mainly comes from the oxidative degradation of carbohydrates, proteins and lipids (De Vasconcelos *et al.*, 2010)).

Proteins and Free Amino Acids

Chestnut protein content is low regarding to wheat reported data (8.0-18.0 %), but it shows a higher range than gluten-free cereals like rice (5.9-7.9 %) (Osborne & Vorhees (1983); Hamaker (1994); Rosell *et al.* (2007)). More detailed results indicate that the main chestnut proteins are globulins and albumins, representing the 20% of total protein content (Tixier & Desmaison, 1980). The amino acids that constitute the proteins in the diet are of high importance. Amino acids are biologically active and have multiple functions in the body: as sources of energy and as precursors of proteins and various important molecules. Amino acids are divided into essential (those that the human body does not synthesize in sufficient quantities, so they are necessary in the diet) and non-essential (the

human body is able to synthesize them in adequate concentrations). Total amino acids, from acid hydrolysis studies of chestnut fruits, have been analysed for European (Portuguese and Italian; *Castanea sativa*), American (*Castanea dentate*) and Chinese (*Castanea mollisima*) chestnuts; the common predominant protein-derived amino acids were aspartic acid and glutamic acid (Borges *et al.*, 2008).

Fibre

Chestnut is a good source of dietary fibre. Its content in fibre varies significantly depending on major or minor presence of internal tegument. Fibre consists of the remnants of edible part cell polysaccharides, lignin and other substances resistant to digestion by the alimentary human enzymes. Dietary fibre is associated with simulation of *Bifidobacterium* and *Lactobacillus* in the intestine, decrease in cholesterol levels, reduction of the risk of cardiovascular diseases, positive regulation of insuline reponse and increase in anticancer mechanisms (Prosky, 2000).

Lipids

Chestnuts contain very small amounts of crude fat content that is low in saturated fatty acids and high in unsaturated fatty acids (Borges *et al.*, 2007). Chestnut fat contains significant levels of monounsaturated fatty acids and polyunsaturated fatty acids. Hence, chestnut is a good source of essential fatty acids (Ferreira-Cardoso *et al.* (1999); Künch *et al.* (1999)). Essential fatty acids are important because of their role in diverse physiological processes affecting normal health and chronic diseases, such as regulation of plasma lipid levels, cardiovascular and immune function, insulin action and neuronal development and visual function (Benatti *et al.*, 2004). The consumption of omega-3 fatty acids can slow the growth of cancerous cells, increase the efficacy of chemotherapy and reduce the side effects of chemotherapy for cancer (Hardman, 2002).

Minerals

The content of minerals found in chestnut fruit is not only associated with the genotype and weather conditions, but is also related to the mineral composition of the soil where the chestnut trees were cultivated. The mineral content was previously analyzed in chestnut fruits, revealing important macro-elements (Ca, P, K, Mg and S), with potassium representing the majority of this group, and also important micro-elements (Fe, Cu, Zn and Mn) (De Vasconcelos *et al.* (2010); Borges *et al.* (2007)).

Other Minor Components
Chestnut fruits are a good dietary source of vitamins C (15.6 mg 100 g^{-1} fresh chestnut) and E (1.9 mg 100 g^{-1} fresh chestnut) (Peña-Méndez *et al.* (2008); Barreira *et al.* (2009)). Nevertheless, these content are close to those found in potato and higher than the corresponding to cereals. Other vitamins previously identified in chestnut fruits in lower amounts are the vitamin A, thiamine, riboflavin, niacin, pyridoxine or folate (Korel & Balaban, 2009).

1.2.1.3 Applications and State of the art

Fresh chestnut fruits are rarely consumed raw. They are processed in various ways, at home or on an industrial scale to improve the organoleptic properties (aroma, flavour, texture), digestibility of the fruits, i.e. making nutrients more bioavailable, and the shelf-life of various products from industrial processes. After collection all cultivars are ready for consumption; however, certain cultivars are more appreciated because of their organoleptic properties, although calibre and maturation time are also factors considered.

To cope with the ever-rising incidence of celiac disease, there is now much interest in the use of chestnut flour for the production of high-quality gluten-free products, especially bread (O'Shea *et al.*, 2014) than the use of chestnut fruit "as is". Moreover, chestnuts are easily subjected to fungal attack during storage and transportation (Zhu, 2016). Processing freshly picked chestnuts into flour provide a way to minimise losses. It also could add value to the product and provide novel chestnut-based products with unique eating and nutritional quality (Rinaldi *et al.*, 2015). Chestnut can also be used as animal feed (e.g. for the weaned piglets) (Ribeiro *et al.*, 2013) however this is out of the focus of this Thesis.

Chestnut flour has been used to formulate various staple and snack-type food products. These products included sourdough, bread, cake, gel, chips, cookie and extruded snack (Zhu, 2017), Table 1.1.

Sourdough
Sourdoughs of chestnut flour with other flours (rye, wheat, buckwheat, rice, and maize) were formulated (e.g. 40–100% of the sourdoughs were made up from chestnut flour) (Aponte *et al.* (2013); Aponte *et al.* (2014)). Principle Component Analysis (PCA) revealed distinctive groups with unique flavour and aroma profiles (Aponte *et al.*, 2014). Chestnut flour-based sourdough (e.g. with buckwheat) remains to be applied for gluten-free products.

Table 1.1. Summary of studies involving the food uses of chestnut flour (Zhu, 2017).

Use	Reference
Sourdough	Aponte *et al.* (2013)
	Aponte *et al.* (2014)
Bread	Rinaldi *et al.* (2015)
	Dall'Asta *et al.* (2013)
Gluten-free bread	Demirkesen *et al.* (2010)
	Demirkesen *et al.* (2011)
	Demirkesen *et al.* (2013)
	Demirkesen *et al.* (2014)
Gluten-free gel	Torres *et al.* (2014b)
	Torres *et al.* (2014a)
Gluten-free cake	Yildiz & Dogan (2014)
Gluten-free chip	Monaco *et al.* (2010)
Cookie	Inkaya *et al.* (2009)

Bread

Chestnut flour was incorporated into wheat flour up to 50% for breadmaking (Rinaldi *et al.* (2015); Dall'Asta *et al.* (2013)). Chestnut flour addition at 50% increased the heterogeneity of crumb structure and hardness, and decreased lightness and yellowness of the bread, enriched the profile of volatile compounds (furans) of the bread due to enhanced Maillard reactions. Chestnut flour addition also increased the antioxidant activity of the bread. Pejcz *et al.* (2015) replaced wheat flour with chestnut flour (up to 15%) and observed a decrease on dough development time and an increase on the stability time assessed by a Brabender farinograph. However, sensory analysis showed that chestnut flour addition decreased the overall sensory scores (by ≈25%) of the bread with darker crumb.

Gluten-free Bread

The development of gluten-free bread from chestnut flour is a major challenge due to the lack of gluten-type protein in these flours giving the desired visco-elasticity of the dough. Various gums (xanthan–locust bean gum, xanthan–guar gum) and emulsifier (diacetyl tartaric acid ester of mono- and diglycerides (DATEM)) were used in chestnut-rice composite flour to improve the visco-elastic properties of dough for bread making (Demirkesen *et al.* (2010), Demirkesen *et al.* (2011), Demirkesen *et al.* (2013), Demirkesen *et al.* (2014)). Xanthan–guar gum blend and DATEM addition (0.5% of flour) into rice-chestnut composite flour (70:30) improved various quality attributes of the bread including hardness, specific

volume, colour, and sensory scores. Further increasing chestnut flour significantly decreased the bread volume, while increasing the darkness and hardness of bread (Demirkesen *et al.*, 2010).

Snack-type foods
Chestnut flour was mixed with rice flour for gluten-free wafer sheet formulation (Mert *et al.*, 2015). Texture and taste scores were comparable to those of other types of flours, but lower than that of wheat flour (Mert *et al.*, 2015).

Chestnut flour was blended with xanthan and guar gum blend, potato starch, and transglutaminase for gluten-free cake production (Yildiz & Dogan, 2014).

Gluten-free gel of chestnut–rice flour was prepared, and the rheological properties were characterised (Torres *et al.* (2014b); Torres *et al.* (2014a)) which indicated that the blend of chestnut (30%) and rice flour (20%) was the most suitable for desert-type gel.

Chips from chestnut flour, lipids, glucose, and albumin were formulated through extreme vertex design (Monaco *et al.*, 2010). However, the resulting chips had a rather low consumer acceptability.

Chestnut flour based cookies (Demirkesen, 2016) and low-fat cookies were made with chestnut flour addition up to 30% (Inkaya *et al.*, 2009) were also made concluding that chestnut flour incorporation increased the hardness and decreased the spread ratio of cookies.

The above-mentioned products with chestnut flour had enhanced nutritional value and/or were gluten-free. As previously mentioned the celiac disease lead to gluten-free products are much required from the market and chestnut flour can aid to this challenge. For both the staple and snack-type foods, the major challenge is to improve the dough rheology as well as the textural and sensory quality of these products for potential commercial applications (Zhu, 2017).

1.2.2 Maize

The cultivation of maize had probably its origin in Central America, particularly in Mexico, from whence it spread northward to Canada and southward to Argentina. Maize was an essential item in Mayan and Aztec civilizations and had an important role in their religious beliefs, festivities and nutrition. They claimed that flesh and blood were made from maize. The survival of the oldest maize and its distribution depended on humans who

harvested the seed for the following planting. At the end of the fifteenth century, after the discovery of the American continent by Christopher Columbus, maize was introduced into Europe through Spain. It then spread through the warmer climates of the Mediterranean and later to northern Europe (FAO 1992). In spite of its great diversity of form, all main types of maize known today were apparently already being produced by the native populations when the American continent was discovered. All maize is botanically classified as *Zea mays*.

1.2.2.1 Market

The world production of maize as crop is around 10^9 tonnes per year, it is the most produced cereal in the world. The highest percentage corresponds to America (≈ 51%), followed by Asia (≈29%) and Europe (≈12%), Figure 1.5. The main producer countries in the world are USA (≈35%), China (21%) and Brazil (≈8%) (FAOSTAT, 2017).

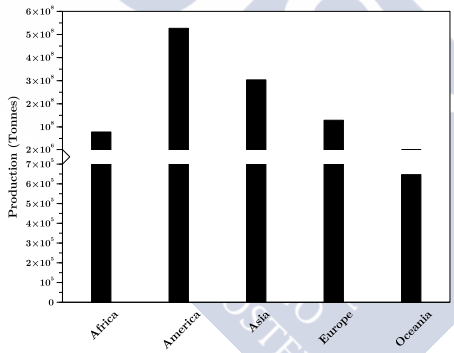

Figure 1.5. World production of maize FAOSTAT (2017).

Maize production in world is in constant increase since 1960, Figure 1.5, as well as their harvesting area. However, in Europe, maize production is increasing whilst the harvesting are is stationary, Figure 1.6.

Spain is placed as 27^{th} country in the world and 9^{th} in Europe with a production of $4.8{\cdot}10^6$ tonnes/year. However, it is an important crop in the northwest of the Iberian Peninsula, where it is cultivated for self consumption in small farms (Revilla *et al.*, 2008). Although most consumers prefer white maize, other types are also used for making bread (Revilla *et al.*, 2008). According to data provided by the Ministerio de Agricultura, Pesca, Alimentación y Medio

Ambiente there were 350,000 ha in Spain dedicated to the cultivation of maize. Castilla y León is the first region in terms of crop area, and the sixth in terms of yield. In Galicia, the recorded area is 18,700 ha (800 ha of cultivation of non-hybrid varieties), the agricultural yield of this cereal being the highest of all.

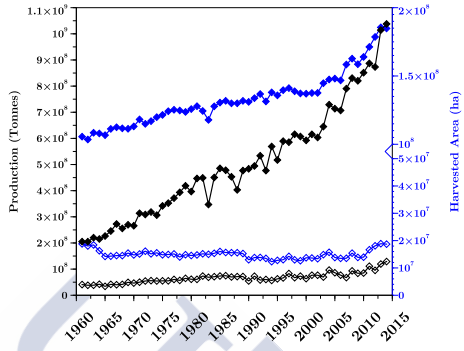

Figure 1.6 Evolution of World (⧫) and European (◇) production of maize from 1960 to 2014.

1.2.2.2 Morphology and Composition

The maize kernel is composed of four primary structures: endosperm, germ, pericarp, and tip cap, representing 83%, 11%, 5%, and 1% of the maize kernel respectively (Gwirtz & Garcia-Casal, 2014), Figure 1.7. There are differences in chemical composition of different parts of kernel. The pericarp has a high fibre content (86%), the endosperm presents the highest starch content (87%) and 8% of proteins. The germ presents high percentage on lipids (33%), protein (20%) and minerals (10.5%) (Watson & Ramstad, 1987).

Chemical composition of several maize kernels is homogeneous but it depends on cultivation conditions, temperature, variety and maize type (white, yellow, purple, black, etc). The main components in maize are (%, w/w w.b.): carbohydrates (≈77), protein (≈7), total fibre (≈7), total lipids (≈4), ash (≈1.5) and other (≈3.5) (Gwirtz & Garcia-Casal, 2014), Figure 1.8. The major chemical component of the maize kernel is starch. This is the main factor that makes maize a product with high nutritional value (either for human and/or animal consumption).

Although starch and proteins are the major compounds of maize grains, several other substances produced by secondary metabolism, such as carotenoids and anthocyanins, have been found, mainly in creoles genotypes (Escribano-Bailon

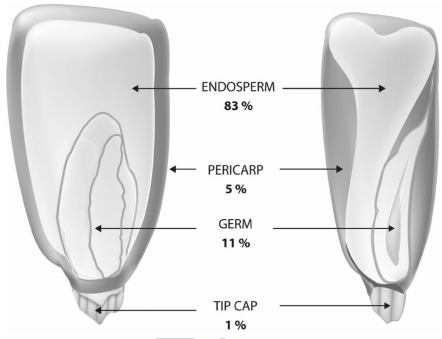

(a)

Figure 1.7. Components of the maize kernel (Gwirtz & Garcia-Casal, 2014).

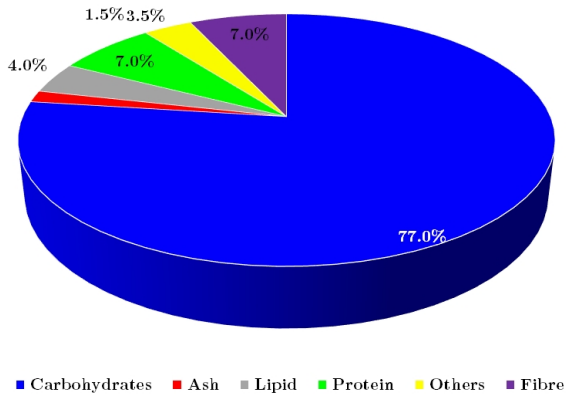

Figure 1.8. Average composition of maize (Gwirtz & Garcia-Casal, 2014).

et al., 2004). The carotenoids are tetraterpenes responsible for the yellow, orange and red colours of several vegetables (Kuhnen *et al.*, 2011). On the other hand, the anthocyanins are water-soluble pigments responsible for the purple, blue and red colors in vegetal tissues, belonging to the class of flavonoids (Escribano-Bailon *et al.*, 2004). Anthocyanin-rich foods and anthocyanin pigments have been suggested as potential agents to reduce the risk of colon cancer by inhibiting proliferation of human colon cancer cells in vitro (Jing *et al.*, 2008).

1.2.2.3 Applications

Maize has three possible uses: as food, as feed for livestock and as raw material for industry. As a food, the whole grain, either mature or immature, may be used; or the maize may be processed by dry milling techniques to give a relatively large number of intermediary products, such as maize grits of different particle size, maize meal, maize flour and flaking grits. These materials in turn have a great number of applications in a large variety of foods. Maize grown in subsistence agriculture continues to be used as a basic food crop (FAO, 1992).

The main use of maize is in form of flour. In the Northwest of the Iberian Peninsula, maize bread is traditionally made with whole grain of maize, following similar procedures as for manufacturing the common wheat bread (Revilla *et al.*, 2008). Three different types of maize kernels are commonly used: white (Rebordanes variety), yellow (Sarreaus variety) and purple (Meiro variety).

1.2.3 Defects associated with gluten-free products and how to face them

Gluten is a proteinaceous material that can be separated from flour when the starch and other minor components of the flour are removed by washing out with running water. It contains the protein fractions glutenin and gliadin (Gallagher *et al.*, 2004). The former is a rough, rubbery mass when fully hydrated, while gliadin produces a viscous, fluid mass on hydration. Gluten, therefore, exhibits cohesive, elastic and viscous properties that combine the extremes of the two components. The gluten matrix is a major determinant of the important properties of dough (extensibility, resistance to stretch, mixing tolerance, gas holding ability), which encloses the starchgranules and fibre fragments.

Gluten is often termed the 'structural' protein for breadmaking. The properties of gluten become apparent when flour is hydrated, giving an extensible dough, with good gas holding properties, and a good crumb structure

in baked bread. The elimination of gluten in baked product is translated into the defects that appear in the product in terms of quality attributes, nutritional characteristics, and consumer acceptance (Naqash *et al.*, 2017). In the production of gluten-free bread deficient gas retention and the resulting low loaf volume are the major challenges encountered. The lack of gluten also leads to a liquid batter instead of dough, which in turn results in baked bread with a crumbling texture, poor color and postbaking quality defects (Gallagher *et al.*, 2004). Such problems are rarely encountered during the manufacture of gluten-free biscuits, as the development of a gluten network in biscuit and cookie dough is minimal and undesirable (apart from some semi-sweet biscuits, which may have a developed gluten system); the texture of baked biscuits is primarily attributable to starch gelatinization and supercooled sugar rather than a protein/starch structure (Gallagher *et al.*, 2002).

Since the gluten-free products do not match gluten containing counterparts in terms of technological attributes and quality, it is a pre-requisite to adopt techniques ensuring their acceptability to the population consuming gluten-free (Naqash *et al.*, 2017). These techniques can be based on the use of new formulations or technologies.

The use of new formulations involves the modification and/or incorporation of additional ingredients to counter the gluten deficiency (Naqash *et al.*, 2017)

- **Incorporation of additives**: several additives have been employed that could mimic the role played by gluten. Different enzymes, emulsifiers, hydrocolloids, etc are added to the gluten-free flours resulting in positive effects on structure, texture, acceptability, and shelf life.

- **Incorporation of proteins**: the use of proteins in order to improve the nutritional profile of gluten-free product have been found to improve their structure and texture (Matos *et al.*, 2014).

- **Incorporation of fibres**: the design of fibre-enriched traditional baked goods has come up against consumers' resistance to accept breads with reduced loaf volume and hard crumb accompanied by certain flavours (Rosell *et al.*, 2010). Their use has led to improvement in the specific volume, brighter crust and crumb of glute-free products (Gularte *et al.*, 2012).

Apart from the formulation directed approach, it is necessary to adopt technologies for gluten-free product improvement, and consider some inherent parameters of the flours used and processes applied that determine the final product quality (Naqash *et al.*, 2017):

- An ideal **particle size** is an important determinant of final product characteristics for example in the case of bread. Coarse maize flour was seen to produce bread with lower crumb hardness and desired loaf volume .

- **Hydrothermal treatments** are being increasingly applied to improve the functionality of starch-based ingredients. Though there are lesser reports of the effect of hydrothermal treatments on gluten-free flours, certain studies do point at some potential for altering gluten-free flour functionality (Gómez & Martínez, 2016). In example, hydrothermal treatment can partially gelatinize the starch, increasing initial flour viscosity, while decreasing the viscosity during heating improving the specific volume of the gluten-free breads, due to a larger capacity of dough to entrap air due to higher initial viscosity (Bourekoua *et al.*, 2016).

- **High pressure treatments** have been reported to be able to create new structures and texture by modifying the functional properties of proteins and starches of gluten-free flours (Ahmed *et al.*, 2007) promoting protein network formation (Kieffer *et al.*, 2007).

- The modification of conditions of some processing steps as **kneading** or **mixing** in comparison with those conditions usually employed in gluten product can also be a good strategy for improving gluten-free dough. In example, among agitators, the wire whip type was more suitable for gluten-free dough than the flat or kneading geometry (Gómez *et al.*, 2013).

Both formulation centric and technological approaches have been able to combat the challenges arising with the elimination of gluten. Production of gluten-free products thus is possible by the application of functional ingredients like starches, hydrocolloids, fibers, proteins, etc, improving them nutritionally as well as functionally. However, alternatives to compositional modifications do exist and prove to be propitious enough for gluten-free products. In example, new processing methods based on starch gelatinization which produce products with better textural attributes, could be adopted as processing technologies for gluten-free baking (Naqash *et al.*, 2017).

1.3 Seaweeds

Edible seaweeds were widely consumed, especially in Asian countries as fresh, dried, or ingredients in prepared foods. Their photosynthetic mechanism is similar to that of land-based plants. They are generally more efficient in converting solar

energy into biomass, mainly because of their simple cellular structure and being submerged in an aqueous environment with access to water, CO_2, and other nutrients. Seaweeds are considered as the food supplement for 21^{st} century due to they contain proteins, lipids, polysaccharides, minerals, vitamins, and enzymes (Kılınç *et al.*, 2013).

Among the three types of algae that exist (red, green and brown, see Section 1.3.1), several red and brown seaweeds are usually employed to produce three main hydrocolloids: agar, alginate and carrageenan. A hydrocolloid is a non-crystalline substance with very large molecules and which dissolves in water to give a thickened (viscous) solution. Alginate, agar and carrageenan are water-soluble carbohydrates that are used to thicken aqueous solutions, to form gels of varying degrees of firmness, to form water-soluble films, and to stabilize some products, such as ice cream (they inhibit the formation of large ice crystals so that the ice cream can retain a smooth texture) (McHugh, 2003). Seaweeds as a source of these hydrocolloids dates back to 1658, when the gelling properties of agar, extracted with hot water from red seaweed, were first discovered in Japan (Kılınç *et al.*, 2013).

Seaweed meal, used an additive to animal feed, has been produced in Norway, where its production was pioneered in the 1960s. It is made from brown seaweeds that are collected, dried and milled. Approximately 50,000 tonnes of wet seaweed are harvested annually to yield 10,000 tonnes of seaweed meal, which is sold for around 4 million *e* (Kılınç *et al.*, 2013).

Fertilizer uses of seaweed date back at least to the nineteenth century. Early usage was by coastal dwellers. The high fibre content of the seaweed acts as a soil conditioner and assists moisture retention, while the mineral content is a useful fertilizer and source of trace elements. The growth area in seaweed fertilizers is in the production of liquid seaweed extracts. These can be produced in concentrated form for dilution by the user. In 1991, it was estimated that about 10,000 tonnes of wet seaweed were used to make 1,000 tonnes of seaweed extracts with a value of around 4 million *e*. However, the market has probably doubled in the last decade because of the wider recognition of the usefulness of the products and the increasing popularity of organic farming, where they are especially effective in the growing of vegetables and some fruits (McHugh, 2003).

Some cosmetic products, such as creams and lotions, sometimes show on their labels that the contents include “marine extract”, “extract of alga”, “seaweed extract” or similar. It means that one of the hydrocolloids extracted from seaweed has been added. Alginate or carrageenan could improve the skin moisture retention properties of the product. Pastes of seaweed, made by cold grinding or freeze crushing, are used in thalassotherapy, where they are applied

to the person's body and then warmed under infrared radiation. This treatment, in conjunction with hydrotherapy, is said to provide relief for rheumatism and osteoporosis (Kılınç *et al.*, 2013).

There are potential uses for seaweed in wastewater treatment. Some seaweeds are able to absorb heavy metal ions such as zinc and cadmium from polluted water. The effluent water from fish farms usually contains high levels of waste that can cause problems to other aquatic life in adjacent waters. Seaweeds can often use much of this waste material as nutrient, so trials have been undertaken to farm seaweed in areas adjacent to fish farms (McHugh, 2003).

1.3.1 Seaweeds Classification

Edible marine macro algae or seaweeds are classified into three types: *Chlorophyceae* (green algae), *Phaeophyceae* (brown algae) and *Rhodophyceae* (red algae) according to their composition of pigments, being brown and red seaweeds the most used algae for human consumption (Li *et al.*, 2011).

Brown seaweeds are usually large, and range from the giant kelp that is often 20 m long, to thick, leather-like seaweeds from 2-4 m long, to smaller species 30-60 cm long. Red seaweeds are usually smaller, generally ranging from a few centimetres to about one meter in length; however, red seaweeds are not always red: they are sometimes purple, even brownish red, but they are still classified by botanists as *Rhodophyceae* because of other characteristics. Green seaweeds are also small, with a similar size range to the red seaweeds (McHugh, 2003). Among all the three types, the highest phytochemical content (such as terpenes, carotenoids and phenolic compounds) has been reported from brown seaweeds (Gupta *et al.*, 2011).

1.3.1.1 Green seaweeds

The green colour of the seaweed is due to the green pigments chlorophyll a and b (Kim, 2011) required for the photosynthesis of light that is why they are also named as *Chlorophyceae*. Using only chlorophyll means that green seaweeds require good levels of light and therefore will not thrive in shadowed areas or too any depth. It does give them an advantage, the ability to live higher up shore without competition from the red or brown seaweeds. The green seaweeds *Ulva sp.*, *Enteromorpha sp.*, *Monostroma sp.*, *Caulerpa sp.* and *Codium sp.* are commonly known as source of food (Kılınç *et al.*, 2013).

Green seaweeds are found on both sandy and rocky beaches. Some of them can tolerate low salinity and will colonize areas where rivers meet the sea.

1.3.1.2 Red seaweeds

Red seaweeds *Rhodophyceae* have had a more diverse evolution than the green and the brown. The red colour of the seaweeds is due to the larger amount of red phycoblin pigments overriding the green pigment chlorophyll (Kılınç *et al.*, 2013). They are water-soluble pigments, the red phycoerythrin and blue phycocyanin. Other pigments present are chlorophyll a, β-carotene and unique xanthophylls. The main biomass of red algae worldwide is provided by the *Corallinaceae* and *Gigartinaceae*.

There are about 8000 species of red algae, most of them are marine. These are found in the intertidal and subtidal zones to depths of up to 40, or occasionally, 250 m (Kim, 2011). Useful red seaweeds are found in cold waters such as Nova Scotia (Canada) and southern Chile; in more temperate waters, such as the coasts of Morocco and Portugal; and in tropical waters, such as Indonesia and the Philippines (McHugh, 2003).

The walls are made of cellulose, agars and carrageenans. Several red algae are edible such as *Palmaria palmata* and *Chondrus crispus* and *Mastocarpus stellatus*. However, "Nori" popularized by the Japanese is the single most valuable marine crop grown by aquaculture with a value in excess of US$ 1·109 (Kim, 2011). Their main uses are as food and as sources of two hydrocolloids: agar (*Gelidium*, *Gracilaria*, *Pterocladis*) (Kılınç *et al.*, 2013) and carrageenan (*Kappaphycus* and *Betaphycus*) (McHugh, 2003). Red algae are considered as the most important source of many biologically active metabolites in comparison to the other algal class (Kim, 2011).

1.3.1.3 Brown seaweeds

Brown algae *Phaeophyceae* vary in colouration from olive–yellow to deep brown. The colouration is due to the accessory carotenoid pigment and fucoxanthin. The amount of fucoxanthin varies in different species of brown algae. Most of the littoral brown algae are rich in xanthophylls and fucoxanthin. The algae rich in fucoxanthin exhibit a much higher rate of phytosynthesis in blue light than the algae with poor fucoxathin (Darghalkar & Kavlekar, 2004).

The other photosynthetic pigments of the brown algae are chlorophyll a and c, β- carotene and xanthophylls. The photosynthetic products of the brown algae

are laminarian and mannitol. Laminarian is a dextrin like polysaccharide, a food reserve; arise from the simple sugar of photosynthesis. Mannitol appears to be not widely distributed and presence of such alcohols may account for extreme scarcity of free sugars as they undergo immediate conversion into alcohol and polysaccharides (Darghalkar & Kavlekar, 2004). The cell walls of these algae are made of cellulose and alginic acid (Kim, 2011).

The main uses of brown seaweeds are as foodstuffs and as the raw material for the extraction of alginates. The most useful brown seaweeds grow in cold waters in both the Northern and Southern Hemispheres. They thrive best in waters up to about 20°C. Brown seaweeds are found in warmer waters, but these are less suitable for alginate production and rarely used as food (McHugh, 2003).

Obtaining ethanol and biogas from brown seaweed would be an interesting option if and when it can be introduced on a commercial scale. Both products would have global applications as transport biofuels or for electricity generation. An additional opportunity is to combine energy production with extraction of alginates (Horn *et al.*, 2000).

1.3.2 Composition

Algae are of particular interest for human consumption for their high content in polysaccharides 33-50%, (g water/ g dry solid, d.b.) and proteins (5-24% in brown algae; 10-47% in red and green algae), and their reduced content in lipids (1-2%) (Gómez-Ordóñez *et al.*, 2010).

1.3.2.1 Polysaccharides

The three types of algae are distinguished by their structural and reserve polysaccharide composition. Many of them cannot be obtained from terrestrial algae and are only produced by marine species, such as sulphated polysaccharides, hardly observed in land plants (Kim, 2011). They are polymeric molecules linked by glycosidic bonds and have many known commercial applications as emulsifiers, thickeners or gelling agents. These polysaccharides can be mostly be considered fibre as they are not digested by the human enzymes in the stomach, although, some of them are partially degraded by enzymes produced by the colon bacteria. Table 1.2 shows the most important polysaccharides of each type of algae. Dietary fibre in brown algae can be divided in four groups: laminarans, alginates, fucans and cellulose (Gómez-Ordóñez *et al.*, 2010).

Table 1.2 Classification of the most important polysaccharides for human consumption present in algae (Gómez-Ordóñez *et al.*, 2010)

Type	Seaweed	Soluble fibre	Insoluble fibre
Green	*Ulva*	Xylan	Cellulose
	Enteromorpha	Sulphated galactans	
Red	*Chondrus*	Agar	Cellulose
	Porphyra	Carrageenan	
	Mastocarpus	Xylan	
Brown	*Fucus*	Laminarin	Cellulose
	Ascophyllum		
	Bifurcaria	Alginate	
	Laminaria		
	Undaria	Fucan	
	Himanthalia		

Additionally, polysaccharides can be classified into three types depending on their role: structural polysaccharide (cellulose), intercellular mucilage (alginate, fucoidan and laminaran) and storage polysaccharides (laminaran).

A brief description of the most important polysaccharides present in brown algae is shown below:

- **Laminarans** are the main reserve polysaccharides of brown algae and they are found in higher quantities in laminarian (*Laminaria* and *Undaria*) and *Fucus* species. The content in laminarans varies depending on environment and season of the year, and it can reach values up to 36% d.b. Highest yields are achieved in autumn, between September and November, while it reaches reduced values in February and June. This variations must be taken into account when laminarans are the compound of interest in the algae. Laminarans are used as dietary fibre and among other properties, they show anticoagulant and antitumor activities (Gómez-Ordóñez *et al.*, 2010).

- **Alginates** constitute the main structural polysaccharide in brown algae cell walls and they cannot be obtained from terrestrial algae. They can reach up to 40-47% d.b. of the seaweed, varying between seasons, reaching maximums in spring and minimums in autumn (Gómez-Ordóñez *et al.*, 2010). This polysaccharide has structural functions, it gives the algae both, mechanical strength and flexibility. They are a family of unbranched binary copolymers of (1-4)-linked-β-D-mannuronic acid (M) and α-L-glucuronic acid (G) residues (Figure 1.9). Proportions of these monomers may vary

depending on the organisms that produces it and the tissue from which it is obtained, exhibiting each different physical properties. High glucuronic acid content is related with high rigidity of the tissue, while a lower content provides a more flexible structure (Stephen *et al.*, 2006).

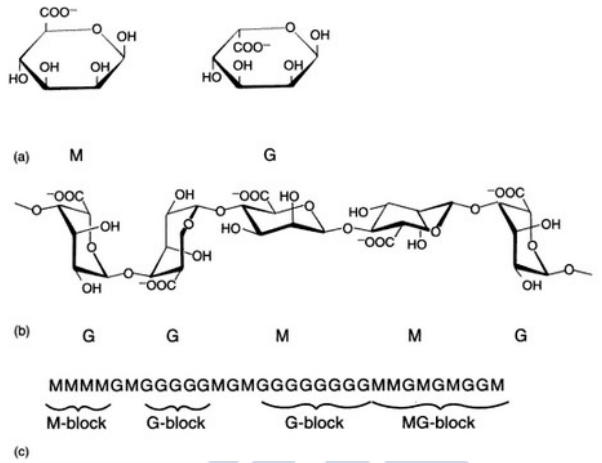

Figure 1.9 a) Alginate monomers. M: β-D-mannuronate; G: α-L-glucuronate. b) Alginate in chair conformation. c) Symbolic representation of an alginate chain.

Alginates are widely used in food industries as thickeners and gelling agents. They also show antihypertensive and anti-inflammatory activities, as well as the capacity to reduce cholesterol levels in blood (Gómez-Ordóñez *et al.*, 2010).

- **Fucodains** are sulphated water-soluble (highly hygroscopic) polysaccharides found in the cell wall or extracellular matrix of brown algae, of which they can contribute up to 40% d.b. It is not possible to fully define a chemical structure for these substances as it changes depending on species, part of the algae or the extraction method (Gómez-Ordóñez 2013). In Figure 1.10, a possible structure of fucoidans from *Fucus vesiculosus* is shown.

The bioactivity of the polysaccharide depends on its molecular weight, quantity, position and conformation of the sulphate groups of the polysaccharides. Different isolated fucoidans have been reported to show anticoagulant, antiviral, antitumor, antioxidant activities and anti-HIV activity (Gómez-Ordóñez *et al.* (2010); Hahn *et al.* (2012), Thuy *et al.* (2015)) and they are summarized in Figure 1.11:

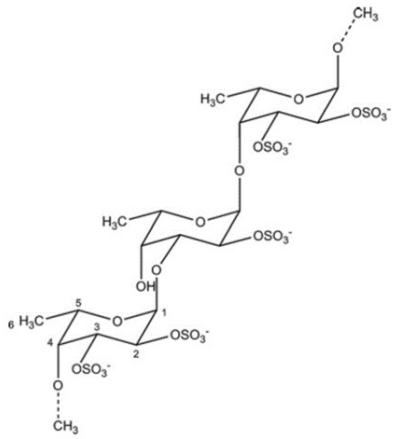

Figure 1.10. Proposed structure of fucoidans from *Fucus vesiculosus* (Hahn *et al.*, 2012)

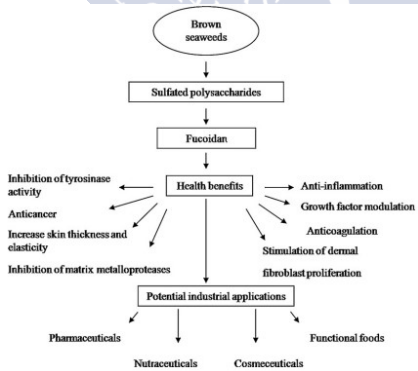

Figure 1.11 Biological properties and potential industrial uses of fucoidans (Wijesinghe & Jeon, 2012)

1.3.2.2 Proteins

Protein, peptide and amino acids content in brown algae is relatively low (5-24% d.b.) and it strongly varies depending on species and season (Gómez-Ordóñez *et al.*, 2010).

1.3.2.3 Lipids

Lipids are present in low quantities in seaweeds (< 5% d.b.) and are responsible of their low calories content. As with protein and polysaccharide content, lipid content depends on the season of the year and other environmental factors. Both, brown and red algae are a valuable source of omega-3 and omega-6, which are recognized for their health benefits (Gómez-Ordóñez *et al.*, 2010).

1.3.2.4 Minerals

Seaweeds accumulate a high amount of minerals (8-40% d.d.) due to the wide variety of these compounds that can be found in marine environments. These minerals include sodium, calcium, magnesium, potassium, chloride, sulphates, phosphorous, fluoride, among others. Therefore, brown algae are a suitable as dietary supplement in foods. The mineral composition of seaweeds can vary depending on species and location. On the other hand, marine algae are good indicators of heavy metals bioaccumulation due to their capacity to hold these substances (Gómez-Ordóñez *et al.*, 2010).

1.3.2.5 Polyphenols

Red and green algae contain little traces of polyphenols (< 1% d.w.). Brown algae have higher fractions, with species like *Ascophyllum* and *Fucus* reaching up to 14% d.b. (Gómez-Ordóñez *et al.*, 2010). Phenolics play a primary role as structural components of cell walls and may have secondary roles in signalling, defence or in responses to environmental stress. Polyphenols are compounds with an aromatic ring bearing one or more hydroxyl substituents and include simple phenols, coumarins, flavonoids, stilbenes, lignans, hydrolysable and condensed tannins, and phlorotannins (Figure 1.12). Phlorotannins have been reported to show anti-inflammatory properties, therapeutic potential in arthritis treatment and antioxidant activities (Balboa *et al.*, 2013).

Phlorotannins are formed by the polymerization of phloroglucinol

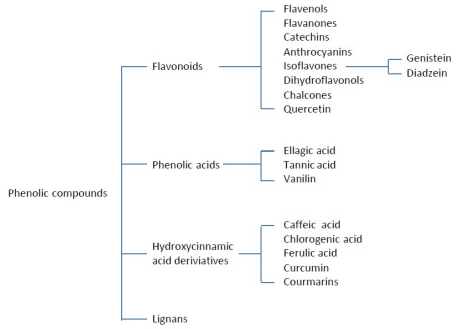

Figure 1.12 Classification of some phenolic compounds from natural sources (Kyung-Tae, 2012).

(1,3,5-trihydroxybenzene) monomer units and biosynthesized through the acetate-malonate pathway (polyketide pathway). They are highly hydrophilic components with a wide range of molecular sizes ranging between 126 Da and 650 kDa. Marine brown algae accumulate a variety of phloroglucinol-based polyphenols, as phlorotannins of low, intermediate and high molecular weight containing both, phenyl and phenoxy units. Depending on linkage, phlorotannins can be classified into four subclasses such as fuhalols and phlorethols (phlorotannins with an ether linkage), fucols (with a phenyl linkage), fucophloroethols (with an ether and phenyl linkage), and eckols (with a dibenzodioxin linkage). Figure 1.13 shows the structure of some phlorotannins found in marine brown algae:

Several species of brown algae, such as *Ecklonia cava*, *Ecklonia kurome*, *Fucus vesiculosus*, *Hizika fusiformis*, and *Sargassum ringgoldianum*, have been found to possess a high content of phlorotannins, which is correlated with the antioxidant activity (Wang *et al.*, 2012).

1.3.2.6 Carotenoids

Carotenoids are a family of pigmented compounds which are synthesized by plants, algae, fungi and microorganisms, but not by animals. They are the most important pigments in nature that are responsible for various colors of different photosynthetic organisms. Carotenoids are related to the prevention of many human diseases including cardiovascular diseases, cancer and other chronic diseases (Ngo *et al.*, 2011).

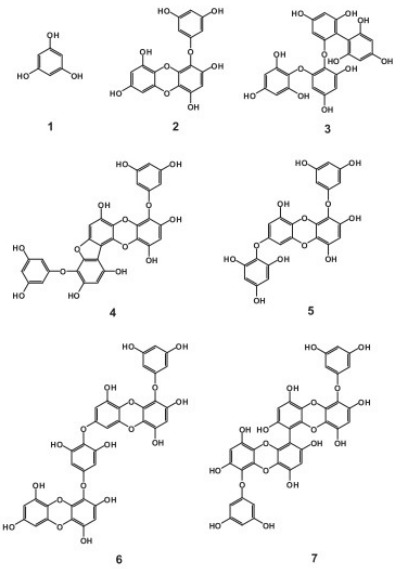

Figure 1.13 Structure of phlorotannins from marine brown algae. (1) phloroglucinol, (2) eckol, (3) fucodiphloroethol, (4) 7-phloroeckol, (6) dieckol and (7) 6,6'-bieckol (Li *et al.*, 2011).

Although chlorophyll is also present in seaweeds, in the case of brown algae, xanthophyll pigment or fucoxanthin (Figure 1.14) is the main responsible for its color (Li *et al.*, 2011).

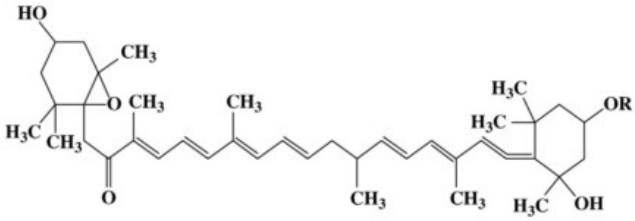

Figure 1.14. Structure of fucoxanthin, carotenoids found in Brown algae (Ngo *et al.*, 2011).

1.3.3 Antioxidant activity

Compounds present in brown seaweeds that have reported to show antioxidant activity and the mechanisms involved are detailed below:

- **Sulphated polysaccharides** are present mostly as fucoidans in brown algae (*Phaeophyceae*), carrageenan in red algae (*Rhodophyceae*), and ulvan in green algae (*Chlorophyceae*). Fucoidans are responsible of the resistance to dryness of brown algae and contribute to the formation of a gel network (Kim 2012). There is a close connection between molecular weight of these molecules and their antioxidant activity. The lower the molecular weight, the higher the antioxidant activity. Low molecular weight molecules are able to easily diffuse through cell membranes to donate protons in a higher effective way. Besides, sulphated polysaccharides are important free-radical scavengers and antioxidants for the prevention of oxidative damage and sulfated groups provide anticoagulant activity (Ngo *et al.*, 2011).

- **Phlorotannins** are mostly extracted from marine brown algae and are responsible for antioxidant activities and have shown protective effects against hydrogen peroxide-induced cell damage. Phlorotannins act as free radical scavengers, reducing agents and metal chelators, inhibiting lipid oxidation.

- Antioxidant activity reported by **carotenoids** is due to its highly unsaturated nature, which leads to their own oxidation instead of other molecules. The antioxidant properties of carotenoids are based on their singlet oxygen quenching properties or their ability to trap free radicals. Antioxidant activity depends on the number of conjugated double bonds of the molecule and carotenoid end groups or the nature of substituents in carotenoids containing cyclic end groups (Ngo *et al.*, 2011).

1.3.4 *Ascophyllum nodosum*

Ascophyllum nodosum (Figure 1.15) is a brown seaweed common on the northwestern coast of Europe (from Svalbard to Portugal) including east Greenland and the northeastern coast of North America (Bertness *et al.*, 2014). It has long fronds with large egg-shaped air-bladders set in series at regular intervals in the fronds and not stalked. The fronds can reach 2 m in length and are attached by a holdfast to rocks and boulders. The fronds are olive-brown in color and somewhat compressed but without a midrib (Hiscock, 1979).

Figure 1.15. *Ascophyllum nodosum*, ©Michael Guiry (Algaebase).

Ascophyllum, also known as rockweed, is a very dark seaweed due to a high content of phenolic compounds. It is likely that the protein is bound to the phenols, giving insoluble compounds that are not attacked by bacteria in the stomach or enzymes in the intestine (McHugh, 2003). Moreover, it is a good source of fucoidans, alginates, ascophyllans and laminarins. *Ascophyllum nodosum* is used as a raw material for alginate production in the hydrocolloid industry and as a fertilizer in the agrochemical industry (Werner & Kraan, 2004). *Ascophyllum nodosum* is one of the most researched brown seaweed species and is proving to be very significant in terms of its potential for agricultural and food applications (Khan *et al.*, 2012). It has traditionally been used as a fertilizer, a soil conditioning agent, animal feed supplement and also as a human nutritional supplement (Fan *et al.*, 2011).

Yuan & Macquarrie (2015) have analyzed the crude seaweed *Ascophyllum nodosum* to determine moisture, protein, ash (mineral content), lipid, phenolic and carbohydrate content. The chemical composition of this seaweed obtained from UK in 2011 showed the results presented in Figure 1.16.

Recent studies carried out by Holdt & Kraan (2011) reported that *Ascophyllum nodosum* present 28% (d.b.) acid alginic 11.6% (d.b.) fucoidan, 4.5% (d.b.) laminarin and 7.5% (d.b.) mannitol.

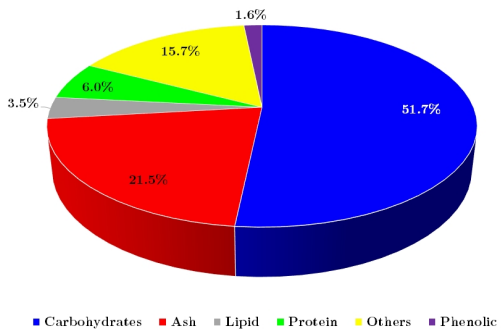

Figure 1.16. Average composition of *Ascophyllum nodosum* (Yuan & Macquarrie, 2015).

1.3.5 *Bifurcaria bifurcata*

Bifurcaria bifurcata (Figure 1.17) is a brown seaweed geographically distribute in Britain and Ireland (Hardy F., 2003), France (Silberfeld *et al.*, 2011), Netherlands (Stegenga & Mol, 1983), Portugal, Western Sahara (van Reine; Tito B. Kostermans, 2004) and Spain (Jiménez-Escrig *et al.*, 2001).

Figure 1.17. *Bifurcaria bifurcata* ©Celtalga.

The main uses of seaweeds in Western countries are traditionally the extraction of compounds used by pharmaceutical, cosmetics, and food industries as raw material to obtain alginate and other products (Mabeau & Fleurence (1993),

Jiménez-Escrig & Sánchez-Muniz (2000)). However, due to its high contents of polysaccharides, proteins and minerals Rupérez & Saura-Calixto (2001); Gómez-Ordóñez *et al.* (2010)) and that they are also currently considered as a good source of antioxidants (Nagai & Yukimoto, 2003), direct human consumption is increasing worldwide in recent years as well as its use as a raw component of functional foods for their nutritional properties materials (Shahidi, 2009).

Human consumption of seaweed *Bifurcaria bifurcata* is not as extended as several edible seaweeds, which are commonly used in the oriental diet, as *Laminaria spp.*, *Porphyra spp.* and *Undaria pinnatifida*. However, its composition, Figure 1.18 a typical composition of brown seaweeds, 34% of ashes, 11% protein, 5.6% lipids, 37% total dietary fibre (14.6% soluble dietary fibre) reveal its suitability to be a good source of food fibre for human consumption (Gómez-Ordóñez *et al.*, 2010).

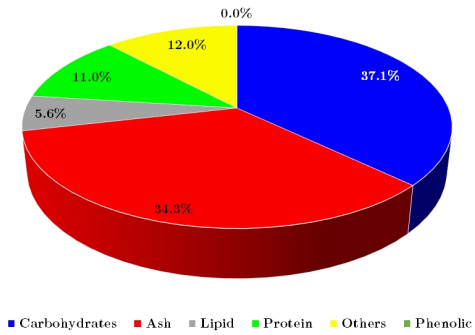

Figure 1.18. Average composition of *Bifurcaria bifurcata* (Gómez-Ordóñez *et al.*, 2010).

1.3.6 *Fucus vesiculosus*

Fucus vesiculosus (Figure 1.19) is commonly known as bladderwrack (gaelic). It is a lower limit intertidal seaweed species and it adheres to and grows on stones (Kim 2012). This brown seaweed is a dominant specie of macroalgae on the coast bathed by the Atlantic Ocean in Europe. Ecologically, it is the most important seaweed, providing shelter and food for associated flora and fauna. It shows a high genetic variability between geographic locations which provides *Fucus* a high capacity to cope with environmental stress (temperature changes, changes in salinity, exposure to sunlight).

Fucus vesiculosus thallus has a strap-like geometry and forks towards the end.

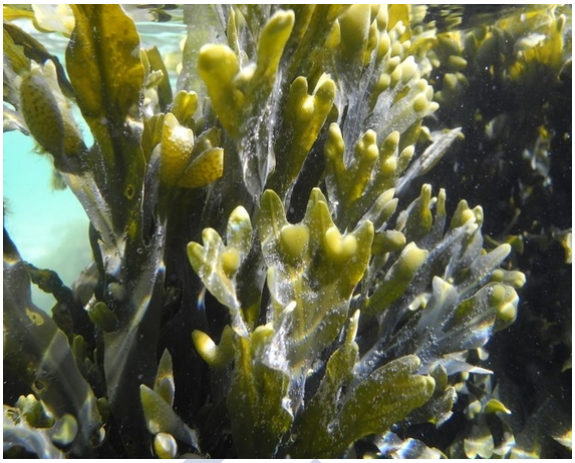

Figure 1.19. *Fucus vesiculosus* underwater (Algae Base Database).

It has a thick midrib (holdfast) which attaches to subtract. Bladders or vesicles appear from the thallus, which helps the seaweed to stand erect underwater. In the tip of the thallus *Fucus* develops the receptacles, which host the conceptacles (fertile parts of the seaweed) (Hoek *et al.*, 1996).

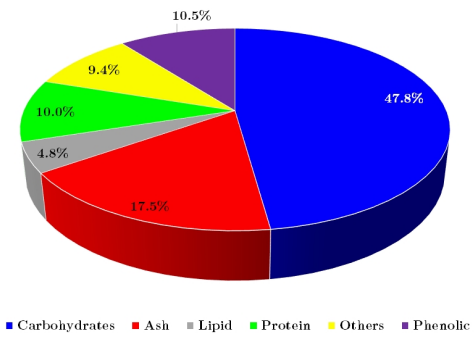

Figure 1.20. Average composition of *Fucus vesiculosus* in dry weight (Hahn *et al.*, 2012).

The European Commission of European Union recently classified the *Fucus vesiculosus*, a brown edible seaweed, like a "novel food" for human consumption and consequently an increase in its demand as food is expected. The average composition of *Fucus vesiculosus* is shown in Figure 1.20. Polysaccharide content

may vary and reach its maximum value after spring (growth season) to generate enough biomass to survive winter. Other authors determine that *Fucus vesiculosus* contains up to 65% of dry weight in polysaccharides (Rioux *et al.*, 2007)).

Fucus vesiculosus is rich in light elements such as Mg, K, Ca and Na, and in halogens (Br, I, Cl). Regarding toxic elements, *Fucus* reported to present high concentrations of As (over 300 ppm in the Baltic Sea) and low contents on Hg, Sb and Se. In addition, mineral content in this algae does not depend on time of the year but on salt concentration of the seawater (Truus *et al.*, 2001).

1.3.7 Applications and State of the art

Seaweeds are generally sundried, process that requires long periods of time. During recent years, an increase of production rates of marine algae requires the application of quicker industrial methods. The most frequently used industrial drying method in food industry is the convective air drying. This process is highly influenced by air temperature and material characteristics, as well as other parameters that must be controlled. For this reason, many researches in convective air drying of several seaweeds were carried out in the recent years, Table 1.3 and 1.4.

Along with the benefits remarked before, drying, and particularly hot air drying, might have some undesirable secondary effects. Under hot air, food products undergo several reactions that alter their physical (rehydration, color loss), chemical (browning reaction, lipid oxidation) and nutritional (vitamin and protein loss, and microbial survival).

As previously mentioned, seaweeds gained attention in the food industry for the antioxidant properties showed by some of their constituent components. In that matter, there are several researches carried out in the last ten years, which study the effect of varied convective drying conditions over antioxidant activity of many marine algae species, Table 1.3 and 1.4.

Convective air drying of algae must be carried out finding a compromise solution to several factors: loss of bioactive properties, energy consumption, time and customer oriented properties.

Table 1.3. Summary of studies involving seaweed drying or its effect on seaweed composition or antioxidant properties.

Reference	Study	Seaweed
Le Lann *et al.* (2008)	Effect of different conditioning treatments (fresh, freezing, freeze-drying, oven-drying and green house drying) on the total phenolic content and antioxidant activities of two brown algae,*Sargassum muticum* and *Bifurcaria bifurcata*.	*Bifurcaria bifurcata*, *Sargassum muticum*
Jiménez-Escrig *et al.* (2001)	Antioxidant activity and total phenolic compounds of fresh seaweeds and dried at 50°C using convective drying technique	*Chondrus crispus*, *Laminaria ochroleuca*, *Fucus vesiculosus*, *Porphyra umbilicalis*, *Undaria pinnatifida*
Uribe *et al.* (2017)	Drying characteristics of seaweed subjected to hot-air drying at 40, 50, 60, 70, and 80°C.	*Durvillaea antarctica*
Sarbatly *et al.* (2010)	Drying kinetics of seaweed dried in convective air drying at 50, 55, 60 and 70°C at different load densities.	*E. spinosum*
Fudholi *et al.* (2012)	Drying kinetics of *Gracilaria cangii* at 50°C and different relative humidities (10, 25 and 40%)	*Gracilaria cangii*
Tello-Ireland *et al.* (2011)	Effect of drying temperature (from 40 up to 70°C) on the antioxidant activity of *Gracilaria chilensis* extracts.	*Gracilaria chilensis*
Cox *et al.* (2012)	Effect of various food processing methods on the phytochemicals of seaweed.	*Himantalia elongata*
Gupta *et al.* (2011)	Phytochemical characteristics of seaweed after drying at temperature (from 20 up to 40°C).	*Himanthalia elongata*
Lee *et al.* (2010)	Total phenol contents and antioxidant activity of dried seaweed using vacuum drying at 20°C and 30°C and hot-air drying at 40°C and 60°C.	*Hizikia fusiformis*

Table 1.4. Summary of studies involving seaweed drying or its effect on seaweed composition or antioxidant properties.

Reference	Study	Seaweed
Ling *et al.* (2015)	Effect of different drying techniques (oven drying (40 and 80°C), sun drying, hang drying, sauna drying, shade drying and freeze drying) on the phytochemical content and antioxidant activity of seaweed.	*Kappaphycus alvarezii*
Neoh *et al.* (2016)	Proximate composition, phytochemical and antioxidant activity of oven dried, sun dried, vacuum dried and freeze dried seaweed.	*Kappaphycus alvarezii*
Cruces *et al.* (2016)	Effect of freeze-drying, silica-drying, oven-drying and air-drying on antioxidant activity of seaweed.	*Lessonia spicata*
Vega-Gálvez *et al.* (2008)	Drying kinetics of the brown algae *Macrocystis pyrifera* at 50, 60, 70, and 80°C and the desorption isotherm at 50°C.	*Macrocystis pyrifera*
Kuda *et al.* (2005)	Total polyphenol content and antioxidant activity of fresh seaweeds.	*Nemacystus decipiens*, *Papenfussiella kuromo*, *Porphyra sp.*, *Scytosiphon lomentaria*
Sappati *et al.* (2017)	Drying kinetics of seaweed at 40 and 70°C, 10 m/s air velocity and at relative humidity of 25, 50 and 80%.	*Saccharina latissima*
Chan *et al.* (1997)	Effect of sun-drying, oven-drying, and freeze-drying methods on the nutritional composition of the seaweed.	*Sargassum hemiphyllum*
Wong & Cheung (2001)	Influence of drying treatment (oven- and freeze-drying) on seaweed composition	*Sargassum hemiphyllum*, *Sargassum henslowianum*, *Sargassum patens*
Norra *et al.* (2016)	Antioxidant properties of sun-dried, oven-dried and freeze-dried seaweeds.	*Sargassum sp.*

As previously mentioned, seaweeds represent a suitable supplement and additive for food due to their high nutritional value and the health benefits they can provide. Moreover, in recent years there has been an increasing interest in natural antioxidants from different sources to replace synthetic additives in foods or nutraceuticals. This fact seems to indicate that once the drying process and its effect on phytochemical characteristics of dried seaweed are studied the next step to be focused on should be the addition of dried seaweed in gluten-free formulations. Very few studies addressed the seaweed addition effect on dough and baked product properties in general and their addition to gluten-free systems seems to be even more limited:

- Mamat *et al.* (2014) reported the effect of red seaweed Kappaphycus alvarezii addition on dough rheological properties and the quality of bread.
- (Allsopp *et al.*, 2016) investigated the effect of consuming the red seaweed Palmaria palmata incorporated into bread on serum markers of inflammation with secondary analysis investigating changes in lipids and antioxidant status ferric reducing antioxidant power.
- Menezes *et al.* (2015) assessed the effect on nutrient composition, caloric value, technological and sensory evaluation of the addition of green seaweed species (*Cladophora spp.* and *Ulva spp.*) to conventional breads.
- Hall *et al.* (2012) investigated the acceptability of brown seaweed *Ascophyllum nodosum* enriched bread as part of a meal, and measured its effect on energy intake and nutrient absorption in overweight, healthy males.
- Różyło *et al.* (2017) assessed the effect of this brown algae addition on the physical, antioxidant and sensory properties of a gluten-free bread.

Considering the actual state of art in this field, a challenge for the coming years would be to introduce these additives and other more innovative in gluten-free products optimising processing conditions and doses of the compounds.

USC
UNIVERSIDADE
DE SANTIAGO
DE COMPOSTELA

Chapter 2

Objectives

The **general objectives** of this Thesis are the obtaining of gluten-free baked products (cookies) with high antioxidant capacity, suitable for celiac population, employing formulations based on Galician native raw materials with socioeconomic interest like chestnut (*Castanea sativa Mill.*), maize (*Zea mays L.* with white, yellow and purple varieties) and brown seaweeds (*Ascophyllum nodosum*, *Birfurcaria bifurcata* and *Fucus vesiculosus*). The influence of seaweed powders addition to chestnut flour on the mixing, rheological and thermomechanical properties of doughs and physicochemical properties (texture, colour, antioxidant activity, etc.) of the final baked product will be studied to determine the maximum seaweed addition levels from a technological point of view.

In order to achieve the general objectives some **specific objectives** are established:

- Reviewing in-depth literature on the characterization, operational conditions, ranges of interest for key variables, among others, for the materials to be employed in this Thesis.
- Set-up and management of experimental equipment and techniques employed for different operations such as drying, milling, sieving, colorimetry, chemical analysis, hygrometric equilibrium, flours mixing, controlled stress rheometry, differential scanning calorimetry, dynamic mechanic-thermal analysis, image methods, texture analysis, etc.
- Study the hygroscopic behaviour of employed seaweeds by determination

of the experimental equilibrium moisture content at different temperatures and water activities, water sorption isotherms modelling and evaluation of the thermodynamic properties of water sorption in order to determine the optimal drying and storage conditions of food materials.

- Determination of the drying kinetics at different conditions and the evaluation of heat and mass transfer coefficients during constant drying rate period and effective coefficients of water diffusion during falling drying rate period of brown seaweeds. Establishment of the adequate air-drying temperatures of seaweeds based on mass transfer rates.

- Physical characterization of seaweeds powders obtained after milling of dried seaweeds. Evaluation of the physical parameters (particle size, water retention capacity, swelling power) of the tested powders and determination of the suitability in comparison to other flour additives commercially employed.

- Evaluation of the physicochemical properties of maize and chestnut flours. Determination of the particle size patterns, colour and chemical composition of these starchy materials in order to explain some doughs properties.

- Obtaining seaweed aqueous extracts by means of Ultrasound Assisted Extraction technique. Determination of the brown seaweed with the highest antioxidant (scavenging activity) and chemical properties (total polyphenols and carbohydrate content) as well as assessing the effect of seaweeds air-drying on these characteristics in order to select the optimal drying temperature to achieve aqueous extracts with optimal characteristics.

- Characterization of the mixing behaviour of flour doughs made from maize, chestnut and chestnut enriched with different levels (3, 6 and 9%) of seaweed powders, manufactured at the same consistency in order to analyse the mixing characteristic parameters (water absorption, development and stability time, etc.). Study of the effect of some variables (particle size of flour, additives employed, seaweed powder addition, etc.) on mixing parameters.

- Evaluation of the rheological behaviour of doughs, employing a stress-controlled rheometer, by means of the mechanical spectra and creep-recovery curves. Mathematical modelling of these curves to quantify the effect of the studied variables (flours particle size, seaweed amount, starch pregelatinization, etc.).

- Determination of thermal transitions (associated to biopolymers in flours) that take place in starchy flours during heating by Differential Scanning Calorimetry (DSC) and Dynamic Mechanic-Thermal Analysis (DMTA) techniques, in order to validate the suitability of DMTA for the study of these processes. Establishment of an experimental protocol.

- Analysis of the effect of storage time of chestnut flours on mixing, rheological and thermomechanical properties of their doughs, in order to establish the shelf-life period.

- Assessment of the effect of baking on colour and antioxidant characteristics of chestnut flour/seaweed powders formulations, employed to obtain cookies. Analysis of the effect of seaweed concentration on colour, antioxidant and textural properties of cookies and compare the obtained results with those of commercial cookies.

Objetivos

Los **objetivos generales** de esta Tesis son la obtención de productos horneados sin gluten con alta capacidad antioxidante, aptos para la población celíaca, empleando formulaciones a base de materias primas nativas gallegas con interés socioeconómico como la castaña (*Castanea sativa Mill.*) y el maíz (*Zea mays L.* con variedades blancas, amarillas y moradas) y algas pardas (*Ascophyllum nodosum*, *Birfurcaria bifurcata* y *Fucus vesiculosus*) para diversificar y aumentar su consumo. Se estudiará la influencia de la adición de polvos de algas a harina de castaña sobre las propiedades de mezcla, reológicas y termomecánicas de las masas y propiedades fisicoquímicas (textura, color, actividad antioxidante, etc.) del producto final horneado para determinar el nivel máximo de adición de algas desde el punto de vista tecnológico.

Para alcanzar los objetivos generales se establecen algunos **objetivos específicos**:

- Hacer una revisión bibliográfica en profundidad sobre la caracterización, las condiciones de operación, los rangos de interés para las variables clave, entre otros, para los materiales a emplear en esta Tesis.

- Establecimiento y manejo de equipos experimentales y técnicas empleadas para diferentes operaciones como secado, molienda, tamizado, colorimetría, análisis químico, equilibrio higrométrico, mezclado y amasado de harinas, reometría de esfuerzo controlado, calorimetría diferencial de barrido, análisis mecánico-térmico dinámico, métodos de imagen, análisis de textura, etc.

- Estudiar el comportamiento higroscópico de las algas empleadas por determinación del contenido de humedad de equilibrio experimental a diferentes temperaturas y actividades de agua, modelización de isotermas de adsorción/desorción de agua y evaluación de las propiedades termodinámicas de la adsorción/desorción de agua para determinar las condiciones óptimas de secado y almacenamiento de los materiales alimenticios.

- Determinación de las cinéticas de secado en diferentes condiciones y la evaluación de los coeficientes de transferencia de calor y masa durante el período de velocidad de secado constante y coeficientes efectivos de difusión de agua durante el período de velocidad de secado decreciente de las algas pardas. Establecimiento de las temperaturas adecuadas de secado por aire convectivo de las algas desde el punto de vista de la transferencia de materia.

- Caracterización física de los polvos de algas obtenidos tras la molienda de algas secas. Evaluación de los parámetros físicos (tamaño de partícula, capacidad de retención de agua, capacidad de hinchazón) de los polvos ensayados y determinación de su idoneidad por comparación con otros aditivos de harina comercialmente empleados.

- Evaluación de las propiedades fisicoquímicas de las harinas de maíz y castaña. Determinación de las distribuciones de tamaño de partícula, color y composición química de estos materiales amiláceos con el fin de explicar algunas propiedades de las masas.

- Obtención de extractos acuosos de algas mediante la técnica de extracción asistida por ultrasonidos. Determinación del alga parda con las mejores propiedades antioxidantes y químicas (contenido total de polifenoles e hidratos de carbono), así como la evaluación del efecto de la temperatura de secado de las algas sobre estas características para seleccionar la temperatura óptima de secado para obtener extractos acuosos con características óptimas.

- Caracterización del comportamiento de mezcla de las masas de harina de maíz, castaña y castaña enriquecidas con diferentes niveles (3, 6 y 9%) de polvos de algas fabricados con la misma consistencia para analizar los parámetros característicos de mezcla (absorción, tiempo de estabilidad, etc.). Estudio del efecto de algunas variables (tamaño de partícula de la harina, aditivos empleados, adición de polvo de algas, etc.) sobre los parámetros de mezcla.

- Evaluación del comportamiento reológico de las masas obtenidas, empleando un reómetro de esfuerzo controlado, mediante la adquisición de los espectros mecánicos y las curvas de fluencia-recuperación. Modelado matemático de estas curvas para cuantificar el efecto de las variables estudiadas (tamaño de partícula de las harinas, cantidad de algas, pregelatinización del almidón, etc.).

- Determinación de las transiciones térmicas (asociadas a los biopolímeros en las harinas) que se producen en las harinas amiláceas ensayadas durante el calentamiento mediante técnicas de Calorimetría de Barrido Diferencial (DSC por sus siglas en inglés) y Análisis Térmico-Mecánico Dinámico (DMTA por sus siglas en inglés) para validar la idoneidad del DMTA para el estudio estos procesos. Establecimiento de un protocolo experimental para la determinación de estas transiciones a través de DMTA.

- Análisis del tiempo de almacenamiento, en condiciones específicas, de las harinas de castaña sobre las propiedades de mezcla, reológicas y

termomecánicas de sus masas, con el fin de establecer el período de conservación de estas harinas.

- Evaluación del efecto del horneado sobre el color y las características antioxidantes de las formulaciones de harina de castaña/algas utilizadas para obtener galletas, el efecto de la concentración de algas sobre el color, las propiedades antioxidantes y texturales de las galletas y comparación de los resultados obtenidos con galletas comerciales.

Obxectivos

Os **obxectivos xerais** desta Tese son a obtención de produtos enfornados sen glute (galletas) con alta capacidade antioxidante, aptos para a poboación celíaca, empregando formulacións a base de materias primas autóctonas galegas con interese socioeconómico como a castaña (*Castanea sativa Mill*), o millo (*Zea mays L.* con variedades brancas, amarelas e moradas) e algas pardas (*Ascophyllum nodosum*, *Birfurcaria bifurcata* e *Fucus vesiculosus*) para diversificar e aumentar os seu consumo. Tamén se estudará a influencia da adición de polvos de algas á fariña de castaña sobre as propiedades de mestura, reolóxicas e termomecánicas das masas e as propiedades fisicoquímicas (textura, cor, actividade antioxidante, etc.) do produto final enfornado para determinar o nivel máximo de adición algas dende un punto de vista tecnolóxico.

Para acadar os obxectivos xerais establécense algúns **obxectivos específicos**:

- Facer unha revisión bibliográfica en profundidade sobre a caracterización, as condicións operativas, os intervalos de interese das variables clave, entre outros, dos materiais que se empregarán nesta tese.
- Configuración e xestión de equipos e técnicas experimentais empregados para diferentes operacións como secado, moenda, tamizado, colorimetría, análise química, equilibrio higrométrico, mezclado de fariñas, reometría de esforzo controlado, calorimetría diferencial de barrido, análise mecánica-térmica dinámica, métodos de imaxe, análise de textura, etc.
- Estudar o comportamento higroscópico das algas empregadas mediante a determinación do contido de humidade de equilibrio experimental a diferentes temperaturas e actividades de auga, isotermas de adsorción/desorción de auga, modelado e avaliación das propiedades termodinámicas da adsorción/desorción de auga para determinar as condicións óptimas de secado e almacenamento de materiais alimentarios.
- Determinación das cinéticas de secado en diferentes condicións e a avaliación dos coeficientes de transferencia de calor e masa durante o período de velocidade de secado constante e os coeficientes efectivos de difusión de auga durante o período de velocidade de secado decrecente das algas pardas. Establecemento das temperaturas de aire adecuadas durante o secado das algas dende o punto de vista da transferencia de materia.
- Caracterización física dos polvos de algas obtidos despois da moenda das algas secas. Avaliación dos parámetros físicos (tamaño de partícula, capacidade de retención de auga, capacidade de inchazón) dos polvos

obtidos e determinación da súa idoneidade en comparación con outros aditivos de fariña comercialmente empregados.

- Avaliación das propiedades fisicoquímicas das fariñas de millo e castaña. Determinación da distribución de tamaños de partícula, cor e composición química destes materiais de amidón para explicar algunhas propiedades de masa.

- Obtención de extractos acuosos de algas mediante a técnica de extracción asistida por ultrasóns. Determinación da alga parda con mellor capacidade antioxidante e propiedades químicas (polifenois totais e contido de hidratos de carbono), así como a avaliación do efecto da temperatura de secado sobre estas características para seleccionar a temperatura de secado ideal para conseguir extractos acuosos con características óptimas.

- Caracterización do comportamento de mestura das masas de fariña de maíz, castaña e castaña enriquecidas con diferentes niveis (3, 6 e 9%) de polvos de algas fabricados coa mesma consistencia para analizar os parámetros característicos da mestura (absorción de auga, desenvolvemento e tempo de estabilidade, etc.). Estudo do efecto dalgunhas variables (tamaño de partícula de fariña, aditivos empregados, adición de algas mariñas, etc.) nos parámetros de mestura.

- Avaliación do comportamento reolóxico das masas obtidas, empregando un reómetro de esforzo controlado, mediante a obtención dos espectros mecánicos e as curvas de fluencia e recuperación. Axuste matemático destas curvas para cuantificar o efecto das variables estudadas (tamaño das partículas de fariña, cantidade de algas, prexelatinización do amidón, etc.).

- Determinación das transicións térmicas (asociadas a biopolímeros na fariña) que se producen en fariñas de amidón durante o quecemento por medio de técnicas de Calorimetría Diferencial de Barrido (DSC, polas súas siglas en inglés) e Análise Dinámica Mecánica-Térmica (DMTA, polas súas siglas en inglés) para validar a adecuación do DMTA para o estudo destes procesos. Establecemento dun protocolo experimental para a determinación destas transicións a través dos datos de DMTA.

- Análise da influencia do tempo de almacenamento, en condicións específicas, da fariña de castaña nas propiedades de mestura, reolóxicas e termomecánicas das súas masas para establecer o período de conservación destas fariñas.

- Avaliación do efecto do enfornado sobre a cor e as características antioxidantes das formulacións de fariña de castaña/polvo de algas empregadas para a obtención de cookies, o efecto da concentración de algas nas propiedades de cor, antioxidantes e texturais das cookies e comparación dos resultados obtidos cos de cookies comerciais.

USC
UNIVERSIDADE
DE SANTIAGO
DE COMPOSTELA

Chapter 3

Theoretical fundamentals

In this section, concepts, definitions and other basic aspects necessary in the development of this Thesis are revised: hygroscopic properties, water activity, convective air drying, viscoelasticity, mechanical models, temperature effects, flour dough rheology, etc.

3.1 Hygroscopic properties

The state of water plays a crucial role in food preservation. The quality of preserved foods depends upon the moisture content, moisture migration, or moisture uptake by the food material during storage. Extent of sorption of water by or desorption from a food product depends on vapour pressure of water present in the food sample and that in the surroundings.

Moisture is bonded to food, mainly, in two ways: to ionic groups, such as carboxyl groups and amino acids, and to hydrogen groups, such as hydroxyl and amides. In foods in which moisture is higher than 50% wet basis (kg water/100 kg wet material), free water exists within the material pores and in intercellular spaces. The former is easier to remove than the latter and is evaporated in the first stages of drying.

Equilibrium moisture content (X_{eq}) of a food material is reached when its internal vapour pressure is in equilibrium with the outside vapour pressure.

The role of moisture in food drying and storage is expressed in terms of water activity (a_w). Water activity is defined in a similar manner as the relative humidity is defined in moist air, that is, the ratio of vapour pressure (p_w) to the saturated vapour pressure (p_w^0) at same temperature Eq. (3.1). It measures the chemical activity of moisture in food during drying and storage.

$$a_w = \left[\frac{p_w}{p_w^0}\right]_T \tag{3.1}$$

The different states of equilibrium at any temperature are usually represented by a X_{eq} *versus* equilibrium related humidity, or water activity.

3.1.1 Sorption Isotherms

The relationship between X_{eq} and corresponding relative humidity at constant temperature yields the so-called moisture sorption isotherm (Basu *et al.*, 2006). By means of sorption isotherm the optimum X_{eq} can be determined at a given temperature and relative humidity. The knowledge of sorption curves is essential to determine the final amount of water needed to stabilize the product. Each foodstuff has its characteristic sorption isotherm at each temperature. The different shapes of sorption isotherms are due to differences in physical structure, chemical composition and water holding

capacity of the food. Thus, knowledge of sorption isotherms is of great importance of food industry since it provides useful information for the optimization of drying process, selection of packaging material, prediction of shelf-life and evolution of food moisture content during storage (Stencl, 2004).

Since the water sorption isotherm is a way to analyze the degree of interaction of water with the substrate, usually it can be divided into three zones based on how water is bounded to food (Figure 3.1). Zone I represents strongly bound water with enthalpy of vaporization considerably higher than that of pure water. The bound water includes structural water (H-bonded water) and monolayer water, which is sorbed by hydrophilic and polar groups of the food components (polysaccharides, proteins, etc.). Bound water is unfreezable and is not available for chemical reactions or as a plasticizer (Basu *et al.*, 2006), it corresponds typically to water activity below 0.2. In zone II water molecules bind less firmly than in the first zone. The vaporization enthalpy is slightly higher than that for pure water. This class of constituent water can be looked upon as the continuous transition of the bound to the free water, it corresponds to a water activity up to 0.8. Properties of water in region III are close to those of the free water that is held in voids, capillaries, crevices, and loosely binds to the food materials and therefore it is easily removed.

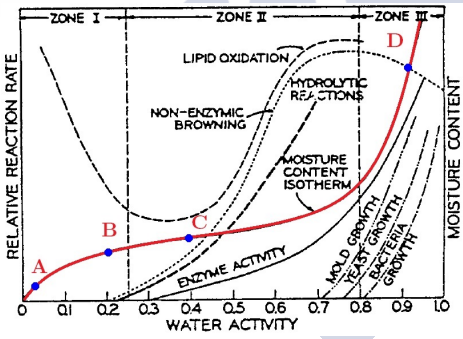

Figure 3.1 Water sorption isotherm zones and its characteristics points combined with the food stability map (adapted from Labuza (1970); Slade & Levine (2004)).

In water sorption isotherm it can be identified four important points (Figure 3.1): A, initial point of the food packaging or processing end point, B, the end of the concave part of the isotherm, corresponding to the monolayer moisture content; C, critical point that should not be exceeded during storage and distribution, and D, point corresponding to equilibrium with the environment. The point A can be located at any point of the isotherm. It can correspond to the end point of a dehydration process. B usually ranges from 0.15 to 0.25 of water activity and

represents the highest relative stability with respect to lipid oxidation, enzymatic reactions and microbial spoilage. D is the intersection of the isotherm with relative humidity of the ambient air. This point is used in packaging calculations. At moisture content corresponding to the critical point, occur certain physical, chemical or biological phenomena so quickly that the spoilage of food is achieved before the end of the storage period. It is important to note that this last point, as well as all isotherm depends on the temperature.

Several researches (Labuza *et al.* (1985); Jayaraman *et al.* (1990); Brennan (1994); Vázquez *et al.* (2003)) showed that the target stability of dehydrated foods during storage is obtained with the moisture content corresponding to a molecular layer of adsorbed water. This layer forms a protective film that prevents the oxidation reactions that can lead to low moisture content. However, it is shown that this monolayer sometimes is not enough, since to cover all points of adsorption, it is necessary higher moisture content to ensure the preservation of a food during storage.

Five types of isotherms were described by Brunauer *et al.* (1940) with interest in the field of food preservation, Figure 3.2:

- **Type 1** is the well-known Langmuir isotherm, obtained assuming monomolecular adsorption of gas by the porous solids in a finite volume of voids. The amount of adsorbate (adsorbed substance, water) increases with relative humidity up to an asymptotic value which is corresponding to a monolayer. It corresponds to chemisorption phenomena that occur in a single layer in the active sites of the surface.

- **Type 2** is the sigmoid isotherm obtained for soluble products, which exhibits asymptotic trend as water activity approaches 1. The inflection point corresponds to the end of the monolayer and the beginning of the sharp decrease of the differential heat of adsorption (Wolf *et al.*, 1985). It is the most common in non-porous food.

- **Type 3**, known as the Flory-Higgins isotherm, accounts for a solvent or plasticizer such as glycerol above the glass transition temperature. The adsorbate content increases without limit for relative humidity equal to one. The curvature of the isotherm can be explained because the heats of adsorption of the first layer of molecules are smaller than normal condensation due to the interactions.

- **Type 4** isotherm describes adsorption by a swellable hydrophilic solid until a maximum of hydration sites are reached.

- **Type 5** is the BET (Brunauer *et al.*, 1938) multilayer adsorption isotherm, observed for adsorption of water vapour on charcoal; it is related to types 2 and 3 isotherms

The two isotherms most commonly found in food products are types 2 and 4.

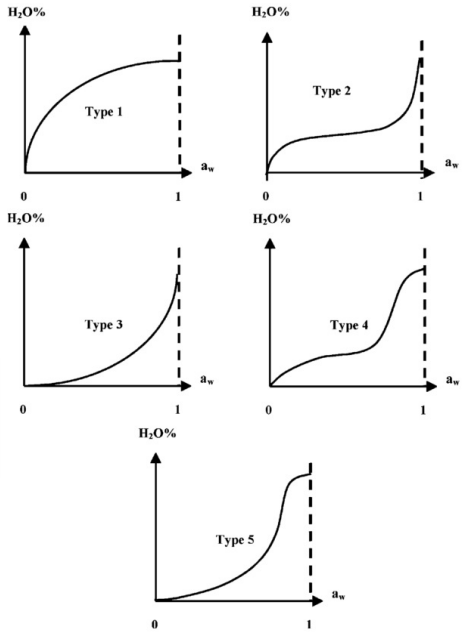

Figure 3.2 Types of isotherms according Brunauer *et al.* (1940) classification. Adapted from Basu *et al.* (2006)).

The sorption curve can be generated from an adsorption process (from a dry system with a_w close to 0) or a desorption process (from a wet system with $a_w > 0.97$). When a foodstuff is exposed to air conditions where vapour pressure of water is higher than vapour pressure of water in the solid, adsorption occurs. At lower vapour pressure of water in atmosphere than in food solids becomes the driving force for desorption. Figure 3.3 shows typical desorption and adsorption curves. At the same vapour pressure, the amount of water for adsorption and desorption processes in the same food may differ. This phenomenon where the X_{eq} during the adsorption and that during the desorption process is different is called "hysteresis". Hysteresis is in fact a thermodynamic impossibility because chemical potential or a_w is a state function, and at the same chemical composition and water content should always occur at a given a_w. A variety of hysteresis

loop shapes can be observed as function of food and the temperature (Wolf *et al.*, 1972)).

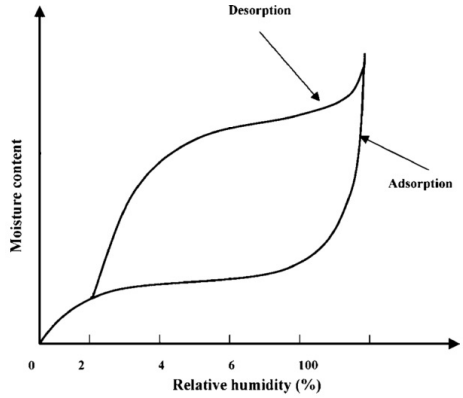

Figure 3.3 A typical sorption isotherm showing the phenomenon of hysteresis (Basu *et al.*, 2006)).

Hysteresis can also depend on the storage time before isotherm measurement, pre-processes, and number of successive adsorption and desorption cycles (Barbosa-Cánovas *et al.*, 2007). Adsorption and desorption rates are governed by the physical and chemical characteristics of the surface boundary. For example, the rate of the fluid molecules to adhere or escape from the surface can depend upon special features of the surface physical structure, such as roughness, smoothness, and porosity. Besides physical adsorption, water can be chemically sorbed (chemisorption). This fact cab enhance or interfere the adsorption or desorption processes, respectively,

Water sorption isotherms are useful with theoretical purposes to calculate heat of sorption, to determine monolayer moisture content and to research the solid structure, but also with practical purposes. In this way, there are specific unit operations (drying, blending, packaging and storage) where practical application of water sorption isotherms are necessary.

3.1.2 Measurement of sorption isotherms

Many methods are available for determination of water sorption isotherm. These methods may be classified into three categories: (1) gravimetric, (2) manometric, and (3) hygrometric. The gravimetric method involves the

measurement of mass changes that can be measured both continuously and discontinuously in dynamic and static systems. Manometric methods involve sensitive manometers to measure vapour pressure of water in equilibrium with a food material of given moisture content. Hygrometric methods measure the equilibrium relative humidity of air in contact with a food material at given moisture content. Dew point hygrometers detect the condensation of cooling water vapour. Electronic hygrometers measure the change of conductance or capacitance of hygrosensors (Troller, 1977).

The most common technique, for which a recommended procedure has been defined in the European project COST 90, uses thermostatted jars filled at the bottom with super- saturated salt solutions to maintain the desired air relative humidity.[20] However, this method encounters some problem at high humidity ranges due to (a) excessive equilibration times and (b) its inability to produce and control high relative humidities.

Baucour & Daudin (2000) developed a rapid but accurate method to measure moisture sorption isotherms of solid foods in the water activity range 0.9–1. This method avoids the drawbacks of saturated salt solution method by blowing calibrated air along thin slices of material at a high velocity to impose an intensive water vapour exchange between air and samples.

3.1.3 Mathematical models of isotherms

Numerous attempts have been made to describe the sorption isotherms mathematically. These correlation models can be classified into several categories: kinetic models based on a monolayer sorption as Brunauer-Emmet-Teller (BET) model (Brunauer *et al.*, 1938) or multilayer sorption and condensed film as Guggenheim-Anderson-de Boer (GAB) model ((van den Ber & Bruin, 1981) grouped as theoretical models; semi-empirical and purely empirical models. The experimental evaluation of the water sorption characteristics of different products, the development and use of mathematical models can help to improve the food processing (McMinn & Magee, 2003).

The mathematical models employed in this Thesis to fit the obtained experimental data of moisture content against water activity are showed below.

The BET isotherm equation (Eq. (3.2)) is one of the most widely used models and gives good fit for a variety of foods over the region $0.05 < a_w < 0.45$ (Basu *et al.*, 2006). It provides an estimate of monolayer value of moisture adsorbed on the surface.

$$X_{eq} = \frac{X_m C a_w}{(1 - a_w)(1 + (C - 1)a_w)} \tag{3.2}$$

where X_m the monolayer moisture content (kg water·(kg dried solid)$^{-1}$, d.b.) and C (dimensionless, -) is a parameter related to heat of sorption of monolayer region.

The theory behind the development of the BET equation has been questioned due to the assumptions that (a) the rate of condensation on the first layer is equal to the rate of evaporation from the second layer, (b) binding energy of all of the adsorbate on the first layer is same, and (c) binding energy of the other layers is equal to that of pure adsorbate. The assumptions of uniform adsorbent surface and absence of lateral interactions between adsorbed molecules are incorrect in view of the heterogeneous food surface interactions (Rizvi, 1986).

van den Ber & Bruin (1981) refined the BET theory and proposed a new equation with three parameters having physical meanings (X_m, C and K), that fit adequately experimental data in the a_w range of 0 to 0.95 for most food materials of practical interest.

$$X_{eq} = \frac{X_m C K a_w}{(1 - K a_w)(1 - K a_w + C K a_w)} \tag{3.3}$$

The three parameters of GAB model depend on the temperature, where X_m represents the monolayer moisture content, C is a constant related to the heat of sorption of the monolayer and K is other constant related to the heat of sorption of the multilayer. Parameters K and C can be expressed by Arrhenius type equations:

$$C = C' exp(\frac{-\Delta H_c}{RT}) \tag{3.4}$$

$$K = K' exp(\frac{-\Delta H_k}{RT}) \tag{3.5}$$

where ΔH_c=ΔH_m-ΔH_q; ΔH_k=ΔH_l-ΔH_q (kJ·mol^{-1}); ΔH_l is the heat of condensation of pure water (kJ·mol^{-1}); ΔH_m is the total heat of sorption of mono layer (kJ·mol^{-1}); ΔH_q is the total heat of sorption of multilayer covering the monolayer (kJ·mol^{-1}); and C', K' are the constants of entropic character.

The GAB model underestimates the water content values at high water activities ($a_w > 0.93$). The discrepancy underlines two facts: (a) this type of model is unsuitable for high humidity range, and (b) the saturated salt solution method does not afford sufficient information to get a complete sorption curve.

Halsey (Halsey, 1948) developed an equation to describe condensation of multilayers, assuming that the potential energy of a molecule varies inversely as the Bth power of its distance from the surface.

$$X_{eq} = \left(\frac{-A}{Tln(a_w)} \right)^{(1/B)} \tag{3.6}$$

where T is the temperature (K), and A ((kg water·K)·(kg dried solid)$^{-1}$) and B (-) parameters of Halsey equation.

3.2 Drying

Drying is one of the most studied processes worldwide as it accounts for about 10-25% of the total energy consumption in manufacturing processes. It represents an important step in the food processing industry. Almost every food product is dried at least once at one point of its preparation (Mujumdar, 2006). The main reasons why food products are dried are detailed below (Brennan, 1994):

- Extended storage life: dried food products are less vulnerable to spoilage caused by bacteria, molds and insects. Activity of several microorganisms is inhibited in systems in which moisture is below certain levels. Additionally, enzymatic and oxidative reactions might not take place under low moisture conditions.
- Quality enhancement: many favourable qualities and nutritional values of food may be enhanced by drying. Palatability and digestibility are improved. Drying changes color, flavour, appearance and texture of a food item. These features may affect the decision of the end user to buy or not a certain food Figure (3.4).
- Ease of handling: packing, handling and transportation of a dried product is considerably easier and cheaper because of weight and volume loss.
- Further processing: food products are dried for improved milling, mixing or segregation. In addition, dry milling is far cheaper than wet milling.
- Sanitation: during drying, insects and other microorganisms are destroyed.

Many foods and, more strictly seaweeds, are generally sundried, process that requires long periods of time. During recent years, an increase of production rates of marine algae requires the application of quicker industrial methods. The

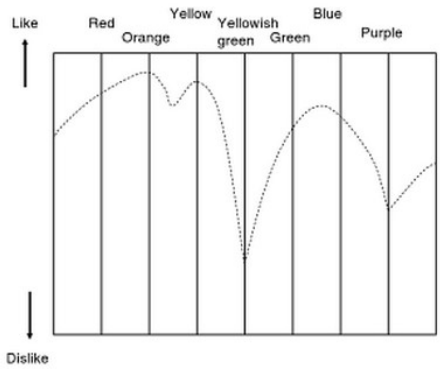

Figure 3.4 Illustration of the impact of the colour of a particular natural food product upon 'Like or dislike' (Birren diagram , Chen & Mujumdar (2009).

most frequently used industrial drying method in food industry is the convective air drying. This process is highly influenced by air temperature and material characteristics, as well as other parameters that must be controlled.

Drying affects physical and chemical properties of food materials. Convective drying can cause changes in appearance. Most food materials shrinkage while drying due to water removal and structural modifications. Besides, colour alterations can occur as a result of chemical reactions, colourants leaching or degradation while drying Figure (3.4). Thereby, it is mandatory to study physical and chemical alterations of food materials along with drying kinetics.

3.2.1 Drying kinetics

The drying kinetics are determined by following the variation of the weight of the product with the processing time. There are multiple operational variables, for the same product that modify the rate of dehydration, such as:

- Air drying temperature: The drying air temperature is the most influential variable in the water removal rate of a product. A high temperature promotes faster drying but can be related to low product quality and high energy cost. The values of the operating temperature depend on the type of product to be dried, too high temperatures can irreversibly damage the thermolabile products or promote degradation reactions (Krokida *et al.*, 2003).

In general, vegetables and fruits are dried at temperatures below 70°C (Ghiaus *et al.*, 1997). On the other hand, too low temperatures would cause a very slow drying rate making the operation economically undesirable given the high drying times.

- Relative humidity: The relative humidity of air is an important variable because it limits the driving force in the drying process between the solid and the surrounding atmosphere. In order to carry out a drying process, the relative humidity of the air during drying must be less than the value of the water activity of the solid during the process which is defined by its sorption isotherm at the selected temperature. If these values are equal equilibrium occurs and if the relative humidity value is higher then the process that takes place is the adsorption.

- Air velocity: The air velocity, together with the direction of the air flow (parallel or perpendicular), has a direct relation with the values of the convective coefficients of mass and heat transfer. In general, a high air velocity favours the drying process as it renews the wet air layers near the surface of the solid, and the resistance to the mass transfer the solid can be neglected (MacGregor, 2005). An excessively low speed would cause the possibility of the existence of local equilibria between the solid and the air which would paralyse the drying. However, too high air velocity could delay drying due to the appearance of a too dry (crust) surface layer that would prevent the removal of water.

- Sample size and configuration in the dryer: A high load density increases the drying process because there is a greater amount of water to be eliminated. A large sample size causes a similar effect. In addition, it does not favour the production of a quality product due to the appearance of moisture gradients resulting in a non-homogeneous dry product. Small dimensions favour drying, but should be limited by the characteristics of the desired end product.

  The basic geometries (cubic cylindrical and spherical) allow to apply different theoretical diffusion equations with analytical solution which helps to a better knowledge of the drying process of the product (Crank, 1975).

  Finally, a very important aspect to take into account during drying is the volume variation of the sample. This reduction can reach 80% of the initial value so it is fundamental to know how this variable is modified with the drying time (Mayor & Sereno, 2004).

The effects of these variables were extensively studied by different authors for

different agroindustrial products (Krokida *et al.* (2003); Kaymak-Ertekin & Gedik (2005)). Thus, for all these variables, there are optimum operating conditions that must be adequately combined to achieve both a high quality product and a minimum time of use of the drying plant with the lowest volume of the equipment.

The evolution of drying process can be follow by different graphical representations, Figure 3.5.

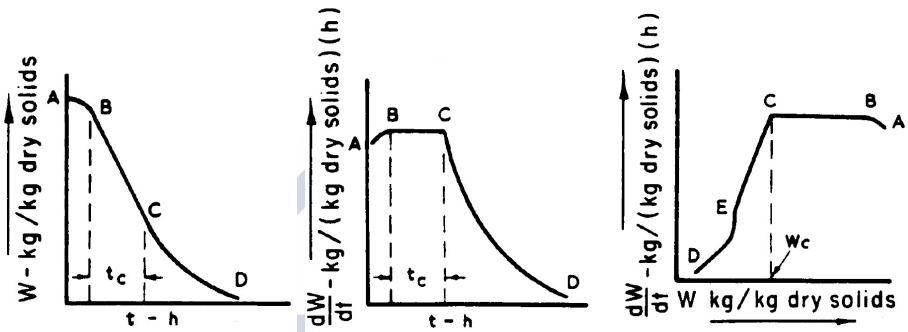

Figure 3.5 Model drying curves: (a) moisture content *vs* time, b) rate of change of moisture content *vs* time, (c) rate of change of moisture content *vs* moisture content (Brennan, 1994).

The most employed representations are (a) named as "drying kinetics" where moisture content *vs* time experimental data is displayed and (c) where drying rate *vs* moisture content is represented. In both figures, different periods can be observed (Brennan, 1994).

Period A-B. This represents a 'settling down' or equilibration period during which the solid surface conditions come into equilibrium with the drying air. The length of this period is usually small compared to the overall drying time.

Period B-C. During this period the rate of drying remains constant. Hence it is known as the constant rate period. During this period the surface of the solid is saturated with water. As water evaporates from the surface it is replaced with water which migrates from within the solid to the surface. The rate of evaporation of water from the surface balances the rate of heat transfer to the surface, from the air, and so a state of equilibrium exists at the surface. Throughout this period the surface temperature remains constant at a value which corresponds to the wet-bulb temperature of the drying air. This state of equilibrium persists as long as the movement of water to the surface is sufficient to maintain it in a saturated condition. Water evaporates into the air stream as a result of a water-vapour

pressure gradient between the surface of the solid and the main stream of the air. The rate of mass transfer (w, kg water·kg d.b.$^{-1}$·s^{-1}) may be described by an expression such as:

$$w = \frac{X_{t_{n-1}} - X_{t_n}}{t_n - t_{n-1}} = \frac{K_t \rho_{air} a}{\rho_s}(Y_i - Y_{air}) \tag{3.7}$$

where K_t (m s^{-1}) is the coefficient of mass transfer of gas phase, Y_i and Y_{air} (kg water kg dry air^{-1}) are the interphase and bulk absolute moisture content of air, respectively, ρ_{air} (kg·m^3) is the air density at drying temperature, ρ_s (kg d.b.·m^{-3}) is the apparent density of the material, a (m^2·m^{-3}) is the total interfacial surface (assuming water transfer by both sides of the layer) per unit of layer volume, T_i and T (°C) are the interphase and dry temperature of air, respectively and ΔH_v (J·kg^{-1}) is the latent heat of vaporization of water at the interphase temperature.

Drying under constant rate conditions can be advantageous when heat sensitive foods are being dried, as high rates of evaporation may be accomplished at relatively low product temperatures. Some solid foods do exhibit constant-rate drying but the length of that period is usually only a small proportion of the total drying time. In the case of many foods no constant rate period of drying is evident.

As drying continues, a point is reached at which the rate of migration of moisture to the surface is no longer adequate to maintain the surface in a saturated condition (point C in Figure 3.5). From this point on, the rate of drying is no longer constant but falls progressively throughout the rest of the drying cycle. Point C is known as the critical point, the moisture content at that point - W,, the critical moisture content and the drying period beyond that point - C-D, the falling-rate period.

In period C-D, the falling-rate period, the temperature at the surface of the solid rises as drying proceeds and approaches a value corresponding to the dry-bulb temperature of the air as the material approaches dryness. Many authors have reported the occurrence of two or more falling rate periods, i.e. points of inflexion in the falling-rate curve (Figure 3.5(c)). Attempts have been made to explain such curves in terms of what is happening within the solid. One such explanation is as follows: just beyond the critical point the surface begins to dry out but moisture is still evaporating from the surface. At some point E (Figure 3.5(c)) the plane of evaporation moves down into the solid. The vapour arising from this plane has to pass through a layer of dry solid which further reduces the rate of drying. This behaviour could account for a two-stage falling-rate period, but there is little experimental evidence to confirm this. Other explanations

relate to the mechanism of moisture movement within the solid. Usually, in food dehydration operations, a large proportion of the drying takes place under falling rate conditions.

Very many mathematical models have been proposed to represent drying under falling-rate conditions. These can be put into two categories: (a) those that relate to the mechanisms of moisture movement within the solid and (b) those that are empirical and are obtained by fitting expressions to drying curves constructed from experimental data. In this Thesis the mathematical model selected to model the falling drying rate period corresponds to category (a). It is based on the mechanism which has received the widest acceptance, diffusion due to concentration gradients. Such diffusion may be represented by Fick's second law:

$$\frac{dX}{dt} = D\frac{d^2X}{dl^2} \tag{3.8}$$

where X = moisture content ; t = time; 1 = characteristic lenght; D = water diffusivity. A well-known solution for this equation for a cylindrical shaped solid is:

$$\frac{X - X_e}{X_c - X_e} = \frac{4}{\pi^{1/2}}\left(\frac{D_{eff}t}{r^2}\right)^{1/2} - \frac{D_{eff}t}{r^2} - \frac{1}{3\pi^{1/2}}\left(\frac{D_{eff}t}{r^2}\right)^{3/2} \tag{3.9}$$

when $(X\text{-}X_e)/(X_c\text{-}X_e) \leqslant 0.6$, and:

$$\frac{X - X_e}{X_c - X_e} = 1 - \sum_{n=1}^{\infty}\frac{4}{\alpha_n^2}e^{-D_{eff}\alpha_n^2 t/r^2} \tag{3.10}$$

when $0.4 < (X\text{-}X_e)/(X_c\text{-}X_e) < 1$, where D_{eff} $(m^2{\cdot}s^{-1})$ is the effective coefficient of water diffusion in the bulk of the material, r (m) is the radius considered for the cylinder and (α) are the roots of the first order Bessel function for each term n.

3.3 Ultrasounds assisted extraction (UAE)

The use of ultrasound technology is widely extended in the food industry. It has been implemented in several large-scale commercial applications such as emulsification, homogenization, extraction, crystallization, dewatering, low-temperature pasteurization, degassing, defoaming, activation and inactivation of enzymes, particle-size distribution and changing viscosity. In the recent years it has attracted the attention for its application for the extraction of

natural products in a short time, which previously required, by conventional methods, many hours or days.

The conventional solvent extraction within the bodies of plants and seeds is based on the right choice of solvent and the use of heat and agitation. The use of ultrasounds improves solvent penetration and disrupts cell walls, releasing its content.

Ultrasound Assisted Extraction (UAE) usually reduces working times, increases yields and the quality of the extract. In recent years, there are several compounds that have been extracted by UAE, especially bioactive compounds in the food industry (Picó, 2013).

3.3.1 Principles of UAE

Ultrasound comprises mechanical waves that need an elastic medium to spread. The difference between sound and ultrasound is the frequency of the wave: sound wave are at human hearing frequencies (16 Hz - 20 kHz) while ultrasound has frequencies above human hearing but below microwave frequencies (20 kHz – 10MHz). The main parameter taken into account for the classification of ultrasound applications is the amount of energy generated: sound power (W), sound intensity (W/m^2) or sound energy density (W/m^3). The applications of ultrasound are divided into two groups: high intensity and low intensity.

Low-intensity, high frequency (100 kHz – 1 MHz, low power ultrasound ($<$ 1 W/cm^2) is employed in non-destructive procedures, especially as an analytical technique to determine food physicochemical properties (firmness, sugar content, acidity). On the other hand, high-intensity, low frequency (16 – 100 kHz), high power ultrasound (10-100 W/cm^2) can affect food properties.

When applying ultrasound to a liquid medium, longitudinal waves are created leading to the formation of regions of compression and rarefaction waves. This way, cavitation takes place and gas bubbles are formed. These bubbles get larger during the rarefaction or expansion step, and collapse when the energy provided by the ultrasounds in the compression stage is not enough to keep the vapour phase in the bubble (Figure 3.6)(Picó, 2013).

Afterwards, the vapour phase rapidly condensates and large amounts of energy are released. The condensed molecules collide creating shock waves. Cavitation can produce micro-streaming, which improves heat and mass transfer. These microjets are useful in terms of improving solvent penetration and occasionally

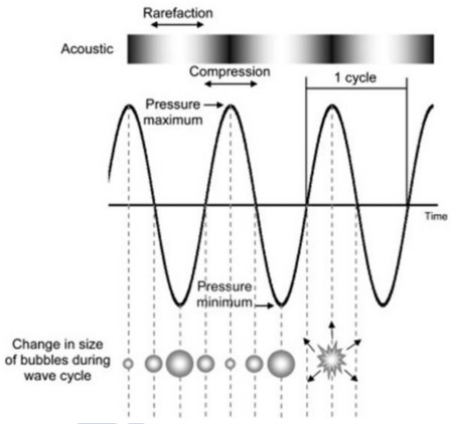

Figure 3.6. Cavitation formation during sonication (Soria & Villamiel, 2010).

break cell walls, facilitating release of bioactives from the biological matrix. In Figure 3.7 it is shown how a bubble is formed (a) and soon thereafter it collapses (b) forming microjets which break down the cell wall (c) and release the cell content (d) (Picó, 2013).

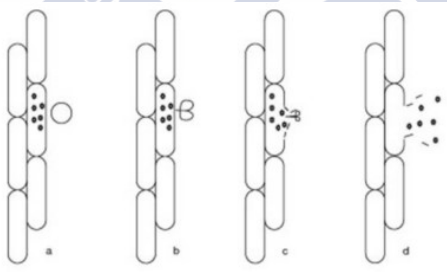

Figure 3.7. Ultrasound assisted extraction process (Picó, 2013).

Ultrasound extraction can be a simple, cost-effective and efficient replacement for traditional technologies employed to extract bioactive compounds from algae. It is a technology already in use for the extraction of lycopene from tomatoes (Lianfu & Zelong, 2008), anthocyanins from raspberries (Chen *et al.*, 2007), phenolic compounds from citrus peel (Ma *et al.*, 2009) and coconut shell (Rodrigues *et al.*, 2008). UAE facilitates the extraction of heat sensitive compounds with minimal damage. Equipment costs are lower than traditional equipment employed for novel extraction techniques and it can be

used in combination with a wide variety of solvents, including water (for water soluble components). One of the drawbacks of the UAE is the weakening of sound waves in dispersed systems, making solid/liquid ratio a critical operation variable. Yet, UAE extraction technology has been employed in both, laboratory and large-scale industrial/commercialized applications (Kadam *et al.*, 2013).

3.4 Rheology

Rheology is defined as the science that studies the flow and deformation of the matter (Steffe, 1996). In the field of food technology, rheology is defined as "the study of the deformation and flow of raw materials, intermediate products and final products of the food industry" (White, 1970). Some concepts are essential for the compression of rheology. The most important ones are:

- Stress (σ). It is defined as the force applied by unit of sample area. It can be of tension, compression or shear. The SI unit for effort is Pascal (Pa) (Steffe, 1996).
- Strain (γ). It is the change, in size or shape, that a material suffers by the application of an effort. Generally expressed in meters (m) or % (Bourne, 2002).
- Shear Stress (σ). It is the component of the effort applied in a tangent way to the plane in which the force acts. Expressed in units of force per unit of area. The unit in SI for cutting effort is Pascal (Pa) (Bourne, 2002).
- Shear rate ($\dot{\gamma}$). It is the gradient of velocity in a fluid resulting from the application of a shear stress. There is transport of amount of movement from the regions of higher speed to those of lower speed, s^{-1}.

The Society of Rheology nomenclature committee recommends using $\dot{\gamma}$ to denote shear velocity, while recommending the use of γ to denote shear deformation.

3.4.1 Elastic behaviour

When force is applied to a solid material and the resulting stress *vs* strain curve is a straight line through the origin, the material is obeying Hooke's law. The relationship may be stated for shear stress and shear strain as:

$$\sigma = G\gamma \tag{3.11}$$

whre G is the shear modulus. Hookean materials do not flow and are linearly elastic (Steffe, 1996). Stress remains constant until the strain is removed and the material returns to its original shape. Hooke's law can be used to describe the behaviour of many solids when subjected to small strains, typically less than 0.01. Large strains often produce brittle fracture or non-linear behaviour.

The behaviour of a Hookean solid may be investigated by studying the uniaxial compression of a cylindrical sample, Figure 3.8. If a material is compressed so that it experiences a change in length and radius, then the normal stress and strain may be calculated:

$$\sigma = \frac{F}{A} = \frac{F}{\pi R_0^2} \tag{3.12}$$

and

$$\varepsilon_c = \frac{\delta h}{h_0} \tag{3.13}$$

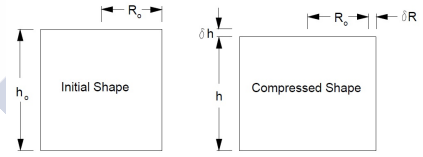

Figure 3.8. Uniaxial compression of a cylindrical sample (Steffe, 1996).

This information can be used to determine Young's modulus (E), also called the modulus of elasticity of the sample:

$$E = \frac{\sigma}{\varepsilon_c} \tag{3.14}$$

taking into account the mentioned relationship, it is clear that the Young's modulus corresponds to the slope of shear stress *vs* strain curve (Bourne, 2002).

3.4.2 Viscous behaviour

The elastic behaviour of food fluids is small or may be negligible, with the exception of flour doughs, leaving the viscosity function as the main area of interest.

This function is related to shear stress and shear rate. The relation between both parameters is based on experimental data. The behaviour is visualized by a representation of shear stress and shear rate. The simplest type of substance to be considered is the Newtonian fluid, for which the shear stress is directly proportional to the shear rate, as expressed through Newton's law, Eq. (3.15):

$$\sigma = \mu\dot{\gamma} \tag{3.15}$$

where μ is the proportionality constant, called the dynamic viscosity for Newtonian fluids, a factor that describes "the slipperiness of a fluid" (Barnes *et al.*, 1993). For this type of fluids, the dynamic viscosity and the viscosity coefficient are synonymous for the term "viscosity" (Steffe, 1996). The dynamic viscosity (μ) is the internal friction of a fluid or the tendency to resist flow (Rao, 2007). According to the International Organization for Standardization (ISO), the unit of measurement of dynamic viscosity is Pa·s. Since, because this unit is a large measure, the most commonly used unit for low viscosity fluids is mPa·s, equivalent to cP.

In Newtonian fluids, the kinematic viscosity ($m^2 \cdot s^{-1}$) is also employed. It is defined as the relationship between the dynamic viscosity the density of the fluid, Eq. (3.16):

$$\upsilon = \frac{\mu}{\rho} = \frac{\sigma}{\dot{\rho}\dot{\gamma}} \tag{3.16}$$

By definition, all Newtonian fluids have a linear relationship between the shear stress and the shear rate. Fluids that do not exhibit this behaviour are known as non-Newtonian fluids (Steffe, 1996). The apparent viscosity (η) is defined as the shear stress divided by the shear rate, Eq. (3.17).

$$\eta = \frac{\sigma}{\dot{\gamma}} \tag{3.17}$$

for Newtonian fluids, η and μ are the same. For non-Newtonian fluids, that follow the Ostwald-de Waale law, their apparent viscosity is defined by Eq. (3.18):

$$\eta = k\dot{\gamma}^{n-1} \tag{3.18}$$

where η is the apparent viscosity (Pa·s), k the consistency index ($Pa \cdot s^n$) and n the flow index (-).

Non-Newtonian fluids are rheologically complex fluids that exhibit one of the following feature (Shenoy, 1999):

- Shear rate dependent viscosities in certain shear rate ranges with or without the presence of an accompanying elastic solid-like behaviour.

- Yield stress with or without the presence of shear rate dependent viscosities.
- Time-dependent viscosities at fixed shear rates.

In Figure 3.9 various types of non-Newtonian time-independent fluids are compared with Newtonian fluids.

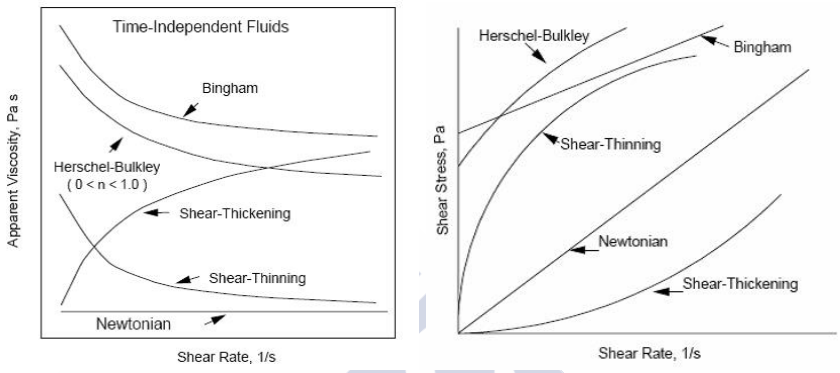

Figure 3.9. Various types of non-Newtonian time-independent fluids (Steffe, 1996).

The shear-thinning or pseudoplastic behaviour is very common in fruit and vegetables as well as melted polymers. During, flow these materials exhibit three different regions, Figure 3.10. At low shear rates the apparent viscosity is constant and is named as zero shear viscosity, η_0. The second region is characterized by a decrease of apparent viscosity with increasing shear rate. In the third region the apparent viscosity is also constant (Newtonian region) as in the first region and is named in this cased infinite shear viscosity, η_∞ (Steffe, 1996).

3.4.3 Viscoelastic behaviour

The word 'viscoelastic' means that the material simultaneously exhibits some of the elastic properties of an ideal solid and some of the flow properties of an ideal liquid. Some authors reserve the word 'viscoelastic' for materials that are more solid-like than liquid-like and use the term 'elastico-viscous' for materials that are more liquid-like than solid-like (Bourne, 2002). A single word 'viscoelastic' will be used in this Thesis.

Figure 3.11 shows schematically the differences between an ideal elastic solid,

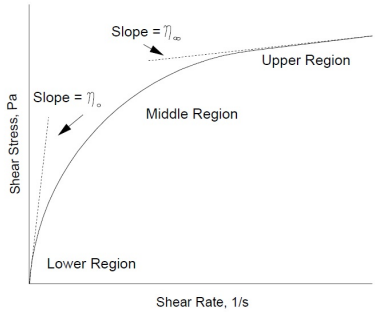

Figure 3.10. Ideal pseudoplastic behaviour (Steffe, 1996).

which is called a Hookean solid after Robert Hooke (1660) who first described elastic deformation, an ideal liquid which is called Newtonian liquid after Isaac Newton (1687) who first described the flow of simple liquids, and a viscoelastic material which combines some of the properties of both. Suppose a uniform block of each of these three materials has a constant stress applied for three time periods and then the stress is removed (Bourne, 2002).

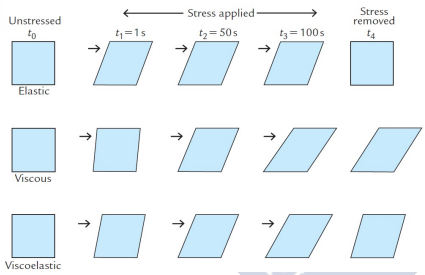

Figure 3.11 Schematic representation of elastic, viscous and viscoelastic responses to the application and removal of a stress. (Bourne, 2002).

- Elastic solid (top line). There is an instantaneous deformation when the deforming force is applied and no further deformation with time. There is complete recovery of the original shape when the force is removed.
- Newtonian liquid (middle line). The material begins to flow as soon as the deforming force is applied and it continues to flow as long as the force is being applied. There is no recovery of shape when the force is removed.
- Viscoelastic solid (bottom line). There is an instantaneous deformation

when the deforming force is first applied, and then the material continues to deform so long as the force is pressing against it. When the force is removed there is some recovery of the original shape (elastic component) but not a full recovery (viscous component).

It can be seen from this figure that the time scale over which the force is applied can seem to affect the relative proportions of elastic deformation and viscous flow. Over a short period of time (t_1) a viscoelastic material will appear to be mostly elastic whereas over a long period of time (t_3) it will seem to be mostly viscous. This demonstrates an important principle in testing of viscoelastic materials: the material will appear to be mostly elastic in nature in an experiment that is performed quickly but in an experiment that is performed slowly it will appear to be more viscous. Since the human testing of foods (squeezing in the hand, chewing with the teeth, manipulating with the tongue) is usually of short duration, many foods that are actually quite viscoelastic will appear to be elastic or close to elastic in sensory tests.

Viscoelastic behaviour can be divided into two general types:

- **Linear viscoelastic** in which the rheological properties are dependent on time alone, and not on the magnitude or rate of application of the stress. Most foods show linear viscoelasticity up to small strains of a few percent.
- **Non-linear viscoelastic** where the mechanical properties are a function of the time the stress is applied, the magnitude of the stress, and often the rate at which the stress is applied. The study of non-linear viscoelasticity is experimentally and theoretically much more difficult than linear viscoelasticity and yet this is the range in which most foods are compressed or sheared in the mouth.

3.4.3.1 Small Amplitude Oscillatory Shear

In oscillatory tests, materials are subjected to deformation (in controlled rate instruments) of stress (in controlled stress instruments) which varies harmonically with time. The test material is usually placed between a cone and plate or parallel plates and the cone or plate is made to oscillate about a central point with a sinusoidal angular velocity at low amplitude while the shear stress is measured, Figure 3.12. This is a non destructive test due the amplitude is small.

Oscillatory tests may be conducted in tension, compression or shear. Several assumptions are necessary in the developing of the mathematical equations in

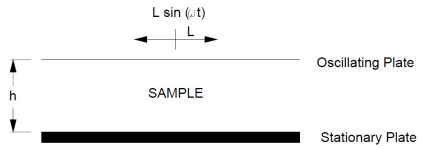

Figure 3.12. Oscillatory shear between parallel plates (Steffe, 1996).

order to describe suitably oscillatory tests: strain is the same at all points in the sample, sample inertia may be neglected and the material behaves as a linear viscoelastic substance (Baltsavias *et al.*, 1997).

In the Figure 3.13 are illustrated the basis of small amplitude tests in parallel plate geometry. Considering that the sample is deformed sinusoidally, within a few cycles the stress, also oscillate sinusoidally at the same frequency. But in general wave stress is shifted by a phase angle, δ with respect to the strain wave.

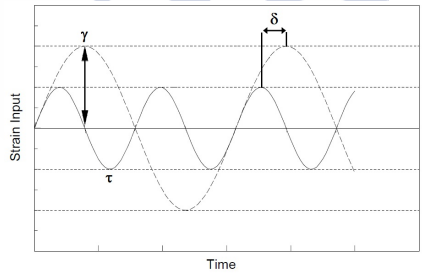

Figure 3.13 Components of the stress wave obtained by sinusoidal oscillating shear strain: γ in phase and τ out of phase with δ.

The oscillatory deformation of the material located between parallel plates is expressed mathematically as follows:

$$\gamma = \gamma_0 sin(\omega t) \tag{3.19}$$

where γ_0 is the amplitude of the strain equal to L/h when the motion of the upper plate is $Lsin(\omega t)$ and ω is the frequency in rad·s^{-1}.

Using the small strain values in order to remain the conditions of linear viscoelasticity range, the following stress is produced by the strain input:

$$\sigma = \sigma_0 sin(\omega t + \delta) \tag{3.20}$$

where σ_0 is the amplitude of stress and δ is the phase lag or phase shift relative to the strain.

The material functions to oscillatory assays of small amplitude are defined on the basis of the response in the shear stress. Expanding the Eq. (3.20) by means of trigonometric functions can be obtained the following expressions:

$$\sigma = \sigma_0(sin\omega t cos\delta + sin\delta cos\omega t) \tag{3.21}$$

$$\sigma = (\sigma_0 cos\delta) sin\omega t + (\sigma_0 sin\delta) cos\omega t \tag{3.22}$$

The Eq. (3.21) includes the material functions obtained by small amplitude tests. It can be noticed that one part of the stress wave is in phase with the fixed deformation (proportional to $sin\omega t$) and the other part of the stress wave is in phase with the fixed strain rate (proportional a $cos\omega t$). In this sense, this observation is in agreement with the definition of viscous and elastic moduli using the Newton's law (Eq. (3.15)) and Hooke's law (Eq. (3.11)), respectively.

For an ideal elastic solid, the shear stress is in phase with the strain and for a Newtonian fluid (ideal viscous liquid) the shear stress is 90° ($pi/2$) out of phase with strain. For a viscoelastic fluid the shear stress lags behind the strain by an angle of difference pi that lies between 0° and 90°. In the Figure 3.14 are clearly illustrated the three types of behaviour.

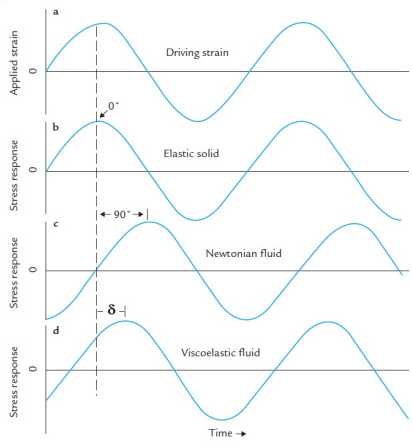

Figure 3.14 Scheme of the fundamentals of oscillatory measurements. (a) applied strain versus time and resultant stress versus time that is measured in (b) a elastic solid, (c) Newtonian liquid and (d) viscoelastic liquid (adapted from Bourne (2002)).

The curve of shear stress against time can be divided in two components or functions which vary with the applied frequency (ω, rad·s^{-1}) (Bourne, 2002):

Stress component in phase with shear strain is defined as the storage or elastic modulus (G$'$, Pa). It is the ratio between shear stress in phase with the strain to the strain.

$$G' = \frac{\sigma'}{\gamma} \tag{3.23}$$

Stress component 90º out of phase with shear strain is defined as the loss or viscous modulus (G", Pa). It is the ratio between shear stress out of phase with the strain to the strain.

$$G'' = \frac{\sigma''}{\gamma} \tag{3.24}$$

The Eqs. (3.23) and (3.24) can be unified in the expression (Eq. (3.25)):

$$\sigma = G'\dot{\gamma} + \frac{G''}{\omega} \tag{3.25}$$

These combination gives rise to several functions depending on the frequency such as the complex modulus (G*, Pa), complex viscosity (η^*, Pa·s), dynamic viscosity (η' Pa·s), out of phase component of the complex viscosity (η'', Pa·s), tangent of the phase shift (tanδ, -)complex compliance (J*, Pa^{-1}), storage compliance (J', Pa^{-1}) and the loss compliance (J", Pa^{-1}):

$$G^* = \frac{\sigma_0}{\gamma_0} = \sqrt{(G')^2 + (G'')^2} \tag{3.26}$$

$$\eta^* = \frac{G^*}{\omega} = \sqrt{(\eta')^2 + (\eta'')^2} \tag{3.27}$$

$$\eta' = \frac{G''}{\omega} \tag{3.28}$$

$$\eta'' = \frac{G'}{\omega} \tag{3.29}$$

$$tan\delta = \frac{G''}{G'} \tag{3.30}$$

$$J^* = \frac{1}{G^*} \tag{3.31}$$

$$J' = \frac{G'}{(G')^2 + (G'')^2} \tag{3.32}$$

$$J'' = \frac{G''}{(G')^2 + (G'')^2} \tag{3.33}$$

Using Eqs. (3.25) and (3.28) can be expressed as Eq. (3.34), which represents clearly the material behaviour by means of its elastic ($G'\gamma$) and viscous nature ($\eta'\gamma$).

$$\sigma = G'\gamma + \eta'\dot{\gamma} \tag{3.34}$$

In qualitative terms, the oscillatory curves give a fingerprint of the state of the microstructure, by identification and quantification of several mechanisms by the position on the frequency axis and the height of the signal. For example, it is possible to obtain η_0 at very low frequencies. This can be used in a number of microstrutural calculations as well as for stability predictions.

3.4.3.2 Mechanical models

Mechanical rheological models consisting of mechanical elements like springs and dashpots can be used to explain and interpret the rheological behaviour of viscoelastic materials.

The spring is considered an ideal solid element obeying Hooke's law (Eq. (3.11), Figure 3.15 (a)). If a force is applied to the spring, it will extend a distance directly proportional to the applied force, with the constant of proportionality (modulus of elasticity) being represented by the spring constant. If the applied force is removed, the spring extension will fully recover . The dashpot is considered an ideal fluid element obeying Newton's law (Eq. (3.15), Figure 3.15 (b)). The application of a constant force to the dashpot, it will extend continuously, representing flow, at a speed directly proportional to the applied force. A greater force will cause it to extend at a faster rate. The constant of proportionality between applied force and extension rate represents the viscosity of a liquid, and is called the viscosity of the viscous element (similar to spring constant for elasticity).

A spring and a dashpot arranged in series (Figure 3.15 (c)) is called a Maxwell element. It is used to simulate stress relaxation in solid materials. This is a time-dependent rheological behaviour characterized by the observation of stress decreasing over time in a sample subjected to a constant applied strain. When a spring and a dashpot are arranged in parallel the result is a Kelvin–Voigt element (Figure 3.15 (d)). It is used to simulate strain retardation (creep) in solid materials. This is also a time-dependent rheological behaviour, but is characterized by the observation of strain increasing over time in a sample subjected to a constant applied stress. Many other models using various combinations of springs, dashpots,

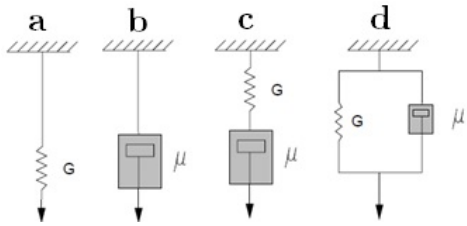

(a)

Figure 3.15 Spring (a), dashpot (b), Maxwell (c) and Kelvin-Voigt (d) mechanical models in viscoelasticity (Steffe, 1996).

Maxwell and Kelvin–Voigt models have been proposed for different foods.

For comparative purposes, both Kelvin and Maxwell model descriptions of creep and stress relaxation behaviour are illustrated side-by-side in Figure 3.16. When a sudden stress is applied to a sample of material and held constant over time, simple creep behaviour is exhibited by the strain beginning to increase rapidly but the rate of increase diminishes over time in the form of an exponential decay. This can be seen in the Kelvin model by noting that the dashpot will control the rate at which the spring can elongate. The initial stress puts target force on the dashpot while the spring is fully recoiled (relaxed).

Thus, the dashpot will begin to move at target speed, allowing the spring to extend along with it. In so doing, the spring begins to take on its share of the applied constant stress with the dashpot being relieved of its share of force. As the force on the dashpot diminishes while being taken up by the spring, the speed of the dashpot likewise diminishes. Thus the rate of strain is retarding exponentially (strain retardation), and is called creep.

Again the period of observation time is important. Application of the Kelvin-Voigt and Maxwell models to creep and stress relaxation will be discussed more extensively in the following section (Section 3.4.3.3).

3.4.3.3 Creep and Recovery

In a creep and recovery test, an stress is applied to a sample and subsequently the change in strain during a period of time is analysed. When the effort is withdrawn, it can be observed as the sample tries to return to the initial form. These types of tests can be useful for studying the behaviour of systems undergoing constant stress such as flour doughs during kneading. This stress can be conducted

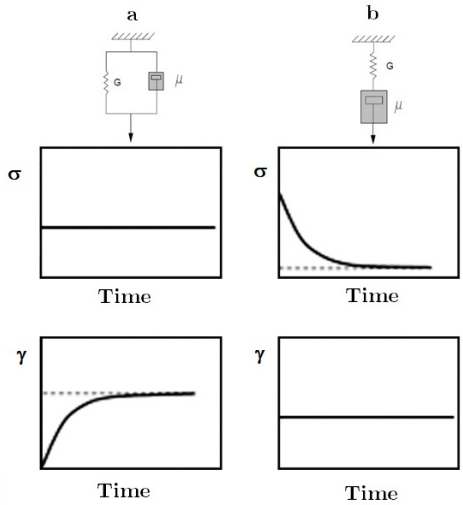

(a)

Figure 3.16 Kelvin (a) and Maxwell (c) mechanical models showing creep and stress relaxation.

in uniaxial tension or compression. Figure 3.17 shows ideal curves of creep and recovery tests.

Mechanical rheological models provide an useful mean of creep data. These data may also be presented in terms of various compliance and modulus distribution functions. In addition, creep curves can be normalized and presented in linear form (Barnes *et al.*, 1993). Creep data may be described in terms of creep compliance function:

$$J = f(t)\frac{\gamma}{\sigma_{constant}} \tag{3.35}$$

Compliance curves generated at different stress levels overlap when data are collected in the range of linear viscoelastic behaviour. With a perfectly elastic solid, $J = 1/G(t)$, the reciprocal of the shear modulus; however, different time patterns in experimental testing mean that $J(t) \neq 1/G(t)$.

To develop a mechanical model describing creep behaviour, the starting point is the Kelving model. When this system is subjected to shear strain, the spring and dashpot are strained equally:

$$\gamma = \gamma_{spring} = \gamma_{dahspot} \tag{3.36}$$

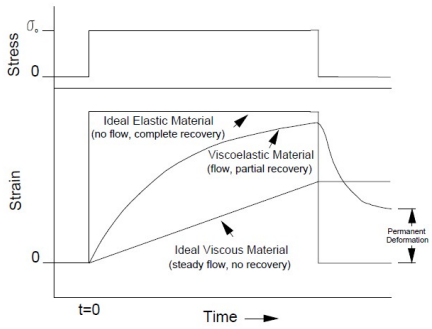

Figure 3.17. Idealized creep and recovery curve (Steffe, 1996).

The total shear stress (σ) caused by the deformation is the sum of the individual shear stress which, using Eqs. (3.15) and (3.11), can be expressed as Eq. (3.34). Differentiating this equation with respect to time yields:

$$\frac{1}{G}\frac{d\sigma}{dt} = \dot{\gamma} + \delta\frac{d\dot{\gamma}}{dt} \tag{3.37}$$

where the retardation time ($\delta = \eta/G$) is unique for any substance. If a material is a Hookean solid, the retardation time would be zero and the target strain would be obtained immediately with the application of stress. Time to achieve target strain in viscoelastic materials is delayed (or retarded).

In creep, where the material is allowed to flow after being subjected to a constant shear stress (σ_0), the variation in stress with time is zero ($d\sigma/dt = 0$) and the solution to Eq. (3.37) is:

$$\gamma = f(t) = \frac{\sigma_0}{G}\dot{(}1 - exp(\frac{-t}{\lambda}) \tag{3.38}$$

Showing that the initial strain is zero (γ=0 at t=0). Eq. (3.38) predicts a strain that asymptotically approaches the target strain (σ_0/G) associated with the spring. δ is the time taken for the delayed strain to reach approximately 63.2% (1-1/e) of the final value. Materials with a large retardation time reach full deformation slowly.

The Kelvin model shows excellent elastic retardation but is not general enough to model creep in many materials. The solution to this problem is to use a Burgers model (Burgers, 1935) (Figure 3.18) which is a Kelvin and a Maxwell model placed in series. Data following this mechanical analogy show an initial elastic response

due to the free spring retarded elastic behaviour related to the parallel spring-dashpot combination, and Newtonian type flow after long periods of time due to the free dashpot (Figure 3.19):

$$\gamma = f(t) = \frac{\sigma_0}{G}\frac{\sigma_0}{G_m}(1 - exp(\frac{-t}{\lambda})) + \frac{\sigma_0 t}{\eta_0} \tag{3.39}$$

where $\lambda = \eta_m/G_m$ is the retardation time of the Kelvin portion of the model.

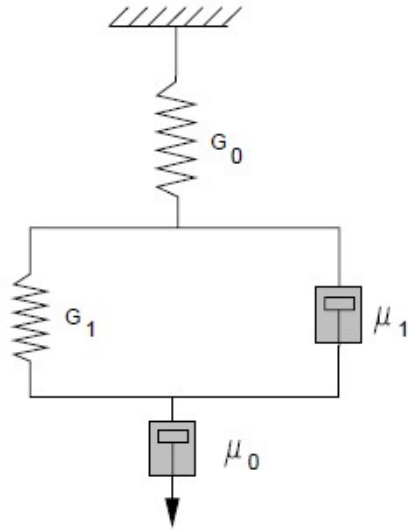

Figure 3.18. Four elements of Burgers model (Steffe, 1996).

The Burgers model can also be expressed in terms of creep compliance by dividing Eq. (3.40) by the constant stress:

$$\frac{\gamma}{\sigma_0} = f(t) = \frac{\sigma_0}{G_0}\frac{1}{G_m}(1 - exp(\frac{-t}{\lambda})) + \frac{t}{\eta_0} \tag{3.40}$$

Writing the result as a creep compliance function (Eq. (3.41)) yields:

$$J(t) = J_0 + J_m(1 - exp(\frac{-t}{\lambda})) + \frac{t}{\eta_0} \tag{3.41}$$

where J_0 is the instantenous compliance, J_m is the retarded compliance, λ is the retardation time (η_m/G_m) of the Kelvin component, and η_0 is the Newtonian

viscosity of the free dashpot. The sum of J_0 and J_m is called the steady state compliance.

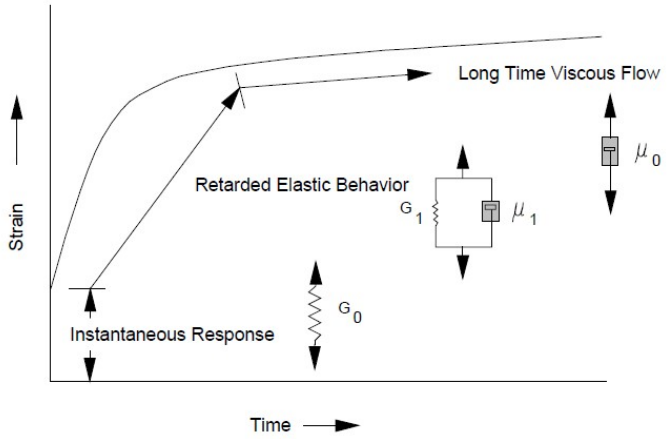

Figure 3.19. Typical creep curve showing the Burgers model elements (Steffe, 1996).

When conducting creep experiments, controlled stress rheometers allow the measure of the strain recovered when the constant stress is removed. The complete creep and recovery curve may be expressed using the Burgers model (Figure 3.18). When calculated as compliance, the creep is given by Eq. (3.41) for $0 < t < t_m$, where t_m is the time when constant stress is removed. At the beginning of creep, there is an instantaneous change in compliance (J_0) due to the spring in the Maxwell portion of the model (Figure 3.20). Then, the Kelvin component produces an exponential change in compliance related to the retardation time. After sufficient time, the independent dashpot 3.18 generates a purely viscous response. Data from the linear portion of the creep curve (Figure 3.20) are related to two parameters the slope is equal to $(1/\eta_0)$ and the intercept, sometimes called the steady state compliance, is equal to $J_0 + J_r$.

At $t = t_m$ the stress is removed ($\sigma = 0$) and there is an instantaneous change in compliance equal to J_0. The free dashpot causes permanent deformation in the material related to a compliance of (t_m/η_0). This factor is directly related to the non-recoverable sample strain of (t_m/η_0). If a substance obeying the Burgers model is tested in the linear viscoelastic region of material behaviour, then the values of J_0 and J_m determined from the creep curve will be equal to those values determined from recovery curve. Writing the result as a 3.20 (Eq. (3.42)) yields:

$$J(t) = J_{max} - J_0 - J_m(1 - exp(\frac{-t}{\lambda})) \tag{3.42}$$

where J_0 is the instantaneous compliance, J_m is the viscoelastic compliance, λ (s) is mean retardation time, t (s) is the pahse time and J_{max} (Pa^{-1}) is the target creep compliance of the recovery phase.

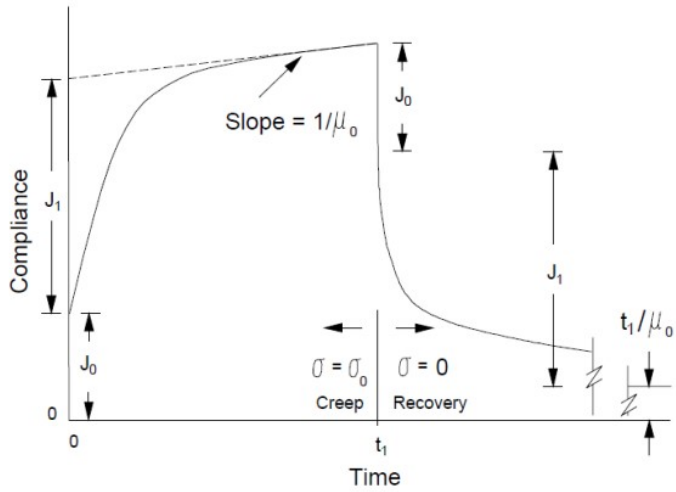

Figure 3.20 Compliance and recovery curves showing compliance parameters for the Burgers model (Steffe, 1996).

3.4.4 Extensional viscosity

A basic knowledge of extensional viscosity is essential for understanding many flow situations found in the food industry. The three basis types of extensional flow are uniaxial, biaxial and planar. One of the most employed experimental methods to determine extensional viscosity is the lubricated squeezing flow (flow between parallel plates being pushed together) due to the relative ease with which this experiment can be conducted in a laboratory.

Squeezing flow between parallel plates can be achieved in many food rheology laboratories. When this deformation is execute between lubricated plates, biaxial extensional flow is achieved and extensional viscosity can be calculated (Steffe, 1996). Figure 3.21 shows the typical configuration of this experiment.

Taking into account the configuration of the experiment, Figure 3.21, the

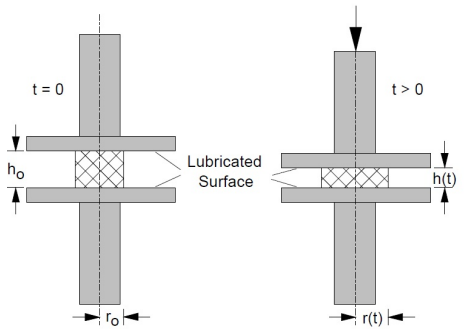

Figure 3.21 Flow between lubricated parallel plates to create sample deformation in biaxial extension (Steffe, 1996).

Hencky strain of the sample is given by:

$$\varepsilon_H = -ln\frac{h(t)}{h_0} \tag{3.43}$$

where h_0 is the intial sample thickness and $h(t)$ the thickness at time t. The biaxial (Hencky) strain ε_b of sample can be then calculated:

$$\varepsilon_b = -\frac{1}{2}ln\frac{h(t)}{h_0} = -\frac{1}{2}ln\frac{V/4\pi r^2}{V/4\pi r_0^2} = -\frac{1}{2}ln\frac{r_0^2}{r^2} = ln\frac{r}{r_0} \tag{3.44}$$

where V is the volume of the sample, r is the radius at time t, and r_0 the initial radius.

Once the biaxial (Hencky) strain ε_b is calculated, it can be related to the time in order to calculate the strain rate, $\dot{\varepsilon_b}$ (s^{-1}). Then $\dot{\varepsilon_b}$ can be related to the stress applied by the plates to compress the sample, calculated as the ratio between the force applied and the surface of the plate, in order to obtain the bi-extensional viscosity, η_e (Pa·s). The variations of η_e with $\dot{\varepsilon_b}$ at constant ε_b, can then be fitted by the Ostwald-de Waele Model, Eq. (3.45):

$$\eta_e = k\dot{\varepsilon_b}^{n-1} \tag{3.45}$$

where k (Pa·s^n) is the consistency index and n (-) the flow behaviour index.

3.5 Temperature behaviour

In this section, the study of the thermal transitions of starch during heating or cooling is provided as well as the use of thermal methods as a suitable tool to characterize the gelatinization and retrogradation of starch. The determination of these properties in flour doughs contribute to a basic understanding of the baking process and their importance in the final baked product.

Although the starch dominates the composition of the most of flour dough, there are other components present that can be expected to exhibit thermal transitions. As described later, several transitions related to starch are possible to analyse using thermal methods, whereas for the other flour components thermal methods give much less information due to the lack of thermal transitions during conditions corresponding to baking.

3.5.1 Gelatinization and Pasting

Gelatinization of starch is responsible for its change properties during the preparation and processing of flour doughs. The following definition was proposed for gelatinization (Atwell *et al.*, 1988):

> Starch gelatinization is the collapse (disruption) of the starch granule manifested in irreversible changes in properties such as granular swelling, native crystallite melting, loss of birefringence, and starch solubilisation. The point of initial gelatinization and the range over which it occurs is governed by starch concentration, method of observation, granular type, and heterogeneity within the granule population under observation.

Similarly, pasting had this proposed definition:

> Pasting is the phenomenon following gelatinization in the dissolution of starch. It involves granular swelling, exudation of molecular components from the granule, and, eventually, total disruption of the granules.

Although the terms gelatinization and pasting have often been applied to all changes that occur when starch is heated in water, gelatinization includes the early changes, according to the proposed definitions, and pasting includes later changes (Kaletunc & Breslauer, 2003).

When the starch granule is heated up to gelatinization temperature in excess water, heat transfer and moisture transfer phenomena occur. The granule swells to several times its initial size as a result of loss of the crystalline order and the absorption of water inside the granular structure.

The swelling behaviour of starches is primarily a property of their amylopectin content, and amylose acts as both a diluent and an inhibitor of swelling, especially in the presence of lipid (Tester & Morrison, 1990). Maximal swelling is also related to the molecular weight and shape of the amylopectin (Tester & Morrison, 1990). Pasting parameters have been used by many researchers for the characterization of native starches from different botanical sources and compared the impacts of other ingredients, including sugars, salts, and lipids (Ai & Jane, 2015).

Starch gelatinization can be studied by measuring the change in viscosity during the application of heat, and several instruments (viscoamylograph, RVA, rheometer or Mixolab®) can be employed for such measurements. Recently, rheometer and differential scanning calorimetry (DSC) are widely used for studying starch gelatinization. Particularly, the samples subjected to a temperature sweep during rheometrical experiments to allow the simulation of some of the changes that take place during baking of flour doughs. Gelatinization involves a range of events with somewhat different onset temperatures, and in the DSC only part of all the aspects of gelatinization is measured. So, a combination of different techniques could be a good option in order to characterize the thermal behaviour of starches (Eliasson, 2004). As example of the modification that can occur during the starch gelatinization process the Figure 3.22 is exposed. More detailed information about DSC assays is below developed (Section 3.5.3).

There is usually a difference in the gelatinization temperature range between the starch and flour, in that T_0 and T_f are shifted toward higher or lower temperatures in the flour suspension compared to the starch-water suspension depending on the type of flour (Eliasson, 2004). The difference in can be around 5°C for the case of wheat flours. This means that components present in the flour will affect starch gelatinization.

3.5.2 Retrogradation

Under low energy input, as in cooling and freezing, further hydrogen bonding may occur, resulting in further tightening of structure with loss of water-holding capacity, known as retrogradation. Starch retrogradation is a process which occurs when the molecules comprising gelatinized starch begin to reassociate in

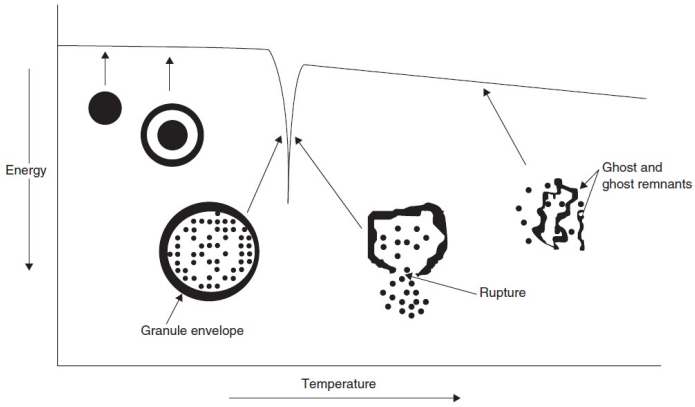

Figure 3.22 Representation of the molecular events of gelatinisation coincident with a hypothetical DSC heating curve (Williams, 2007).

an ordered structure. In its initial phases, two or more starch chains may form a simple juncture point that may then develop into more extensively ordered regions. Ultimately, under favourable conditions, a crystalline order appears (Atwell *et al.*, 1988).

It is generally accepted that retrogradation is involved in the staling of baked products such as bread (Edwards, 2007). Amylose has been thought to impart stiffness to food systems, especially after retrogradation. Amylose was reported to be the main factor in short-term (several hours) development of the starch gel structure, while amylopectin was correlated with long-term (several days or weeks) development of the starch gel structure (Orford *et al.*, 1987). It is believed that amylopectin does not substantially associate or retrograde upon standing because the outer branches are sufficiently long enough and therefore waxy starch pastes are nongelling (Pomeranz, 1991) or form very weak gels. However, a role for amylopectin in retrogradation had been reported. The short amylopectin side-chains undergo a shift from coil to a helix transition (Winter & Kwak, 1987). These changes were due to a slow association of the double helices and were studied for potato and wheat starch by transmission electron microscopy, DSC, and rheology (Keetels *et al.*, 1996). Ring *et al.* (1987) demonstrated that amylopectin staling within the gelatinized granule is the cause of increased firmness of the starch gel during storage. Varietal differences in rate and extent of amylopectin staling may help explain the variation in texture during storage of heat processed rice products (Perez *et al.*, 1993).

3.5.3 Thermodynamic Analysis by Differential Scanning Calorimetry

Differential scanning calorimetry (DSC) is a thermal analysis technique that detects and monitors thermally induced conformational transitions and phase transitions as a function of temperature. A pair of sample pans, one containing the sample and other serving as reference, is heated in tandem. As a dough is heated, its temperature increases, depending on the heat capacity of the content of the dough. At temperatures where an endothermic transition occurs, the thermal energy supplied to the dough is consumed by that transition and the temperature of the sample cell lags behind the reference cell temperature. Conversely, the reference cell temperature lags when an exothermic transition occurs in the sample. A temperature difference between the cells results in heat flow between the cells. DSC measures the differential heat flow between the sample and reference crucibles as a function of temperature at a fixed heating rate. DSC thermograms are normalized to yield the specific heat capacity (C_p) as a function of temperature Kaletunc & Breslauer (2003).

Differential scanning calorimetry (DSC) is used to detect and define those temperatures that correspond to significant thermally induced transformations (glass, melting, and gelatinization transitions), over temperature and moisture content ranges. The basis for thermodynamic study of starches is that the relevant initial and final states can be defined and the energetic and/or structural differences between these states can be measured using calorimetric instrumentation. The temperatures for the endothermic or exothermic transitions and the heat involved in such transitions can be measured in DSC experiments. The transition temperatures (T_p) are points of target heat capacity of endotherms or minimum heat capacity of exotherms. From a DSC thermogram, heat capacity (C_p) *vs* temperature curve, one can extract values for the thermal (temperature of transition) and thermodynamic changes in free energy (ΔG), enthalpy (ΔH), entropy (ΔS), and heat capacity (ΔC_p) of the various transitions, in addition to determination of the bulk heat capacity of the material. A typical DSC thermogram, displaying initial (T_0) and final (T_f) gelatinization temperatures (°C), T_p (°C), ΔC_p (J/Kg °C) and ΔH (J/g starch) is given in Figure 3.23. The transition enthalpy, ΔH, is calculated from the area below the transition endotherm.

The enthalpy change of a transition, at any temperature T, is extracted using:

$$\Delta H = \Delta H_{T_0} + \int_{T_0}^{T} \Delta C_p dT \tag{3.46}$$

where T_0 is the midpoint of the transition and ΔC_p is the difference in heat

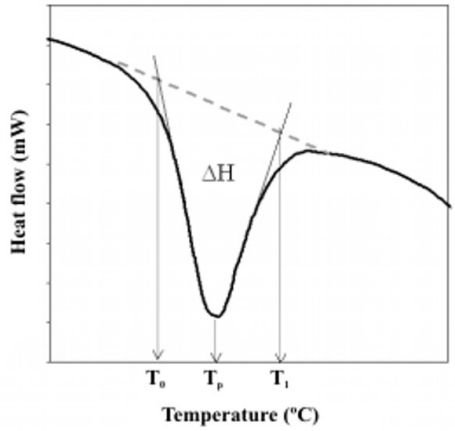

Figure 3.23 Typical DSC curve with the main interesting parameters to the thermodynamic characterization.

capacity between the pre- and post-transition material.

A similar analysis is employed to extract the entropy change (ΔS) for the transition:

$$\Delta S = \frac{\Delta H}{T_0} + \int_{T_0}^{T} \frac{\Delta C_p}{T} dT \tag{3.47}$$

The free energy change is obtained from the relation: A similar analysis is employed to extract the entropy change (ΔS) for the transition:

$$\Delta G = \Delta H - T\Delta S \tag{3.48}$$

Taken together these data provide a complete thermodynamic characterization of the material. The advantages of the calorimetric approach to studying thermodynamics are that direct measurements are made of ΔH and ΔC_p, the data collection and analysis are not specific to particular materials, and the materials require neither destructive nor elaborate sample preparation before analysis.

3.5.3.1 Thermal transitions of doughs determined by DSC

Dough heating causes structural changes in the starch granules during gelatinization (Orlowska & Randzio, 2010). Nowadays, the DSC is seen as one of the most suitable methods to observe changes in starch during gelatinization (Campanha & Franco, 2011).

When the starch is heated in excess of water, a transition endotherm, called G, is usually found at low temperatures. When the amount of free water decreases, another transition usually appears (M1) as a shoulder overlapped with the G endother. When the water content is further reduced, the first peak (G) disappears and it is only possible to observe peak M1 at a higher temperatures. There are several models to explain the nature of the transitions G and M1 in the absence of water (Tananuwong & Reid, 2004). In the first model (Donovan, 1979), the G transition is considered to be induced by the swelling of the amorphous regions of the starch granules. This swelling process removes the amorphous component from the surface of the crystals. The remaining crystals after the dissolution of the amorphous region are subsequently melted at higher temperatures, which causes the M1 transition. The second model (Evans & Haisman, 1982) suggests that peak G represents the fusion of the least perfect crystals (less stable), while peak M1 represents the fusion of the most perfect (most stable). The third model (Slade & Levine, 1988) suggests that the peak G first reflects the plasticity of the amorphous region, while peak M1 reflects the fusion in non-equilibrium of the amylopectin crystals.

At higher temperatures, another transition (M2) is observed related to amylose-lipid interactions (Svensson & Eliasson, 1995). Finally, according to the results shown by Liu *et al.* (2006), there may be a fourth peak called M3 corresponding to the amylose fusion, although said peak was only observed for samples with more than 80% amylose.

As discussed above, there are numerous studies of the effect of the temperature on the starch granules through DSC. These studies were conducted in a temperature range of 110-200°C. However, studies where the influence of temperature was studied by means of reometry (DMTA), the maximum study temperature was 100-110°C while studies of the phenomena that occur in doughs at higher temperatures were not found in the bibliography which signifies an interesting challenge to face with the objective of making a comparison between the results obtained and a verification of whether the observed phenomena coincide.

USC
UNIVERSIDADE
DE SANTIAGO
DE COMPOSTELA

Chapter 4

Experimental

This chapter presents the employed materials, equipment and experimental techniques classified as function of the different experimental procedures employed to carry out the experimentation. Firstly, it is exposed a detailed description of the employed materials and subsequently, the corresponding experimental conditions and the main equipment used for each procedure. Finally, the statistical analysis of the experimental data obtained is described.

4.1 Water Sorption Isotherms

4.1.1 Materials

The materials employed for the water sorption isotherms determination were fresh and dried brown seaweeds *Bifurcaria bifurcata*(BB), *Fucus vesiculosus* (FV) and *Ascophyllum nodosum* (AN). Fresh BB seaweeds (82.7 ± 1.2 g water·(100 g wet solid)$^{-1}$), w.s.) were purchased from a local fishermen's association of the Northwest of Spain (Corcubión, A Coruña) in October and November of 2013. Fresh FV seaweeds (84.4 ± 2.9 w.s.) were collected in the Northwest coast of Spain (Noia, A Coruña, geographical coordinates 42.782255 N, -8.929705 W) in October and November of 2014. Fresh AN seaweeds (79.38 ± 2.70 w.s.) were purchased from the seaweeds canning Mar de Ardora of the Northwest of Spain (Ortigueira, A Coruña) in November and December of 2015.

The other materials employed for the water sorption isotherms determination were: LiCl, $MgCl_2$, $Mg(NO_3)_2$, NH_4NO_3, NaCl, KCl, $BaCl_2$, thymol (analytical grade, Panreac, Barcelona, Spain) and distilled water.

4.1.2 Experimental Conditions and Equipment

All fresh brown seaweed samples were carefully washed with tap water to remove sand, epiphytes and bugs and selected according to their size and colour. Then they were employed for experimentation or stored (during a maximum of 1 week) at 5°C until further processing. They were employed for water desorption (fresh seaweeds) and adsorption (dried seaweeds) experiments.

Dried seaweeds were obtained after drying in an oven at 40°C until to achieve constant weight (≈12 h). Seaweeds were cut using a thin blade to shorten the time to reach the equilibrium, *Bifurcaria bifurcata* were cut into small cylinders (5.0 mm length and 1.5–2.0 mm diameter) and *Fucus vesiculosus* and *Ascophyllum nodosum* were cut into small slabs (5.0 mm length and 1.5-2.0 mm width).

The equilibrium moisture content of seaweed (X_{eq}) for water sorption isotherms of seaweeds were determined by a static gravimetric method. Saturated salt solutions prepared according to recommendations (Greenspan, 1977), were used to hold constant water activity (a_w) values, Figure 4.1.

These saturated solutions give a range of a_w from 0.10 to 0.93 in the range of tested temperatures (5, 25, 45, and 65°C) (Labuza *et al.*, 1985). Triplicate samples (≈0.6 ± 0.1 g for desorption and ≈0.2 ± 0.1 g for adsorption experiments) were

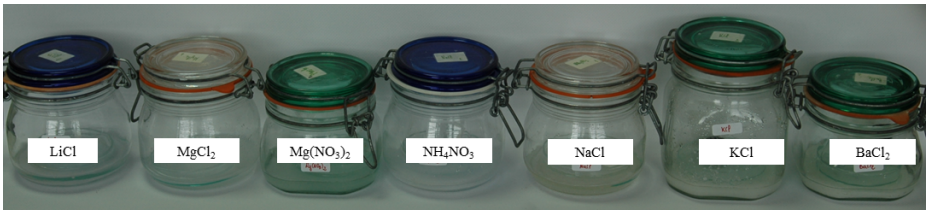

Figure 4.1. Saturated salt solutions.

placed on Petri dishes inside the jars at constant relative humidity atmosphere and were periodically weighed until to reach constant weight (±0.0005 g) in an analytical balance (Denver Instrument, model SI-234, USA, accuracy ± 0.0001 g), Figure 4.2.

At $a_w > 0.5$, small amounts of crystalline thymol were placed into the jar in order to avoid microbial spoilage of samples. Around 14 weeks were necessary to achieve the equilibrium.

Dry solid was determined by weighing after vacuum drying using an oven (Heraeus Vacutherm, model VT 6025, Germany), Figure 4.2, at 70°C and 15 kPa (AOAC, 1995).

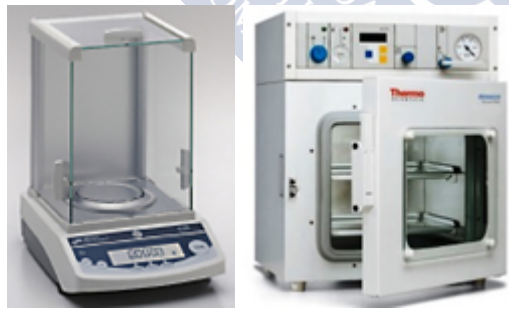

(a) (b)

Figure 4.2 Analytical balance SI-234 (Denver Instrument, Germany) (a) and Vacuum oven Vacutherm VT650 (Heraeus Hanau, Germany) (b).

4.1.3 Data Treatment

The employed models to fit water sorption experimental data (equilibrium moisture content, X_{eq}, and water activity, a_w) were those proposed by Brunauer-Emmett-Teller (BET, $a_w < 0.5$) (Brunauer *et al.*, 1940), Eq. (3.2) and Halsey (Halsey, 1948), Eq. (3.6).

$$X_{eq} = \frac{X_m C a_w}{(1-a_w)(1+(C-1)a_w)}$$

$$X_{eq} = \left(\frac{-A}{Tln(a_w)}\right)^{(1/B)}$$

where T is the temperature (K), X_m the monolayer moisture content (kg water·(kg dried solid)$^{-1}$, d.b.) and C (dimensionless, -) parameters of BET equation and A ((kg water·K)·(kg dried solid)$^{-1}$) and B (-) parameters of Halsey equation.

The net isosteric heat of sorption (ΔH_s, kJ·mol^{-1}) is the difference of total heat of sorption (ΔH_d, kJ·mol^{-1}) in the sample and the heat of vaporization of water (ΔH_{vap}, kJ·mol^{-1}) associated with the sorption process and can be calculated using Clausius-Clapeyron equation, Eq. (4.1), (Tsami, 1991), where ΔH_s is associated with sorbed molecules at a particular moisture content (X). Plotting the $ln(a_w)$ *vs* T^{-1}, ΔH_s was obtained by the slope of the resulted straight line.

$$\Delta H_s = -R\left[\frac{dln(a_w)}{d(1/T)}\right]_{X_{eq}} \tag{4.1}$$

with R (8.314 J·mol^{-1}·K^{-1}) as the ideal gas constant.

The fit of data of ΔH_s and X_{eq} were carried out using an empirical exponential model proposed by Tsami (Tsami, 1991), Eq. (4.2).

$$\Delta H_s = \Delta H_0 e^{\frac{-X_{eq}}{X_0}} \tag{4.2}$$

where ΔH_0 is the net isosteric heat of sorption (kJ·mol^{-1}) of the first molecule of water in the sample and X_0 is a characteristic moisture content of the food material (d.b.), at which this net isosteric heat of sorption was reduced by 63%.

The differential entropy, ΔS_d, as change in molar differential entropy, was determined at constant moisture content as follows, Eq. (4.3) McMinn & Magee (2003):

$$ln(a_w)|_X = \frac{\Delta H_s}{RT} - \frac{\Delta S_d}{R} \tag{4.3}$$

Leffer & Grunwald (1963) proposed the enthalpy-entropy compensation theory (called as isokinetic relationship) to evaluate physical and chemical phenomena that prevail in the sorption processes. This theory proposes a linear relationship between ΔH_d and ΔS_d, Eq. (4.4).

$$\Delta H_d = T_I \Delta S_d + \alpha \tag{4.4}$$

where T_I is the isokinetic temperature, representing the temperature at which all reactions in the sorption series proceed at the same rate, and α parameter may be neglected due to its negligible contribution to the enthalpy change.

Krug *et al.* (1976) recommended a test for the compensation theory which establishes that this theory can only be applied if the isokinetic temperature (T_I) is different of the harmonic temperature (T_{hm}, Eq. (4.5)).

$$T_{hm} = \frac{n}{\sum_{i=1}^{n} \frac{1}{T}} \tag{4.5}$$

where n is the number of isotherms. If $T_I > T_{hm}$ the process is enthalpy driven, while in the opposite condition, the process is entropy controlled.

The net integral enthalpy, or net equilibrium heat of sorption, ΔH_{eq} (kJ·mol^{-1}), can be calculated in a similar manner to the differential heat of sorption, but at a given spreading pressure, θ (J·m^{-2}), instead of constant moisture content (Rizvi, 1986). In the range of water activities tested, the spreading pressure was estimated using an analytical procedure as function of the isotherm model that best fits equilibrium data. Following the procedure described by Iglesias *et al.* (1976) for Halsey model, θ was estimated using Eq. (4.6), that needs Halsey parameters A and B^{-1} (Eq. (3.6)),

$$\theta = \frac{K_B T}{A_m} A^{1/B} \left[\frac{1}{(\frac{1}{B} - 1)(-ln(a_w))^{\frac{1}{B}-1}} \right]_{a_{w_i}}^{a_{w_f}} \tag{4.6}$$

with K_B ($1.38 \cdot 10^{-23}$ J·K^{-1}) as the Boltzmann constant and A_m as the area of a water molecule ($1.06 \cdot 10^{-19}$ m^2).

Net equilibrium heat of sorption (ΔH_{eq}) was calculated using Eq. (4.7). At a particular spreading pressure value (θ), plotting the $ln(a_w)$ *vs* T^{-1}, a straight line is obtained from whose slope ΔH_{eq} can be calculated.

$$\Delta H_{eq} = -R \left[\frac{d(ln(a_w))}{d(1/T)} \right]_{\theta} \tag{4.7}$$

Finally, net integral entropy was also calculated using Eq. (4.8) (Mazza & Le Magger, 1978).

$$\Delta S_{eq} = \frac{-\Delta H_{eq}}{T} - Rln(a_w) \tag{4.8}$$

where a_w is the water activity obtained at constant spreading pressure at different temperatures.

4.2 Drying Assays

4.2.1 Materials

The systems employed for drying experiments were fresh chestnut fruits *Castanea sativa* (1.29 ± 0.13 d.b.) and fresh brown seaweeds selected on the basis of having similar sizes *Bifurcaria bifurcata* (4.59 ± 0.28 d.b.), 100-150 mm length and 1.5–2.0 mm diameter), *Fucus vesiculosus* (5.68 ± 1.20 d.b., length: 150 mm, width: 30 mm) and *Ascophyllum nodosum* (3.59 ± 0.54 d.b., length: 150 mm, width: 30 mm).

4.2.2 Experimental Conditions and Equipment

Chestnut fruits were dried in a hot air convective dryer (Angelantoni, Challenge 250, Italy), Figure 4.3 (a), maintaining constant the temperature (45°C), the relative humidity (30%) and the air velocity (2 $m \cdot s^{-1}$). Previously to drying, chestnuts were manually peeled and cut in small pieces (3-4 mm edge cubes) using a blender (Waring Blender HGBTWT, USA), Figure 4.3 (b). Then they were placed in a metallic mesh with a load density of 6.3 ± 0.1 $kg \cdot m^{-2}$ and dried until a sample moisture content of 0.13-0.16 d.b. was achieved.

(a) (b)

Figure 4.3 Air convective dryer Challenge 250 (Angelantoni Industries, Italy) (a) and Laboratory blender (Waring HGBTWT, USA) (b).

Drying experiments of seaweeds were carried out in the same dryer, Figure 4.3, at four air temperatures (35, 50, 60 and 75°C). Relative humidity (30%) and air velocity (2 $m \cdot s^{-1}$) remained constant in all experiments. Seaweed samples of each specie were selected with similar sizes arranged in a metallic mesh (45x45 cm^2) allowing a transversal air flow to carry out drying experiments. Two different configurations were applied in drying experiments of seaweeds, deep-bed configuration (load density of 14.9 ± 0.1 $kg \cdot m^{-2}$) and thin layer configuration, that involved the use minimum amount of seaweed to cover the drier tray (load density of 2.04 ± 0.02 $kg \cdot m^{-2}$ for *Bifurcaria bifurcata*, 1.25 ± 0.10 $kg \cdot m^{-2}$ for *Fucus vesiculosus* and 2.43 ± 0.02 $kg \cdot m^{-2}$ for *Ascophyllum nodosum*). Additionally, experiments with intermediate load densities (5 and 10 $kg \cdot m^{-2}$) were performed at 35°C for *Ascophyllum nodosum* seaweed.

Samples were weighed using a balance (Cobos D-6000-CS, ± 0.1 g, Spain), every few minutes in the first stages of drying and every hour towards the end. All experiments were performed, at least in triplicate, until moisture content was close to equilibrium.

At the end of drying step 13 different dried products have been obtained: dried chestnut (CT) and brown seaweeds dried at different temperatures (35, 50, 60 and 75°C) *Bifurcaria bifurcata* (BB35, BB50, BB60 and BB75), *Fucus vesiculosus* (FV35, FV50, FV60 and FV75) and *Ascophyllum nodosum* (AN35, AN50, AN60 and AN75).

Ascophyllum nodosum was also freeze dried during 24 h in a Telstar LyoQuest lyophilizer -55 (Telstar Technologies, Spain), Figure 4.4, at -55°C and 0.5 Pa.

Figure 4.4. Telstar LyoQuest lyophilizer -55, Telstar Technologies, Spain.

4.2.3 Data Treatment

Data of moisture content at different drying times for deep-bed configuration and thin layer configuration were modelled by Eq. (4.9), (Page, 1949):

$$MR = e^{-kt^n} \tag{4.9}$$

where k (min^{-n}) and n (-) are the model parameters. The dimensionless moisture content or moisture ratio, MR (-), was calculated by Eq. (4.10):

$$MR = \frac{X_t - X_{eq}}{X_0 - X_{eq}} \tag{4.10}$$

where X_t is the moisture content (d.b.) at any drying time, X_0 is the initial moisture content (d.b.) and X_{eq} is the equilibrium moisture content of the sample (d.b.) evaluated from water desorption experiments previously obtained, Section 4.1.

Sample surface area and shrinkage determination

Sample surface area and shrinkage of the different seaweed were estimated following the same procedure. Seaweed samples (0.5-1.5 g) at different drying times were immersed in a probe filled with n-heptane at room temperature (21±1°C). The initial volume (V_0, m^3) of the samples and those corresponding to the samples dried at different times (V),were measured applying Archimedes' principle and a volumetric shrinkage with seaweed moisture content (V/V_0 *vs* X) relationship was obtained. External surface area of the seaweed monolayer during drying was estimated by means of the assumption of a cylindrical geometry of the seaweed considering that the tray surface is fully covered initially. For this purpose, the average initial radius of fresh seaweed branches (r_0 of 4.0±0.3 10^{-3} for *Ascophyllum nodosum* and *Fucus vesiculosus* and 2.3±0.3 10^{-3} for *Bifurcaria bifurcata*) was determined. It was assumed that volume shrinkage was mainly governed by radius decrease ($L/r_0 > 100$) and Eq. (4.11) was obtained:

$$\frac{V}{V_0} = \frac{\pi r_X^2 L}{\pi r_0^2 L} \Rightarrow r_X = \sqrt{\frac{V r_0^2}{V_0}} \tag{4.11}$$

where L (m) is the length, r_0 and r_X (m) the initial and the corresponding radius of seaweed at different moisture content. The surface area ratio of seaweeds monolayer can be calculated by Eq. (4.12):

$$\frac{S_X}{S_0} = \frac{2\pi r_X L N_s}{2\pi r_0 L N_s} = \frac{r_X}{r_0} \tag{4.12}$$

where S_X (m^2) is the surface area of seaweed monolayer at each moisture content, S_0 the initial surface area of the monolayer and N_s is the number of seaweed samples that can be placed in the monolayer ($L/(2r_0)$). Employing the Eq (4.11), the relationship between surface area of seaweed monolayer and volumetric seaweed shrinkage resulted on Eq. (4.13):

$$\frac{S_X}{S_0} = \sqrt{\frac{V}{V_0}} \tag{4.13}$$

The determination of surface area of the both seaweeds monolayers allowed the specific drying rate, w_s (kg water kg d.b.$^{-1}$ m^{-2} min^{-1}) evaluation by means of Eq. (4.14):

$$w_s = \frac{1}{S_X}\frac{X_{t_{n-1}} - X_{t_n}}{t_n - t_{n-1}} \tag{4.14}$$

The plotting of w_s *vs* X allowed the determination of the critical moisture content (X_c, d.b.) at different tested temperatures which defines the end of the constant drying rate period and the beginning of the falling drying rate period.

Constant drying rate period modelling

During the constant drying rate period, the water removal mechanism is governed by the external resistances (gas phase) and the drying rate is defined by the evaporation rate, proportional to the heat flow. Constant drying rate period was modelled in order to obtain the respective coefficients of mass transfer of gas phase (K_t, m s^{-1}) and the convective heat transfer coefficient (h_t, W·m^2·K^{-1}), defined by the Eq. (4.15) and Eq. (4.16), respectively:

$$w = \frac{X_{t_{n-1}} - X_{t_n}}{t_n - t_{n-1}} = \frac{K_t \rho_{air} a}{\rho_s}(Y_i - Y_{air}) \tag{4.15}$$

$$w = \frac{h_t a}{\Delta H_v \rho_s}(T_i - T) \tag{4.16}$$

where w (kg water·kg d.b.$^{-1}$·s^{-1}) is the mass flow of evaporated water, Y_i and Y_{air} (kg water kg dry air^{-1}) are the interphase and bulk absolute moisture content of air, respectively, ρ_{air} (kg·m^3) is the air density at drying temperature, ρ_s (kg d.b.·m^{-3}) is the apparent density of seaweed layer, a (m^2·m^{-3}) is the total interfacial surface (assuming water transfer by both sides of the layer) per unit of layer volume, T_i and T (°C) are the interphase and dry temperature of air, respectively and ΔH_v (J·kg^{-1}) is the latent heat of vaporization of water at the interphase temperature. Note here that the interphase properties (Y_i and T_i), during pre-critical drying period, were considered as the corresponding wet-bulb properties of the air employed for drying.

Falling drying rate period modelling

The falling drying rate period of drying was modelled employing the analytical solutions to Fick's diffusion equation to determine the effective coefficients of water diffusion through the sample under some assumptions (Crank, 1975). Briefly, the distribution of the moisture within the product is uniform; at t > 0 surface reaches equilibrium moisture and all resistances to water removal are inside the material (the external resistances are negligible). Moreover, the shrinking effect on the characteristic dimension of seaweeds was taken into account. The fitting of the experimental data of the falling drying rate period was carried out employing the following ratio, Eq. (4.17):

$$\frac{M_t}{M_\infty} = \frac{X_t - X_c}{X_{eq} - X_c} \tag{4.17}$$

where M_t (g) is the amount of water removed at time t (min), M_∞ (g) is the total amount of water removed until the equilibrium is reached.

The chosen geometry to carry out the modelling was cylinder geometry, based on seaweeds shape. According to (Crank, 1975), for cylinder geometry it is considered a long circular cylinder in which diffusion is everywhere radial.

The analytical solutions associated to this geometry for short, when $M_t/M_\infty \leqslant 0.6$, Eq. (4.18) and long times, when $0.4 < M_t/M_\infty < 1$, Eq. (4.19) are:

$$\frac{M_t}{M_\infty} = \frac{4}{\pi^{1/2}}\left(\frac{D_{eff}t}{r^2}\right)^{1/2} - \frac{D_{eff}t}{r^2} - \frac{1}{3\pi^{1/2}}\left(\frac{D_{eff}t}{r^2}\right)^{3/2} \tag{4.18}$$

$$\frac{M_t}{M_\infty} = 1 - \sum_{n=1}^{\infty}\frac{4}{\alpha_n^2}e^{-D_{eff}\alpha_n^2 t/r^2} \tag{4.19}$$

where D_{eff} $(m^2 \cdot s^{-1})$ is the effective coefficient of water diffusion in the bulk of the material, r (m) is the radius considered for the cylinder and (α) are the roots of the first order Bessel function for each term n. In this case, three terms (α_1, α_2 and α_3 are 2.405, 5.520 and 8.654) of the Eq. (4.19) were considered enough to fit the experimental data.

The final values of water diffusivity for the whole falling rate period were calculated by the weighted arithmetic mean (as function of the number of data for each time) of the water diffusivity obtained with the corresponding models for short and long times.

4.3 Flours Manufacture and Characterization

4.3.1 Manufacture

4.3.1.1 Materials

The materials employed on milling operation in order to obtain flours were three different maize varieties obtained from Spanish maize kernels, white (WM, *Rebordanes* variety), yellow (YM, *Sarreaus* variety) and purple (PM, *Meiro* variety) and those materials obtained after drying operation: the dried chestnuts (CT) and dried seaweeds *Bifurcaria bifurcata* (BB35, BB50, BB60 and BB75), *Fucus vesiculosus* (FV35, FV50, FV60 and FV75) and *Ascophyllum nodosum* (AN35, AN50, AN60 and AN75).

4.3.1.2 Experimental Conditions and Equipment

Milling was carried out using a centrifugal mill (ZM 200, Retsch GMBH, Germany), Figure 4.5 (a). The rotor speed was adjusted to 8000 rpm and two different standard sieves differentiated in its mesh size, 200 and 500 μm, were employed. Dried seaweeds (BB35, BB50, BB60, BB75, FV35, FV50, FV60, FV75, AN35, AN50, AN60 and AN75) were milled using the 500 μm standard sieve. The different maize varieties (WM, YM and PM) were milled using the two standard sieves in order to obtain two different particle size distributions for each maize variety, obtaining six different systems of flours WM200F, WM500F, YM200F, YM500F, PM200F and PM500F. Finally, dried chestnut (CT) was milled using the 200 μm standard sieve. The milled systems were stored in polyethylene plastic bags under vacuum with a vacuum-packer (Sammic V201, Spain), Figure 4.5 (b), and stored at 5^{o}C for further utilization.

4.3.2 Physical Characterization

4.3.2.1 Materials

All powders and flours obtained after milling (BB35P, BB50P, BB60P, BB75P, FV35P, FV50P, FV60P, FV75P, AN35P, AN50P, AN60P, AN75P, WM200F, WM500F, YM200F, YM500F, PM200F, PM500F and CTF) were subjected to physical characterization.

(a) (b)

Figure 4.5 Centrifugal mill (ZM 200, Retsch GMBH, Germany)(a) and Vacuum-packer (Sammic V201, Spain) (b).

4.3.2.2 Experimental Conditions and Equipment

The determination of the particle size distribution of each flour was performed using different standard sieves (Standard ISO-3310.1, 500, 250, 200, 125, 80, 63 and 40 μm, Cisa Cedacería Industrial, Spain), Figure 4.6 (a). Flour particles were passed through the different sieves and the corresponding fraction of particles retained in each sieve were weighed in order to obtain the corresponding mass fraction associated to each particle size.

The study of the colour of flours and flour fractions was carried out using a colorimeter (Chroma Meter CR-400, Konika Minolta, Japan), Figure 4.6 (b). Colour was measured by means of CIELab coordinates (ISO 11664-4:2008): L^* (whiteness ($L^* = 0$) or brightness ($L^* = 100$)), a^* (redness ($a^* > 0$) or greenness ($a^* < 0$) and b^* (yellowness ($b^* > 0$) or blueness ($b^* < 0$)).

(a) (b)

Figure 4.6 Standard ISO-3310.1 sieves (Cisa Cedacería Industrial, Spain) (a) and Colorimeter (Chroma Meter CR-400, Konika Minolta, Japan) (b).

Seaweed powders (BB35P, FV35P and AN35P) were also physically characterized by means of water retention capacity (WRC) determined following an established protocol (Robertson *et al.*, 2000) and swelling power (SP) determined using the method proposed by Leach *et al.* (1959).

4.3.2.3 Data Treatment

For analysing sieving data it was assumed that the particles were spherical and the diameter corresponded to the side of the square sieve openings. The mass mean diameter D_w, Eq. (4.20), the volume mean diameter D_v, Eq. (4.21), and the surface mean diameter D_s, Eq. (4.22), were calculated for all flours.

$$D_w = \sum_{i=1}^{i=n} x_i D_{pi} \tag{4.20}$$

$$D_v = \sum_{i=1}^{i=n} \left(\frac{x_i}{D_{pi}} \right)^{-\frac{1}{3}} \tag{4.21}$$

$$D_s = \frac{1}{\sum_{i=1}^{i=n} \frac{x_i}{D_{pi}}} \tag{4.22}$$

where D_{pi} (μm) is the mean diameter for each fraction and x_i (-) is the weight fraction calculated as the ratio between corresponding mass of each fraction and the total mass of flour employed in the sieving.

In addition, total colour difference (ΔE^*) was calculated at each drying time with fresh seaweed as control value Eq. (4.23):

$$\Delta E^* = \sqrt{(L^* - L_r^*)^2 + (a^* - a_r^*)^2 + (b^* - b_r^*)^2} \tag{4.23}$$

where suffix r corresponded to the reference system (as it will be explained in Chapter 6). Calibration of the colorimeter is done by measuring the colour parameters of a standardized white glossy ceramic tile (L^*=97.00, a^*=0.00 and b^*=1.85). Each colour measurement was made nine times (three triplicates on three different surface points).

4.3.3 Chemical Characterization

4.3.3.1 Materials

Seaweed powders (BB35P, BB50P, BB60P, BB75P, FV35P, FV50P, FV60P, FV75P, AN35P, AN50P, AN60P and AN75P) and the starchy flours (WM200F,

WM500F, YM200F, YM500F, PM200F, PM500F and CTF) were chemically characterized by means of moisture content. Additionally, total starch, damaged starch and amylose-amylopectin content were also measured for starchy flours.

The materials needed to carried out the chemical characterization were: aqueous ethanol (80% v·v^{-1}), thermostable α-amylase, amyloglucosidase, high purity glucose oxidase-peroxidase reagent, fungal α-amylase, dilute sulphuric acid solution (0.2% v·v^{-1}), distilled water, aqueous solution of sodium sulphite 0.5% (w·w^{-1}), dimethylsulphoxide (DMSO) and a solution of iodine (0.0025 mol·L^{-1}) in potassium iodide (0.0065 mol·L^{-1}).

4.3.3.2 Experimental Conditions and Equipment

Moisture Content Determination
Moisture content was determined as previously explained in section 4.1.2. All determinations were carried out at least by duplicate.

Starch Characterization
Starch characterization was carried out by means of total starch, damaged starch and amylose-amylopectin ratio:

- Total starch content (TS, % g starch·(g dry flour)$^{-1}$) was determined using an enzymatic assay kit (Total Starch, Megazyme, Ireland) based on standard methods (AOAC Method 996.11, AACC Method 76-13.01). In these methods starchy flour (0.1 g) were washed with aqueous ethanol (0.2 mL, 80% v·v^{-1}) before analysis. Then 3 mL of thermostable α-amylase was added to samples and incubated in a boiling water bath for 12 min to hydrolyse starch into soluble branched and unbranched maltodextrins. Then amyloglucosidase (0.1 mL) was added and the resulting solution incubated at 50^{o}C during 30 min in order to hydrolyse maltodextrins to D-glucose. The glucose was specifically measured with a high purity glucose oxidase-peroxidase reagent mixture (3 mL) by absorbance at 510 nm with a glucose control against the reagent blank using a spectrophotometer (Genesys 10S UV, ThermoFisher Scientific, Spain), Figure 4.7.

- Damaged starch content (DS, % g damaged starch·(g dry flour)$^{-1}$) was obtained using an enzymatic assay kit (Starch Damage, Megazyme, Ireland) based on standard methods (ICC Method No. 164, AACC Method 76-31.01). In these methods damaged starch granules of a flour

sample (0.1 g) are hydrated and hydrolysed to maltosaccharides plus α-limit dextrins by carefully controlled treatment, 40°C for exactly 10 min, with purified fungal α-amylase (1.0 mL, 50 U·mL^{-1}). The fungal α-amylase treatment is designed to give near complete solubilisation of damaged granules with minimum breakdown of undamaged granules. This reaction is terminated on addition (8.0 mL) of a dilute sulphuric acid solution (0.2% v·v^{-1}), and aliquots (0.1 mL) are treated with excess levels of purified amyloglucosidase (0.1 mL, 2 U) at 40°C for 10 min to give complete degradation of starch-derived dextrins to glucose. The glucose is specifically measured with a high purity glucose oxidase-peroxidase reagent mixture (4.0 mL) by absorbance at 510 nm with a glucose control against the reagent blank using a spectrophotometer (Genesys 10S UV, ThermoFisher Scientific, Spain), Figure 4.7.

- The starch extraction from maize and chestnut flours was carried out according to the method of Singh & Singh (2001) with minor modifications. Maize and chestnut powder (10 g) was added into 100 ml of distilled water with 0.5% (w·w^{-1}) of sodium sulphite. The slurry was filtered through a 63 μm sieve. The residue on the sieve was washed with distilled water for three times. The filtrate was precipitated over night at 4°C. Then, the supernatant was discarded and the starch was washed with distilled water and precipitated again for two times. The starch was collected and dried at 40°C up to constant weight. The amylose-amylopectin ratio was determined according to the procedure previously established in bibliography (McGrance *et al.*, 1998). This method is based on starch digestion (0.1 g) with 4.4 mL of DMSO at 85°C during 15 min in a water bath. When dissolved, this solution was diluted to 25.0 mL with distilled water. Then an aliquot (1.0 mL) of this solution was diluted with 50.0 mL of water, 5.0 mL of a solution of iodine (0.0025 mol·L^{-1}) in potassium iodide (0.0065 mol·L^{-1}) added with mixing and the absorbance of a sample of this solution was measured at 600 nm in a spectrophotometer (Genesys 10S UV, ThermoFisher Scientific, Spain), Figure 4.7. All the tests were made at least in duplicate.

Figure 4.7. Spectrophotometer Genesys 10S UV (Thermo Fisher Scientific, Spain).

4.4 Seaweed Extracts Manufacture and Characterization

4.4.1 Extraction

4.4.1.1 Materials

Seaweed aqueous extracts were obtained from the different dried seaweed powders: BB35P, BB50P, BB60P, BB75P, FV35P, FV50P, FV60P, FV75P, AN35P, AN50P, AN60P and AN75P. Additionally, different particles size fractions of the systems FV35P and the particle size fraction corresponded to 250-500 μm for AN35P, AN50P, AN60P and AN75P were employed as well to obtain the extracts.

The other necessary materials to carry out this experimentation consisted of distilled water and acetone.

4.4.1.2 Experimental Conditions and Equipment

Samples of powdered seaweed, were processed with an ultrasound processor (Hielscher, UIP-1000 hdT, Germany), Figure 4.8 (a), to enhance the extraction of polyphenols and carbohydrates. All experiments were carried out in batch, the procedure starting with a 15 minutes rehydration step before extraction. Then extraction operation took place using a 200 mL beaker at controlled temperature ($< 35^{o}$C) employing a cold water bath to avoid that temperatures increased could affect antioxidant activity. All extractions were performed using water as solvent, excepting in the cases that acetone-water (70:30 v$\cdot$v^{-1}) was used as solvent to obtain reference extracts according to (Koivikko *et al.*, 2007). The equipment operated with a frequency of 20 kHz and the irradiation power (< 1000 W) was regulated in the ultrasound generator at 80% amplitude. Preliminary tests were carried out, using *Fucus vesiculosus* powder formerly dried at 35^{o}C, varying liquid-solid ratio (20, 30 and 40 w$\cdot$w^{-1}) and contacting time (4, 12, and 20 min) and analysing polyphenols and carbohydrates content to establish the most adequate extraction conditions for further studies. The selected conditions were 4 min of contact time and 30 w$\cdot$w^{-1} of liquid-solid ratio.

Finally, obtained extracts were centrifuged at 12400 rpm for 15 minutes using a high speed laboratory centrifuge (2-15, Sigma, UK), Figure 4.8 (b), and the supernatant obtained was then filtered by pressure using syringe filters with a pore size of 0.25 μm and used for characterization analysis.

(a) (b)

Figure 4.8 Ultrasound processor UIP-1000 hdT (Hielscher, Germany) (a) and High speed laboratory centrifuge Type 2-15 (Sigma, UK) (b).

4.4.2 Phytochemical Characterization

4.4.2.1 Materials

All seaweed aqueous extracts were analysed by means of DPPH scavenging activity, total solids, polyphenols and carbohydrate content.

The materials employed for seaweed aqueous extracts characterization were acetone, sodium carbonate, *Folin-Ciocalteau* reagent, sulphuric acid, phenol, sodium tetraborate, sulfamic acid and 3-hydroxybiphenyl (Panreac, Barcelona, Spain).

4.4.2.2 Experimental Conditions and Equipment

Total Solids Content
The total solids content in the extracts was determined after samples drying at 104 ± 1°C in an oven. Samples were weighed daily until constant weight was reached after two consecutive measurements (Symons & Morey, 1941).

Polyphenols content
The quantitative determination of total polyphenols content (TP) was measured as phloroglucinol (PHL) equivalents following a colorimetric method (Singleton & Rossi, 1965). This method is based on the absorbance changes of the *Folin Ciocalteu* reagent when reacting whit the hydroxyl groups of the polyphenolic substances. TP was evaluated in reference to raw seaweed powder sample (mg PHL·(100 g dry powder)$^{-1}$, TP_w) and also to total solids content in the extract (mg PHL·(100 g dry solids)$^{-1}$, TP_s).

DPPH Scavenging Activity

The DPPH scavenging activity assay measures the capacity of a system to react with a free radical agent (2, 2-diphenyl-1-picrylhydrazyl, DPPH). It was employed a method previously proposed (Brand-Williams *et al.*, 1995). In its radical form, DPPH· shows an absorption peak at 515 nm, but upon reduction by an antioxidant (AH) or a radical species (R·) the absorption disappears. As the reaction takes time to fully develop, for the determination of the DPPH scavenging activity absorbance is measured every 5 minutes until it reaches the stationary state. Scavenging activity, SA, is evaluated by means of Eq. (4.24):

$$SA(\%) = \frac{(A_0 - A_f)100}{A_0} \tag{4.24}$$

where A_0 (-) is the absorbance at time 0 and A_f is the absorbance after one hour.

Carbohydrates Content

Carbohydrates content of the extracts was determined using the DuBois *et al.* (1956) method that employs sulphuric acid and phenol as reagents. In the presence of strong acids and heat, carbohydrates form furan derivatives such as furanaldehyde and hydroxymethyl furaldehyde. These compounds react with phenol, leading to the formation of orange-coloured compounds. Furan derivatives from pentoses and hexoses exhibit peaks of light absorbance in the range of 480–490 nm (Brummer & Cui, 2005). Samples were evaluated measuring the absorbance read at 485 nm and glucose was used for the calibration curve. Hence, carbohydrates content was expressed as glucose equivalents (GL) referred to raw seaweed powder sample (mg GL·(100 g dry powder)$^{-1}$, CHO_w) and also to total solids content in the extract (mg GL·(100 g dry solids)$^{-1}$, CHO_s).

4.5 Gluten-free Doughs Manufacture and Characterization

4.5.1 Manufacture

4.5.1.1 Materials

Preparation of gluten-free doughs were carried out employing three different maize flours, white (WM, *Rebordanes* variety), yellow (YM, *Sarreaus* variety)

and purple (PM, *Meiro* variety) and chestnut flour (CT, *Castanea sativa Mill.*) as flour basis for dough, seaweed powders obtained from milling of seaweeds formerly dried at 35°C *Bifurcaria bifurcata* (BB35P), *Fucus vesiculosus* (FV35P) and *Ascophyllum nodosum* (AN35P), guar gum, salt and tap water.

Different formulations were assayed, simple formulations consisted of CT, WM, YM and PM flours with tap water, respectively, and blends based on CT enriched with seaweed powders BB35P, FV35P and AN35P added at different levels (3, 6 and 9% g seaweed powder·(g chestnut flour)$^{-1}$, flour basis, f.b.), guar gum (2% f.b.), salt (1.8% f.b.) and tap water.

4.5.1.2 Experimental Conditions and Equipment

The preparation and characterization of gluten-free flour doughs was conducted by means of two standard and one proposed methods carried out employing Mixolab® laboratory kneader, Figure 4.9.

(a) (b) (c)

Figure 4.9. Mixolab® laboratory kneader (Chopin Technologies, France).

Simple Curve Standard Protocol

According to ICC-Standard Method No. 173 (2008) this standard method establishes the protocol necessary for determining the rheological behaviour of wheat flour (*Triticum aestivum*) as a function of mixing and temperature by means of Mixolab®. Named as mixing curve, it consists of water addition to a flour in order to obtain a dough with a consistency of 1.10 N·m (equivalent to 500 Brabender units) at constant mixing rate (80 rpm) and temperature (30°C) during 30 min, Table 4.1. It provides similar information on dough behaviour that experiments carried out with farinograph (a typical apparatus to carry out doughs mixing behaviour characterization). Several dough parameters can be obtained:

Table 4.1. Mixolab® simple curve protocol

Mixing speed (rpm)	Temperature (°C)	Time (min)
80	30	30

- Target consistency, C1 (N·m): the consistency is defined as the resistance opposed by the dough to a constant mechanical action. The torque, measured in N·m, is proportional to the consistency.

- Water absorption level, WA (g water·(100 g flour)$^{-1}$): quantity of water added to 100 g of flour (with 14% of moisture content) to form dough with the target consistency, C1.

- Development time, DT (min): time interval from the water addition to the achievement of C1.

- Stability time, ST (min): time interval at which the dough consistency is kept at 1.10±0.07 N·m.

- Departure time, DPT (min): time required to decrease the torque produced by the dough passage below 1.10±0.07 N·m.

Complete Curve Standard Protocol

The second standard test consisted on different mixing steps involving heating and cooling cycles. This kind of test gives information about mechanical and proteins weakening, amylase activity, cooking stability and protein network weakening, starch gelatinization and enzymatic degradation rates. As well as the first standard protocol, this method, commonly named as complete curve, involves water addition to a flour in order to obtain a dough with a consistency of 1.10 N·m at constant mixing rate (80 rpm). The first step is a typical mixing during 8 min at 30°C. Then a heating step is applied (15 min) from 30°C to 90°C at constant heating rate (4°C·min^{-1}). Subsequently, a constant temperature step (90°C) is performed for 7 min followed by a cooling step (10 min) from 90°C to 50°C at constant cooling rate (4°C·min^{-1}). Finally a constant temperature step at 50°C is performed during 5 min that implies a total duration of the method of 45 min, Table 4.2.

Table 4.2. Mixolab® complete curve protocol

Step	Mixing speed (rpm)	Initial temperature (°C)	Final temperature (°C)	Time (min)	Heating rate (°C·min^{-1})
1		30	30	8	0
2		30	90	15	4
3	80	90	90	7	0
4		90	50	10	-4
5		50	50	5	0

An example of data acquired with the application of this procedure is shown in Figure 4.10. Five different sections can be observed in Figure 4.10. In section

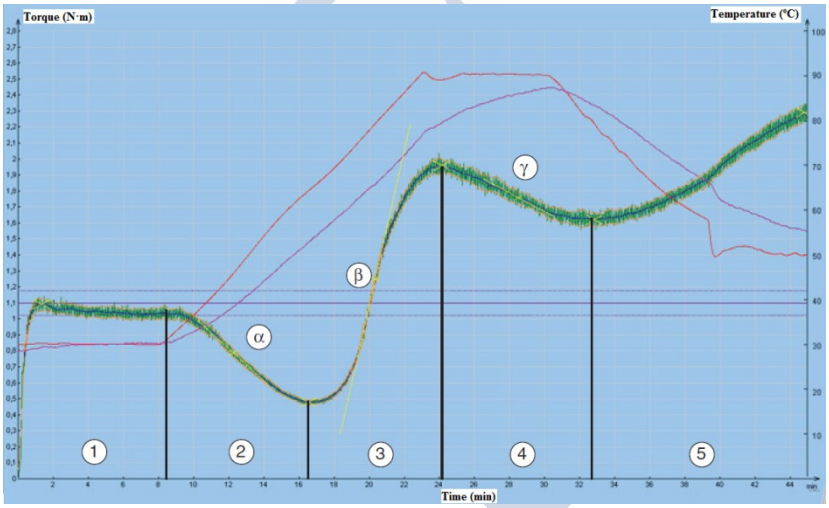

Figure 4.10. Example of Mixolab® complete curve for a wheat flour dough.

1, the torque increases with the adapted hydration level reaching the target value 1.10±0.07 N·m, C1. Mixing characteristics of doughs such as development time (DT), stability time (ST) and departure time (DPT) can be determined. Additionally, water absorption level (WA) can also be calculated indirectly as the amount of water employed to achieve the target consistency C1. The continuous mixing, above dough stability time, produces changes in dough properties from suitable (consistent, stable and elastic) to unsuitable (slack, sticky) (Rosell *et al.*, 2007). In section 2, the consistency of the dough decreases due to mixing and

heating of dough that promotes protein weakening (Kahraman *et al.*, 2008) until achieve a minimum, C2. In section 3, that starts in C2, the dough consistency increases due to the starch gelatinization until a maximum of consistency, C3. Then in section 4, the consistency of dough can decrease to a minimum, C4, or remain constant mainly as function of amylase activity. Finally, in section 5 (from C4 to C5), temperature decreases and consistency increases as result of gelling processes and retrogradation of starch. From Mixolab® complete curves, as in the case of the mixing curve, WA, DT, ST and DPT of dough can be obtained. Additionally, other dough parameters can be attained related to thermal and non-thermal processes that take place in dough:

- C2 (N·m): minimum torque achieved due to protein weakening as a function of mechanical work and temperature.
- C3 (N·m): maximum torque achieved as a result of starch gelatinization.
- C4 (N·m): torque related to the hot gel stability.
- C5 (N·m): final consistency of the dough related to starch retrogradation in the cooling phase.
- Protein network weakening rate, α (N·m·min^{-1}): slope of curve between end of period at 30°C and C2. It represents the protein weakening speed under the effect of heat.
- Starch gelatinization rate, β (N·m·min^{-1}): slope of curve between C2 and C3.
- Enzymatic degradation rate, γ_e (N·m·min^{-1}): slope of curve between C3 and C4.
- Cooking stability, C4/C3 (-)
- Setback, C5-C4 (N·m): it represents retrogradation of dough.
- Initial gelatinization temperature, T_0 (°C): temperature associated to C2. It represents the beginning of the starch gelatinization process.
- Final gelatinization temperature, T_{fg} (°C): temperature associated to C3. It represents the end of the starch gelatinization process.

Proposed Protocol
The proposed protocol consisted on three different steps, all of them carried out at constant mixing speed (80 rpm). The first step involved mixing at constant temperature, 50°C, during 5 min. Then a heating step is performed from 50 to 90°C at constant heating rate, 4 °C·min^{-1} (during 10 min). Finally a 4 min step at constant temperature of 90°C. The whole proposed protocol had a total duration of 19 min, Table 4.3.

Table 4.3. Mixolab® proposed protocol

Step	Mixing speed (rpm)	Initial temperature (°C)	Final temperature (°C)	Time (min)	Heating rate (°C·min^{-1})
1		50	50	5	0
2	80	50	90	10	4
3		90	90	4	0

4.5.1.3 Data Treatment

The analysis of mixing data of gluten-free flour doughs was carried out using Microsoft Excel software.

4.5.2 Rheological Characterization

4.5.2.1 Materials

The systems rheologically assayed corresponded to flour doughs obtained after mixing the different components in Mixolab®. gluten-free flour doughs (YM, WM, PM and CT) were studied at the target consistency C1. Flour dough blends (CT+AN, CT+BB and CT+FV) with different levels of seaweed addition were analysed at two different consistencies, the typical target consistency (C1) and the final consistency of the dough obtained applying the proposed protocol of mixing.

Liquid paraffin (Panreac, Barcelona, Spain) was also employed to carry out rheological experiments of gluten-free doughs.

4.5.2.2 Experimental Conditions and Equipment

Rheological characterization consisted on three different rheological studies. Firstly, the the linear viscoelastic region (LVER) of the samples was determined applying a strain sweep test. Subsequently, Small Amplitude Oscillatory Shear (SAOS) and Creep and Recovery rheological tests were carried out in order to study viscoelastic properties of doughs inside the LVER. All tests, were carried out using a controlled stress rheometer (MCR 301, Anton Paar, Austria) with parallel plates (50 mm diameter, 2 mm gap) at 30°C (±0.1°C), Figure 4.11. Doughs obtained with Mixolab® at the target consistency were placed between the plates. Excess volume of dough sample, in relation to the volume given by gap between plates, was trimmed and the edge was coated with paraffin to prevent water evaporation during the measurement. A rest time of 5 min was applied to all samples before measuring. All measurement was carried out at least in triplicate.

Strain Sweep

The linear viscoelastic region (LVER) was determined by means of a strain sweep (γ, 0.01–10%) at frequency of 1 Hz. The critical strain (γ_c) of each studied system was calculated as those corresponded to a diminution of $G^{'}$ plateau value of 10%.

Small Amplitude Oscillatory Shear (SAOS)

The mechanical spectra of doughs were obtained by Small Amplitude Oscillatory Shear (SAOS) test. This test consisted on a frequency sweep from 1 to 100 rad·s^{-1} of angular frequency (ω) at 0.1% strain (inside the LVER of the samples) to determine the storage, $G^{'}$ (Pa), and loss, $G^{''}$ (Pa), moduli, the damping factor ($\tan\delta = G^{'}\cdot(G^{''})^{-1}$), the complex modulus and the complex viscosity.

As additional verification of the linear viscoelasticity and stability conditions of the sample for tested sample, the frequency sweep was applied following decreasing-increasing angular frequency sweeps, in order to verify the satisfactory superposition of the spectra and that any modification of the sample was produced.

Creep & Recovery

Creep and recovery tests consisted on the application of a constant stress (σ) of 50 Pa during 60 s (creep phase) and allowing strain recovery during 180 s after stress removal, $\sigma = 0$ (recovery phase).

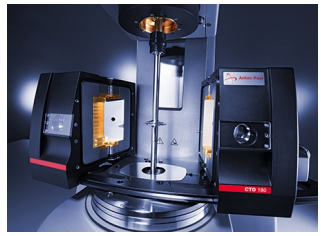

Figure 4.11. Anton Paar MCR 301 Rheometer with CTD 450 Chamber (Physica, Austria).

4.5.2.3 Data Treatment

Values of storage modulus ($G^{'}$), loss modulus ($G^{''}$), damping factor ($\tan\delta$) and compliance (J(t)) were determined with Rheoplus/32 software (version 3.21, Anton Paar, Ostfildern, Germany).

Experimental data of $G^{'}$ and $G^{''}$ *vs* ω obtained by SAOS tests application were fitted by Eqs. (4.25) and (4.26):

$$logG^{'} = loga^{'} + b^{'} log\omega \tag{4.25}$$

$$logG^{''} = loga^{''} + b^{''} log\omega \tag{4.26}$$

where $a^{'}$ (Pa·s$^{-b'}$), $a^{''}$ (Pa·s$^{-b''}$), $b^{'}$ (-) and $b^{''}$ (-) are the fitting parameters.

Experimental data of creep and recovery were analysed by creep compliance rheological parameters J(t) (Pa^{-1}) = $\gamma\sigma^{-1}$ (Steffe, 1996) and modelling by Burgers model (Burgers, 1935) using the Eqs. (4.27) and (4.27) for creep and recovery phases, respectively:

$$J(t) = J_0 + J_m(1 - e^{\frac{-t}{\lambda}}) + \frac{t}{\eta_0} \tag{4.27}$$

$$J(t) = J_{max} + J_0 + J_m(1 - e^{\frac{-t}{\lambda}}) \tag{4.28}$$

where J_0, J_m and J_{max} (Pa^{-1}) are the instantaneous, viscoelastic and maximum creep compliance, respectively, t (s) is the phase time, λ_c (s) and λ_r (s) are the mean retardation time of creep and recovery steps, respectively, and η_0 (Pa·s) is the zero-shear viscosity. The recovery compliance, J_r (Pa^{-1}), is calculated by the sum of J_0 and J_m corresponding to recovery phase, Eq. (4.28). The $J_r{\cdot}J_{max}^{-1}$ ratio gives information on relative elastic component of the maximum creep compliance.

4.5.3 Thermal Characterization

4.5.3.1 Dynamic Mechanic-Thermal Analysis (DMTA)

Materials
Flour doughs obtained after mixing the different components of each system in Mixolab® were analysed. gluten-free flour doughs (YM, WM, PM and CT) were studied at the target consistency C1. Flour dough blends (CT+AN, CT+BB and CT+FV) were analysed at two different consistencies, C1 corresponding to the typical target consistency and C5, the final consistency of the dough obtained applying the proposed protocol of mixing. Liquid paraffin (Panreac, Barcelona, Spain) was also necessary to carry out DMTA experiments.

Experimental Conditions and Equipment
Flour doughs at the aforementioned consistency were tested in the same machine employed for rheological characterization (see 4.5.2). The thermomechanical assays were performed in the linear viscoelastic region of the doughs (0.1% of strain, 1 Hz of frequency). Temperature was increased from 30 to 180°C with a constant heating rate of $4°C \cdot min^{-1}$. All rheological assays were performed at least in duplicate.

Data Treatment
Values of storage modulus (G') loss modulus (G'') and damping factor ($\tan\delta$) were determined to analyse the temperatures associated with thermal transitions using Rheoplus/32 software (version3.21, Anton Paar, Ostfildern, Germany).

4.5.3.2 Differential Scanning Calorimetry (DSC)

Materials
Flour doughs of YM, WM, PM and CT with the same water content of the same doughs studied by DMTA were studied.

Experimental Conditions and Equipment
Samples were prepared using the same method described in bibliography (Liu *et al.*, 2006). The solid (∼1 g), in a glass vial, was weighted in an analytical balance (Denver Instruments SI-234), the water needed to obtain the desired water absorption was added with a micropipette and mixed well with a small spatula. Water absorption levels were calculated by weight. The glass vial was

sealed and the mixture was equilibrated for 24 h at room temperature. Then, a small portion of the sample (12.6–16.2 mg) was introduced in a steel pan, sealed with a lid and equilibrated at room temperature for 1 h. Thermal properties of these samples were studied using a differential scanning calorimeter (TA Q200, TA Instruments, New Castle, USA), Figure 4.12. An empty steel pan was used as reference. The sample pan and the empty pan were placed in two identical compartments of the furnace unit. The assay realized consisted of equilibrating the sample during 5 min at 40°C and then heating to 180°C at a constant heating rate of 4°C·min^{-1}.

Figure 4.12. DSC TA Q200 (TA Instruments, USA).

Data Treatment
All temperatures and enthalpy changes associated with thermal transitions observed in each endothermic curve were determined using TA Instruments Universal Analysis 2000 Software (version 4.7A, TA Instruments Waters LLC, New Castle, USA).

4.6 Wheat Doughs Manufacture and Charaterization

4.6.1 Manufacture

4.6.1.1 Materials

The employed materials for preparation of wheat doughs were wheat flour (*Triticum aestivum*) supplied by Moulin Girardeau (France) as basis of dough,

seaweed powder obtained from milling of *Fucus vesiculosus* formerly dried at 35°C (FV35P), fresh yeast, ascorbic acid and tap water.

Five different systems were assayed corresponded to blends based on wheat flour: one of wheat flour used as reference, and four with FV35 seaweed powder added to wheat flour at different levels.

4.6.1.2 Experimental Conditions and Equipment

Control formulation consisted of 300 g wheat flour, 192 g tap water, 6 g fresh yeast, 5.4 g salt and 0.006 g ascorbic acid. Several seaweed powder amounts were added to obtain different doughs composition, labelled as $FV0X$, with X as 2, 4, 6 and 8 (% of seaweed powder (f.b.)). Tap water addition was adjusted by an expert baker for each formulation in view of dough behaviour in order to obtain a comparable dough consistency at the end of mixing (AFNOR, 2002).

Mixing was carried out in a spiral mixer (Kitchen Aid, USA), Figure 4.13, in three different steps. Initially, wheat flour and powder seaweed were mixed at 60 rpm for 1 min in order to homogenize the solid mixture. Then, yeast, ascorbic acid and water were added and a pre-mixing step was carried out at 60 rpm during 2 min. Finally, a texturing step was developed for 7 min at 120 rpm. Salt was added 4 min before the end of the texturing step. Experiments were carried out at least in triplicate.

Figure 4.13. Kitchen Aid Artisan, USA.

4.6.2 Rheological Characterization

4.6.2.1 Materials

Wheat flour doughs enriched with different levels of FV35P (FV00, FV02, FV04, FV06 and FV08) were rheologically studied. Paraffin oil (Panreac, Barcelona, Spain) was also necessary to carry out rheological characterization.

4.6.2.2 Experimental Conditions and Equipment

Elongational viscosity of doughs was carried out at large bi-extensional deformations by Lubrificated Squeezing Flow test (LSF). A traction-compression machine (Instron Corporation, Type 1122, USA), Figure 4.14, with a plate-plate geometry (20 mm diameter, 15 mm gap) equipped with a force sensor (0-100 N) was employed. At the end of mixing, unyeasted dough samples (≈5 g) were placed in Teflon cylinders (14 mm height, 20 mm diameter) lubricated with paraffin oil and kept at room temperature (≈25°C) for 30 min (Launay & Michon, 2008). Then the homogeneous samples were removed from the cylinders and placed between the plates also lubricated with paraffin oil. The cylindrical samples were compressed by the upper plate, attached with a movable crosshead, until a final height of 1 mm, at several constant speeds (5, 10 or 100 mm·min^{-1}). The force and applied was recorded as function of sample displacement.

Figure 4.14. Instron Universal Test Machine, Type 1122, Instron Corporation (USA).

4.6.2.3 Data Treatment

Data were processed according to a previous procedure (van Vliet, 2008). The biaxial (Hencky) strain ε_b was calculated and related to the time in order to calculate the strain rate, $\dot{\varepsilon}_b$ (s^{-1}). Then $\dot{\varepsilon}_b$ was related to the stress, calculated as the ratio between the force applied and the surface of the plate, in order to obtain the bi-extensional viscosity, η_e (Pa·s). The variations of η_e with $\dot{\varepsilon}_b$ at constant ε_b, were fitted by the power law equation, Eq. (4.29):

$$\eta_e = K(\varepsilon_b)^{n-1} \tag{4.29}$$

where K(Pa·s^n) is the consistency index and n (-) the flow behaviour index.

4.6.3 Thermal Characterization

4.6.3.1 Dynamic Mechanic-Thermal Analysis (DMTA)

Materials
Wheat flour doughs enriched with different levels of *Fucus vesiculosus* seaweed formerly dried at 35°C (FV00, FV02, FV04, FV06 and FV08).

Experimental Conditions and Equipment
Thermomechanical viscoelastic properties of doughs (without yeast) were studied by dynamic mechanical thermal analysis (DMTA) using a controlled stress rheometer (MCR 301, Anton Paar, Austria) equipped with a chamber (CTD 450, Anton Paar, Austria) with parallel plates (50 mm diameter, 2 mm gap). After mixing dough rested 20 min at ambient temperature (≈25°C). Then a dough sample was placed between the plates, excess volume of dough sample, in relation to the volume given by gap between plates, was trimmed and the edge was coated with paraffin to prevent water evaporation during the measurement. A rest time (5 min) was applied to all samples before measuring. Experiments were carried out at 1 Hz, 0.1% of strain (inside the linear viscoelastic region). Temperature was increased from 25 to 115°C with a constant heating rate of 3°C·(min)$^{-1}$. Values of viscoelastic moduli where determined. Initial, minimum and maximum values of G' were determined and their ratio calculated to provide an interpretation of gelatinization and gluten reticulation (Angioloni & Dalla Rosa, 2005). All measurements were carried out at least in duplicate.

Data Treatment
Values of storage modulus (G'), loss modulus (G'') and damping factor (tanδ)

were determined to analyse the temperatures associated with thermal transitions using Rheoplus/32 software (version3.21, Anton Paar, Ostfildern, Germany).

4.6.4 Fermentation Analysis

4.6.4.1 Materials

Fermentation analysis was performed for all wheat flour systems obtained after mixing result of addition of salt, tap water, yeast and different quantities of FV35 to wheat flour: FV00, FV02, FV04, FV06 and FV08.

4.6.4.2 Experimental Conditions and Equipment

Fermentation process of wheat doughs and enriched wheat doughs with FV35P was studied using the procedure describe by Shehzad *et al.* (2010). Images of a rounded dough sample (25 g) during proofing in a controlled atmosphere (27°C, 75% RH) were acquired every minute during 210 min through a digital camera (JVC TK-C750U, Japan), Figure 4.15.

Figure 4.15. Digital camera (JVC TK-C750U, Japan).

4.6.4.3 Data Treatment

Volume of dough sample was estimated by image analysis and converted into porosity by Eq. (4.30):

$$P(t) = 1 - \frac{m_d/V_d}{d_m} \tag{4.30}$$

where P is the porosity (-), m_d is the dough mass (g), V_d is the dough volume (cm^3) at any time of proofing and ρ_m is the matrix dough density ($g \cdot cm^{-3}$) calculated by Eq. (4.31):

$$\rho_m = \frac{1}{\sum_{i=1}^{i=n} \frac{x_i}{\rho_i}} \tag{4.31}$$

where x_i is the mass fraction (-) and ρ_i the density ($g \cdot m^{-3}$) of every component of dough. The porosity curves were modelled using a Gompertz function (Romano *et al.*, 2007), Eq. (4.32):

$$P(t) = ae^{-e^{-\frac{-2.72b}{a}(t-c)}} \tag{4.32}$$

where a (-) is an approximation of the final porosity increase from the initial value, b (min^{-1}) is the maximum volume expansion growth rate (the slope at inflection point), c (min) is the time for inflection point and d is the theoretical porosity when $t \to \infty$ (that makes $a + d = P(t \to \infty)$).

The dough shape ratio, $S(t)$ (-), was defined H/L_{max} with H as the height and L_{max} the maximum width of the dough sample at a given time. When $t <$ 90 min, the curve $S(t)$ *vs* t can be fitted by Eq. (4.33), (Kansou *et al.*, 2014):

$$S(t) = (a^{'} - c^{'})e^{-t/b^{'}} + c^{'} \tag{4.33}$$

where $a^{'}$ and $c^{'}$ are the stability at $t = 0$ and $t \to \infty$, respectively, that makes $(a^{'} - c^{'})$ the overall loss of dough stability, and $b^{'}$ is the starting time (min) of the stationary phase. To avoid any differences due to hand rounding of the dough prior to measurement, all curves were modelled with the same value of $a^{'}$ (0.60). Experiments were carried out at least in duplicate.

4.7 Gluten-free Baked Product Manufacture and Characterization

4.7.1 Manufacture

4.7.1.1 Materials

The different chestnut doughs enriched with seaweed powder at different levels (CHD, CBB03D, CBB06D, CBB09D, CFV03D, CFV06D, CFV09D, CAN03D, CAN06D and CAN09D) at the final consistency after application of the proposed mixing protocol in Mixolab® were then baked in order to achieve the final baked product.

4.7.1.2 Experimental Conditions and Equipment

Doughs at the final consistency achieved after application of the proposed protocol of mixing were allowed to cool (≈30°C). Subsequently they were manually moulded, cut in disks of 34 mm diameter and 3.6 mm height and scarified. Finally they were baked in an oven (Balay 3HB569XC, BSH, Spain), Figure 4.16, at 180°C during 25 min.

Figure 4.16. Oven Balay 3HB569XC, BSH, Spain.

4.7.2 Textural Characterization

4.7.2.1 Materials

The different cookies (CTC, BB03C, BB06C, BB09C, FV03C, FV06C, FV09C, AN03C, AN06C and AN09C) obtained after baking were texturally characterized.

4.7.2.2 Experimental Conditions and Equipment

Textural properties of cookies were studied by means of hardness, measured as the force needed to break the cookie. Textural tests, carried out in a texture analyser (TA-TXPlus, Stable Microsystems), Figure 4.17, employing a cylinder probe P/3 (3 mm diameter), consisted of a compression of cookie with the probe at a constant velocity of 2 mm·s^{-1} recording the force applied until break of cookie was achieved.

Figure 4.17. Texture analyser (TA-TXPlus, Stable Microsystems).

4.7.3 Phytochemical Characterization

4.7.3.1 Materials

Phytochemical characterization of the different obtained cookies (CTC, BB03C, BB06C, BB09C, FV03C, FV06C, FV09C, AN03C, AN06C and AN09C) was performed by means of moisture content, colour and antioxidant activity, polyphenols and total solids content of their extracts. Moreover, the same formulations employed for cookies were evaluated by means of polyphenols content and antioxidant activity before baking in order to obtain the baking effect on antioxidants properties of cookies.

4.7.3.2 Experimental Conditions and Equipment

Water Content

Water content of cookies was determined according to AOAC method (1995). It was evaluated by the weight loss of a sample determined when dried at 70°C using a vacuum oven Vacutherm VT650 (Heraeus Hanau, Germany), Figure 4.2, until to reach constant weight (±0.0005 g) in an analytical balance SI-234 (Denver Instrument, Germany), Figure 4.2. All determinations were carried out at least by duplicate.

Colour

Colour of cookies was evaluated using a colorimeter (CR-400, Konica Minolta) employing CIELab as coordinates system. Total colour difference (ΔE^*) was calculated by Eq. (4.23), where L_r^*, a_r^*, b_r^* are colour parameters of cookie without seaweed addition (reference) and L_i^*, a_i^*, b_i^* the colour parameters of cookies. Cookie colour was measured six times on three different positions of

cookie surface. At least 6 different cookies with the same composition were evaluated.

Characterization of Cookies Extracts
Cookies were milled using a laboratory blender (Figure 4.3) and then a centrifugal mill (Figure 4.5). The resulted powders were employed to obtain the extracts that were obtained and characterized by means of polyphenols and total solid content and the DPPH scavenging activity employing the same experimental procedure previously mentioned in section 4.2.

4.8 Wheat Bread Manufacture and Characterization

4.8.1 Materials

Different wheat breads were obtained after baking wheat flour doughs result of mixing salt, tap water, yeast and quantities of FV35P with wheat flour: FV00, FV02, FV04, FV06 and FV08.

4.8.2 Experimental Conditions and Equipment

After mixing, first dough fermentation was performed in a proofing cabinet (Panem, France) for 35 min at 27°C and 75% of relative humidity (RH). Then the dough was manually rounded and moulded mechanically (Tregor Merand, France), Figure 4.18, and proofed for 70 min at 27°C and 75% RH. Finally, dough pieces were scarificated and baked in an oven (Bongard, France), Figure 4.18, for 21 min at 245°C (hearth and vault temperatures). 300 mL of steam were added before and after loading. Before characterization, breads were cooled at room temperature for 2 h.

4.8.2.1 Physical Characterization

Texture
Bread texture was analysed by means of compression assays. About 16 h after baking, bread slices cut at the same diameter as the compression plate, were submitted to a compression using a plate-plate geometry (40 mm of diameter) set

on a universal testing machine (Instron type 1122, Instron Corporation, USA). The maximum height of slices (H_0) was measured and the crosshead was moved down at a speed of 50 mm·min^{-1} and stopped after a distance equal to 2/3 H_0. After compression, the bread was relaxed for 180 s. The apparent modulus, E_{crumb} (kPa), derived from the initial slope of the stress-strain curve, $\sigma_{critical}$ (kPa) at the peak of stress and $\sigma_{residual}$ (kPa) as the apparent residual stress at the end of the relaxation step were obtained.

Density

Bread density, ρ^* (g·cm^{-3}) was calculated from mass-volume ratio. When 2 h of cooling after baking were achieved, bread volume was measured based on rapeseeds displacement in a bread volumeter (Chopin Technologies, France). Bread mass was measured using a balance (±0.01 g, Mettler, Switzerland).

Colour

Colour of bread was evaluated using a colorimeter (CR-400, Konica Minolta) employing CIELab as coordinates system. Total colour difference (ΔE^*) was calculated by Eq. (4.23), where L_r^*, a_r^*, b_r^* are colour parameters of bread without FV (reference) and L_i^*, a_i^*, b_i^* the colour parameters of FV breads. Bread colour was measured six times on three different positions of each bread crust. At least 4 different breads with the same composition were evaluated.

(a) (b)

Figure 4.18. Tregor moulder, Merand (France) (a) and Bongard oven (France) (b).

4.9 Statistical Analysis

Experimental data were statistically analysed. All obtained data was treated as mean ± standard deviation. Differences among means were identified by one factor analysis of variance (ANOVA), followed by the Scheffe test and considering significant P-values ≤ 0.05 (IBM SPSS Statistics 22). The goodness of the adjustment of each model was determined based on coefficient of determination (R^2) and root mean square error (E_{RMS}, Eq. (4.34)).

$$E_{RMS} = \left[\frac{1}{N} \sum_{i=1}^{i=N} (X_{exp} - X_{cal})^2 \right]^{1/2} \tag{4.34}$$

where N is the number of data points, X_{exp} the experimental data point and X_{cal} the calculated data point using the corresponding model. The values of models parameters were obtained using Microsoft Excel 2013 (Solver add-on) by means of non-linear programming in which E_{RMS} is minimized. Units of E_{RMS} corresponded to the unit of the parameter to be analysed.

USC
UNIVERSIDADE
DE SANTIAGO
DE COMPOSTELA

Chapter 5

Assayed systems

The diagrams presented in this chapter aim to summarize the assayed systems, the main characterizations carried out and the operation conditions employed to perform the experimentation. Firstly, a general diagram as a resume of this Thesis is presented in order to facilitate its comprehension, see Figure 5.1.

5.1 Nomenclature

In this section, the nomenclature employed in the following diagrams is presented in order to facilitate its comprehension.

∇T	—	Heating rate (ºC·min^{-1})
A	—	Acetone (-)
a_w	—	Water activity (-)
C	—	Compression velocity (mm·min^{-1})
D	—	Dissolvent (-)
d	—	Diameter (mm)
$DMTA$	—	Dynamic Mechanic-Thermal Analysis (-)
DSC	—	Differential Scanning Calorimetry (-)
f	—	Frequency (Hz)
g	—	Gap (mm)
H	—	Height (mm)
L/S	—	Liquid-Solid ratio (-)
P	—	Power (W)
T	—	Temperature (ºC)
t	—	Time (min)
v	—	Speed or velocity (rpm or m·s^{-1})
W	—	Water (-)
X	—	Moisture content (kg water·(kg dry solid)$^{-1}$)

Subscript

0	—	Initial
a	—	Agitation
eq	—	Equilibrium
f	—	Final
r	—	Rotation

Greek letters

γ	—	Strain (%)
φ	—	Relative humidity (%)
σ	—	Shear stress (Pa)
τ	—	Contact time (min)
ω	—	Angular frequency (rad·s^{-1})

5.2 Hygroscopic Assays

Figure 5.2 shows the studied systems and the employed experimental conditions to determine the hygroscopic properties of three brown seaweeds: *Ascophyllum nodosum* (AN), *Bifurcaria bifurcata* (BB) and *Fucus vesiculosus* (FV). Desorption experiments were carried out employing fresh seaweed. For adsorption experiments seaweeds previously dried at 40°C up to constant weight were employed. Four temperatures and seven different salt solutions were employed to generate different relative humidity atmospheres in order to obtain water sorption isotherms experimental data (X_{eq} *vs* a_w).

5.3 Drying Assays

Figure 5.3 presents the diagram that summarises the experimental conditions and the employed systems in drying assays. Some air conditions remained constant for all experiments (30% relative humidity, 2 $m \cdot s^{-1}$ velocity). Fresh chestnut was dried at one temperature (45°C) and load density (6 $kg \cdot m^{-2}$) whilst fresh seaweeds were dried at four temperatures (35, 50, 60, and 75°C) and two different load densities (thin layer and deep bed configuration). The experimental data of moisture content *vs* time were obtained.

Thirteen different systems were obtained by means of employing this procedure to be used in subsequent experiments, one of dried chestnut (CT) and twelve corresponding to seaweeds (AN, FV and BB) dried at different temperatures (35, 50, 60 and 75°C) at constant load density (15 $kg \cdot m^{-2}$): AN35, AN50, AN60, AN75, FV35, FV50, FV60, FV75, BB35, BB50, BB60 and BB75.

5.4 Flours and Powders

Figure 5.4 displays the materials employed to obtain the different flours (from dried starchy materials: chestnut *Castanea sativa*, Yellow *Zea mays*, Purple *Zea mays* and White *Zea mays*) and powders (from dried seaweeds: AN35, AN50, AN60, AN75, FV35, FV50, FV60, FV75, BB35, BB50, BB60 and BB75) employed in the experimentation of this Thesis.

All dried materials were milled using standard sieves obtaining different flours and powders: CTF, YM200F, YM500F, PM200F, PM500F, WM200F, WM500F, AN35P, AN50P, AN60P, AN75P, FV35P, FV50P, FV60P, FV75P, BB35P, BB50P,

BB60P and BB75P. These systems were physically characterized by means of particle size and colour. Additionally, starchy systems were also characterized by means of damaged and total starch and amylose-amylopectin ratio.

5.5 Seaweed Extracts

Figure 5.5 shows the experimental conditions employed in the procedure to obtain seaweed extracts from twelve different seaweed powders studied in this Thesis (AN35P, AN50P, AN60P, AN75P, FV35P, FV50P, FV60P, FV75P, BB35P, BB50P, BB60P and BB75P). Seaweeds dried powders obtained as mentioned in the previous section (Section 5.4) were rehydrated and then subjected to an ultrasounds assisted extraction (UAE).

The obtained aqueous extracts (AN35E, AN50E, AN60E, AN75E, FV35E, FV50E, FV60E, FV75E, BB35E, BB50E, BB60E and BB75E) were clarificated and phytochemically characterized by means of total solids, total polyphenols and carbohydrate content and antioxidant activity.

5.6 Gluten-free Doughs

Figure 5.6 presents the procedure to manufacture and characterization of gluten-free doughs obtained from starchy flours: CTF, YM200F, YM500F, PM200F, PM500F, WM200F and WM500F.

These flours were added with water and mixed in a laboratory kneader and the doughs obtained (CTD, YM200D, YM500D, PM200D, PM500D, WM200D and WM500D) were then rheologically and thermally characterized.

5.7 Seaweed-enriched gluten-free Doughs

Figure 5.7 displays the main steps performed for manufacture and characterization of gluten-free doughs based on chestnut flour enriched with seaweed powder at different levels (3, 6 and 9% f.b.).

Chestnut flour was mixed with powders obtained from seaweeds dried at 35°C (AN35P, FV35P and BB35P), guar gum and salt. Then water was added in

Mixolab® laboratory kneader and three different tests were performed: simple curves, complete curves and a proposed protocol.

The doughs obtained by combination of chestnut flour with seaweed powder resulted in 9 different systems: CAN03D, CAN06D, CAN09D, CFV03D, CFV06D, CFV09D, CBB03D, CBB06D and CBB09D that were rheologically and thermally characterized.

5.8 gluten-free Product

Figure 5.8 shows the corresponding diagram to the manufacture and characterization process of the gluten-free product: a cookie based on chestnut flour enriched with seaweed powders (AN35P, FV35P and BB35P) at different levels (3, 6 and 9% f.b.).

Chestnut doughs enriched with seaweed powders obtained by the application of the procedure previously mentioned (Section 5.7) were baked and the cookies (CAN03C, CAN06C, CAN09C, CFV03C, CFV06C, CFV09C, CBB03C, CBB06C and CBB09C) obtained were characterized by means of water content, colour and textural properties. Phytochemical characterization of cookies was carried out in order to determine the baking effect on their antioxidant properties. With this goal, cookies were milled and the UAE method was applied to obtain aqueous extracts (AN00CE, FV00CE, BB00CE, AN03CE, FV03CE, BB03CE, AN06CE, FV06CE, BB06CE, AN09CE, FV09CE and BB09CE) that had been characterized by means of total polyphenols and DPPH scavenging activity.

5.9 Wheat Bread Enriched with *Fucus vesiculousus* Powder

Figure 5.9 presents the process to carry out the manufacture and characterization of wheat bread enriched with *Fucus vesiculosus* powder (FV35P) at different levels (2, 4, 6 and 8% f.b.): FV00B, FV02B, FV04B, FV06B and FV08B. In order to determine the effect of FV35P addition to wheat flour doughs the obtained doughs were characterized by means of Lubricated Squeezing Flow (LSF), Dynamic Mechanic-Thermal Analysis (DMTA) and their fermentation process. Finally, after baking, water content, density, colour and textural properties of enriched bread were determined.

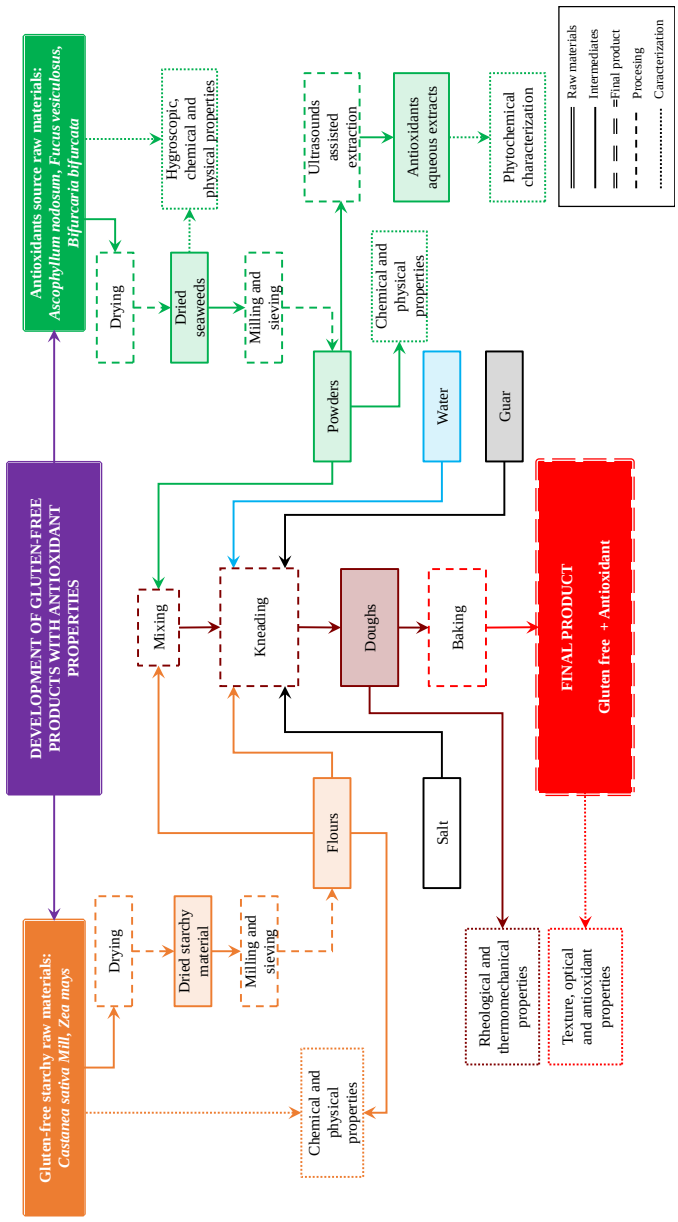

Figure 5.1. General diagram of the Thesis.

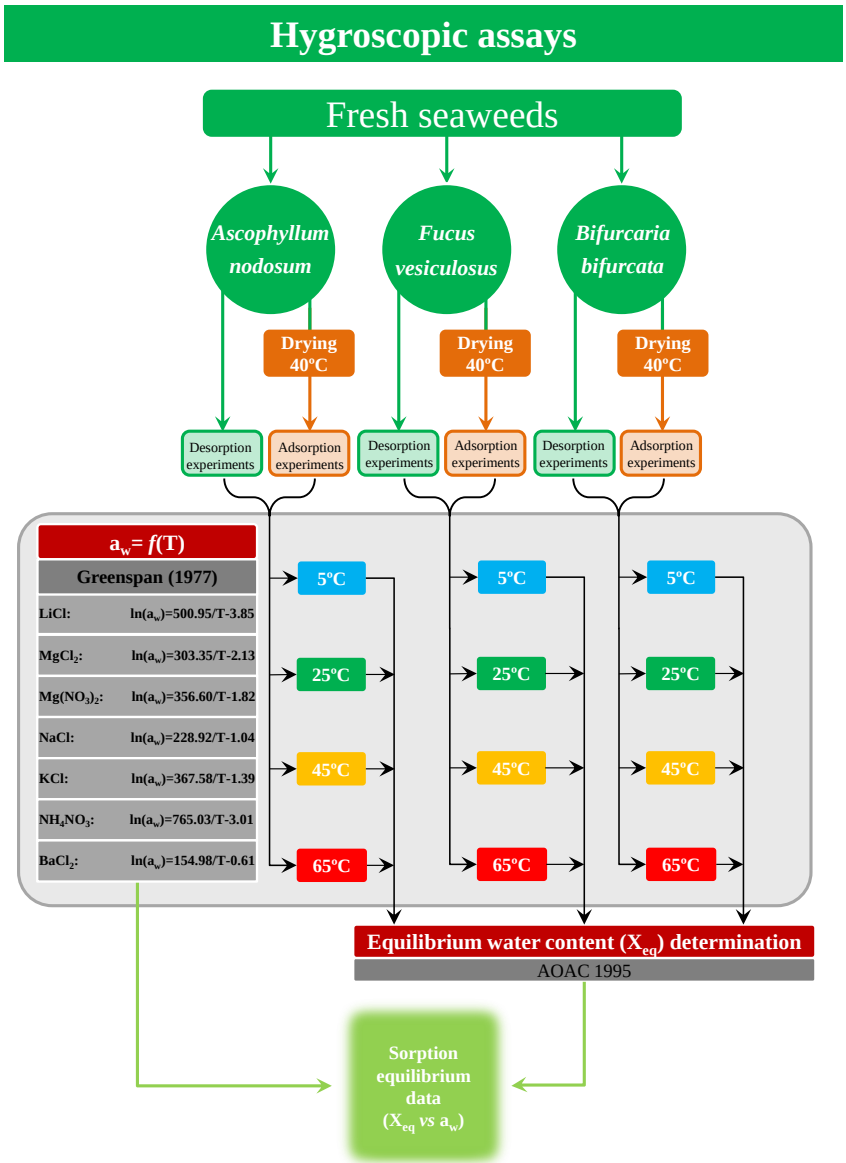

Figure 5.2. Seaweeds experimentally analysed in order to obtain water sorption isotherms.

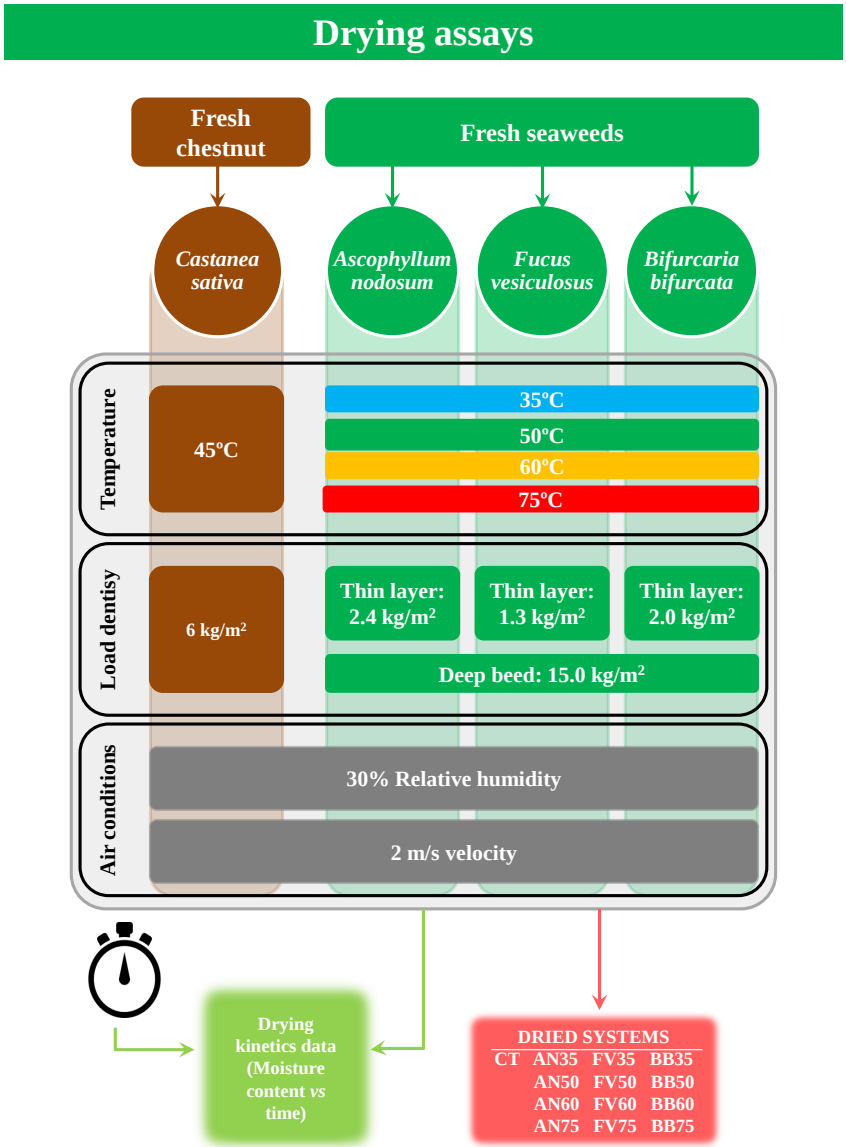

Figure 5.3 Systems experimentally dried in order to obtain air drying kinetics and dried products.

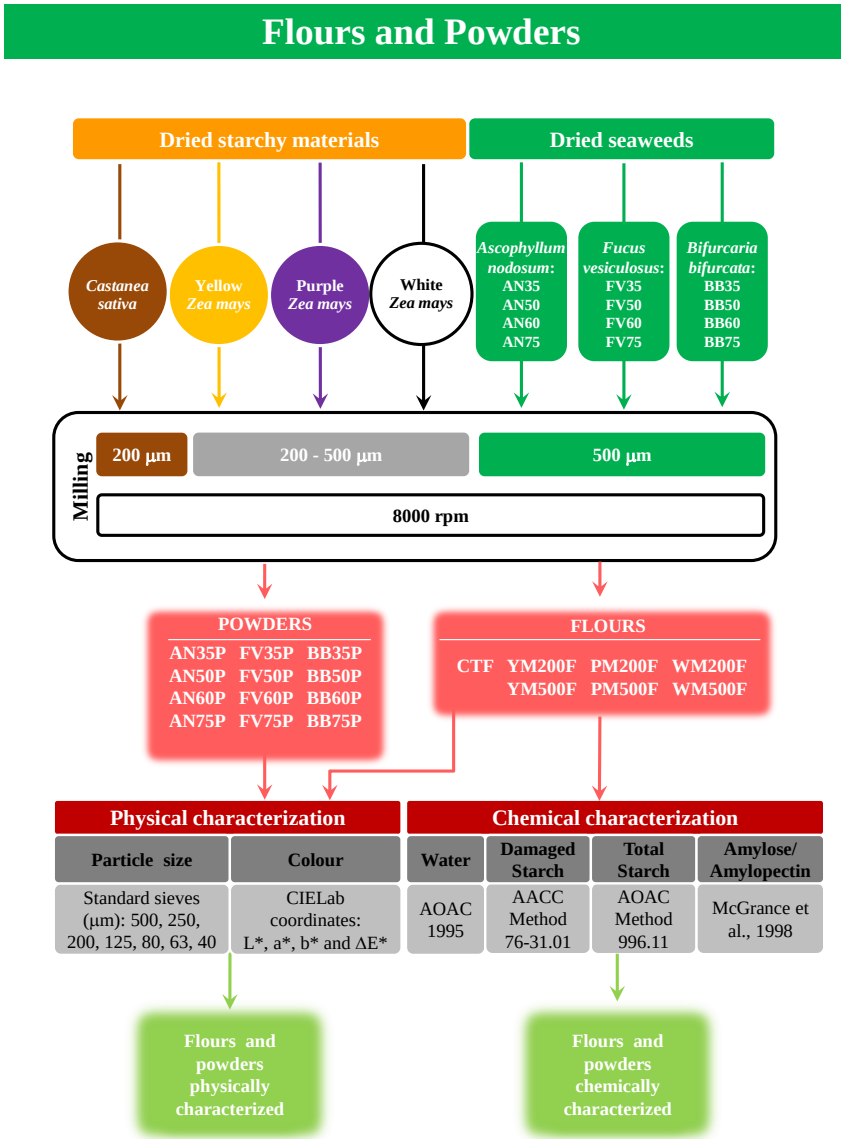

Figure 5.4 Obtained flours and powders from dried systems and the corresponding performed characterization.

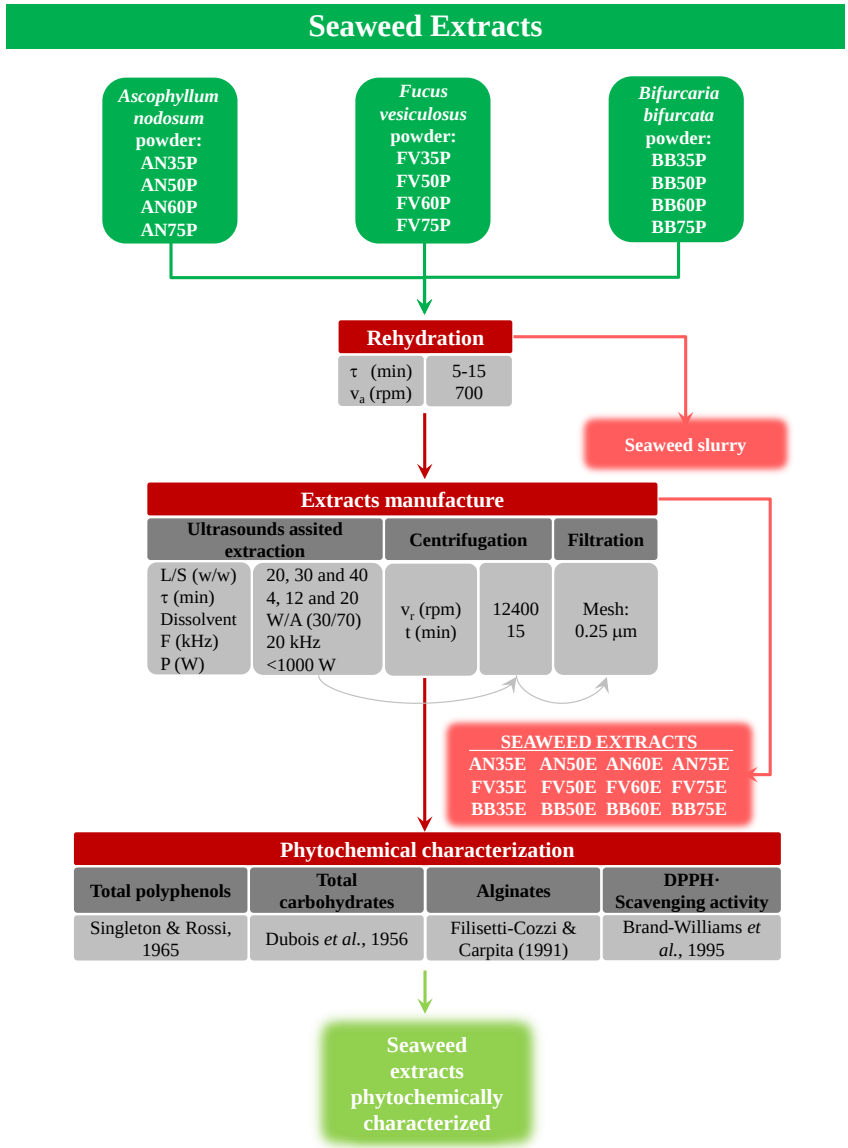

Figure 5.5 Employed systems for seaweed extracts obtention, procedure conditions and performed characterization.

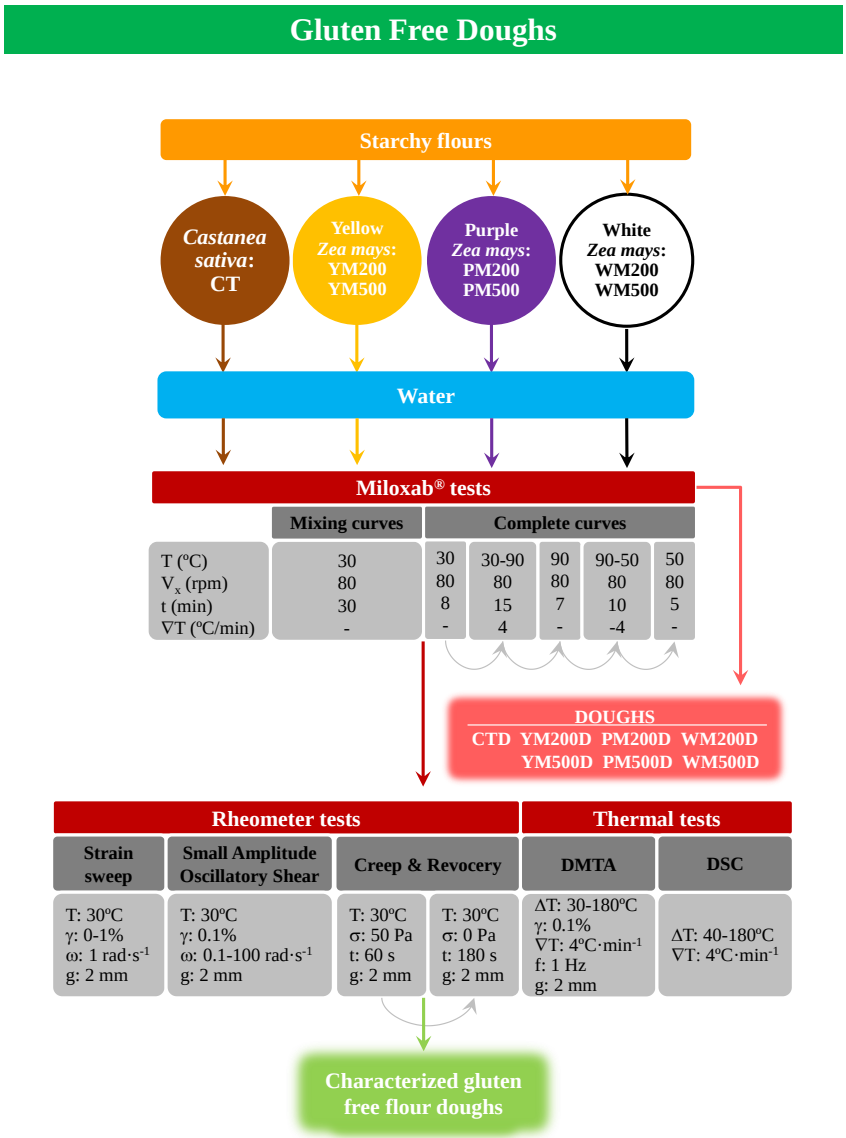

Figure 5.6. Assayed gluten-free flour doughs and the corresponding tests performed.

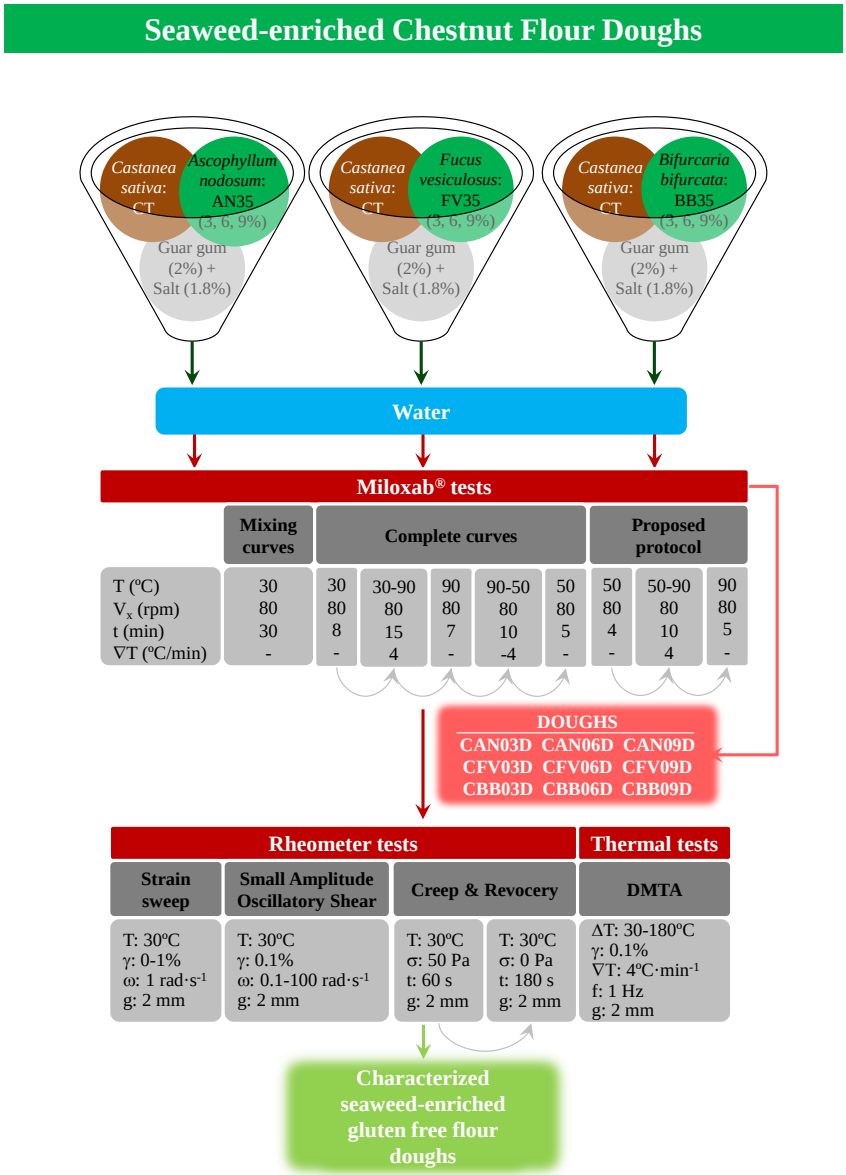

Figure 5.7 Assayed gluten-free doughs from flour blends (chestnut flour + seaweed powders) and the corresponding tests performed.

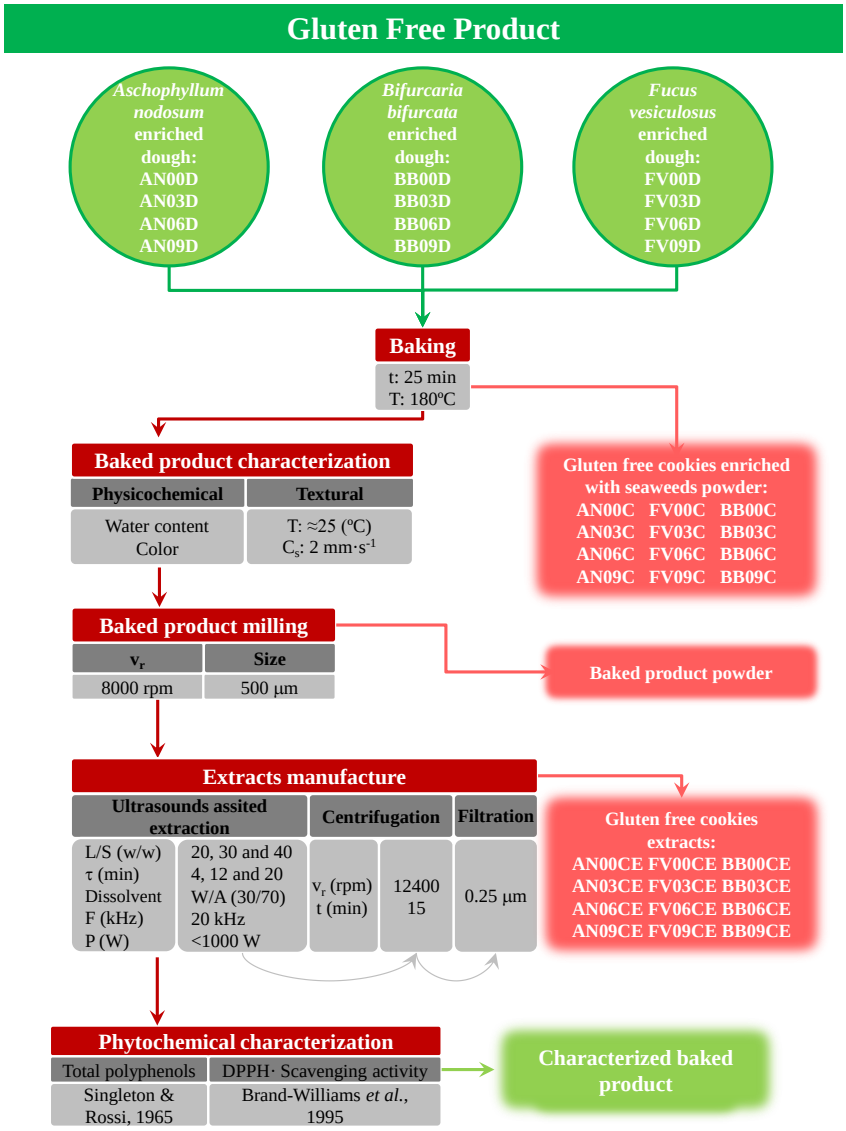

Figure 5.8 Assayed gluten-free products, procedure conditions and performed characterization.

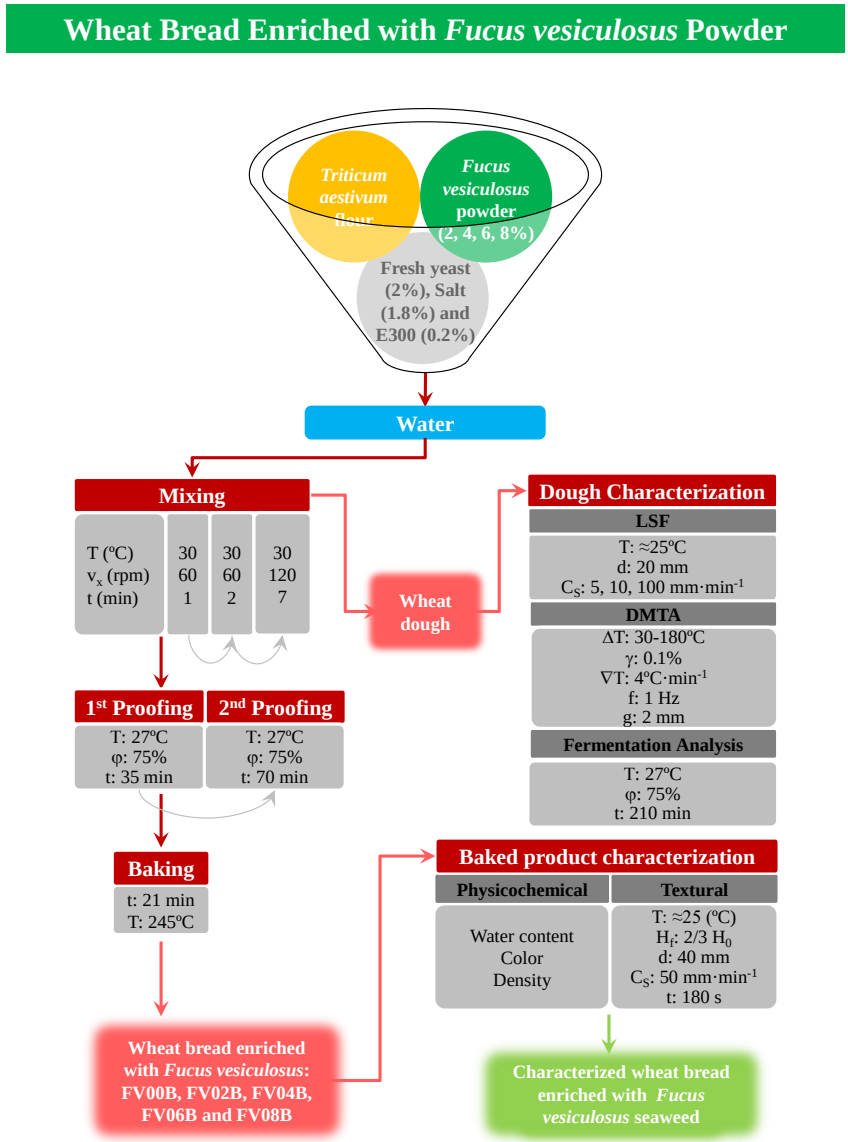

Figure 5.9 Assayed wheat bread enriched with *Fucus vesiculosus* powder, procedure conditions and performed characterization.

Chapter 6

Results and Discussion

In the present chapter the experimental data analysis and treatment as well as mathematical modelling are exposed. It is divided into 10 different sections where the results of hygroscopic properties of seaweed, drying data of fresh materials, physicochemical characterization of milled dried materials, seaweed extracts properties, flour dough mixing behaviour, effect of storage on doughs characteristics, rheological characterization and thermomechanical properties of doughs, baking effect on antioxidant properties of cookies and seaweed addition effect on wheat bread are presented. Each section begins with a brief introduction, subsequently the results and its discussion are showed and finally the main conclusions are presented.

6.1 Hygroscopic characterization: water sorption isotherms and thermodynamic properties

Water adsorption and desorption isotherms at 5, 25, 40 and 55°C for *Bifurcaria bifurcata* and at 5, 25, 45 and 65°C for *Ascophyllum nodosum* and *Fucus vesiculosus* were obtained and fitted by two-parameters Halsey and BET models. A model to estimate equilibrium moisture content for adsorption and desorption processes as function of water activity and temperature simultaneously was obtained by means of linear correlations of Halsey model parameters with temperature.

Water sorption isotherms were analysed by a thermodynamic approach to obtain properties such as net isosteric heats of sorption, net equilibrium heats, differential and integral entropies. Monolayer moisture content evaluated by BET model corresponded to the moisture content at which local minimum integral entropy value was observed for sorption processes. The goodness of the fits was evaluated by means of statistical parameters such as coefficient of determination and root mean square error.[1]

[1]This section has been adapted from the following papers:
MOREIRA, R., CHENLO, F., SINEIRO, J., SÁNCHEZ, M. & ARUFE, S. (2016). Water sorption isotherms and air drying kinetics modelling of the brown seaweed *Bifurcaria bifurcata*. *Journal of Applied Phycology* **28**, 609-618. DOI: http://doi.org/10.1007/s10811-015-0553-1.
MOREIRA, R., CHENLO, F., SINEIRO, J., ARUFE, S. & SEXTO, S. (2016). Water sorption isotherms and air drying kinetics of *Fucus vesiculosus* brown seaweed. *Journal of Food Processing and Preservation* IN PRESS. DOI: http://doi.org/10.1111/jfpp.12997.
MOREIRA, R., SINEIRO, J., CHENLO, F., ARUFE, S. & DÍAZ, D. (2016). Aqueous extracts of *Ascophyllum nodosum* obtained by ultrasound assisted extraction: effect of drying temperature of seaweed on their properties. *Journal of Applied Phycology*. IN PRESS. DOI: http://doi.org/10.1007/s10811-017-1159-6.

Nomenclature

Parameters

a_w	–	Water activity, -.
X_{eq}	–	Equilibrium moisture content, kg water·(kg dried solid)$^{-1}$, d.b.
X_m	–	Monolayer moisture content, Eq. (3.2), d.b.
A	–	Parameter of Halsey model, Eq. (3.6), (kg water·K)·(kg dried solid)$^{-1}$.
B	–	Parameter of Halsey model, Eq. (3.6), -.
C	–	Parameter of BET model, Eq. (3.2), -.
D	–	Parameter of new model, Eq. (6.1), d.b.·K^{-1}.
E	–	Parameter of new model, Eq. (6.1), d.b.
F	–	Parameter of new model, Eq. (6.1), K^{-1}.
J	–	Parameter of new model, Eq. (6.1), -.
T_I	–	Isokinetic temperature, Eq. (4.4), K.
T_{hm}	–	harmonic temperature, Eq. (4.5), K.
ΔH_s	–	Net isosteric heat of sorption, Eq. (4.1), kJ·mol^{-1}.
ΔS_d	–	Differential entropy, Eq. (4.3), kJ·mol^{-1}·K^{-1}.
ΔH_{eq}	–	Net equilibrium heat of sorption, Eq. (4.7), kJ·mol^{-1}.
θ	–	Spreading pressure, Eq. (4.6), J·m^{-2}.

6.1.1 Introduction

The demand of seaweed products for human consumption makes necessary to determine the preservation conditions of this food material. The knowledge of the water sorption is necessary to select the end of drying operation. Moreover, the determination of water sorption isotherms at different temperatures is essential in regard to stability and acceptability of food products, determination of moisture changes which may occur during storage, and for the selection of packaging materials (Bahloul *et al.*, 2008). From water sorption isotherms, some thermodynamic properties such as differential enthalpy (isosteric heat of sorption), differential entropy, integral enthalpy and integral entropy can be estimated to predict physical properties and storage stability. The isosteric heat of sorption is essential to estimate the energy requirement during dehydration process and provides information on the state of water in food products (Vega-Gálvez *et al.*, 2014). The differential entropy of a material is proportional to the number of available sorption sites corresponding to a specific energy level (Moreira *et al.*, 2008). The integral enthalpy provides information of the total energy available to do work, and is related to the energy balance of drying operations, its variation with moisture content indicates the level to which water/substrate interactions is greater than the interactions between water molecules (Fasina *et al.*, 1999). The integral entropy describes the degree of disorder and randomness of motion of water molecules (McMinn & Magee, 2003).

No studies about water sorption isotherms of *Ascophyllum nodosum*, *Bifurcaria bifurcata* and *Fucus vesiculosus* seaweeds were found in the bibliography. Consequently, the aims of the present chapter are to provide at different temperatures experimental equilibrium moisture content (*i*), water sorption isotherms modelling (*ii*) and determine the corresponding thermodynamic properties (*iii*) for the three seaweeds of the present Thesis.

6.1.2 Sorption Isotherms

Experimental data of hygroscopic equilibrium (equilibrium moisture content (X_{eq}) *vs* water activity (a_w)) for desorption and adsorption processes for the three brown seaweeds studied in this Thesis at four temperatures are shown in Figure 6.1. As expected, X_{eq} increased with water activity (a_w) at constant temperature. A more detailed data analysis allows the identification of two different regions for both desorption and adsorption isotherms. At low and intermediate a_w (≤ 0.5) moisture content increases with decreasing temperatures for a constant a_w.

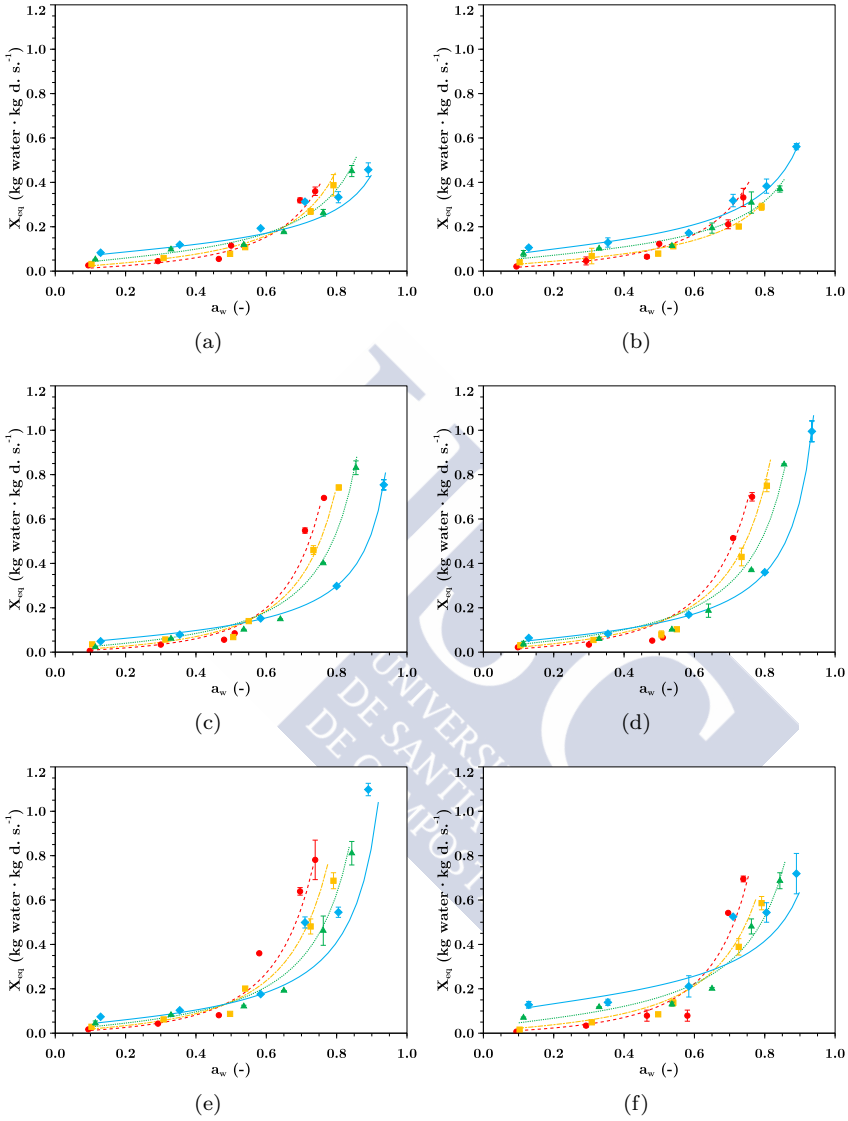

Figure 6.1 Experimental data of X_{eq} for adsorption (a, c and e) and desorption (b, d and f) processes of brown seaweeds *Ascophyllum nodosum* (a, b), *Bifurcaria bifurcata* (c, d) and *Fucus vesiculosus* (e, f) at 5°C (◆), 25°C (▲), 45°C(■, 40°C for *Bifurcaria bifurcata*) and 65°C (●, 55°C for *Bifurcaria bifurcata*). Lines correspond to proposed model (Eq. (6.1)).

At intermediate a_w values (0.5-0.6) there is a crossover point from which the temperature effect is reversed. This behaviour can be related to the solubility of the polysaccharides (mainly alginates, fucoidan, and mannitol) and proteins present in the material. Other researchers reported previously this behaviour for some food materials such as loquat and quince fruits (Moreira *et al.*, 2008) and seaweeds such as *Gelidium sesquipedale* (Ait Mohamed *et al.*, 2005) and *Gracilaria* (Lemus *et al.*, 2008).

The comparison of water adsorption and desorption isotherms at the same temperature allow the determination of hysteresis cycles. In general, different behaviours of hysteresis cycle can be observed depending on temperature, Figure 6.2. Specifically, for *Ascophyllum nodosum* water sorption isotherms at a_w <0.5 no important differences between desorption and adsorption were observed whereas at higher a_w the higher moisture contents corresponded to water desorption equilibrium, when temperature was $\leq$ 25°C, and to water adsorption equilibrium when temperature was $\geq$ 45°C.

Bifurcaria bifurcata water sorption isotherms displayed a similar behaviour. In the range of a_w between 0.10 and 0.50 no differences between water adsorption and desorption equilibrium data were observed indicating the absence of the hysteresis cycle. At high a_w ($>$ 0.5) and temperatures above 40°C higher moisture content corresponded to water adsorption equilibrium. At 25°C no cycle was observed and at 5°C the behaviour was reversed.

In the case of *Fucus vesiculosus* water sorption isotherms at low a_w range ($<$ 0.5), the differences between water adsorption and desorption isotherms were noticeable. At low temperatures ($<$ 25°C), desorption isotherms showed larger water content than adsorption isotherms at the same a_w whereas this hysteresis cycle was not noticeable for temperatures $>$ 45°C. In the same range of a_w, at constant a_w value, X_{eq} decreased with increasing temperature. A crosspoint (from 0.6 to 0.7 for desorption and from 0.5 to 0.6 for adsorption) of sorption isotherms was observed. After cited crosspoint, adsorption and desorption isotherms displayed the opposite thermal effect.

These results could be related to structural changes during dehydration processes of samples used for adsorption experiments where hydrophilic compounds are more accessible (on surface) to water or by the process of solubility of some compounds in water promoted by temperature and structural changes (Bell & Labuza, 2000). In general, brown seaweeds contain relevant amounts of polysaccharides, alginates and fucoidans, among others (Heffernan *et al.*, 2014). This behaviour was also observed in other seaweeds with high polysaccharides content such as *Gracilaria chilensis* (Lemus *et al.*, 2008), *Gelidium sesquipedale* (Ait Mohamed *et al.*, 2005) and *Macrocystis Pyrifera*

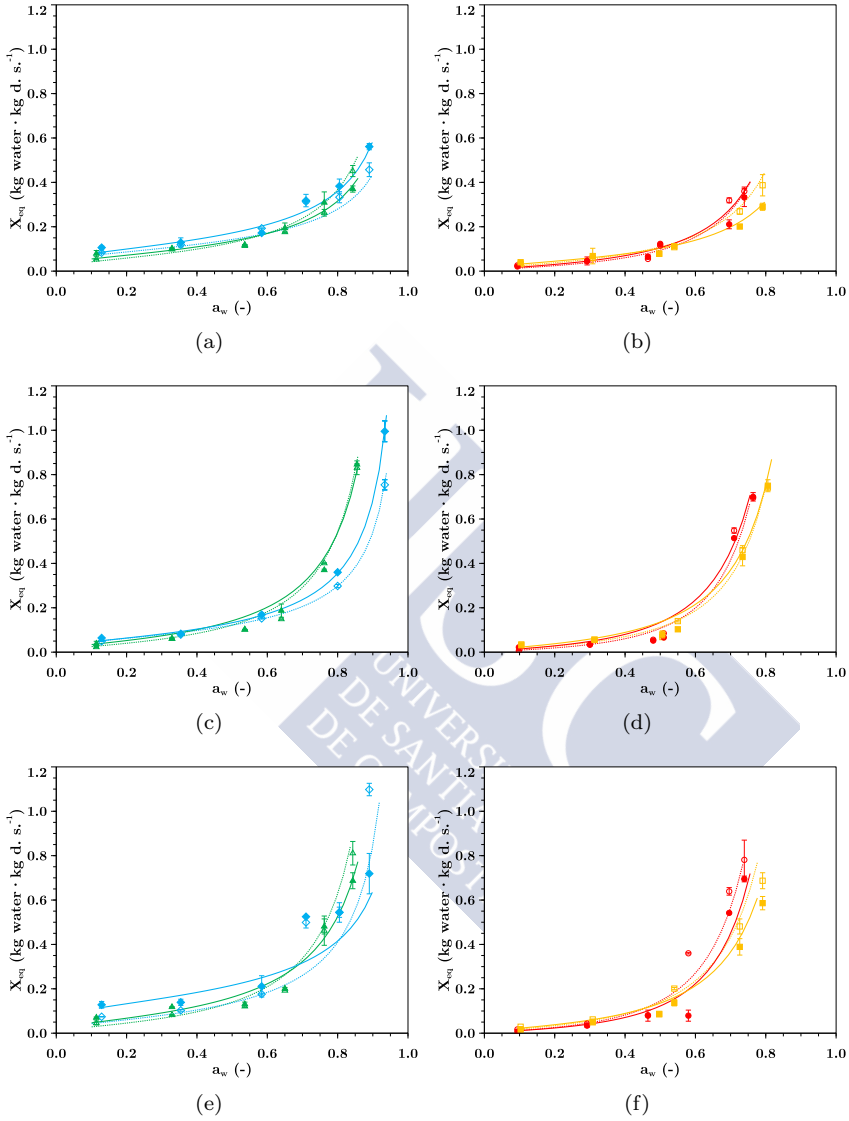

Figure 6.2 Hysteresis cycles of brown seaweeds *Ascophyllum nodosum* (a, b), *Bifurcaria bifurcata* (c, d) and *Fucus vesiculosus* (e, f) at different temperatures: 5°C (◆), 25°C (▲), 45°C(■, 40°C for *Bifurcaria bifurcata*) and 65°C (●, 55°C for *Bifurcaria bifurcata*). Empty symbols correspond to adsorption process. Lines correspond to proposed model (Eq. (6.1)).

(Vega-Gálvez *et al.*, 2014). These results suggest that the hysteresis phenomenon could depend on temperature.

Water sorption isotherms were satisfactorily fitted, at a_w <0.5, employing BET model ($R^2 \geq 0.90$). In general, all water sorption isotherms presented a C parameter of BET model higher than 1. That indicates that all water sorption isotherms are type II according to the BET classification (Brunauer *et al.*, 1940). In general, this parameter decreased as temperature increased indicating a certain trend to change from type II to type III isotherm. Namely, for *Ascophyllum nodosum* seaweed, the monolayer water content (X_m) decreased linearly with absolute temperature from 0.08±0.01 to 0.04±0.01 d.b with temperature (5-65°C) for water desorption and from 0.08±0.01 up to 0.03±0.01 d.b for water adsorption. For *Bifurcaria bifurcata* seaweeds X_m decreases (from ≈0.07 to ≈0.03 d.b.) with increasing temperature for adsorption and desorption processes and in the case of *Fucus vesiculosus* X_m values decreased with increasing temperature from 5°C (0.07±0.01 d.b. for adsorption; 0.09±0.02 d.b., for desorption) up to 65°C (0.06±0.01 d.b., for adsorption and 0.06±0.01 for desorption).

The magnitude of X_m (monolayer water content) is related to the optimum moisture content at which food spoilage processes are minimized and allows the estimation of the most suitable air conditions for storage (Bell & Labuza, 2000) or processing. Hence, by means of the corresponding a_w for each X_m from the water adsorption-desorption isotherms data the most suitable air conditions for processing and storage can be established. Namely, for *Ascophyllum nodosum*, relative humidity of air around 7% is equally necessary for wetter and drier seaweeds than monolayer moisture content, where water desorption and adsorption processes take place, respectively, during storage in order to achieve the equilibrium at 5°C. A relative humidity of air about 25% is necessary for drier seaweeds than monolayer moisture content at temperatures ≥ 25°C. When desorption process takes place, a linear increase of relative humidity of air from 11% (25°C) to 31% (65°C) is necessary to minimize spoilage processes in the material. In the case of *Bifurcaria bifurcata* seaweeds, the adequate relative humidity for seaweeds that desorb water is 20% (independently on temperature) and a range from 23 to 30% with increasing temperature in the tested range when adsorption of water takes place. For *Fucus vesiculosus*, atmospheres with relative humidity around 8% at 5 and 25°C and around 30% at 45 and 65°C are adequate for seaweeds that desorb water during storage (or processing). In the case that water adsorption takes place, relative humidity of surrounding atmosphere increases from 13 up to 25 % with increasing temperature.

Halsey model was employed to fit water sorption isotherms data throughout the whole range of water activities. Several models like Caurie, Oswin, Henderson,

Halsey and GAB were also tested to fit the experimental data throughout the whole range of water activities but Halsey model was finally selected based on the highest coefficients of determination ($R^2 \geq 0.963$) at low E_{RMS} (≤ 0.077) obtained. The values of the corresponding parameter for each model are presented, at the end of this Section, in Tables 6.2, 6.3 and 6.4 for *Ascophyllum nodosoum*, *Bifurcaria bifurcata* and *Fucus vesiculosus*, respectively. Additionally, except in the case of *Ascophyllum nodosum* water desorption data, the Halsey model parameters, A and $1/B$ were found to show linear trends with temperature. These linear correlations allowed the generation of a four-parameters model, Eq. (6.1), for water adsorption and desorption equilibria of three seaweeds:

$$X_{eq} = \left(\frac{-(D + ET)}{Tln(a_w)} \right)^{(FT+J)} \tag{6.1}$$

where D (d.b.·K^{-1}), E (d.b.), F (K^{-1}) and J (-) are the model parameters and the corresponding values are shown in Tables 6.2, 6.3 and 6.4. The coefficient of determination ($R^2 > 0.95$) and root mean square error ($E_{RMS} < 0.099$) are acceptable taking into account that the model can be used to determine equilibrium data for any temperature and water activity jointly in the range tested.

Water desorption and adsorption equilibrium moisture content fitting of brown seaweeds employing Eq. (6.1) are plotted in Figure 6.1.

6.1.3 Thermodynamic Properties

The net isosteric heat of sorption (ΔH_s, kJ·mol^{-1}) was determined using Eq. (4.1) for water desorption and adsorption processes. The results at a mean temperature of 35ºC were acceptably fitted (R^2 >0.953) using the Tsami model (Eq. (4.2)).

In Figure 6.3 it can be observed that, in general, there is an exponential decrease in ΔH_s with X_{eq} increases. At high X_{eq} the ΔH_s approaches to zero, meaning that the value of the heat of sorption is the same as the heat of vaporisation/condensation of water.

Namely, for *Ascophyllum nosodum* ΔH_s decrease from 13.2 to 0.2 kJ·mol^{-1} with an increase of X_{eq} from 0.11 to 0.30 d.b. and from 27.1 to 0.04 kJ·mol^{-1} with an increase of X_{eq} from 0.08 to 0.24 d.b. for water desorption and adsorption data, respectively. *Bifurcaria bifurcata* presented a ΔH_s decrease from 18.7 to 0.04 kJ·mol^{-1} with an increase of X_{eq} from 0.05 to 0.17 d.b., and from 16.6 to 0.01 kJ·mol^{-1} with an increase of X_{eq} from 0.07 to 0.16 d.b. for water adsorption

and desorption data, respectively. Regarding *Fucus vesiculosus*, ΔH_s decreased from 13.4 to 0.01 kJ·mol^{-1} increasing X_{eq} from 0.13 to 0.24 d.b. for desorption and from 21.2 to 0.01 kJ·mol^{-1} from 0.07 to 0.34 d.b. for adsorption.

Similar effects of moisture content on the net isosteric heat of sorption were reported by Tsami (1991) for dried currants, figs, prunes and apricots, Ait Mohamed *et al.* (2005) for the seaweed *Gelidium sesquipedale* and Lemus *et al.* (2008) for the red seaweed *Gracilaria chilensis* which, *i.e.*, reported values in the case of water desorption experiments where an increase on X_{eq} from 0.07 up to 0.22 d.b. decreased ΔH_s from 15.90 to 0.26 kJ·mol^{-1}. The physical explanation for the rapid increase in ΔH_s at low X_{eq} may be that in the initial stages of sorption there are highly active polar sites on the surface of the food material, which are covered with water molecules to form a monomolecular layer. These molecules are tightly bound to the food and the amount of energy involved in sorption process is very high. As the moisture content increases the strength of water molecule binding decreases such as the ΔH_s.

ΔS_d is proportional to the number of available sorption sites at a specific energy level, and the corresponding values can be calculated using Eq. (4.3) at different moisture content. Differential entropy depends strongly on moisture content with an exponential trend in the same way exhibited for the differential enthalpy. This trend is in agreement with literature data (Moreira *et al.* (2008) and Vega-Gálvez *et al.* (2014)).

The acceptable linear ($R^2 > 0.992$) relationships between ΔH_s (Eq. (4.1)) and ΔS_d (Eq. (4.3)), allowed the determination of the isokinetic temperature of sorption, T_I by Eq. (4.4). T_I for *Ascophyllum nodosum* varied from 355.8 K for desorption to 341.2 K for adsorption processes. The values obtained for *Bifurcaria bifurcata* experiments were 331.4 K and 404.4 K for water desorption and adsorption experiments, respectively and, in the case of *Fucus vesiculosus*, the corresponding values of T_I for water desorption and adsorption processes were 342.8 K and 363.2 K, respectively.

These values are in the range of reported data for pullulan-sodium alginate films (Xiao & Tong, 2013). Using Eq. (4.5), harmonic mean temperature (T_{hm}) was 303.3 K for both water desorption and adsorption experiments for *Bifurcaria bifurcata* and 306.5 for *Ascophyllum nodosum* and *Fucus vesiculosus*. The T_{hm} value is significantly lower than the values of T_I obtained confirming the suitability of the isokinetic theory. These results indicated that compensation theory can be applied throughout the range of water activities tested for all seaweeds. Additionally, in all cases $T_I > T_{hm}$, leading to the conclusion that the processes can be characterised as enthalpy driven.

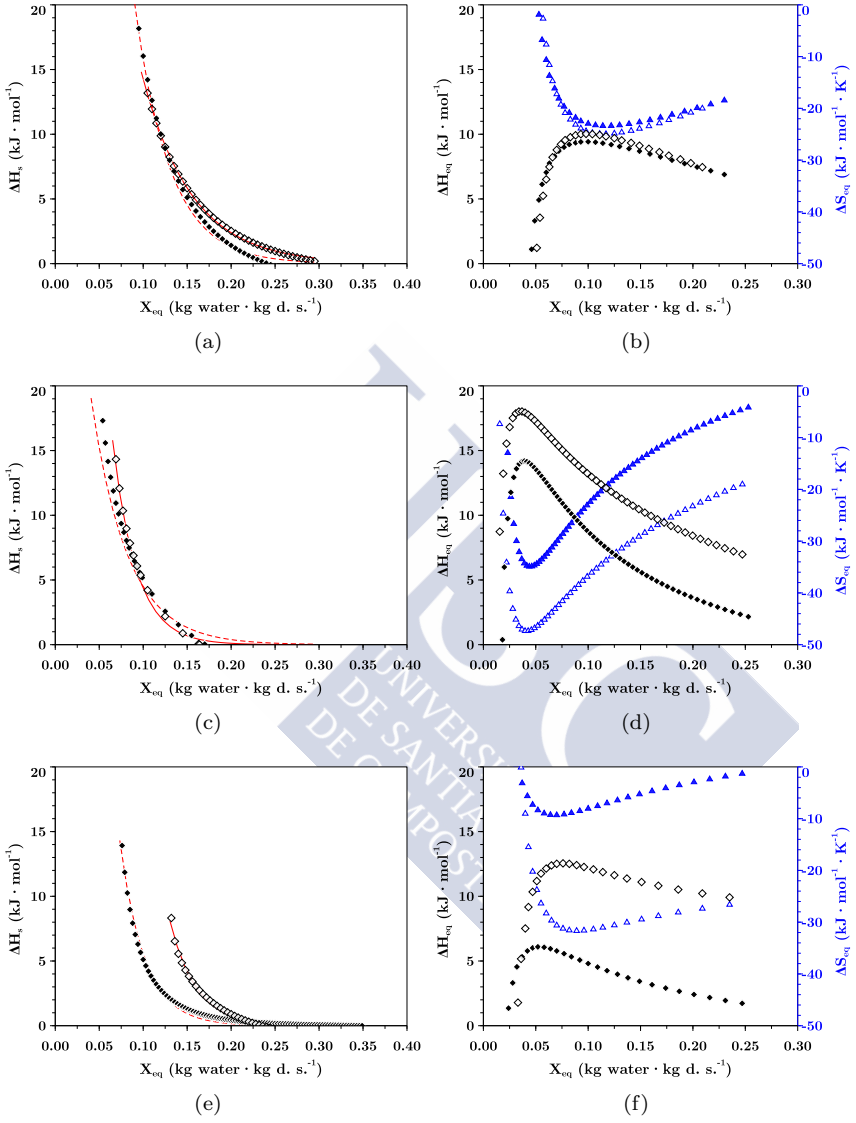

Figure 6.3 Net isosteric heat of sorption ((desorption (◇), adsorption (♦)), integral enthalpy (desorption (◇), adsorption (♦)) and integral entropy (desorption (△), adsorption (▲)) *vs* X_{eq} at 35°C for brown seaweeds *Ascophyllum nodosum* (a, b), *Bifurcaria bifurcata* (c, d) and *Fucus vesiculosus* (e, f). Tsami model (Eq. (4.2)), desorption (−) and adsorption (−−).

The spreading pressure was calculated using Eq. (4.6). The results as it can be seen in Figure 6.4 in the case of *Ascophyllum nodosum* seaweed in example, indicate that the spreading pressure increases with water activity, and decreases with temperature, at a given water activity. The spreading pressure values and its trends with respect to temperature and water activity are comparable to those reported for carboxymethyl cellulose and tragacanth gums (Torres *et al.*, 2012).

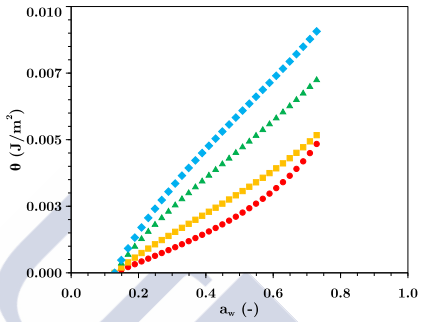

Figure 6.4 Spreading pressure (θ) *vs* water activity (a_w) for *Ascophyllum nodosum* brown seaweed at different temperatures (5°C (♦), 25°C (▲), 45°C (■) and 65°C (●).

The net integral enthalpy (ΔH_{eq}) at each spreading pressure was obtained by fitting Eq. (4.6) to the equilibrium data. The variation in ΔH_{eq} with X_{eq} for water desorption and adsorption experiments at a mean temperature of 35°C is shown in Figure 6.3 (a, b, c). In general, ΔH_{eq}) increases until achieve a maximum and then decreases with increasing X_{eq}. This behaviour can be explained, because at low moisture contents, water is absorbed on the most accessible locations on the surface area of the solid. The increase of moisture content causes swelling of material, and then new high energy sites are opened, and new water binding can be developed. This behaviour explains the increasing of ΔH_{eq} at low moisture contents. The decreasing of ΔH_{eq} is due to the fact that less favourable locations are covered with water molecules, forming multiple layers of sorbed water. A similar trend has been reported for potato (McMinn & Magee, 2003) and carboxymethyl cellulose and tragacanth gums (Torres *et al.*, 2012). ΔH_{eq} for water desorption was higher than the corresponding parameter for water adsorption (Figure 6.3). A similar trend was obtained for potato starch and highly amylose powder starch (Al-Muhtaseb *et al.*, 2004).

Ascophyllum nodosum presented a maximum value of ΔH_{eq} of 10.0 and 9.4 kJ·mol^{-1} corresponding to X_{eq} values of 0.10 and 0.09 d.b. for desorption and adsorption, respectively. For *Bifurcaria bifurcata* at low X_{eq}, ΔH_{eq} increases until maximum values of 18.0 and 14.2 kJ·mol^{-1} at moisture contents of 0.04

and 0.03 d.b. for desorption and adsorption, respectively. In the case of *Fucus vesiculosus* at low X_{eq} values, ΔH_{eq} increased up to 12.6 and 6.1 kJ·mol^{-1} at moisture content of 0.09 and 0.06 d.b. for desorption and adsorption, respectively.

The net integral entropy (ΔS_{eq}) was calculated using Eq. (4.8). ΔS_{eq} trend with moisture content for water desorption and adsorption experiments are also shown in Figure 6.3 (a, b, c). In general, ΔS_{eq} values descends until to achieve a minimum value. The negative entropy values are associated to the existence of chemical adsorption and/or structural modifications of the adsorbent (Iglesias *et al.*, 1976). At low water activity range, a decrease in the net integral entropy values is possibly caused by localization of water (loss of rotational freedom and degree of randomness) due to the strongest binding sites with water molecules and solid (McMinn & Magee, 2003).

Ascophyllum nodosum presented a minimum value of ΔS_{eq} of -25.0 and -23.4 kJ·mol^{-1}·K^{-1} associated to X_{eq} of 0.12 and 0.10 d.b. for desorption and adsorption experiments, respectively. For *Bifurcaria bifurcata*, ΔS_{eq} reaches a minimum value of -47.4 and -34.9 kJ·mol^{-1}·K^{-1} associated to X_{eq} of 0.05 and 0.04 d.b. for desorption and adsorption experiments, respectively. In the case of *Fucus vesiculosus* ΔS_{eq} reached a minimum value of -31.7 and -9.3 kJ·mol^{-1}·K^{-1} at X_{eq} of 0.10 and 0.07 d.b. for desorption and adsorption experiments, respectively. A similar trend has been reported for other food materials previously (Moreira *et al.* (2008); Torres *et al.* (2012)).

The minimum ΔS_{eq} can be interpreted as the water activity at which the product has the best stability for a food product (Domínguez *et al.* (2007); Nunes & Rotstein (1991)) that could help to establish the best storage or processing conditions as in the case of X_m parameter of BET model. In fact, X_{eq} that corresponded to the minimum ΔS_{eq} was very close to X_m parameter of BET model for all studied seaweeds (Tables 6.2, 6.3 and 6.4), that leads to the conclusion that both analyses were in god agreement.

Table 6.2 BET (Eq. (3.2)), Halsey (Eq. (3.6)) and proposed model (Eq. (6.1)) parameters and their corresponding statistical coefficients (R^2, E_{RMS}) values for water sorption isotherms data fitting of brown seaweed *Ascophyllum nodosum*.

Model	**Parameter**	**Desorption**				**Adsorption**			
		5°C	**25°C**	**45°C**	**65°C**	**5°C**	**25°C**	**45°C**	**65°C**
BET* (3.2)	X_m (d.b.)	0.090±0.008	0.070±0.003	0.044±0.014	0.039±0.010	0.088±0.003	0.060±0.004	0.043±0.002	0.030±0.001
	C (-)	35.0±3.5	32.0±2.5	49.5±5.3	10.0±0.1	49.7±8.7	30.4±3.7	31.1±4.3	46.5±0.4
	R^2	0.988	0.922	0.910	0.995	0.999	0.910	0.977	0.951
	E_{RMS} (d.b.)	0.026	0.021	0.006	0.001	0.013	0.009	0.004	0.003
Halsey Eq. (3.6)	A (d.b.·K)	13.8±0.04	14.3±0.3	20.80±3.4	45.2±6.5	8.4±1.8	21.9±2.3	36.0±2.8	54.9±2.9
	1/B (-)	0.65±0.05	0.75±0.06	0.995±0.16	1.43±0.05	0.55±0.03	0.98±0.03	1.29±0.13	1.56±0.02
	R^2	0.98	0.96	0.99	0.97	0.963	0.988	0.994	0.974
	E_{RMS} (d.b.)	0.023	0.021	0.01	0.02	0.025	0.015	0.01	0.024
Model Eq. (6.1)	D (d.b.·K)	-	-	-	-	-206.5±13.84			
	E (d.b.)	-	-	-	-	0.768±0.044			
	F (K^{-1})	-	-	-	-	0.017±0.001			
	J (-)	-	-	-	-	-4.05±0.35			
	R^2	-	-	-	-	0.959	0.986	0.993	0.974
	E_{RMS} (d.b.)	-	-	-	-	0.049	0.025	0.023	0.027

*BET model was applied for $a_w \leq 0.5$; d.b.:kg water·(kg dried solid)$^{-1}$

Table 6.3 BET (Eq. (3.2)), Halsey (Eq. (3.6)) and proposed model (Eq. (6.1)) parameters and their corresponding statistical coefficients (R^2, E_{RMS}) values for water sorption isotherms data fitting of brown seaweed *Bifurcaria bifurcata*.

Model	Parameter	Desorption				Adsorption			
		5°C	**25°C**	**40°C**	**55°C**	**5°C**	**25°C**	**40°C**	**55°C**
BET* Eq. (3.2)	X_m (d.b.)	0.072±0.006	0.047±0.008	0.041±0.007	0.027±0.001	0.065±0.001	0.055±0.002	0.047±0.011	0.043±0.001
	C (-)	11.9±2.1	20.1±3.4	16.7±3.3	23.8±5.4	11.5±2.9	5.1±0.7	3.4±1.2	2.4±0.1
	R^2	0.977	0.995	0.999	0.996	0.994	0.999	0.901	0.99
	E_{RMS} (d.b.)	0.011	0.004	0.002	0.002	0.005	0.002	0.015	0.003
Halsey Eq. (3.6)	A (d.b.·K)	18.9±2.2	41.7±0.1	57.9±1.0	76.2±1.2	13.4±2.5	41.5±1.3	57.0±0.7	75.7±0.4
	B^{-1} (-)	0.87±0.08	1.47±0.07	1.77±0.09	2.09±0.04	0.79±0.06	1.47±0.04	1.63±0.02	1.96±0.01
	R^2	0.990	0.999	0.995	0.981	0.999	0.996	0.991	0.976
	E_{RMS} (d.b.)	0.007	0.011	0.019	0.039	0.004	0.019	0.027	0.046
Model Eq. (6.1)	D (d.b.·K)	-297.9±4.2				-328.3±11.5			
	E (d.b.)	1.139±0.010				1.232±0.041			
	F (K^{-1})	0.024±0.001				0.022±0.002			
	J (-)	-5.84±0.16				-5.38±0.32			
	R^2	0.999	0.998	0.995	0.981	0.998	0.994	0.990	0.975
	E_{RMS} (d.b.)	0.016	0.015	0.021	0.040	0.021	0.030	0.028	0.047

*BET model was applied for $a_w \leq 0.5$; d.b.:kg water·(kg dried solid)$^{-1}$

Table 6.4 BET (Eq. (3.2)), Halsey (Eq. (3.6)) and proposed model (Eq. (6.1)) parameters and their corresponding statistical coefficients (R^2, E_{RMS}) values for water sorption isotherms data fitting of brown seaweed *Fucus vesiculosus*.

Model	**Parameter**	**Desorption**				**Adsorption**			
		5°C	**25°C**	**45°C**	**65°C**	**5°C**	**25°C**	**45°C**	**65°C**
	X_m (d.b.)	0.092±0.023	0.066±0.005	0.057±0.007	0.064±0.002	0.073±0.003	0.060±0.001	0.064±0.040	0.062±0.002
BET*	C (-)	116.0±1.4	93.5±2.1	2.9±0.9	1.7±1.1	41.0±2.9	12.0±1.4	8.8±4.5	2.6±0.2
Eq. (3.2)	R^2	0.948	0.943	0.996	0.983	0.997	0.993	0.991	0.997
	E_{RMS} (d.b.)	0.019	0.013	0.004	0.007	0.004	0.006	0.016	0.002
	A (d.b.·K)	21.2±4.9	29.5±8.5	53.5±2.2	87.4±0.1	26.3±4.0	44.0±3.2	65.9±2.1	92.9±6.7
Halsey	B^{-1} (-)	0.69±0.03	1.05±0.07	1.56±0.06	2.07±0.09	0.93±0.10	1.38±0.03	1.53±0.06	2.08±0.19
Eq. (3.6)	R^2	0.985	0.999	0.996	0.992	0.966	0.994	0.990	0.996
	E_{RMS} (d.b.)	0.043	0.048	0.014	0.026	0.042	0.026	0.077	0.040
	D (d.b.K)	-295.2±2.9				-284.1±1.0			
	E (d.b.)	1.110±0.060				1.110±0.210			
Model	F (K^{-1})	0.023±0.004				0.018±0.007			
Eq. (6.1)	J (-)	-5.82±0.02				-4.04±0.04			
	R^2	0.952	0.983	0.997	0.996	0.986	0.996	0.989	0.991
	E_{RMS} (d.b.)	0.099	0.043	0.057	0.052	0.176	0.046	0.079	0.047

*BET model was applied for $a_w \leq 0.5$; d.b.:kg water·(kg dried solid)$^{-1}$

The section in tweets

- At water activities (a_w) lower than 0.5, equilibrium moisture content (X_{eq}) increases with decreasing temperatures.
- At constant a_w and above a crossover point, the temperature effect on X_{eq} is reversed.
- Temperature affects differently the hysteresis cycles amongst adsorption-desorption equilibrium for each seaweed.
- Halsey model successfully correlates water sorption isotherms data of all studied seaweeds throughout the whole range of water activity.
- Net isosteric heat of sorption decreases with increasing moisture content.
- Water desorption and adsorption processes on the studied seaweeds are enthalpy driven.
- The best storage conditions for the studied seaweeds as function of their moisture content can be established through thermodynamic studies.

USC
UNIVERSIDADE
DE SANTIAGO
DE COMPOSTELA

6.2 Seaweeds drying

Air drying kinetics at 35, 50, 60 and 75°C of brown seaweeds *Bifurcaria bifurcata*, *Fucus vesiculosus* and *Ascophyllum nodosum* using two different configurations (deep bed and thin layer) and seaweed shrinkage during drying at these temperatures were determined. Additionally, in the case of *Ascophyllum nodosum* seaweed, drying studies at 35°C using different load densities were carried out. Page model was used to fit seaweed drying kinetics data. Moreover, thin layer configuration drying data of constant drying rate period were employed to evaluate heat and mass transfer coefficients whilst falling drying rate period data were employed for determination of effective coefficients of water diffusion on seaweed assuming cylinder geometry.[2]

[2]This section has been adapted from the following papers and others in writing process:
MOREIRA, R., CHENLO, F., SINEIRO, J., SÁNCHEZ, M. & ARUFE, S. (2016). Water sorption isotherms and air drying kinetics modelling of the brown seaweed *Bifurcaria bifurcata*. *Journal of Applied Phycology* **28**, 609-618. DOI: http://doi.org/10.1007/s10811-015-0553-1.
MOREIRA, R., CHENLO, F., SINEIRO, J., ARUFE, S. & SEXTO, S. (2016). Water sorption isotherms and air drying kinetics of *Fucus vesiculosus* brown seaweed. *Journal of Food Processing and Preservation* IN PRESS. DOI: http://doi.org/10.1111/jfpp.12997.
CHENLO, F., ARUFE, S., DÍAZ, D., TORRES, M. D., SINEIRO, J. & MOREIRA, R. (2017). Air drying and rehydration characteristics of *Ascophylum nodosum* and *Undaria Pinnatifida* brown seaweeds. Submitted to: *Journal of Applied Phycology*.

Nomenclature

Parameters

D_0	–	Arrhenius factor, $m^2 \cdot s^{-1}$.
D_{eff}	–	Effective water diffusion coefficient, $m^2 \cdot s^{-1}$.
E_a	–	Activation energy, J·mol−1.
h_t	–	Heat transfer coefficient during constant drying rate period, $W \cdot m^{-2} \cdot K^{-1}$.
k	–	Page model parameter, min^{-n}.
K_t	–	Mass transfer coefficient during constant drying rate period, $m \cdot s^{-1}$.
MR	–	Moisture ratio, (-).
n	–	Page model parameter, (-).
r	–	Characteristic dimension of seaweeds (radio), m.
R	–	Universal gas constant, $J \cdot mol^{-1} \cdot K^{-1}$.
S_X	–	Monolayer surface area at each moisture content, m^2.
T	–	Temperature, ºC.
w	–	Mass flow of evaporated water, kg water·kg d.b.$^{-1} \cdot s^{-1}$.
w_s	–	Specific drying rate, kg water kg d.b.$^{-1}$ m^{-2} min^{-1}.
X	–	Moisture content, kg water·(kg dried solid)$^{-1}$, d.b..

6.2.1 Introduction

The experimental determination of drying kinetics under different conditions allows the knowledge of drying time and the existence of constant and falling drying rate periods. Usually, the end of drying operation is given by the equilibrium moisture content of the material during storage. This fact makes necessary the knowledge of the equilibrium moisture value, which is obtained by the desorption isotherm of the product, see Section 6.1.

Traditionally, the drying of seaweeds is carried out by solar methods, but the increasing demand of stable products can be satisfied with the use of other industrial methods like convective hot air drying.

Ascophyllum nodosum is harvested for use as an alginate source or fertilizer and for the manufacture of seaweed meals for animal and human consumption. From *Ascophyllum nodosum* seaweed sodium alginate can be obtained which is a very commonly used industrial product. As a stock feed additive its may make up to represent 5% of the diet for sheep, pigs, cattle and horses. As fertilizer *Ascophyllum nodosum* was used as a soil conditioner. Its extracts have proven chelating properties which improve the utilization of minerals.

Human consumption of seaweed *Bifurcaria bifurcata* is not as extended as several edible seaweeds, which are commonly used in the oriental diet, as *Laminaria spp.*, *Porphyra spp.* and *Undaria pinnatifida*. However, its composition, a typical composition of brown seaweeds, 34% of ashes, 11% protein, 5.6% lipids, 37% total dietary fibre (14.6% soluble dietary fibre) reveal its suitability to be a good source of food fibre for human consumption (Gómez-Ordóñez *et al.*, 2010).

Dried *Fucus vesiculosus* seaweed is commonly used as a food in Japan. In Europe and North America it is added in powder form to soups for flavour. The main uses of *Fucus vesiculosus* in Europe are related to medicinal or food purposes, typically as a dry powdered substance for oral use including auxiliary measure for weight loss, treatment of gastritis, the management of constipation, colitis, etc. The European Commission (EC) of European Union recently classified the *Fucus vesiculosus* seaweed like a "novel food" for human consumption and an increase in its demand as food is expected (EC, 2015). Recent studies are also focused on the potential antioxidant capacity of some *Fucus vesiculosus* seaweed components (Hahn *et al.*, 2012).

A limited number of reported studies on mathematical modelling of drying kinetics of seaweed can be found in literature. Brown seaweed *Eucheuma cottonii* drying curves were studied by Fudholi *et al.* (2012), (Gupta *et al.*, 2011) air

drying kinetics of *Himantalia elongata* seaweed, Kadam *et al.* (2015b) studied the of ultrasound pre-treatment on the drying kinetics of the brown seaweed *Ascophyllum nodosum* also employed in this Thesis and red seaweed *Gracilaria chilensis* drying kinetics and desorption isotherms were determined by Lemus *et al.* (2008). No studies on drying kinetics of fresh *Bifurcaria bifurcata*, *Fucus vesiculosus* and *Ascophyllum nodosum* employing hot air convective drying were found in the literature.

The aims of the present work are to determine the drying kinetics at different conditions and the evaluation of heat and mass transfer coefficients during constant drying rate period and effective coefficients of water diffusion during falling drying rate period of drying at different temperatures for *Ascophyllum nodosum*, *Bifurcaria bifurcata* and *Fucus vesiculosus* brown seaweeds.

6.2.2 Deep Bed Configuration studies

Experimental drying data of *Ascophyllum nodosum*, *Bifurcaria bifurcata* and *Fucus vesiculosus* for deep-bed configuration (load density of 14.9 ± 0.1 kg·m^{-2}) at four different temperatures (35, 50, 60 and 75°C) are shown in Figure 6.5. In all cases drying time was shortened with increasing air temperature. Drying at 35°C exhibited the largest drying time to achieve a MR of 0.03 while the lowest corresponded to 75°C for all assayed seaweed. The corresponding drying time to achieve a certain MR value at the same temperature was significantly different for the different seaweeds. In example, the necessary drying time to achieve a MR of 0.03 at 35°C for *Ascophyllum nodosum* was the lowest (480 min) compared to *Bifurcaria bifurcata* (700 min) and *Fucus vesiculosus* (1400 min). In addition, air drying temperature effect was significantly higher for *Fucus vesiculosus* for which a temperature increase from 35°C to 75°C lead to a decrease of ≈ 42% (from 1400 to 810 min) on drying time followed by *Bifurcaria bifurcata* (≈34%, from 700 to 460 min) and *Ascophyllum nodosum* (≈13%, from 480 to 420 min).

Drying kinetics curves for deep-bed configuration were modelled by means of the Page model, Eq. (4.9). Table 6.6 shows the values of model parameters along with statistical parameters which make clear that the experimental data was satisfactorily modelled ($R^2 \geq 0.994$ and $E_{RMS} \leq 0.02$). Air drying temperature significantly modified air drying kinetics of seaweeds, as it can be clearly seen on the significantly different values of Page model parameters. Two different behaviours were observed.

Ascophyllum nodosum showed a clear effect of air drying temperature on Page model parameters when drying above 35°C. Specifically, n parameter varied from

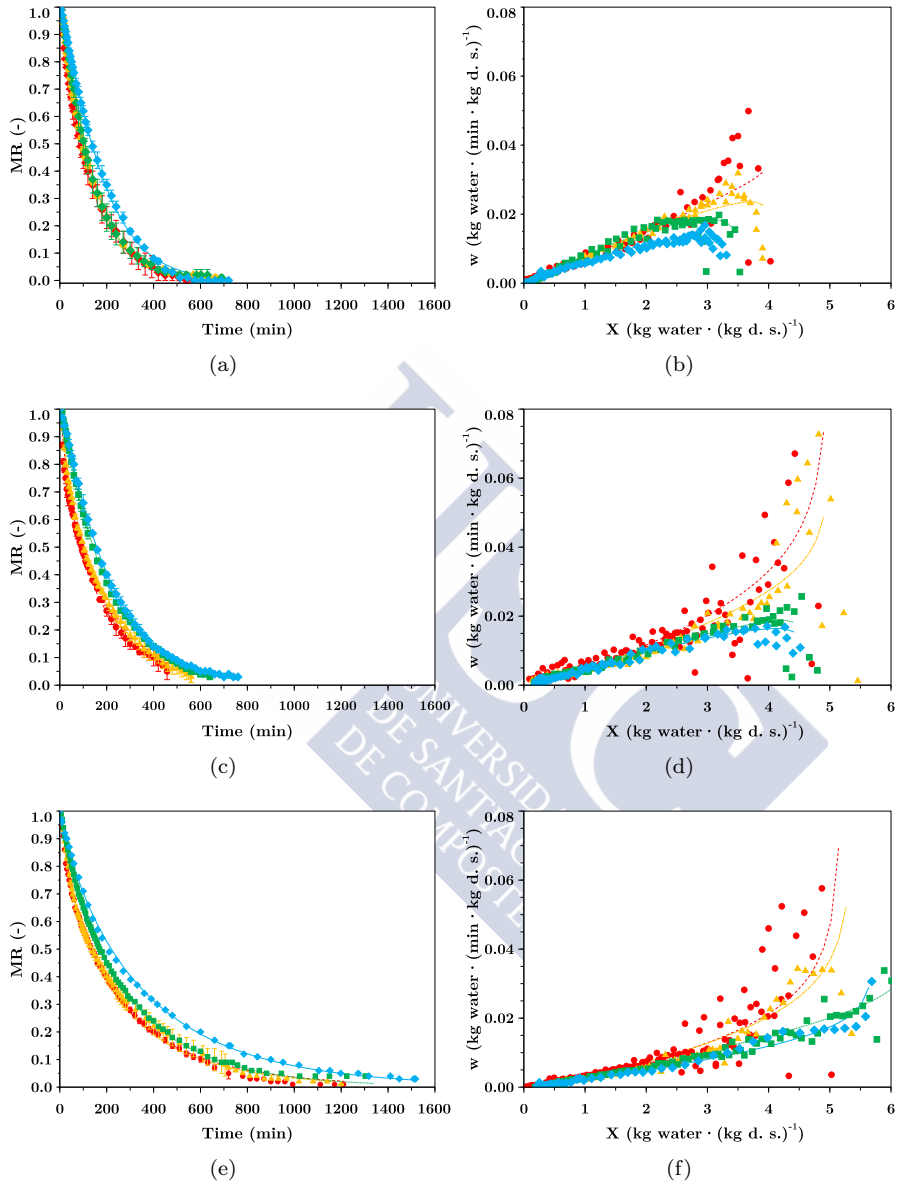

Figure 6.5 Experimental drying and drying rate curves of brown seaweeds *Ascophyllum nodosum* (a, b), *Bifurcaria bifurcata* (c, d) and *Fucus vesiculosus* (e, f) at 35°C (♦), 50°C (■), 60°C(▲) and 75°C (●) using deep bed configuration. Page model (—), Eq. (4.9).

Table 6.6 Values of the Page model, Eq. (4.9), parameters (k, n) and statistical coefficients (R^2, E_{RMS}) for drying curves of*Ascophyllum nodosum* (AN), *Bifurcaria bifurcata* (BB) and *Fucus vesiculosus* (FV) brown seaweeds.♣

Seaweed	**T** (°C)	k·**10**^{3} (min^{-n})	n (-)	$\mathbf{E}_{RMS}$ (-)	$\mathbf{R}^2$
AN	35	2.10±0.33^b	1.18±0.02^a	0.01	0.998
	50	7.61±0.69^a	0.98±0.03^b	0.01	0.997
	60	7.93±0.65^a	0.98±0.02^b	0.01	0.999
	75	8.69±0.82^a	0.98±0.01^b	0.01	0.998
BB	35	2.73±0.87^c	1.14±0.01^a	0.01	0.998
	50	4.70±0.20^c	1.07±0.06^a	0.01	0.999
	60	12.52±0.42^b	0.85±0.03^b	0.02	0.996
	75	19.13±0.32^a	0.78±0.04^b	0.02	0.994
FV	35	6.61±0.50^b	0.86±0.01^a	0.01	0.998
	50	6.97±0.13^b	0.89±0.01^a	0.01	0.999
	60	14.62±0.46^a	0.79±0.01^b	0.02	0.997
	75	15.77±1.23^a	0.77±0.02^b	0.01	0.998

♣Data are presented as means±standard deviation. Data value of each parameter with different superscript letters in columns (for each seaweed) are significantly different (P≤ 0.05).

0.98 to 1.18 and k parameter increased from 2.10 to > 7.61·10^3 min^{-n}. No significant differences on n and k were observed for drying temperatures > 35°C.

On the other hand, *Bifurcaria bifurcata* and *Fucus vesiculosus* drying kinetics showed a similar trend with temperature. For both seaweeds air drying temperature significantly modified drying kinetics parameters when > 50°C. Moreover, in the case of *Bifurcaria bifurcata* seaweeds air drying at 75°C significantly reduced drying time (higher k values and no significantly differences on n value compared to 60°C). In the case of *Fucus vesiculosus* a gap between drying kinetics at 35-50°C and 60-75°C was observed. In fact, in the case of *Fucus vesiculosus* n varied from ≈0.78 to ≈0.87 and k parameter from ≈6.79·10^{-3} min^{-n} to ≈15.3·10^{-3} min^{-n} for < 50°C and > 60°C, respectively.

The k values are similar of those observed by Vega-Gálvez *et al.* (2008) for other brown algae (*Macrocystis Pyrifera*) at temperatures between 70 and 80°C. There is no data in literature that assessed the air drying kinetics of *Fucus vesiculosus* and *Bifurcaria bifurcata*. However, Kadam *et al.* (2015b) obtained the Page model parameters for drying at 50°C of *Ascophyllum nodosum*, previously treated by ultrasounds. The reported results, k=7·10^{-3} min^{-n} and n=1.03 are in the range of those obtained for *Ascophyllum nodosum* drying between 60°C and 75°C. However, it has to be mentioned that the results are hardly comparable due to the different amounts of seaweed (20 g) employed in the mentioned study.

Drying rate curves Figure 6.5 (b, d and f) displayed an initial induction period (at high moisture content) corresponding to the unsteady state heating of the seaweed samples. Then, drying rates achieve maximum values depending on air drying temperature, and after that, a falling drying rate period is observed at all tested temperatures in which the water flow from the bulk to the surface of the seaweed sample is lower than the evaporation flow and consequently surface dries and its temperature increases. This stage lasts until the equilibrium moisture was reached. It is interesting to note that no temperature effect on drying rate below 3 (kg water·(kg dried solid)$^{-1}$, d.b.) for *Fucus vesiculosus* and *Bifurcaria bifurcata* and below 1 d.b. for *Ascophyllum nodosum*, was observed. These invariant rates could be related to phase transitions of polymers (i.e. alginate, commonly present in brown seaweeds) promoted by temperature that could change the internal structure of seaweed and hence modify the water transport characteristics inside the semi-dried seaweed during drying, avoiding the well known drying rate increase with temperature.

6.2.3 Effect of load density on drying kinetics

The effect of load density on drying kinetics of seaweeds was studied for *Ascophyllum nodosum* seaweed at 35°C. Therefore, drying at 35°C was carried out using four different load densities: approximately 2.5, 5, 10 and 15 kg·m^{-2}.

The experimental drying kinetics data and the corresponding curves employing Page model are shown in Figure 6.6. After a first modelling, the corresponding ANOVA analysis of n values showed that this parameter varied with load density in narrow interval (1.17-1.20) with no significant differences. These results lead to the assumption of a constant mean value of n =1.18 that allowed a new modelling employing the same procedure explained in the previous section. The corresponding values of k are presented in Table 6.7.

Table 6.7 Values of the Page model, Eq. (4.9), parameters (k, n) and statistical coefficients (R^2, E_{RMS}) for drying curves of *Ascophyllum nodosum* at 35°C and different load densities (LD).♣

LD (kg·m^{-2})	k·**10**^{3} (min^{-n})	n (-)	$\mathbf{E}_{RMS}$ (-)	$\mathbf{R}^2$ (-)
2.5	9.10±0.78^a	1.18	0.01	0.998
5.0	5.16±0.08^b		0.01	0.999
10.0	2.86±0.36^c		0.01	0.999
15.0	2.10±0.33^c		0.02	0.997

♣Data are presented as means±standard deviation. Data value of each parameter with different superscript letters in rows are significantly different (P≤ 0.05).

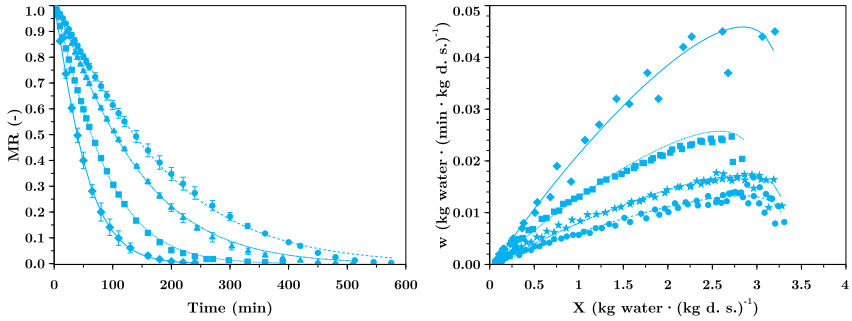

(a) (b)

Figure 6.6 Experimental drying and drying rate curves for brown seaweed *Ascophyllum nodosum* at 2.5 kg·m^{-2} (♦), 5.0 kg·m^{-2} (■), 10 kg·m^{-2} (★) and 15 kg·m^{-2} (●) at 35°C. Lines correspond to Page model, Eq. (4.9).

As it can be seen, load density significantly varied k parameter. The higher the load density, the lower the value of k and consequently the higher the time to achieve a certain MR. In fact, the different drying times required to achieve a moisture ratio of 0.03 were 200 min at load density of 2.5 kg·m^{-2}, 375 min at 5 kg·m^{-2}, 420 min at 10 kg·m^{-2} and 480 min at 15 kg·m^{-2}. Due to in this case n was considered constant for all experiments, k values represents well the load density effect on drying kinetics. In fact, it has been found an exponential relationship ($R^2 > 0.96$) between k parameter and the employed load density (LD), Eq. (6.2):

$$k = 3.07 - 2.459ln(LD) \tag{6.2}$$

where k is the well known Page model parameter (min^{-n}) and LD is the employed load density (Kg·m^{-2}).

6.2.4 Thin layer configuration studies

Drying kinetics of brown seaweeds employing thin layer configuration, that involved the use minimum amount of seaweed to cover the drier tray (load density of 2.43±0.02 kg·m^{-2} for *Ascophyllum nodosum*, 2.04±0.02 kg·m^{-2} for *Bifurcaria bifurcata* and 1.25±0.10 kg·m^{-2} for *Fucus vesiculosus*) were satisfactorily fitted employing Page model, Table 6.8. In general, the drying time was shortened with increasing air temperature for all assayed seaweeds. However, some differences in comparison with deep bed configuration have to be mentioned.

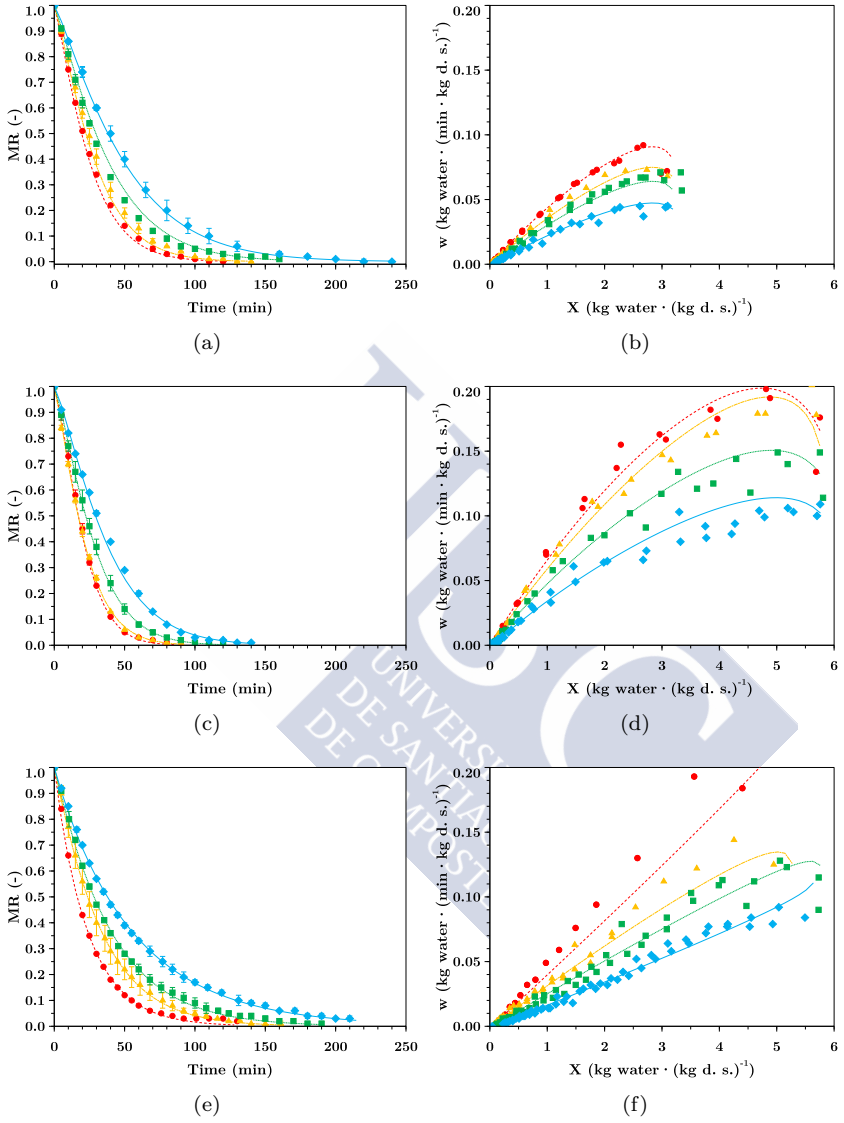

Figure 6.7 Experimental drying and drying rate curves for brown seaweed *Ascophyllum nodosum* (a, b), *Bifurcaria bifurcata* (c, d) and *Fucus vesiculosus* (e, f) at 35°C (♦), 50°C (■), 60°C(▲) and 75°C (●) employing thin layer configuration. Lines correspond to the proposed model for each seaweed: Eqs. (6.3), (6.4) and (6.5).

First of all, it is necessary to indicate that in this case the comparison between the different studied seaweeds is troublesome due to the different load densities employed for each one. The necessary drying time to achieve a MR of 0.03 for *Ascophyllum nodosum* significantly decreased from 160 to 80 min with increasing temperatures from 35°C to 75°C (a decrease of drying time of ≈50%). For *Bifurcaria bifurcata* and *Fucus vesiculosus*, drying time to achieve a MR of 0.03 was shortened from 100 to 60 min and 210 to 110 min, respectively, and no differences were observed between drying at 60°C or 75°C. As in the case of deep-bed configuration, the air drying temperature effect was significantly higher for *Fucus vesiculosus* (a decrease of ≈48%) compared to *Bifurcaria bifurcata* (≈40%).

Regarding water removal flow, a different drying temperature effect is observed between deep-bed and thin layer drying, Figure 6.5 (b, d and f) and Figure 6.7 (b, d and f), respectively. For thin layer configuration, higher drying temperatures resulted in higher water removal even at low moisture contents whilst for deep-bed configuration no sensible differences were observed in water removal flow at low moisture contents. This can be attributed to the additional resistance of water migration through the bed to arrive at the bed surface when drying in deep-bed configuration.

Table 6.8 Values of the Page model parameters (k, n), Eq. (4.9), and statistical coefficients (R^2, E_{RMS}) for drying curves of *Ascophyllum nodosum* (AN), *Bifurcaria bifurcata* (BB) and *Fucus vesiculosus* (FV) brown seaweeds in thin layer configuration.♣

Seaweed	**T** (°C)	$k \cdot \mathbf{10^3}$ (min^{-n})	n (-)	$\mathbf{E_{RMS}}$ (-)	$\mathbf{R^2}$
AN	35	9.10 ± 0.78^{c}	1.18	0.00	0.999
	50	13.90 ± 0.09^{b}		0.01	0.999
	60	16.20 ± 1.13^{b}		0.01	0.999
	75	19.80 ± 0.27^{a}		0.01	0.999
BB	35	8.7 ± 0.08^{c}	1.28	0.01	0.999
	50	12.8 ± 1.15^{b}		0.01	0.999
	60	17.8 ± 0.65^{a}		0.01	0.999
	75	18.6 ± 0.77^{a}		0.01	0.999
FV	35	17.3 ± 0.62^{c}	1.01	0.01	0.999
	50	$23.5 \pm 0.58^{b,c}$		0.01	0.998
	60	29.0 ± 3.67^{b}		0.01	0.999
	75	40.1 ± 0.15^{a}		0.01	0.998

♣Data are presented as means±standard deviation. Data value of each parameter with different superscript letters in columns (for each seaweed) are significantly different ($P \leq 0.05$).

After a first modelling of drying kinetics curves employing Page model, Eq. (4.9), where k and n were obtained, the ANOVA analysis shows that no significant

effect of drying temperature on n parameter existed for each seaweed (data not shown). This allows the mathematical assumption that n was constant for the different temperatures employed. Consequently, a new fitting was performed and k values were obtained, Table 6.8. The statistical parameters of fitting ($R^2 > 0.997$ and $E_{RMS} < 0.012$) for the model obtained can be considered acceptable taking into account that it can be used to estimate the drying kinetics of these seaweeds at any drying temperature in the tested range.

Finally, a linear relationship between k and temperature was found ($R^2 > 0.97$). This fact, allowed the generation of an unified model able to fit drying kinetics throughout the range of temperatures tested for each seaweed:

- *Ascophyllum nodosum*:

$$MR = e^{-(1.65\cdot10^{-4}+2.65\cdot10^{-4}T)t^{1.18}} \tag{6.3}$$

- *Bifurcaria bifurcata*:

$$MR = e^{-(-1.36\cdot10^{-3}-2.90\cdot10^{-4}T)t^{1.28}} \tag{6.4}$$

- *Fucus vesiculosus*:

$$MR = e^{-(-3.87\cdot10^{-3}+5.61\cdot10^{-4}T)t^{1.01}} \tag{6.5}$$

6.2.4.1 Sample surface area and shrinkage during drying determination

The specific drying rate in thin layer configuration was evaluated using Eq. (4.14) considering that the surface area of drying varied with seaweed moisture content according to the following empirical non-linear relationships for *Ascophyllum nodosum* (Eq. (6.6)), *Bifurcaria bifurcata* (Eq. (6.7)) and *Fucus vesiculosus* (Eq. (6.8)) seaweeds obtained as previously explained in Section 4.2.

$$\frac{S_X}{S_0} = \sqrt{4.8 - 4.49e^{-0.05X}} \tag{6.6}$$

$$\frac{S_X}{S_0} = \sqrt{-1.0 + 1.06e^{0.11X}} \tag{6.7}$$

$$\frac{S_X}{S_0} = \sqrt{0.1 + 0.07e^{0.41X}} \tag{6.8}$$

Different non-linear surface (S_X/S_0) ratio relationships were previously reported for shrinkage modelling for foodstuffs (Mayor & Sereno, 2004). Latter authors indicated that at high moisture content, shrinkage almost entirely compensates for moisture loss and volume of the material decreases linearly with moisture content. At low moisture content the rate and extension of shrinkage decreases dramatically. This behaviour may explain deviations from linearity in the assessment of the relative change of sample volume *vs* moisture content during the final stage of convective drying. No significant differences on shrinkage behaviour of seaweeds with temperature were observed indicating that this properties is more related to moisture content than to air drying rate. Non-linear surface (S_X/S_0) ratio relationships can be observed for all studied seaweeds in Figure 6.8 (a, b and c).

The specific drying rate *vs* moisture content for all seaweeds at tested temperatures is shown in Figure 6.8. It can be clearly observed the common drying periods. Namely, at high moisture content the constant drying rate period and below X_c begins the falling rate period. No noticeable variations were observed on X_c (d.b.) with temperature for *Ascophyllum nodosum* (1.3±0.2 d.b.) and *Bifurcaria bifurcata* (1.6±0.2 d.b.). In the case of *Fucus vesiculosus* X_c values increased linearly ($R^2 > 0.99$) with increasing air temperature (1.8±0.1 d.b at 35ºC, 2.0±0.1 d.b at 50ºC, 2.3±0.1 d.b at 60ºC and 2.5±0.2 d.b at 75ºC) (Figure 6.8 (f)).

The shrinkage of samples during drying significantly reduced the characteristic dimension (r) of seaweeds. Concerning *Ascophyllum nodosum*, r decreased from $4.0\pm0.3\cdot10^{-3}$ m (initial value) to $3.0\pm0.2\cdot10^{-3}$ m at X_c. For *Bifurcaria bifurcata*, r was reduced from $1.2\pm0.1\cdot10^{-3}$ to $5.8\pm0.3\cdot10^{-4}$ m at X_c. Regarding *Fucus vesiculosus* initial value of r was $4.0\pm0.2\cdot10^{-3}$ m and it was reduced to 2.1-$2.3\cdot10^{-3}$ at the corresponding X_c. During the falling-rate period this shrinking effect on the characteristic dimension was taken into account in order to obtain the water diffusion coefficient through the seaweed. Experimental shrinkage data in terms of the variation of characteristic dimension with time were correlated with moisture content for *Ascophyllum nodosum* (Eq. (6.9)), *Bifurcaria bifurcata* (Eq. (6.10)) and *Fucus vesiculosus* (Eq. (6.11)) seaweeds as follows:

$$r = \sqrt{4.8 - 4.49e^{-0.05MR}(4.010^{-3})^2} \tag{6.9}$$

$$r = \sqrt{-1.0 + 1.06e^{0.11MR}(1.210^{-3})^2} \tag{6.10}$$

$$r = \sqrt{0.1 + 0.07e^{0.41MR}(4.010^{-3})^2} \tag{6.11}$$

where MR is evaluated by the Eq. (4.10) with the corresponding parameters of Page model shown in Table 6.8 for each seaweed and drying temperature.

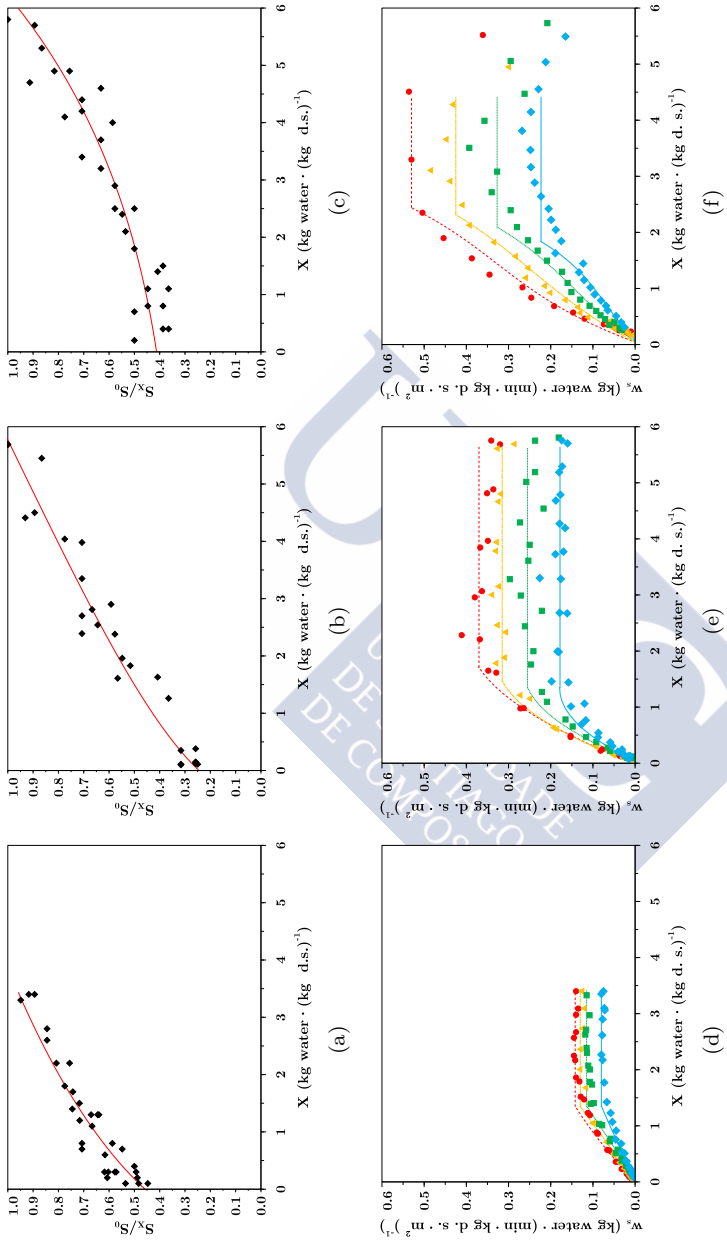

Figure 6.8 S_X/S_0 *vs* X curve and specific drying rate curves of *Ascophyllum nodosum* (a, d), *Bifurcaria bifurcata* (b, e) and *Fucus vesiculosus* (c, f) at 35°C (◆), 50°C (■), 60°C(▲) and 75°C (●). Lines correspond to difusional model (postcritical period) and Eq. (4.15) (precritical period) for cylindrical geometry.

6.2.4.2 Constant drying rate period: mass and heat transfer coefficients

The modelling of constant drying rate period employing Eqs. (4.15) and (4.16) showed that no significant differences were found in the convective mass (K_t) and heat (h_t) transfer coefficients with temperature for each tested seaweed.

Regarding mass transfer coefficient, no significant differences were observed for drying of different seawees, $13.7 \pm 1.6 \cdot 10^{-3}$ m·s^{-1} for *Ascophyllum nodosum*, $21.8 \pm 2.0 \cdot 10^{-3}$ m·s^{-1} for *Bifurcaria bifurcata* and $18.1 \pm 1.0 \cdot 10^{-3}$ m·s^{-1} for *Fucus vesiculosus*. These values are higher than those observed by da Silva *et al.* (2013) who reported values of K_t from $0.8 \cdot 10^{-3}$ to $1.9 \cdot 10^{-3}$ m·s^{-1} for pear drying in a forced air oven at higher temperatures (between 68 and 92°C).

The corresponding values of h_t were 12.9 ± 1.6 W·m^{-2}·K^{-1} for *Ascophyllum nodosum*, 19.9 ± 0.9 W·m^{-2}·K^{-1} for *Bifurcaria bifurcata* and 16.6 ± 1.5 W·m^{-2}·K^{-1} for *Fucus vesiculosus*. These values are in the range reported by Bird *et al.* (2002) who indicated that a typical magnitude of convective heat transfer coefficient varies from 3 to 20 W·m^{-2}·K^{-1}.

Note here that obtained h_t and K_t values accomplished satisfactorily the Chilton-Colburn analogy of heat and mass transfer with a relative deviation of parameters lower than 10.5%. The Eq. (4.15) with the mass transfer coefficients here determined reproduced satisfactorily the drying kinetics above the critical moisture content as can be observed in the Figure 6.8.

6.2.4.3 Falling drying rate period: effective coefficient of water diffusion through the seaweed

In the case of the drying during the falling rate periods, it was considered that drying is governed by water diffusion in the bulk of seaweeds. Diffusional modelling of drying during post-critical period for thin layer configuration was performed ($R^2 > 0.98$ and $E_{RMS} < 0.05$) by diffusional model for cylindrical geometry (Eqs. (4.18) and (4.19)). Table 6.9 shows the effective coefficients of diffusion of water through *Ascophyllumn nodosum*, *Bifurcaria bifurcata* and *Fucus vesiculosus* seaweeds at each tested temperature.

Water diffusion coefficient (D_{eff}) of *Ascophyllum nodosum* significantly increased with increasing drying temperature from $281.3 \pm 38.7 \cdot 10^{-12}$ m^2·s^{-1} at 35°C up to $537.2 \pm 22.3 \cdot 10^{-12}$ m^2·s^{-1} at 75°C. In the case of *Bifurcaria bifurcata* seaweeds D_{eff} significantly increased when drying at > 50°C but no difference was observed between drying at 60°C and 75°C. Concerning *Fucus vesiculosus*,

Table 6.9 Effective coefficient of difussion of water (D_{eff}) and statistical coefficients (R^2, E_{RMS}) for *Ascophyllum nodosum* (AN), *Fucus vesiculosus* (FV) and *Bifurcaria bifurcata* (BB) seaweed drying at different temperature.♣

Seaweed	T (°C)	D_{eff}·10^{12} ($m^2 \cdot s^{-1}$)	E_{RMS}	R^2
AN	35	281.3±38.7^d	0.02	0.993
	50	372.7±41.7^c	0.02	0.989
	60	476.9±9.7^b	0.01	0.993
	75	537.2±22.3^a	0.03	0.983
BB	35	12.43±0.64^c	0.02	0.988
	50	18.14±0.92^b	0.03	0.998
	60	21.97±0.27^a	0.03	0.986
	75	20.35±1.31^{a,b}	0.03	0.989
FV	35	104.0±15.4^b	0.03	0.983
	50	154.8±22.1^b	0.03	0.985
	60	207.3±13.9^{a,b}	0.03	0.983
	75	268.4±17.1^a	0.03	0.982

♣Data are presented as means±standard deviation. Data value of each parameter with different superscript letters in columns (for each seaweed) are significantly different ($P \leq 0.05$).

temperature had to be incremented to > 60°C in order to significantly increase D_{eff}. This trend of D_{eff} with temperature could be related to a structural collapse of seaweed when drying above > 60°C takes place. This structural collapse can led to a more difficult diffusion of water molecule through the seaweed structure and consequently the typical increment of water diffusion with drying temperature is eliminated.

In general the comparison of D_{eff} values with literature is troublesome mainly due to the strong dependence of its value with the chosen geometry for drying kinetics modelling and other additional considerations like in example the employed machine to carry out the drying operation. Nevertheless, other authors determined D_{eff} values for other seaweed species. Employing plane sheet geometry Gupta *et al.* (2011) reported values of D_{eff} from $5.6 \cdot 10^{-7}$ to $12.2 \cdot 10^{-7}$ $m^2 \cdot s^{-1}$ with increasing temperature from 25 to 40°C for *Himanthalia elongata* seaweed, significantly higher than those obtained in this Thesis, and Vega-Gálvez *et al.* (2008) reported more similar values of D_{eff}, from 5.6 to 10.2^{-9} $m^2 \cdot s^{-1}$ for temperatures between 50 and 80°C for the brown seaweed *Macrocystis Pyrifera*. Employing cylindrical geometry, Vega-Gálvez *et al.* (2007) presented values of D_{eff} from 2.8 to $22.4 \cdot 10^{-9}$ $m^2 \cdot s^{-1}$ for temperatures from 30 to 70°C for *Gracilaria chilensis* seaweed. As it can be seen, by comparison with literature, D_{eff} values varied in a large range. However, it can be said that the

obtained values of D_{eff} are in the range of the typical values for food stuff reported by (Rizvi, 1986), from 10^{-9} to 10^{-11} $m^2 \cdot s^{-1}$.

Additionally, it has been found that in the case of *Ascophyllum nodosum* and *Fucus vesiculosus* seaweeds, D_{eff} followed an Arrhenious relatioship with temperature ($R^2 > 0.97$), Eq. (6.12):

$$ln(D_eff) = ln(D_0) - \frac{E_a}{R(T + 273.1)} \tag{6.12}$$

where D_0 ($m^2 \cdot s^{-1}$) the Arrhenius factor, E_a (J·mol−1) the energy of activation and R ($J \cdot mol^{-1} \cdot K^{-1}$) the universal gas constant.

The energy of activation was 14.6 and 22.1 $kJ \cdot mol^{-1}$ for *Ascophyllum nodosum* and *Fucus vesiculosus*, respectively, which is within the reported range, from 12.7 to 110 $kJ \cdot mol^{-1}$, obtained by other foodstuffs (Zogzas *et al.*, 1996). Also, it was similar to energy of activation for other seaweeds like *Macrocystis pyrifera*, 19.8 $kJ \cdot mol^{-1}$ or *Gracilaria chilensis*, 39.9 $kJ \cdot mol^{-1}$ (Vega-Gálvez *et al.*, 2008).

The section in tweets

- Pagel model satisfactorily fits *Ascophyllum nodosum* (AN), *Bifurcaria bifurcata* (BB) and *Fucus vesiculosus* (FV) drying kinetics.
- Employing deep-beed configuration (15 kg·m^2) during drying, AN has the lowest drying time to achieve a MR of 0.03 and FV the highest.
- When drying employing thin layer configuration, the lowest drying time corresponds to *Bifurcaria bifurcata*.
- A model able to fit drying kinetics of the studied brown seaweed from 35 to 75°C has been developed (Eqs. (6.3), (6.4) and (6.5)).
- The effect of increasing load density (LD) on drying kinetics of AN seaweed was found to follow a logarithmic relationship between k and LD.
- Volume shrinkage of seaweeds can be modelled as function of moisture content by means of a non linear equation.
- The critical moisture content increases linearly with increasing air temperature for FV and remains constant for AN and BB.
- Mass transfer coefficients are assessed for constant drying rate periods modelling.
- Falling drying rate period are fitted by diffusional model considering shrinkage for thin layer configuration
- Effective diffusivity of water on seaweed (D_{eff}) increased with air temperature for AN and FV following and Arrhenius relationship.
- For BB seaweeds no significant differences were observed on D_{eff} when drying at > 60°C.

USC
UNIVERSIDADE
DE SANTIAGO
DE COMPOSTELA

6.3 Physicochemical characterization of dried milled systems

The dried materials (seaweeds and starchy products) have been milled in order to obtain systems with small particle size that could be employed to obtain doughs or extracts. Powders, obtained by milling of dried seaweeds, and flours, obtained by milling of dried starchy materials, have been physically and chemically characterized, in each case, by means of particle size, colour, water retention capacity, swelling power, total and damaged starch and amylose/amilopectin ratio.[3]

[3]This section has been adapted from the following papers and others in writing process:
MOREIRA, R., CHENLO, F. & ARUFE, S. (2015). Starch transitions of different gluten free flour doughs determined by dynamic thermal mechanical analysis and differential scanning calorimetry. *Carbohydrate polymers* **127**, 160-167. DOI: http://doi.org/10.1016/j.carbpol.2015.03.062.
MOREIRA, R., CHENLO, F., ARUFE, S. & RUBINOS, S. (2015). Physicochemical characterization of white, yellow and purple maize flours and rheological characterization of their doughs. *Journal of Food Science and Technology-Mysore* **12**, 7954–7963. DOI: http://doi.org/10.1007/s13197-015-1953-6.
MOREIRA, R., CHENLO, F., SINEIRO, J., ARUFE, S. & SEXTO, S. (2016). Drying temperature effect on powder physical properties and aqueous extract characteristics of *Fucus vesiculosus*. *Journal of Applied Phycology* **28**, 2485–2494. DOI: http://doi.org/10.1007/s10811-015-0744-9.
MOREIRA, R., SINEIRO, J., CHENLO, F., ARUFE, S. & DÍAZ, D. (2016). Aqueous extracts of *Ascophyllum nodosum* obtained by ultrasound assisted extraction: effect of drying temperature of seaweed on their properties. *Journal of Applied Phycology*. IN PRESS. DOI: http://doi.org/10.1007/s10811-017-1159-6.

Nomenclature

Powders

AN35P	–	*Ascophyllum nodosum* (AN) powder obtained from AN35.
AN50P	–	AN powder obtained from AN50.
AN60P	–	AN powder obtained from AN60.
AN75P	–	AN powder obtained from AN75.
BB35P	–	*Bifurcaria bifurcata* (BB) powder obtained from BB35.
BB50P	–	BB powder obtained from BB50.
BB60P	–	BB powder obtained from BB60.
BB75P	–	BB powder obtained from BB75.
FV35P	–	*Fucus vesiculosus* (FV) powder obtained from FV35.
FV50P	–	FV powder obtained from FV50.
FV60P	–	FV powder obtained from FV60.
FV75P	–	FV powder obtained from FV75.

Flours

CTF	–	Chestnut flour (*Castanea sativa*)
YM200F	–	Yellow maize flour obtained with a 200 μm standard mesh during milling.
YM500F	–	Yellow maize flour obtained with a 500 μm standard mesh during milling.
PM200F	–	Purple maize flour obtained with a 200 μm standard mesh during milling.
PM500F	–	Purple maize flour obtained with a 500 μm standard mesh during milling.
WM200F	–	White maize flour obtained with a 200 μm standard mesh during milling.
WM500F	–	White maize flour obtained with a 500 μm standard mesh during milling.

Parameters

D_w	–	Mass mean diameter, Eq. (4.20).
D_v	–	Volume mean diameter, Eq. (4.21).
D_s	–	Surface mean diameter, Eq. (4.22).
SP	–	Swelling power (mL·g d.s.$^{-1}$)
WRC	–	Water retention capacity (g water·g d.s.$^{-1}$)
Y_i	–	Measured colour parameter.
w_i	–	Mass fraction of powders and flours.
Y_c	–	Calculated colour parameter.
TS	–	Total Starch
DS	–	Damaged Starch

6.3.1 Introduction

Chestnut (*Castanea sativa Mill.*) is a gluten-free seasonal nut that is mainly consumed fresh, however, some ways of processing like drying make chestnuts available outside the traditional season (Moreira *et al.*, 2015). It is a typical product of Mediterranean countries where its production is focused mainly in Turkey, Italy and Iberian Peninsula. Chestnut is mainly composed by high-quality protein with essential amino acids (4-7%), a relatively high amount of sugar (20-32%), starch (50-60%), dietary fibre (4-10%) and fat (2-4%). It also contains vitamin E, B vitamins, potassium, phosphorus and magnesium (Sacchetti *et al.* (2004)) which make this nut a healthy and nutritional product.

Despite the chestnut flour has a high nutritional quality and aroma, the baked products have usually low volume and an undesirable dark colour (Demirkesen *et al.*, 2010). These defects can be related to an unwanted starch gelatinization and a high sugar and fibre content. However, the main disadvantage of technological chestnut flour are its low protein content and particularly the absence of proteins with viscoelastic properties like gluten (Borges *et al.*, 2007).

Maize (*Zea mays L.*) is the most produced cereal in the world. Corn is used for many food (human and animal) and non-food (pharmaceutical, cosmetics, chemical, among others) applications. Specifically, in the northwest of Spain, maize is cultivated for self-consumption in small farms. Maize bread is traditionally made with whole grain of maize, following similar procedures as for manufacturing the common wheat bread (Revilla *et al.*, 2008). Although most consumers prefer white maize (Rebordanes variety), other types are also used for making bread, like yellow (Sarreaus variety) and purple (Meiro variety) maize. Chemical composition of different maize kernels can be considered homogeneous but it depends on cultivation conditions, temperature, variety and maize variety (white, yellow, purple, black, etc). The main components in maize are (%, w/w wet basis, w.b.): carbohydrates (≈77), water (≈11), protein (≈7), total fibre (≈7), total lipids (≈4) and ash (≈1.5) (Gwirtz & Garcia-Casal, 2014). The main compound of the maize is the starch and is responsible of the high nutritional value.

The maize kernel is composed of four primary structures: endosperm, germ, pericarp, and tip cap, representing 83, 11, 5, and 1% of the maize kernel respectively (Gwirtz & Garcia-Casal, 2014). There are differences in composition between these structures. For example, the pericarp has high fibre content (86%, w/w dry basis, d.b), the endosperm presents the highest starch content (87%, d.b.) and ca. 8% d.b. of proteins. The germ presents high percentage (d.b.) in lipids (33%), proteins (20%) and minerals (11%) (Watson & Ramstad, 1987).

Although starch and proteins are the major compounds of maize grains, several other compounds produced by secondary metabolism, such as carotenoids and anthocyanins, have been found, mainly in cereals genotypes ((Escribano-Bailon *et al.*, 2004)). The carotenoids are tetraterpenes responsible for the yellow, orange and red colours of several vegetables (Kuhnen *et al.*, 2011). Otherwise, the anthocyanins are water-soluble pigments responsible for the purple, blue and red colours in vegetable tissues, belonging to the class of flavonoids (Escribano-Bailon *et al.*, 2004). Anthocyanin-rich foods and anthocyanin pigments have been suggested as potential agents to reduce the risk of colon cancer (Jing *et al.*, 2008).

The aforementioned starchy flours (chestnut and maize) are very interesting from a researcher point of view, due to the absence of gluten in these systems. Celiac disease is characterized by inflammation of the small intestinal mucosa that results from a genetically based immunologic intolerance to ingested gluten. This fact promotes the development of new products with no presence of gluten suitable for celiac patients which makes that in the last decade the interest in gluten-free products, like it could be chestnut and maize, is growing due to the increase in celiac disease (Lazaridou *et al.*, 2007).

As consequence of this increasing demand, several studies are focused on gluten-free flours development in the last few years. However, very few studies are focused on enhancing the functional properties of gluten-free products which we consider that constitute an important task for research and development, and is a concomitant challenge towards the improvement of technological and sensory characteristics. In this sense, the use of seaweed powders to be added to gluten-free starchy flours in order to improve antioxidant properties of the final product is proposed. Bearing this in mind, the physicochemical characterization of flours and powders is a very important task in order to facilitate the comprehension on possible behaviours of flours blends (starchy flour + seaweed powder) during manufacture process.

Namely, in the case of starchy products, it is important to determine the modifications of the chemical properties promoted during drying or milling operations in order to obtain the corresponding flours (such as the amylose/amylopectin ratio, the total and damaged starch content, etc.). On the other hand, physical properties such as particle size, colour, swelling power or water retention capacity of flours and powders are very important to control due to, usually, technological aptitude of the product depends on these parameters. Some of them can be notably altered by the processing conditions (Moreira *et al.*, 2013b) and consequently thermal and rheological behaviours of gluten-free doughs from these flours and powders can be also altered. Others, like colour

properties, are directly related to customer acceptance of the final product (Demirkesen, 2016).

The main aim of this work is to characterize physically and chemically maize and chestnut flours and the different seaweeds powders obtained from three different seaweeds dried at different temperatures.

6.3.2 Seaweed powders

The three seaweed species studied in this Thesis were dried at different temperatures as previously explained (see Section 3.2) and four different dried systems as function of employed drying temperature for each seaweed specie were obtained. These systems were milled (see section 4.3) and the corresponding powders were physically characterized by means of their particle size, colour, swelling power and water retention capacity.

6.3.2.1 Physical characterization

Particle size

Particle size distribution of sieved powders obtained after the milling of seaweeds dried at different temperatures are shown in Figure 6.9. In addition, the corresponding values of these data are presented at the end of this Section in Table 6.16. In general, two different particle size distribution curves were obtained. *Ascophyllum nodosum* and *Fucus vesiculosus* seaweeds powders showed a similar behaviour, an unimodal curve, whereas particle size distribution of *Bifurcaria bifurcata* seaweed powders were bimodal curves.

In the case of *Ascophyllum nodosum* and *Fucus vesiculosus*, seaweeds powders fraction from 250 to 500 μm represents the highest mass fraction, independently of the temperature employed to obtain them. Mass fractions varied from 29.2% (AN35P) to 42.7% (AN75P) and from 38.1% (FV60P) to 46.7% (FV35P, FV75P) for these seaweeds. The particle size fraction with the second highest mass fraction percentage corresponded to a range of sizes from 125 to 200 μm. For *Ascophyllum nodosum* it varied from 14.3% (AN35P) up to 17.7% (AN60P) and for *Fucus vesiculosus* from 14.1 (FV35P) up to 19.3% (FV60P). The minimum mass fraction was obtained for particles with a size < 40 μm (1.3–4.3%) considering residual the particle size higher than 500 μm. Regarding *Bifurcaria bifurcata* seaweed powders, Figure 6.9 shows that their particle size distribution curves corresponded to bimodal curves where the highest mass fractions corresponded

to particles sizes inside the range from 250 to 500 μm and from 125 to 250 μm.

In contrast to the similarity of the particle size distribution curves, significant differences between *Ascophyllum nodosum* and *Fucus vesiculosus* mean diameters were observed and drying temperature <50°C, Table 6.11. FVP obtained employing drying temperature $\leqslant$ 50°C had larger values of D_s and D_w compared to the corresponding ANP. However, when drying temperature increased, no differences were observed. In the case of BBP, mean diameter showed intermediate values between ANP and FVP.

Table 6.11 Mean diameters D_w, D_v and D_s (Eqs. (4.20), (4.21) and (4.22), respectively), for seaweed powders of *Ascophyllum nodosum* (AN), *Bifurcaria bifurcata* (BB) and *Fucus vesiculosus* (FV) obtained after milling of seaweeds previously dried at different temperatures.♣

System	D_w (μm)	D_v (μm)	D_s (μm)
AN35P	191 ± 7^b	39 ± 1^b	77 ± 1^b
AN50P	201 ± 3^b	40 ± 2^b	80 ± 2^b
AN60P	231 ± 6^a	45 ± 1^a	103 ± 2^a
AN75P	238 ± 5^a	46 ± 1^a	108 ± 2^a
BB35P	175 ± 14^a	66 ± 5^b	106 ± 5^b
BB50P	193 ± 14^a	75 ± 6^b	122 ± 6^b
BB60P	211 ± 17^a	115 ± 9^a	156 ± 7^a
BB75P	185 ± 15^a	60 ± 5^b	109 ± 5^b
FV35P	244 ± 20^a	79 ± 23^a	133 ± 31^a
FV50P	231 ± 7^a	91 ± 21^a	139 ± 20^a
FV60P	234 ± 39^a	75 ± 6^a	136 ± 19^a
FV75P	231 ± 11^a	91 ± 32^a	147 ± 33^a

♣Data are presented as means±standard deviation. Data value of each parameter with different superscript letters in columns (for each seaweed) are significantly different ($P\leq 0.05$).

Regarding drying temperature effect on mean diameter values of seaweeds powders, two different behaviours were observed. In the case of *Fucus vesiculosus* and *Bifurcaria bifurcata* none of the diameters showed significant differences as function of employed temperature. This result seems to indicate that no notorious textural differences are developed during drying at different conditions that could affect final particle size of powders. On the contrary, in the case of *Ascophyllum nodosum* it can be clearly observed that particle size of AN35P and AN50P were similar and significantly different compared to AN60P and AN75P, which also showed similar distributions among them. This lead to a significant increase of the mean diameter of the powder when they were obtained after drying at temperatures above 50°C, Table 6.11.

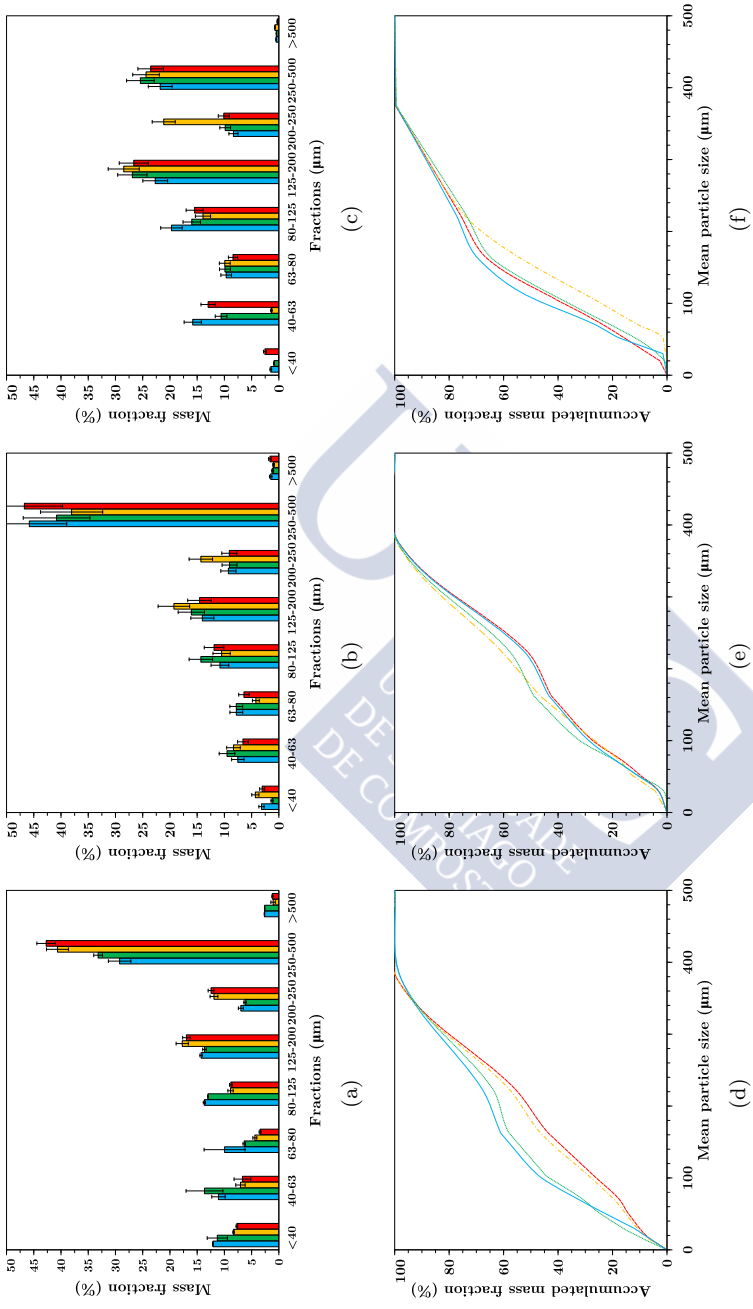

Figure 6.9 Differential and accumulated particle size distribution curves for seaweeds powders obteined from brown seaweed *Ascophyllum nodosum* (a, d), *Fucus vesiculosus* (b, e) and *Bifurcaria bifurcata* (c, f) previously dried at 35°C (—), 50°C (···), 60°C(-·-·) and 75°C (- - -).

This fact seems to indicate that some textural modifications could be thermally promoted during drying at temperatures above this value, probably due to samples are more difficult to be milled when drying is performed at higher temperatures.

The differences observed in mean diameters of powders and particles size distribution as function of each specie could be related to their structure and composition. In fact, *Ascophyllum nosodum* and *Fucus vesiculosus* seaweed have very similar shape which could led to a more similar structure of dried seaweed previously to milling and justify the obtaining of similar particle size distribution curves (unimodal) whilst the shape of *Bifurcaria bifurcata* seaweeds are very different compared to the first ones which could also indicate a different structure of the seaweed that could lead to the different particle size distribution curves obtained.

Taking into account future uses of these powders, it has to be mentioned that the obtained particle sizes are in the same range of several food additives such as bran (Le Bleis *et al.*, 2015), chia (Moreira *et al.*, 2013a), etc. This fact, led to the conclusion that, based on their particle size, these type of powders could be employed as food additive.

Colour

The trends for colour parameters values of powders from seaweeds dried at 35, 50, 60 and 75°C and their corresponding particle size fractions are displayed in Figures 6.10 and 6.11. Additionally, their values and the corresponding ANOVA analysis are presented at the end of this Section in Tables 6.17, 6.18 and 6.19). ΔE^* parameter for each size fractions was estimated using as reference the colour coordinates of the seaweed powder prior to sieving (whole).

Seaweed powders exhibited in all cases a slight trend to whiteness, more than brightness ($L^* < 50$),greenness ($a^* < 0$) and yellowness ($b^* > 0$) predominance. Except in the case of some fractions of *Fucus vesiculosus* seaweed powders which showed a brightness trend ($L^* > 50$) and *Bifurcaria bifurcata* seaweed powders BB60P and BB75P which values of a^* were positive but close to zero indicating a slightly redness trend. Colour characteristics varied differently for each seaweed powder.

It can be seen that L^* parameter significantly decreased with increasing particle size up to 200-250 μm for all drying temperatures. Similar values of L^* were observed for the studies species. Regarding drying temperature effect, no clear trends were observed.

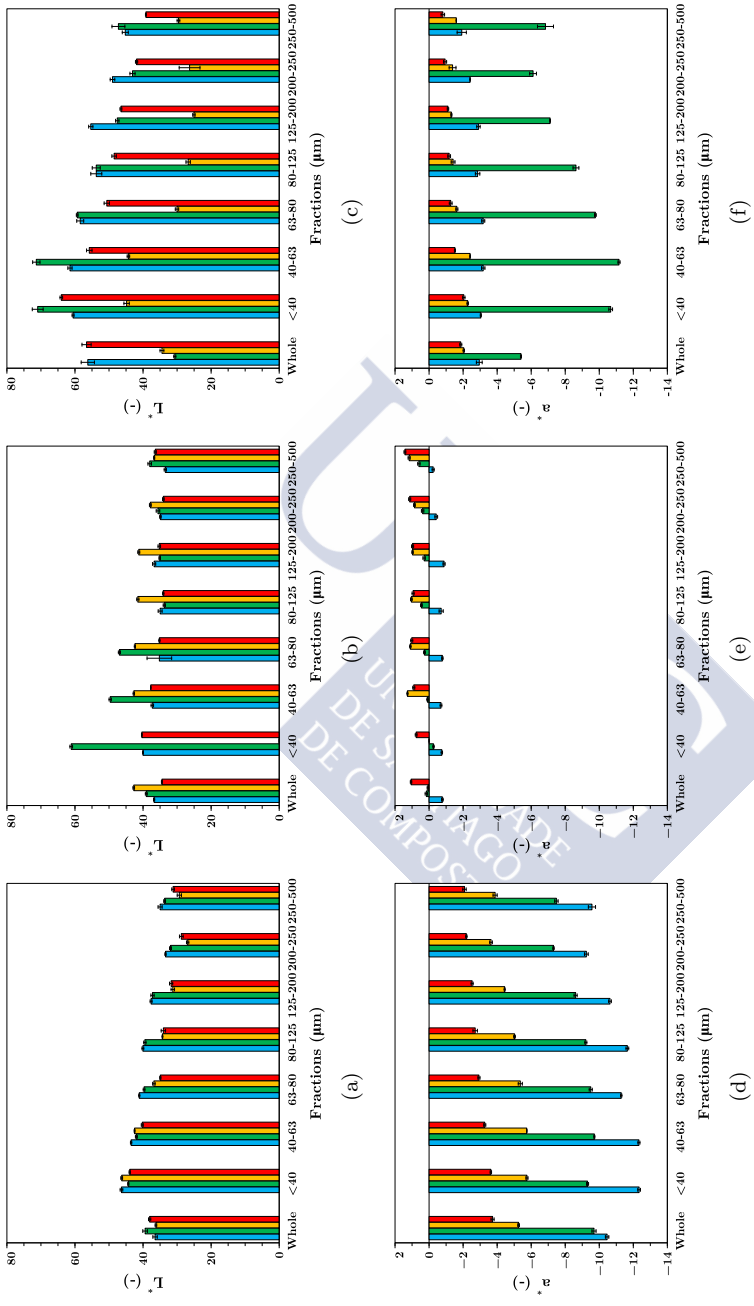

Figure 6.10 L^* and a^* colour parameters for *Ascophyllum nodosum* (a, d), *Bifurcaria bifurcata* (b, e) and *Fucus vesiculosus* (c, f) powders obtained after seaweed drying at different temperatures 35°C (■), 50°C (■), 60°C(■) and 75°C (■).

Specifically, a^* parameter values increased with increasing drying temperature for all assayed seaweed. *Ascophyllum nosodum* and *Bifucaria bifurcata* seaweed powders, Table 6.17 and Table 6.18, respectively, showed a similar influence of drying temperature althought *Bifucaria bifurcata* values of a^* parameter were larger than those obtained for *Ascophyllum nodosum* powders and even the trend of a^* changes from green to red with drying temperatures above 35°C. In the case of *Fucus vesiculosus* powders, their a^* values are similar to those obtained for *Ascophyllum nodosum* powders, however, powders from *Fucus vesiculosus* seaweed dried at 50°C revealed a relevant decrease, Table 6.19. This fact can be explained because during dehydration, the tonoplast, the plasmalemma and the chloroplast membrane may suffer structural damage, and as result, a solute loss of chlorophyll and carotenoids, among others components, can occur (Burritt *et al.* (2002); Oliver *et al.* (1998)). In raw brown seaweeds, fucoxanthin is an important component, responsible of its colouration, that covers the pigmentation of chlorophyll. However, the chlorophyll leaching during drying may expose its colour, and consequently, the parameter a^* drastically decreases. During drying at higher temperatures (> 60°C), the released chlorophyll undergoes degradation reactions. Chlorophylls are easily degraded in the presence of dilute acids, heat, light and oxygen. Along with degradation produced by external agents, it is also degraded by chlorophyllase enzyme (Erge *et al.*, 2008). Degradation of the chlorophyll is manifested as yellowing, as it allows the preponderance of carotenoid colouration (Drazkiewicz & Krupa, 1991). At room temperature, this enzyme only acts in the presence of high concentrations of organic solvents. However, its optimum activity is found to be within the range of 60–82°C (Erge *et al.*, 2008). It is difficult to distinguish if chlorophyll breakdown is produced by enzymatic or non-enzymatic reactions but, eventually, they both lead to the formation of non-colourant species (Delgado-Vargas & Paredes-Lopez, 2002). Regarding particle size effect, a^* increased in general for all assessed seaweed powders.

Regarding b^*, it decreased for *Ascophyllum nodosum* and *Fucus vesiculosus* powders obtained with drying temperatures above 60°C. This attenuation in yellowness (b^*) related to employed drying temperature in these powders may be linked, as explained previously, to the reactions of carotenoids or other pigments, which could result in their degradation, or in the formation of alternative coloured substances or volatile compounds (Landrum, 2009). Particularly, in FV75P it is observed a relevant increase in b^* compared to those values obtained for FV60P, this additional b^* coordinate increase may be induced by Maillard's reactions. In the case of *Bifurcaria bifurcata* seaweed powders the effect of drying temperature did not cause relevant changes in b^* values. Regarding colour properties of size fractions, b^* decreased significantly for all systems as mean size increased. Both trends might be related to the presence of still structurally undamaged parts of the seaweed in the biggest particles.

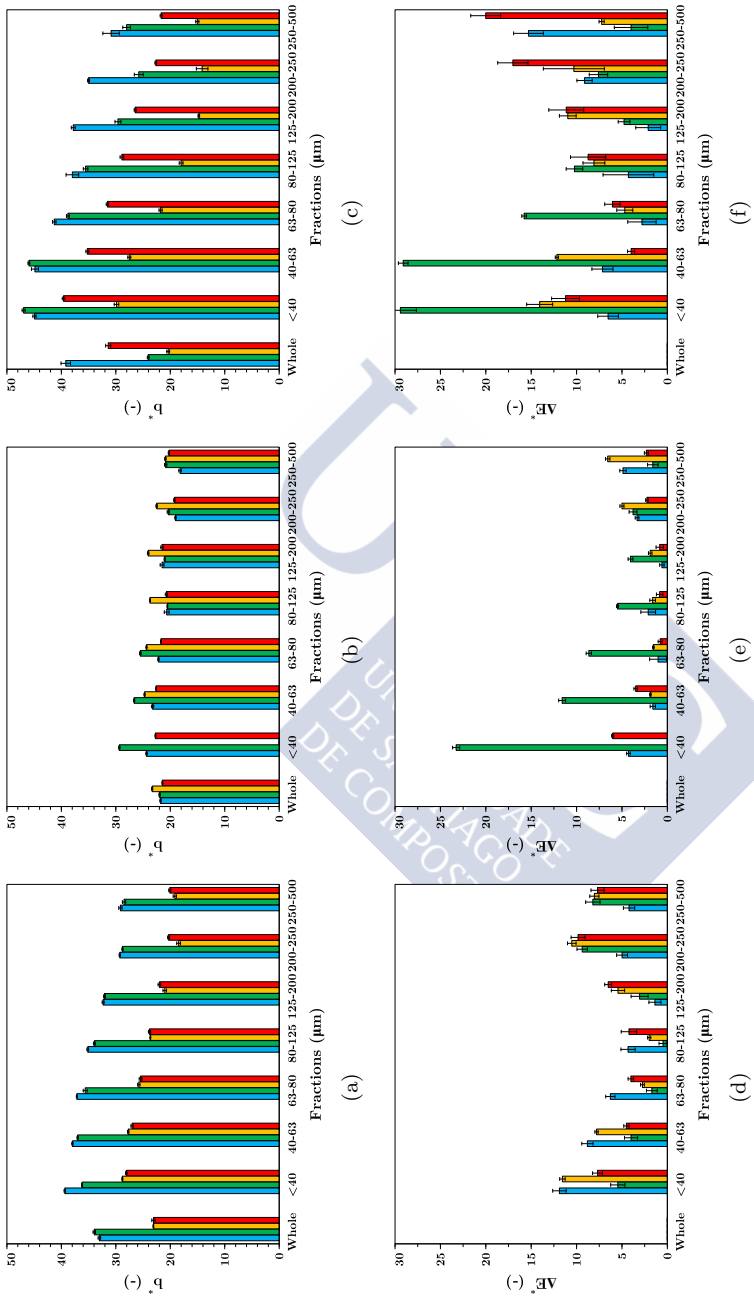

Figure 6.11 b^* and ΔE^* colour parameters for *Ascophyllum nodosum* (a, d), *Bifurcaria bifurcata* (b, e) and *Fucus vesiculosus* (c, f) powders obtained after seaweed drying at different temperatures 35°C (■), 50°C (■), 60°C(■) and 75°C (■).

The evaluation of total colour difference (ΔE^*) trend showed minimum values at intermediate particle sizes (from 63 to 125 μm). Particularly, colour difference clasifications for *Ascophyllum nosodum* varied from small for AN35P ($\Delta E^* = 1.37$) and AN50P ($\Delta E^* = 0.48$), distinct for AN60P ($\Delta E^* = 2.01$) and very distinct for AN75P ($\Delta E^* = 4.02$); for *Bifurcaria bifurcata* were all small $\Delta E^* = 0.60$, 1.60, 1.54 and 0.79 for BB35P, BB50P, BB60P and BB75P, respectively, and for *Fucus vesciculosus* were all very distinct except in the case of FV35P that was distinct ($\Delta E^* = 2.11$), according to classification proposed by Adekunte *et al.* (2010).

It is noticeable that, except in the case of *Bifurcaria bifurcata*, D_s values are into the range of particle size fraction that corresponds to the lowest ΔE^* values. This fact, seeems to indicate that these characteristic diameter could be adequate to estimate approximately the colour properties of the mixtures of seaweed powder formerly dried at 35, 60, and 75°C. In the case of drying at 50°C, this relationship was not met (except for *Ascophyllum nodosum*), and the largest size fractions showed the minimum colour differences. Tello-Ireland *et al.* (2011) reported that drying *Gracilaria chilensis* at 50°C resulted in the highest ΔE^* value, and drying at higher temperatures showed similar colorimetric coordinates to sample dried at low temperature (35°C).

The obtained colour data of the particle size fractions allows the estimation of the colour characteristics of whole-seaweed powders. The weighted arithmetic mean is employed to calculate each colour parameter, Y_c, Eq. 6.13:

$$Y_c = \sum_{i=1}^{n} w_i Y_i \tag{6.13}$$

where Y_i is the measured colour parameter (a^*, b^*, or L^*) at each particle size fraction (Tables 6.17, 6.18 and 6.19) and w_i is the corresponding mass fraction (Table 6.16).

Calculated values are also shown in Tables 6.17, 6.18 and 6.19. Specifically, estimated values of colour parameters employing Eq. (6.13) for *Ascophyllum nodosum* and *Bifurcaria bifurcata* seaweed powders showed a good agreement with experimental data of whole-seaweed powders ($\Delta E^* \leqslant 5.37$ and 3.44, respectively) whereas for *Fucus vesiculosus* seaweed powders the estimation was less satisfactorily ($\Delta E^* \leqslant 13.72$).

Bifurcaria bifurcata seaweed powders showed the best estimation values. The colour difference between the experimental values of colour parameters for whole-seaweed powders and the calculated ones can be classified as small for 50°C and

75°C, distinct for 35°C and very distinct for 60°C. The good prediction of the Eq. (6.13) for colour parameter values could be related to the particle size distribution of the powders. As it can be seen in Table 6.16, *Bifurcaria bifurcata* seaweed powders shows a bimodal curve where none mass fraction represents a percentage higher than 28.5%. This more homogeneous distribution, compared to the others seaweed powders, helps the estimation of an average weighted value for each colour parameter.

Ascophyllum nodosum seaweed powders showed ΔE^* values that allow the classification of the difference as distinct ($1.5 < \Delta E^* < 3.0$) for temperatures lower than 50°C and very distinct ($\Delta E^* > 3.0$) for temperatures above this value. The modelled values for samples dried at higher temperatures are slightly poor (mainly in relation to L^* and a^* parameters). This result can be explained by the high percentage (> 40% w/w) of particles with size higher than 250 μm in the samples dried at 60 and 75°C, Table 6.16. Colour measurements need to have a minimum thickness to avoid negative optical effects related to transparency. Large particles tend to settle to the bottom and the corresponding relative surface population decreases; consequently, the colour measurement can be distorted. The same explanation can be applied in the case of *Fucus vesiculosus* seaweed powders were the differences between the experimental values and the calculated ones were higher than 5.63 probably due to to the high percentage (> 38% w/w) of particles with size higher than 250 μm, Table 6.16.

Swelling power, water retention capacity ans insolubility

Regarding the results obtained for swelling power (SP), water retention capacity (WRC) and solubility index (SI), Table 6.12, different trends can be observed as function of studied seaweed. In the case of *Ascophyllum nodosum* seaweed powder both SP and WRC increased when particle size decreased. No clear effect of particle size was observed on the same parameters for *Bifurcaria bifurcata* and *Fucus vesiculosus* seaweed powders.

The comparison between whole powders for each seaweed indicated that BB35P had the largest SP (16.7 mL·g d.s.$^{-1}$) and WRC (14.29 g water·g d.s.$^{-1}$) with no clear differences between AN35P and FV35P. On the other hand, insolubility index was significantly larger for FV35P.

The obtained seaweeds powders had higher SP and WRC of those reported by Gómez-Ordóñez *et al.* (2010) for *Bifurcaria bifurcata* powders 7.75 mL·g d.s.$^{-1}$ and 4.89 g water·g d.s.$^{-1}$, respectively, and by Rupérez & Saura-Calixto (2001) for *Fucus vesiculosus*, 5.77 mL·g d.s.$^{-1}$ and 5.48 g water·g d.s.$^{-1}$, respectively. These differences could be due to the different milling and drying operation employed to obtain the seaweed powders.

The rise of SP with particle size decrease could be explained by means of specific surface area of particles. Due to water absorption is a superficial phenomenon, the use of smaller particles could led to an increase on this parameter due to the higher specific surface area compared to larger particles. Hence particles could proportionally absorb more water and consequently the SP rise. In the case of WRC values, their heterogeneity could be related to the different compositions of the seaweeds and particle size fractions.

Table 6.12 Swelling power (SP), water retention capacity (WRC) and insolubility index (II) of seaweed powders from *Ascophyllum nodosum* (AN), *Bifurcaria bifurcata* (BB) and *Fucus vesiculosus* (FV) previously dried at 35°C.♣

Seaweed	Fraction (μm)	SP (mL·g d.s.$^{-1}$)	WRC (g water·g d.s.$^{-1}$)	II (g·100 g d.s.$^{-1}$)
AN35P	63-40	14.9±0.1^{a}	12.10±0.02^{a}	-
	200-125	10.7±0.3^{b}	9.79±0.59^{b}	-
	500-250	6.8±0.1^{c}	8.79±0.02^{b}	-
	Whole	11.2±0.4^{b}	10.57±0.15^{b}	79.81±0.86^{a}
BB35P	63-40	17.4±2.5^{a}	12.76±0.58^{a}	-
	200-125	20.0±1.7^{a}	16.63±0.22^{b}	-
	500-250	16.8±1.3^{a}	17.09±0.58^{b}	-
	Whole	16.7±0.2^{a}	14.29±0.08^{b}	78.30±0.23^{a}
FV35P	63-40	11.4±0.1^{a}	10.48±0.15^{a}	-
	200-125	11.4±0.1^{a}	11.83±1.31^{a}	-
	500-250	10.9±0.1^{b}	11.40±0.78^{a}	-
	Whole	10.2±0.1^{b}	10.40±0.16^{a}	90.27±0.98^{b}

♣Data are presented as means±standard deviation. Data value of each parameter with different superscript letters in rows are significantly different (P≤ 0.05).

6.3.3 Starchy flours

Starchy flours were obtained after milling of dried maize and chestnut milling. Their physicochemical characterization consisted on particle size, colour and total and damaged starch determination.

6.3.3.1 Physical characterization

Particle size

Particle size distribution curves of flours obtained from different dried maize

varieties and dried chestnut, are shown in Figure 6.12. Additionally, the corresponding values of these data are presented in Table 6.20, at the end of this Section. As it can be seen, different trends as function not only of the employed mesh during milling (200 μm or 500 μm) but also of the nature of the starchy material were obtained.

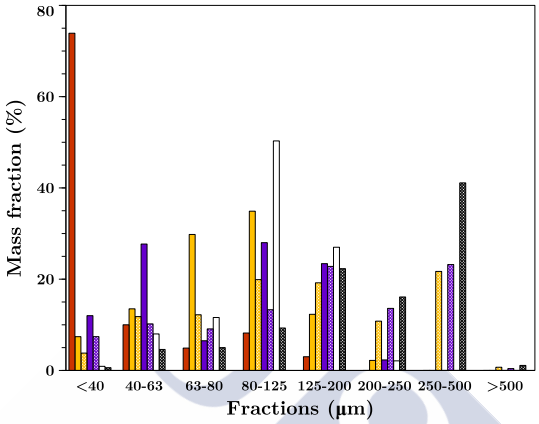

Figure 6.12 Particle size distribution CTF (■), YM200F (■), YM500F (☒), PM200F (■), PM500F (☒), WM200F (□) and WM500F (☒).

Maize flours obtained after milling dried maize kernels with an internal sieve of 500 μm showed a maximum mass fraction (21.7 – 41.1%) for particles with size from 250 to 500 μm, Table 6.20. The second more important mass fraction corresponded to particles with size between 125 and 200 μm (19.2 – 22.8%). The lower mass fraction corresponded to particles with size below 40 μm for all flours (considering residual the fraction with particle size > 500 μm). The average particle diameter by mass, D_w (Eq. (4.20)), for maize flours showed no differences between YM500F (176 μm) and PM500F (184 μm), but it was higher for WM500F (250 μm).

In maize flours obtained employing a sieve of 200 μm the maximum mass fraction percentage (from 28.0 to 50.3%) of particles was from 80 to 125 μm of particle size, Table 6.20. WM200F also showed an important population (27.0%) in the range of 125 to 200 μm. Maize flour particles with size between 63 and 80 μm were the second more important (29.8%) in YM200F flour while PM200F flour showed two fractions with high weight percent; 40 to 63 μm and 125 to 200 μm, with 27.7% and 23.4%, respectively. However, as in flours obtained with an internal sieve of 500 μm no differences in D_w was observed between YM200F (90 μm) and PM200F (93 μm) and the highest average diameter corresponded to

WM200F (113 μm). Higher values for WM flours, Table 6.13, were probably due to the higher hardness of WM kernels in comparison to YM and PM kernels.

CTF showed a particle size distribution curves completely different compared to those observed for maize flours. The most important mass fraction (73.9%) of CTF flour was < 40 μm and the average particle size (37.8 μm) of CTF was smaller than maize flours, indicating that dried chestnut is a softer material than dried maize.

Table 6.13 Mean diameters, D_w, D_v and D_s (Eqs. (4.20), (4.21) and (4.22), respectively), for starchy flours.♣

	$\mathbf{D}_w$ (μm)	$\mathbf{D}_v$ (μm)	$\mathbf{D}_s$ (μm)
CTF	44.1	32.8	35.4
YM200F	90.3	44.4	67.8
YM500F	176.1	54.5	99.2
PM200F	93.4	38.5	60.4
PM500F	183.5	45.8	91.9
WM200F	112.8	73.2	97.1
WM500F	249.7	89.4	166.7

Colour

Colour characteristics of maize flours showed differences between them. The measured parameters (L^*, a^* and b^*) values of whole flours showed the same behaviour independently on the average particle size, Table 6.21. PM flours showed the lowest value of L^* (53.80 and 54.49 for PM500F and PM200F, respectively) and WM the highest (65.25 and 66.41 for WM500F and WM200F, respectively). PM flours showed the highest value of a^* (2.22 and 2.94 for PM500F and PM200F, respectively) indicating the domination of red over the green colour in this flour. This could be related to the high anthocyanin content of PM (Yang *et al.*, 2008). For WM flours a^* values (0.19-0.12) were near to zero indicating no domination of red over green colour. The lowest values of a^*, corresponded to YM (-0.79 and -0.87 for YM200F and YM500F, respectively), were negative which indicates the presence of green over red colour in these flours. Values of b^* parameter were much higher than a^* for all studied flours except PM flour. YM flour showed the highest b^* values (20.92 and 17.24 for YM500F and YM200F, respectively) that is indicative of its yellow colour due to the presence of high amount of carotenoids (Sandhu *et al.*, 2007). The lowest b^* value corresponded to PM (2.54 and 0.55 for PM500F and PM200F, respectively).

L^* in PM was lower than YM and WM flours at every particle size studied,

Figure 6.13. L^* decreased with particle size increasing in YM and PM flours. In the case of YM and WM flours a^* increased with particle size and for PM flours remained almost constant. Parameter b^* showed the same trend for all studied flours and their values increased with particle size. The same trend has been reported for other maize flours (Bolade *et al.*, 2009). Particle size fractions of PM flours showed the lowest b^* values. These values, near to zero, indicate the tendency to blue colour of these flours compared the other studied flours. All fractions from WM and YM flours showed much higher b^* values that indicates the clearly predomination of yellow colour respect to blue colour. It also remarkable the fact that, for particle size fractions of PM flours less than 125 μm, b^* values were lower than a^* values indicating that red-green colour dominates yellow-blue colour.

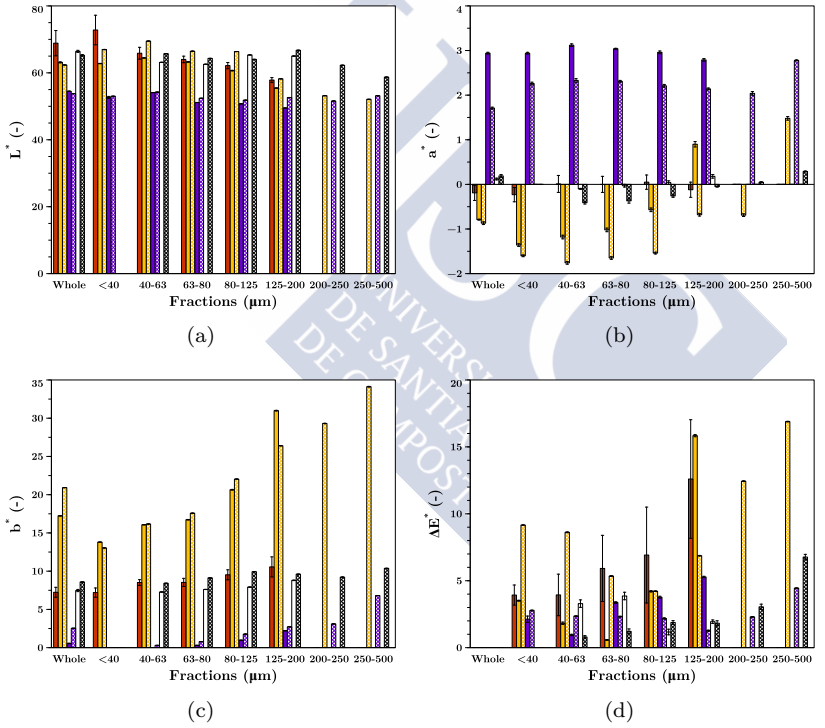

Figure 6.13 L^* (a), a^* (b), b^* (c) and ΔE^* (d) colour parameters for CTF (■), YM200F (■), YM500F (☒), PM200F (■), PM500F (☒), WM200F (□) and WM500F (☒).

Regarding ΔE^* values, calculated employing the whole flour as the reference flour, it was observed that the minimum value for each flour varied from 0.58 for

YM200F to 4.22 for YM500F. Moreover it was observed a correlation between minimum values of ΔE^* and D_s values. Except in the case of WM500F, D_s values are into the interval that corresponds to the lower ΔE^* values. This fact, indicates that these characteristic diameter could be adequate to estimate approximately the colour properties of the whole flours.

A model is proposed in order to obtain the whole flour colour parameters employing the colour parameters values and the mass fraction of each particle size fraction by using Eq. (6.14).

$$Y_c = \sum_{i=1}^{n} \left(\frac{w_i}{Y_i^3} \right)^{-1/3} \tag{6.14}$$

where Y_i is the measured colour parameter (a^*, b^*, or L^*) at each particle size fraction (Table 6.21), and w_i is the corresponding mass fraction (Table 6.20).

It can be observed that the employed model predicts satisfactorily the colour parameter values in comparison to experimentally measured values of whole flours, Table 6.21. Particularly, for L^* and a^* high accuracy was observed among WF calculated values and WF data. Total colour difference, ΔE^* (Eq. (4.23)), between experimental and calculated values was evaluated. In tested flours, ΔE^* values were low inside the range of 1.5 and 3.0 and can be classified as distinct (Adekunte *et al.*, 2010).

Additionally, the comparison between YM, WM and CTF with commercial yellow, white and wheat flours, respectively, taken as reference (Collar *et al.*, 2014) was done. No comparison was performed for PM due to the absence of bibliographic data. ΔE^* parameter, Eq. (4.23), showed that the difference between every whole flour obtained could be considered very distinct (ΔE^* = 6.0 - 12.0) compared to its respective commercial flour taken as reference, Table 6.14, with exception of some fractions (80-63 and 63-40 μm) of YM500F and CTF that can be classified as distinct ($\Delta E^* = 1.5$-3.0). This result indicates that these fractions are the most similar to commercial flours according to their colour. These colour differences could be justified by the use in this work of whole maize flours and flours used as reference could be refined during processing.

6.3.3.2 Chemical characterization

Chemical characterization of flour was carried out by means of starch characterization. Taking into account that starch is one of the main components that could affect mixing and baking behaviour of flour doughs, its control is very important in order to understand the modifications on these processes.

Table 6.14. ΔE^* values for starchy flours compared to commercial starchy flours.

Fraction	CTF	YM200F	WM200F	YM500F	WM500F
250-500	-	-	-	22.34±0.02	11.76±0.02
200-250	-	-	-	18.19±0.03	8.03±0.01
125-200	10.80±1.08	17.71±0.03	5.41±0.01	12.43±0.02	4.50±0.01
80-125	6.42±0.66	7.60±0.06	4.74±0.01	3.69±0.01	6.75±0.01
63-80	4.38±0.81	5.11±0.04	7.31±0.02	1.84±0.05	6.09±0.02
40-63	2.88±1.27	4.38±0.02	6.69±0.03	2.99±0.02	4.51±0.01
< 40	5.02±4.09	7.11±0.03	-	5.74±0.02	-

Total starch (TS) corresponds to the starch amount without gelatinize before the analysis. Total starch of the maize flours varied from 60.1 to 75.2 (% w/w, d.b.), Table 6.15. These values are in concordance with those reported by other authors for different maize flours: 66.9-74.1% (Hasjim *et al.*, 2009) and 77.5 % (Malumba *et al.*, 2015) whereas specifically, WM flours showed total starch content (60.1 to 73.8) slightly higher than those reported by other authors for white maize (57.88 %), (Flores-Silva *et al.*, 2014). CTF flour showed lower total starch content (50.9%) than maize flours due to mainly its high sugar content. In both cases, high total starch content were found and it can be related to the mild conditions during processing, particularly, the use of low drying temperatures (45°C) that avoided the occurrence of starch gelatinization.

Table 6.15. Total (TS) and damaged starch (DS) of tested flours.

	TS (% w/w, d.b.)	**DS** (% w/w, d.b.)
CTF	50.9±3.1	7.3±0.8
YM200F	68.1±2.2	8.6±0.2
YM500F	71.6±6.0	2.6±0.7
PM200F	75.2±6.3	18.2±0.5
PM500F	71.3±0.28	8.3±0.6
WM200F	73.8±2.2	25.0±2.1
WM500F	60.1±7.6	12.6±0.6

Damaged starch (DS) measures the starch fraction that is thermal or mechanically modified during processing (mainly drying and milling operations). Damaged starch varied from 7.3 to 25.0% (% w/w, d.b.) for all tested flours, Table 6.15. Same values were previously obtained for maize, 10.1-17.4% (Bolade *et al.*, 2009), and chestnut flour (Torres *et al.*, 2014c) with similar particle size. Regardless of the average particle size of the flour (given by the used sieve during milling, 200 or 500 μm), WM variety always showed the highest (25.0 %

and 12.6 % for WM200 and WM500, respectively) and YM the lowest (8.6 % and 2.6 % for YM200 and YM500, respectively) DS content, similar values were obteined for CTF (7.3%). This fact can be related to the different hardness and friability of maize variety. It was also notice that DS content of maize flours decreased with increasing average particle size (employing the same sieve during milling). The milling operation affects directly the starch structure (Li *et al.*, 2014). It can be observed that the flours obtained with a sieve of 200 μm showed higher DS content than 500 μm flours due to higher mechanical and thermal damage caused during milling. Bolade *et al.* (2009) observed the same trends, lower particle size fraction of flours showed higher DS content (from 12.2 to 17.4 % d.b. for 450 to $<$ 75 μm fractions, respectively).

Amylose/amylopectin ratio of starch from tested sources varied in a narrow interval among (17.8$\pm$0.7 for PM and 19.5$\pm$0.3 for CH). Consequently, this ratio value cannot be considered relevant in order to discuss differences related to starch transitions between different samples.

6.3.4 Tables

In this section, supplementary Tables are presented, as previously mentioned, in order to facilitate the comprehension of the reader.

Table 6.16 Particle size distribution of powders obtained after milling from dried *Ascophyllum nodosum* (AN), *Bifurcaria bifurcara* (BB) and *Fucus vesiculosus* (FV) seaweeds at different temperatures.

Seaweed	Fraction	Mass fraction (w_i,% w/w)			
		35°C	**50°C**	**60°C**	**75°C**
AN	> 500	2.6±0.1	2.6±0.1	1.1±0.4	1.2±0.1
	250 - 500	29.2±2.1	33.2±0.8	40.6±2.0	42.7±1.7
	200 - 250	7.0±0.4	6.2±0.2	11.9±0.7	12.5±0.5
	125 - 200	14.3±0.2	13.7±0.3	17.7±1.1	17.0±0.7
	80 - 125	13.7±0.2	13.0±0.0	8.9±0.5	8.8±0.2
	63 - 80	10.0±3.8	6.4±0.2	4.4±0.4	3.4±0.2
	40 - 63	11.1±1.2	13.7±3.4	7.1±0.9	6.7±1.5
	< 40	12.1±0.1	11.3±1.9	8.3±0.1	7.7±0.2
BB	> 500	0.5±0.1	0.4±0.1	0.7±0.2	0.3±0.1
	250 - 500	21.8±3.5	25.4±5.6	24.4±3.8	23.5±1.5
	200 - 250	8.3±0.8	9.9±0.7	21.1±2.1	10.1±0.5
	125 - 200	22.7±0.8	26.9±1.2	28.5±3.0	26.6±1.3
	80 - 125	19.7±0.4	16.0±1.2	13.9±1.3	15.5±1.4
	63 - 80	9.7±0.5	9.9±1.6	9.9±0.6	8.4±0.6
	40 - 63	15.8±2.2	10.6±1.1	1.4±0.9	13.0±1.9
	< 40	1.5±1.3	0.9±0.4	0.0±0.0	2.6±0.8
FV	> 500	1.5±0.1	1.1±0.6	1.0±0.3	1.6±0.2
	250 - 500	45.8±4.9	40.8±0.5	38.1±5.6	46.7±1.3
	200 - 250	9.3±1.2	9.1±2.2	14.3±3.5	9.1±0.4
	125 - 200	14.1±0.5	16.1±1.9	19.3±4.8	14.6±1.8
	80 - 125	10.8±0.8	14.3±3.1	10.5±2.0	11.9±2.6
	63 - 80	7.8±0.6	7.8±2.1	4.2±0.7	6.4±0.9
	40 - 63	7.5±1.3	9.5±7.7	8.3±0.9	6.6±2.2
	< 40	3.2±0.2	1.3±0.5	4.3±1.1	3.1±1.4

Table 6.17 Colour parameters of seaweed powder obtained from *Ascophyllum nodosum* previously dried at 35, 50, 60 and 75°C and the corresponding size fractions.♣

T(°C)			Fractions(μm)							Whole
		Whole	**< 40**	**40-63**	**63-80**	**80-125**	**125-200**	**200-250**	**250-500**	**Eq. 6.13**
35	L^*	36.47±0.64^{f}	46.34±0.38^{a}	43.51±0.19^{b}	41.11±0.16^{c}	40.0±0.26^{d}	37.64±0.28^{e}	33.40±0.17^{h}	34.99±0.59^{g}	38.99±3.50
	a^*	-10.46±0.10^{c}	-12.34±0.08^{f}	-12.33±0.06^{f}	-11.29±0.04^{d}	-11.65±0.08^{e}	-10.63±0.08^{c}	-9.24±0.11^{a}	-9.57±0.21^{b}	-10.83±0.98
	b^*	33.02±0.22^{e}	39.37±0.12^{a}	37.97±0.11^{b}	37.16±0.08^{c}	35.15±0.15^{d}	32.33±0.17^{f}	29.28±0.10^{g}	29.16±0.30^{g}	33.57±2.86
	ΔE^*	-	11.89±0.74	8.81±0.62	6.28±0.51	4.33±0.78	1.37±0.66	4.99±0.60	4.22±0.62	2.61±0.75
50	L^*	39.39±0.68^{c}	44.34±0.16^{a}	41.96±0.28^{b}	39.70±0.25^{c}	39.47±0.34^{c}	37.22±0.47^{d}	31.93±0.29^{f}	33.66±0.26^{e}	37.66±3.06
	a^*	-9.69±0.12^{e,f}	-9.31±0.06^{c,d}	-9.71±0.03^{f}	-9.50±0.09^{e,d}	-9.21±0.06^{c}	-8.61±0.09^{b}	-7.31±0.04^{a}	-7.48±0.10^{a}	-8.53±0.66
	b^*	33.95±0.22^{d}	36.21±0.09^{b}	37.01±0.11^{a}	35.62±0.36^{c}	33.94±0.17^{d}	32.08±0.18^{e}	28.78±0.10^{f}	28.49±0.30^{f}	32.33±2.59
	ΔE^*	-	5.46±0.78	4.00±0.72	1.71±0.59	0.48±0.43	3.06±0.93	9.38±0.57	8.21±0.79	2.72±0.75
60	L^*	36.22±0.23^{c}	46.27±0.25^{a}	42.49±0.11^{b}	36.82±0.37^{c}	34.30±0.11^{d}	31.26±0.51^{e}	26.90±0.34^{g}	29.34±0.62^{f}	32.53±2.24
	a^*	-5.26±0.05^{e}	-5.75±0.06^{f}	-5.74±0.01^{f}	-5.36±0.12^{e}	-5.02±0.05^{d}	-4.44±0.03^{c}	-3.64±0.08^{b}	-3.88±0.12^{a}	-4.41±0.27
	b^*	23.10±0.06^{d}	28.80±0.08^{a}	27.72±0.12^{b}	25.78±0.21^{c}	23.66±0.07^{d}	21.01±0.32^{e}	18.47±0.35^{g}	19.16±0.30^{f}	21.53±1.51
	ΔE^*	-	11.56±0.30	7.80±0.18	2.74±0.21	2.01±0.18	5.44±0.73	10.53±0.47	8.04±0.50	4.10±0.09
75	L^*	38.07±0.33^{c}	43.91±0.18^{a}	40.23±0.28^{b}	34.93±0.17^{d}	34.03±0.64^{d}	31.76±0.47^{e}	28.76±0.54^{f}	31.18±0.39^{e}	32.96±2.06
	a^*	-3.73±0.09^{e}	-3.63±0.04^{e}	-3.27±0.06^{d}	-2.93±0.06^{c}	-2.71±0.13^{b}	-2.53±0.06^{b}	-2.19±0.04^{a}	-2.08±0.10^{a}	-2.46±0.19
	b^*	23.08±0.31^{e}	28.08±0.12^{a}	27.01±0.21^{b}	25.46±0.24^{c}	23.81±0.20^{d}	22.00±0.23^{f}	20.31±0.18^{g}	20.09±0.19^{g}	22.05±1.30
	ΔE^*	-	7.69±0.55	4.51±0.29	4.02±0.30	4.23±0.85	6.52±0.38	9.84±0.76	7.69±0.72	5.37±0.48

♣Data are presented as means±standard deviation. Data value of each parameter with different superscript letters in rows are significantly different ($P \leq 0.05$).

Table 6.18 Colour parameters of seaweed powder obtained from *Bifurcaria bifurcata* previously dried at 35, 50, 60 and 75°C and the corresponding size fractions.♣

T (°C)			Fractions (μm)							Whole
		Whole	**< 40**	**40-63**	**63-80**	**80-125**	**125-200**	**200-250**	**250-500**	**Eq. 6.13**
35	L^*	36.76±0.17^{b,c}	40.20±0.12^{a}	37.28±0.36^{b}	35.21±3.61^{c,d}	34.98±0.57^{c,d}	36.75±0.46^{b,c}	34.90±0.22^{d}	33.46±0.33^{d}	35.50±0.21
	a^*	-0.78±0.05^{c}	-0.75±0.04^{c}	-0.70±0.05^{c}	-0.78±0.04^{c}	-0.71±0.12^{c}	-0.88±0.06^{d}	-0.42±0.08^{b}	-0.24±0.06^{a}	-0.57±0.03
	b^*	21.79±0.12^{d}	24.36±0.13^{a}	23.26±0.20^{b}	22.18±0.11^{c}	20.66±0.44^{e}	21.51±0.34^{d}	19.04±0.12^{g}	18.21±0.22^{g}	20.72±0.11
	ΔE^*	-	4.29±0.20	1.60±0.29	1.02±0.93	2.11±0.81	0.60±0.24	3.34±0.20	4.89±0.35	1.79±0.20
50	L^*	39.05±0.27^{c}	61.10±0.39^{a}	49.65±0.34^{b}	46.94±0.31^{b}	33.75±0.32^{e}	35.10±0.21^{d,e}	35.62±0.51^{c,d,e}	38.04±0.52^{c,d}	38.64±0.22
	a^*	0.16±0.07^{d}	-0.26±0.04^{e}	0.09±0.04^{d}	0.27±0.05^{c}	0.45±0.05^{b}	0.29±0.07^{c}	0.38±0.07^{b}	0.60±0.07^{a}	0.38±0.02
	b^*	21.96±0.12^{d}	29.36±0.12^{a}	26.64±0.11^{b}	25.50±0.14^{c}	20.53±0.06^{f}	21.03±0.09^{e}	20.37±0.19^{f}	20.85±0.21^{e}	21.95±0.07
	ΔE^*	-	23.27±0.39	11.59±0.38	8.66±0.29	5.49±0.11	4.06±0.26	3.78±0.43	1.60±0.58	0.87±0.22
60	L^*	42.73±0.23^{a}	-	42.71±0.20^{a}	42.39±0.17^{b}	41.54±0.32^{c}	41.26±0.28^{c}	37.86±0.26^{d}	36.73±0.15^{e}	39.57±0.16
	a^*	0.07±0.04^{g}	-	1.27±0.03^{b}	1.10±0.04^{c}	1.04±0.05^{d}	0.97±0.04^{e}	0.86±0.05^{f}	1.17±0.06^{a}	1.02±0.02
	b^*	23.33±0.10^{e}	-	24.72±0.10^{a}	24.37±0.10^{b}	23.73±0.08^{d}	24.06±0.13^{c}	22.50±0.12^{f}	20.90±0.12^{g}	22.93±0.06
	ΔE^*	-	-	1.87±0.08	1.54±0.08	1.62±0.31	1.89±0.19	5.00±0.22	6.57±0.24	3.44±0.15
75	L^*	34.46±0.14^{b,c}	40.34±0.10^{a}	37.74±0.07^{a,b}	35.19±0.17^{a,b}	34.07±0.19^{c}	35.23±0.37^{b,c}	34.04±0.24^{b,c}	36.40±0.30^{b}	35.66±0.16
	a^*	1.06±0.04^{c,b}	0.76±0.05^{f}	0.90±0.06^{e}	1.02±0.06^{c,d}	0.94±0.06^{e}	0.97±0.06^{e,d}	1.14±0.06^{b}	1.42±0.05^{a}	1.08±0.02
	b^*	21.45±0.08^{c}	22.73±0.07^{a}	22.62±0.06^{a}	21.72±0.07^{b}	20.72±0.19^{d}	21.53±0.22^{c}	19.25±0.11^{f}	20.26±0.10^{e}	21.06±0.09
	ΔE^*	-	6.03±0.11	3.49±0.19	0.79±0.22	0.85±0.35	0.84±0.40	2.25±0.14	2.31±0.22	1.33±0.13

♣Data are presented as means±standard deviation. Data value of each parameter with different superscript letters in rows are significantly different ($P \leq 0.05$).

Table 6.19 Colour parameters of seaweed powder obtained from *Fucus vesiculosus* previously dried at 35, 50, 60 and 75°C and the corresponding size fractions.♣

T (°C)		Fractions (μm)								Whole
		Whole	**< 40**	**40-63**	**63-80**	**80-125**	**125-200**	**200-250**	**250-500**	**Eq. 6.13**
35	L^*	56.23±1.94^{d,e}	60.56±0.28^{a,b}	61.47±0.61^{a}	58.46±1.02^{c,d}	53.74±1.61^{f}	55.36±0.62^{e,f}	48.98±0.67^{g}	45.22±0.88^{h}	50.68±0.32
	a^*	-2.95±0.17^{c}	-3.04±0.03^{c}	-3.18±0.10^{c}	-3.18±0.09^{c}	-2.85±0.13^{c}	-2.90±0.10^{c}	-2.41±0.01^{b}	-1.92±0.27^{a}	-2.43±0.12
	b^*	39.19±0.87^{b,c}	44.94±0.29^{a}	44.85±0.64^{a}	41.30±0.31^{b}	37.98±1.15^{c}	37.82±0.35^{c}	35.01±0.18^{d}	30.87±1.51^{e}	35.34±0.72
	ΔE^*	-	6.53±1.14	7.15±1.16	2.80±1.56	4.29±2.79	2.11±1.37	9.12±0.84	15.30±1.64	6.79±2.39
50	L^*	50.68±0.31^{c,d}	70.95±1.59^{a}	71.36±1.07^{a}	59.34±0.25^{b}	53.75±1.17^{c}	47.58±0.50^{d}	43.10±0.75^{e}	47.24±1.89^{d}	51.44±0.81
	a^*	-6.40±0.30^{a}	-10.67±0.11^{d}	-11.16±0.06^{d}	-9.77±0.05^{c,d}	-8.63±0.17^{b,c}	-7.11±0.02^{a,b}	-6.11±0.20^{a}	-6.84±0.47^{a}	-7.77±0.20
	b^*	26.05±0.36^{e,f}	46.93±0.27^{a}	45.96±0.16^{a}	38.80±0.26^{b}	35.55±0.42^{c}	29.61±0.54^{d}	25.79±0.81^{f}	28.02±0.70^{d,e}	31.99±0.37
	ΔE^*	-	29.41±1.76	29.10±0.53	15.78±0.25	10.23±0.91	4.77±0.64	7.59±1.01	4.00±1.84	5.83±0.87
60	L^*	34.45±0.56^{b}	44.83±0.79^{a}	44.30±0.36^{a}	30.03±0.49^{c}	26.74±0.64^{c,d}	25.06±0.35^{c,d}	26.33±3.05^{c,d}	29.60±0.39^{c}	29.86±0.33
	a^*	-2.04±0.04^{c}	-2.27±0.04^{c,d}	-2.41±0.01^{d}	-1.63±0.06^{b}	-1.41±0.11^{a,b}	-1.31±0.03^{a}	-1.38±0.20^{a,b}	-1.60±0.01^{a,b}	-1.59±0.03
	b^*	20.39±0.26^{c}	29.88±0.41^{a}	27.53±0.27^{b}	21.78±0.28^{c}	18.01±0.34^{d}	14.76±0.14^{e}	14.15±1.06^{e}	15.04±0.29^{e}	17.16±0.06
	ΔE^*	-	14.07±1.43	12.17±0.17	4.69±0.88	8.09±1.20	10.97±0.92	10.30±3.36	7.24±0.28	5.63±0.84
75	L^*	56.60±1.34^{b}	64.02±0.38^{a}	55.80±0.80^{b}	50.65±0.78^{c}	48.50±0.65^{c}	46.50±0.26^{d}	41.91±0.32^{e}	39.16±0.13^{f}	44.27±0.17
	a^*	-1.86±0.06^{e}	-2.04±0.07^{e}	-1.52±0.03^{e}	-1.27±0.08^{c}	-1.18±0.08^{c}	-1.11±0.04^{b,c}	-0.94±0.09^{a,b}	-0.81±0.10^{a}	-1.03±0.05
	b^*	31.40±0.47^{c}	39.60±0.23^{a}	35.23±0.26^{b}	31.54±0.21^{c}	28.89±0.32^{d}	26.45±0.17^{e}	22.66±0.15^{f}	21.68±0.17^{f}	25.45±0.13
	ΔE^*	-	11.22±1.53	3.99±0.39	6.05±0.85	8.73±1.94	11.14±1.92	17.02±1.67	20.01±1.65	13.72±1.33

♣Data are presented as means±standard deviation. Data value of each parameter with different superscript letters in rows are significantly different ($P \leq 0.05$).

Table 6.20 Particle size distribution of chesnut flour (CTF) and maize flours dried maize milling with two different sieves, 200 μm (YM200, WM200 and PM200) and 500 μm (YM500, WM500 and PM500).

Fraction (μm)	**Mass fraction (w_i, % w/w)**						
	CTF	**YM200F**	**YM500F**	**PM200F**	**PM500F**	**WM200F**	**WM500F**
> 500	-	-	0.7	-	0.4	-	1.1
250 - 500	-	-	21.7	-	23.2	-	41.1
200 - 250	0.0	2.2	10.8	2.3	13.6	2.1	16.1
125 - 200	3.0	12.3	19.2	23.4	22.8	27.0	22.3
80 - 125	8.2	34.9	19.9	28.0	13.3	50.3	9.3
63 - 80	4.9	29.8	12.2	6.5	9.1	11.6	5.0
40 - 63	10.0	13.5	11.8	27.7	10.2	8.0	4.6
< 40	73.9	7.4	3.8	12.0	7.4	0.9	0.6

Table 6.21 Colour parameters of chestnut flour (CTF) and maize flours obtained after dried maize milling with two different sieves, 200 μm (YM200F, WM200F and PM200F) and 500 μm (YM500F, WM500F and PM500F).♣

Flours		Fractions (μm)								Whole
		Whole	**500-250**	**250-200**	**200-125**	**125-80**	**80-63**	**63-40**	**< 40**	**Eq. 6.14**
CTF	L^*	68.87±3.77^{a,b}	-	-	57.84±0.74^{d}	62.16±0.93^{c}	64.00±0.98^{b}	65.86±1.76^{b,c}	72.80±4.41^{a}	69.67±3.11
	a^*	-0.19±0.17^{a,b}	-	-	-0.12±0.17^{a,b}	0.05±0.16^{b}	0.00±0.18^{a,b}	0.01±0.19^{a,b}	-0.24±0.16^{c}	-0.14±0.09
	b^*	7.24±0.65^{c}	-	-	10.56±1.31^{a}	9.53±0.65^{a,b}	8.53±0.53^{b}	8.52±0.37^{b}	7.20±0.60^{c}	7.53±0.60
	ΔE^*	-	-	-	12.56±3.42	7.16±2.67	5.13±2.63	3.47±1.65	3.93±0.64	0.91±0.60
YM200F	L^*	63.13±0.15^{b}	-	-	55.45±0.01^{e}	60.67±0.08^{d}	63.26±0.04^{d}	64.46±0.03^{a}	62.78±0.04^{c}	61.68±0.03
	a^*	-0.79±0.01^{c}	-	-	0.90±0.06^{a}	-0.57±0.04^{b}	-1.02±0.04^{d}	-1.18±0.04^{e}	-1.36±0.03^{f}	-0.78±0.03
	b^*	17.24±0.03^{c}	-	-	30.99±0.04^{a}	20.65±0.04^{b}	16.73±0.03^{d}	16.07±0.01^{e}	13.80±0.01^{f}	18.12±0.02
	ΔE^*	-	-	-	15.84±0.08	4.21±0.05	0.58±0.03	1.82±0.09	3.51±0.03	1.70±0.09
YM500F	L^*	62.35±0.02^{e}	52.09±0.01^{h}	53.17±0.02^{g}	58.22±0.01^{f}	66.36±0.01^{d}	66.46±0.05^{c}	69.49±0.02^{a}	66.96±0.04^{b}	59.28±0.03
	a^*	-0.87±0.03^{c}	1.48±0.04^{a}	-0.69±0.03^{b}	-0.68±0.03^{d}	-1.54±0.02^{d}	-1.65±0.03^{e}	-1.76±0.03^{f}	-1.60±0.02^{d,e}	-1.01±0.03
	b^*	20.92±0.00^{e}	34.12±0.04^{a}	29.31±0.03^{b}	26.40±0.01^{c}	22.04±0.01^{d}	17.58±0.02^{f}	16.17±0.02^{g}	13.04±0.02^{h}	21.12±0.02
	ΔE^*	-	16.89±0.02	12.44±0.02	6.87±0.02	4.22±0.02	5.35±0.03	8.62±0.03	9.16±0.02	3.09±0.02
PM200F	L^*	54.49±0.06^{a}	-	-	49.49±0.01^{f}	50.75±0.02^{e}	51.13±0.02^{d}	54.11±0.02^{b}	52.67±0.28^{c}	51.95±0.08
	a^*	2.94±0.02^{c}	-	-	2.79±0.03^{d}	2.96±0.03^{c}	3.04±0.01^{b}	3.12±0.03^{a}	2.94±0.02^{c}	2.98±0.02
	b^*	0.55±0.03^{c}	-	-	2.22±0.02^{a}	0.97±0.01^{b}	0.30±0.01^{d}	-0.30±0.02^{e}	-0.56±0.01^{f}	-0.49±0.01
	ΔE^*	-	-	-	5.28±0.05	3.77±0.07	3.37±0.06	0.95±0.05	2.13±0.23	2.75±0.06
PM500F	L^*	53.79±0.03^{b}	53.16±0.04^{c}	51.59±0.03^{h}	52.61±0.03^{e}	51.82±0.03^{g}	52.40±0.02^{f}	54.23±0.05^{a}	53.01±0.02^{d}	52.72±0.03
	a^*	1.71±0.02^{b}	2.78±0.01^{a}	2.04±0.04^{f}	2.14±0.02^{e}	2.21±0.03^{e,f}	2.31±0.02^{b,c}	2.33±0.04^{b}	2.26±0.03^{c,d}	2.28±0.03
	b^*	2.54±0.00^{d}	6.81±0.01^{a}	3.11±0.02^{b}	2.73±0.02^{c}	1.77±0.02^{e}	0.79±0.01^{f}	0.30±0.01^{g}	-0.07±0.02^{h}	-0.16±0.02
	ΔE^*	-	4.45±0.01	2.30±0.02	1.27±0.04	2.18±0.05	2.32±0.03	2.36±0.02	2.78±0.03	2.97±0.05
WM200F	L^*	66.41±0.31^{a}	-	-	65.02±0.03^{c}	65.35±0.03^{b}	62.56±0.03^{e}	63.13±0.04^{d}	-	65.36±0.02
	a^*	0.12±0.02^{b}	-	-	0.18±0.04^{a}	0.04±0.04^{c}	-0.03±0.03^{d}	-0.10±0.01^{e}	-	0.07±0.02
	b^*	7.47±0.14^{d}	-	-	8.80±0.03^{a}	7.92±0.01^{b}	7.61±0.01^{c}	7.28±0.01^{e}	-	8.10±0.01
	ΔE^*	-	-	-	1.94±0.13	1.17±0.21	3.86±0.28	3.29±0.28	-	1.25±0.18
WM500F	L^*	65.25±0.21^{c}	58.72±0.03^{g}	62.27±0.03^{f}	66.74±0.04^{a}	64.02±0.03^{e}	64.31±0.04^{d}	65.73±0.03^{b}	-	62.23±0.02
	a^*	0.19±0.03^{b}	0.29±0.01^{a}	0.05±0.01^{c}	-0.05±0.01^{e}	-0.26±0.03^{b}	-0.37±0.05^{a}	-0.41±0.03^{a}	-	-0.13±0.02
	b^*	8.59±0.01^{a}	10.37±0.01^{f}	9.22±0.03^{c}	9.61±0.01^{d}	9.93±0.01^{a}	9.12±0.03^{d}	8.42±0.01^{f}	-	9.80±0.01
	ΔE^*	-	6.77±0.20	3.05±0.20	1.83±0.18	1.88±0.14	1.22±0.18	0.80±0.10	-	3.26±0.19

♣Data are presented as means±standard deviation. Data value of each parameter with different superscript letters in rows are significantly different (P≤ 0.05).

The section in tweets

- *Ascophyllum nodosum* (ANP) and *Fucus vesiculosus* (FVP) powders show similar particle size distribution curves (unimodal).
- *Bifurcaria bifurcata* powders (BBP) show bimodal curves, different to ANP and FVP, probably due to its different structure and composition.
- Seaweed powders show a trend to whiteness, greenness and yellowness colour predominance.
- Brightness, greenness and yellowness of seaweed powders decrease with increasing particle size.
- Increasing drying temperature decreases brightness and yellowness (only for ANP and FVP when $> 60^{o}$C) and greenness for all seaweed powders.
- A model to estimate powders colour from colour of their size fractions when none mass fraction represents $> 40\%$ is proposed, Eq. (6.13).
- Particle size of starchy flours depends not only on the employed mesh during milling but also on the nature of the starchy material.
- White maize flour (WMF) presents higher particle size than yellow (YMF) and purple (PMF) maize flours.
- Chestnut flour (CTF) presents lower particle size compared maize flours and indicating that it is softer.
- PMF show redness and YMF yellowness predominance probably due to its high anthocyanin and carotenoids content, respectively.
- Increasing particle size decrease brightness and increase redness and yellowness predominance in all flours colour.
- A model to estimate powders colour from colour of their size fractions is proposed, Eq. (6.14).
- CTF show lower total starch content than maize flours.
- Milling process affects damaged starch (DS) of flours. The lower the mesh employed during milling the higher the DS.
- WMF show the highest and YMF the lowest values of DS, this difference could be due to different hardness and friability of maize variety.

USC
UNIVERSIDADE
DE SANTIAGO
DE COMPOSTELA

6.4 Seaweeds extracts

Aqueous extracts of *Ascophyllum nodosum*, *Bifurcaria bifurcata* and *Fucus vesiculosus* seaweeds powders were obtained by Ultrasounds-Assisted Extraction (UAE) (Section 4.4). Firstly, preliminary assays were carried out in order to establish the optimal conditions (liquid/solid ratio and contact time) to carry out the UAE that generates aqueous extracts with the highest total polyphenols content. Subsequently, the effect of air-drying temperature (35, 50, 60 and 75°C) and seaweed powders particle size as well as the effect of freeze-drying of *Ascophyllum nodosum*, on the antioxidant activity (SA), total polyphenols (TP) and carbohydrates (CHO) content of the aqueous extracts was assessed. Two different parameters were employed for TP and CHO evaluation: one referred to raw powder employed to obtain the seaweed extracts (TP_w and CHO_w) and other referred to the dry solids content in the extracts (TP_s and CHO_s). This differentiation allows to determine whether differences of TP or CHO content could be due to the effect of drying temperature/particle size or due to differences in the extraction yield. Finally, aqueous extracts properties were also related to physicochemical properties of seaweed powders previously described in Section 6.3 of this Thesis.[4]

[4]This section has been adapted from the following papers and others in writing process:
MOREIRA, R., CHENLO, F., SINEIRO, J., ARUFE, S. & SEXTO, S. (2016). Drying temperature effect on powder physical properties and aqueous extract characteristics of *Fucus vesiculosus*. *Journal of Applied Phycology* **28**, 2485–2494. DOI: http://doi.org/10.1007/s10811-015-0744-9.
MOREIRA, R., SINEIRO, J., CHENLO, F., ARUFE, S. & DÍAZ, D. (2016). Aqueous extracts of *Ascophyllum nodosum* obtained by ultrasound assisted extraction: effect of drying temperature of seaweed on their properties. *Journal of Applied Phycology*. IN PRESS. DOI: http://doi.org/10.1007/s10811-017-1159-6.

6.4.1 Nomenclature

Powders

AN35P	–	*Ascophyllum nodosum* (AN) powder obtained from AN35.
AN50P	–	AN powder obtained from AN50.
AN60P	–	AN powder obtained from AN60.
AN75P	–	AN powder obtained from AN75.
BB35P	–	*Bifurcaria bifurcata* (BB) powder obtained from BB35.
BB50P	–	BB powder obtained from BB50.
BB60P	–	BB powder obtained from BB60.
BB75P	–	BB powder obtained from BB75.
FV35P	–	*Fucus vesiculosus* (FV) powder obtained from FV35.
FV50P	–	FV powder obtained from FV50.
FV60P	–	FV powder obtained from FV60.
FV75P	–	FV powder obtained from FV75.

Aqueous extracts

AN35E	–	Aqueous extract (AE) obtained from AN35P.
AN50E	–	AE obtained from AN50P.
AN60E	–	AE obtained from AN60P.
AN75E	–	AE obtained from AN75P.
BB35E	–	AE obtained from BB35P.
BB50E	–	AE obtained from BB50P.
BB60E	–	AE obtained from BB60P.
BB75E	–	AE obtained from BB75P.
FV35E	–	AE obtained from FV35P.
FV50E	–	AE obtained from FV50P.
FV60E	–	AE obtained from FV60P.
FV75E	–	AE obtained from FV75P.
FVACE	–	Acetone extract obtained from FV35P.
ANFDE	–	AE obtained from AN freeze-dried milled seaweed.
AN35EF	–	AE obtained from AN35P's sizes between 250-500 μm.
AN50EF	–	AE obtained from AN50P's sizes between 250-500 μm.
AN60EF	–	AE obtained from AN60P's sizes between 250-500 μm.
AN75EF	–	AE obtained from AN75P's sizes between 250-500 μm.

Parameters

TP_w	–	Total polyphenols content (TP), mg PHL·(g dry powder)$^{-1}$.
TP_s	–	Total polyphenols content (TP), mg PHL·(g dry solids)$^{-1}$.
CHO_w	–	Carbohydrate content (CHO), mg GL·(g dry powder)$^{-1}$.
CHO_s	–	Carbohydrate content (CHO), mg GL·(g dry solids)$^{-1}$.
SA	–	Antioxidant activity, %.

6.4.2 Introduction

In recent years, there has been an increasing interest in natural antioxidants to replace synthetic additives in foods or nutraceuticals. One reason that can explain this trend is the safety and toxicity issues related with synthetic antioxidants (Khairy & El-Sheikh, 2015). Natural antioxidants are effective in protecting the body against damage caused by Reactive Oxygen Species (ROS) and extending the storage time of food (Heo *et al.*, 2005). They have the capability not only to improve oxidative stability but also to provide a wide variety of additional health benefits (Wang *et al.*, 2012). They inhibit or prevent the oxidation of a substrate and evolve to protect biological systems against damage induced by ROS.

Although marine algae are exposed to light and oxygen, causing the formation of free radicals, there is no presence of oxidative damage in the structural components of seaweeds. This fact suggests that their cells have protective antioxidative defense systems (Jiménez-Escrig *et al.*, 2001). In fact, there are several substances (mainly, polyphenols) present in marine algae that are strongly related to the antioxidant activity (Keyrouz *et al.* (2011) and Hahn *et al.* (2012)). It has been demonstrated that some marine algal extracts have strong antioxidant properties (Chew *et al.*, 2008) that were related to the composition of the seaweed from which they were obtained, such as pigments (fucoxanthin, astaxanthin, carotenoid e.g.) and polyphenols (phenolic acids, phlorotannins e.g.) (Heo *et al.*, 2005). The composition of seaweeds and hence their antioxidant compounds depends on species, geographic area, season (Peinado *et al.*, 2014), environmental parameters such as light, nutritional history, salinity, temperature, contaminants (Stengel *et al.*, 2011) and even natural variability in biochemical composition exists within individual thalli (Stengel & Dring, 1998).

It has been demonstrated that antioxidant compounds from seaweeds have health benefits such as antimutagenic, anti-viral, amelioration of diabetic complication, bactericides, etc. (Cornish & Garbary, 2010). Some types of polyphenols and tannins (i.e. phlorotannins) have strong antioxidant activities, and they are abundant in brown macroalgae, such as *Sargassum*, *Fucus* and *Ascophyllum* species, which have high concentrations (from 1 - 14% dry solid, d.s.) of polyphenols. *Ascophyllum* and *Fucus* are the species with the maximum content (14% and 12% d.s., respectively). Some of them have been also reported to work as preventative medicines for problems like cardiovascular diseases, cancers and arthritis (Holdt & Kraan, 2011) and were reported to have anti-inflammatory properties (Balboa *et al.*, 2013). These biological activities, attributed to the phlorotannins, contributed for the reputation of brown seaweed as a source of healthy food (Pádua *et al.*, 2015).

Regarding the potential uses of brown seaweeds, due to their interesting antioxidant properties, it is necessary to study how the processing (including operations such as collection, preservation (drying) and storage, among others) affects the biological activity of certain compounds. Traditionally, seaweeds are sundried for long periods of time. In particular, drying is the most common preservation method of fresh, harvested biomass which decreases the water activity of the material. It represents one of the most employed industrial operations worldwide as it accounts for about 10-25% of the total energy consumption in manufacturing processes (Mujumdar, 2006). There are several reasons for drying biological products, extending storage time reducing spoilage processes, enhancing the final quality, facilitating the handling and transport, to improve further processing and, finally, to destroy micro-organisms (improve sanitation)(Brennan, 1994).

The current increase of marine algae production rates requires the application of faster and controlled industrial methods. In this sense, in order to overcome these long periods of natural sun drying (days), several alternatives can be useful such as freeze-drying and convective hot air drying, which is the most widely employed method for preserving biological materials, where the air conditions (temperature, relative humidity and velocity) are controlled (Santchurn et al., 2012). Compared to air convective drying, freeze-drying leads, in general, to much less shrinkage (Mayor & Sereno, 2004). During drying, the solid material can undergo several processes that modify the physical (rehydration, color loss), chemical (browning reaction, lipid oxidation) and also nutritional (vitamin and protein loss) properties (Bonazzi & Dumoulin, 2011). Particularly, colour is a main attribute with respect to the quality of dried materials and can change during drying due to chemical and biochemical reactions. As it was discussed in section 6.3 of this Thesis, colour characteristics as a measure of the processes promoted during drying, could be related to the properties of the extracts. In particular, antioxidant activity can be affected during thermal drying and the effects must be determined for specific seaweed species.

The use of ultrasound technology is widely extended in the food industry. It has been implemented in several large-scale commercial applications such as emulsification, homogenization, extraction, crystallization, etc. It has gained the attention for its application for the extraction of natural products. Particularly, Ultrasound-Assisted Extraction (UAE) is considered as "green technique", as it complies with standards set by Environmental Protection Agency, USA (Talmaciu *et al.*, 2015). The high degree of UAE development is due to its requirement for relatively inexpensive equipment, simple operation, and high efficiency (Mason *et al.*, 2011). UAE allows the extraction of natural products in a short time by means of the improvement of solvent penetration and cell walls disruption

that aids the release of its content. UAE usually increases yields and the quality of the extract and can replace efficiently the traditional technologies to extract bioactive compounds from natural sources (Picó (2013) and Corbin *et al.* (2015)). Yield and extraction rates increase with smaller particle size, but milling is an intensive energy operation that must operate without denaturing the material and commensurate with separation from the solvent post-extraction (Balachandran *et al.*, 2006). In recent years, there are several compounds that have been extracted by UAE using water as solvent, especially bioactive compounds in the food industry. UAE has been used, *i.e.*, for lycopene extraction from tomatoes (Lianfu & Zelong, 2008), anthocyanins from raspberries (Chen *et al.*, 2007), phenolic compounds from citrus peel (Ma *et al.*, 2009)) and seaweeds (Kadam *et al.* (2015a), Kadam *et al.* (2015c) and Rodrigues *et al.* (2015)).

Several authors studied the effect of different drying techniques in the antioxidant properties of seaweeds extracts. Norra *et al.* (2016) reported for *Sargassum sp.* that extracts obtained employing oven-dried seaweed at 50°C had higher antioxidant properties that those obtained from sun-dried and freeze-dried seaweeds. Ling *et al.* (2015) studied the effect of different drying techniques (oven drying (40 and 80°C), sun drying, hang drying, sauna drying, shade drying and freeze drying) on the phytochemical content and antioxidant activity of *Kappaphycus alvarezii.* They reported that oven-dried and shade-dried samples contained the highest values of phytochemical content and antioxidant activity compared to other dried samples tested. Cruces *et al.* (2016) analysed the effect of freeze-drying, silica-drying, oven-drying and air-drying on antioxidant activity of *Lessonia spicata* and reported freeze-drying as the best method. Other authors focused their studies on the effect of drying temperature with the same drying technique: Tello-Ireland *et al.* (2011) studied the effect of drying temperature (from 40 up to 70°C) on the antioxidant activity of *Gracilaria chilensis* extracts, indicating that antioxidant activity showed a decreasing pattern as the drying temperature increased; Gupta *et al.* (2011) evaluated the phytochemical characteristics of *Himanthalia elongata* seaweed after drying at low temperature (from 20 up to 40°C) and reported that drying caused a significant decrease in the antioxidant activity of the extracts. Some of these results are partially contradictory and experiments must be carried out for the study of each seaweed.

No studies assessing the effect of drying conditions on phytochemical properties of *Ascophyllum nodosum*, *Bifurcaria bifurcata* and *Fucus vesiculosus* were found in literature. Consequently, the main objective of this section is to determine the effect of the air drying temperature on phytochemical constituents of the aqueous extracts obtained from these three brown seaweeds by means of UAE method using water as solvent.

6.4.3 Preliminary assays

Preliminary assays were undertaken to establish the optimal liquid/solid (L/S) ratio and contact time to carry out the polyphenols and carbohydrates extraction, Figure 6.14. The L/S ratio was established between 20 and 40 (w/w) and contact time of extraction between 4 and 20 min employing *Fucus vesiculosus* seaweed powders obtained from *Fucus vesiculosus* previously dried at 35°C (FV35P).

6.4.3.1 Total polyphenols content

In the case of TP content, Table 6.23, it was observed that L/S ratios $\geq$ 30 significantly increased TP content of the extracts. Besides, no significant increase was observed on TP content when L/S was increased from 30 to 40 w/w. For contact time period, the highest TP_w values corresponded to contact times $\leq$ 12 min. However, TP_s values indicated that a contact time of 4 min implies significantly higher polyphenols content values respect to dry solids in the extracts than the other contact times applied. This behaviour is likely caused by a potential degradation undergone by polyphenols due to longer periods of exposure to ultrasounds once they were extracted to the liquid phase than a lower yield of extraction when employing higher contact times.

Regarding these results, the optimal conditions to obtain seaweeds extracts with large polyphenols content seems to be those with high L/S ratio ($\geq$ 30) and low contact times (4 min).

Table 6.23 Total polyphenolic (TP) and carbohydrate (CHO) content of extracts obtained from *Fucus vesiculosus* previously dried at 35°C using different liquid/solid ratio and contact times (τ) during UAE.♣

L/S (w/w)	τ (min)	**TP_w**	**TP_s**	**CHO_w**	**CHO_s**
20	4	1007 ± 46^b	1433 ± 65^b	5424 ± 344^a	8574 ± 544^a
30	4	1571 ± 76^a	2940 ± 141^a	5152 ± 260^a	8218 ± 414^a
40	4	1772 ± 19^a	2371 ± 34^a	5204 ± 882^a	7763 ± 1315^a
30	4	1571 ± 76^a	2940 ± 141^a	5152 ± 260^b	8218 ± 414^b
30	12	1514 ± 68^b	2029 ± 92^b	7383 ± 839^a	11211 ± 1044^a
30	20	1331 ± 5^c	1759 ± 7^b	7096 ± 168^a	10427 ± 248^a

TP_w is referred to raw powder (mg PHL/100 g dry powder), TP_s is referred to total solids content in the extract (mg PHL/100 g dry solids), CHO_w is referred to raw powder (mg GL/100 g dry powder) and CHO_s to total solids content in the extract (mg GL/100 g dry solids).♣Data are presented as means±standard deviation. Data value of each parameter with different superscript letters in columns are significantly different ($P\leq 0.05$).

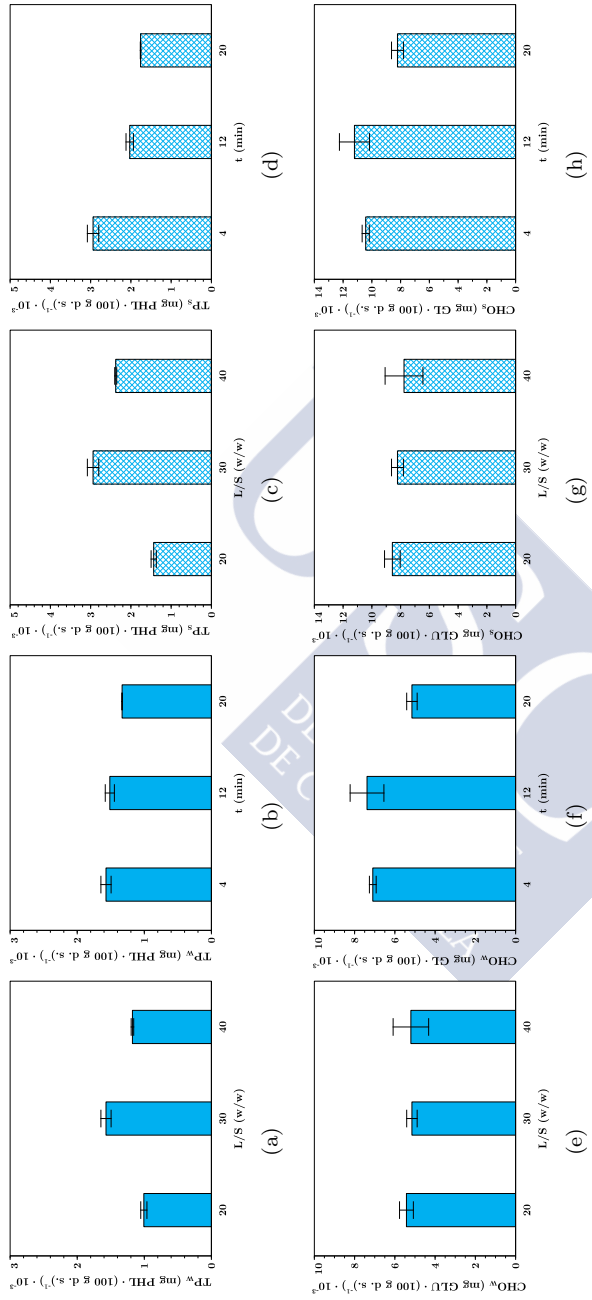

Figure 6.14 Total polyphenols (TP) and carbohydrate content (CHO) of aqueous extracts obteined with different L/S ratios (a, c, e, g) and conctact times (b, d, f, h) of *Fucus vesiculosus* powders formerly dried at 35°C: referred to raw powder (mg PHL·(100 g dry powder)$^{-1}$, TP_w and (mg Gl·(100 g dry powder)$^{-1}$, CHO_w (■) and total solids content in the extract (mg PHL·(100 g dry solids)$^{-1}$, TP_s and (mg GL·(100 g dry solids)$^{-1}$, CHO_s (☒).

6.4.3.2 Carbohydrates content

Concerning carbohydrates content, no significant differences were observed when employing liquid/solid ratios from 20 to 40 w/w, Table 6.23. However, regarding contact time influence in CHO content, it was observed that larger contact times than 4 min significantly increased CHO_w and CHO_s content. Compared to TP results, it can be said that carbohydrates extraction seems to be a slower process than polyphenols extraction because it could be improved by increasing contact time from 4 to 12 min whilst for polyphenols extraction it was observed that higher contact times did not increas TP content in the extracts.

Taking into account these results, the optimal conditions to obtain seaweeds extracts with the objective of obtaining large carbohydrate contents would be those with contact times $\geq$ 12 min together with liquid/solid ratios that could varied indistinctly between 20 and 40 w/w.

6.4.3.3 Selection of Ultrasounds Assisted Extraction conditions

Regarding the obtained results, the most adequate conditions for seaweeds extracts obtaining employing UAE can be establish. Taking into account that the present work aims to obtain seaweeds extracts with the larger antioxidant activity and this property is often related to the TP in the extracts as reported by several authors (Matanjun *et al.* (2008); (Igual *et al.* (2010); Bahorun *et al.* (2004)); Rubilar *et al.* (2006); (Rubilar *et al.*, 2007); (Connan *et al.*, 2007)), the selected conditions corresponded to a contact time of 4 min and a liquid/solid ratio of 30 w/w.

6.4.4 Influence of air-drying temperature on chemical properties of extracts

The influence of air-drying temperature on seaweeds extracts was studied to establish the temperature that leads to the highest TP and CHO.

6.4.4.1 Total polyphenols content

Total polyphenols content values (TP) of aqueous extracts from *Ascophyllum nodosum*, *Bifurcaria bifurcata* and *Fucus vesiculosus* are shown in Figure 6.15 and Table 6.24.

The highest TP (TP_w and TP_s) values were achieved for the extracts obtained from AN50P (3180±131 mg PHL/100 dry powder and 13383±552 mg PHL/100 g dry solids, respectively). AN35E reported a slightly lower TP content (below ≈12%). Increasing the drying temperature to 75°C decreased TP ≈31%. When freeze-dried samples (ANFDE) were employed TP_w was reduced by up to 53% (1500±99 mg PHL/100 dry powder and 5799±382 mg PHL/100 g dry solids). TP_s in the extracts showed the same trend. These results indicated that the significant differences in TP can be attributed to the combined effect of the dehydration method (*i.e.* freeze-drying or convective air-drying) and temperature (in the case of convective air-drying) and not to differences in the extraction yields. Moreover, their lead to the conclusion that, regarding samples affected from air-drying technique, the air-drying temperatures $\leq$ 60°C did not affect noticeably TP content of extracts from *Ascophyllum nodosum*.

Table 6.24 Total polyphenolic (TP) and carbohydrate (CHO) content of extracts from *Ascophyllum nodosum*, *Bifurcaria bifurcata* and *Fucus vesiculosus* dried at different temperatures.♣

Extract	TP_w	TP_s	CHO_w	CHO_s	SA (%)
ANFDE	1500±99^{d}	5799±382^{d}	5136±649^{b}	14890±1742^{d}	70.9±5.5^{a,b}
AN35E	2802±147^{b}	12003±766^{b}	5267±1078^{b}	22167±4537^{b}	74.7±2.4^{a}
AN50E	3180±131^{a}	13383±552^{a}	6472±574^{a}	27238±2416^{a}	76.2±5.0^{a}
AN60E	2584±52^{b}	9233±185^{c}	4182±706^{b,c}	14945±2522^{c}	67.0±8.6^{a,b}
AN75E	2194±339^{c}	8147±1260^{c}	3951±493^{c}	14671±1832^{c}	62.9±8.4^{b,c}
BB35E	1041±48^{a}	2317±99^{a}	2394±167^{a}	5211±363^{a}	58.3±2.3^{b,c}
BB50E	985±69^{a}	2207±155^{a}	2228±176^{b,c}	4993±394^{a}	54.7±7.2^{b,c}
BB60E	1037±61^{a}	2270±134^{a}	2275±181^{b,c}	4980±396^{a}	55.4±0.7^{b,c}
BB75E	848±13^{b}	1784±28^{b}	2103±143^{c}	4426±301^{b}	45.3±2.5^{c,d}
FVACE	11428±1124^{a}	-	11388±156	-	-
FV35E	1571±76^{b}	2940±141^{a}	5152±994^{a}	8218±414^{b}	57.7±3.4^{b,c}
FV50E	983±33^{c}	2006±68^{b}	4592±225^{a}	10144±511^{a,b}	31.0±1.3^{d,e}
FV60E	943±66^{c,d}	2056±143^{b,c}	5192±524^{a}	12588±1269^{a}	30.8±3.2^{d,e}
FV75E	847±73^{d}	1670±145^{c}	5883±357^{a}	12895±783^{a}	26.0±1.7^{e}

TP_w is referred to raw powder (mg PHL/100 g dry powder), TP_s is referred to total solids content in the extract (mg PHL/100 g dry solids), CHO_w is referred to raw powder (mg GL/100 g dry powder) and CHO_s to total solids content in the extract (mg GL/100 g dry solids).♣Data are presented as means±standard deviation. Data value of each parameter with different superscript letters in columns (for each seaweed) are significantly different ($P \leq 0.05$).

It was unexpected that extracts from the hot air-drying treatment gave larger TP compared to those obtained employing the freeze-drying technique for AN extracts. This behaviour was also observed for the red seaweed *Kappaphycus alvarezii*, which produced a 45% lower TP for freeze-dried material, compared with samples dried at 80°C, by convective air-drying and 47% lower TP than seaweed dried at 40°C (Ling *et al.*, 2015). These differences could be related

to different extraction yields as consequence of employed drying techniques that could affect differently seaweed structure.

In the case of TP content of BB extracts, the air-drying temperature effect showed a similar trend as those observed for *Ascophyllum nodosum* extracts. Air-drying temperatures lower than 60°C did not significantly change TP content.

With regards to *Fucus vesiculosus* extracts, air-drying temperatures higher than 35°C significantly caused a TP decrease. The significantly highest TP was obtained for the extract made employing FV35P (1571±76 TP_w, 2940±141 TP_s). A reduction of TP_w of 37% was produced when employing FV50P and up to 54% when FV75P was employed. That indicates a more sensible behaviour of this parameter with air-drying temperature, compared to the others seaweeds. Extractions were also carried out with acetone/water mixture (70/30 v/v) to achieve the theoretical highest extraction yield as reported by Koivikko *et al.* (2007), replicating the remaining operation conditions. TP attained was 11428±1124 TP_w, which is within the interval of 8–13% of dry matter reported by Ragan & Jensen (1978) and is comparable to TP_w achieved by Díaz-Rubio *et al.* (2009) in extractions with acetone/water and methanol/water mixtures using *Fucus vesiculosus*. The maximum TP obtained employing only water as solvent in the ultrasound extraction accounted for 14.4±1% of TP_w achieved with an acetone/water mixture. Acetone may contribute to a higher solubility of these compounds due to its low polarity, viscosity, surface tension, etc. In addition, polyphenols exhibit a wide difference among their composition and structure and, as a result, in polarity. The use of water as the only solvent allows the extraction of water-soluble polyphenols, while the addition of acetone promotes the extraction of the non-polar fraction as well (López *et al.*, 2011)).

Comparing all studied seaweed extracts and taking into account that the same procedure was applied, it can be concluded that *Ascophyllum nodosum* aqueous extracts have the highest polyphenolic content followed by *Fucus vesiculosus* (51% of reduction in TP_w) and *Bifurcaria bifurcata* (67% of reduction in TP_w).

Extracts obtained from seaweeds dried at 75°C rendered the lowest TP values for all studied species, thus indicating that air-drying temperature clearly influences TP content of the extracts, independently of the seaweed species. The use of a hot air-drying technique can lead to thermally-promoted physical and chemical processes (*i.e.* structural collapse of cells during drying, textural modifications, migrations of chemical compounds, accumulation of substances in cell membranes and several chemical reactions) during this step, which make difficult the subsequent extraction of phenolic compounds.

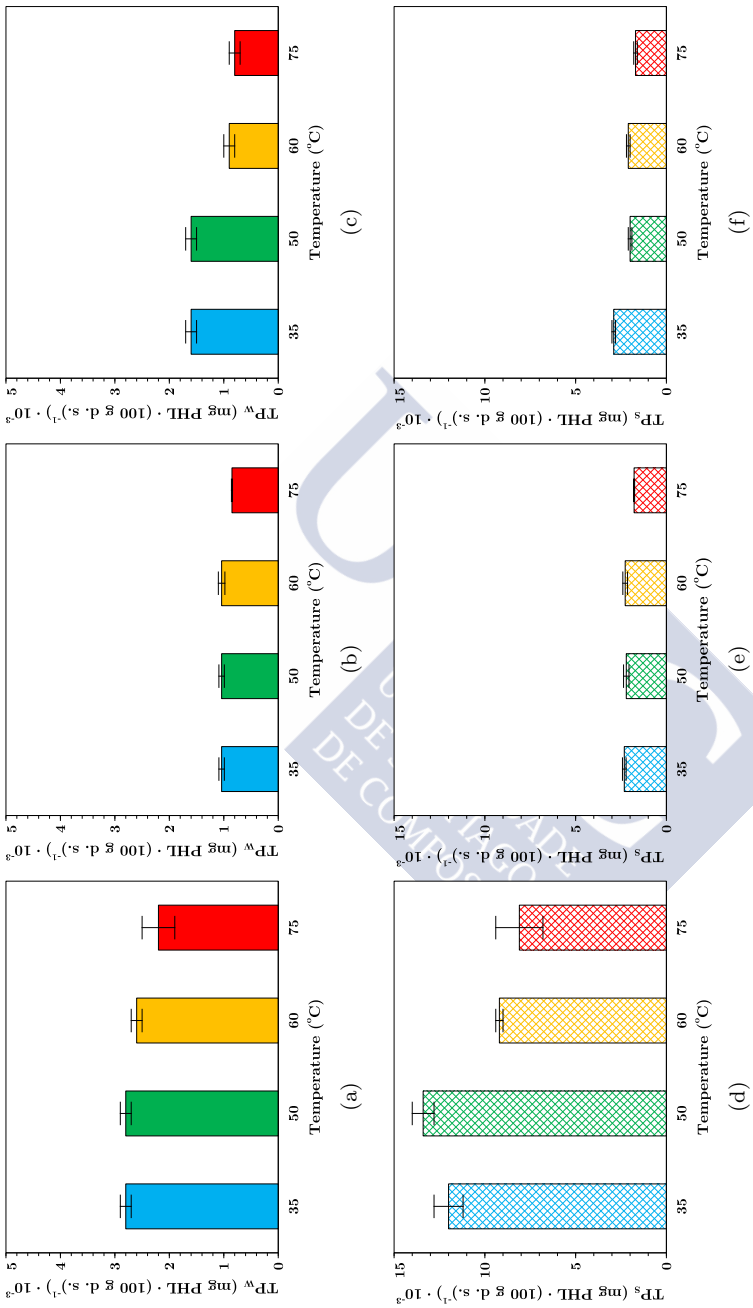

Figure 6.15 Total polyphenols content (TP) of aqueous extracts of *Ascophyllum nodosum* (a, d), *Bifurcaria bifurcata* (b, e) and *Fucus vesiculosus* (c, f) powders formerly dried at different temperatures (35 (■), 50 (■), 60 (■) and 75°C (■)): referred to raw powder (mg PHL·(100 g dry powder)$^{-1}$, TP_w (■) and total solids content in the extract (mg PHL·(100 g dry solids)$^{-1}$, TP_s (☒).

The different trends observed for TP values as function of air temperature for each seaweed suggest that these thermally promoted processes are affected by morphology, seaweed composition, etc.

TP_s in the extract showed the same trend as TP_w for all analyses seaweed extracts. This result implies that differences in TP can be attributed to the effect of drying temperature, and not to a difference in extraction yield.

6.4.4.2 Carbohydrate content

The effect of drying temperature on carbohydrate content (CHO) of extracts can be observed in Figure 6.16. Moreover, ANOVA analysis of these data is presented in Table 6.24.

In the case of *Ascophyllum nodosum* extracts, the highest carbohydrate content (*e.g.* CHO_w 6465±579 mg eq. GL/100 g dry powder or CHO_s 27212±2435 mg eq. GL/100 g dry solid) were obtained in AN50E. The carbohydrate content in the extracts decreased dramatically with increasing drying temperature with no significant difference between AN60 and AN75, indicating that 60°C could be a threshold temperature when no decrease on CHO content is desired. AN35E showed intermediate values.

Regarding *Bifurcaria bifurcata*, carbohydrate content showed a similar trend with air-drying temperature as *Ascophyllum nodosum* extracts. Air-drying temperatures higher than 60°C significantly decreased CHO content, BB75E showing the minimum values of CHO_w and CHO_s (2103±143 mg eq. GL/100 g dry powder and 4426±301 mg eq. GL/100 g dry solid, respectively). However, in this case the maximum value of CHO content was observed for BB35E (2394±167 mg eq. GL/100 g dry powder and 521±363 mg eq. GL/100 g dry solid, respectively). These results might be related to the physical and chemical processes that may difficult the extraction of carbohydrates, in the same mode than the phenolic compounds. Similarly, to the TP content results, CHO obtained results indicated that their differences should be attributed to the effect of drying conditions (temperature) and not to the differences in the extraction yields, because trends of CHO_w and CHO_s values with temperature were similar.

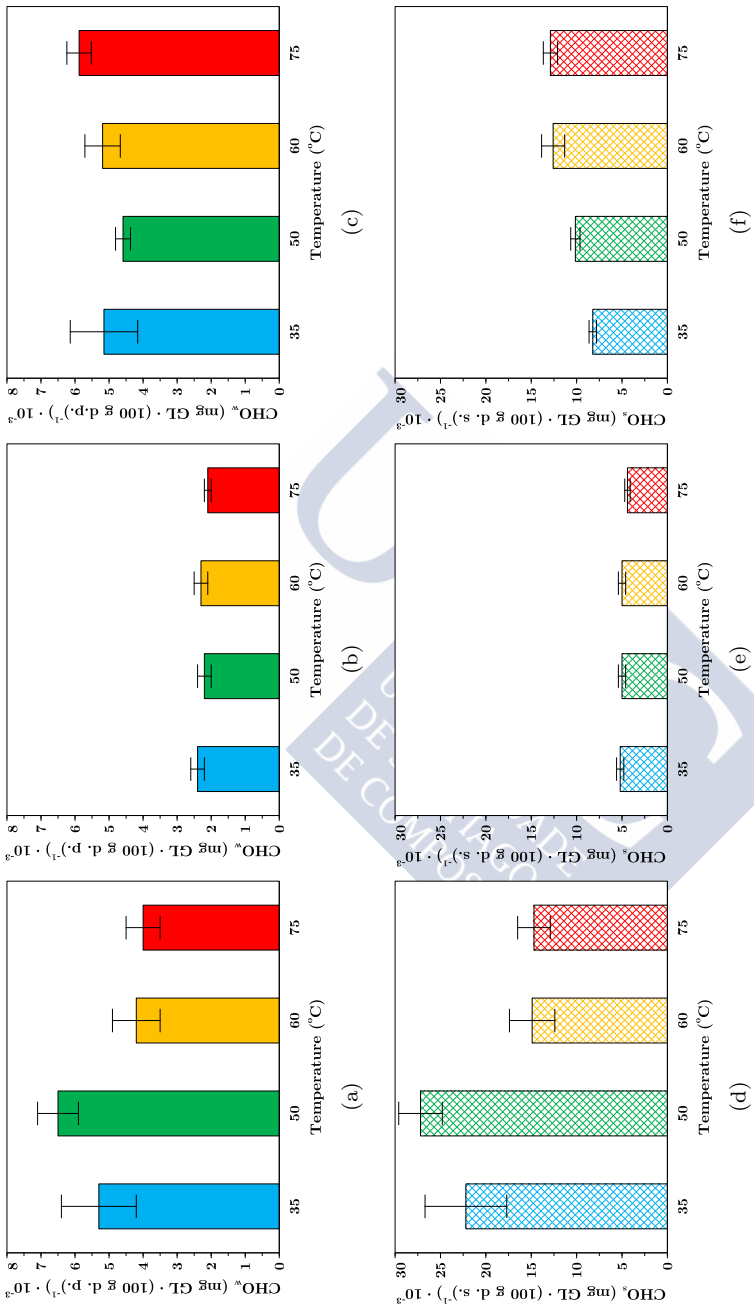

Figure 6.16 Carbohydrate content (CHO) of aqueous extracts of *Ascophyllum nodosum* (a, d), *Bifurcaria bifurcata* (b, e) and *Fucus vesiculosus* (c, f) powders formerly dried at different temperatures (35 (■), 50 (■), 60 (■) and 75°C (■)): referred to raw powder (mg GL·(100 g dry powder)$^{-1}$, CHO$_w$ (■) and total solids content in the extract (mg GL·(100 g dry solids)$^{-1}$, CHO$_s$ (☒).

With regards to *Fucus vesiculosus*, the relationship between carbohydrates content and air-drying temperature showed a completely different behaviour. CHO_w values were no significantly different (mean value: 5204 mg eq. GL/100g dry powder) when analysing the effect of drying temperature. The content of carbohydrates referred to total solids content (CHO_s) was significantly lowest for those samples obtained from FV35P (8217±414 mg eq. GL/100g dry powder). The significantly highest value corresponded to FV60E and FV75E samples (12588±1269 and 12895±784 mg eq. GL/100g dry powder, respectively). No significant differences in CHO_s values between samples FV60E and FV75E were observed. Although extraction yields referred to raw seaweed powder were similar, there should be compounds already extracted or degraded during drying at 60 and 75°C. If these substances are not removed at lower drying temperatures, they are extracted during ultrasound-assisted extraction thus increasing the total solids content of the extract. The extraction with acetone/water (70/30 v/v) of FV35P gave CHO_w of 11388±156 mg eq. GL/100g dry powder. The aqueous extraction of *Fucus vesiculosus* seaweed dried at 75°C exhibited the highest yield in relation to the acetone/water extract (≈52%). As most polysaccharides present in the seaweed are structural substances, a higher drying temperature (75°C) might have contributed to a better subsequent extraction of carbohydrates.

6.4.4.3 Antioxidant Activity

The antioxidant activity of aqueous seaweed extracts was evaluated by means of total DPPH radical scavenging activity (SA) and related to total polyphenols content.

For *Ascophyllum nodosum*, the influence of air-drying temperature and freeze-drying operation was assessed (Table 6.24). Note here that ANOVA analysis was carried out with all studied systems in order to differentiate the seaweed with the highest SA. Regarding air-drying temperature effect, extracts obtained from AN75P showed significantly lower SA than samples dried at lower temperature or freeze-dried. Taking into account the trends mentioned for TP with temperature, these results indicated that freeze-dried samples produced aqueous extracts with the lowest TP (see section 6.4.4.1) values, but their polyphenols were more active than those extracted from air-dried samples because of a lower thermal degradation.

Radical scavenging activity of *Bifurcaria bifurcata* extracts showed lower values compared to *Ascophyllum nodosum* extracts obtained at lower temperatures (< 50°C), Table 6.24. Namely, SA values of *Bifurcaria bifurcata* extracts are in the

range of those obtained for AN75E which makes clear the higher antioxidant capacity of *Ascophyllum nodosum* extracts. No significant effect of air-drying temperature on SA values of *Bifurcaria bifurcata* extracts were observed.

Concerning *Fucus vesiculosus* extracts, FV35E exhibited the highest radical scavenging activity (57.7±3.4%) similar to those obtained from *Bifurcaria bifurcata* seaweed powders $< 60^{o}$C and *Ascophyllum nodosum* ($\geqslant 60^{o}$C). As in the case of polyphenols, an increase in drying temperature gave as result a significant decrease of radical scavenging activity up to the lowest value (26.0±1.7%) in FV75E.

The results obtained clearly indicated a large antioxidant capacity under the tested conditions for aqueous extracts of *Ascophyllum nodosum* compared to those reported for *Fucus vesiculosus* and *Bifurcaria bifurcata*.

Linear correlations (R^2 >0.97) were established between TP_s and radical scavenging activity of *Ascophyllum nodosum* (Eq. 6.15), *Bifurcaria bifurcata* (Eq. 6.16) and *Fucus vesiculosus* (Eq. 6.17) extracts:

$$SA(\%) = 0.0026TP_S + 42.64 \tag{6.15}$$

$$SA(\%) = 0.0228TP_S + 4.54 \tag{6.16}$$

$$SA(\%) = 0.044TP_S - 11.90 \tag{6.17}$$

Freeze-dried samples were not included in these correlations due to they did not follow the same behaviour. These positive linear relationships were also found in green and red seaweeds (Matanjun *et al.*, 2008) in fruits (Igual *et al.* (2010); Bahorun *et al.* (2004)), hulls (Rubilar *et al.*, 2007), leaf extracts Rubilar *et al.* (2006) and brown seaweeds (Connan *et al.*, 2007).

The reduction in TP content and SA at high drying temperatures may be due to several factors: release of phenolic compounds bound to cell wall during drying; thermal degradation by oxidative enzymes; phenolic compounds may rapidly degrade at drying temperatures above 40°C; binding of polyphenols to other substances (proteins) or alterations in their chemical structure (Gupta *et al.* (2011); Tello-Ireland *et al.* (2011); Le Lann *et al.* (2008)). Tello-Ireland *et al.* (2011) reported a loss of antioxidant activity when drying *Gracilaria chilensis* at high temperatures (70°C) and Gupta *et al.* (2011) a 30% decrease in TP of *Himanthalia elongata* when dried at 40°C in comparison with fresh seaweed.

6.4.5 Influence of powder particle size on extracts properties

The effect of particle size of seaweed powders on aqueous extracts properties was also assessed. Two different types of studies were carried out: the first one employing the particle size fraction (250-500 μm) of *Ascophyllum nosodum*, that corresponds to the highest mass fraction of seaweed powders obtained employing different air-drying temperatures, in order to determine if the antioxidant activity of final extract is mainly bounded to this fraction. The second employing different particle size fractions of *Fucus vesiculosus* powders obtained from seaweed drying at 35°C, in order to study the effect of particle size in extraction process of polyphenols compounds.

In the case of *Ascophyllum nodosum*, TP values were higher for the whole-seaweed powders (section 6.4.4.1) rather than those from the 375 μm average particle size, Table 6.25. Nevertheless, the same trend with temperature was found, Figure 6.17. Using this fraction, maximum TP values (2792±244 mg PHL/100 dry powder and 11751±1027 mg PHL/100 dry solid) were also obtained with AN50E samples. No significant differences between AN35E samples were observed (only a reduction of 4% of TP_w was measured). By applying a drying temperature of 75°C, a reduction of 35% in TP_w was observed.

The extracts obtained from the highest particle size fraction of AN35P exhibited the highest SA (70.6±5.4%), a similar value to those of extracts obtained from whole-powders AN35P and AN50P, Table 6.25. Extracts from the highest particle size fraction of AN50P showed no significant difference in SA whilst temperature up to 60°C significantly decreased SA values of extracts. A linear correlations (R^2 >0.97) was established between TP_s and radical scavenging activity of *Ascophyllum nodosum* extracts obtained from highest particle size fraction of powders, Eq. (6.18):

$$SA(\%) = 0.0026 TP_S + 37.54 \tag{6.18}$$

Regarding carbohydrate content of the extracts of *Ascophyllum nodosum* obtained from the highest particle size fraction of the seaweed powders, the same trend with air-drying temperature as those obtained from the whole-seaweed powders were observed but the corresponding carbohydrate content was always lower (around 25-30%).

Total polyphenols content of aqueous extracts obtained from different particle size fractions of *Fucus vesiculosus* powder formerly dried at 35°C are shown in the Table 6.26. The size fraction between 80 and 125 μm exhibited the significantly

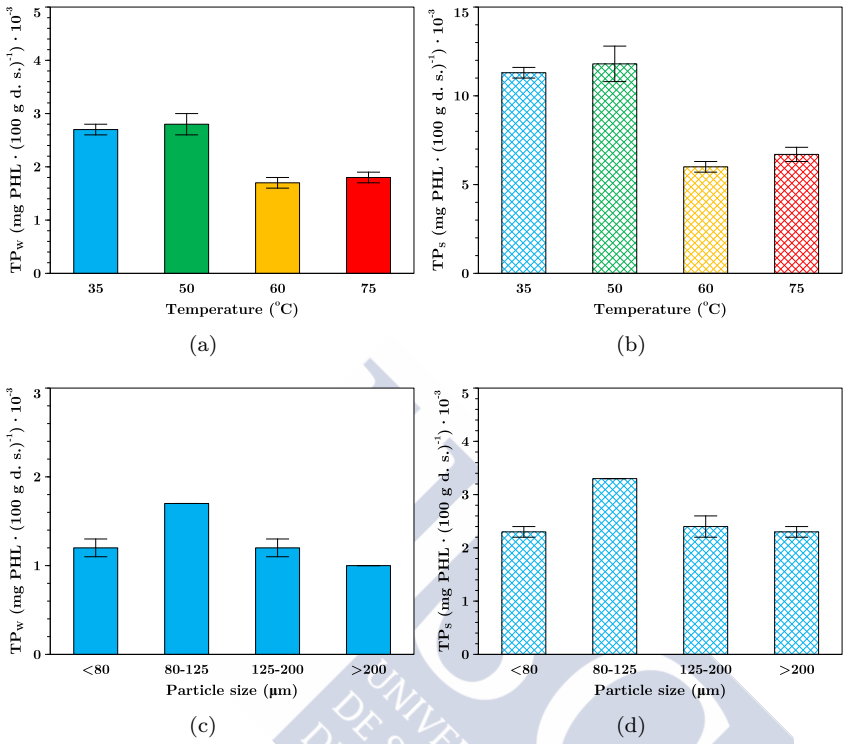

Figure 6.17 Total polyphenols content (TP) of aqueous extracts of *Ascophyllum nodosum* (a, b) powders (fraction 250-500 μm) formerly dried at different temperatures (35 (■), 50 (■), 60 (■) and 75°C (■)) and *Fucus vesiculosus* different fractions of powders dried at 35°C (c, d): referred to raw powder (mg PHL·(100 g dry powder)$^{-1}$, TP_w (■) and total solids content in the extract (mg PHL·(100 g dry solids)$^{-1}$, TP_s (☒).

Table 6.25 Total polyphenols (TP) and carbohydrate (CHO) of extracts from fractions (250-500 μm) of *Ascophyllum nodosum* previously dried at different temperatures.♣

Extract	TP_w	TP_s	CHO_w	CHO_s	SA (%)
FAN35FE	2687±82^a	11310±343^b	2729±135^b	12304±609^b	70.6±5.4^a
FAN50FE	2792±244^a	11751±1027^a	3984±1004^a	17754±4474^a	65.0±3.3^a
FAN60FE	1691±88^b	6041±313^b	2403±195^b	10002±813^b	51.9±1.0^b
FAN75FE	1803±112^b	6696±414^b	2428±155^b	9998±639^b	56.5±0.4^b

TP_w is referred to raw powder (mg PHL/100 g dry powder), TP_s is referred to total solids content in the extract (mg PHL/100 g dry solids), CHO_w is referred to raw powder (mg GL/100 g dry powder) and CHO_s to total solids content in the extract (mg GL/100 g dry solids).♣Data are presented as means±standard deviation. Data value of each parameter with different superscript letters in columns are significantly different ($P \leq 0.05$).

highest total polyphenols content (TP_w of 1672±13 mg PHL/100 g dry powder and TP_s of 326±20 mg PHL/100 g dry solids), Figure 6.17. The fraction with the significantly lowest TP_w was that with the highest particle diameter (> 200 μm). No significant differences were found among the remaining size fractions. The smallest and the biggest fractions exhibited a reduction in total polyphenols content. The first observation may be attributed to the accumulation of inorganic substances, like salts in the smallest fractions. In the largest fractions, seaweed cells could not be totally degraded and, polyphenols, along with other substances, might not have been released indicating that higher extraction times would be necessary for particles this size. Hence, polyphenols are better extracted when intermediate fractions are employed.

Table 6.26 Total polyphenols content (TP) of extracts of *Fucus vesiculosus* powder fractions with different particle size previously dried at 35°C.♣

Fraction (μm)	**TP_w**	**TP_s**
< 80	1222±56^b	2334±107^b
80-125	1672±13^a	3258±24^a
125-200	1216±75^b	2412±150^b
> 200	1042±26^c	2265±57^b

TP_w is referred to raw powder (mg PHL/100 g dry powder)and TP_s is referred to total solids content in the extract (mg PHL/100 g dry solids).♣Data are presented as means±standard deviation. Data value of each parameter with different superscript letters in columns are significantly different (P≤ 0.05).

6.4.6 Antioxidant activity *vs* seaweed powder colour

Antioxidant activity of aqueous seaweed extracts of studied seaweeds (*Ascophyllum nodosum*, *Bifurcaria bifurcata* and *Fucus vesiculosus*) obtained from whole or sieved powders and colour of air-dried seaweed powder from which they were obtained was found to be related. A linear trend between the greenness colour of powders (a^*) and the scavenging activity of seaweeds aqueous extracts is observed, Figure 6.18, when antioxidant activity is larger than 40%. As previously mentioned in Section 6.3 fucoxanthin is an important component on brown seaweed responsible of its green colouration and it is also known to be an antioxidant compound in edible seaweeds (YAN *et al.*, 1999).

This fact seems to indicate that colour could be a useful parameter for applications where extracts with high antioxidant activity have to be obtained from this seaweeds because the seaweed powders can be previously selected (by

colorimetric technique) in order to obtain the extracts with the best qualities.

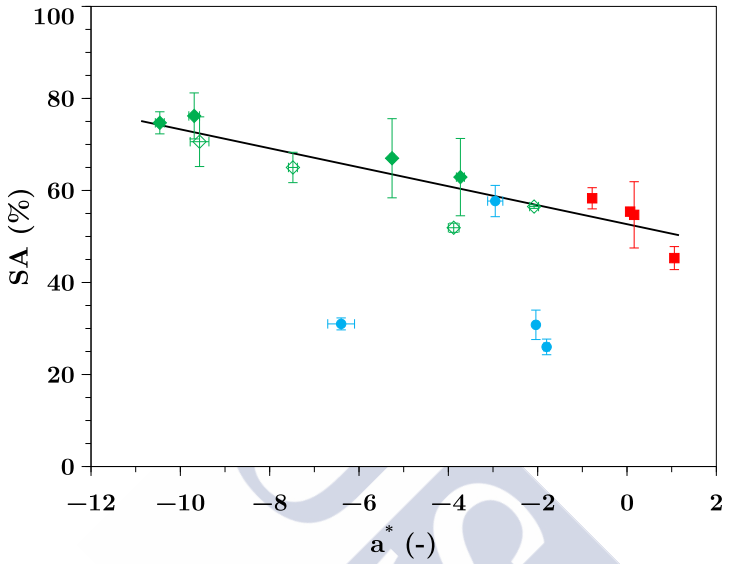

Figure 6.18 Relationship between scavenging activity (SA) and green colour parameter (a^*) of aqueous seaweeds extracts obtained from *Ascophyllum nodosum* (whole ♦ and sieved ◊), *Bifurcaria bifurcata* (■) and *Fucus vesiculosus* (●) seaweeds powders.

6.4.7 The section in tweets

- *Ascophyllum nodosum* (AN) aqueous extracts present the highest polyphenols content (TP) of all studied seaweed extracts.
- Air-drying temperature significantly modifies antioxidant properties, TP and carbohydrate content (CHO) of seaweed aqueous extracts.
- In general, TP content significantly decrease when drying at temperatures higher than 60°C.
- Increasing temperature decreases CHO of AN and *Bifurcaria bifurcara* (BB) aqueous extracts. *Fucus vesiculosus* (FV) present the reverse trend.
- The particle size of powders influences TP; polyphenols are better extracted when intermediate fractions (80-125 μm) are employed.
- Freeze-drying technique decreases TP and CHO in extracts compared to those obtained from seaweeds air-dried at low temperatures.
- Green colour of seaweed powders can be a good indicator of high antioxidant activity of obtained extracts.

6.5 Preparation of flour doughs: mixing characteristic curves

Mixing properties of gluten-free flour doughs based on maize flours, chestnut flour and chestnut flour blends consisting of chestnut flour enriched with seaweed powders of *Ascophyllum nodosum*, *Bifurcaria bifurcata* and *Fucus vesiculosus* obtained from seaweeds dried at 35°C has been studied employing Mixolab® apparatus. Moreover, the thermal mixing properties of those doughs with better mixing properties has also been studied and discussed as function of flour nature and additives employed.[5]

[5]This section has been adapted from the following papers published and in writing process: MOREIRA, R., CHENLO, F., ARUFE, S. & RUBINOS, S. (2015). Physicochemical characterization of white, yellow and purple maize flours and rheological characterization of their doughs. *Journal of Food Science and Technology-Mysore* **12**, 7954–7963. DOI: http://doi.org/10.1007/s13197-015-1953-6.
MOREIRA, R., CHENLO, F., SINEIRO, J., TORRES, M. D. & ARUFE, S. (2017). Mixing, rheological and thermomechanical characterization of seaweed-enriched chestnut flour doughs. To be submitted to: *Journal of Food Engineering*.
MOREIRA, R., CHENLO, F., SINEIRO, J., TORRES, M. D. & ARUFE, S. (2017). Physico-Chemichal Properties of seaweed-enriched chestnut flour cookies obtained from pregelatinized doughs. To be submitted to: *Journal of Texture studies*.

Nomenclature

Powders

AN35P	–	*Ascophyllum nodosum* (AN) powder obtained from AN35.
BB35P	–	*Bifurcaria bifurcata* (BB) powder obtained from BB35.
FV35P	–	*Fucus vesiculosus* (FV) powder obtained from FV35.
GG	–	Guar gum.

Doughs

CAN03D	–	Chestnut flour dough with 3% f.b. of AN35P.
CAN06D	–	Chestnut flour dough with 6% f.b. of AN35P.
CAN09D	–	Chestnut flour dough with 9% f.b. of AN35P.
CBB03D	–	Chestnut flour dough with 3% f.b. of BB35P.
CBB06D	–	Chestnut flour dough with 6% f.b. of BB35P.
CBB09D	–	Chestnut flour dough with 9% f.b. of BB35P.
CTD	–	Chestnut flour dough.
CTSD	–	Chestnut flour dough with 1.8% f.b. of sodium chloride (S).
CTSGD	–	Chestnut flour dough with 1.8% f.b. of S and 2% f.b. of GG.
CFV03D	–	Chestnut flour dough with 3% f.b. of FV35P.
CFV06D	–	Chestnut flour dough with 6% f.b. of FV35P.
CFV09D	–	Chestnut flour dough with 9% f.b. of FV35P.
PM200D	–	Purple maize dough (flour obtained with 200 μm mesh during milling).
PM500D	–	Purple maize dough (flour obtained with 500 μm mesh during milling).
WM200D	–	White maize dough (flour obtained with 200 μm mesh during milling).
WM500D	–	White maize dough (flour obtained with 500 μm mesh during milling).
YM200D	–	Yellow maize dough (flour obtained with 200 μm mesh during milling).
YM500D	–	Yellow maize dough (flour obtained with 500 μm mesh during milling).

Parameters

α	–	Protein network weakening rate, N·m·min^{-1}.
β	–	Starch gelatinization rate, N·m·min^{-1}.
γ_e	–	Enzymatic degradation rate, N·m·min^{-1}.
C1	–	Target consistency, N·m.
C2	–	Minimum torque achieved due to protein weakening, N·m.
C3	–	Maximum achieved due to starch gelatinization, N·m.
C4	–	Minimum torque achieved as consequence of enzymatic degradation, N·m.
C4/C3	–	Cooking stability, (-).
C5	–	Final dough consistency when applying complete curve protocol, N·m.
D_w	–	Mass mean diameter, Eq. (4.20), μm.
DPT	–	Departure time, min.
DS	–	Damaged Starch, g damaged starch· (g dry flour)$^{-1}$.
DT	–	Development time, min.
MW	–	Mechanical weakening, N·m·min^{-1}.
SP	–	Swelling power, mL·(g d.s.)$^{-1}$.
ST	–	Stability time, min.
T_0	–	Initial gelatinization temperature, ^{o}C.
T_{fg}	–	Final gelatinization temperature, ^{o}C.
WA	–	Water absorption, % f.b..
WRC	–	Water retention capacity, g water·(g d.s.$^{-1}$).

6.5.1 Introduction

Traditionally, dough is a blend of flour, water and mechanical energy to obtain a final mixed product. In bakery products, this process is one of the most important steps that influence the final product quality (Bushuk *et al.*, 1997). Mixing process of flour doughs is mainly constituted by several steps (Feigl *et al.*, 2003). Firstly, to mix and distribute ingredients of the formulation (flour, water, salt, sugars, additives, etc.) in order to obtain a homogeneous system. Secondly, the dough has to develop a continuous three-dimensional viscoelastic structure with good properties to retain gas production caused by yeast during fermentation (in the case of fermented doughs) or at the beginning of the baking process.

In order to obtain high quality products, doughs dedicated to bread production need protein structures developed to achieve the objective of retention capability of gas, parameter that is not so important for pastry-making doughs. The gluten in wheat flour is able to form these structures during hydration but in the case of gluten-free flours, additives (hydrocolloids, polymers, etc.) may have to be included to allow the action to replace the gluten. The mixing time is also important for the quality of dough, depends on the composition of the flour, the type of mixer and the formulation of the dough, to obtain optimal values. Considering all mentioned above, the rheological study of this type of material becomes imperative to understand their behaviour and thus to improve their properties to get a better technological skills.

Gluten-free flours from cereals (maize and rice) and beans (chickpea) are commonly manufactured (Moreira *et al.*, 2013b). Some studies on these flour doughs are available (Lazaridou *et al.*, 2007) but no comparative studies on different types of maize have been reported. Moreover, seaweed enrichment of gluten-free doughs as a new source to develop new products suitable for people with coeliac disease has not been studied yet, up to our knowledge.

The main aim of this work is to characterize the mixing behaviour of flour doughs made from three types of maize (purple, yellow and white), from chestnut flour and from blends of chestnut flour enriched with different levels (3, 6 and 9%) of seaweed powders (*Ascophyllum nodosum*, *Bifurcaria bifurcata* and *Fucus vesiculosus*) manufactured at the same consistency using a laboratory kneader. Furthermore, the results obtained will be discussed in relation to physical and chemical properties of flours and additives employed and compared to some commercial gluten and gluten-free flour doughs.

6.5.2 Gluten-Free flour doughs based on chestnut flour

Experimental mixing curves (see Section 4.5.1) of chestnut flour doughs obtained from chestnuts previously dried at 45°C and milled in a centrifugal mill employing a 200 μm standard sieve are shown in Figure 6.19 (a). All curves showed a similar behaviour. Firstly, the consistency (torque) of dough increases as consequence of water absorption by flour components that leads to a structure-formation process which binds starch and other flour components (Létang *et al.* (1999); Maeda *et al.* (2015)). Subsequently, after achieve a maximum; a softening stage characterized by the continuous decrease on consistency begins due to of mechanical weakening of dough caused by mixing.

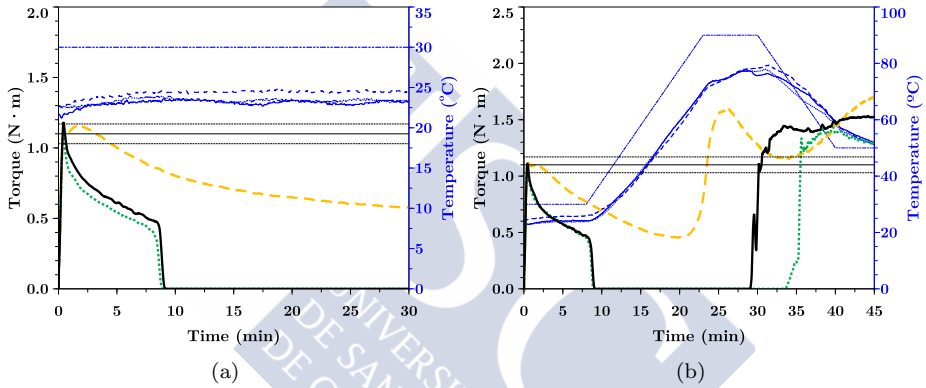

Figure 6.19 Mixolab® simple (a) and complete (b) curves for chesnut flour dough (—), with salt (···) and with salt and guar gum (– – –). Blue lines correspond to bowl (-·-·-) and dough temperatures.

Parameters obtained after experimental data analysis are presented in Table 6.28. Water absorption of chestnut dough (CTD) was significantly higher of those reported by Moreira *et al.* (2010a) for commercial chestnut flour 41.9%. Note here that this difference could be due to chestnut flour employed in this Thesis had noticeable lower D_w (44.1 μm) than those employed in the aforementioned work (168.6 μm). In fact, the same authors reported WA of 56.3% for doughs from flours with lower particle size (76.8 μm) elaborated by mixing of two different sieved fractions (200–80 and < 80 μm) of commercial chestnut flours. This indicates that the obtained WA for chestnut flours is in accordance with literature although the obtained flours after drying and milling of chestnut had lower particle size. Similar WA have been reported for wheat flour dough obtained in similar conditions, 54.6% (Rosell *et al.*, 2007).

Regarding development time (DT, defined as the time interval from water addition to the achievement of C1), departure time (DPT, defined as the time at which the consistency of dough decrease below 1.10±0.07 N·m) and stability (ST, elapsed time at which the torque produced is kept at 1.10±0.07 N·m), very low values of these parameters (0.44, 0.63 and 0.28 min, respectively) were obtained in comparison to commercial chestnut flours (4.70 and 12.2 min for DT and ST, respectively, Moreira *et al.* (2010a)) or commercial wheat flours (1.35 and 5.05 min for DT and ST, respectively, Rosell *et al.* (2007)). Moreover, mechanical weakening (MW, calculated as the torque difference between the maximum torque at 30°C and the torque after 8 min of mixing) of chestnut flour doughs was higher (0.67 N·m) than those obtained for commercial chestnut and wheat flour (*i. e.*, 0.27 N·m, Rosell *et al.* (2007)).

Table 6.28 Mixing curves parameters of chestnut flour doughs based on chestnut flour (CTD) with salt (CTSD) and salt+guar gum (CTSGD) obtained in Mixolab® apparatus.♣

Dough	CTD	CTSD	CTSGD
WA (%, f.b.)	57.3±1.4^a	59.8±1.4^a	56.4±0.8^a
C1 (N·m)	1.14±0.04^a	1.10±0.01^a	1.12±0.03^a
DT (min)	0.44±0.01^b	0.42±0.01^b	1.68±0.20^a
DPT (min)	0.63±0.03^b	0.52±0.01^b	3.61±0.42^a
ST (min)	0.28±0.05^b	0.17±0.01^b	3.22±0.40^a
MW (N·m)	0.67±0.03^a	0.81±0.25^a	0.29±0.03^b
C2 (N·m)	-	-	0.45±0.03
α (Nm·min^{-1})	-	-	-0.029±0.003
C3 (N·m)	-	-	1.69±0.11
β (N·m·min^{-1})	-	-	0.191±0.008
C4 (N·m)	-	-	1.40±0.03
γ (N·m·min^{-1})	-	-	-0.035±0.004
C4/C3 (-)	-	-	0.83±0.03
C5 (N·m)	-	-	2.04±0.07
$\mathbf{T}_0$ (°C)	-	-	56.5±0.6
$\mathbf{T}_{fg}$ (°C)	-	-	75.3±0.8

♣Data are presented as means±standard deviation. Data value of each parameter with different superscript letters in rows are significantly different (P≤ 0.05).

Summarising, CTD showed a very poor mixing behaviour compared to commercial flours established as target. WA was in the range of commercial flours. Nevertheless, CTD showed noticeable lower values of ST and larger values of MW compared to commercial flours doughs indicating that its mixing characteristics are not acceptable. Moreover, as it can be seen in Figure 6.19 (b), no experimental data were obtained employing the complete curve protocol, that

assessed the thermal effect on doughs during mixing (see Section 4.5.1) corroborating the poor mixing quality of this flour.

In order to improve mixing characteristics of chestnut flour, it was added with 1.8% (flour basis, f.b.) of sodium chloride and 2% (f.b) of guar gum (GG) obtaining a new formulation named as CTSGD. As it can be observed in Figures 6.19 (a) and (b), mixing behaviour have been significantly improved.

Regarding simple mixing curve experimental data, Table 6.28, GG addition did not significantly influence WA of doughs. However, characteristics paremters of doughs related to time significantly increased for doughs with GG (*i.e.* DT: 1.68 *vs* 0.44 min). In this case, DT, ST and DPT values were closer to those obtained by Rosell *et al.* (2007) for wheat flour doughs which indicate that mixing behaviour of CTD was improved by adding GG. Note here that two peaks were observed when GG was added to chestnut flour, Figure 6.20.

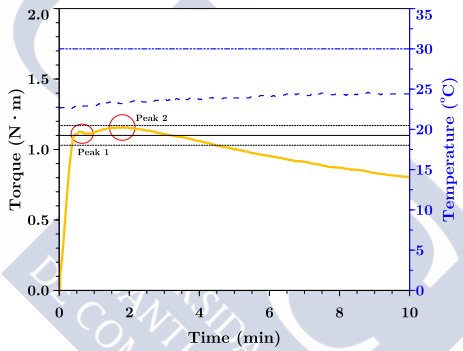

Figure 6.20 Mixolab® simple curve of CTSGD. Blue lines correspond to bowl (-·--) and dough temperatures.

Several authors (Bonet *et al.* (2006); Marco & Rosell (2008); Miś *et al.* (2017)) have already reported that addition of additives of different nature (protein, fibres, etc) to flour could lead to higher characteristic times of doughs since their addition led to a more complex hydration process that needs more time to complete development of dough. In fact, Miś *et al.* (2017) clearly explain that in the case of dietary fibre addition to wheat dough, dough development process can be separated in two steps: an initial stage characterised by highly dynamic changes in the dough consistency, induced probably by hydration of fibre particles added and inclusion thereof into the gluten network obtaining a first peak of consistency, and a second stage consisted in molecular interactions between the fibres and other dough components where a second peak is observed. Processes that take place during mixing due to interaction with gluten not applied in our

case due to the absence of this protein in our systems. However, the achievement of two differents peaks during mixing seems to indicate that a similar hydration process could also taken place when GG was added.

Concerning MW of CTSGD, it was significantly decreased when comparing to CTD. Compared to wheat flour dough as target dough, similar values were obtained (0.29 *vs* 0.27, (Rosell *et al.*, 2007)) which is also indicative of the improving effect of GG addition on chestnut doughs. This indicates that GG addition to chestnut flour aids to strength the dough which consequently caused lower mechanical degradation probably due by molecular interaction between GG and components present in flour.

In the case of thermal behaviour during mixing, note here that CTSGD successfully performed complete curve tests, Figure 6.19 (b). However, in order to facilitate the comprehension of the reader, the analysis and discussion of these experimental data will be carried out together with the effect of seaweed addition to CTSGD in the following section 6.5.4.

6.5.3 Gluten-Free flour doughs based on maize flours

Table 6.29 shows mixing curves parameters obtained in Mixolab® for all assayed gluten-free flour doughs based on different varieties of maize, Figure 6.21 (a). Doughs with the target consistency could not be obtained from YM500 and PM500 flours (the consistency was low). These flours had the highest particle size (D_w: 176 and 250 μm, respectively, Table 6.13) which seems to indicate that flour particle size was critical for the dough formation capacity.

The obtained flour doughs showed water absorption (WA) values significantly different. The lowest WA corresponded to WM500 (48.7%). This value was similar to WA of other gluten-free flour doughs (chestnut) with the same flour particle size (Moreira *et al.*, 2010a). The results showed that WA decreased with increasing flour particle size by comparison of WM samples (WM200, 90.0%). Regarding the effect of maize variety, WA was 63% for YM200 which was in the range to those observed for wheat, rice and yellow maize flours doughs (Rosell *et al.* (2007); Hadnadev *et al.* (2011); Moreira *et al.* (2012)) whilst WM200 and PM200 doughs showed higher WA (> 80%). This trend could be explained by the high values (> 18%) of damaged starch of the respective flours (Table 6.15) that was reported to increase WA (Greer & Stewart, 1959). In fact, a linear relationship (R^2 >0.98) was found among WA and DS for flour doughs with similar average particle size (D_s: 60-90 μm, kernels milled with 200 μm sieve).

Development time of dough (DT) values (< 1 min) were significantly lower

for maize flour doughs with small average particle size (obtained with a 200 μm sieve) and no significant differences among maize varieties were observed. These DT values were similar to those found for some gluten-free commercial flour doughs like rice (1.13 min, Moreira *et al.* (2012)). WM500 showed the highest DT value (7.6 min) and was similar to those observed for whole wheat flour doughs by Moreira *et al.* (2012). This noticeable difference between flours with different particle size can be explained by two main factors. The fact that low particle size of flours is often related to high surface area compared to flours with higher particle size and the high WA of flours obtained with a 200 μm sieve that increased the water availability of flour particles. This led to the conclusion that water absorption rate of flours was higher for those flours with low particle size and high WA values, which was reflected in lower values of DT.

Table 6.29 Mixing curves parameters, obtained in Mixolab® apparatus, of purple (PM), yellow (YM) and white (WM) maize doughs based on flours obtained after milling employing mill's sieves of 200 (PM200, YM200 and WM200) and 500 (WM500) μm .♣

Dough	PM200D	YM200D	WM200D	WM500D
WA (%, f.b)	81.1±1.4^b	63.0±1.0^c	90.0±2.0^a	48.7±2.0^d
C1 (N·m)	1.05±0.04^a	1.09±0.02^a	1.11±0.03^a	1.13±0.04^a
DT (min)	0.72±0.06^b	0.89±0.06^b	0.75±0.02^b	7.62±1.58^a
DPT (min)	1.67±0.12^c	2.61±0.17^b	1.97±0.26^c	9.13±2.28^a
ST (min)	1.10±0.10^b	2.00±0.12^{a,b}	1.50±0.10^{a,b}	2.90±1.20^a
MW (N·m)	0.74±0.04^a	0.49±0.01^b	0.59±0.02^b	0.11±0.14^c
C2 (N·m)	-	-	-	0.16±0.11
α (N·m·min^{-1})	-	-	-	-0.080±0.009
C3 (N·m)	-	-	-	2.01±0.09
β (N·m·min^{-1})	-	-	-	0.251±0.072
C4 (N·m)	-	-	-	2.54±0.46
γ (N·m·min^{-1})	-	-	-	-0.071±0.024
C4/C3 (-)	-	-	-	1.26±0.17
C5 (N·m)	-	-	-	4.09±0.61
$\mathbf{T}_0$ (°C)	-	-	-	57.15±2.62
$\mathbf{T}_{fg}$ (°C)	-	-	-	78.15±1.48

♣Data are presented as means±standard deviation. Data value of each parameter with different superscript letters in rows are significantly different (P≤ 0.05).

Departure time and stability time of doughs are associated. High values are usually related to the strength of flours (Marco & Rosell, 2008). ST values increased with increasing average particle size (from 1.5 min for WM200 to 2.9 min for WM500), a similar trend as obtained in the case of DT values. This behaviour could be explained by the same reason previously exposed for DT values trends. The higher water absorption rates of flours with low particle size implied that

doughs obtained from these flours quickly achieved the target consistency. Hence, dough mechanical weakening begins before for these doughs compared to WM500 dough and consequently ST showed lower values. Stability time (ST) values obtained are in the same range (from 1.1 up to 2.9 min) than those observed for soft wheat, rice and amaranth flour doughs (Moreira *et al.* (2012); Hadnadev *et al.* (2011)). Note here that wheat flour doughs usually have larger DT values than gluten-free doughs precisely by the presence of gluten on the formulation that aids the formation of more strengthen doughs due to gluten network formation. In our case, the absence of gluten on WM flours seems to be covered up by the increasing on particle size of flour, that results in lower WA and consequently more strengthen doughs which showed higher DT values.

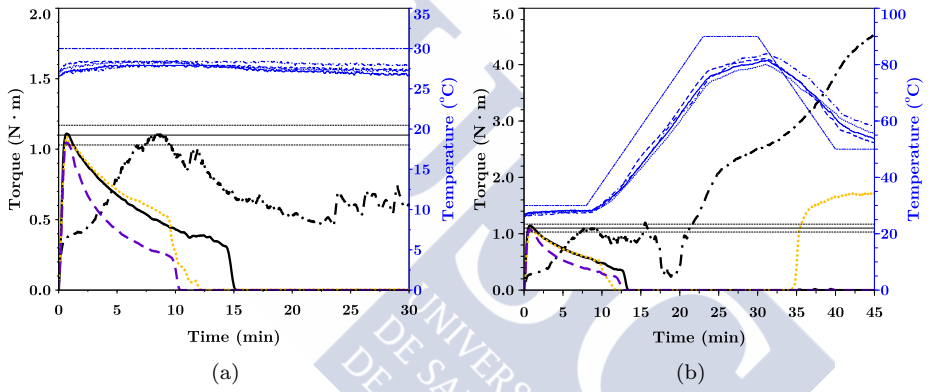

Figure 6.21 Mixolab® simple (a) and complete (b) curves for purple maize (PM200D, - - -), yellow maize (YM200D, ···) and white maize (WM200, —; WM500, - - -). Blue lines correspond to bowl (-·-·-) and dough temperatures.

Mechanical weakening (MW) of dough was also affected by particle size of flours from which they were obtained. As it can be seen, WM doughs showed higher values of MW for doughs obtained from flours with lower particle size (0.59 *vs* 0.11). This fact also confirm that increasing particle size of flours resulted in more strengthen doughs. No clear relationship was found between MW and WA of studied doughs which seems to indicate that maize variety also affected this parameter, probably due to their different compositions.

Regarding thermal properties of doughs during mixing, it has to be noted that only WM500D successfully performed complete curves test. Consequently no comparison between maize varieties could have been done. Regarding proteins network weakening rate, α, its value (-0.080 N·m·min^{-1}) was similar of those obtained for commercial wheat flour and gluten-free formulations such as starch

from corn, however it was higher than those observed for chestnut, rice and yellow maize flours (Moreira *et al.*, 2012). C3 and C4 were similar to those obtained for these commercial flours whilst C5 was larger. β value was lower than to those obtained for the aforementioned commercial flour whilst λ was similar to those obtained for whole wheat. Finally, gelatinaztion temperature obtained showed that WM500D had similar characteristics temperatures of wheat flour and lower T_0 compared to other gluten-free formulations, *i.e.*: chestnut, rice and yellow maize flours doughs (Moreira *et al.*, 2012).

6.5.4 Seaweed-enriched flour doughs based on chestnut flour

Experimental mixing curves of chestnut flour enriched with seaweeds powders of *Ascophyllum nodosum*, *Bifurcaria bifurcata* and *Fucus vesiculosus* obtained applying the simple curve standard protocol using Mixolab® apparatus are shown in Figure 6.22 (a), (b) and (c). All obtained curves showed a similar behaviour of those reported previously for CTSGD.

The parameters obtained after the data analysis as previously explained (see Section 4.5.1) are shown in Table 6.30. In general, seaweed powder addition to control dough (a flour blend consisting of chestnut flour + salt + guar gum, CTSGD) required larger amounts of water to be added in order to obtain doughs with the same consistency. WA of CTSGD was 56.4±0.8 % d.b. which is in the range to those observed for wheat (Rosell *et al.*, 2007) or other gluten-free matrices like rice (Sivaramakrishnan *et al.*, 2004) and yellow maize flours doughs (Moreira *et al.*, 2012). Specifically, water absorption of dough (WA) varied as function of employed seaweed powder. Concerning AN35P, WA significantly increased for doughs with $\geq$ 6% of seaweed powder addition (> 63.0%). BB35P addition had the strongest influence on WA of all seaweed powders. In fact, just a 3% of seaweed powder addition already produced a significantly increase on WA (62.5±0.9%) and the CBB09D had the highest WA of all assayed doughs (70.8±0.8%). Finally, FV35P addition influenced lesser the WA and this parameter was significantly higher to those of control formulation only when large amounts of seaweed powder (9%) were added (64.0±0.1%). Although, WA was significantly modified by seaweed powder addition, all WA values obtained for these series of experiments were in the range of other gluten-free doughs such as wholegrain buckwheat or amaranth flour (Hadnadev *et al.*, 2011) and wheat flour doughs enriched with red seaweed (*Kappaphycus alvarezii*) powder incorporated at levels from 2 to 8%, whose WA varied even in a wider range from 58.5±0.1 to 77.6±0.2% (Mamat *et al.*, 2014).

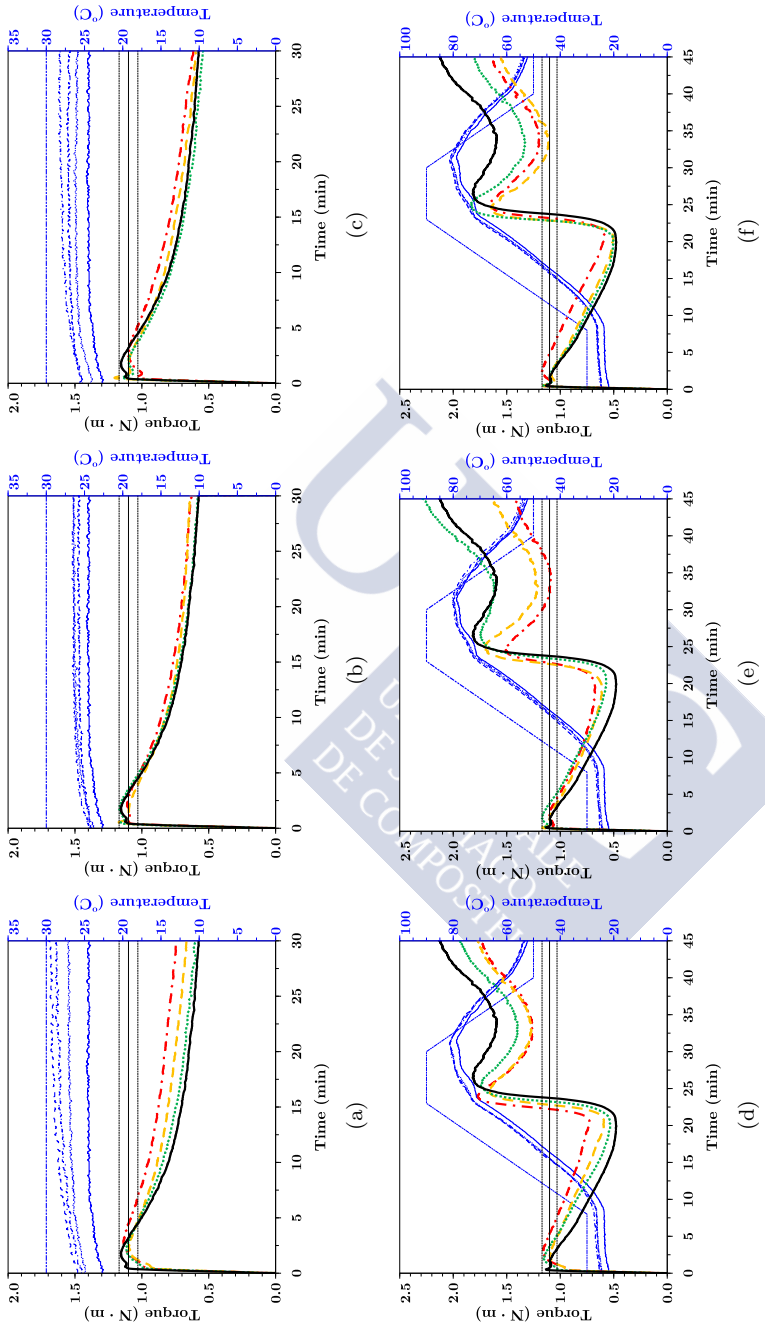

Figure 6.22 Mixolab® simple (a, b, c) and complete (d, e, f) curves for CF control dough (—) and doughs with seaweed powders (*Ascophyllum nodosum* (a, d), *Bifurcaria bifurcata* (b, e) and *Fucus vesiculosus* (c, f)) added at different levels (3% (···), 6% (- - -) and 9% (-·-·-)). Blue lines correspond to bowl (-·-·-) and dough temperatures.

Table 6.30 Mixing curves parameters of chestnut flour seaweed-enriched doughs obtained in Mixolab® apparatus (target torque, C1: 1.10±0.07 Nm).♣

Dough	WA (%, f.b.)	DT (min)	DPT (min)	ST (min)	MW (N·m)
CTSGD	56.4 ± 0.8^{a}	$1.68\pm0.20^{d,e}$	3.61 ± 0.42^{c}	$3.22\pm0.40^{b,c}$	0.29 ± 0.03^{a}
CAN03D	$58.3\pm0.6^{a,b}$	$2.11\pm0.19^{b,c,d}$	$4.22\pm0.24^{b,c}$	3.02 ± 0.52^{c}	$0.22\pm0.01^{b,d,e}$
CAN06D	63.2 ± 0.3^{d}	$2.33\pm0.15^{a,b,c}$	$4.85\pm0.14^{b,c}$	$3.70\pm0.23^{b,c}$	$0.17\pm0.01^{d,e,f}$
CAN09D	$68.7\pm0.5^{e,f}$	2.81 ± 0.05^{a}	6.89 ± 0.71^{c}	5.65 ± 0.87^{a}	0.13 ± 0.01^{f}
CBB03D	$62.4\pm0.7^{c,d}$	$1.75\pm0.12^{d,e}$	$4.82\pm0.39^{b,c}$	$4.47\pm0.38^{a,b,c}$	$0.28\pm0.03^{a,b}$
CBB06D	67.5 ± 1.3^{e}	1.57 ± 0.09^{e}	$3.87\pm0.06^{b,c}$	$3.53\pm0.06^{b,c}$	$0.22\pm0.01^{b,c,d}$
CBB09D	70.4 ± 1.0^{f}	$2.09\pm0.05^{b,c,d}$	$4.60\pm0.05^{b,c}$	$4.22\pm0.08^{a,b,c}$	$0.20\pm0.01^{d,e}$
CFV03D	$58.9\pm0.7^{a,b}$	$1.84\pm0.15^{c,d,e}$	$3.72\pm0.47^{b,c}$	$3.38\pm0.45^{b,c}$	$0.27\pm0.01^{a,b,c}$
CFV06D	$60.5\pm1.0^{b,c}$	$1.95\pm0.04^{c,d,e}$	$3.98\pm0.25^{b,c}$	$3.66\pm0.27^{b,c}$	$0.22\pm0.01^{c,d,e}$
CFV09D	64.0 ± 0.5^{d}	$2.50\pm0.18^{a,b}$	4.92 ± 0.48^{b}	$4.50\pm0.46^{b,c}$	$0.16\pm0.01^{e,f}$

♣Data are presented as means±standard deviation. Data value of each parameter with different superscript letters in columns are significantly different ($P\leq 0.05$).

The increase of WA of doughs with seaweed powder addition could be explained by higher water affinity of seaweed powders compared to chestnut flour. This can be observed in their different WRC. Although the reported values of WRC are determined after 18h of hydration and with no competence with other matherials for water (Robertson *et al.*, 2000), and during mixing the times are lower (1.57-2.50 min) and seaweed particles compete with flours components for water, the larger WRC of seaweed powders ($\geq$ 10.40 g water·(g d.s)$^{-1}$, Table 6.12) compared chestnut flour $\leq$ 3.80 g water·(g d.s)$^{-1}$ clearly highlight this difference. Moreover, this trend can also be observed on the high hygroscopicity of seaweed showed up by their water adsorption isotherms compared to chestnut flour water adsorption isotherms previously reported by Moreira *et al.* (2010b), Figure 6.23.

The different trends of WA as function of the employed seaweed powder could be also explained by the different WRC together with the mean particle size of each seaweed powder. BB35P addition produced a higher influence on WA because of its higher WRC (14.40±0.08 g water·g d.s^{-1}) compared to those of AN35P and FV35P ($\leq$ 10.57 g water·g d.s^{-1}), Table 6.12. Due to the limitations of WRC values previously mentioned in order to understand WA behaviour of doughs. If it is considered that all water added goes directly to seaweed powders an effective WRC inside the blends during mixing could be calculated. This $WRC_{effective}$ would be 2.9±0.3, 2.0±0.2 and 1.7±0.1 g water·(g seaweed powder)$^{-1}$ for BB35P, AN35P and FV35P, respectively. These values are lower than those reported in Table 6.12 due to in this case seaweed powders compete with other flour components for water during mixing. However, the trends of $WRC_{effective}$ with seaweed specie are corroborated due to the largest WRC also corresponded for BB35P followed by AN35P and FV35P. Finally, the fact that AN35P influenced

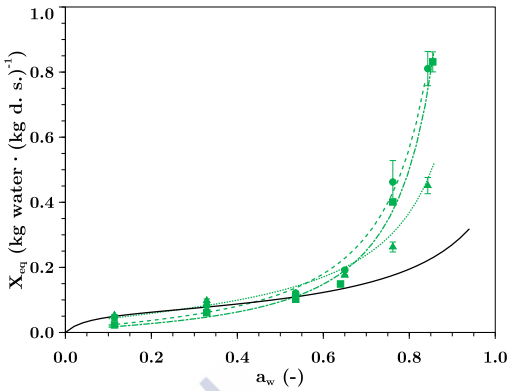

Figure 6.23 Water adsorption isotherms of brown seaweeds *Ascophyllum nodosum* (▲, ···), *Bifurcaria bifurcata* (■, - · -) and *Fucus vesiculosus* (●, - - -) and chestnut flour (—, Moreira *et al.* (2010b)) at 25°C. Green lines correspond to proposed model (Eq. (6.1), Section 6.1).

stronger WA than FV35P, even if they have a similar WRC at 18h, could be explained by the different particle size of these powders. AN35P had a significantly lower particle size compared to FV35P (*i.e.*, D_s: 77±1 *vs* 133±31 μm for AN35P and FV35P, respectively). As previously mentioned in section 6.5.3, low particle sizes of powders are often related to high surface area of these systems that could enhance their water absorption, in this case leading to a larger effective WRC for AN35P.

Regarding the development time (DT), significant increases were observed on DT values ($\geq$ 2.09±0.05 min) for doughs enriched with large quantities of *Ascophyllum nodosum* ($\geq$ 6%), *Bifurcaria bifurcata* (9%) and *Fucus vesiculosus* (9%) compared to control dough (1.68±0.20 min). The increase of WA caused by seaweed powder addition could lead to expect a decrease on DT values, as previously reported by Marco & Rosell (2008) for rice flour doughs with different WA maintaining constant the composition of dough. However, in our case this trend was not observed because the composition of doughs varied as consequence of different levels of seaweed powder addition. In fact, several authors (Marco & Rosell (2008); Miś *et al.* (2017); Bonet *et al.* (2006)) have already reported that addition of additives of different nature (protein, fibres, etc) to flour could lead to higher development times of doughs since they are also involved in water absorption process showing different consistency peaks, as previously explained in Section 6.5.2. This could explain the mentioned increase on DT values of seaweed-enriched doughs compared to CTSGD.

The effect of the seaweed powders on departure time (DPT) was closely related to the one observed on the stability time (ST). A significant increase on these parameters was observed on AN09D (6.89±0.71 min compared to 3.61±0.42 min for control dough) which represents a high percentage of seaweed powder addition. Moreover, it has to be mentioned that even no significant differences were observed on ST and DPT for the remaining doughs it seems to exist a slight increase on ST values due to seaweed powder addition, Table 6.30. The same trend was previously reported by Mamat *et al.* (2014) for wheat flour doughs enriched with red seaweed powder (*Kappaphycus alvarezii*). The fact that the same trend had been observed for gluten-free and non gluten-free doughs could indicate that the main effect of seaweed powder addition on ST could be due to interactions between this added particles and flour components like starch or other proteins different to gluten.

The ST is an indicator of flour strength. The higher the values of this parameter, the stronger the dough. This regard is corroborated by the mechanical weakening (MW) values that were lower for those doughs with large seaweed powder content. The control dough and doughs with the lowest content of seaweed powder addition (3%) showed the significantly highest values of MW ($\geq$ 0.22±0.01 N·m), whilst the lowest values of MW ($\leq$ 0.20±0.01 N·m) corresponded to those doughs with the highest seaweed powder content (9%). Note here that a linear relationship was found between seaweed powder addition (%, taking into account control dough as 0% of addition) and MW ($R^2 > 0.92$). The obtained values of MW were in the same range of those obtained by Moreira *et al.* (2012) for gluten (soft wheat, hard wheat and whole wheat) and gluten-free flour doughs (chestnut, rice and yellow corn), all of them obtained from commercial flours.

Summarizing, seaweed powder addition significantly modified dough mixing properties. WA increased with seaweed powder addition due to the higher hygroscopicity and WRC of seaweed powder compared to chestnut flour. DT values increased by seaweed powder addition due to a more complex mixing process is produced by the hydration of the particles added and interactions between this added particles with other dough components. Finally, seaweed powder addition produced strengthens doughs as it was observed by the larger ST and lower MW values of seaweed-enriched doughs that seems to indicate that seaweed addition did not cause negative effects on chestnut flour based doughs.

Regarding thermal properties of doughs during mixing, a clear influence of seaweed powder addition on doughs was also observed.

Table 6.31 Mixing curves parameters of chestnut flour seaweed-enriched doughs obtained in Mixolab® apparatus (target torque, C1: 1.10±0.07 Nm).♣

Dough	**C2** (N·m)	**C3** (N·m)	**C4** (N·m)	**C5** (N·m)
CTSGD	0.45 ± 0.03^{c}	1.69 ± 0.11^{a}	1.40 ± 0.03^{a}	2.04 ± 0.07^{a}
AN03D	$0.52\pm0.02^{a,b}$	1.61 ± 0.07^{a}	$1.32\pm0.01^{a,b}$	$1.83\pm0.02^{a,b,c}$
AN06D	$0.59\pm0.01^{a,b}$	1.72 ± 0.08^{a}	$1.32\pm0.07^{a,b}$	$1.79\pm0.02^{a,b,c}$
AN09D	0.67 ± 0.07^{a}	1.73 ± 0.06^{a}	$1.24\pm0.02^{a,b}$	$1.74\pm0.02^{a,b,c}$
BB03D	$0.56\pm0.01^{a,b,c}$	1.68 ± 0.09^{a}	$1.27\pm0.04^{a,b}$	$1.93\pm0.11^{a,b}$
BB06D	$0.61\pm0.01^{a,b}$	1.72 ± 0.01^{a}	$1.21\pm0.01^{a,b}$	$1.63\pm0.01^{b,c}$
BB09D	0.68 ± 0.01^{a}	1.63 ± 0.16^{a}	$1.21\pm0.01^{a,b}$	1.50 ± 0.11^{c}
FV03D	$0.51\pm0.02^{b,c}$	1.77 ± 0.10^{a}	1.19 ± 0.02^{b}	$1.73\pm0.11^{a,b,c}$
FV06D	$0.50\pm0.02^{b,c}$	1.77 ± 0.17^{a}	1.16 ± 0.07^{b}	1.58 ± 0.03^{c}
FV09D	$0.57\pm0.02^{a,b}$	1.70 ± 0.16^{a}	1.16 ± 0.05^{b}	1.54 ± 0.06^{c}

♣Data are presented as means±standard deviation. Data value of each parameter with different superscript letters in columns are significantly different ($P \leq 0.05$).

Concerning C2, which represents the minimum torque achieved due to protein weakening as function of mechanical work and temperature, the addition of seaweed powder significantly increased C2, Figure 6.22 (d, e and f). From a technological point of view this can be considered as an improving effect. *Ascophyllum nodosum* and *Bifurcaria bifurcata* powder addition affected similarly C2, seaweed powder addition $\geq$ 3% significantly increased C2 whilst the effect of *Fucus vesiculosus* addition on C2 was less influential and only when addition $\geq$ 9% C2 was significantly increased, Table 6.31. The fact that protein network weakening rate, α, slightly varied with seaweed powder addition (Table 6.32) seems to indicate that protein weakening of doughs due to thermal effects is similar for all studied doughs. The upgrade on C2 values is mainly due to a mechanical improvement related to strengthen doughs by seaweed powder addition than any thermal interactions between proteins present in flour and some components of the seaweed powder added.

Process related to starch gelatinization can be analysed focusing on C3 (maximum torque achieved as a result of starch gelatinization), the starch gelatinization rate β and temperatures associated to the beginning and the end of this process (T_0 and T_{fg}, respectively). Seaweed powder addition did not significantly influenced C3 and T_f values and no clear trends were observed for T_{fg} and β.

The effect of seaweed powder addition on characteristics temperatures of gelatinization will be discussed in the coming Section 6.7 more in detail due to

the technique applied (Dynamic Mechanic-Thermal Analysis) is more sensible to thermal transition compared to Mixolab® apparatus. However, it could be said that characteristic temperatures of gelatinization in doughs are often related to their WA. T_0 determines the beginning of gelatinization process related to swelling of starch granules which implies the necessity of available water. In our case, when seaweed powder is added, the water added to form the dough can be attracted by the seaweed powder due to its higher WRC compared to chestnut flour which implies a lower water availability to swell the starch granules and hence a T_0 rise due to this phenomenon (Donovan, 1979). This could explain the rise of T_0 when AN35P and FV35P are added. However, in the case of BBP addition, this effect of water privation by seaweed powder could have been covered up by the high WA needed to obtain the dough, Table 6.30

Table 6.32 Mixing curves parameters of chestnut flour seaweed-enriched doughs obtained in Mixolab® apparatus (target torque, C1: 1.10±0.07 Nm).♣

Dough	α (N·m/min)	β (N·m/min)	γ_e (N·m/min)
CTSGD	-0.029±0.003^{a,b}	0.191±0.008^{b,c}	-0.035±0.004^{a}
AN03D	-0.029±0.002^{a,b}	0.219±0.001^{a,b,c}	-0.035±0.007^{a}
AN06D	-0.027±0.001^{a,b}	0.277±0.012^{a}	-0.048±0.002^{a,b}
AN09D	-0.021±0.004^{a,b}	0.300±0.011^{a}	-0.056±0.001^{a,b}
BB03D	-0.028±0.003^{a,b}	0.185±0.014^{b,c}	-0.042±0.006^{a,b}
BB06D	-0.023±0.001^{a,b}	0.192±0.000^{b,c}	-0.062±0.000^{b}
BB09D	-0.020±0.001^{b}	0.170±0.040^{c}	-0.062±0.005^{b}
FV03D	-0.028±0.001^{a,b}	0.257±0.001^{a,b}	-0.061±0.001^{b}
FV06D	-0.029±0.002^{a,b}	0.298±0.005^{a}	-0.055±0.003^{a,b}
FV09D	-0.032±0.003^{a}	0.255±0.028^{a,b,c}	-0.053±0.008^{a,b}

♣Data are presented as means±standard deviation. Data value of each parameter with different superscript letters in columns are significantly different (P≤ 0.05).

The fact that β increased with seaweed powder addition in the case of AN35P and FV35P is mainly due to temperature gelatinization range (T_{fg}-T_0) was lower for those doughs due to the delay on T_0 by seaweed addition (and consequently the time associated to gelatinization process was shortened due to the use of a constant heating rate of dough) and that C3 was independent of seaweed powder addition. This makes that a similar increase on torque values was obtained with lower times and hence a rise on gelatinization rate.

The reduction on dough consistency after starch gelatinization (C4), is the result of the physical breakdown of the granules due to mechanical shear stress and the temperature constraint. This breakdown torque is also represented by the enzymatic degradation rate, γ_e. As it can be seen in Tables 6.31 and 6.32,

Table 6.33 Mixing curves parameters of chestnut flour seaweed-enriched doughs obtained in Mixolab® apparatus (target torque, C1: 1.10±0.07 Nm).♣

Dough	$\mathbf{T}_0$ (°C)	$\mathbf{T}_{fg}$ (°C)	**C4/C3** (-)	**Setback** (N·m)
CTSGD	56.5±0.6^{b}	75.3±0.8^{a}	0.83±0.03^{a}	0.65±0.05^{a}
AN03D	60.3±0.8^{a,b}	75.2±0.2^{a}	0.82±0.03^{a,b}	0.51±0.01^{a,b}
AN06D	61.1±1.2^{a}	74.5±0.1^{a}	0.77±0.01^{a,b}	0.47±0.05^{a,b}
AN09D	61.0±1.1^{a}	73.7±0.4^{a}	0.72±0.01^{a,b}	0.49±0.01^{a,b}
BB03D	57.8±1.0^{a,b}	75.7±0.6^{a}	0.76±0.02^{a,b}	0.65±0.07^{a}
BB06D	56.1±0.1^{b}	74.3±0.1^{a}	0.71±0.01^{a,b}	0.42±0.01^{a,b}
BB09D	56.6±0.6^{b}	73.2±0.8^{a}	0.74±0.07^{a,b}	0.29±0.10^{b}
FV03D	58.6±0.1^{a,b}	74.5±0.4^{a}	0.67±0.03^{a,b}	0.55±0.09^{a,b}
FV06D	61.5±0.8^{a}	74.4±0.7^{a}	0.66±0.02^{b}	0.42±0.04^{a,b}
FV09D	59.3±0.1^{a,b}	74.0±0.1^{a}	0.69±0.03^{a,b}	0.38±0.11^{a,b}

♣Data are presented as means±standard deviation. Data value of each parameter with different superscript letters in columns are significantly different (P≤ 0.05).

C4 tends to decrease which means that dough consistency is lower for seaweed-enriched doughs. This is due to the filler effect of seaweed particles which impairs the aggregation of dough after gelatinization and consequently provokes a higher reduction on dough consistency due to mechanical and thermal weakening. This effect is also observable on γ_e which, in general, increased with seaweed powder addition.

Cooking stability (C4/C3) was worsened as consequence of seaweed powder addition, Tables 6.33. As previously explained the addition of seaweed particles could impair dough aggregation process caused by gelatinization and consequently negatively affected dough consistency and hence dough cooking stability. However, values obtained are in the range of those obtained for other gluten-free doughs (Moreira *et al.*, 2012).

Final consistency of dough was also affected by seaweed powder addition, Table 6.30. In this case, a slight trend was observed. C5 decreased with seaweed powder addition which means that seaweed particles impair starch retrogradation of dough and consequently consistency increased due to this phenomenon was lower. This fact, can be also observed on setback (Tables 6.33) trend where it was observed a lower value of this parameter when seaweed powder amount on dough was increased. The explanation to this behaviour could be related to high WRC of seaweed powders that increased the capacity of dough to retain water even during heating and hence impaired starch retrogradation of dough.

6.5.5 New protocol

In order to evaluate the possibility of use of chestnut flour doughs and seaweed-enriched chestnut flour doughs previously gelatinizated in order to obtain the desired baked product, a new protocol is proposed. This protocol aims the obtaining of gelatinized doughs employing a short time of mixing as previously explained in Section 4.5.

Tables 6.34 and 6.35 present the mixing and thermal parameters of doughs during mixing employing the aforementioned protocol. Moreover, experimental data curves can be observed in Figure 6.24 (a), (b) and (c).

Table 6.34 Mixing curves parameters of chestnut flour doughs and seaweed-enriched chestnut flour doughs obtained in Mixolab® apparatus employing the proposed protocol (target torque, C1: 1.10±0.07 N·m).♣

Dough	WA (%, f.b.)	DT (min)	DPT (min)	ST (min)	MW (N·m)	C2 (N·m)
CTSGD	56.0±0.1^{e}	1.12±0.19^{b,c}	3.11±0.25^{b,c}	2.76±0.22^{a,b,c,d}	0.52±0.01^{a}	0.64±0.01^{d}
AN03D	59.0±0.1^{d}	1.64±0.11^{a,b}	3.36±0.01^{b}	2.47±0.12^{a,b,c,d}	0.36±0.02^{b,c,d}	0.73±0.02^{a,b,c}
AN06D	63.0±0.1^{c}	1.73±0.01^{a,b}	3.32±0.01^{b}	2.32±0.01^{a,b,c,d}	0.37±0.01^{b,c,d}	0.72±0.01^{b,c}
AN09D	69.0±0.1^{a}	1.97±0.07^{a}	4.30±0.16^{a}	3.38±0.12^{a}	0.29±0.03^{b,c,d}	0.81±0.03^{a}
BB03D	63.5±0.7^{c}	1.12±0.28^{b,c}	2.48±0.06^{b,c}	2.04±0.11^{a,b,c,d}	0.41±0.01^{c,d}	0.69±0.01^{b,c,d}
BB06D	67.3±0.4^{b}	1.33±0.05^{a,b}	2.69±0.11^{b,c}	2.18±0.06^{a,b,c,d}	0.41±0.01^{c,d}	0.69±0.01^{b,c,d}
BB09D	69.8±0.4^{a}	1.49±0.06^{a,b}	3.33±0.15^{b}	2.87±0.24^{a,b,c}	0.35±0.01^{b,c,d}	0.75±0.01^{a,b}
FV03D	59.3±0.4^{d}	0.54±0.01^{b,c}	1.48±0.07^{d}	1.11±0.06^{e}	0.47±0.02^{a,b}	0.63±0.02^{d}
FV06D	60.0±0.2^{d}	1.28±0.14^{a,b}	2.58±0.18^{b,c}	2.17±0.26^{c,d}	0.44±0.04^{a,b,c}	0.66±0.02^{c,d}
FV09D	64.0±0.2^{c}	1.51±0.15^{a,b}	3.38±0.15^{b}	2.97±0.09^{a,b}	0.41±0.02^{b,c}	0.69±0.01^{b,c,d}

♣Data are presented as means±standard deviation. Data value of each parameter with different superscript letters in columns are significantly different (P≤ 0.05).

As it can be observed in Table 6.34 similar changes in WA values were obtained in order to obtain the desired consistency of dough, compared to the standard mixing protocol presented in the previous sections. The addition of seaweed powders significantly increased WA and also DT and DPT. The explanation of this behaviour is the same as explained before. The addition of a new ingredient to doughs led to a more complex mixing process and hence to larger values of DT and DPT. Moreover, ST values were improved when adding large amounts (9% d.b) of seaweed powders were added, specially in the case of *Ascophyllum nodosum* seaweed. Note here that the values of ST here obtained are not comparable to those previously obtained employing the standard protocol due to this mixing step was shortened and hence all parameters related to time will present lower values. Finally, mechanical weakening of doughs was also shortened and consequently C2 values were higher for seaweed-enriched seaweeds.

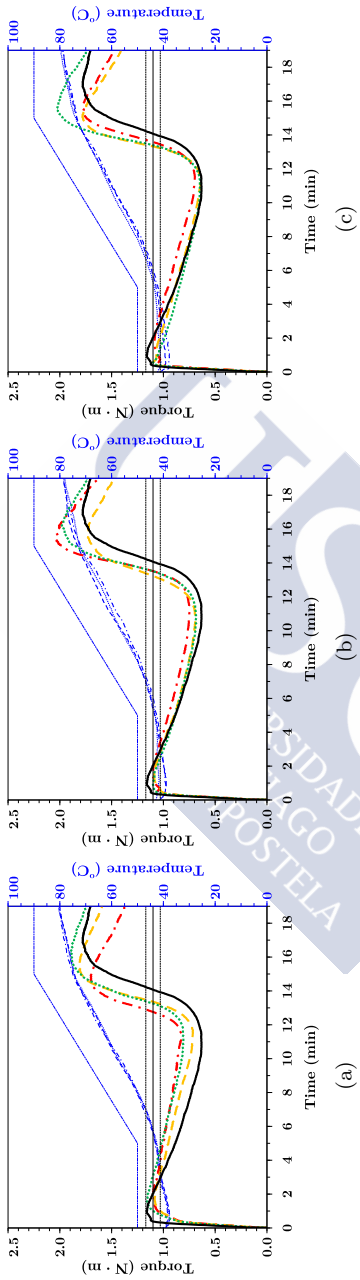

Figure 6.24 Mixolab® proposed curves for CF control dough (—) and doughs with seaweed powders (*Ascophyllum nodosum* (a), *Bifurcaria bifurcata* (b) and *Fucus vesiculosus* (c)) added at different levels (3% (···), 6% (- - -) and 9% (-·-·-)). Blue lines correspond to bowl (-···-) and dough temperatures.

Table 6.35 Thermal curves parameters of chestnut flour doughs and seaweed-enriched chestnut flour doughs obtained in Mixolab® apparatus employing the proposed protocol (target torque, C1: 1.10±0.07 N·m).♣

Dough	α (N·m/min)	**C3** (N·m)	β (N·m/min)	$\mathbf{T}_0$ (°C)	$\mathbf{T}_{fg}$ (°C)
CTSGD	-0.037±0.002^{a}	1.77±0.02^{a}	0.183±0.004^{c}	59.3±0.2^{a}	76.1±0.3^{a}
AN03D	-0.028±0.003^{a}	1.85±0.03^{a}	0.193±0.018^{c}	60.4±0.3^{a}	74.7±2.5^{a}
AN06D	-0.035±0.002^{a}	1.82±0.01^{a}	0.282±0.002^{a,b}	62.7±0.1^{a}	75.0±0.1^{a}
AN09D	-0.031±0.005^{a}	1.75±0.06^{a}	0.260±0.032^{a,b,c}	61.5±0.3^{a}	74.1±0.3^{a}
BB03D	-0.029±0.002^{a}	1.88±0.15^{a}	0.204±0.026^{b,c}	58.4±1.2^{a}	75.1±1.4^{a}
BB06D	-0.025±0.003^{a}	1.84±0.14^{a}	0.222±0.015^{a,b,c}	58.4±1.1^{a}	74.6±0.3^{a}
BB09D	-0.027±0.002^{a}	1.96±0.11^{a}	0.285±0.012^{a,b}	58.9±2.1^{a}	73.5±1.1^{a}
FV03D	-0.025±0.001^{a}	2.06±0.04^{a}	0.289±0.002^{a}	60.6±0.4^{a}	74.3±1.3^{a}
FV06D	-0.032±0.003^{a}	1.80±0.01^{a}	0.283±0.004^{a,b}	61.1±1.6^{a}	74.5±1.3^{a}
FV09D	-0.036±0.001^{a}	1.77±0.01^{a}	0.259±0.011^{a,b,c}	61.3±0.6^{a}	74.5±0.4^{a}

♣Data are presented as means±standard deviation. Data value of each parameter with different superscript letters in columns are significantly different (P≤ 0.05).

Regarding Table 6.35, it can be seen that no significant differences existed in protein network weakening rate (α) and final consistency after gelatinization (C3) with seaweed powder addition. This invariant gelatinization behaviour with seaweed powder addition is also observed in T_0 and T_{fg}, which remained constant for all assayed doughs. Finally, it has to be mentioned that β varied with a similar trend as previously reported with seaweed addition.

The section in tweets

- Chestnut flour doughs show poor mixing characteristics (low stability time, high mechanical weakening) and thermal properties.
- Guar gum addition to chestnut flour improves mixing properties of doughs increasing stability time and reducing mechanical weakening.
- The analysis of maize flour doughs mixing behaviour indicates that milling process is critical because it affects dough mixing properties.
- Maize flours with low particle size have high damaged starch content and hence larger water absorption (WA) is needed to obtain doughs.
- Maize flours with high particle size generate strengthen doughs and consequently their mechanical weakening during mixing is reduced.
- Seaweed powder addition significantly modifies mixing properties of seaweed-enriched chestnut doughs compared to non-seaweed-enriched.
- Mixing of seaweed-enriched doughs components is a complex process which involves high development times and two peaks of consistency.
- Higher water retention capacity (WRC) of seaweed powder implies larger WA to obtain seaweed-enriched doughs at the same consistency.
- For seaweeds powders with similar WRC the particle size is critical. The higher the particle size, the lower the WA.
- Seaweed powder addition reduces mechanical weakening of dough; mainly by a mechanical improvement due to strengthened doughs are obtained.
- Cooking stability worsens with seaweed powder addition because this addition impairs dough aggregation after gelatinization process.
- Starch retrogradation is lower for doughs with high seaweed powder content, they retain more water due to the high WRC of these powders.

USC
UNIVERSIDADE
DE SANTIAGO
DE COMPOSTELA

6.6 Rheology of gluten-free flour doughs

Rheological properties of gluten-free flour doughs based on maize flours, chestnut flour and chestnut flour blends consisting on chestnut flour enriched with seaweed powders of *Ascophyllum nodosum*, *Bifurcaria bifurcata* and *Fucus vesiculosus* obtained from seaweeds dried at 35°C has been studied by means of small amplitude oscillatory shear (SAOS) and creep-recovery experiments. [6]

[6]This section has been adapted from the following papers published and in writing process: MOREIRA, R., CHENLO, F., ARUFE, S. & RUBINOS, S. (2015). Physicochemical characterization of white, yellow and purple maize flours and rheological characterization of their doughs. *Journal of Food Science and Technology-Mysore* **12**, 7954–7963. DOI: http://doi.org/10.1007/s13197-015-1953-6.
MOREIRA, R., CHENLO, F., SINEIRO, J., TORRES, M. D. & ARUFE, S. (2017). Mixing, rheological and thermomechanical characterization of seaweed-enriched chestnut flour doughs. To be submitted to: *Journal of Food Engineering*.
MOREIRA, R., CHENLO, F., SINEIRO, J., TORRES, M. D. & ARUFE, S. (2017). Physico-Chemichal Properties of seaweed-enriched chestnut flour cookies obtained from pregelatinized doughs. To be submitted to: *Journal of Texture studies*.

Nomenclature

Powders

AN35P	–	*Ascophyllum nodosum* (AN) powder obtained from AN35.
BB35P	–	*Bifurcaria bifurcata* (BB) powder obtained from BB35.
FV35P	–	*Fucus vesiculosus* (FV) powder obtained from FV35.
GG	–	Guar gum.

Doughs

CAN03D	–	Chestnut flour dough with 3% f.b. of AN35P.
CAN06D	–	Chestnut flour dough with 6% f.b. of AN35P.
CAN09D	–	Chestnut flour dough with 9% f.b. of AN35P.
CBB03D	–	Chestnut flour dough with 3% f.b. of BB35P.
CBB06D	–	Chestnut flour dough with 6% f.b. of BB35P.
CBB09D	–	Chestnut flour dough with 9% f.b. of BB35P.
CFV03D	–	Chestnut flour dough with 3% f.b. of FV35P.
CFV06D	–	Chestnut flour dough with 6% f.b. of FV35P.
CFV09D	–	Chestnut flour dough with 9% f.b. of FV35P.
CTSGD	–	Chestnut flour dough with 1.8% f.b. of NaCl and 2% f.b. of GG.
CAN0XPD	–	Pregelatinized CAN0XD.
CBB0XPD	–	Pregelatinized CBB0XD.
CFV0XPD	–	Pregelatinized CFV0XD.
CTSGPD	–	Pregelatinized CTSGD.
PM200D	–	Purple maize dough (flour obtained with 200 μm mesh during milling).
PM500D	–	Purple maize dough (flour obtained with 500 μm mesh during milling).
WM200D	–	White maize dough (flour obtained with 200 μm mesh during milling).
WM500D	–	White maize dough (flour obtained with 500 μm mesh during milling).
YM200D	–	Yellow maize dough (flour obtained with 200 μm mesh during milling).
YM500D	–	Yellow maize dough (flour obtained with 500 μm mesh during milling).

Parameters

a'	–	Fitting parameter of SAOS data, Pa·s$^{-b'}$, Eq. (4.25).
a''	–	Fitting parameter of SAOS data, Pa·s$^{-b''}$, Eq. (4.26).
b'	–	Fitting parameter of SAOS data, Eq. (4.25).
b''	–	Fitting parameter of SAOS data, Eq. (4.26).
G'	–	Storage modulus, Pa.
G''	–	Loss modulus, Pa.
J(t)	–	Compliance, Pa^{-1}, Eqs. (4.27) and (4.28).
J_0	–	Instantaneous compliance, Pa^{-1}, Eq. (4.27).
J_m	–	Viscoelastic compliance, Pa^{-1}, Eqs. (4.27) and (4.28).
J_{max}	–	Maximum creep compliance, Pa^{-1}, Eq. (4.28).
J_r	–	Recovery compliance, Pa^{-1}, Eq. (4.28).
LVER	–	Linear viscoelastic region.
tanδ	–	Damping factor.
γ_c	–	Critical strain, %.
λ_c	–	Mean retardation time of creep phase, s, Eq. (4.27).
λ_r	–	Mean retardation time of recovery phase, s, Eq. (4.28).
η_0	–	Zero shear viscosity, Pa·s, Eq. (4.27).
η_c	–	Complex viscosity, Pa·s.
σ	–	Shear stress, Pa.
ω	–	Angular frequency, s^{-1}.

6.6.1 Introduction

Given the increasing demand of gluten-free products adequate for people suffering some of the three pathologies associated with the gluten intake (i.e. gluten allergy, coeliac disease, and gluten sensitivity), the development of new formulations is necessary. In this sense, the use of gluten-free sources like maize and chestnut becomes a very interesting starting point. Moreover, the development of enriched gluten-free products could enhance its comsumption. In this sense, brown seaweeds such as *Ascophyllum nodosum*, *Bifurcaria bifurcata* and *Fucus vesiculosus* represent a suitable supplement for food because of their high nutritional value as source of dietary fibre and healthy benefits (Jiménez-Escrig & Sánchez-Muniz (2000) and Rupérez & Saura-Calixto (2001)). They can be employed in gluten-free formulations based on flour, *i.e.* made from dried and milled chestnut fruits (*Castanea sativa*), an autochthonous Mediterranean raw material, to improve nutritional and antioxidants properties.

Recent studies on chestnut flour indicated that the presence of this flour may be a promising frontier to improve overall appearance, quality, sensory properties and shelf life of gluten-free baked products (Paciulli *et al.*, 2016). Overall, chestnut flour and brown seaweed powder offer a range of excellent choices, both as a base or additive, for gluten-free baked products. A challenge for the coming years would be to introduce these and other novel additives with attractive antioxidant properties in gluten-free products, optimising processing conditions and doses of the compounds (Torres *et al.*, 2017). One of the steps to carry out in order to optimise the processing is to determine possible changes on the product due to the addition of the new ingredient.

Particularly, in the case of gluten-free products based on chestnut flour, the behaviour of enriched chestnut flour dough during processing is essential. This fact makes imperative the study of rheological properties of these doughs in order to determine possible changes and also a threshold value of the addition of the new ingredients that not worsen the doughs properties.

In this context, the main objective of this work is to study the rheological behaviour of gluten-free flour doughs based on different maize varieties and chestnut flour and the effect of *Ascophyllum nodosum*, *Bifurcaria bifurcata* and *Fucus vesiculosus* seaweed powder addition on rheological characteristics of chestnut flour doughs.

6.6.2 Rheology of gluten-free flour doughs based on maize flours

Strain sweep tests established that linear viscoelasticity range was at strain $< 0.4\%$ for all flour doughs. To ensure that all tests were carried out within the linear viscoelastic range, a strain of 0.1% was employed.

Figure 6.25 shows the mechanical spectra (data of storage modulus (G'), loss modulus (G'') and damping factor ($\tan\delta$) at 30°C for all maize flour doughs obtained at target consistency (1.10±0.07 N·m). In all cases, in the studied range, G' and G'' values increased with increasing ω. This behaviour can be attributed to the absence of binding agents in the dough (absence of gluten) and repulsive forces between starch granules are predominant (Sivaramakrishnan *et al.*, 2004). For all maize flour doughs G' values were higher than G'' indicating that elastic proportion was dominant over the viscous one, ($\tan\delta < 1$). This behaviour is according to the solid behaviour for other gluten-free flours like rice (Pruska-Kedzior *et al.*, 2008) and chestnut (Moreira *et al.*, 2013b) flour doughs. In tested doughs, $\tan\delta$ varied in a restricted range indicating that the viscoelasticity is slightly modified with the angular frequency.

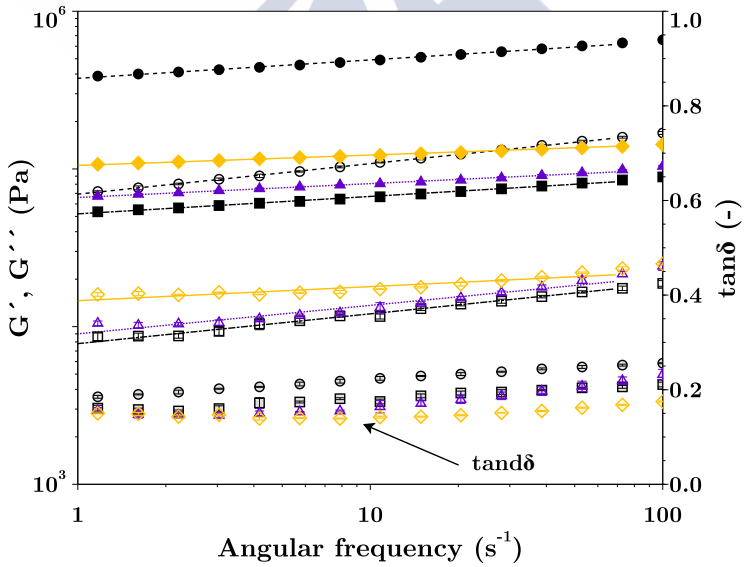

Figure 6.25 Experimental data of G' (filled markers), G'' (empty markers) and $\tan\delta$ (dot filled markers). YM200D (◇), WM200D (□), PM200D (△) and WM500D (○). Lines correspond to Eqs. (4.25) and (4.26): YM200D (-), WM200D (- · -), PM200D (···) and WM500D (- - -).

Oscillatory data were successfully fitted ($R^2 > 0.96$) by means of Eqs. (4.25) and (4.26), Table 6.37. The analysis of the fitting parameters values allows the better discussion on the differences of the flour doughs viscoelastic behaviour. WM500D showed higher values for a' and a'' parameters than WM200D demonstrating that average particle size of flour modifies strongly the viscoelastic character of dough. This increase might be attributed to different interactions between starch granules with different particle size distribution and the integrity of flour particles produces stiffer doughs (Moreira *et al.*, 2010a). Flour doughs with smaller average particle size (milled with a 200 μm sieve) were also significantly different between them. YM200D showed the highest a' and a'' values, and WM200D and PM200D the lowest ones. This could be related to the high WA required for WM200D and PM20D0 flour doughs, Table 6.29. G' and G'' values of studied doughs are comparable to those observed for chestnut flour doughs (Moreira *et al.*, 2013b), but they are higher than those observed for commercial wheat (Hadnadev *et al.*, 2013) and maize (Pruska-Kedzior *et al.*, 2008) flour doughs with similar WA. On the other hand, the slopes (b' and b'') indicated that flour doughs of white maize variety, independently on particle size (WM200D and WM500D), showed greater dependence of both moduli (higher values of b' and b'') on angular frequency than yellow and purple maize flour doughs.

Table 6.37 Parameters of oscillatory shear modelling, Eqs. (4.25) and (4.26), of maize flour doughs.♣

Dough	$a'\cdot10^{-3}$ ($Pa\cdot s^{-b'}$)	$b'\cdot10^{3}$	R^2	$a''\cdot10^{-3}$ ($Pa\cdot s^{-b''}$)	$b''\cdot10^{3}$	R^2
YM200D	105.2 ± 2.0^{b}	66.1 ± 0.2^{c}	0.998	14.6 ± 0.2^{b}	89.4 ± 0.6^{c}	0.948
WM200D	51.9 ± 1.1^{c}	110.5 ± 2.7^{a}	0.994	7.8 ± 0.3^{c}	$189.0\pm4.5^{a,b}$	0.991
PM200D	65.9 ± 0.4^{c}	88.1 ± 2.1^{b}	0.992	9.0 ± 0.3^{c}	$180.5\pm0.2^{a,b}$	0.955
WM500D	375.6 ± 10.2^{a}	116.7 ± 0.6^{a}	0.996	69.2 ± 0.9^{a}	193.3 ± 0.8^{a}	0.999

♣Data are presented as means±standard deviation. Data value of each parameter with different superscript letters in columns are significantly different ($P \leq 0.05$).

Experimental data of creep and recovery tests for all assayed doughs are shown in Figure 6.26. During creep step (first 60 s) creep compliance increased and after stress removal (recovery step, last 180 s) creep compliance decreased until almost to achieve stationary state. The curves shape is similar to other gluten-free systems previously studied (Lazaridou *et al.* (2007), Moreira *et al.* (2013b)).

The parameters of Burgers model for creep and recovery curves parameters, Eqs. (4.27) and (4.28) respectively, for the tested flour doughs are shown in Table 6.38. Creep step was successfully modelled ($R^2 > 0.95$). WM200D and PM200D showed the highest ($\approx 14\cdot10^{-6}$ Pa^{-1}) instantaneous creep compliance

(J_0). This value is comparable to those obtained for gluten-free doughs, with similar WA, made from chestnut flour (Moreira *et al.*, 2013b). The lowest value of J_0 ($3.6{\cdot}10^{-6}$ Pa^{-1}) corresponded to dough with highest particle size (WM500D). These results are in good agreement with the elastic modulus values obtained in the sweep frequency test discussed above. Stiffer flour doughs showed lower J_0. The same trend was observed before in other gluten-free flour doughs (Moreira *et al.*, 2010a). Viscoelastic creep compliance (J_m) was significantly different for all assayed doughs. The highest ($11.2{\cdot}10^{-6}$ Pa^{-1}) and lowest ($1.9{\cdot}10^{-6}$ Pa^{-1}) value of J_m corresponded to WM200D and WM500D, respectively indicating one more time that particle size of flour strongly affected viscoelastic behaviour of doughs. J_m increased linearly ($R^2 > 0.94$) with WA in the tested flour doughs. Moreover, for maize flour doughs with smaller average particle size (obtained with 200 μm sieve), J_m increased with increasing damaged starch (DS).

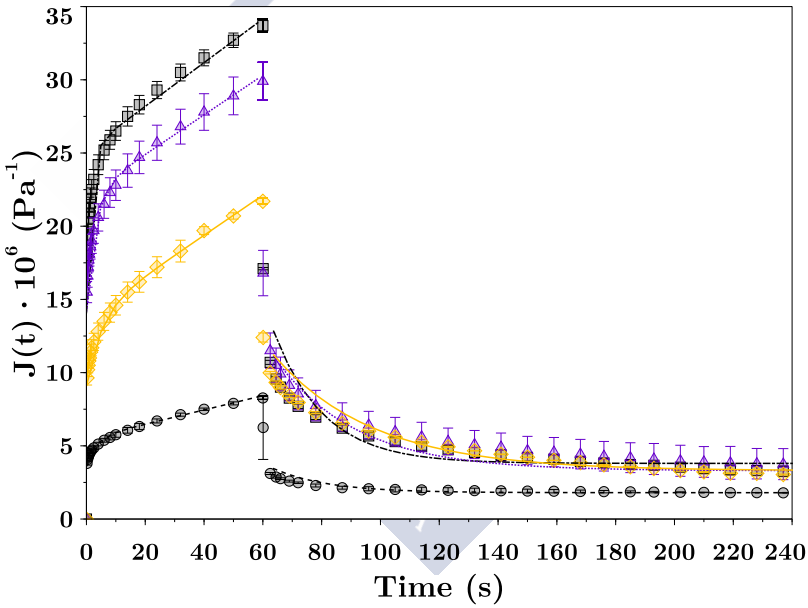

Figure 6.26 Experimental creep and recovery data at 30°C of YM200D (◇), WM200D (□), PM200D (△) and WM500D (○). Lines correspond to Eqs. (4.27) and (4.28): YM200D (-), WM200D (- · -), PM200D (···) and WM500D (- - -).

The mean retardation time of creep step (λ_c) varied from 1.5 up to 5.0 s. These values were in the range reported in literature for gluten-free doughs (Lazaridou *et al.*, 2007). For flour doughs with similar particle size (YM200D, WM200D and PM200D), δ_c decreased with increasing DS. Regarding particle size effect, it was

observed that the dough from flour with higher average particle size, WM500D, showed higher value of λ_c (3.2 s) compared to dough from the same variety with lower particle size (WM200D).

Zero shear viscosity parameter (η_0) was significantly higher for WM500D ($20.5 \cdot 10^6$ Pa·s) dough and no significant differences ($6.7\text{-}7.4 \cdot 10^6$ Pa·s) among remaining flour doughs were observed. This fact confirms that flow resistance of doughs depends strongly on average particle size of flour from which they are obtained (Moreira *et al.*, 2010a).

Table 6.38 Parameters of creep (Eq. (4.27)) and recovery (Eq. (4.28)) phase modelling of maize flour doughs.♣

Phase	Parameters	YM200D	WM200D	PM200D	WM500D
Creep	$\mathbf{J_0 \cdot 10^6}$ (Pa^{-1})	9.1 ± 0.1^b	14.1 ± 0.2^a	14.2 ± 0.9^b	3.6 ± 0.2^c
	$\mathbf{J_m \cdot 10^6}$ (Pa^{-1})	4.8 ± 0.1^c	11.2 ± 0.5^a	8.0 ± 0.3^b	1.9 ± 0.1^d
	λ_c (s)	5.0 ± 0.1^a	1.5 ± 0.1^c	2.9 ± 0.2^b	3.2 ± 0.3^b
	$\eta_0 \cdot \mathbf{10^{-6}}$	7.3 ± 0.9^b	6.7 ± 0.2^b	7.4 ± 0.2^b	20.5 ± 1.1^a
	$\mathbf{R^2}$	0.98	0.95	0.96	0.97
Recovery	$\mathbf{J_{max} \cdot 10^6}$ (Pa^{-1})	21.7 ± 0.3^b	32.0 ± 1.4^a	30.5 ± 0.7^a	8.1 ± 0.3^c
	$\mathbf{J_0 \cdot 10^6}$ (Pa^{-1})	9.6 ± 0.2^b	17.0 ± 1.4^a	18.3 ± 0.4^a	4.3 ± 0.1^c
	$\mathbf{J_m \cdot 10^6}$ (Pa^{-1})	8.8 ± 0.1^b	11.2 ± 0.1^a	8.9 ± 0.2^b	2.0 ± 0.1^c
	λ_r (s)	34.0 ± 1.4^a	17.0 ± 0.1^c	27.5 ± 0.7^b	18.5 ± 0.7^c
	$\mathbf{J_r / J_{max}}$ (%)	83.1 ± 0.1^c	87.6 ± 1.3^a	86.5 ± 0.9^b	75.8 ± 1.1^d
	$\mathbf{R^2}$	0.95	0.85	0.91	0.86

♣Data are presented as means±standard deviation. Data value of each parameter with different superscript letters in rows are significantly different ($P \leq 0.05$).

Recovery phases of tested flours were acceptably fitted ($R^2 > 0.86$) by means of Eq. (4.28) and the corresponding parameters are shown in Table 6.38. The maximum creep compliance (J_{max}) was significantly lower ($8.1 \cdot 10^{-6}$ Pa^{-1}) for WM500D indicating that doughs obtained from flour with large particle size had less deformation capacity. J_{max} increased linearly ($R^2 > 0.94$) with increasing WA in the tested flour doughs. This could be related to the formation of weaker material structures promoted by high WA (Lazaridou *et al.*, 2007). Instantaneous recovery compliance (J_0, $4.3\text{-}18.3 \cdot 10^{-6}$ Pa^{-1}) and viscoelastic recovery compliance (J_m, $2.0\text{-}11.2 \cdot 10^{-6}$ Pa^{-1}) values were in the same range as those observed in creep step. In both cases, the values obtained for WM500D were significantly lower which corroborate the same trend observed during creep phase.

Values of mean retardation time of recovery step, *lambda*$_r$, were higher than those observed for λ_c. These differences can be explained because the creep phase was performed outside the LVER and irreversible changes in the structure of the flours were produced. The highest

value of λ_r, as in the creep phase, corresponded to YM200D (34.0 s). Similar values were obtained for gluten-free doughs, with WA in the same range, from rice flour (38.1 s) (Lazaridou *et al.*, 2007). Note here that no differences were observed as function of flour particles size. However, WM500D and WM200D showed the lowest value of λ_r meaning that this dough variety needs less time to achieve the stationary state. On the other hand, J_r/J_{max} ratio values increased with WA in the tested flour doughs. All of them showed higher values (75.8 – 87.6 %) than wheat doughs (65%) indicating a higher elastic character of doughs.

6.6.3 Rheology of seaweed-enriched flour doughs based on chestnut flour

Small amplitude oscillatory shear (SAOS) tests showed that G' and G'' values increased with angular frequency (ω) for all assayed doughs, Figure 6.27. Moreover, all doughs presented a dominant elastic behaviour over the viscous one, a typical behaviour of flour doughs. This trend can be also observed on damping factor (tanδ) values which were < 1 ($\approx$0.2). Moreover the trend of tanδ with ω indicates that the elastic/viscous predominance of doughs was constant and independent of ω.

The mentioned behaviour of doughs can be also observed regarding values of Eqs.(4.25) and (4.26) parameters ($R^2 > 0.87$) and their ANOVA analysis, Table 6.39. The increasing trend of G' and G'' with ω can be observed in the positive values of b' and b'', which represent the slopes of the linear model. On the other hand, the domination of elastic behaviour over the viscous one can be also observed, in this case paying attention to the larger values of a' (which represents the elastic character at 1 s^{-1}) compared to a'' (which represents the viscous character at 1 s^{-1}). Moreover, the trend of tanδ with ω, which in this case presents a constant value independent of ω, can be also deduced from Table 6.39 due to b' and b'' values were very similar for each dough.

Regarding the effect of each seaweed powder addition to chestnut flour, different behaviour can be mentioned. In the case of *Ascophyllum nodosum* and *Fucus vesiculosus*, the addition of AN35P and FV35P significantly decreased elastic character of dough (a' values). On the other hand, both elastic and viscous dependence with ω were significantly increased (b' and b''). This could be related to the larger WA of these seaweed-enriched doughs compared to CTSGD dough, Table 6.28.

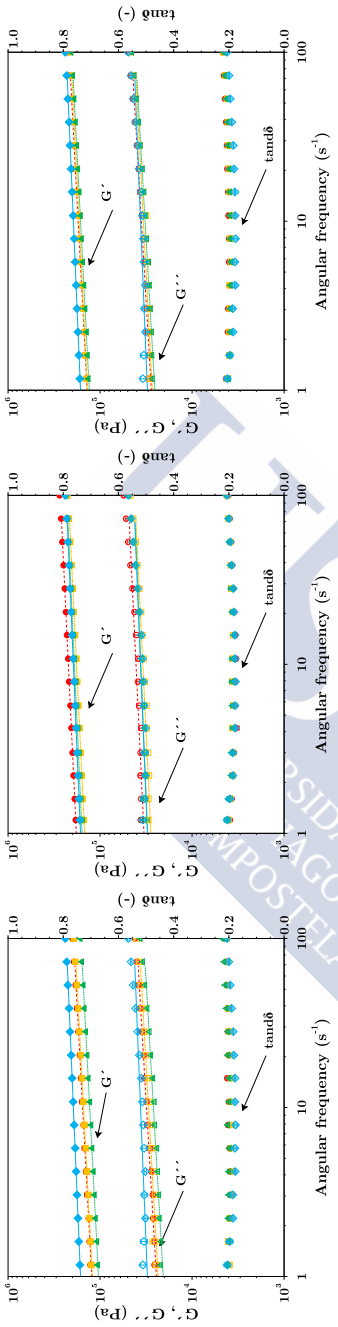

Figure 6.27 Experimental data of G′ (filled markers), G″ (empty markers) and tanδ (dot filled markers) at 30°C of chestnut flour doughs (◇) and chestnut flour doughs enriched with *Ascophyllum nodosum* (a), *Bifurcaria bifurcata* (b) and *Fucus vesiculosus* (c) seaweed powders at different levels: 3% (△), 6% (□) and 9% (○). Lines correspond to Eqs. (4.25) and (4.26).

Regarding *Bifurcaria bifurcata*, BB35P addition effect on elastic character of dough was the opposite compared to AN35P and FV35P addition. BB35P additions larger than 6% significantly increased G' values whilst G'' values remained invariant for all assayed doughs. No significant differences existed on moduli dependence with ω caused by BB35P. In this case, WA of CBB doughs was even larger than those observed for CAN and CFV doughs. Up to this, lower G' values could be expected for CBB doughs. However, the different physical properties of BB35P could explain this behaviour. BB35P had larger swelling powder (SP) compared to AN35P and FV35P, Table 6.12. The larger WA of CBB, due to its larger WRC, combined with its larger SP led to a swelling of CBB particles that results in doughs with higher elastic character. This swollen particles could have a similar effect on doughs properties of those related to the particle size increase observed maize doughs (Section 6.6.2), where it was observed that higher particle size of flours led to more elastic doughs.

Although seaweed addition modified moduli values of seaweed-enriched chestnut flour doughs, the values obtained were in the range of those previously reported for gluten-free doughs such as maize flour doughs in this Thesis or rice flour doughs (Moreira *et al.*, 2013b). Moreover, they were also in accordance with those values reported for non gluten-free doughs based on wheat (Salvador *et al.*, 2006) and (Tarancón *et al.*, 2015).

Table 6.39. Parameters of oscillatory shear modelling, Eqs. (4.25) and (4.26).♣

Dough	$\mathbf{a'\cdot 10^{-3}}$ ($Pa\cdot s^{-b'}$)	$\mathbf{b'\cdot 10^{3}}$	$\mathbf{R^2}$	$\mathbf{a''\cdot 10^{-3}}$ ($Pa\cdot s^{-b''}$)	$\mathbf{b''\cdot 10^{3}}$	$\mathbf{R^2}$
CTSGD	163.2 ± 3.8^{b}	77.9 ± 1.2^{b}	0.997	$30.6\pm2.2^{a,b}$	74.3 ± 12.6^{a}	0.902
CAN03D	103.5 ± 1.2^{e}	95.7 ± 0.6^{a}	0.997	20.6 ± 0.5^{c}	$106.3\pm2.7^{a,b}$	0.960
CAN06D	$121.1\pm8.8^{d,e}$	97.0 ± 4.0^{a}	0.998	$23.4\pm1.9^{b,c}$	$103.8\pm6.5^{a,b}$	0.962
CAN09D	$123.4\pm6.8^{d,e}$	99.5 ± 0.5^{a}	0.998	$24.4\pm1.1^{b,c}$	108.4 ± 2.9^{a}	0.980
CBB03D	$157.1\pm12.5^{b,c}$	$83.3\pm8.8^{a,b}$	0.998	$30.4\pm2.5^{a,b}$	79.3 ± 19.6^{b}	0.849
CBB06D	$147.2\pm2.5^{b,c,d}$	$88.9\pm1.6^{a,b}$	0.999	$28.0\pm0.2^{a,b}$	88.1 ± 1.0^{b}	0.919
CBB09D	180.9 ± 1.2^{a}	$87.1\pm1.9^{a,b}$	0.999	33.3 ± 0.9^{a}	86.9 ± 0.9^{b}	0.871
CFV03D	$130.6\pm0.6^{c,d,e}$	94.7 ± 1.2^{a}	0.998	$25.4\pm0.1^{b,c}$	106.2 ± 2.1^{a}	0.958
CFV06D	$137.0\pm6.7^{c,d}$	90.9 ± 0.4^{a}	0.997	$27.0\pm1.5^{a,b}$	$97.4\pm0.6^{a,b}$	0.932
CFV09D	$137.9\pm6.6^{c,d}$	98.2 ± 0.6^{a}	0.998	$27.7\pm1.2^{a,b}$	108.3 ± 3.8^{a}	0.964

♣Data are presented as means±standard deviation. Data value of each parameter with different superscript letters in columns are significantly different ($P\leq 0.05$).

Creep and recovery results revealed similar viscoelastic behaviour of doughs, Figure 6.28. During creep phase compliance increased and then, during recovery phase, a sensible decrease on compliance was observed until almost achieved the steady state. Similar curves were also reported in this Thesis for maize flour doughs or by other authors for other gluten-free doughs (Lazaridou *et al.*, 2007).

Values of parameters obtained after fitting of experimental data employing Eqs. (4.27) and (4.28) (R^2 >0.95) for creep and recovery are shown in Table 6.40 and 6.41, respectively.

Concerning *Ascophyllum nodosum* addition to chestnut flour doughs, J_0 and J_m were increased highlighting the higher deformation capacity of dough due to the lubricant effect of water and the higher WA and lower WRC values. Regarding recovery properties, J_{max} was significantly higher, also by lubricant effect of AN35P on dough associated to larger values of WA were necessary to obtain these doughs. As well as on creep phase J_0 and J_m were also increased. This increase was proportional in both phases, as it can be observed on J_r/J_{max} parameter which remained constant and not significantly different for all AN35P enriched-dough compared to CTSGD. Taking into account the mentioned variations, AN35P addition up to 9% could be employed without worsening creep-recovery characteristics of seaweed-enriched doughs.

Table 6.40. Parameters of creep phase modelling, Eq. (4.27).♣

Dough	$\mathbf{J_0 \cdot 10^6}$ (Pa^{-1})	$\mathbf{J_m \cdot 10^6}$ (Pa^{-1})	λ_c (s)	$\eta_0 \cdot \mathbf{10^{-6}}$ (Pa·s)	$\mathbf{R^2}$
CTSGD	5.9 ± 0.2^{d}	$3.7\pm0.1^{d,e}$	4.8 ± 0.1^{a}	10.1 ± 0.2^{b}	0.984
CAN03D	8.1 ± 0.1^{a}	6.0 ± 0.2^{a}	4.1 ± 0.1^{c}	6.9 ± 0.2^{c}	0.984
CAN06D	$6.9\pm0.1^{b,c}$	$4.6\pm0.1^{b,c}$	4.1 ± 0.1^{c}	9.6 ± 0.5^{b}	0.980
CAN09D	$7.4\pm0.2^{a,b}$	5.1 ± 0.1^{b}	4.0 ± 0.1^{c}	9.3 ± 0.1^{b}	0.978
CBB03D	$6.7\pm0.1^{b,c}$	$4.4\pm0.1^{b,c,d}$	$4.3\pm0.1^{b,c}$	9.2 ± 0.2^{b}	0.982
CBB06D	$6.3\pm0.1^{c,d}$	$4.2\pm0.1^{c,d}$	$4.4\pm0.1^{a,b}$	9.9 ± 0.1^{b}	0.982
CBB09D	5.5 ± 0.1^{e}	3.4 ± 0.1^{e}	$4.5\pm0.2^{a,b}$	12.1 ± 0.1^{a}	0.981
CFV03D	$6.8\pm0.2^{b,c}$	$4.6\pm0.1^{b,c}$	$4.3\pm0.1^{b,c}$	9.4 ± 0.3^{b}	0.981
CFV06D	$6.5\pm0.3^{b,c}$	$4.3\pm0.3^{b,c,d}$	$4.3\pm0.1^{b,c}$	9.6 ± 0.5^{b}	0.981
CFV09D	$6.4\pm0.2^{c,d}$	$4.4\pm0.4^{b,c,d}$	$4.2\pm0.1^{b,c}$	10.3 ± 0.3^{b}	0.980

♣Data are presented as means±standard deviation. Data value of each parameter with different superscript letters in columns are significantly different ($P \leq 0.05$).

In the case of *Bifurcaria bifurcata* addition it was observed a significant difference on instantaneous and viscoelastic compliance (J_0 and J_m) and zero shear viscosity (η_0) for additions > 6% compared to control dough, Table 6.40. J_0 and J_m significantly decreased when added > 6% of BB35P, this was in accordance with those observed in SAOS measurements, due to due to J_0 decreased in a similar proportion that $G^{'}$ increased. Moreover, BB35P addition increased η_0, Bonnand-Ducasse *et al.* (2010) reported an increase on viscosity when fibre was added to wheat flour doughs and suggested to be due to a filler like effect of particles added. This phenomenon could be happening in our case.

As previously explained for SAOS experiments, the large values of SP of BB35P could aid to formation of more strengthen doughs which could explain that this effect was more important when BB35P was added compared to AN35P and FV35P addition. Concerning recovery characteristics, Table 6.41, J_0 and J_m showed similar behaviour of those corresponding for creep step whilst J_{max} showed its maximum value for doughs enriched with 3% of BB35P and then decreased to lower values with BB35P addition of 9%. This seems to indicate that BB addition < 6% did not significantly worsen the recovery behaviour of doughs.

Table 6.41. Parameters of recovery phase modelling, Eq. (4.28).♣

Dough	$J_{max}\cdot10^6$ (Pa^{-1})	$J_0\cdot10^6$ (Pa^{-1})	$J_m\cdot10^6$ (Pa^{-1})	λ_r (s)	J_r/J_{max} (%)	R^2
CTSGD	$13.4\pm0.1^{c,d}$	5.9 ± 0.1^{d}	$4.9\pm0.3^{b,c}$	41.9 ± 3.7^{a}	80.6 ± 1.7^{a}	0.961
CAN03D	19.3 ± 0.1^{a}	8.1 ± 0.2^{a}	7.2 ± 0.2^{a}	40.8 ± 0.7^{a}	79.5 ± 1.1^{a}	0.959
CAN06D	15.0 ± 0.6^{b}	$6.9\pm0.1^{b,c}$	5.5 ± 0.3^{b}	39.9 ± 1.5^{a}	82.6 ± 0.2^{a}	0.956
CAN09D	15.9 ± 0.3^{b}	$7.4\pm0.1^{a,b}$	5.8 ± 0.1^{b}	38.7 ± 0.2^{a}	82.9 ± 1.1^{a}	0.952
CBB03D	15.5 ± 0.1^{b}	$7.4\pm0.2^{a,b}$	6.0 ± 0.2^{b}	47.5 ± 0.4^{a}	86.2 ± 2.6^{a}	0.961
CBB06D	14.4 ± 0.1^{c}	$6.8\pm0.1^{b,c}$	$5.1\pm0.5^{b,c}$	41.7 ± 0.2^{a}	82.1 ± 2.8^{a}	0.957
CBB09D	12.6 ± 0.1^{d}	6.3 ± 0.1^{d}	4.3 ± 0.1^{c}	39.7 ± 1.0^{a}	84.0 ± 1.1^{a}	0.955
CFV03D	15.1 ± 0.4^{c}	$6.8\pm0.2^{b,c}$	5.5 ± 0.1^{b}	41.5 ± 0.7^{a}	81.2 ± 1.4^{a}	0.954
CFV06D	$14.4\pm0.7^{b,c}$	$6.5\pm0.1^{c,d}$	$5.3\pm0.2^{b,c}$	41.6 ± 0.3^{a}	82.3 ± 0.2^{a}	0.958
CFV09D	$14.2\pm0.1^{b,c}$	$6.4\pm0.1^{c,d}$	$5.3\pm0.3^{b,c}$	41.1 ± 0.4^{a}	83.0 ± 0.4^{a}	0.957

♣Data are presented as means±standard deviation. Data value of each parameter with different superscript letters in columns are significantly different (P≤ 0.05).

Regarding *Fucus vesiculosus* seaweed powder addition to chestnut flour doughs no significant differences were observed on creep and recovery characteristics of doughs. This behaviour could be related to the large insolubility of FV35P which indicates a very low interaction between seaweed particles and chestnut flour which could led to small modifications of creep characteristics of enriched-doughs. This fact seems to indicate that FV35P could be added up to 9% f.b. without impairing the creep-recovery behaviour of doughs.

Summarising, AN35P and FV35P additions up to 9% f.b. and BB35P up to 6% did not significantly modify creep-recovery dough characteristics. In general, seaweed-enriched dough had larger capacity to be deformed (larger J_{max} values)compared to control dough, probably due to the larger WA of these doughs. On the other hand, higher seaweed addition levels corresponded with an increasing trend of η_0 and a decreasing trend of J_{max} values due to a filler like effect of seaweed particles on dough matrix. In fact, a linear relationship was observed between η_0 *vs* J_{max} ($R^2 > 0.90$).

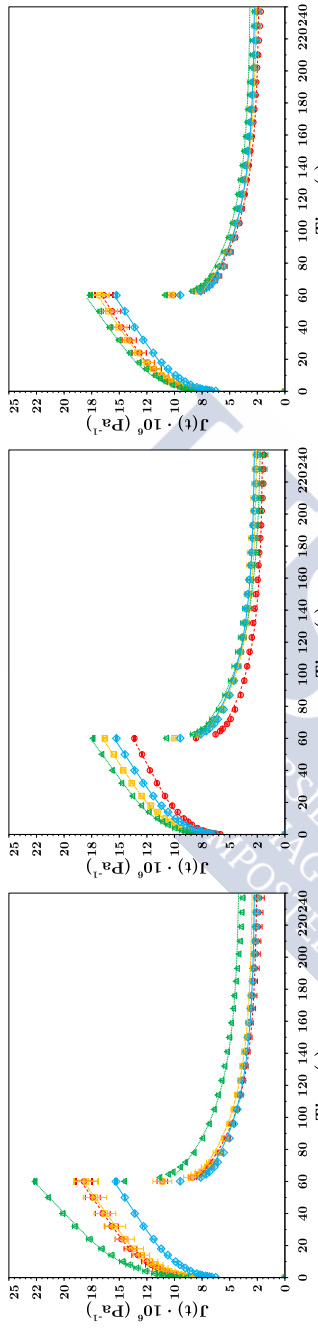

Figure 6.28 Experimental creep and recovery data at 30°C of chestnut flour doughs (◇) and chestnut flour doughs enriched with *Ascophyllum nodosum* (a), *Bifurcaria bifurcata* (b) and *Fucus vesiculosus* (c) seaweed powders at different levels: 3% (△), 6% (□) and 9% (○). Lines correspond to Eqs. (4.27) and (4.28).

Compared to other gluten-free doughs, seaweed-enriched chestnut flour doughs showed, in general, lower values of J_{max}, J_0 and J_m and larger values of η_0 compared to maize flour doughs with similar particle size (YM200D, WM200D and PM200D). Hadnadev *et al.* (2013) also reported higher values of J_{max}, J_0 and J_m for gluten-free cookie doughs based on rice/buckwheat flour blends. However, in this case similar values of η_0 were obtained.

Finally, it is important to note that a linear relationship ($R^2 > 0.78$) between complex viscosity η^* (at 0.1 s^{-1}) obtained from SAOS data and η_0 of creep data was found. Figure 6.29.

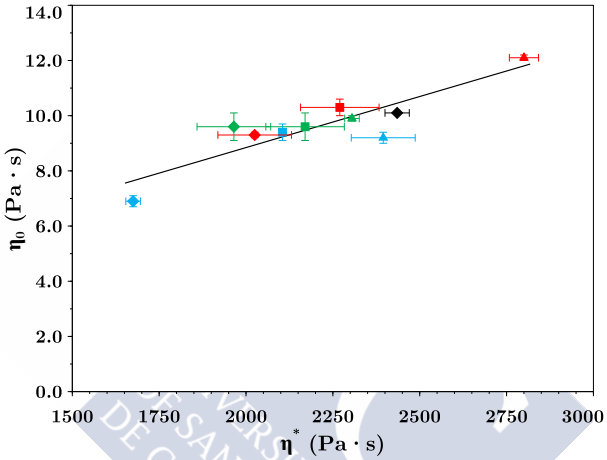

Figure 6.29 η_0 *vs* η^* chestnut flour doughs (♦) and chestnut flour doughs enriched with *Ascophyllum nodosum* (diamonds), *Bifurcaria bifurcata* (triangles) and *Fucus vesiculosus* (squares) seaweed powders at different levels: 3% (blue), 6% (green) and 9% (red).

These results suggest that creep-recovery measurements were carried out inside the LVER of doughs.

6.6.4 Rheology of seaweed-enriched pregelatinized flour doughs based on chestnut flour

Small amplitude oscillatory shear (SAOS) data of pregelatinized doughs employing the protocol presented in Section 6.5.5 are presented in Tables 6.42 and Figure 6.30. These data were successfully fitted ($R^2 > 0.90$) by means of Eqs. (4.25) and (4.26). As it can be seen, these doughs presented in general a similar behaviour of those previously analysed. They showed an elastic character predominant over the viscous character ($G' > G''$). However, compared to the same doughs analysed without pregelatinization (C1 point of mixing curve, Section 6.6.3) some differences have to be noted.

Table 6.42. Parameters of oscillatory shear modelling, Eqs. (4.25) and (4.26).♣

Dough	$\mathbf{a'\cdot 10^{-3}}$ ($Pa\cdot s^{-b'}$)	$\mathbf{b'\cdot 10^{3}}$	$\mathbf{R^2}$	$\mathbf{a''\cdot 10^{-3}}$ ($Pa\cdot s^{-b''}$)	$\mathbf{b''\cdot 10^{3}}$	$\mathbf{R^2}$
CTSGPD	166.1 ± 10.2^{b}	62.7 ± 2.5^{a}	0.985	14.5 ± 1.6^{a}	191.8 ± 2.7^{a}	0.937
CAN03PD	165.7 ± 9.8^{a}	64.3 ± 2.0^{a}	0.984	15.8 ± 3.4^{a}	193.6 ± 0.1^{a}	0.901
CAN06PD	$146.3\pm2.2^{a,b}$	62.4 ± 1.5^{a}	0.992	13.6 ± 0.6^{a}	165.6 ± 0.4^{b}	0.962
CAN09PD	130.2 ± 3.8^{b}	65.2 ± 0.5^{a}	0.991	12.7 ± 1.2^{a}	172.6 ± 0.6^{b}	0.958
CBB03PD	127.8 ± 2.1^{b}	62.6 ± 1.9^{a}	0.993	11.8 ± 0.2^{a}	$169.1\pm1.2^{a,b}$	0.957
CBB06PD	128.1 ± 8.1^{b}	61.6 ± 0.0^{a}	0.993	11.7 ± 1.2^{a}	$161.2\pm14.2^{a,b}$	0.941
CBB09PD	128.8 ± 8.3^{b}	64.8 ± 3.9^{a}	0.994	13.2 ± 0.7^{a}	138.9 ± 8.5^{c}	0.930
CFV03PD	161.6 ± 1.0^{a}	63.3 ± 1.5^{a}	0.995	15.2 ± 0.2^{a}	$164.8\pm0.1^{b,c}$	0.961
CFV06PD	165.4 ± 6.1^{a}	63.3 ± 1.2^{a}	0.995	16.0 ± 0.6^{a}	157.6 ± 0.1^{c}	0.948
CFV09PD	142.1 ± 3.8^{a}	67.2 ± 3.1^{a}	0.992	14.4 ± 1.5^{a}	171.2 ± 1.7^{b}	0.959

♣Data are presented as means±standard deviation. Data value of each parameter with different superscript (for each seaweed) letters in columns are significantly different ($P \leq 0.05$).

Firstly, it is remarkable the fact that for control dough (CTSDG) no great differences were observed on elastic behaviour compared to pregelatinized dough (CTSGPD). a′ values were very similar for both doughs 166.1 *vs* 163.2. However, concerning viscous properties of doughs, a significant decrease was observed on viscous character (lower a″) for pregelatinized doughs compared to non-pregelatinized doughs. Moreover, viscous character dependence with angular frequency was risen (larger values of b″). These significant differences between both doughs could be attributed to a less hydration of pregelatinized doughs, Table 6.43 compared to the non-pregelatinized, Table 6.28. During application of the new protocol, dough are submitted to a heating process that enhance water evaporation and also starch gelatinization. This could lead to doughs with lower hydration levels and hence to a doughs with a lower viscous character (lower values of G″).

Table 6.43 Water content of chestnut flour seaweed-enriched doughs obtained in Mixolab® apparatus after application of new protocol of mixing.♣

Dough	Water content (%, f.b.)
CTSGPD	47.7 ± 1.0^{e}
CAN03PD	$53.0 \pm 2.3^{b,c,d}$
CAN06PD	$53.3 \pm 2.2^{b,c,d}$
CAN09PD	58.4 ± 2.0^{a}
CBB03PD	$51.5 \pm 3.7^{c,d}$
CBB06PD	$55.3 \pm 2.0^{a,b,c}$
CBB09PD	$56.3 \pm 1.8^{a,b}$
CFV03PD	$51.6 \pm 1.4^{c,d,e}$
CFV06PD	$49.6 \pm 0.9^{c,d,e}$
CFV09PD	$55.0 \pm 0.7^{b,c,d}$

♣Data are presented as means±standard deviation. Data value of each parameter with different superscript letters in columns are significantly different ($P \leq 0.05$).

Regarding seaweed enriched doughs, different trends could be mentioned. Concerning viscous behaviour, it was observed the same trend as those previously described for CTSGPD. However, elastic character of seaweed-enriched doughs was also modified by application of the new protocol. Two different behaviours were observed as function of employed seaweed. In the case of AN35P and FV35P addition, elastic character was increased after the application of the new protocol of mixing. This fact can be explained, as in the case of the viscous character, by the combined effect of water evaporation and starch gelatinization promoted by application of new protocol of mixing which in this case reduced viscous character and increased the elastic one. On the other hand, CBBPD showed a decrease on elastic character compared to CBBD. This phenomenon could be attributed to the larger WA of BB35P-enriched doughs and the high SP of BB35P particles. The high SP of these particles resulted, as previously explained (Section 6.6.3) in more elastic doughs when no thermal process occurs in doughs. However, when a heating step is applied to the dough and gelatinization of starch takes place, this swollen particles are pressured by the swollen particles of starch hence losing water. This, together with the fact that BB35P-enriched doughs had the largest WA levels could led to a larger contents of free water on dough matrix that could provoke the lubricant effect observed on G' decrease. These larger amounts of available water on BB35P-enriched doughs will be also corroborated by their thermomechanical properties, more details will be presented in the next Section 6.7.

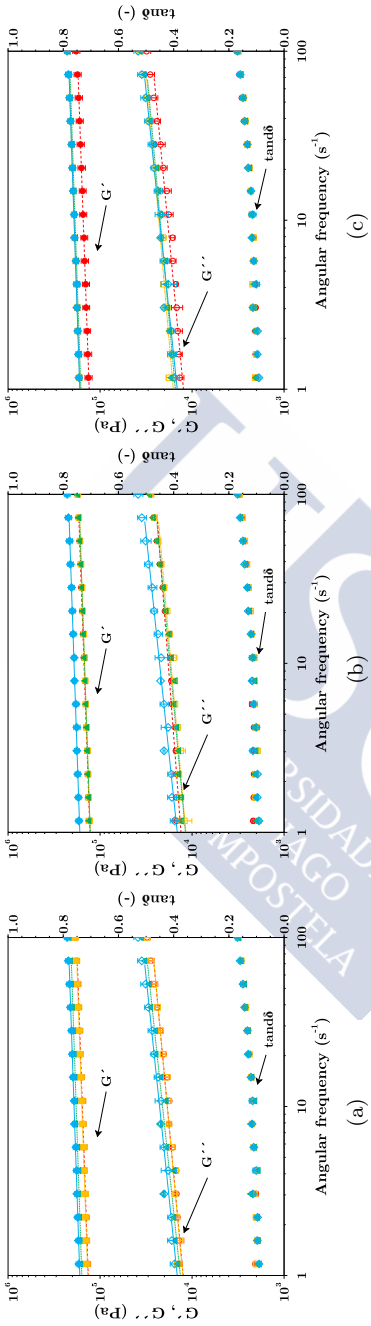

Figure 6.30 Experimental data of G′ (filled markers), G″ (empty markers) and tanδ (dot filled markers) at 30°C of chestnut flour doughs (◇) and chestnut flour doughs enriched with *Ascophyllum nodosum* (a), *Bifurcaria bifurcata* (b) and *Fucus vesiculosus* (c) seaweed powders at different levels: 3% (△), 6% (□) and 9% (○). Lines correspond to Eqs. (4.25) and (4.26).

Concerning creep and recovery properties, different behaviours have been observed (Tables 6.44 and 6.45 and Figure 6.31).

Table 6.44. Parameters of creep phase modelling, Eq. (4.27).♣

Dough	$\mathbf{J_0 \cdot 10^6}$ (Pa^{-1})	$\mathbf{J_m \cdot 10^6}$ (Pa^{-1})	λ_c (s)	$\eta_0 \cdot \mathbf{10^{-6}}$ (Pa·s)	$\mathbf{R^2}$
CTSGPD	6.3 ± 0.3^{b}	1.4 ± 0.1^{b}	1.5 ± 0.1^{b}	$33.5\pm4.3^{a,b}$	0.784
CAN03PD	6.0 ± 0.2^{b}	$1.6\pm0.2^{a,b}$	2.1 ± 0.1^{a}	40.8 ± 0.6^{a}	0.817
CAN06PD	$7.2\pm0.2^{a,b}$	1.9 ± 0.1^{a}	2.2 ± 0.1^{a}	28.1 ± 1.4^{b}	0.851
CAN09PD	7.8 ± 0.6^{a}	2.1 ± 0.1^{a}	2.4 ± 0.1^{a}	29.5 ± 0.2^{b}	0.837
CBB03PD	8.2 ± 0.2^{a}	2.3 ± 0.1^{a}	2.2 ± 0.1^{a}	26.7 ± 0.6^{b}	0.982
CBB06PD	8.0 ± 0.4^{a}	2.3 ± 0.1^{a}	2.1 ± 0.2^{a}	23.2 ± 1.4^{b}	0.982
CBB09PD	$7.6\pm0.6^{a,b}$	2.4 ± 0.1^{a}	2.5 ± 0.1^{a}	25.3 ± 5.6^{b}	0.981
CFV03PD	6.5 ± 0.1^{b}	1.8 ± 0.1^{a}	2.4 ± 0.1^{a}	34.4 ± 3.0^{b}	0.981
CFV06PD	6.5 ± 0.1^{b}	$1.7\pm0.1^{a,b}$	2.4 ± 0.1^{a}	30.3 ± 1.1^{b}	0.981
CFV09PD	7.0 ± 0.2^{b}	2.1 ± 0.2^{a}	2.2 ± 0.2^{a}	28.9 ± 0.2^{b}	0.980

♣Data are presented as means±standard deviation. Data value of each parameter with different superscript letters (for each seaweed) in columns are significantly different ($P \leq 0.05$).

Firstly, instantaneous compliance was in concordance with SAOS data, larger values of $G^{'}$ in SAOS experiments were concomitant with lower values of J_0 as it was also observed for non-pregelatinized doughs. Viscoelastic compliance, J_m decreased for all studied doughs compared to non-pregelatinized indicating the reduction of viscous character of doughs. This reduction can be also observed in the lower values of λ_c for pregelatinized doughs. Finally, zero shear viscosity, η_0, increased after the application of the new protocol of mixing probably due to the effect of gelatinization. In the case of recovery parameters, J_0, J_m and λ_c presented the same trend as in creep phase. J_{max} was slightly reduced, highlighting the lower deformation capacity of dough, probably due to their viscous character reduction. Finally, J_r/J_{max} ratio was increased overall ≈10% compared to doughs analysed at C1 which indicates that pregelatinized doughs presented higher recuperation capacity. All trends previously mentioned can be attributed, as in the case of SAOS analysis, to the combined effect of water evaporation and gelatinization.

Regarding seaweed addition effect on pregelatinizated chestnut flour doughs, it seems that the application of the new protocol of mixing seems to smoothed the differences between all studied doughs. In fact, it was observed no huge differences on doughs properties as function of seaweed addition. As explained in SAOS test, doughs enriched with BB35P showed the most different behaviour. In this case, they presented larger values of J_0, J_{max} and J_m reinforcing the idea that BB35P particles aids to a more lubricant effect of water due to their swollen

particles are pressured after gelatinization process and can release water that aids to a higher capacity of deformation of doughs.

Table 6.45. Parameters of recovery phase modelling, Eq. (4.28).♣

Dough	$\mathbf{J}_{max}\cdot\mathbf{10}^{6}$ (Pa^{-1})	$\mathbf{J}_{0}\cdot\mathbf{10}^{6}$ (Pa^{-1})	$\mathbf{J}_{m}\cdot\mathbf{10}^{6}$ (Pa^{-1})	λ_r (s)	$\mathbf{J}_r/\mathbf{J}_{max}$ (%)	$\mathbf{R}^2$
CTSGD	8.3 ± 0.7^{b}	6.3 ± 0.3^{b}	1.4 ± 0.3^{b}	30.6 ± 19.1^{a}	91.9 ± 2.2^{a}	0.675
CAN03D	7.9 ± 0.1^{b}	6.0 ± 0.2^{b}	$1.5\pm0.1^{a,b}$	33.3 ± 2.0^{a}	94.4 ± 0.6^{a}	0.770
CAN06D	$10.0\pm0.1^{a,b}$	$7.2\pm0.2^{a,b}$	1.8 ± 0.1^{a}	17.7 ± 1.4^{a}	90.1 ± 1.4^{a}	0.729
CAN09D	10.6 ± 0.8^{a}	7.8 ± 0.6^{a}	2.0 ± 0.1^{a}	20.9 ± 1.5^{a}	92.2 ± 0.8^{a}	0.733
CBB03D	11.2 ± 0.1^{a}	8.2 ± 0.2^{a}	$2.1\pm0.1^{a,b}$	22.3 ± 3.6^{a}	91.5 ± 0.9^{a}	0.757
CBB06D	11.4 ± 0.6^{a}	8.0 ± 0.1^{a}	$2.1\pm0.1^{a,b}$	17.8 ± 9.1^{a}	88.5 ± 3.7^{a}	0.675
CBB09D	10.8 ± 1.2^{b}	$7.6\pm0.4^{a,b}$	2.3 ± 0.4^{a}	30.2 ± 10.9^{a}	91.8 ± 1.9^{a}	0.802
CFV03D	$8.8\pm0.3^{a,b}$	6.5 ± 0.1^{b}	$1.7\pm0.1^{a,b}$	28.0 ± 3.5^{a}	92.8 ± 1.3^{a}	0.782
CFV06D	$9.1\pm0.1^{a,b}$	6.5 ± 0.1^{b}	$1.7\pm0.1^{a,b}$	19.5 ± 2.6^{a}	89.7 ± 2.2^{a}	0.667
CFV09D	9.8 ± 0.1^{a}	7.0 ± 0.2^{b}	1.8 ± 0.1^{a}	24.3 ± 14.4^{a}	90.1 ± 3.8^{a}	0.747

♣Data are presented as means±standard deviation. Data value of each parameter with different superscript letters (for each seaweed) in columns are significantly different ($P\leq 0.05$).

The differences observed by seaweed powder addition could be considered as acceptable and considering creep and recovery properties it could be said that seaweed addition levels up to 9% can be employed to chestnut flour doughs enrichment without impairing these properties.

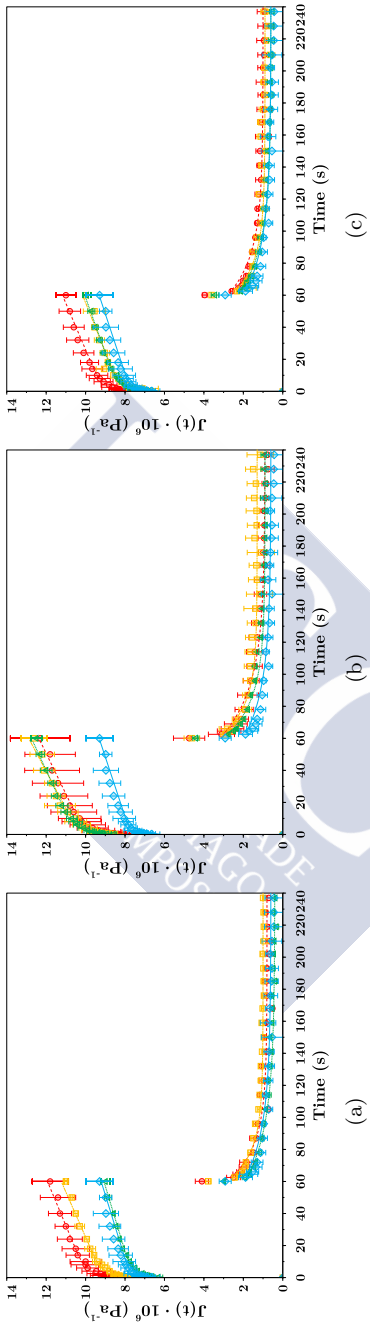

Figure 6.31 Experimental creep and recovery data at 30°C of chestnut flour doughs (◇) and chestnut flour doughs enriched with *Ascophyllum nodosum* (a), *Bifurcaria bifurcata* (b) and *Fucus vesiculosus* (c) seaweed powders at different levels: 3% (△), 6% (□) and 9% (○). Lines correspond to Eqs. (4.27) and (4.28).

The section in tweets

- All gluten-free flour doughs showed G' higher than G'' values indicating that elastic proportion was dominant over the viscous one.
- G' and G'' increase with angular frequency (ω) for all assayed doughs.
- The higher the average particle size of flour, the larger the G' and G'' values of flour doughs.
- The higher the water absorption of doughs, the lower the values of G' and G''.
- Stiffer doughs showed lower instantaneous compliance on creep and recovery phases.
- Viscoelastic compliance increase with increasing damaged starch content.
- AN35P and FV35P addition significantly decrease moduli values compared to control dough.
- Addition of BB35P $\geq 6\%$ significantly increases elastic character of doughs.
- Water retention capacity and swelling power of seaweed powders affect G' and G'' values of seaweed-enriched doughs.
- Seaweed powder addition up to 9% f.b. for ANP and FVP and 6% f.b. for BBP does not impair viscoelastic properties of doughs.
- Pregelatinized doughs showed lower viscous character than non-pregelatinized flour doughs.
- Seaweed powder addition of 9% f.b does not impair viscoelastic properties of pregelatinized doughs.

USC
UNIVERSIDADE
DE SANTIAGO
DE COMPOSTELA

6.7 Thermomechanical properties of gluten-free flour doughs

Starch transitions of flour doughs based on maize flours and chestnut flour were studied by differential scanning calorimetry (DSC) and Dynamic Mechanic-Thermal Analysis (DMTA) in order to establish a new method to study the thermal transitions on gluten-free dough employing only DMTA. Moreover, chestnut flour blends consisting on chestnut flour enriched with seaweed powders of *Ascophyllum nodosum*, *Bifurcaria bifurcata* and *Fucus vesiculosus* obtained from seaweeds dried at 35°C has been studied by means DMTA. [7]

[7] This section was adapted from the following papers and others in writing process:
MOREIRA, R., CHENLO, F. & ARUFE, S. (2015). Starch transitions of different gluten free flour doughs determined by dynamic thermal mechanical analysis and differential scanning calorimetry. *Carbohydrate polymers* **127**, 160-167. DOI: http://doi.org/10.1016/j.carbpol.2015.03.062.
MOREIRA, R., CHENLO, F., SINEIRO, J., TORRES, M. D. & ARUFE, S. (2017). Mixing, rheological and thermomechanical characterization of seaweed-enriched chestnut flour doughs. To be submitted to: *Journal of Food Engineering*.
MOREIRA, R., CHENLO, F., SINEIRO, J., TORRES, M. D. & ARUFE, S. (2017). Physico-Chemichal Properties of seaweed-enriched chestnut flour cookies obtained from pregelatinized doughs. To be submitted to: *Journal of Texture studies*.

Nomenclature

Powders

AN35P	–	*Ascophyllum nodosum* (AN) powder obtained from AN35.
BB35P	–	*Bifurcaria bifurcata* (BB) powder obtained from BB35.
FV35P	–	*Fucus vesiculosus* (FV) powder obtained from FV35.
GG	–	Guar gum.

Doughs

CAN03D	–	Chestnut flour dough with 3% f.b. of AN35P.
CAN06D	–	Chestnut flour dough with 6% f.b. of AN35P.
CAN09D	–	Chestnut flour dough with 9% f.b. of AN35P.
CBB03D	–	Chestnut flour dough with 3% f.b. of BB35P.
CBB06D	–	Chestnut flour dough with 6% f.b. of BB35P.
CBB09D	–	Chestnut flour dough with 9% f.b. of BB35P.
CFV03D	–	Chestnut flour dough with 3% f.b. of FV35P.
CFV06D	–	Chestnut flour dough with 6% f.b. of FV35P.
CFV09D	–	Chestnut flour dough with 9% f.b. of FV35P.
CTD	–	Chestnut flour dough.
CTSGD	–	Chestnut flour dough with 1.8% f.b. of NaCl and 2% f.b. of GG.
CAN0XPD	–	Pregelatinized CAN0XD.
CBB0XPD	–	Pregelatinized CBB0XD.
CFV0XPD	–	Pregelatinized CFV0XD.
CTSGPD	–	Pregelatinized CTSGD.
PM200D	–	Purple maize dough (flour obtained with 200 μm mesh during milling).
PM500D	–	Purple maize dough (flour obtained with 500 μm mesh during milling).
WM200D	–	White maize dough (flour obtained with 200 μm mesh during milling).
WM500D	–	White maize dough (flour obtained with 500 μm mesh during milling).
YM200D	–	Yellow maize dough (flour obtained with 200 μm mesh during milling).
YM500D	–	Yellow maize dough (flour obtained with 500 μm mesh during milling).

Techniques

DSC	–	Differential Scanning Calorimetry.
DMTA	–	Dynamic Mechanic-Thermal Analysis.

Parameters

DS	–	Damaged Starch, (g damaged starch·(g dry flour)$^{-1}$).
G'	–	Storage modulus, Pa.
G''	–	Loss modulus, Pa.
LVER	–	Linear viscoelastic region.
tanδ	–	Damping factor.
TS	–	Total Starch, g starch·(g dry flour)$^{-1}$.
T'_0	–	Temperature of beginning of starch granules swelling determined by DMTA, ^{o}C.
T_0	–	Onset transition temperature, ^{o}C.
T_p	–	Peak transition temperature, ^{o}C.
T_f	–	Final transition temperature, ^{o}C.
WA	–	Water absorption, % f.b..
WRC	–	Water retention capacity, g water·(g dry solid)$^{-1}$.

6.7.1 Introduction

Gluten-free products based on starchy foods are in increasing demand due to the growing number of people diagnosed with coeliac disease. The research on the transformations experienced by these materials during thermal processes is essential to estimate and control the final product properties. The use of traditional and world starch source like maize or alternative and local sources like chestnut is necessary to increase the supply of products with high quality to a growing market.

The main component of maize and chestnut is the starch. Starch is present in form of granules with crystalline and amorphous structures. Physicochemical properties and thermal behaviour of starch depend on the amorphous/crystalline ratio and the arrangement of the structure in the granule (Tahir *et al.*, 2010). Chemically, starch is constituted by two carbohydrate polymers, amylose (linear) and amylopectin (branched) (French, 1984) with different behaviour during thermal processing and also depending on the water content.

Differential scanning calorimetry (DSC) is the most common method to study the thermal behaviour of isolated starches for determining temperature of transitions and the corresponding enthalpies (Donovan (1979); Eliasson (1980)). Particularly, gelatinization of different starch is well studied in the bibliography by its importance in starch processing for food and non-food purposes. At high water content one broad endothermic peak, G, by the swelling of the amorphous region and subsequent melting of crystallites is observed, but at intermediate water content, this last transition is partially postponed to higher temperatures resulting M1 transition (Jang & Pyun, 1996). Other thermal transitions, due to biopolymer interactions, can be determined at higher temperatures as the reversible dissociation of lipid-amylose complexes in the range from 100 to 120°C (Liu *et al.* (2006); Torres *et al.* (2013)) and also melting amylose above 140°C (Jang & Pyun, 1996). These transitions also depend on water content of the sample.

Nevertheless, some endothermic peaks associated to the thermal transitions are very weak and consequently their determination and evaluation is troublesome. This fact is pronounced in samples with high water content because the limited dry mass amount and DSC is not sensitive to changes affecting to mechanical properties of the material (Warren *et al.*, 2012).

The study of the starch transitions in cereal doughs like maize and chestnuts flour doughs is more complex than the study of isolated starch from different sources. The presence of other biopolymers in a relevant proportion like proteins

and lipids together with the particle size of the flour affect significantly the water absorption of the samples to achieve a determined consistency. At these conditions, doughs can be submitted to different industrial thermal processes involving operations such as baking, extrusion of floury products and the material properties depend on starch gelatinization and other transitions promoted by temperature. The chemical, physical and viscoelastic properties of the final starchy products depend mainly on the extension of water-starch and water-biopolymers interactions developed during processing.

Dynamic Mechanic-Thermal Analysis (DMTA) is an experimental method in which a sinusoidal force is applied to the sample at fixed angular frequency measuring the stress and strain inside the linear viscoelaticity region (LVER) at constant heating/cooling rate. This analysis was employed by other authors to evaluate the starch gelatinization due to strong structural changes takes place during the plasticizing process promoted by water (Bogracheva *et al.*, 2002). In fact, gelatinization temperatures range can be clearly observed by peaks of the storage modulus, G', complex viscosity, G^* or $\tan\delta$ (Moreira *et al.* (2011); Chanvrier *et al.* (2013)).

The experimental determinations of the phase transitions at high temperatures (above 100°C) of flour doughs by using DMTA or DSC methods may lead to different results, beyond the physical fundamentals of each technique, by the fact of the water evaporation. Water during DSC is evaporated generating an overpressure inside the sealed pan and equilibrium between sample and surrounding is achieved. In DMTA experiments, water is also removed by evaporation and sample dries. Both methods are interesting because DSC analysis can be useful to understand the crumb formation and DMTA tests can be related to the crust generation.

The aim of this work is to determine the starch transitions of several gluten-free flour doughs (three from different maize varieties and one from chestnut fruit) processed at the same consistency level with different water absorption by two different experimental techniques (DSC and DMTA) in order to establish comparisons between the results obtained with both tested methods and develop a new protocol to determine thermal transitions through DMTA analysis. Results on starch transitions are discussed in relation to chemical and physical properties of flours and doughs also experimentally determined. Moreover, the developed protocol will be employed to determine thermal transitions on seaweed-enriched gluten-free flour doughs.

6.7.2 Differential Scanning Calorimetry (DSC)

Figure 6.32 shows the thermograms of the tested flour doughs divided into two temperature ranges (a, from 40 to 115°C and b, from 115 to 150°C) in order to observe clearer the peaks. All samples showed the typical gelatinization endotherm, G, which appears at relative low temperature (66.7 up to 69.1°C, Table 6.47). This endotherm at high water content mainly corresponds to the gelatinization of amylopectin (Russell (1987); Liu *et al.* (2006)). When available water is restricted, gelatinization can be partly postponed to higher temperatures due to the melting of the remaining amylopectin crystallites (Shogren, 1992) giving as result M1 peak. At intermediate water content, M1 peak can appear as a shoulder overlapped with the G peak giving as result a broad temperature range of gelatinization. At lower moisture content, M1 is clearly separated from G and shifted to higher temperatures up to disappear at dry conditions (Liu *et al.*, 2006).

Table 6.47 Onset (T_o), peak (T_p) and final (T_1) temperatures and enthalpy, ΔH_i, of thermal starch transitions determined by DSC for tested maize and chestnut flour doughs.♣

		YM200D	WM200D	PM200D	CTD
WA	(% f.b.)	63.0 ± 1.0^c	90.0 ± 2.0^a	81.1 ± 1.4^b	52.9 ± 0.5^d
G	T_o (°C)	66.7^b	66.7^b	68.2^a	69.1^a
	T_p (°C)	74.0^c	76.7^b	78.8^a	77.5^b
	T_f (°C)	82.6^c	90.6^b	93.3^a	90.2^b
	ΔH_G (J/g starch)	2.9^c	4.2^c	9.2^b	11.2^a
M1	T_o (°C)	83.0	-	-	-
	T_p (°C)	91.7	-	-	-
	T_1 (°C)	100.7	-	-	-
	ΔH_{M1} (J/g starch)	2.0	-	-	-
M2	T_o (°C)	100.7^b	94.6^d	97.8^c	102.8^a
	T_p (°C)	109.6^b	102.1^d	105.0^c	114.0^a
	T_1 (°C)	117.6^b	112.0^c	112.4^c	122.2^d
	ΔH_{M2} (J/g starch)	0.6^a	1.1^a	1.1^a	1.7^a
M3	T_o (°C)	140.1^a	130.2^c	129.0^c	134.6^b
	T_p (°C)	140.2^a	130.3^c	129.1^c	134.7^b
	T_1 (°C)	146.4^a	137.9^b	132.5^d	136.0^c
	ΔH_{M3} (J/g starch)	6.6^a	3.7^b	2.9^b	3.5^b
$\Delta H_{G+M1+M2+M3}$ (J/g starch)		12.1^a	9.0^b	13.2^a	16.4^c

♣ Standard deviations of temperature data were ±0.2°C and enthalpy data ±0.3 J/g. Yellow (YM), white (WM) and purple (PM) maize flour doughs and chestnut (CH) flour doughs. Data value with different letters in rows are significantly different, $P \leq 0.05$.

In the maize flour doughs, YM200D showed separately G and M1 peaks and WM200D and PM200D only one peak (G + M1). This result agrees with the

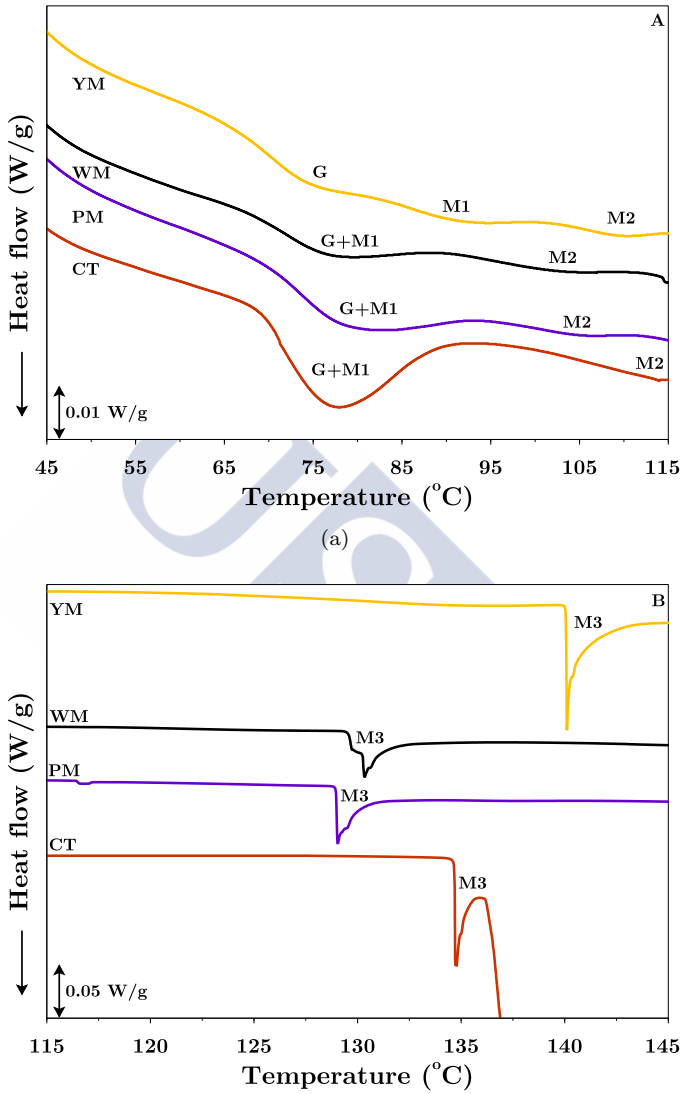

Figure 6.32 DSC thermograms for yellow (YM, —), white (WM, —) and purple (PM, —) maize flour doughs and chestnut (CH, —) flour doughs. (A) Temperatures from 45 up to 115°C, (B) temperatures from 115 up to 145°C.

explained trend of both peaks with water content due to YM200D flour doughs is the sample with lower hydration (63% w/w) while WM200D and PM200D hydration is higher than 80% w/w, Table 6.29. CTD also showed a peak with shoulder (G + M1), in spite of it is the sample with the lowest hydration (53% w/w). This result reveals that the different nature of starch (average molecular weights of amylose and amylopectin, etc) and its interactions with other hydrophilic components (mainly carbohydrates, protein and fibre) modify the available water for starch gelatinization. Consequently the thermal behaviour of the dough is modified and the temperature ranges for each starch thermal transition must be experimentally determined for each starchy material. Samples with peaks overlap showed a broad temperature range for the glass transition (from 66.7 to 93.3 °C), Table 6.47. M1 peak of YM flour dough took place between 83.0 and 100.7 °C that agrees with reported data for maize starch at similar hydration (52% w/w) (Liu *et al.*, 2007).

Gelatinization enthalpy is related to the proportion of ordered/disorder material in the starch (Bogracheva *et al.*, 2002). The sum of the associated enthalpy values of G and M1 peaks varied for maize flour doughs between 4.2 and 9.2 J/g and they are in the range of previously reported data (Liu *et al.*, 2007). In the case of CTD the enthalpy value was higher (11.2 J/g) and also is according to those reported for chestnut starch (Cruz *et al.*, 2013).

Other transition at higher temperature, denominated M2, was observed in all flour doughs. This transition varied between 94.6 to 122.2°C and corresponds to the melting of amylose-lipid complexes (Biliaderis *et al.* (1986); Jovanovich & Añón (1999)). Enthalpy values (from 0.6 up to 1.7 J/g) are lower than the transitions at lower temperatures and the range are also according to bibliography (Liu *et al.*, 2007). No clear relationship was found between enthalpy values and lipid or total starch or damaged starch content. The required energy for the melting of amylose-lipid complexes depends rather on microstructural characteristics of both biopolymers and the accessibility among them.

Figure 6.32 (b) shows the appearance of a new peak, M3, at high temperatures (from 129 to 147°C) corresponding to the melting of amylose (Liu *et al.*, 2007). This endotherm sets in a narrow interval of temperatures (< 7°C) and in maize flours the peak temperatures showed an inversely relationship with hydration of flour. So, M3 for PM200D was into 129.0-132.5°C and for YM200D flour dough was 140.1-146.4°C. M3 peak of CTD flour dough was shorter and at intermediate temperature (134.6-136.0°C) in spite of its low hydration, showing again the importance of the starch nature on its thermal behaviour. Enthalpy values of M3 for maize flours varied between 6.6 J/g for YM200D and 2.9 J/g for PM200D. This result reveals a relationship between hydration and damaged

starch proportion and enthalpy values of M3 endotherm. The presence of high proportion of damaged starch gives as result high hydration level to achieve the target consistency and leached amylose interacts easily with other biopolymers and undergoes thermal stress. At low hydration level, amylose is preserved and the corresponding melting heat is higher. CTD flour doughs showed an intermediate value for the enthalpy value of M3 endotherm regarding to maize flours.

The total enthalpy, $\Delta H_{G+M1+M2+M3}$, calculated as the sum of the individual enthalpy values of the determined peaks is shown in Table 6.47. Average enthalpy value for maize flours was 11.5±2.2 J/g and no significant differences were observed between them. Other authors found a proportional trend between hydration and total enthalpy (with values in the same range), but this result was not found in the tested samples (Liu *et al.*, 2006). Total enthalpy (16.4±0.2 J/g) for CTD flour doughs was significantly higher, revealing again the specific features of starch from different sources.

CTD sample showed a differenced behaviour regarding to maize flour doughs at higher temperatures (> 135ºC). A broad endotherm among 138 and 168ºC appears corresponding to the melting of sugars (mainly sucrose) of chestnut (data partially shown), Figure 6.32 (b). This peak was not observed in the maize flour doughs due to the low sugar content of the samples.

6.7.3 Dynamic Mechanic-Thermal Analysis (DMTA)

6.7.3.1 Chestnut and maize flour doughs

The same maize and chestnut flour doughs were also evaluated by DMTA in order to carry out a comparison between both methods to evaluate the suitability of DMTA to determine the starch transition properties of doughs. In order to carry out the analysis minimum, maximum and inflection points of G$'$ and tandδ *vs* temperature curves were determined.

G+M1 transition

Figure 6.33 shows the elastic modulus (a) and tanδ (b) peaks during heating of PM200D and YM200D samples, as example of starch gelatinization transition of doughs (G+M1).

At low temperatures G$'$ values decreases slightly with increasing temperature due to proteins weakening up to achieve a minimum. This point is labelled like T'_o, Table 6.48, and determines the beginning of the physical phenomena that

take place during starch gelatinization, mainly the swelling of the starch granules. This can be observed in Figure 6.33 (c) where a typical curve of dough normal force applied to the plates of rheometer *vs* temperature during DMTA analysis is plotted. As it can be observed at temperatures closer to T'_o the normal force of the dough between the plates increased, indicating a tendency of dough to increase its volume due to swelling of starch granules. In the tested flour doughs, elastic modulus values sharply increase from 50-57°C, Table 6.48. This point was not detected during DSC experiments, because the involved processes do not modify significantly the thermal properties of the system.

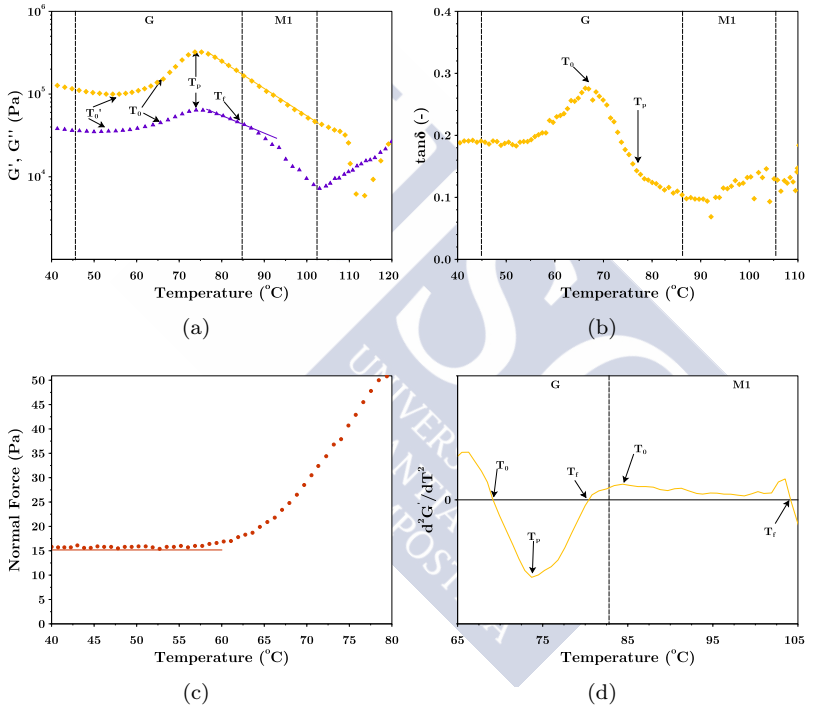

Figure 6.33 G' and tanδ evolution with temperature for yellow (YM200D, ♦) and purple (PM200d, ▲) maize flour doughs (a, b), normal force during DMTA analysis of CTD dough (c) and d^2G'/dT^2 *vs* temperature curve (d).

After T'_o G' increases due to the growing turgor of starch granules. Nevertheless, starch gelatinization is also originated by the disintegration of the granules and starchy polymers melting with a generation of a continuous matrix of leached amylose molecules that increases the viscosity and consequently the

viscous character of the multi-phased system (Ring, 1985). The beginning of this process was measured by DSC due to it involved thermal changes in the sample and labelled as T_o. It could be also determined employing DMTA technique. It corresponded to inflexion point of $G^{'}(T)$ as it can be observed in Figure 6.33 (a) or by the determination of $d^2G^{'}/dT^2$=0, Figure 6.33 (d).

The peak temperature of G transition, T_p, can be determined by the relative maximum of $G^{'}$, Figure 6.33 (a).

Final temperature, T_f, can be evaluated through the inflexion point of $G^{'}(T)$ curve (the point in which the slope (straight line in Figure 6.33 (a)) of $G^{'}$ changes after T_p) which corresponded to $d^2G^{'}/dT^2$=0, Figure 6.33 (d).

This first peak corresponds, as it was explained during discussion of the DSC results, to the addition of two transitions G and M1 for WM200D, PM200D and CTD flour doughs while YM200D sample showed separated peaks. During DMTA both peaks of YM200D flour dough were not observed at first glance, G′ showed a broader temperature interval with constant slope. However characteristic temperatures of M1, T_0 and T_f could be determined as the relative maximum of $d^2G^{'}/dT^2$ curve and the inflexion point of G′ ($d^2G^{'}/dT^2$=0), respectively, Figure 6.33 (d).

Table 6.48 Onset (T_o), peak (T_p) and final (T_1) of thermal starch transitions determined by DMTA following the elastic modulus ($G^{'}$) and the damping factor (tanδ) for tested maize and chestnut flour doughs.♣

Transition			YM200D	WM200D	PM200D	CTD
G	T_0' (°C)	$G^{'}$	53.6±0.1^a	50.0±1.3^a	56.1±0.2^a	56.9±2.5^a
		tanδ	-	-	-	-
	T_o (°C)	$G^{'}$	69.1±0.1^b	68.1±0.1^b	72.5±0.8^a	71.0±0.7^a
		tanδ	66.9±0.1^a	68.6±1.9^a	71.5±0.6^a	71.0±0.7^a
	T_p (°C)	$G^{'}$	74.4±0.1^b	74.5±0.3^b	77.3±0.5^a	76.9±0.2^a
		tanδ	74.0±0.4^a	75.8±2.0^a	77.7±0.6^a	78.0±0.6^a
	T_f (°C)	$G^{'}$	81.4±0.7^a	86.8±0.2^a	85.0±0.4^a	84.5±0.3^a
		tanδ	78.8±1.7^a	83.0±0.2^a	84.5±1.5^a	85.4±0.1^a
M1	T_o (°C)	$G^{'}$	86.2±1.4	-	-	-
		tanδ	-	-	-	-
	T_p (°C)	$G^{'}$	-	-	-	-
		tanδ	-	-	-	-
	T_1 (°C)	$G^{'}$	102.5±2.1	-	-	-
		tanδ	-	-	-	-

♣ Yellow (YM), white (WM) and purple (PM) maize flour doughs and chestnut (CH) flour doughs. Data value with different letters in rows are significantly different, P≤ 0.05.

Additionally, characteristics temperatures of G transition (T_0, T_p and T_F) could be also determined through tanδ analysis. This factor increases below the temperature corresponding to the onset temperature of gelatinization, T_o, measured by DSC up to a maximum value, T_p. The onset temperature of gelatinization, T_o, corresponded to the relative maximum of tanδ(T) and the peak temperature of this transition, T_p, to the inflexion point of tanδ(T) curve, Figure 6.33 (b). Finally, the final temperature, T_f, could be evaluated through the relative maximum of $d^2\text{tan}\delta/dT^2$ (data not shown).

The characteristic temperatures of G transition determined by $G^{'}$ and tanδ were in accordance, Table 6.48. Moreover, it is noteworthy that the tanδ peaks are relatively small, because the starch transitions are more limited by the presence of other hydrophilic polymers in the dough together with the restricted amount of water and a significant fraction of starch crystallites melt at higher temperature (Xie *et al.*, 2008).

Furthermore, the presence of amylose helps to maintain starch granule integrity during gelatinization and more transitions can be observed at higher temperatures (Debet & Gidley, 2007). Other authors have studied isolated starches with different amylose to amylopectin ratio and, in the case of starches with a normal ratio (0.15-0.25), peaks in $G^{'}$ and tanδ are reliably obtained (Warren *et al.*, 2012). These authors also found, using these kind of starches and with excess of water, good agreement among $G^{'}$ peak and T_p evaluated by DSC. Nevertheless, they found that T_p measured by tanδ was in agreement with T_o measured by DSC, result that was no observed in the tested samples in this work. Nevertheless, these results are not rigorously comparable because flour doughs are complex materials and with restricted water accessible the peaks are shifted at higher temperatures and occur into a broader temperature interval.

M2 transition

M2 peak is difficult to observe because is coincident with the water evaporation from the dough sample. In these circumstances, simultaneous processes that affect to mechanical properties take place and the elastic modulus data show some dispersion due to the important physical and structural changes (fracturing by the rupture of the matrix porosity) promoted by the water removal (Jefferson *et al.*, 2007). Furthermore, $G^{'}$ passes through a minimum value that is labelled like peak temperature of M2 transition, T_p. T_o was determined as the inflection point of $G^{'}$(T) and T_f by means of slope changes of $G^{'}$(T) before and after T_p, respectively, Figure 6.34 (a) and (b).

The peaks took place in a narrow interval of temperatures varying from 99 to

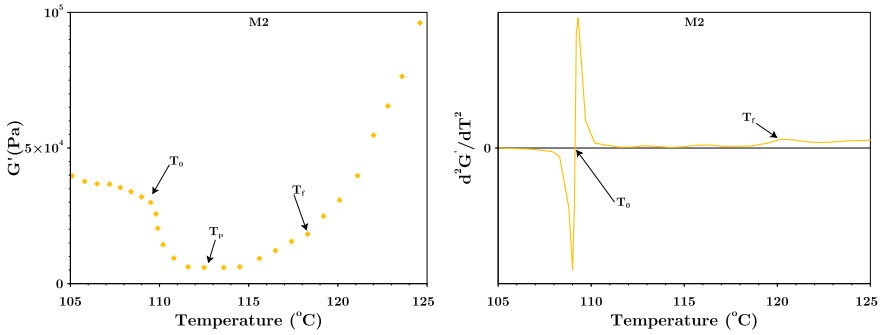

(a) (b)

Figure 6.34 G´ and tanδ evolution with temperature for yellow (YM200D, ♦) maize flour doughs (a) and d^2G'/dT^2 *vs* T (b).

111°C for WM200D flour dough and from 109 to 122°C for CTD flour doughs. It was observed that T_o and T_p determined by DMTA corresponding to M2 peak shifted to higher temperatures than those measured by DSC. This result indicates that the melting of amylose-lipid complexes is accompanied with an elastic modulus decrease, depending on moisture content of the dough because this transition is retarded when water content diminishes. Nevertheless, the ends of the M2 transition, T_f, were the same by means of both methods for the tested flour doughs, Tables 6.47 and 6.49.

Table 6.49 Onset (T_o), peak (T_p) and final (T_1) of M2 transition determined by DMTA through G´ and tanδ for tested maize and chestnut flour doughs.♣

Transition			YM200D	WM200D	PM200D	CTD
M2	T_o (°C)	G´	109.5±0.5^a	99.1±1.2^c	102.8±0.1^b	110.6±0.3^a
		tanδ	-	-	-	-
	T_p (°C)	G´	113.7±0.1^a	103.7±0.2^c	108.5±0.5^b	116.5±1.6^a
		tanδ	-	-	-	-
	T_1 (°C)	G´	119.8±0.5^a	111.4±2.8^a	111.7±2.4^a	121.8±1.3^a
		tanδ	-	-	-	-

♣ Yellow (YM), white (WM) and purple (PM) maize flour doughs and chestnut (CH) flour doughs. Data value with different letters in rows are significantly different, P≤ 0.05.

M3 transition

Above M2 transition, G´ values increase sharply during baking by the complex phenomena related to the crust formation that give as result a more rigid and stiff

material. Regarding to M3 peak, corresponding to the melting of amylose, it can be monitored by tanδ or G$'$ as function of the curve obtained. As it can be seen, two different types of curves were obtained Figure 6.35 (a) and (b). For WM200D and PM200D the determination of the characteristic temperatures could be done by means of tanδ due to a clear transition was observed. Onset temperature corresponded with the maximum value of tanδ, T_p was the temperature associated to the change of the slope and T_f with temperature associated to a stabilization of tanδ values, Figure 6.35 (b). T_o varied between 131.5 and 137.8°C and T_f from 152.7 and 156°C for WM200D and PM200D doughs, respectively.

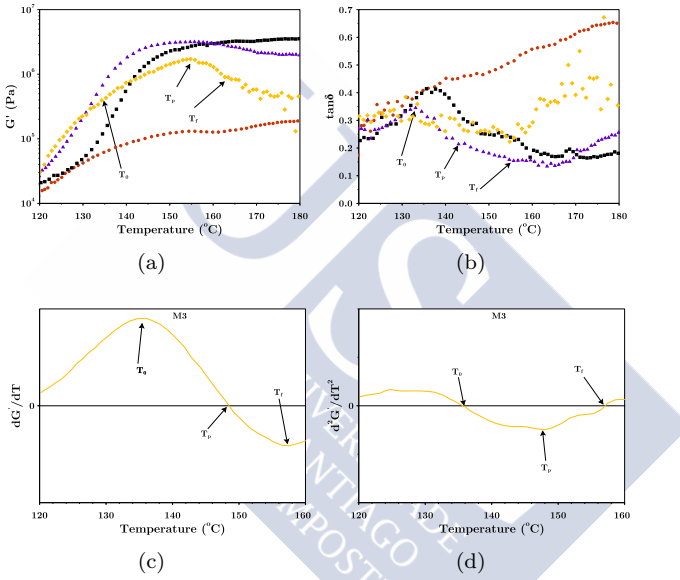

Figure 6.35 DMTA rheograms ((a) and (b)) for yellow (YM, ♦), white (WM, ■), purple (PM, ▲) maize and chestnut (CTD, ●) flour doughs and correspond to dG$'$/dT (c) and d^{2}G$'$/dT^2 (d) curves for YM200D.

In the case of YM200D and CTD doughs no M3 peak was observed in tanδ. This result can be related to lower hydration levels of both doughs. However, the characteristic temperatures of M3 transition for these kind of doughs could be determined by means of G$'$. T_o and T_f were determined by the corresponding inflexion points of the G$'$(T) (Figure 6.35 (d)) whilst T_p was calculated as the relative maximum of G$'$(T) (6.35 (c)). M3 peaks determined by DMTA are broader than those obtained by DSC due to the associated structural changes and rearrangements of the transitions take place in an extensive range of temperatures.

Table 6.50 Onset (T_o), peak (T_p) and final (T_1) of M3 thermal starch transitions determined by DMTA following the elastic modulus ($G^{'}$) and the damping factor (tanδ).♣

Transition			YM200D	WM200D	PM200D	CTD
M3	T_o (°C)	$G^{'}$	136.6±0.8	-	-	141.8±3.5
		tanδ	-	131.5±3.1	137.8±3.1	-
	T_p (°C)	$G^{'}$	146.1±2.6	-	-	154.5±0.6
		tanδ	-	139.1±1.6	145.2±1.5	-
	T_1 (°C)	$G^{'}$	156.2±0.5	-	-	157.0±0.4
		tanδ	-	152.7±2.9	156.0±1.4	-

♣ Yellow (YM), white (WM) and purple (PM) maize flour doughs and chestnut (CH) flour doughs. Data value with different letters in rows are significantly different, P≤ 0.05.

6.7.3.2 Determination Protocol of Characteristic Temperatures of Thermal Transitions by DMTA

Table 6.51 Determination protocol of Onset (T_o), peak (T_p) and final (T_f) characteristic temperatures of thermal transitions employing DMTA data following the elastic modulus ($G^{'}$) and the damping factor (tanδ) for tested maize and chestnut flour doughs.♣

		G transition	**Figure**
$T_0^{'}$	–	Minimum of $G^{'}(T)$	Figure 6.33 (a)
T_0	–	Inflexion point of $G^{'}(T)$	Figure 6.33 (a)
T_p	–	Local maximum of $G^{'}(T)$	Figure 6.33 (a)
T_f	–	Inflexion point of $G^{'}(T)$	Figure 6.33 (a)
		M1 transition	**Figure**
T_0	–	Local maximum of $d^2G^{'}/dT^2$ *vs* T	Figure 6.33 (d)
T_f	–	Inflexion point of $G^{'}(T)$	Figure 6.33 (d)
		M2 transition	**Figure**
T_0	–	Local minimum of $dG^{'}/dT$ *vs* T	Figure 6.34 (b)
T_p	–	Minimum of $G^{'}(T)$	Figure 6.34 (a)
T_f	–	Inflexion point of $G^{'}(T)$	Figure 6.34 (a)
		M3 transition	**Figure**
T_0	–	Inflexion point of $G^{'}(T)$	Figure 6.35 (d)
		Maximum of tanδ(T)	Figure 6.35 (b)
T_p	–	Local maximum of $G^{'}(T)$	Figure 6.35 (c)
		Slope change of tanδ(T)	Figure 6.35 (b)
T_f	–	Inflexion point of $G^{'}(T)$	Figure 6.35 (d)
		Slope change of tanδ(T)	Figure 6.35 (b)

6.7.3.3 Seaweed-enriched flour doughs based on chestnut flour

The thermal transitions of seaweed-enriched doughs of this Thesis were evaluated employing the protocol previously developed to carry out the analysis of characteristic temperatures of thermal transitions on gluten-free flour doughs by DMTA, Table 6.51.

Evolution of storage modulus (G') and damping factor tanδ of seaweed-enriched chestnut doughs with temperature are presented in Figure 6.37. As it can be seen, these curves presented a similar shape of those obtained for gluten-free doughs based on chestnut flours. Analysing G' and tanδ behaviour with increasing temperature all transitions previously mentioned could have been obtained for doughs enriched with *Ascophyllum nodosum*, *Bifurcaria bifurcata* and *Fucus vesiculosus* seaweed powders, Tables 6.52, 6.53 and 6.54, respectively.

Table 6.52 Onset (T_o), peak (T_p) and final (T_f) temperatures of thermal starch transitions determined by DMTA following the elastic modulus (G') for chestnut flour doughs enriched with *Ascophyllum nodosum* seaweed powders.♣

		CTSGD	CAN03D	CAN06D	CAN09D
WA	(%, f.b.)	56.4±0.8^{d}	58.3±0.6^{c}	63.2±0.3^{b}	68.7±0.5^{a}
G	T'_0(°C)	60.2±1.0^{a}	59.0±0.9^{a}	61.4±0.1^{a}	62.5±1.5^{a}
	T_0 (°C)	71.5±0.3^{a}	70.7±0.1^{a}	70.3±0.2^{a}	69.9±0.7^{a}
	T_p (°C)	75.2±0.3^{a}	74.7±0.2^{a,b}	73.7±0.4^{b,c}	72.6±0.1^{a}
	T_f (°C)	79.1±0.4^{a}	78.1±0.1^{a,b}	77.4±0.5^{b}	76.9±0.1^{b}
M1	T_0 (°C)	81.6±0.2^{a}	80.5±0.2^{b}	79.7±0.3^{b,c}	79.0±0.1^{c}
	T_p (°C)	86.0±0.8^{a}	84.4±0.6^{a,b}	83.0±0.6^{b}	82.4±0.3^{b}
	T_f (°C)	93.8±0.7^{c}	94.3±0.2^{b,c}	98.3±1.6^{a,b}	101.2±0.5^{a}
M2	T_0 (°C)	118.1±0.4^{a}	105.9±0.2^{b}	105.7±0.4^{b}a	105.8±0.4^{b}
	T_p (°C)	121.8±0.5^{a}	110.5±0.8^{b}	110.2±0.4^{b}	112.1±0.1^{b}
	T_f (°C)	125.1±0.5^{a}	122.0±1.8^{b}	122.8±0.4^{b}	125.8±1.1^{a}
M3	T_0 (°C)	135.4±1.4^{a}	137.3±3.2^{a}	134.4±1.9^{a}	135.0±0.2^{a}
	T_p (°C)	146.0±0.2^{a}	149.7±1.7^{a}	146.9±2.0^{a}	142.76±1.5^{a}
	T_f (°C)	160.0±0.1^{a}	159.2±1.2^{a}	153.3±0.4^{a}	156.1±1.8^{a}

♣Data value with different letters in rows are significantly different, P≤ 0.05.

Regarding gelatinization process (G + M1 transition), both G and M1 transitions could have been determined separately. Even in the case of control dough (CTSGD), although CTD dough previously analysed aslo based on chestnut flour showed only one transition G+M1. This difference could be due to the addition of GG that could interact with water limiting it to starch and hence leading to some crystallites of amilopectin to be melt at higher

temperatures (M1 transition determined separately).

Concerning G transition, it was observed that no significant differences existed on the corresponding temperature of the beginning of swelling of starch granules (T_0'). This fact seems to indicate that, although larger WA values were necessary to obtain doughs with similar consistency when seaweed powders were added (Table 6.28), the water availability to starch granules present in chestnut flours was the same in all assayed doughs. In other words, the additional amount of water added to obtain the dough when adding seaweed powders seems to interact directly with seaweed powder particles and not to starch present in flour favouring the swelling of these particles at lower temperatures.

Table 6.53 Onset (T_o), peak (T_p) and final (T_f) temperatures of thermal starch transitions determined by DMTA following the elastic modulus (G') for chestnut flour doughs enriched with *Bifurcaria bifurcata* seaweed powders.♣

		CTSGD	CBB03D	CBB06D	CBB09D
WA	(%, f.b.)	56.4 ± 0.8^{d}	62.4 ± 0.7^{c}	67.5 ± 1.3^{b}	70.4 ± 1.0^{a}
G	$\mathbf{T}_0'$ (°C)	60.2 ± 1.0^{a}	60.9 ± 0.1^{a}	58.2 ± 0.2^{a}	59.6 ± 0.1^{a}
	$\mathbf{T}_0$ (°C)	71.5 ± 0.3^{a}	71.5 ± 0.3^{a}	$69.9\pm0.7^{a,b}$	69.3 ± 0.1^{b}
	$\mathbf{T}_p$ (°C)	75.2 ± 0.3^{a}	75.1 ± 0.1^{a}	72.9 ± 0.3^{b}	72.5 ± 0.1^{b}
	$\mathbf{T}_f$ (°C)	79.1 ± 0.4^{a}	79.2 ± 0.8^{a}	$77.1\pm0.4^{a,b}$	76.0 ± 0.4^{b}
M1	$\mathbf{T}_0$ (°C)	81.6 ± 0.2^{a}	81.3 ± 0.8^{a}	$79.2\pm0.4^{a,b}$	78.7 ± 0.6^{c}
	$\mathbf{T}_p$ (°C)	86.0 ± 0.8^{a}	84.8 ± 0.4^{a}	82.3 ± 0.4^{b}	82.5 ± 0.1^{b}
	$\mathbf{T}_f$ (°C)	93.8 ± 0.7^{a}	94.5 ± 0.8^{a}	95.1 ± 2.3^{a}	94.9 ± 0.1^{a}
M2	$\mathbf{T}_0$ (°C)	118.1 ± 0.4^{a}	106.6 ± 2.4^{b}	105.3 ± 0.5^{b}	105.5 ± 1.6^{b}
	$\mathbf{T}_p$ (°C)	121.8 ± 0.5^{a}	112.6 ± 0.3^{b}	109.8 ± 1.0^{b}	110.6 ± 0.8^{b}
	$\mathbf{T}_f$ (°C)	125.1 ± 0.5^{a}	122.9 ± 0.3^{b}	120.8 ± 0.6^{b}	120.4 ± 0.5^{b}
M3	$\mathbf{T}_0$ (°C)	135.4 ± 1.4^{a}	136.1 ± 2.3^{a}	135.4 ± 3.1^{a}	137.7 ± 0.6^{a}
	$\mathbf{T}_p$ (°C)	146.0 ± 0.2^{a}	145.7 ± 2.1^{a}	145.6 ± 0.5^{a}	147.8 ± 0.3^{a}
	$\mathbf{T}_f$ (°C)	160.0 ± 0.1^{a}	158.5 ± 0.1^{a}	159.2 ± 0.6^{a}	159.5 ± 1.1^{a}

♣Data value with different letters in rows are significantly different, P≤ 0.05.

On the other hand, the corresponding temperature of disintegration of the starch granules and starchy polymers melting (T_0) seems to be slightly influenced by seaweed powder addition in the case of doughs enriched with BB35P. Seaweed powder addition ≥ 6% significantly decreased T_0 values. A similar behaviour was observed in the case of T_p and T_f for all studied seaweed-enriched doughs. This behaviour could be due to larger WA absorption of these doughs. Due to swelling there is an increase in turgor of starch granules that could lead to a higher pressure against the hydrated seaweed particles. This fact, together with the increasing temperature could favour a water leach on seaweed particles and consequently a

large quantity of available water in dough matrix that could facilitate the thermal process associated to melting of starch granules and hence lead to a decrease on the characteristic temperatures values. In fact, it was observed that the effect of WA on T_p values of seaweed-enriched chestnut flour doughs is the same of those observed for chestnut starch dispersions at different hydration levels by Moreira *et al.* (2013b). In Figure 6.36 can be observed the same relationship between WA increase and T_p decrease for seaweed-enriched chestnut flour doughs and chestnut starch dispersions. This lead to the conclusion that seaweed powder addition only modified physical process of starch swelling in doughs, avoiding the well known decrease of T_0' with increasing WA due to the high WRC of added particles.

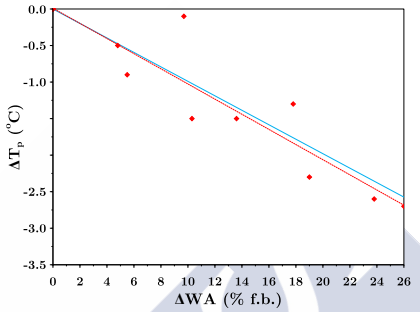

Figure 6.36 Relationship between WA increase and T_p decrease for seaweed-enriched chestnut flour doughs (♦) and chestnut starch dispersions (—, (Moreira *et al.*, 2013b)).

In the case of M1 transition, defined as the process where melting of the remaining amylopectin crystallites occurred (Shogren, 1992), it was observed that seaweed powder addition significantly reduced T_0 values for all studied doughs. In all cases, T_0 decreased from ≈86°C for control dough to ≈79°C being the main difference that for CAN and CBB doughs it was necessary to obtain this behaviour addition levels ≥ 6% of seaweed powder and for CFV doughs only ≥ 3%. A similar trend was observed in the case of T_p whilst T_f did not significantly varied for doughs enriched with BB35P and FV35P and it was increased from 93.8 to 101.2°C in the case of doughs enriched with AN35P. The differences on T_0 and T_p could be attributed, as previously explained, to a larger quantity of available water on seaweed-enriched doughs due to an increase of pressure of starch granules against seaweed particles and a water loss of these particles due to heating. The different trends observed as function of the employed seaweed powder could be explained by means of their physical properties. T_0 and T_0 of FV35P-enriched doughs were more influenced due to the higher particle size of these particles which made the steric effect of starch granules against seaweed particles more important. In the case of BB35P-enriched doughs, the higher

WRC of these doughs could led to a delay on this effect whilst in the case of AN35P-enriched dough, the steric effect would be less important due to the lower particle size of AN35P compared to FV35P.

Table 6.54 Onset (T_o), peak (T_p) and final (T_f) temperatures of thermal starch transitions determined by DMTA following the elastic modulus ($G^{'}$) for chestnut flour doughs enriched with *Fucus vesiculosus* seaweed powders.♣

		CTSGD	CFV03D	CFV06D	CFV09D
WA	(%, f.b.)	56.4 ± 0.8^{c}	58.9 ± 0.7^{b}	60.5 ± 1.0^{b}	64.0 ± 0.5^{a}
G	$\mathbf{T}_0'$ (°C)	60.2 ± 1.0^{a}	58.2 ± 0.3^{a}	58.4 ± 0.4^{a}	61.2 ± 0.9^{a}
	$\mathbf{T}_0$ (°C)	71.5 ± 0.3^{a}	70.8 ± 0.8^{a}	70.8 ± 0.2^{a}	70.4 ± 0.4^{a}
	$\mathbf{T}_p$ (°C)	75.2 ± 0.3^{a}	$74.3\pm0.4^{a,b}$	73.7 ± 0.1^{b}	73.9 ± 0.1^{b}
	$\mathbf{T}_f$ (°C)	79.1 ± 0.4^{a}	77.7 ± 0.1^{b}	77.3 ± 0.1^{b}	77.6 ± 0.1^{b}
M1	$\mathbf{T}_0$ (°C)	81.6 ± 0.2^{a}	79.8 ± 0.1^{b}	79.4 ± 0.1^{b}	79.9 ± 0.3^{b}
	$\mathbf{T}_p$ (°C)	86.0 ± 0.8^{a}	83.7 ± 0.3^{b}	83.4 ± 0.3^{b}	83.4 ± 0.1^{b}
	$\mathbf{T}_f$ (°C)	93.8 ± 0.7^{a}	97.1 ± 0.9^{a}	95.9 ± 0.6^{a}	95.3 ± 1.6^{a}
M2	$\mathbf{T}_0$ (°C)	118.1 ± 0.4^{a}	106.2 ± 1.2^{b}	105.0 ± 2.0^{b}	106.4 ± 0.4^{b}
	$\mathbf{T}_p$ (°C)	121.8 ± 0.5^{a}	110.7 ± 0.8^{b}	111.0 ± 0.4^{b}	110.6 ± 1.7^{b}
	$\mathbf{T}_f$ (°C)	125.1 ± 0.5^{a}	125.2 ± 0.8^{a}	121.2 ± 0.8^{a}	122.9 ± 0.7^{a}
M3	$\mathbf{T}_0$ (°C)	135.4 ± 1.4^{a}	136.2 ± 0.4^{a}	139.8 ± 0.5^{a}	134.3 ± 0.5^{a}
	$\mathbf{T}_p$ (°C)	146.0 ± 0.2^{a}	146.8 ± 3.3^{a}	147.5 ± 3.1^{a}	151.9 ± 1.1^{a}
	$\mathbf{T}_f$ (°C)	160.0 ± 0.1^{a}	158.9 ± 0.8^{a}	158.1 ± 0.1^{a}	158.9 ± 1.2^{a}

♣Data value with different letters in rows are significantly different, $P \leq 0.05$.

M2 transition was observed in all flour doughs. This transition corresponds to the melting of amylose-lipid complexes. It varied between 105 to 125°C and the begining of this process was signicantly advanced by seaweed powder addition in doughs, probably due to the larger WA of these dough compared to control. As previously reported by Gómez-Ordóñez *et al.* (2010), brown seaweeds have a relevant percentage of lipids which could led to expect that some interactions between seaweed-lipids and amylose of flour could occur. However, the fact that this transition ends at the same temperature for all assayed seaweeds, seems to indicate that these interactions did not take place, probably due to the high insolubility of seaweed particles (>80%). The temperature range observed was similar of those previosly reported in literature (Biliaderis *et al.* (1986); Jovanovich & Añón (1999)).

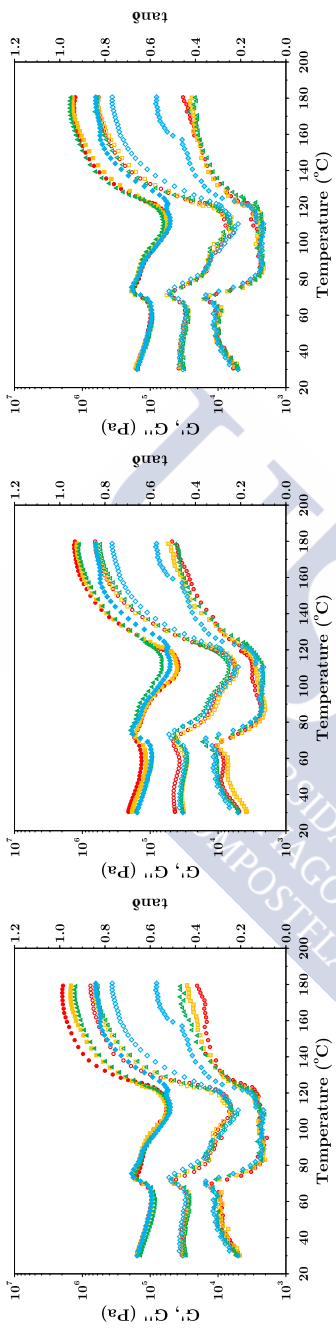

Figure 6.37 DMTA rheograms of chestnut flour doughs (◇) and chestnut flour doughs enriched with *Ascophyllum nodosum* (a), *Bifurcaria bifurcata* (b) and *Fucus vesiculosus* (c) seaweed powders at different levels: 3% (△), 6% (□) and 9% (○). G′ (solid symbol), G″ (emphy symbols) and tanδ (doted symbols).

Finally, M3 defined as melting of amylose polymers was also determined for all assayed doughs. The temperature range varied from 134 to 160°C, a typical range of temperatures to this transition, as previously reported by (Liu *et al.*, 2007). No significant differences were observed due to seaweed powder addition. Note here that this transition only depends on amylose and at these temperatures, the studied doughs presented low water content and hence no modifications on dough behaviour due to seaweed powder addition could be expected.

6.7.3.4 Seaweed-enriched pregelatinized chestnut flour doughs

Thermal profiles of storage modulus (G') and damping factor tanδ of pregelatinized seaweed-enriched chestnut flour doughs are presented in Figure 6.38. As it can be seen, these curves differ from those obtained for seaweed-enriched chestnut flour doughs analysed at C1. No transition associated to gelatinization (G) was observed. This confirmed that gelatinization of starch was carried out during mixing process applying the new protocol. Applying the same method of G' and tanδ evaluation previously explained different transition could be determined, Tables 6.55, 6.56 and 6.57, respectively.

Table 6.55 Onset (T_o), peak (T_p) and final (T_f) temperatures of thermal starch transitions determined by DMTA following the elastic modulus (G') and the damping factor (tanδ) for pregelatinized chestnut flour doughs enriched with *Ascophyllum nodosum* seaweed powders.♣

Transition			CTSGD	CAN03PD	CAN06PD	CAN09PD
M1	T_0	G'	87.7±0.6^a	81.7±0.4^b	82.6±1.1^b	83.7±0.2^b
	T_p	G'	92.4±0.6^a	92.9±0.7^a	93.0±0.3^a	92.0±0.5^a
	T_f	G'	95.0±1.3^a	97.9±0.2^a	98.5±2.3^a	97.8±3.3^a
New	T_0	G'	108.2±0.4^a	108.4±0.2^a	108.1±0.4^a	108.1±0.4^a
		tanδ	108.7±0.3^a	107.6±2.5^a	108.9±0.1^a	109.1±0.1^a
	T_p	G'	111.4±0.5^a	110.4±2.0^a	111.3±0.4^a	111.1±0.1^a
		tanδ	110.9±0.1^a	110.8±1.3^a	111.6±0.1^a	111.0±0.0^a
	T_f	G'	112.1±0.0^a	110.9±2.1^a	111.9±0.1^a	111.9±0.4^a
		tanδ	112.0±0.2^a	112.2±0.6^a	111.8±0.1^a	111.8±0.2^a
M2	T_0	G'	113.3±0.1^a	112.8±0.5^a	112.6±0.4^a	112.9±0.5^a
	T_p	G'	120.5±0.5^a	118.5±0.4^a	117.2±2.4^a	116.7±0.4^a
	T_f	G'	121.9±0.8	123.0±0.9	-	122.4±1.5
M3	T_0	G'	-	-	-	-
		tanδ	131.9±3.0	-	132.8±0.3	135.4±1.6
	T_p	G'	-	-	-	-
		tanδ	-	-	-	-
	T_f	G'	155.4±0.8	155.8±1.6	157.4±1.3	-
		tanδ	151.0±1.3^a	153.8±1.7^a	155.7±4.5^a	156.4±1.6^a

♣Data value with different letters in rows are significantly different, P≤ 0.05.

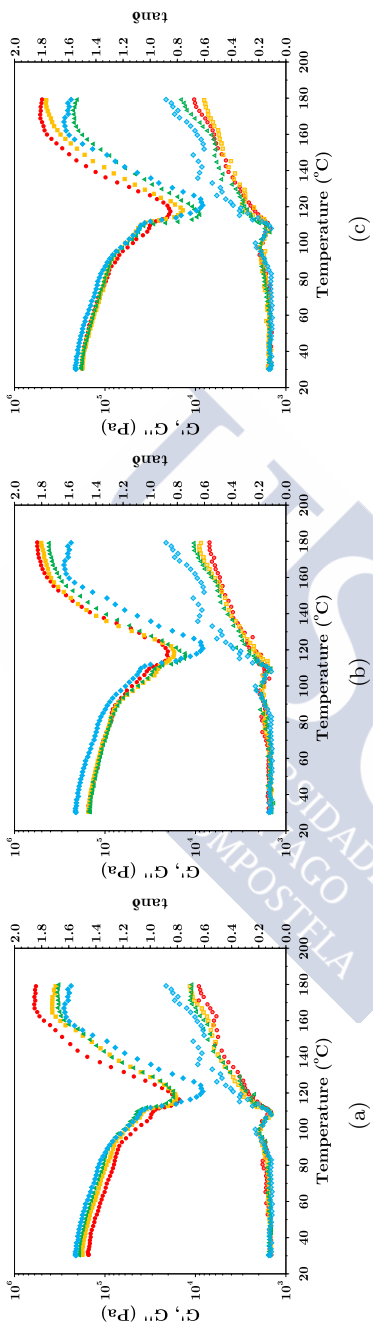

Figure 6.38 DMTA rheograms of chestnut flour doughs (◇) and chestnut flour doughs enriched with *Ascophyllum nodosum* (a), *Bifurcaria bifurcata* (b) and *Fucus vesiculosus* (c) seaweed powders at different levels: 3% (△), 6% (□) and 9% (○). G′ (solid symbol), G″ (emphy symbols) and tanδ (doted symbols).

Firstly, M1 was observed in all studied doughs indicating that although gelatinization of starch was mainly carried out during mixing step, some of amylopectin remained without melting. At higher temperatures (108-112°C) a new transition named as GT was observed. Finally, M2 (113-122°C) and M3 (124-158°C) were also observed in all studied doughs.

Table 6.56 Onset (T_o), peak (T_p) and final (T_f) temperatures of thermal starch transitions determined by DMTA following the elastic modulus (G') and the damping factor (tanδ) for pregelatinized chestnut flour doughs enriched with *Bifurcaria bifurcata* seaweed powders.♣

Transition			CTSGD	CBB03PD	CBB06PD	CBB09PD
M1	$\mathbf{T}_0$	G'	87.7±0.6^a	80.0±0.2^b	81.4±1.0^b	83.1±0.7^b
	$\mathbf{T}_p$	G'	92.4±0.6^a	92.3±1.0^a	90.2±2.7^a	88.0±1.1^a
	$\mathbf{T}_f$	G'	95.0±1.3^a	96.1±0.7^a	93.8±1.2^a	93.0±0.7^a
New	$\mathbf{T}_0$	G'	108.2±0.4^a	107.9±0.8^a	109.5±0.6^a	107.2±0.1^a
		tanδ	108.7±0.3^a	108.9±1.1^a	108.7±0.6^a	107.6±0.7^a
	$\mathbf{T}_p$	G'	111.4±0.5^a	110.9±0.2^a	111.0±0.1^a	110.7±0.0^a
		tanδ	110.9±0.1^a	111.1±1.6^a	110.6±0.6^a	110.6±0.1^a
	$\mathbf{T}_f$	G'	112.1±0.0^a	112.1±0.8^a	112.3±0.4^a	111.6±0.4^a
		tanδ	112.0±0.2^a	112.2±1.5^a	112.4±0.6^a	111.7±0.2^a
M2	$\mathbf{T}_0$	G'	113.3±0.0^a	113.3±1.1^a	113.8±0.5^a	113.2±0.1^a
	$\mathbf{T}_p$	G'	120.5±0.5^a	117.3±1.6^a	117.5±0.9^a	117.2±0.7^a
	$\mathbf{T}_f$	G'	121.9±0.8	122.6±86.6	-	119.9±1.1
M3	$\mathbf{T}_0$	G'	-	-	-	-
		tanδ	131.9±3.2^a	132.4±0.6^a	135.1±1.9^a	136.0±0.8^a
	$\mathbf{T}_p$	G'	-	-	-	-
		tanδ	-	-	-	-
	$\mathbf{T}_f$	G'	155.4±0.8^a	153.6±0.7^a	154.8±2.5^a	154.0±1.7^a
		tanδ	151.0±1.3^a	150.3±1.5^a	153.0±2.5^a	153.9±3.0^a

♣Data value with different letters in rows are significantly different, P≤ 0.05.

Concerning M1 transition, a significant decrease on T_0 was observed in the case of AN35P and BB35P-enriched doughs. This behaviour could be related to the higher initial WA of these doughs that resulted in higher hydration at the end of mixing process compared to CTSGPD and CFVPD, Table 6.43. This higher hydration levels of CANPD and CBBPD aid to come early the temperature of the beginning of amylopectin crystallites melting. Compared to doughs analysed at C1 it was observed, in general, a delay in the characteristic temperatures associated to this transition. This result could be due to lower hydration of doughs (Table 6.43) compared to doughs analysed at C1 (Table 6.28).

In the case of GT transition, it has to be noted that this transition was not determined separately from M2 transition when the analysis of non-pregelatinized doughs was done. Taking into account the characteristic temperatures values of

this transition (108-112°C) it could be related to the glass transition of guar gum added to doughs as previously reported in literature (Torres *et al.* (2013) and Kumar *et al.* (2015)) who reported characteristics temperature values for these transition between (96 and 115°C). The fact that this transition was not determined separately from M2 for non-pregelatinized doughs could be due to the high WA of these doughs. Once doughs reduced their hydration due to the application of the new protocol of mixing M2 was delayed to higher temperatures and hence GT could be determined.

Table 6.57 Onset (T_o), peak (T_p) and final (T_f) temperatures of thermal starch transitions determined by DMTA following the elastic modulus (G') and the damping factor (tanδ) for pregelatinized chestnut flour doughs enriched with *Fucus vesiculosus* seaweed powders.♣

Transition			CTSGPD	CFV03PD	CFV06PD	CFV09PD
M1	$\mathbf{T}_0$	G'	87.7±0.6^a	86.0±0.8^a	83.3±3.7^a	83.6±2.4^a
	$\mathbf{T}_p$	G'	92.4±0.6^a	91.2±2.1^a	92.1±0.9^a	92.2±0.9^a
	$\mathbf{T}_f$	G'	95.0±1.3^a	94.5±2.4^a	95.8±1.7^a	97.1±1.2^a
New	$\mathbf{T}_0$	G'	108.2±0.4^a	107.4±1.2^a	107.6±1.6^a	108.8±0.1^a
		tanδ	108.7±0.3^a	108.7±0.1^a	107.1±1.0^a	109.0±1.2^a
	$\mathbf{T}_p$	G'	111.4±0.5^a	110.3±0.8^a	110.8±1.3^a	111.9±0.1^a
		tanδ	110.9±0.1^a	111.1±0.4^a	112.1±0.1^a	111.0±0.5^a
	$\mathbf{T}_f$	G'	112.1±0.0^a	111.1±0.6^a	112.2±0.1^a	112.5±0.3^a
		tanδ	112.0±0.2^a	111.5±0.5^a	113.0±0.4^a	112.4±0.1^a
M2	$\mathbf{T}_0$	G'	113.3±0.0^a	111.8±0.4^a	112.9±0.1^a	113.6±0.7^a
	$\mathbf{T}_p$	G'	120.5±0.5^a	117.2±1.6^a	116.7±0.9^a	117.4±0.6^a
	$\mathbf{T}_f$	G'	121.9±0.8	119.4±1.4	-	120.8±1.3
M3	$\mathbf{T}_0$	G'	-	-	-	-
		tanδ	131.9±3.2^a	133.2±0.7^a	132.2±1.5^a	133.6±0.3^a
	$\mathbf{T}_p$	G'	-	-	-	-
		tanδ	-	-	-	-
	$\mathbf{T}_f$	G'	155.4±0.8^a	156.6±0.1^a	154.8±2.9^a	155.0±0.9^a
		tanδ	151.0±1.3^a	154.3±0.5^a	155.4±1.1^a	158.1±0.1^a

♣Data value with different letters in rows are significantly different, P≤ 0.05.

Finally, both amylose-lipids complex melting (M2) and amylose melting transition (M3) remained invariant with seaweed powder addition. Compared to non-pregelatinized doughs, the beginning of M2 seems to be delayed over ≈8°C from 105 to 113°C whilst final transition temperature (T_f) remained constant. In the case of M3, final transition temperature did not significantly varied ≈155°C *vs* ≈160°C . These results could be also related to a lower hydration of pregelatinized doughs compared to C1 doughs. It has been reported that initial WA could have an influence in these transition at higher temperatures (Liu *et al.*, 2006) indicating that lower initial WA could led to higher characteristics temperature values for these transitions as it would be happening in our case.

The section in tweets

- Thermal transitions of gluten-free flour doughs can be determined by both DSC and DMTA techniques.
- Gelatinization transition (G+M1) can be observed differently as function of WA of doughs.
- High WA resulted in a transition G+M1 determined jointly.
- Low WA resulted in determination of G and M1 determined separately.
- Seaweed powder addition does not significantly change the physical process of starch granules swelling.
- The melting of starch granules is enhanced by the water increase on dough matrix as consequence of seaweed powder addition.
- Seaweed powder addition does not modify thermal transitions associated to amylose-lipid complex and amylose melting.
- DMTA analysis of pregelatinized doughs confirms that gelatinization takes places during dough mixing employing the new protocol.
- A new transition (GT) related to guar gum glass transition is determined separately for pregelatinized doughs.
- M2 and M3 thermal transition of pregelatinized doughs are delayed as consequence of lower hydration of doughs.

6.8 Effect of storage time on chestnut flour doughs characteristics

The effect of storage time on chestnut flour doughs characteristics was assessed by means of mixing, rheological and thermomechanical assays. Chestnut flour doughs were analysed at 0, 6 and 12 months after flours manufacturing. Chestnut flours were stored at 4°C in vacuum sealed bags until assessment.

Nomenclature

Parameters

a''	–	Fitting parameter of SAOS data, Pa·s$^{-b''}$, Eq. (4.26).
a'	–	Fitting parameter of SAOS data, Pa·s$^{-b'}$, Eq. (4.25).
b''	–	Fitting parameter of SAOS data, Eq. (4.26).
b'	–	Fitting parameter of SAOS data, Eq. (4.25).
C1	–	Target consistency, N·m.
C2	–	Minimum torque achieved due to protein weakening, N·m.
C3	–	Maximum achieved due to starch gelatinization, N·m.
C4	–	Minimum torque achieved as consequence of enzymatic degradation, N·m.
C4/C3	–	Cooking stability, (-).
C5	–	Final dough consistency when applying complete curve protocol, N·m.
D_w	–	Mass mean diameter, Eq. (4.20).
DPT	–	Departure time, min.
DS	–	Damaged Starch, g damaged starch·(g dry flour)$^{-1}$.
DT	–	Development time, min.
G''	–	Loss modulus, Pa.
G'	–	Storage modulus, Pa.
J_{max}	–	Maximum creep compliance, Pa^{-1}, Eq. (4.28).
J_0	–	Instantaneous compliance, Pa^{-1}, Eq. (4.27).
J_m	–	Viscoelastic compliance of creep or recovery phase, Pa^{-1} Eqs. (4.27) and (4.28).
J_r	–	Recovery compliance, Pa^{-1}, Eq. (4.28).
J(t)	–	Compliance, Pa^{-1}, Eqs. (4.27) and (4.28).
LVER	–	Linear viscoelastic region.
MW	–	Mechanical weakening, N·m·min^{-1}.
SP	–	Swelling power, (mL·g d.s.$^{-1}$).
ST	–	Stability time, min.
T_{ig}	–	Initial gelatinization temperature, °C.
T_0	–	Onset transition temperature, °C.
T_0'	–	Temperature of beginning of starch granules swelling determined by DMTA, °C.
T_{fg}	–	Final gelatinization temperature, °C.
T_f	–	Final transition temperature, °C.
T_p	–	Peak transition temperature, °C.
tanδ	–	Damping factor.
TS	–	Total starch content, g starch·(g flour)$^{-1}$.
WA	–	Water absorption, % f.b..
WRC	–	Water retention capacity, g water·(g d.s.$^{-1}$).
α	–	Protein network weakening rate, N·m·min^{-1}.
β	–	Starch gelatinization rate, N·m·min^{-1}.
λ_c	–	Mean retardation time of creep phase, s, Eq. (4.27).
λ_r	–	Mean retardation time of recovery phase, s, Eq. (4.28).
η_0	–	Zero shear viscosity, Pa·s, Eq. (4.27).
η_c	–	Complex viscosity, Pa·s.
γ_c	–	Critical strain, %.
γ_e	–	Enzymatic degradation rate, N·m·min^{-1}.
ω	–	Angular frequency, s^{-1}.
σ	–	Shear stress, Pa.

6.8.1 Introduction

Chestnut is a seasonal nut that in 2014 was mainly produced in Asia (86.5% of total world production) and Europe (9.6%) (FAOSTAT, 2017). Regarding countries, China (82.0% of total world production), Bolivia (3.8%) and Turkey (3.1%) are the three main producers of chestnut fruit in the world. In this field, Spain is classified as 10^{th} chestnut producer in the world with 0.79%.

Chestnut contains relatively high amount of sugar (20–32%), starch (50–60%), dietary fiber (4–10%) and low amount of fat (2–4%). It has proved to be a rich source of high quality proteins with essential amino acids (4–7%) and also has some important of vitamins (vitamin E, vitamin B group), minerals (potassium, phosphorous, and magnesium) and phenolics (gallic and ellagic acid) (Demirkesen, 2016). This composition makes it a very interesting raw material to be used in gluten-free products development, suitable for people with coeliac disease.

In fact, in last years some works focused on the study of chestnut flour doughs behaviour (Moreira *et al.*, 2013b) or baked chestnut products such as cookies (Demirkesen, 2016), gluten-free bread (Paciulli *et al.*, 2016), snacks (Sacchetti *et al.*, 2004) obtained from chestnut flours have been carried out which confirms its suitability to be used at industrial scale. The main disadvantage of using chestnut is the seasonal character of this fruit that only can be collected few months of the year, which impairs the production of chestnut derived products to be commercialized over the whole year. This fact highlights that studies on the storage process to preserve chestnut flour properties to supply the market over the year until the new chestnut harvesting arrives are necessary.

Some studies assessed the effect of storage conditions on technological properties of flours. In example, Zarzycki & Sobota (2015) studied the effect of storage of wheat flour at -20, 4 and 20°C during 6 weeks on viscosity of wheat flour gruels and reported an increase on this parameter with no influence of storage temperature. Kim *et al.* (2017) carried out an study evaluating consumer acceptance of cookies made from whole flour of immature wheat (WFIW) stored at different temperatures (0-45°C) and reported that consumers prefer cookies made with WFIW stored at relatively low temperature (0-25°C). However, no studies on effect of chestnut flour storage on their technological aptitudes had been carried out, up to our knowledge.

In this context, the main aim of this work is to study the effect of storage time of chestnut flour at controlled conditions (4°C, vacuum) on its chemical properties and mixing, rheological and thermomechanical behaviour of their doughs in order to determine the suitability of these conditions.

6.8.2 Mixing properties

Chestnut flour doughs mixing parameters are presented in Table 6.59. Moreover, experimental data are presented on Figure 6.39. As it can be seen, no significant differences were obtained when employing chestnut flours previously storage during 6 (II) or 12 (III) months compared to chestnut flours that were analysed once the chestnut flour was obtained after milling dried chestnuts (I). Additionally, thermal behaviour could not have been measured for the studied doughs as previously explained in Section 6.5.

Table 6.59 Mixing curves parameters of chestnut flour doughs at different storage times (I: 0, II: 6 and III: 12 months) obtained in Mixolab® apparatus.♣

Dough	I	II	III
WA (%, f.b.)	52.8 ± 1.2^a	50.7 ± 0.6^a	51.0 ± 0.1^a
C1 (N·m)	1.11 ± 0.02^a	1.10 ± 0.04^a	1.08 ± 0.03^a
DT (min)	0.40 ± 0.01^a	0.41 ± 0.01^a	0.43 ± 0.02^a
DPT (min)	0.60 ± 0.05^a	0.68 ± 0.04^a	0.60 ± 0.09^a
ST (min)	0.28 ± 0.05^a	0.34 ± 0.05^a	0.25 ± 0.11^a
MW (N·m)	0.61 ± 0.03^a	0.56 ± 0.03^a	0.53 ± 0.03^a

♣Data are presented as means±standard deviation. Data value of each parameter with different superscript letters in rows are significantly different ($P\leq 0.05$).

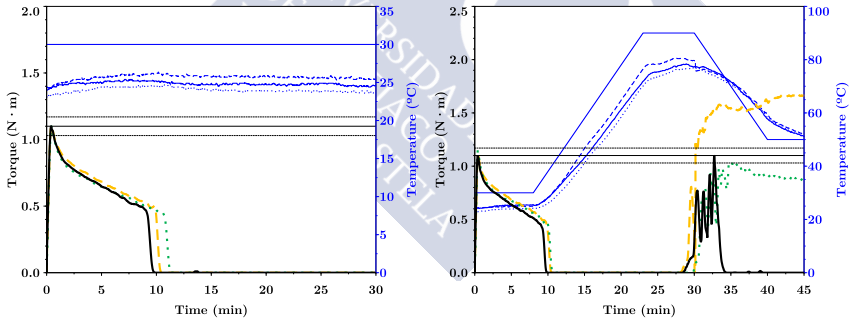

Figure 6.39 Mixolab® simple (a) and complete (b) curves for chesnut flour dough at 0 (—), 6 (···) and 12 (- - -)) months of storage at 4°C in vacuum-sealed plastis bags. Blue lines correspond to bowl (-·-·-) and dough temperatures.

These absence of significant differences on mixing properties of dough during 1 year of storage could be related to chestnut flour composition did not significantly

varied in the tested period. As it can observed in Table 6.60, no significant differences existed on total starch (TS) and damaged starch (DS) of flours at different storage times. As previously mentioned, DS is a key parameter which determines gluten-free doughs behaviour due to it clearly influences WA of doughs. In this case, the fact that DS content was invariant over the period of time tested led to the same WA value for all studied doughs to obtain the same consistency. Moreover, the others parameters (DT, DPT, ST and MW) also related to interactions between flours compounds (*i.e* proteins, fibre, etc) and water did not significantly varied over the tested period of time indicating that flour doughs behaviour was the same.

Table 6.60 Mixing curves parameters of chestnut flour doughs at different storage times (I: 0, II: 6 and III: 12 months) obtained in Mixolab® apparatus.♣

Dough	I	II	III
TS (g starch·(g flour)$^{-1}$)	54.9±6.9^a	50.1±4.3^a	49.6±4.9^a
DS (g damaged starch·(g flour)$^{-1}$)	6.2±1.3^a	5.8±1.3^a	5.8±1.4^a

♣Data are presented as means±standard deviation. Data value of each parameter with different superscript letters in rows are significantly different (P≤ 0.05).

From a point of view based on mixing operation these results led to the conclusion that chestnut flour can be used from 0 to 12 months of storage at 4°C in vacuum sealed bags without impairing mixing properties of doughs.

6.8.3 Rheological properties

Rheological properties of chestnut flour doughs obtained from chestnut flour storage at 4°C at different times was determined by means of Small Amplitude Oscillatory Shear (SAOS) and Creep and Recovery tests.

Table 6.61 presents the parameters of oscillatory shear modelling, Eqs. (4.25) and (4.26). As it can be seen obtained doughs presented a dominant elastic character ($a' > a''$). This trend was maintained over the whole angular frequency tested range as it can also observed in Figure 6.40.

Regarding the effect of storage time on chestnut flour doughs it was clearly observed that no significant differences existed between doughs obtained at 0, 6 and 12 months of storage. This trend is also in accordance with the behaviour obtained of these doughs during mixing where it was observed no significant changes neither.

In the case of creep and recovery parameters, Table 6.62, the same trend

Table 6.61 Parameters of oscillatory shear modelling, Eqs. (4.25) and (4.26), of chestnut flour doughs at different storage times (I: 0, II: 6 and III: 12 months).♣

	Parameter	CTDI	CTDII	CTDIII
G′	$\mathbf{a'{\cdot}10^{-3}}$ (Pa·s$^{-b''}$)	139.4±1.3^a	147.7±3.9^a	146.3±1.5^a
	$\mathbf{b'{\cdot}10^{3}}$	60.1±6.9^a	55.9±3.1^a	64.8±0.9^a
	$\mathbf{R^2}$	0.988	0.990	0.996
G″	$\mathbf{a''{\cdot}10^{-3}}$ (Pa·s$^{-b''}$)	18.3±0.3^a	19.2±1.0^a	21.0±0.3^a
	$\mathbf{b''{\cdot}10^{3}}$	108.2±4.0^a	112.1±15.5^a	95.5±0.5^a
	$\mathbf{R^2}$	0.858	0.888	0.817

♣Data are presented as means±standard deviation. Data value of each parameter with different superscript letters in rows are significantly different (P≤ 0.05).

was observed. No significant differences existed on doughs viscoelastic behaviour as function of storage time of chestnut flour. All studied chestnut flour doughs presented similar parameter values of creep and recovery phase modelling, Eq. (4.27) and Eq. (4.28), respectively.

Table 6.62 Parameters of creep (Eq. (4.27)) and recovery (Eq. (4.28)) phase modelling of chestnut flour doughs at different storage times (I: 0, II: 6 and III: 12 months).♣

	Parameter	CTDI	CTDII	CTDIII
Creep	$\mathbf{J_0{\cdot}10^{6}}$ (Pa^{-1})	8.2±0.1^a	7.7±0.3^a	8.8±1.2^a
	$\mathbf{J_m{\cdot}10^{6}}$ (Pa^{-1})	4.8±0.1^a	5.8±0.6^a	4.7±0.7^a
	λ_c (s)	6.2±1.0^{a,b}	8.6±0.6^a	5.4±0.3^b
	$\eta_0{\cdot}\mathbf{10^{-6}}$ (Pa·s)	8.1±0.7^a	6.7±0.1^a	7.0±0.6^a
	$\mathbf{R^2}$	0.985	0.991	0.985
Recovery	$\mathbf{J_{max}{\cdot}10^{6}}$ (Pa^{-1})	18.2±0.3^a	20.9±1.1^a	19.7±1.1^a
	$\mathbf{J_0{\cdot}10^{6}}$ (Pa^{-1})	8.2±0.1^a	7.7±0.3^a	8.8±1.2^a
	$\mathbf{J_m{\cdot}10^{6}}$ (Pa^{-1})	5.4±0.4^a	7.1±0.7^a	6.2±0.8^a
	λ_r (s)	44.1±9.6^a	35.4±5.2^a	42.1±4.3^a
	$\mathbf{J_r/J_{max}}$ (%)	74.8±3.1^a	71.0±1.2^a	75.6±5.9^a
	$\mathbf{R^2}$	0.941	0.972	0.955

♣Data are presented as means±standard deviation. Data value of each parameter with different superscript letters in rows are significantly different (P≤ 0.05).

It has to be noted that both SAOS and creep and recovery parameter values are in the same range of those observed for maize flour doughs previously reported in this Thesis (See Section 6.6 or other gluten-free doughs (Lazaridou *et al.*, 2007).

These results confirmed not only that chestnut flour doughs rheological properties were invariant throughout a period of time of one year but also that

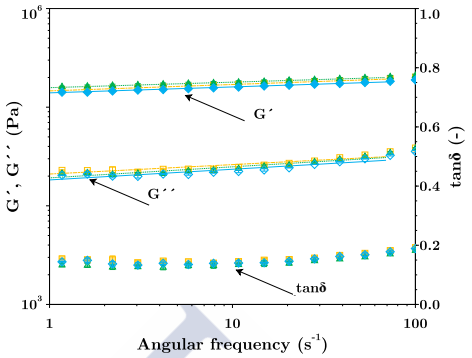

Figure 6.40 Experimental data of $G^{'}$ (filled markers), G'' (empty markers) and tanδ (dot filled markers) at 30°C of chestnut flour doughs at different storage times (0 (◇), 6 (△) and 12 (□) months). Lines correspond to Eqs. (4.25) and (4.26).

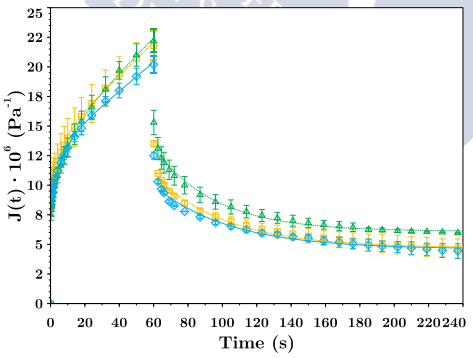

Figure 6.41 Experimental creep and recovery data at 30°C of chestnut flour doughs at different storage times (0 (◇), 6 (△) and 12 (□) months). Lines correspond to Eqs. (4.27) and (4.28).

their properties are similar of those observed for other gluten-free doughs such as maize, rice, etc.

6.8.4 Thermomechanical properties

Thermal transitions of chestnut flour doughs were determined by DMTA technique employing the same method previously mentioned in Section 6.7. As it can be seen in Table 6.63, all thermal transitions G, M1, M2 and M3 could be determined. Moreover, G' and tanδ variations with temperature can be also observed in Figure 6.42.

Table 6.63 Onset (T_o), peak (T_p) and final (T_f) temperatures (°C) of thermal starch transitions determined by DMTA following the elastic modulus (G') for chestnut flour doughs at different storage times (I: 0, II: 6 and III: 12 months).♣

Transition		CTDI	CTDII	CTDIII
G	$\mathbf{T}'_0$	64.4±4.4^a	61.8±0.7^a	68.5±0.5^a
	$\mathbf{T}_0$	74.4±0.7^a	74.3±0.7^a	75.6±0.4^a
	$\mathbf{T}_p$	77.5±0.4^a	77.7±0.7^a	78.4±0.1^a
	$\mathbf{T}_f$	79.8±0.5^a	80.7±0.4^a	81.1±0.5^a
M1	$\mathbf{T}_0$	82.7±1.2^a	84.1±0.6^a	85.1±0.7^a
	$\mathbf{T}_p$	87.5±1.3^a	88.0±0.5^a	89.1±2.0^a
	$\mathbf{T}_f$	94.4±0.2^a	95.5±1.1^a	94.4±0.5^a
M2	$\mathbf{T}_0$	112.4±2.0^a	110.7±2.6^a	112.0±1.1^a
	$\mathbf{T}_p$	117.4±1.0^a	118.5±0.4^a	118.3±0.8^a
	$\mathbf{T}_f$	121.3±1.6^a	122.1±0.4^a	121.6±0.8^a
M3	$\mathbf{T}_0$	126.9±0.7^a	126.2±0.5^a	125.2±0.1^a
	$\mathbf{T}_p$	136.4±0.5^a	136.3±0.1^a	134.6±1.9^a
	$\mathbf{T}_f$	153.1±0.2^a	153.5±1.0^a	152.6±0.6^a

♣Data are presented as means±standard deviation. Data value of each parameter with different superscript letters in rows are significantly different ($P \leq 0.05$).

Non significant differences were observed in thermal transitions of doughs during heating indicating the suitability of the employed conditions for storage. Gelatinization transition carried out from 62°C up to 81°C, amylopectin crystallites melting was also observed between 82.7 and 95.5°C, amylose-lipid complex melting from 110.7 to 122.1 and amylose melting from 125.2 up to 153.5°C. All transitions were observed into their typical range tempearture values (Donovan (1979), Liu *et al.* (2006)).

Following the same behaviour as previously explained in mixing and rheological

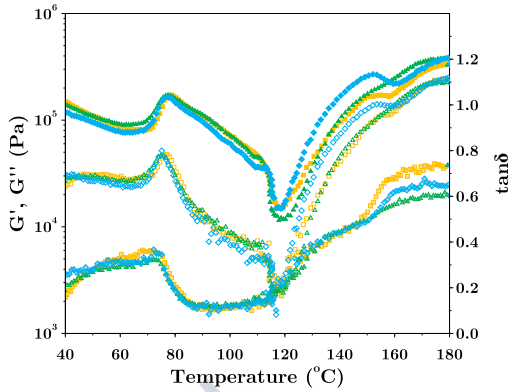

Figure 6.42 DMTA rheograms data of G′ (filled markers), G″ (empty markers) and tanδ (dot filled markers) at 30°C of chestnut flour doughs at different storage times (0 (◇), 6 (△) and 12 (□) months).

properties, the invariant thermal transitions on chestnut flour doughs storage at different times observed by DMTA confirmed, once again, the suitability of the employed storage conditions.

The section in tweets

- Mixing, rheological and thermomechanical properties of chestnut flour doughs remained invariant during 12 months after chestnut flour manufacturing.
- No changes on starch characteristics of chestnut flour exist during the studied period.
- No significant differences on doughs technological properties confirms the suitability of the employed storage conditions (4°C and vacuum).
- Results shows that chestnut flours can be storage for a period of 1 year.

6.9 Physico-Chemical Properties of Seaweed-Enriched Chestnut Flour Cookies

The textural and colorimetric properties as well as the antioxidant activity and polyphenols content of the cookies obtained after the baking of pregelatinized doughs at 180°C for 25 min were determined in order to evaluate the effect of the seaweed addition. Additionally, colorimetric properties, antioxidant activity and polyphenols content of flour blends previous to baking were also determined in order to evaluate the effect of baking process in these properties by comparison with those obtained for baked cookies.[8]

[8]This section was adapted from the following paper in writing process:
MOREIRA, R., CHENLO, F., SINEIRO, J., TORRES, M. D. & ARUFE, S. (2017). Physico-Chemichal Properties of seaweed-enriched chestnut flour cookies obtained from pregelatinized doughs. To be submitted to: *Journal of Texture studies*.

Nomenclature

Powders

AN35P	–	*Ascophyllum nodosum* (AN) powder obtained from AN35.
BB35P	–	*Bifurcaria bifurcata* (BB) powder obtained from BB35.
FV35P	–	*Fucus vesiculosus* (FV) powder obtained from FV35.

Doughs

CAN0XB	–	Chestnut flour blend with X% f.b. of AN35P.
CBB0XB	–	Chestnut flour blend with X% f.b. of BB35P.
CTSGB	–	Chestnut flour blend with 1.8% f.b. of sodium chloride and 2% f.b. of GG.
CFV0XB	–	Chestnut flour blend with X% f.b. of FV35P.
CAN0XBE	–	Chestnut flour blend extract with X% f.b. of AN35P.
CBB0XBE	–	Chestnut flour blend extract with X% f.b. of BB35P.
CTSGBE	–	Chestnut flour blend with 1.8% f.b. of sodium chloride and 2% f.b. of GG.
CFV0XBE	–	Chestnut flour blend extract with X% f.b. of FV35P.
CAN0XC	–	Chestnut flour cookie with X% f.b. of AN35P.
CBB0XC	–	Chestnut flour cookie with X% f.b. of BB35P.
CTSGC	–	Chestnut flour cookie with 1.8% f.b. of sodium chloride and 2% f.b. of GG.
CFV0XC	–	Chestnut flour cookie with X% f.b. of FV35P.
CAN0XCE	–	Chestnut flour extract with X% f.b. of AN35P.
CBB0XCE	–	Chestnut flour extract with X% f.b. of BB35P.
CCTSGCE	–	Chestnut flour extract with 1.8% f.b. of sodium chloride and 2% f.b. of GG.
CFV0XCE	–	Chestnut flour extract with X% f.b. of FV35P.

Parameters

SA	–	Antioxidant activity, %.
TP_w	–	Total polyphenols content (TP), (mg PHL·(g dry powder)$^{-1}$).
TP_s	–	Total polyphenols content (TP), (mg PHL·(g dry solids)$^{-1}$).
WA	–	Water absorption, % f.b..
WRC	–	Water retention capacity, g water·g dry solid^{-1}.

6.9.1 Introduction

Chestnut flour employed as basis of gluten-free baked products development can be a very interesting raw material due to its lack of gluten and its health and nutritional benefits (Demirkesen, 2016). However, precisely this absence of gluten, that could aid the dough to retain the gas generated during fermentation process in order to increase its volume, made this flour non suitable to be employed as the only source to obtain bread, the most commonly consumed baked product. Some studies addressed the obtaining of gluten-free breads from flour blends where chestnut flour is added at different ratios (Paciulli *et al.* (2016) and Demirkesen *et al.* (2010)) but reported that elevated levels of chestnut flour led to some deterioration in quality parameters (volume, texture and colour) of these products.

Taking into account these characteristics, a good alternative of use for chestnut flour can be as source to develop gluten-free cookies due the lower requirements of gas retention of this type of products. In fact, Demirkesen (2016) has already assessed the formulation of gluten-free cookies based on chestnut/rice flour blends and their rheological and quality characteristics and reported that using 40% of chestnut flour replacement significantly enhanced sensory properties of the cookie samples. In this Thesis, it has been studied the effects of brown seaweed powder addition as source of antioxidant compounds, on gluten-free doughs based on chestnut flour with regards to their mixing, rheological and thermomechanical properties. It was observed that, i.e., mixing parameters of seaweed-enriched doughs were enhanced respect to chestnut flour doughs employed as control. Taking this into account, it seems interesting the determination of the final properties of the product: antioxidant activity, polyphenols content, colour or texture of a baked product based on the previously studied formulations.

Several studies reported the effect of addition of some compounds on physicochemical properties of cookies. For example, Krystyjan *et al.* (2015) studied the effect of bee pollen addition on chemical properties of wheat cookies, reporting an increase on its antioxidant properties. Kaur *et al.* (2015) addressed the effect of the incorporation of several gums on physicochemical and sensory properties of gluten-free biscuits, prepared from buckwheat flour. Inglett *et al.* (2015) studied the physical properties of gluten-free sugar cookies made from amaranth-oat composites. Žilić *et al.* (2016) analysed the effects of baking conditions and dough formulations on phenolic compounds stability, antioxidant capacity and colour of cookies made from anthocyanin-rich corn flour. However, no studies have been carried out based on chestnut flour cookies enrichment with brown seaweed powders, up to our knowledge.

Taking into account all previously mentioned, the main aim of this work is to

study the effect of baking operation on antioxidant properties of gluten-free cookies based on chestnut flour and seaweed-enriched chestnut flour blends. Moreover, the effect of seaweed powder addition on texture properties of seaweed-enriched chestnut cookies will be assessed.

6.9.2 Antioxidant properties of flour blends

Acetone/water extracts from blends of chestnut flour enriched with AN35P, BB35P and FV35P were analysed by means of Total polyphenolic content (TP_w, TP_S) and Scavenging Activity (SA), Table 6.65 and Figure 6.43.

Table 6.65 Total polyphenolic (TP) and scavenging activity (SA) of acetone:water (70:30) extracts of chestnut flour enriched with AN35P, BB35P and FV35P.♣

Flour blend extract	TP_w	TP_s	SA
CTSGBE	155 ± 16^{d}	755 ± 77^{d}	16.9 ± 3.1^{c}
CAN03BE	282 ± 14^{c}	1389 ± 69^{c}	24.7 ± 2.8^{c}
CAN06BE	472 ± 39^{b}	2235 ± 182^{b}	39.9 ± 4.7^{a}
CAN09BE	622 ± 34^{a}	2804 ± 154^{a}	48.6 ± 2.9^{a}
CBB03BE	206 ± 20^{c}	927 ± 89^{c}	18.5 ± 5.0^{c}
CBB06BE	320 ± 7^{b}	1461 ± 34^{b}	30.8 ± 2.5^{b}
CBB09BE	419 ± 15^{a}	1803 ± 65^{a}	43.8 ± 1.1^{a}
CFV03BE	188 ± 6^{d}	867 ± 26^{d}	$16.0\pm2,2^{c}$
CFV06BE	249 ± 34^{b}	1164 ± 157^{b}	33.0 ± 7.4^{a}
CFV09BE	386 ± 14^{a}	1664 ± 60^{a}	37.9 ± 7.5^{a}

TP_w is referred to raw powder (mg PHL/100 g dry powder), TP_s is referred to total solids content in the extract (mg PHL/100 g dry solids) and SA as % of total inhibition after 1 hour.

♣Data are presented as means±standard deviation. Data value of each parameter with different superscript letters in columns (for each seaweed compared to control) are significantly different ($P\leq 0.05$).

Seaweed powder addition significantly increased TP of flour blends. AN35P addition signified the largest increase in TP, followed by BB35P and FV35P. Specifically for each seaweed, for AN35P and BB35P addition and addition of 3% significantly increased TP whilst for FV35P addition a minimum of addition of 6% is necessary to increase TP.

A minimum of 6% was needed in order to increase SA of flour blends extract for all seaweed powders. However, two different behaviours were observed. For AN35P and FV35P SA was not increased significantly when adding larger contents than 6% whereas in the case of BB35P, an addition of 9% significantly increased SA compared to an addition of 6%.

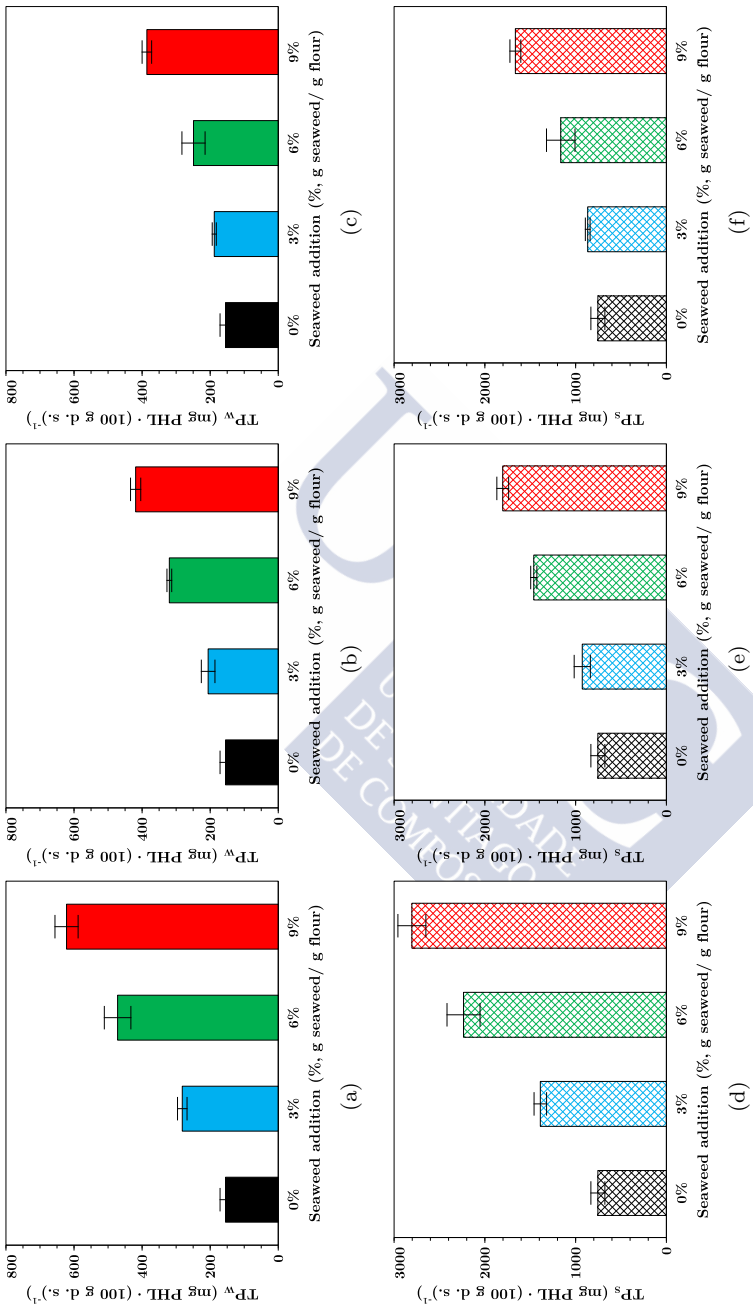

Figure 6.43 Total polyphenols content (TP) of acetone:water extracts of chestnut flour enriched at different levels (0%, 3% (■), 6% (■) and 9% (■), g seaweed·(g chestnut flour)$^{-1}$ with *Ascophyllum nodosum* (a, d), *Bifurcaria bifurcata* (b, e) and *Fucus vesiculosus* (c, f) powders formerly dried at 35°C.

In this context, based on SA results it can be said that the optimum value of seaweed addition before baking is 6% for chestnut flour blends enriched with AN35P and FV35P and 9% for BB35P. It is worth mentioning that, regarding SA values, the largest SA values were obtained for flour blends enriched with AN35P, followed by BB35P and FV35P. This was in accordance with the previously reported in Section 6.4 where AN35P extracts showed the highest antioxidant activity (Table 6.24).

In Figure 6.44 it can be seen the relationship between TP and SA for the analysed flour blends. A linear relationship was obtained between SA and both TP_w and TP_s. This fact seems to indicate that antioxidant activity of flour blends is mainly related to their TP. A similar relationship between TP and SA was already reported in Section 6.4 of this Thesis for the aqueous extracts of the studied seaweeds and also in other authors' publications for green and red seaweeds (Matanjun *et al.*, 2008). This seems to indicate that once seaweed powders are added to chestnut flours the SA of chestnut flour blends are mainly defined by the antioxidant capacity of seaweed powder added and not to the chestnut flour antioxidant properties.

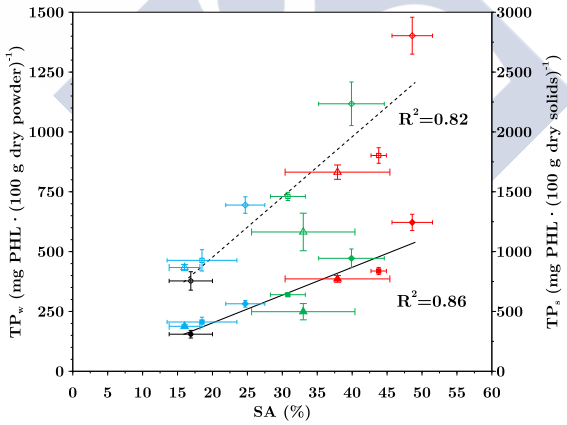

Figure 6.44 Relationship between Total polyphenolic content (TP) and scavenging activity (SA) of acetone:water (70:30) extracts of chestnut flour enriched at different levels (0%, 3% (■), 6% (■) and 9% (■) f.b. with AN35P, BB35P and FV35P. TP_w (filled symbols) and TP_s (empty symbols).

6.9.3 Antioxidant properties of baked cookies

Total polyphenolic content (TP) and Scavenging activity (SA) of cookies extracts are shown in Table 6.66 and Figure 6.45.

Table 6.66 Total polyphenolic (TP) and scavenging activity (SA) of acetone:water (70:30) extracts of chestnut cookies enriched with with AN35P, BB35P and FV35P.♣

Cookie extract	TP_w	TP_s	TP_{wgae}	SA
CTSGE	876 ± 71^{a}	3025 ± 239^{a}	1.722 ± 0.109^{a}	75.9 ± 5.1^{a}
CAN03CE	926 ± 94^{a}	3024 ± 308^{a}	1.791 ± 0.183^{a}	76.0 ± 0.7^{a}
CAN06CE	601 ± 113^{b}	1699 ± 318^{b}	1.162 ± 0.218^{b}	52.8 ± 3.4^{b}
CAN09CE	430 ± 34^{c}	1154 ± 91^{c}	0.831 ± 0.066^{c}	43.8 ± 1.7^{b}
CBB03CE	$769\pm68^{a,b}$	1124 ± 99^{c}	$1.486\pm0.131^{a,b}$	72.8 ± 1.8^{a}
CBB06CE	716 ± 78^{b}	2536 ± 276^{b}	1.385 ± 0.151^{b}	68.5 ± 2.1^{a}
CBB09CE	646 ± 57^{b}	3175 ± 278^{a}	1.248 ± 0.109^{b}	70.6 ± 2.8^{a}
CFV03CE	$740\pm85^{a,b}$	$1752\pm201^{b,c}$	$1.431\pm0.164^{a,b}$	71.0 ± 1.4^{a}
CFV06CE	672 ± 79^{b}	1375 ± 162^{c}	1.299 ± 0.153^{b}	70.3 ± 5.4^{a}
CFV09CE	$746\pm63^{a,b}$	1800 ± 151^{b}	$1.442\pm0.121^{a,b}$	68.0 ± 2.7^{a}

TP_w is referred to raw powder (mg PHL/100 g dry powder) and TP_wgae (mg GAE/g dry powder), TP_s is referred to total solids content in the extract (mg PHL/100 g dry solids) and SA as % of total inhibition after 1 hour.

♣Data are presented as means±standard deviation. Data value of each parameter with different superscript letters in columns (for each seaweed compared to control) are significantly different ($P \leq 0.05$).

Compared to flour blends from which cookies were obtained, TP and SA values increased after baking, except in the case of CAN09C. The increase of SA induced by baking is explained by the Maillard's reactions that take place during this operation, because control samples have shown a significantly hihger SA values compared to the same samples before baking. The action of baking process has been previously reported. Žilić *et al.* (2016) reported an increase on TP due to baking process. As they clearly explained, baking process increased content of TP compounds by affecting the solubility of bound forms of phenolic acids. Moreover, certain Maillard reaction products are Folin-Ciocalteu reactive substances thus increasing the total phenolic compounds measured by Folin-Ciocalteu assay. These Maillard reaction products are also responsible of the increase of SA of baked products compared to flour blends. Lindenmeier & Hofmann (2004) and Şensoy *et al.* (2006) already reported that these products are responsible of increase on antioxidant activity of bakery products.

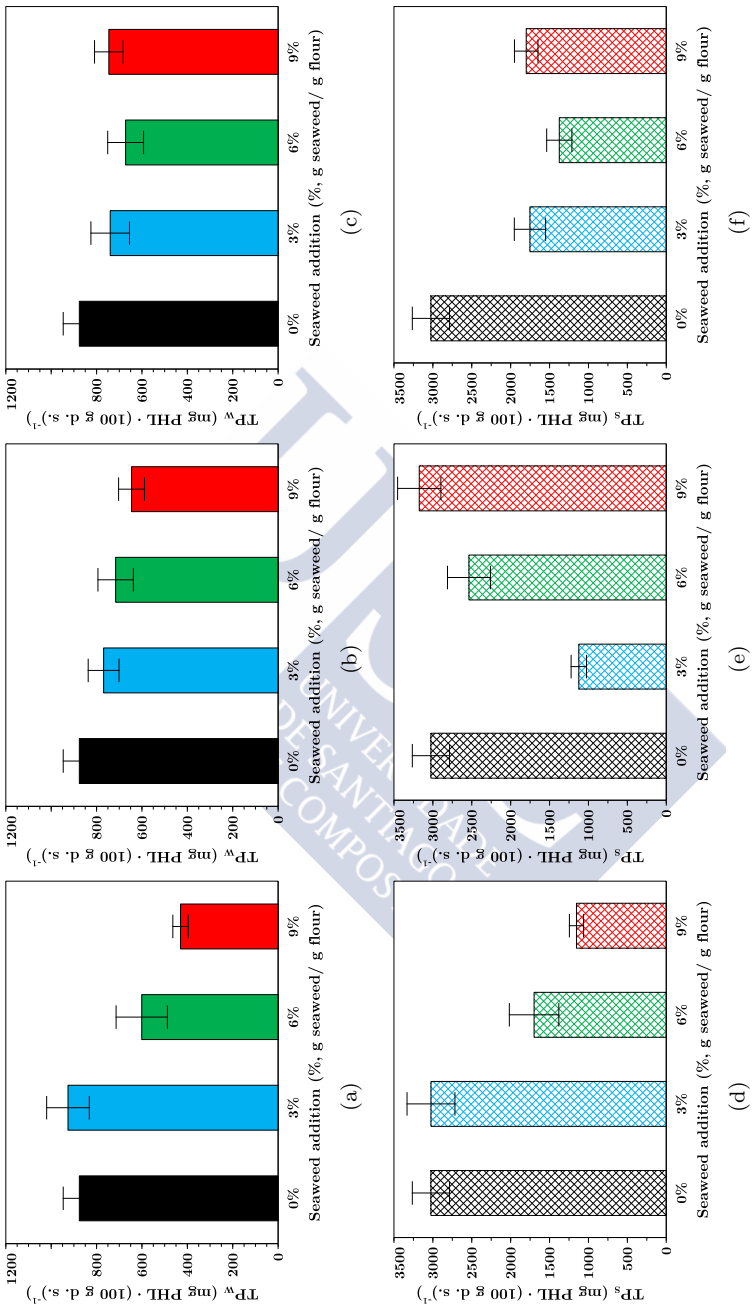

Figure 6.45 Total polyphenols content (TP) of acetone:water extracts of chestnut cookies enriched with powdered seaweeds at different levels (0%, 3% (■), 6% (■) and 9% (■), g seaweed·(g chestnut flour)$^{-1}$. *Ascophyllum nodosum* (a, d), *Bifurcaria bifurcata* (b, e) and *Fucus vesiculosus* (c, f) powders formerly dried at 35°C.

Regarding the effect of seaweed addition on TP, in general it decreased TP values of cookies in comparison with control. This behaviour is the opposite of that obtained for seaweed-enriched flour blends, where seaweed powder addition significantly increased TP content. This difference may be due to the formation of Maillard reaction products, as it was previously explained. Yeo & Shibamoto (1991) reported that moisture content is a key parameter that determines the browning intensity. The lower the moisture content, the higher the intensity of browning. Control cookies had higher TP values due to their WA values are lower compared to other doughs.Moreover they have no seaweed particles that could aid to retain some water during baking. Although during baking higher temperatures are achieved and water is evaporated in all doughs, having lower WA could led to lower water content for longer periods of time during baking thus favouring the generation of these type of reaction products compared to seaweed-enriched cookies. As it could be observed at intermediate temperatures for pregelatinized doughs (Table 6.43) seaweed-enriched doughs had higher water content.

In order to facilitate the comparison with other studies in literature, TP content was also reported as gallic acid equivalents/ g dry solid. As it can be seen, the values varied between 0.831 and 1.791 mg GAE/g dry powder with a similar trend observed for TP_w. Compared to other works, seaweed enriched cookies presented higher polyphenols content than rice cookies and gluten-free rice and buckwheat cookies ($\approx$ 1.0 mg GAE/g dry powder, Sakac *et al.* (2015)), wheat flour cookies (not detected, (Jan *et al.*, 2016)). Similar values than those reported by Žilić *et al.* (2016) (1.8 mg GAE/g dry powder) for dark red corn based cookies and lower than blue corn cookies Žilić *et al.* (2016) and *Chenopodium* flour based cookies (Jan *et al.*, 2016) ($\approx$ 3.0 mg GAE/g dry powder). This led to the conclusion that seaweed-enriched chestnut cookies can be considered as cookies with high polyphenols content with regards to other commercial gluten-free and non gluten-free cookies.

For SA, two different trends were observed. For chestnut cookies enriched with BB35P and FV35P, non significant effect of addition was observed on SA values. Moreover, it has to be noted that in this case the previously mentioned relationship of SA *vs* TP was not observed, Figure 6.46. This leads to the conclusion that the SA value achieved by these cookies after baking was mainly due to compounds related to seaweed powder generated during baking not measured as TP and not to Maillard reaction products. However, in the case of chestnut cookies enriched with *Ascophyllum nodosum*, seaweed addition significantly decreased SA and the aforementioned relationship of SA with TP remained after baking, indicating that, for this seaweed, powder addition >3% significantly worsen antioxidant characteristics of cookies.

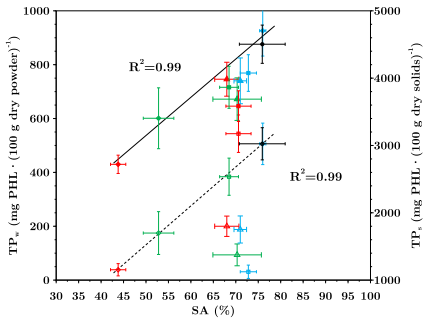

Figure 6.46 Relationship between TP and SA of acetone:water (70:30) extracts of chestnut cookies enriched at different levels (0%, 3% (■), 6% (■) and 9% (■)f.b. with AN35P, BB35P and FV35P. TP_w (filled symbols) and TP_s (empty symbols).

6.9.4 Colour properties of cookies

Colour parameters values of seaweed-enriched chestnut flour blends and cookies are showed in Tables 6.67 and 6.68 respectively and in Figure 6.47.

The addition of seaweed powders significantly modified colour parameters values of cookies doughs before baking. It reduced their brightness (L*), more pronounced in the case of FV35P. Their green colour (a*) and yellow colour (b*) predominance was significantly increased in all cases due to the large green and yellow colour predominance of seaweed powders added, Tables 6.17, 6.18 and 6.19.

Table 6.67. Colour parameters of seaweed-enriched chestnut flour doughs.♣

Dough	L*	a*	b*	ΔE^*
CTSGC	54.68±0.95^a	7.62±0.16^a	17.76±0.27^c	-
CAN03C	51.76±1.16^b	4.64±0.20^b	21.70±0.44^b	5.74
CAN06C	48.61±0.77^c	2.84±0.18^c	23.99±0.57^a	9.92
CAN09C	47.55±1.49^c	1.82±0.22^d	24.56±0.89^a	11.43
CBB03C	49.30±0.94^b	3.93±0.10^b	22.62±0.35^a	8.14
CBB06C	44.52±0.74^c	2.77±0.16^c	22.52±0.55^a	12.23
CBB09C	40.73±1.03^d	2.37±0.17^d	21.28±0.79^b	15.31
CFV03C	46.50±1.11^b	3.42±0.25^b	21.65±0.52^a	9.98
CFV06C	42.25±0.60^c	2.21±0.08^c	22.23±0.36^a	14.27
CFV09C	39.38±0.98^d	1.51±0.11^d	20.53±0.49^b	16.71

♣Data are presented as means±standard deviation. Data value of each parameter with different superscript letters in columns (for each parameter compared to control) are significantly different (P≤ 0.05).

After baking, in general a* decreased and b* increased with seaweed powder addition, the same trend of cookies doughs previously to baking process, although this effect was less pronounced. The effect of seaweed powder addition on brightness of baked cookies was the opposite of those observed for non-baked cookies. In general, brightness of seaweed-enriched cookies was larger than control cookies. This fact could be due to the larger periods of time with high water content of seaweed-enriched doughs during baking as consequence of their higher WA and the WRC of seaweed particles which led to a less degradation of some components during baking resulting in cookies with larger values of L*.

In both cases, before and after baking, seaweed-enriched cookies showed a colour difference that could be clasiffied as very distinct (>3.5, Adekunte *et al.* (2010)), indicating that colour of cookies was significantly changed due to seaweed powder addition.

Table 6.68 Colour parameters values of chestnut cookies, enriched with AN35P, BB35P and FV35P, after baking.♣

Cookie	L*	a*	b*	ΔE^*
CCTSGC	$38.19\pm3.01^{b,c}$	14.12 ± 0.24^{a}	28.37 ± 2.28^{a}	-
CAN03C	36.35 ± 2.61^{c}	12.25 ± 0.30^{a}	25.26 ± 2.29^{b}	4.07
CAN06C	46.59 ± 1.95^{a}	8.35 ± 1.91^{b}	29.65 ± 0.69^{a}	10.28
CAN09C	42.00 ± 2.74^{b}	8.96 ± 1.07^{b}	28.63 ± 1.12^{a}	6.43
CBB03C	45.24 ± 2.70^{a}	10.87 ± 2.01^{b}	30.93 ± 1.38^{a}	8.17
CBB06C	44.58 ± 1.05^{a}	8.23 ± 1.56^{c}	29.09 ± 0.80^{a}	8.78
CBB09C	$42.09\pm1.44^{a,b}$	6.13 ± 0.67^{c}	27.48 ± 0.74^{a}	8.94
CFV03C	45.89 ± 2.57^{a}	$9.70\pm1.45^{b,c}$	31.20 ± 1.02^{a}	9.32
CFV06C	43.86 ± 1.99^{a}	7.84 ± 1.49^{c}	30.23 ± 0.95^{a}	8.67
CFV09C	36.53 ± 3.84^{b}	9.93 ± 0.51^{b}	24.24 ± 3.71^{b}	6.17

♣Data are presented as means±standard deviation. Data value of each parameter with different superscript letters in columns (for each parameter compared to control) are significantly different ($P\leq 0.05$).

The baking operation significantly modified colour characteristics. Before baking process seaweed-enriched chestnut doughs presented larger values of L* and lower values of a* and b* compared to baked cookies. This represents doughs with larger brightness, greenness and blueness. After baking, cookies presented in general lower L* and higher a* and b*. This is an usual trend of CIE parameters during browning proceeds (Romani *et al.*, 2009). Moreover, it has to be noted that baking process reduced colour differences of seaweed-enriched cookies compared to control. In general, ΔE^* values were lower for baked cookies compared to cookies dough before baking. This fact, can be considered as a positive effect on cookies colour. Figure 6.48 shows images of obtained cookies as example.

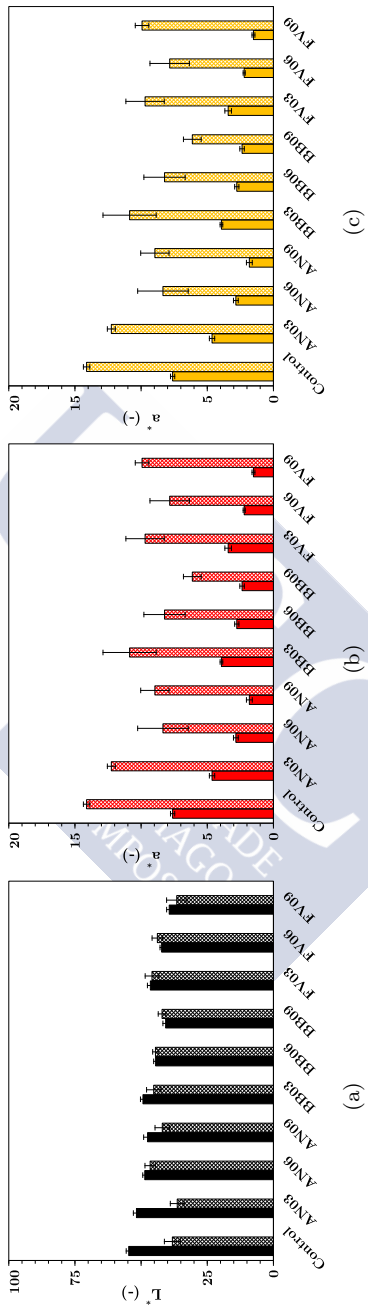

Figure 6.47. Colour parameter values of seaweed enriched chestnut cookies before (■) and after baking (☒).

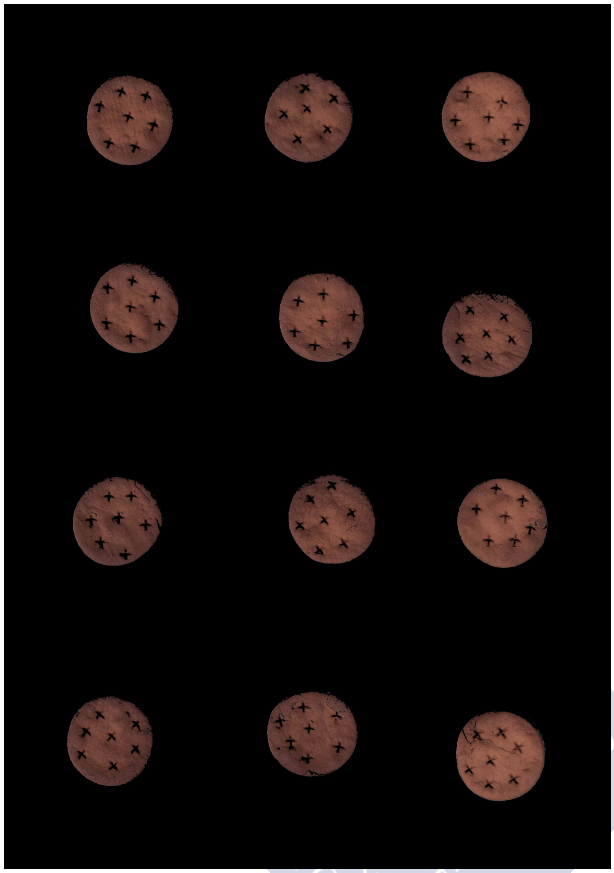

(a)

Figure 6.48. Images of cookies based on chestnut flour.

Compared to literature, the obtained cookies had lower values of L^* and higher values of a^* parameters compared to cookies based on rice flour (Mancebo *et al.*, 2016). However, colour parameter values were similar of those obtained by Šaponjac *et al.* (2016) for wheat flour based cookies incorporated with sour cherry pomace extract encapsulated in whey and soy proteins, Chauhan *et al.* (2015) for gluten-free cookies made from raw and germinated amaranth (*Amaranthus spp.*) and wheat flour cookies employed as control and Gerzhova *et al.* (2016) for gluten-free cookies of rice-buckwheat flour blends incorporated with canola proteins. These results led to the conclusion that with regards to cookies colour the obtained values for seaweed-enriched chestnut cookies could be acceptable.

6.9.5 Effect of seaweed powder addition on textural properties of cookies

Hardness of seaweed-enriched chestnut cookies are shown in Table 6.69. It was necessary and addition of seaweed powder >6% to significantly increase cookie hardness, except in the case of CBBC where an addition of 6% already caused a significant change. Mamat *et al.* (2014) also reported and increase in hardness due to seaweed powder addition, in this case on bread crumb. As the authors explained, this effect could be attributed to the thickening of the walls surrounding gas cells due to a higher water content of breads with higher amounts of seaweed powder that could promotes starch re-crystallization. In our case, a similar effect of that presented by Mamat *et al.* (2014) could be happening due to, as it was reported in Section 6.5, seaweed enriched doughs presented significantly higher WA.

Table 6.69 Hardness of chestnut cookies enriched with *Ascophyllum nodosum*, *Bifurcaria bifurcata* and *Fucus vesiculosus* seaweed powders previously dried at 35°C.♣

Cookie	**Hardness** (g)	**Young modulus** (Pa)
CCTSGC	8116 ± 1139^{b}	$83.4\pm12.3^{a,b}$
CAN03C	$8738\pm1206^{a,b}$	64.1 ± 8.3^{c}
CAN06C	$8906\pm1069^{a,b}$	$73.6\pm13.5^{a,b}$
CAN09C	9392 ± 427^{a}	$75.1\pm17.3^{a,b}$
CBB03C	$9137\pm615^{a,b}$	$75.1\pm14.7^{a,b}$
CBB06C	9294 ± 560^{a}	$77.7\pm9.8^{a,b}$
CBB09C	9882 ± 921^{a}	85.0 ± 6.5^{a}
CFV03C	$8332\pm777^{a,b}$	$81.2\pm12.2^{a,b}$
CFV06C	$9047\pm789^{a,b}$	$74.1\pm11.5^{a,b}$
CFV09C	9479 ± 1121^{a}	$80.2\pm9.8^{a,b}$

♣Data are presented as means±standard deviation. Data value of each parameter with different superscript letters in columns (for each parameter compared to control) are significantly different ($P\leq 0.05$).

The comparison of texture data with literature works is troublesome due to the different accessories employed for hardness determination. Seaweed-enriches chestnut cookies showed higher hardness than gluten-free cookies based on buckwheat flour and carboxymethyl cellulose (Hadnadev *et al.*, 2013), Indian water chestnut flour added with whey protein concentrate and potato starch (Sarabhai & Prabhasankar, 2015), buckwheat flour added with transglutaminase (Altindag *et al.*, 2015) and cookies based on rice flour, maize starch and pea protein (Mancebo *et al.*, 2016). However, they were in the same range reported for wheat flour cookies enriched with dried *Tinospora* leaf powder (Sharma

et al., 2013) and cookies based on fine-grained maize,coarse-grained maize, buckwheat and teff flours (Mancebo *et al.*, 2015).

In addition, linear relationships ($R^2 > 0.77$) between Young's modulus and rheological parameters such as zero shear viscosity η_0 and maximum creep compliance (J_{max}) of doughs was found, Figure 6.49. As it can be seen, the higher the η_0 the higher the Young's modulus of cookie. Demirkesen (2016) reported for gluten-free cookies based on chestnut/rice flour blends that very high viscosity of chestnut cookie dough prevented air incorporation on dough matrix during the mixing and resulted in hard texture. On the other hand, the higher the J_{max} of dough, the lower the Young's modulus of cookie. This seems to indicate that doughs with higher capacity to deformation result in cookie with lower Young's modulus after baking. These correlations can be useful because they can be employed to estimate the differences on cookies texture (Young's modulus) only by measuring the viscoelastic properties of the corresponding doughs without the evaluation of dough through thermal processes.

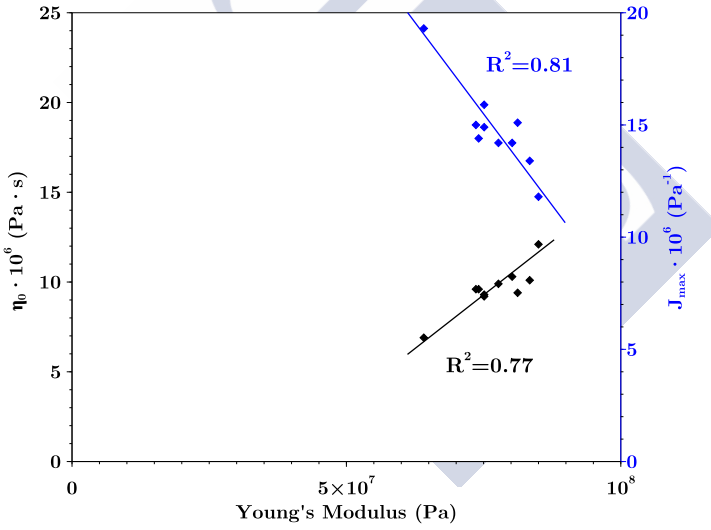

Figure 6.49. Relationship between Young's modulus of cookie and η_0 and J_{max} of doughs.

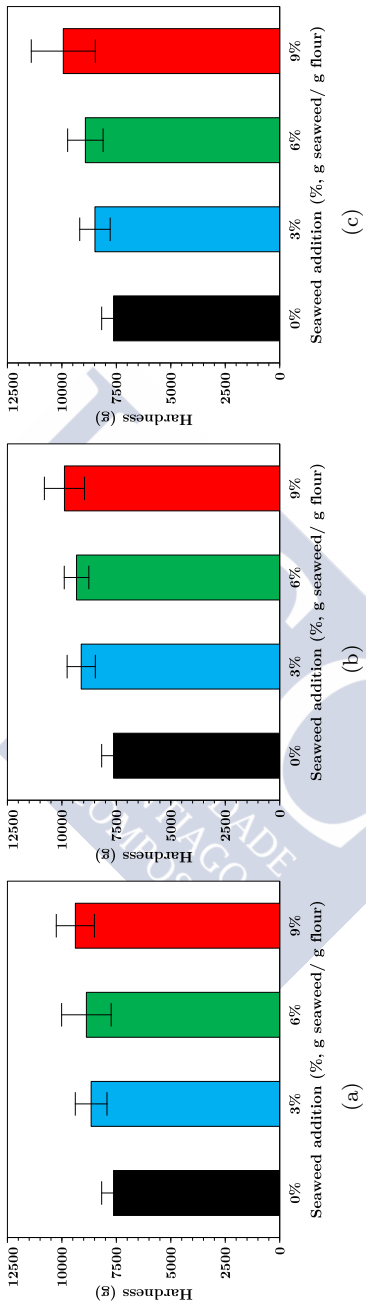

Figure 6.50 Hardness of chestnut cookies enriched with *Ascophyllum nodosum* (a), *Bifurcaria bifurcata* (b) and *Fucus vesiculosus* (c) seaweed powders previously dried at 35°C.

The section in tweets

- The optimum value of seaweed addition before baking is 9% for chestnut flour blends enriched with AN35P and FV35P and 6% for BB35P.
- In general, TP and SA of baked cookies increased compared to flour blends analysed before baking.
- Seaweed powder addition decreased TP values of baked cookies compared to control due to they impair Maillar's reaction products formation.
- BB35P and FV35P-enriched cookies have similar SA of control with lower TP contents.
- Seaweed powder addition significantly increases green colour of cookies.
- Baking process reduces L^* and increases a^* and b^* parameters of cookies due to browning proceeds.
- Baking process reduces colour differences of seaweed-enriched cookies compared to control.
- Young's modulus of cookies is directly related to η_0 and J_{max} of doughs obtained after mixing at 30°C.

6.10 Effect of Brown Seaweed Powder on Physical and Textural Properties of Wheat Bread

This study addresses the effect of *Fucus vesiculosus* seaweed powder addition up to 8% (flour basis, f.b.) on wheat flour dough and bread properties. Rheological properties and proofing behaviour of dough and density, colour and crumb texture of bread were determined. Compared to a typical wheat bread formulation, the addition of *Fucus vesiculosus* seaweed powder raised elongational dough viscosity, which was responsible of a lower porosity of dough at the end of proofing. The wheat dough consistency index (power law) increased from 6.6 to $22.1 \cdot 10^{-3}$ Pa·s^n with FV addition and the flow index values were low (0.24-0.29) showing a strong shear-thinning behaviour. *Fucus vesiculosus* seaweed powder addition significantly increased density from 0.23 g·cm^{-3} ($\leq$ 2% f.b.) up to 0.40 g·cm^{-3} (8% f.b.), crumb firmness from $\approx$ 18 kPa ($\leq$ 4% f.b.) up to 45 kPa (8% f.b.) and green colour of bread crust. The results showed that a maximum of (4% f.b.) *Fucus vesiculosus* seaweed powder could be added, without impairing the density and crumb texture of enriched breads.[9]

[9]This section has been adapted from the following paper:
ARUFE, S., DELLA VALLE, G., CHIRON, H., CHENLO, F., SINEIRO, J. & MOREIRA, R. (2017). Effect of Brown Seaweed Powder on Physical and Textural Properties of Wheat Bread. *European Food Research and Technology*. IN PRESS. DOI: http://doi.org/10.1007/s00217-017-2929-8.

Nomenclature

Powders

FV35P – *Fucus vesiculosus* (FV) powder obtained from FV35.

Doughs

FV00D – Wheat flour dough.
FV02D – Wheat flour dough enriched with 2% f.b. of FV35P.
FV04D – Wheat flour dough enriched with 4% f.b. of FV35P.
FV06D – Wheat flour dough enriched with 6% f.b. of FV35P.
FV08D – Wheat flour dough enriched with 8% f.b. of FV35P.

Breads

FV00B – Wheat bread.
FV02B – Wheat bread enriched with 2% f.b. of FV35P.
FV04B – Wheat bread enriched with 4% f.b. of FV35P.
FV06B – Wheat bread enriched with 6% f.b. of FV35P.
FV08B – Wheat bread enriched with 8% f.b. of FV35P.

Parameters

a – Approximation of the final porosity increase from the initial value, Eq. (4.30), -.
$a^{'}$ – Stability at $t = 0$, Eq. (4.33), -.
b – Maximum volume expansion growth rate, Eq. (4.30), min^{-1}.
$b^{'}$ – Starting time of the stationary phase, Eq. (4.33), min.
c – Time for the inflexión point, Eq. (4.30), min.
$c^{'}$ – Stability at $t \to \infty$, Eq. (4.33), -.
d – Theoretical porosity when $t \to \infty$, Eq. (4.30), -.
K – Consistency index, Eq. (4.29), Pa·s^n.
n – Flow behaviour index, Eq. (4.29), -.
P – Porosity of dough, Eq. (4.30), -.
S – Dough shape ratio, Eq. (4.33), -.
η_e – Bi-extensional viscosity, Eq. (4.29), Pa·s.
ρ^* – Bread density, g·cm^{-3}.
ε_b – biaxial Hencky strain, %.
$\dot{\varepsilon}_b$ – Strain rate, s^{-1}.

6.10.1 Introduction

Wheat, in the form of bread, provides more nutrients to the world population than any other single food source (Peña, 2002). Nutritional properties of bread can be improved by the use of new ingredients which has become a common practice in the baking industry in order to improve also dough handling properties, bread quality and to extend the shelf life of stored bread (Mamat *et al.*, 2014).

In recent years, a growing interest is observed about natural antioxidants to replace synthetic additives in foods or nutraceuticals able to improve oxidative stability and to provide a wide variety of additional health benefits (Wang *et al.*, 2012). In this sense, brown seaweeds represent a suitable supplement for food because of their high nutritional value as source of dietary fibre and healthy benefits (Jiménez-Escrig & Sánchez-Muniz (2000), Rupérez & Saura-Calixto (2001)), high polyphenol content (Holdt & Kraan (2011), Rodríguez-Bernaldo de Quirós *et al.* (2010)) and phlorotannins that have been reported to show anti-inflammatory properties and high antioxidant activities (Balboa *et al.*, 2013). They can also be considered as ingredients for glycaemic control because they decrease the rate of starch digestibility in bread (Goñi *et al.*, 2002).

The European Commission of European Union recently classified the *Fucus vesiculosus*, a brown edible seaweed, like a "novel food" for human consumption and consequently an increase in its demand as food is expected. This brown seaweed is a dominant specie of macroalgae on the coast bathed by the Atlantic Ocean in Europe. It is mainly constituted by (% dry mass): 47.8 carbohydrates, 17.5 minerals, 10.5 polyphenols, 10 proteins, 4.8 lipids and 9.4 other components (Hahn *et al.*, 2012). Recent studies stand out the large antioxidant capacity of some of its components (Hahn *et al.*, 2012). *Fucus vesiculosus* is commonly used as food in Japan. In Europe and North America it is added in powder form to soups for flavouring. Besides these uses, further research is needed to increase *Fucus vesiculosus* applications and alternative uses, to improve the nutritional properties of traditional foods, like wheat breads.

However, the use of fibre ingredients in breadmaking process can modify dough processing such as mixing, fermentation and baking steps, and dough and bread properties like dough viscosity and bread density, colour and crumb texture (Poutanen *et al.*, 2014). High-quality bakery products have various attributes, including high volume, uniform crumb structure, tenderness, shelf life, and tolerance to staling (Mamat *et al.*, 2014). The main problems are the major increase of density and crumb elasticity (Pomeranz *et al.*, 1977) that could affect consumer's acceptability. In this sense, rheological properties of dough represent a key parameter during breadmaking process because of their effect on density

and crumb texture of bread. This is why it is necessary to study these properties in order to understand and control the variations of the final properties of baked product when a new additive or ingredient is added.

Fibre ingredients can alter gluten network formation and physical properties of the gluten network during mixing by a combination of both physical and chemical mechanism (Noort *et al.* (2010), Miś *et al.* (2017)). During proofing, an essential step of breadmaking due to its relation with cellular structure development, dough expansion can be also limited (Cavella *et al.*, 2008), like in the case of bran addition (Le Bleis *et al.*, 2015). Dough expansion can be studied at macroscopic scale by different image methods that allow the measurement of dough volume evolution (Romano *et al.* (2007), Chevallier *et al.* (2012), Shehzad *et al.* (2010)). Dough elongational properties play an important role on proofing (Bloksma (1990), Turbin-Orger *et al.* (2016)), and they can be also affected by the addition of fibres. These properties have currently been measured as they have been considered as an important tool for the analysis of breadmaking (Turbin-Orger *et al.* (2016), van Vliet (2008)).

Very few studies addressed the seaweed addition effect on dough and enriched wheat bread properties. Mamat *et al.* (2014) reported the effect of red seaweed *Kappaphycus alvarezii* addition on dough rheological properties and the quality of bread. The effect of consuming the red seaweed *Palmaria palmata* incorporated into bread on serum markers of inflammation with secondary analysis investigating changes in lipids and antioxidant status ferric reducing antioxidant power was studied by Allsopp *et al.* (2016). The addition of green seaweed species (*Cladophora spp.* and *Ulva spp.*) to conventional breads was evaluated by the effect on nutrient composition, caloric value, technological and sensory evaluation (Menezes *et al.*, 2015). Hall *et al.* (2012) investigated the acceptability of brown seaweed *Ascophyllum nodosum* enriched bread as part of a meal, and measured its effect on energy intake and nutrient absorption in overweight, healthy males. Moreover, a very recent study reported by Różyło *et al.* (2017) assessed the effect of this brown algae addition on the physical, antioxidant and sensorial properties of a gluten-free bread. Nevertheless, no studies related to brown seaweeds, specifically *Fucus vesiculosus*, that addressed the effect of seaweed addition on dough rheological properties and bread density and crumb texture were found in literature.

The main aim of this study is to determine the influence of *Fucus vesiculosus* powder addition to wheat flour at different levels on the final properties of the enriched wheat breads. Therefore, dough rheological properties and proofing behaviour are studied in order to establish the maximum addition limit of *Fucus vesiculosus* without impairing the final properties of breads.

6.10.2 Elongational and thermomechanical properties

The biaxial extension measurements of all studied doughs were satisfactorily fitted ($R^2 > 0.94$) using power law equation, Eq. (4.29). At constant strain value ($\varepsilon_b = 1$), elongational viscosity increased with seaweed powder addition, Fig. 6.51. Moreover, it decreased with increasing shear rate for all assayed doughs (e.g. from $1.2{\cdot}10^5$ to $1.2{\cdot}10^4$ Pa·s for FV00 and from $3.5{\cdot}10^5$ to $3.9{\cdot}10^4$ Pa·s for FV08).

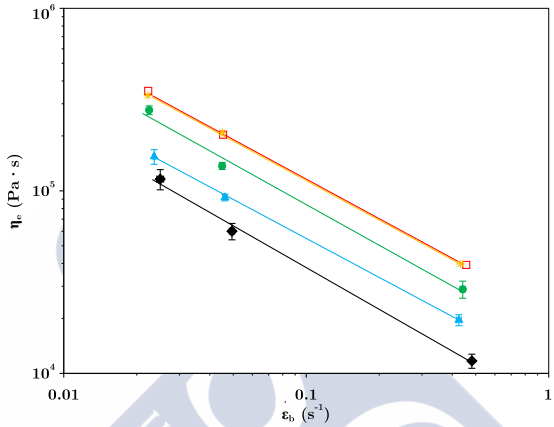

Figure 6.51 Elongational viscosity, η_e, at constant strain value ($\epsilon_b = 1$) of wheat flour dough (♦) and enriched wheat flour dough with different levels of *Fucus vesiculosus* powder seaweed (2%, ▲; 4%, ●; 6%, ✶; 8%, □). Solid line corresponds to Eq. (4.29).

The values of consistency index (K) varied between 6.6 and $22.1{\cdot}10^3$ Pa·s^n (Table 6.71) in the same interval as those reported for wheat flour doughs containing different bran amounts (Le Bleis *et al.*, 2015). The flow index (n) values varied in a narrower interval (0.24-0.29), which were lower than those encountered by Le Bleis *et al.* (2015) and reflected a clear shear-thinning behaviour for all assayed doughs. A previous work (Turbin-Orger *et al.*, 2016) has reported slightly larger values of n for wheat flour doughs obtained employing different mixing conditions (mixing time from 3 to 11 min and mixing speed from 80 to 320 rpm). In our case, the increase of K, and consequently of elongational viscosity, due to seaweed powder addition, can be explained by the physical action of seaweed powder particles. Indeed, this is in agreement with the results reported by Cavella *et al.* (2008) and Bonnand-Ducasse *et al.* (2010) which showed that, for elongational and shear viscosities, respectively, solid particles could increase dough viscosity through a filler-like effect in the dough matrix. In this case, the FV particles could perform this role. A similar increase

in the elongational viscosity of wheat flour dough, by adding bran, was reported by Le Bleis *et al.* (2015) and related to the high water absorption capacity and insolubility of the added particles. Given this, it could be suggested that, in this case, *Fucus vesiculosus* seaweed powder could play the same role as bran particles due to its high WRC and insolubility (Table 6.12).

Table 6.71 Composition and LSF parameters Eq. (4.29) wheat flour doughs and enriched wheat flour doughs with *Fucus vesiculosus* (FV) brown seaweed powder.♣

Bread	Composition			LSF parameters			
	Dough (g)	**FV** (g)	**Water** (g)	$K\cdot\mathbf{10}^{-3}$ (Pa·s^n)	n (-)	$\mathbf{R}^2$	$\mathbf{E}_{\mathrm{RMS}}\cdot\mathbf{10}^{-3}$
FV00D	300	0	192	6.6 ± 0.01^{d}	0.24 ± 0.01^{b}	0.991	4.87
FV02D	300	6	196	10.7 ± 0.01^{c}	0.29 ± 0.01^{a}	0.999	1.87
FV04D	300	12	200	15.3 ± 0.02^{b}	$0.26\pm0.01^{a,b}$	0.983	16.09
FV06D	300	18	204	21.7 ± 0.03^{a}	0.28 ± 0.01^{a}	0.998	4.41
FV08D	300	24	208	22.1 ± 0.01^{a}	0.28 ± 0.01^{a}	0.998	7.2

♣Data are presented as means±standard deviation. Data value of each parameter with different superscript letters in rows are significantly different ($P\leq 0.05$).

To have a better insight on the possible structural mechanisms governing the changes of dough extensional properties, we have examined, by DMTA, its properties in the viscoelastic domain (small strains). In this purpose, G'_{max}/G'_{min} ratio was measured and it has been considered as a possible indicator of gluten network structuration or cross-linking. Indeed, a lower value of the ratio is related to a less efficient heat effect promoting thermal aggregation of proteins, showing that the gluten network was already cross-linked before heating (Turbin-Orger *et al.* (2016), Angioloni & Dalla Rosa (2005)). Temperatures associated to the minimum and maximum values of G$'$ varied in a narrow range for all assayed doughs, 41.9±0.8°C and 72.9±0.8°C, respectively. In our case, the modulus ratio strongly decreased with FV content, from 28 (FV00) to 8 (FV08).

Figure 6.52 shows the correlation between the G'_{max}/G'_{min} ratio, measured at low strains, and K obtained at large strains (LSF). Data from literature measured for wheat dough obtained under different mixing conditions (Turbin-Orger *et al.*, 2016) were also plotted on Figure 6.52. The same trend is observed for both data series. Acceptable correlation ($R^2 > 0.90$) was found between the G'_{max}/G'_{min} ratio and K by an Arrhenius type equation, Eq. (6.19):

$$K = 4.79e^{\left(\frac{13.65}{G'_{max}/G'_{min}}\right)} \tag{6.19}$$

Large values of elongational viscosity are coincident with low G'_{max}/G'_{min} values that indicate a high structuration of dough gluten network, according to Turbin-Orger *et al.* (2016), since in their case gluten network formation was likely influenced by the mixing conditions. In our case, such mechanism is still

questionable because solid particles, like FV powder, are better known to preclude the formation of gluten network either by competing for available water or because of steric hindrance (Noort *et al.* (2010), Le Bleis *et al.* (2015)). The obtained result could be related to the physical effect of seaweed particles which impairs gluten aggregation during heating by DMTA.

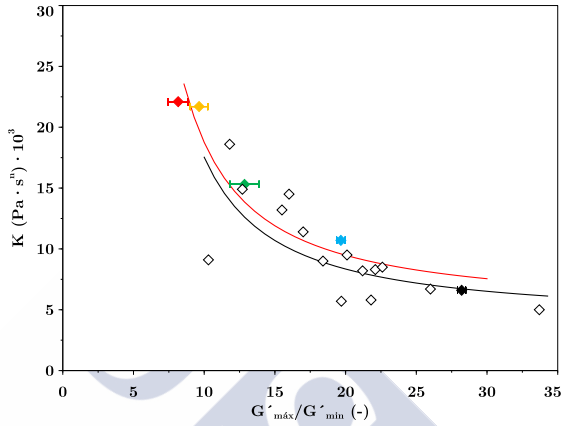

Figure 6.52 Consistency index, K, Eq. (4.29), correlation with G'_{max}/G'_{min} ratio for wheat flour dough enriched with different levels of *Fucus vesiculosus* powder seaweed (0%, (♦); 2%, (♦); 4%, (♦); 6%, (♦); 8%, (♦)) and wheat flour doughs under different mixing conditions (Turbin-Orger *et al.* (2016)), ◇. Solid red line corresponds to Eq.(6.19).

6.10.3 Dough behaviour during proofing

Porosity curves were satisfactorily fitted ($R^2 > 0.995$) employing the Compertz model, Eq. (4.32), Table 6.72. They had a sigmoid shape with an initial porosity value between 0.05 and 0.12 and a final value that varied from 0.64 to 0.80, Figure 6.53 (a). For FV00 dough, the asymptotic value of porosity ($a + d$) corresponded to a value 0.80, *app.* This asymptotic value is in agreement with those previously reported for wheat flour doughs with different mixing conditions (Turbin-Orger *et al.*, 2016). The total porosity increase (a parameter) significantly decreased from 0.76±0.02 (FV00) to 0.58±0.03 (FV08) with seaweed powder addition indicating that seaweed powder addition has a negative effect on dough expansion and final porosity. This trend can be related to high elongational viscosity associated to FV addition. Indeed, the low solubility of FV powder particles precludes glucose release from seaweed and thus the increase of gas production by yeast. The increase of porosity during proofing can be explained by the mechanisms of

gas bubble growth in a viscous medium according to which a high elongational viscosity decreases the bubble growth and limit dough expansion (Kansou *et al.*, 2014). This observation is in agreement with those reported by Cavella *et al.* (2008) and Le Bleis *et al.* (2015) who reported that bran addition can lead to a decrease on expansion of dough during proofing. The maximum volume expansion growth rate (b parameter) and the time for the inflection point (c parameter) were not significantly different for all assayed doughs. It is important to note that in the case of FV08 dough c parameter shows no significant difference due to the large standard deviation, probably due to the addition of a large quantity of seaweed that makes doughs fermentation less repetitive. Finally, d parameter slightly increased with seaweed powder addition.

Table 6.72 Porosity parameters of wheat flour doughs and enriched wheat flour doughs with *Fucus vesiculosus* (FV) brown seaweed powder.♣

Bread	a **(-)**	$b{\cdot}\mathbf{10^3}$ **(min^{-1})**	c **(min)**	d **(-)**	$\mathbf{R^2}$	$\mathbf{E_{RMS}{\cdot}10^3}$
FV00	0.77 ± 0.05^{a}	8.3 ± 0.3^{a}	38.8 ± 2.0^{a}	0.03 ± 0.02^{c}	0.997	12.4
FV02	$0.71\pm0.01^{a,b}$	7.3 ± 0.2^{a}	48.9 ± 5.0^{a}	$0.07\pm0.01^{b,c}$	0.999	10.7
FV04	$0.62\pm0.01^{b,c}$	7.5 ± 1.0^{a}	44.8 ± 7.7^{a}	$0.09\pm0.01^{a,b}$	0.998	9.1
FV06	$0.59\pm0.03^{b,c}$	8.2 ± 1.0^{a}	37.6 ± 6.7^{a}	$0.06\pm0.01^{b,c}$	0.996	12.2
FV08	0.52 ± 0.01^{c}	8.4 ± 3.2^{a}	37.7 ± 13.1^{a}	0.12 ± 0.01^{a}	0.993	12.0

♣Data are presented as means±standard deviation. Data value of each parameter with different superscript letters in rows are significantly different ($P \leq 0.05$).

The shape ratio kinetics during proofing were appropriately fitted ($R^2 > 0.987$) employing, Eq. (4.33) for $t \leqslant 90$ min, Table 6.71. Doughs exhibited a continuous decrease of the shape ratio S(t) indicating a loss of stability of the fermenting dough, Figure 6.53 (b). The starting time of the stationary phase (b′), Table 6.71, was significantly larger for FV08 dough suggesting that the seaweed powder addition contributed to a slow but continuous loss of stability of the dough during proofing. Lower values of stability loss ($a^{'} - c^{'}$) of dough reflect the capacity of dough to maintain its shape whereas larger values reflect dough spreading during proofing (Turbin-Orger *et al.*, 2016). In our case, ($a^{'} - c^{'}$) values decreased with FV addition $> 2\%$ from 0.19±0.01 (FV00 and FV02) to 0.15±0.02 (FV04, FV06 and FV08). This result shows that larger concentrations of seaweed powder have a positive effect on dough stability, which could be due to a larger elongational viscosity. Le Bleis *et al.* (2015) observed the opposite effect, when adding larger level of bran particles. They attributed it to coalescence, due to the destabilization of the gas bubbles structure by bran particles, which could pierce the bubbles films. In our case, the absence of destabilisation effect could be attributed to a lower size of seaweed particles (130μm on average).

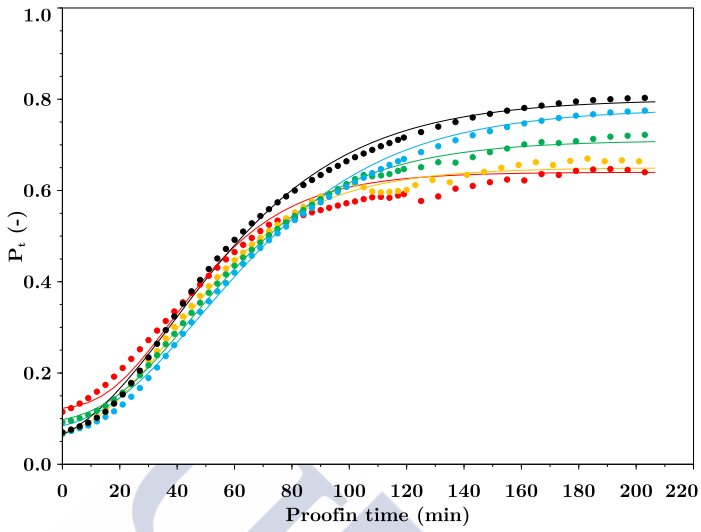

(a)

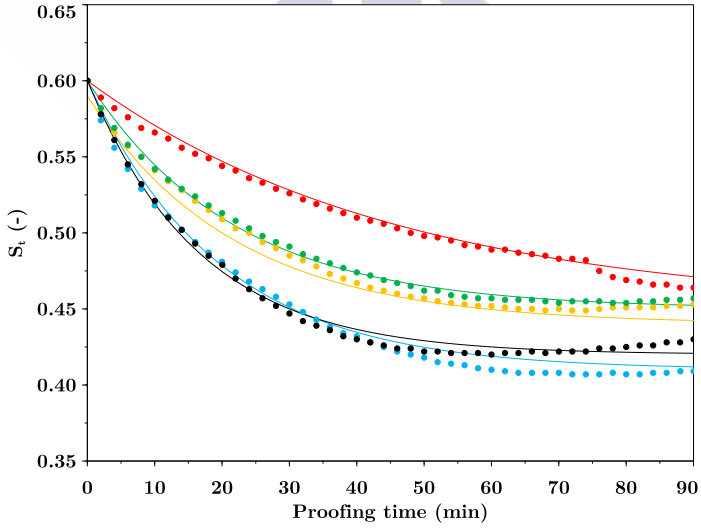

(b)

Figure 6.53 Porosity (a) and shape (b) kinetics for wheat flour dough and wheat flour dough enriched with different levels of *Fucus vesiculosus* powder seaweed (0%, (●); 2%, (●); 4%, (●); 6%, (●); 8%, (●)). Lines correspond to Eq. (4.32) for Figure (a) and to Eq. (4.33) for Figure (b).

Table 6.73 Stability parameters of wheat flour doughs and enriched wheat flour doughs with *Fucus vesiculosus* (FV) brown seaweed powder.♣

Bread	$b^{'}$ (min)	$c^{'}$ (-)	$a^{'} - c^{'}$ (-)	$\mathbf{R}^2$	$\mathbf{E}_{\mathrm{RMS}}\cdot\mathbf{10}^3$
FV00	16.75 ± 0.50^{b}	0.42 ± 0.01^{a}	$0.18\pm0.01^{a,b}$	0.999	4.3
FV02	19.57 ± 1.88^{b}	0.41 ± 0.01^{a}	0.19 ± 0.01^{a}	0.993	4.7
FV04	21.73 ± 3.93^{b}	0.45 ± 0.01^{a}	0.15 ± 0.01^{b}	0.992	3.6
FV06	21.81 ± 3.02^{b}	0.44 ± 0.01^{a}	0.15 ± 0.01^{b}	0.993	3.3
FV08	45.99 ± 2.55^{a}	0.45 ± 0.02^{a}	0.15 ± 0.02^{b}	0.987	4.1

♣Data are presented as means±standard deviation. Data value of each parameter with different superscript letters in rows are significantly different ($P\leq 0.05$).

6.10.4 Bread characterization

Bread characterisation was carried out by mean of bread density, bread crust colour and bread crumb texture.

6.10.4.1 Density

Bread with 2% of seaweed powder had same density as control (FV00), Table 6.74. The values of bread density obtained for these samples (0.22-0.23 g·cm^{-3}, respectively) were similar to those previously reported for wheat bread (Besbes *et al.*, 2014). Seaweed addition larger than 2% significantly increased bread density, this trend contrasts with those obtained by Różyło *et al.* (2017) who reported that *Ascophyllum nodosum* seaweed powder addition to a gluten-free formulation based on rice, corn and millet flours significantly incremented bread volume and hence reduced its density. An addition of *Fucus vesiculosus* powder content up to 4% increased bread density up to 0.27 g·cm^{-3} which represents an increase of 23% in comparison to control bread. Addition of seaweed powder larger than 4% increased bread density to more than 0.30 g·cm^{-3} (> 36%). These values are close to those reported for wheat breads with added fibres like pear, apple and date fibre (Bchir *et al.*, 2014) or bran (Le Bleis *et al.*, 2015). These results suggest that 4% of seaweed powder could be a maximum limit of addition to obtain wheat bread enriched with FV seaweed powder with density typical of wheat bread.

Figure 6.54 displays the experimental data of this study and the bibliographic data of wheat bread enriched with wheat bran (Le Bleis *et al.*, 2015) of the final porosity increase (a) *vs* the final bread density ratio (ρ^*/ρ^*_{max}), defined as the ratio between the bread density and the maximum bread density of each data

series in order to facilitate the comparison. For FV enriched breads, a strong correlation ($R^2 > 0.97$) was found between bread density and the final porosity on proofing step by an Arrhenius type equation, Eq. 6.20:

$$a = 0.32e^{\left(\frac{0.47}{\rho^*/\rho^*_{max}}\right)} \tag{6.20}$$

Both data series show similar trends, the lower the porosity at the end of proofing, the higher the bread density. This mentioned trend also connects the bread density to the elongational viscosity due to, as mentioned before, higher elongational viscosity leads to lower porosity of dough at the end of proofing. This result indicates that, in the case of bread enriched with FV powder, bread density was not influenced by baking operation and that seaweed particles influence more proofing operation.

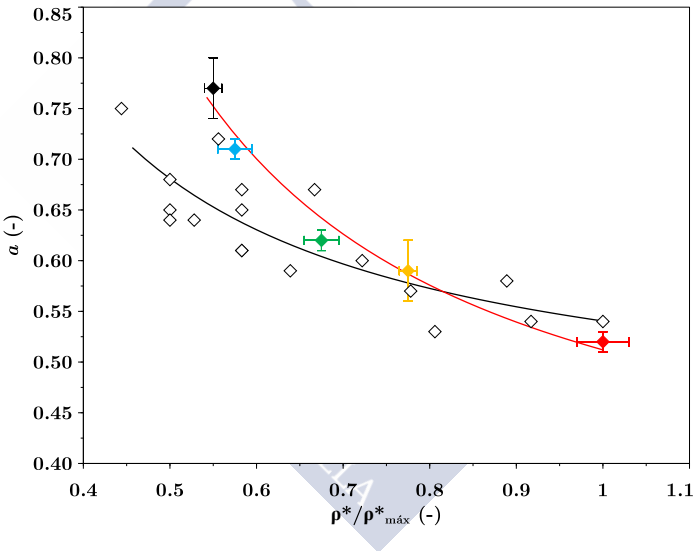

Figure 6.54 Porosity increase (a parameter of Gompertz model, Eq. (4.32)) as function of bread density ratio for wheat flour dough enriched with different levels of *Fucus vesiculosus* powder seaweed (0%, (♦); 2%, (♦); 4%, (♦); 6%, (♦); 8%, (♦)) and wheat flour dough enriched with wheat bran at different levels (Le Bleis *et al.* (2015)), ◇. Red line correspond to Eq.(6.20).

6.10.4.2 Bread crust colour

Bread crust colour was significantly modified due to *Fucus vesiculosus* powder addition, Table 6.74 and Figure 6.55. Compared to FV00, L^* value of FV08 was significantly lower and FV04 and FV06 L^* values were close whereas the maximum value was obtained for FV02. Regarding a^*, it can be clearly seen that seaweed addition significantly increased green colour of bread crust (low a^* values), as it could be expected due to green colour of the powder added, a^*: -2.95±0.17 (Table 6.19). In addition, a linear relationship was found between a^* and the mass percentage of seaweed powder for FV $\geq$ 2% ($R^2 > 0.95$). The yellow colour of bread crust decreased, as shown by a linear decrease in b^* value with FV mass fraction ($R^2 > 0.88$). This fact can be explained by the pigments of FV powder particles and also components released in soluble fraction which reduced the yellow proportion of bread associated to wheat flour colour. The colour difference of all seaweed enriched breads in comparison to standard wheat bread can be classified as very distinct ($\Delta E^* > 3$).

Table 6.74 Colour parameters and density of wheat breads and enriched wheat breads with *Fucus vesiculosus* (FV) brown seaweed powder.♣

Bread	L^*	a^*	b^*	ΔE^*	ρ^* $(g \cdot cm^{-3})$
FV00	49.80±1.32^{c}	16.19±0.38^{a}	30.25±0.83^{a,b}	-	0.22±0.01^{d}
FV02	58.31±1.15^{a}	8.58±1.03^{b}	30.92±1.24^{a}	11.4	0.23±0.02^{d}
FV04	53.13±1.40^{b}	7.43±0.56^{b,c}	28.38±0.21^{b}	9.6	0.27±0.02^{c}
FV06	48.90±0.70^{c}	7.04±0.38^{c}	25.74±0.64^{c}	10.2	0.31±0.01^{b}
FV08	42.75±3.94^{d}	6.33±0.55^{c}	22.36±2.24^{d}	14.5	0.40±0.03^{a}

♣Data are presented as means±standard deviation. Data value of each parameter with different superscript letters in rows are significantly different (P≤ 0.05).

6.10.4.3 Crumb texture

Figure 6.56 shows the results of E_{crumb}, $\sigma_{critical}$ and $\sigma_{residual}$ obtained from the compression essays for the tested breads. Moreover, images of crumb of differents breads are presented in Figure 6.57.

A FV addition > 4% significantly modified bread crumb texture parameters. In fact ANOVA analysis showed that for the apparent modulus, E_{crumb}, there were significant differences between FV08 (45.0±4.0 kPa) and FV06 (33.6±1.0 kPa) whereas no significant differences were found for system with a FV fraction ≤ 4%, with an average value for the 3 systems equal to 18.1±2.5 kPa. Similar values of E_{crumb} (≈14.0 kPa) were previously reported for similar breads (Besbes

Figure 6.55 Images of wheat bread, FV00, (a) and wheat bread enriched with *Fucus vesiculosus* seaweed at 2%, (FV02, b), 4% (FV04, c), 6% (FV06, d) and 8% d.b., (FV08, e).

et al., 2014). On the contrary, the observed trend of crumb firmness increasing with seaweed powder addition was the opposite of that observed by Różyło *et al.* (2017) for gluten-free bread added with *Ascophyllum nodosum* powder.

The peak of stress, $\sigma_{critical}$, and the apparent residual stress at the end of the relaxation step, $\sigma_{residual}$, showed the same trend of E_{crumb}. This fact may suggest that crumb texture properties of wheat bread enriched with FV seaweed are not modified with an addition of seaweed powder $\leq 4\%$.

A good correlation was found between E_{crumb} and ρ^* ($R^2 > 0.91$) which suggests that the increase of bread crumb firmness was mainly due to an increase of bread density that, as mentioned before, is related to the increase of elongational viscosity of dough caused by FV powder addition.

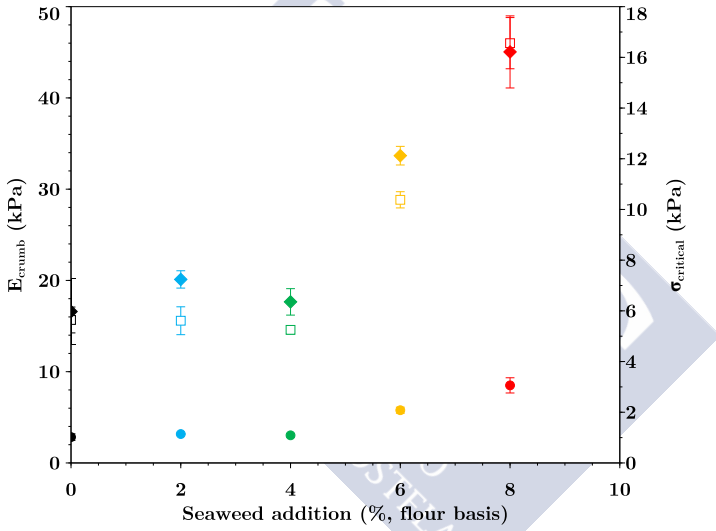

Figure 6.56 Apparent modulus, E_{crumb} (0%, (♦); 2%, (♦); 4%, (♦); 6%, (♦); 8%, (♦)), critical stress, $\sigma_{critical}$ (0%, (□); 2%, (□); 4%, (□); 6%, (□); 8%, (□)), residual stress $\sigma_{residual}$ (0%, (●); 2%, (●); 4%, (●); 6%, (●); 8%, (●)) of wheat bread crumb enriched with different levels of *Fucus vesiculosus* powder seaweed.

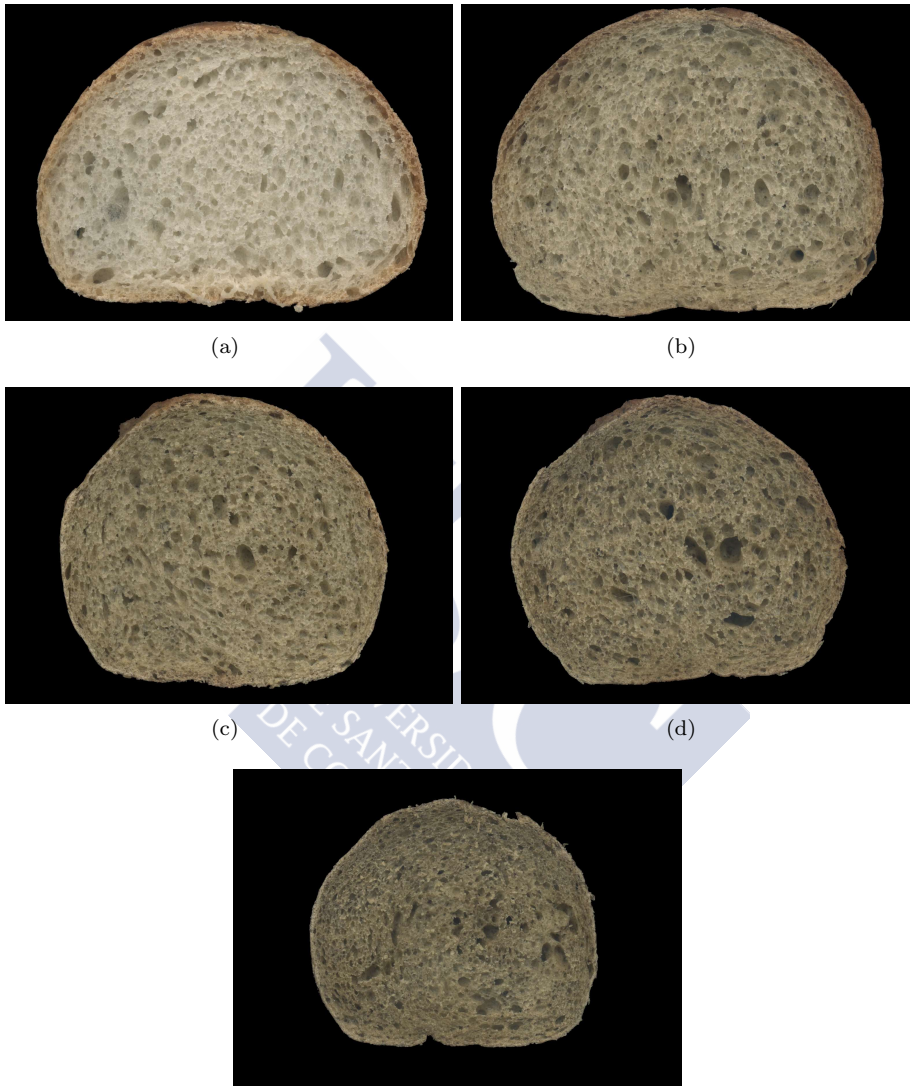

(a) (b)

(c) (d)

(e)

Figure 6.57 Images of crumb for wheat bread, FV00, (a) and wheat bread enriched with *Fucus vesiculosus* seaweed at 2%, (FV02, b), 4% (FV04, c), 6% (FV06, d) and 8% d.b., (FV08, e).

The section in tweets

- *Fucus vesiculosus* seaweed powder (FV) addition increments elongational viscosity and improves the stability of dough.
- FV addition is negative for dough final porosity due to the high elongational viscosity reduces the bubble growth limiting dough expansion.
- FV additions larger than 4% (flour basis) significantly leads to an increase of bread density and bread crumb firmness.
- Green colour of bread crust is increased by FV addition which could be a non-positive effect on consumer's acceptance.
- A range of FV addition up to 4% can be employed to bread enrichment without impairing bread properties.

USC
UNIVERSIDADE
DE SANTIAGO
DE COMPOSTELA

Chapter 7

Conclusions

As a consequence of the proposed objectives and the experimental work carried out, as well as the analysis of the results achieved, the following conclusions are established as the most relevant ones:

- Tested seaweeds have different **hygroscopic properties** and must be dried and stored (at room temperature) at different equilibrium moisture content values ≈ 0.10 dry basis (d.b) for *Ascophyllum nodosum* (AN) and *Fucus vesiculosus* (FV) and ≈ 0.05 d.b for *Bifurcaria bifurcata* (BB).

- The water sorption isotherms of tested seaweeds in the temperature range (5-65°C) are classified as type II and adequately fitted by the Halsey model. At water activities < 0.5, BET model is suitable to fit the experimental data. Equilibrium moisture content decreases with increasing temperature at water activities < 0.5; at higher water activities the behaviour is reverted.

- **Seaweed drying** experiments in deep-bed configuration (from 35°C up 75°C) indicate that the maximum water removal rates are achieved at the following temperatures: 75°C for BB, 50°C for AN and 60°C for FV.

- The falling drying rate period of monolayer seaweeds drying can be satisfactorily modelled by means of Fick's Law equation, assuming cylindrical geometry and shrinkage. Diffusion coefficients of water ($m^2 \cdot s^{-1}$) for AN seaweed were the highest ($2.8 - 5.4 \cdot 10^{-10}$) followed by FV ($1.0 - 2.7 \cdot 10^{-10}$) and BB ($1.2 - 2.0 \cdot 10^{-11}$). Mass transfer coefficients ($m \cdot s^{-1}$) on constant drying rate period (mass transfer rate governed by external

resistances) are similar (13.7 - 21.8·10^{-3}) for all seaweeds in the employed dryer.

- Powders **physical characteristics** were different as function of tested seaweed: the surface mean diameter (μm) of FV powder is the highest (133 - 147) compared to BB (106 - 126) and AN (77 - 108) with bimodal particle size distributions for FV and AN and unimodal for BB. These values are in the range of flour additives. Colour parameters of whole flours can be estimated through colour parameters of the corresponding mass fractions by means of a mixing rule. BB powder has the highest water retention capacity and swelling power with no significant differences on these parameters between AN and FV powders.

- **Flour characteristics** depend on employed starchy raw materials: the surface mean diameter (μm) of flours from white maize is the highest (97.1 - 166.7) compared to yellow (67.8 - 99.8) and purple (60.4 - 91.9) and chestnut (35.4) with bimodal particle size distributions. Colour parameters of whole flours can be estimated through colour parameters of the corresponding mass fractions by means of a mixing rule. No significant differences on total starch (TS, d.b.) for all maize flours (60 - 75 %) are observed. Chestnut flours present lower TS (51%). Damaged starch (d.b.) of flours obtained employing the same milling conditions is higher for white maize (25%) than purple maize (18%) and yellow maize and chestnut ($\approx$ 8%).

- High drying temperatures dramatically decrease (up to 54% at 75°C in comparison to 35°C) total polyphenolic (TP) content and antioxidant activity (SA) of **seaweeds aqueous extracts**. The most adequate drying temperatures are 35°C for BB and FV and $\leqslant$ 50°C for AN. The highest TP ($\approx$ 3000 mg PHL/100 g dry powder) and SA correspond to AN ($\approx$ 75%) followed by BB and FV extracts. There is a linear relationship between SA ($>$ 45%) of extracts and green colour (a^* parameter) of seaweed powders. Carbohydrate content (CHO) decreases (up to 25%) with increasing drying temperature ($>$ 60°C) for AN and BB and remains constant for FV. The highest CHO corresponds to FV and AN ($\approx$ 6000 mg GL/100 g dry powder).

- **Mixing flour-water characteristics** of different maize flours are specific. Water absorption (WA, 55 - 91% flour basis, f.b.) depends on damaged starch content (DS, 3 - 25% d.b.), so, the higher DS the higher WA. The higher particle size, the lower WA and the higher development and stability time of doughs.

- Guar gum (2% f.b.) is necessary to obtain chestnut flour doughs with adequate mixing characteristics. Seaweed powder addition (up to 9% f.b.)

significantly increases WA and improves mixing characteristic of chestnut flour doughs: better stability (higher times), mechanical weakening and retrogradation (lower C2 and C5 values, respectively).

- **Mechanical spectra** of gluten-free doughs are adequate due to they have the elastic proportion (storage modulus, $G^{'}$) higher than the viscous one (loss modulus, $G^{''}$) as well as it occurs in doughs with gluten. At the same consistency, flour doughs from chestnut have the highest moduli, followed by yellow, purple and white maize. In all cases, higher particle size of flour results in higher moduli values. In general, the presence of seaweeds powders in chestnut flour doughs significantly decreases both moduli. The presence of gelatinized starch modifies viscoelasticity of doughs (lower viscous character).

- **Creep and recovery** experimental data are in accordance with those observed in mechanical spectra. Stiffer doughs (high $G^{''}$ values) show lower instantaneous compliance on creep and recovery phases and lower capacity to deformation. Different amounts of seaweeds powders can be added to chestnut flour doughs without impairing their creep-recovery properties: 9% of AN and FV and 6% of BB. Gelatinized starch enhances the relative total strain recovery of doughs (from 80% to 90%). All obtained values are in the same range to those obtained for gluten-free flour doughs.

- **Dynamic Mechanic-Thermal Analysis (DMTA)** is validated like a valuable experimental technique to determine the thermal transitions (starch swelling and gelatinization (G, 50 - 85°C and M1, 85 - 104°C), amylose-lipid complex (M2, 104 - 124°C) and amylose (M3, 131 - 160°C) melting) of starchy products. A full protocol for determination of these transitions is proposed by means of evaluation (maximum, minimum and inflexion points) of thermal trends of $G^{'}$ and/or tanδ.

- The transitions of maize and chestnut doughs depend on WA. In general, high WA implies lower values of characteristic temperatures of transitions. Low WA values lead to determine the gelatinization transition separately (G and M1). Seaweed powder addition to chestnut flour dough significantly anticipate ($\approx$ 2°C, by high WA) the breakdown of starch granules. The found peaks are related to the processes involved in the crust formation during baking of starchy products.

- Chestnut flour can be **stored** during at least one year, at 4°C in vacuum sealed bags, after its manufacturing. During this period, mixing, rheological and thermomechanical properties of their doughs remains constant.

- Seaweed powder significantly increases SA (15-30%) of obtained flour blends but, no differences on SA of **baked cookies** are observed. Green colour of baked cookies increases by the presence of seaweed powders. Hardness and Young's modulus of cookies increase by seaweed additions higher than 6% (f.b.) and both remain invariant below this value. Baking process increases TP (from $\approx$ 100 to $\approx$ 700 mg PHL/100 g dry powder) and SA (from $\approx$ 12% to $\approx$ 59%) of cookies compared to pre-baked flour blends.
- *Fucus vesiculosus* seaweed powder addition significantly increases elongational viscosity (from $1.2{\cdot}10^5$ to $3.5{\cdot}10^5$ Pa·s at 0.025 s^{-1}) and stability ($\approx$ 20%) of wheat dough. It has a negative effect on dough final porosity (lower values, from 0.77 to 0.52) leading to an increase of bread density and crumb apparent modulus. An addition of seaweed powder larger than 4% (f.b.) significantly increased bread density (> 36%) and bread crumb firmness (46%).

Summarising, the mixing and rheological features of obtained gluten-free doughs from chestnut and maize flours indicate that they can be classified like pastrymaking flours. Keeping this in mind, cookies from chestnut flour and seaweed-enriched chestnut flour blends were manufactured in order to analyse and compare their characteristics with other commercial cookies (with or without gluten) reported in literature. The results obtained allow establishing some important remarks for obtained baked products (**cookies**):

- **Phenolic content**: seaweed-enriched chestnut cookies showed higher polyphenols content than wheat flour and other gluten-free such as rice and buckwheat cookies. In this sense, seaweed-enriched chestnut cookies are suitable.
- **Colour properties**: cookies showed greenness and yellowness trends like other commercial cookies. The main handicap of tested chestnut cookies is the low value of brightness, although is acceptable.
- **Textural properties**: hardness and elasticity of cookies are in the upper limit of the usual commercial range values for cookies. The improvement of texture quality of these cookies will be a future challenge by the new formulations and/or different processing conditions.

Finally, the obtained cookies or the improved products considering the previous remarks will need additional studies previous to commercialization. A complete nutritional characterisation, packaging and storage studies as well as sensory analysis and consumer's acceptance of baked product should be performed by corresponding researchers.

Conclusiones

Como consecuencia de los objetivos propuestos y del trabajo experimental realizado, así como del análisis de los resultados obtenidos, se establecen las siguientes conclusiones como las más relevantes:

- Las algas estudiadas tienen diferentes **propiedades higroscópicas** y deben ser secadas y almacenadas (a temperatura ambiente) a diferentes valores de humedad de equilibrio $\approx$ 0,10 base seca (b.s.) para *Ascophyllum nodosum Fucus vesiculosus* (FV) y $\approx$ 0,05 b.s. para *Bifurcaria bifurcata* (BB).

- Las isotermas de adsorción/desorción de algas estudiadas en el rango de temperatura (5-65°C) están clasificadas como de tipo II y se ajustan adecuadamente mediante el modelo Halsey. En las actividades de agua $<$ 0,5, el modelo BET es adecuado para ajustar los datos experimentales. El contenido de humedad en equilibrio disminuye con el aumento de la temperatura en las actividades de agua $<$ 0,5; en las actividades de agua más altas el comportamiento se invierte.

- El **secado de algas** en la configuración de lecho denso (desde 35°C hasta 75°C) indican que la máxima velocidad de eliminación de agua se consigue a las siguientes temperaturas: 75°C para BB, 50°C para AN y 60°C para FV.

- El período de secado de velocidad de secado decreciente de algas en configuración de monocapa puede ser modelado satisfactoriamente mediante la ecuación de Fick suponiendo geometrías cilíndricas y teniendo en cuenta el encogimiento de las algas. Los coeficientes de difusión del agua ($m^2 \cdot s^{-1}$) para AN son los más altos (2,8 - 5,4$\cdot 10^{-10}$) seguido de FV (1.0 - 2.7$\cdot 10^{-10}$) y BB (1,2 - 2,0$\cdot 10^{-11}$). Los coeficientes de transferencia de masa ($m \cdot s^{-1}$) en el período de velocidad de secado constante (transferencia de masa gobernada por resistencias externas) son similares (13.7 - 21.8$\cdot 10^{-3}$) para el secado de las estudiadas en el secadero empleado.

- Las **características físicas** de los polvos son diferentes en función de las algas empleadas: el diámetro medio de superficie (μm) del polvo de FV es el más alto (133 - 147) en comparación con BB (106 - 126) y AN (77 - 108) con distribuciones de tamaño de partícula bimodal para FV y AN y unimodal para BB. Estos valores están en el rango de aditivos comerciales para harina. Los parámetros de color de las harinas integrales se pueden estimar mediante parámetros de color de las fracciones de masa correspondientes mediante una regla de mezcla. BB tiene la mayor capacidad de retención de agua y

capacidad de hinchamiento sin diferencias significativas en estos parámetros entre los polvos AN y FV.

- Las **características de la harina** dependen de las materias primas amiláceas empleadas: el diámetro medio de superficie (μm) de las harinas del maíz blanco es el más alto (97.1 - 166.7) en comparación con el amarillo (67.8 - 99.8) y el morado (60,4 - 91,9) y la castaña (35,4) con distribuciones bimodales de tamaño de partícula. Los parámetros de color de las harinas enteras se pueden estimar mediante parámetros de color de las fracciones de masa correspondientes mediante una regla de mezcla. No se observan diferencias significativas en el almidón total (TS, b.s.) para todas las harinas de maíz (60 - 75 %). Las harinas de castaña presentan una TS inferior (51 %). El almidón dañado (b.s.) de las harinas obtenidas empleando las mismas condiciones de molienda es mayor para el maíz blanco (25 %) que el maíz morado (18 %) y el maíz amarillo y ela castaña ($\approx$ 8 %).

- Las altas temperaturas de secado disminuyen drásticamente (hasta 54 % a 75°C en comparación con 35°C) el contenido total de polifenoles (TP) y la actividad antioxidante (SA) de los **extractos acuosos de las algas**. Las temperaturas de secado más adecuadas son 35°C para BB y FV y $\leqslant$ 50°C para AN. El valor más alto de TP ($\approx$ 3000 mg PHL / 100 g de polvo seco) y SA corresponden a AN ($\approx$ 75 %) seguido de los extractos de BB y FV. Existe una relación lineal entre la SA ($>$ 45 %) de los extractos y el color verde (parámetro a*) de los polvos de algas. El contenido de carbohidratos (CHO) disminuye (hasta 25 %) con el aumento de la temperatura de secado ($>$ 60°C) para AN y BB y permanece constante para FV. El CHO más alto corresponde a FV y AN ($\approx$ 6000 mg GL / 100 g de polvo seco).

- Las **características de mezcla harina-agua** de las diferentes harinas de maíz son específicas. La absorción de agua (WA, 55 - 91 % base de harina, b.h.) depende del contenido de almidón dañado (DS, 3 - 25 % d.b.). A mayor tamaño de partícula, menor WA y mayor tiempo de desarrollo y estabilidad de las masas.

- La goma guar (2 % f.b.) es necesaria para obtener masas de harina de castaña con características de mezcla adecuadas. La adición de polvo de alga (hasta 9 % b.h.) aumenta significativamente WA y mejora las características de mezcla de las masas de harina de castaña: mejor estabilidad (tiempos más altos), debilitamiento mecánico y retrogradación (valores C2 y C5 inferiores, respectivamente).

- Los **espectros mecánicos** de las masas sin gluten son adecuados debido a que tienen la proporción elástica (módulo de almacenamiento, G$'$) más

alta que la viscosa (módulo de pérdida, G'') así como ocurre en las masas con gluten. A la misma consistencia, las masas de harina de castaña tienen los módulos más altos, seguidos del maíz amarillo, morado y blanco. En todos los casos, un mayor tamaño de partícula de harina da como resultado unos valores de los módulos superiores. En general, la presencia de polvos de algas en masas de harina de castaña disminuye significativamente ambos módulos. La presencia de almidón gelatinizado modifica la viscoelasticidad de las masas (carácter viscoso inferior).

- Los datos experimentales de **Fluencia y recuperación** están de acuerdo con los observados en los espectros mecánicos. Las masas más rígidas (altos valores de G') muestran menor deformación instantánea de fluencia y recuperación y menor capacidad de deformación. Se pueden añadir diferentes cantidades de polvos de algas a las masas de harina de castaña sin perjudicar sus propiedades de recuperación de fluencia: 9 % de AN y FV y 6 % de BB. El almidón gelatinizado mejora la recuperación relativa de la deformación total de las masas (de 80 % a 90 %). Todos los valores obtenidos están en el mismo rango que los obtenidos para las masas de harina sin gluten.

- El **Análisis Dinámico Mecánico-Térmico** (DMTA, por sus siglas en inglés) se valida como una técnica experimental válida para determinar las transiciones térmicas (hinchamiento y gelatinización del almidón (G, 50 - 85°C y M1, 85 - 104°C), fusión de complejos de amilosa - lípido M2, 104 - 124°C) y fusión de la amilosa (M3, 131 - 160°C) de productos amiláceos. Se propone un protocolo completo para la determinación de estas transiciones mediante la evaluación (máximos, mínimos y puntos de inflexión) de las tendencias térmicas de G' y/o tanδ.

- Las transiciones térmicas en las masas de maíz y castaña dependen de WA. En general, WA altas implican valores más bajos de las temperaturas características de las transiciones. Los valores bajos de WA conducen a determinar la transición de gelatinización separadamente (G y M1). La adición de polvo de algas a la masa de harina de castaña anticipa significativamente (≈ 2°C, por WA alta) la rotura de gránulos de almidón. Los picos encontrados están relacionados con los procesos implicados en la formación de la corteza durante el horneado de productos almidonados.

- La harina de castaña puede ser **almacenada** durante al menos un año, a 4°C en bolsas selladas al vacío, después de su fabricación. Durante este período, las propiedades de mezcla, reológicas y termomecánicas de sus masas no varían.

- La adición de polvo de algas marinas aumenta significativamente la SA (15-30 %) de las mezclas de harina obtenidas, pero no se observan diferencias en la SA de **galletas** después de hornear. El color verde de las galletas horneadas aumenta por la presencia de polvos de algas. La dureza y el módulo de Young de las galletas aumentan por la adición de la algas por encima del 6 % (f.b.) y ambos permanecen invariantes debajo de este valor. El proceso de horneado aumenta significativamente el TP (de $\approx$ 100 a $\approx$ 700 mg PHL / 100 g de polvo seco) y la SA (desde $\approx$ 12 % a $\approx$ 59 %) en comparación con las mezclas de harina sin hornear.

- La adición de polvo de *Fucus vesiculosus* incrementa significativamente la viscosidad elongacional (de $1{,}2{\cdot}10^5$ a $3{,}5{\cdot}10^5$ Pa·s a 0,025 s^{-1}) y la estabilidad ($\approx$ 20 %) de las masas de trigo. Tiene un efecto negativo sobre la porosidad final de la masa (valores más bajos, de 0,77 a 0,52), dando lugar a un aumento de la densidad del pan y del módulo aparente de la miga. Una adición de polvo de algas superior al 4 % (b.h.) aumenta significativamente la densidad del pan ($>$ 36 %) y la firmeza de la miga de pan (46 %).

Finalmente, las galletas obtenidas o los productos mejorados considerando las observaciones anteriores necesitarán estudios adicionales previos a la comercialización. Los investigadores correspondientes deberán llevar a cabo una completa caracterización nutricional, los estudios de envasado y almacenamiento, así como el análisis sensorial y de aceptación por parte de los consumidores de los productos horneados.

Conclusións

Como consecuencia dos obxectivos propostos e do traballo experimental realizado, así como a análise dos resultados obtidos, establécense as seguintes conclusións como as máis relevantes:

- As algas estudadas teñen diferentes **propiedades higroscópicas** e deben ser secadas e almacenadas (a temperatura ambiente) a diferentes valores de contido de humidade de equilibrio $\approx$ 0,10 base seca (b.s.) para *Ascophyllum nodosum* (AN) e *Fucus vesiculosus* (FV) e $\approx$ 0,05 b.s. para *Bifurcaria bifurcata* (BB).
- As isotermas de adsorción/desorción de auga das algas estudadas no rango de temperatura (5-65ºC) son clasificadas como tipo II e axustadas polo modelo Halsey. Para actividades de auga $<$ 0,5, o modelo BET é axeitado para axustar os datos experimentais. O contido de humidade de equilibrio diminúe co aumento da temperatura para actividades de auga $<$ 0,5; en actividades de auga máis elevadas o comportamento invírtese.
- Os experimentos de **secado de algas** na configuración de leito denso (de 35ºC a 75ºC) indican que a máxima velocidade de eliminación de auga conséguese nas seguintes temperaturas: 75ºC para BB, 50ºC para AN e 60ºC para FV.
- O período de de velocidade de secado decrecente de algas en configuración de monocapa pódese modelar satisfactoriamente mediante a ecuación de Fick asumindo xeometrías cilíndricas e tendo en conta o encollemento. Os coeficientes de difusión de auga ($m^2 \cdot s^{-1}$) para AN son os máis altos (2,8 - 5,4$\cdot 10^{-10}$) seguidos por FV (1,0 - 2,7$\cdot 10^{-10}$) e BB (1,2 - 2,0$\cdot 10^{-11}$). Os coeficientes de transferencia de masa (m$\cdot s-1$) no período de velocidade de secado constante (transferencia de masa gobernada por resistencias externas) son similares (13,7 - 21,8$\cdot 10^{-3}$) para todas as algas no secadoiro empregado.
- As **características físicas** dos pos son diferentes en función das algas empregadas: o diámetro medio de superficie (μm) do po de FV é o máis alto (133 - 147) en comparación con BB (106 - 126) e AN (77 - 108) con distribucións bimodales de tamaño de partícula para FV e AN e unimodal para BB. Estes valores están no rango de aditivos comerciais para fariña. Os parámetros de cor da fariña integral poden ser estimados a través dos parámetros de cores das fraccións de masa correspondentes mediante unha regra de mestura. O po de BB ten a maior capacidade de retención de auga e capacidade de inchazón, sen diferenzas significativas nestes parámetros entre os pos de AN e FV.

- As **características das fariñas** dependen das materias primas amidáceas empregadas: o diámetro medio de superficie (μm) das fariñas de millo branco é o máis alto (97.1 - 166.7) en comparación co amarelo (67.8-99.8) e morado (60,4 - 91,9) e a castaña (35,4) con distribucións bimodales de tamaño de partícula. Os parámetros de cor da fariña enteira poden ser estimados a través dos parámetros de cor das fraccións de masa correspondentes mediante unha regra de mestura. Non se observan diferenzas significativas no amidón total (TS, b.s.) para tódalas fariñas de millo (60-75 %). As fariñas de castaña presentan menor TS (51 %). O amidón danado (b.s.) de fariñas obtidas empregando as mesmas condicións de moenda é maior para o millo branco (25 %) que o millo morado (18 %) e o millo amarelo e a castaña ($\approx$ 8%).

- As altas temperaturas de secado diminúen drasticamente (ata un 54% a 75°C en comparación con 35°C) o contido total polifenólico (TP) e actividade antioxidante (SA) de **extractos acuosos das algas**. As temperaturas de secado máis axeitadas son 35°C para BB e FV e $\leqslant$ 50°C para AN. O máis alto valor de TP ($\approx$ 3000 mg de PHL /100 g de po seco) e SA corresponde a AN ($\approx$ 75 %) seguido dos extractos de BB e FV. Hai unha relación lineal entre a SA ($>$ 45 %) dos extractos e a cor verde (parámetro a*) do po de algas. O contido de hidratos de carbono (CHO) diminúe (ata un 25 %) coa temperatura de secado crecente ($>$ 60°C) para AN e BB e permanece constante para FV. O maior CHO corresponde a FV e AN ($\approx$ 6000 mg GL /100 g de po seco).

- As **características de mestura fariña-auga** das distintas fariñas de millo son específicas. A absorción de auga (WA, 55 - 91 % base de fariña, b.f.) depende do contido de amidón danado (DS, 3-25 % d.b.), polo tanto, canto máis elevado é o DS maior e a WA. A maior tamaño das partículas, o WA é máis baixo e maior tempo de desenvolvemento e a estabilidade das masas.

- A goma de guar (2 % b.f.) é necesaria para obter masas de fariña de castaña con características de mestura adecuadas. A adición de po de algas (ata 9 % b.f.) aumenta significativamente a WA e mellora as características de mestura das masas de fariña de castaña: mellor estabilidade (tempos superiores), debilitamento mecánico e retrogradación (valores inferiores C2 e C5, respectivamente).

- Os **espectros mecánicos** das masas libres de glute son axeitados debido a que teñen a proporción elástica (módulo de almacenamento, $G^{'}$) superior ao viscoso (módulo de perda, $G^{''}$) así como ocorre nas masas con glute. Para unha mesma consistencia, as masas de fariña de castaña teñen os máis altos módulos, seguidos de millo amarelo, vermello e branco. En todos os

casos, o maior tamaño das partículas de fariña resulta en valores superiores dos módulos. En xeral, a presenza de pos de algas na masa de fariña de castaña diminúe significativamente os dous módulos. A presenza de amidón xelatinizado modifica a viscoelasticidade das masas (carácter viscoso máis baixo).

- Os datos experimentais de **fluencia e recuperación** están dacordo cos observados nos espectros mecánicos. As masas máis ríxidas (altos valores de G') mostran unha menor deformación instantánea de fluencia e recuperación e menor capacidade de deformación. Diferentes cantidades de algas poden ser engadidas á fariña de castaña sen perxudicar as propiedades de recuperación das masas: 9 % de AN e FV e 6 % de BB. O amidón xelatinizado mellora a recuperación relativa de deformación das masas (de 80 % a 90 %). Todos os valores obtidos están no mesmo rango aos obtidos para masas de fariña sen glute.

- O **Análise Dinámico Mecánico-Térmico** (DMTA, polas súas siglas en inglés) é validado como unha válida técnica experimental para determinar as transicións térmicas (inchazón e xelatinización do almidón (G, 50 - 85°C e M1, 85 - 104°C), fusión de complexos amilosa-lípido (M2, 104 - 124°C) e amilosa (M3, 131 - 160°C)). Proponse un protocolo completo para a determinación destas transicións mediante a avaliación (puntos máximos, mínimos e de inflexión) das tendencias térmicas de G' e/ou tanδ.

- As transicións térmicas nas masas de millo e castaña dependen da WA. En xeral, a WA alta implica valores máis baixos das temperaturas características das transicións. Os valores baixos de WA permiten determinar a transición de gelatinización por separado (G e M1). A adición de algas á masa de fariña de castaña anticipa significativamente ($\approx$ 2°C, debido ás altas WA) a rotura dos gránulos de amidón. Os picos atopados están relacionados cos procesos implicados na formación de codia durante o enfornado de produtos de almidón.

- A fariña de castaña pode ser **almacenada** durante polo menos un ano, a 4°C en bolsas seladas ao baleiro, despois da súa fabricación. Durante este período, as propiedades de mestura, reolóxicas e termomecánicas das súas masas son invariantes.

- A adición de po de algas aumenta significativamente a SA (15-30 %) das mesturas de fariña obtidas pero non se observan diferenzas na SA das **galletas** unha vez enfornadas. A cor verde das galletas enfornadas aumenta coa presenza de pos de algas. A dureza e o módulo de Young das galletas aumentan con adición de algas superiores ao 6 % (b.f.) e ámbolos dous

permanecen invariantes por baixo deste valor. O proceso de enfornado aumenta significativamente o TP (de ≈ 100 a ≈ 700 mg de PHL /100 g de po seco) e a SA (de ≈ 12 % a ≈ 59 %) das galletas en comparación coas mesturas de fariña antes de enfornar.

- A adición *Fucus vesiculosus* aumenta significativamente a viscosidade elongacional (de $1{,}2{\cdot}10^5$ a $3{,}5{\cdot}10^5$ Pa·s a 0,025 s^{-1} e a estabilidade (≈ 20 %) de masa de trigo. Ten un efecto negativo sobre a porosidade final da masa (valores inferiores, de 0.77 a 0.52) o que leva a un aumento da densidade do pan e do módulo aparente da miga. Unha adición de algas superior ao 4 % (b.f.) aumenta significativamente a densidade do pan (> 36 %) e a dureza da miga do pan (46 %).

Resumindo, a mestura e as características reolóxicas das masas sen glute obtidas a partir de fariña de castaña e de millo indican que se poden clasificar como fariñas de pastelería. Tendo en conta isto, elaboráronse galletas de fariña de castañas e mesturas de fariña de castañas enriquecidas con algas para analizar e comparar as súas características con outras galletas comerciais (con ou sen glute) da bibliografía. Os resultados obtidos permiten establecer algúns comentarios importantes para os produtos enfornados obtidos (**galletas**):

- **Propiedades antioxidantes**: as galletas de castaña enriquecidas con algas mostraron un contido de polifenoles máis elevado que as de fariña de trigo e outras sen glute, como as galletas de arroz e trigo sarraceno. Neste sentido, as galletas de castañas enriquecidas con algas son axeitadas.
- **Propiedades de cor**: as galletas amosaron tendencias á cor verde e amarela como outras galletas comerciais. O principal diferencia das galletas de castaña analizadas é o baixo valor do brillo, aínda que é aceptable.
- **Propiedades texturais**: a dureza e a elasticidade das cookies están no límite superior dos valores de intervalo comercial habitual para as galletas. A mellora da calidade da textura destas cookies será un desafío futuro polas novas formulacións e/ou condicións de procesamento diferentes.

Finalmente, as galletas obtidas ou os produtos mellorados tendo en conta as observacións anteriores necesitarán estudos adicionais previos á comercialización. Os investigadores correspondentes deben realizar un completo estudo de caracterización nutricional, embalaxe e almacenamento, así como a análise sensorial e de aceptación do produto enfornado por parte dos consumidores.

Bibliography

Adekunte, A. O., Tiwari, B. K., Cullen, P. J., Scannell, A. G. M. & O'Donnell, C. P. (2010). Effect of sonication on colour, ascorbic acid and yeast inactivation in tomato juice. *Food Chemistry* **122**, 500 – 507. DOI: http://dx.doi.org/10.1016/j.foodchem.2010.01.026.

Adua, M. (1999). The sweet chestnut throughout history from the miocene to the third millennium. *Acta Horticulturae* **494**, 29–36. DOI: http://doi.org/10.17660/ActaHortic.1999.494.2.

AFNOR (2002). *BIPEA standard method for French breadmaking, V03 716*. Paris, France: Association Française de Normalisation.

Ahmed, J., Ramaswamy, H. S., Ayad, A., Alli, I. & Alvarez, P. (2007). Effect of high-pressure treatment on rheological, thermal and structural changes in basmati rice flour slurry. *Journal of Cereal Science* **46**, 148 – 156. DOI: http://dx.doi.org/10.1016/j.jcs.2007.01.006.

Ai, Y. & Jane, J.-l. (2015). Gelatinization and rheological properties of starch. *Starch - Stärke* **67**, 213–224. DOI: http://doi.org/10.1002/star.201400201.

Ait Mohamed, L., Kouhila, M., Lahsasni, S., Jamali, A., Idlimam, A., Rhazi, M., Aghfir, M. & Mahrouz, M. (2005). Equilibrium moisture content and heat of sorption of *Gelidium sesquipedale*. *Journal of Stored Products Research* **41**, 199 – 209. DOI: http://dx.doi.org/10.1016/j.jspr.2004.03.001.

Al-Muhtaseb, A. H., McMinn, W. & Magee, T. (2004). Water sorption isotherms of starch powders. part 2: Thermodynamic characteristics. *Journal of Food Engineering* **62**, 135 – 142. DOI: http://dx.doi.org/10.1016/S0260-8774(03)00202-4.

Allsopp, P., Crowe, W., Bahar, B., Harnedy, P. A., Brown, E. S., Taylor, S. S., Smyth, T. J., Soler-Vila, A., Magee, P. J., Gill, C. I. R., Strain, C. R., Hegan, V., Devaney, M., Wallace, J. M. W., Cherry, P., FitzGerald, R. J., Strain, J. J., O'Doherty, J. V. & McSorley, E. M. (2016). The effect of consuming *Palmaria palmata*-enriched bread on inflammatory markers, antioxidant status, lipid profile and thyroid function in a randomised placebo-controlled intervention trial in healthy adults. *European Journal of Nutrition* **55**, 1951–1962. DOI: http://doi.org/10.1007/s00394-015-1011-1.

Altindag, G., Certel, M., Erem, F. & Ilknur Konak, U. (2015). Quality characteristics of gluten-free cookies made of buckwheat, corn, and rice flour with/without transglutaminase. *Food science and technology international* **21**, 213–220. DOI: http://doi.org/10.1177/1082013214525428.

Angioloni, A. & Dalla Rosa, M. (2005). Dough thermo-mechanical properties: influence of sodium chloride, mixing time and equipment. *Journal of Cereal Science* **41**, 327 – 331. DOI: http://dx.doi.org/10.1016/j.jcs.2004.10.004.

AOAC (1995). *Official methods of analysis of AOAC International*. Washington, USA: Association of Official Analytical Chesmist, 16th ed.

Šaponjac, V. T., Ćetković, G., Čanadanović Brunet, J., Pajin, B., Djilas, S., Petrović, J., Lončarević, I., Stajčić, S. & Vulić, J. (2016). Sour cherry pomace extract encapsulated in whey and soy proteins: Incorporation in cookies. *Food Chemistry* **207**, 27 – 33. DOI: http://dx.doi.org/10.1016/j.foodchem.2016.03.082.

Aponte, M., Boscaino, F., Sorrentino, A., Coppola, R., Masi, P. & Romano, A. (2013). Volatile compounds and bacterial community dynamics of chestnut-flour-based sourdoughs. *Food Chemistry* **141**, 2394 – 2404. DOI: http://dx.doi.org/10.1016/j.foodchem.2013.05.052.

Aponte, M., Boscaino, F., Sorrentino, A., Coppola, R., Masi, P. & Romano, A. (2014). Effects of fermentation and rye flour on microstructure and volatile compounds of chestnut flour based sourdoughs. *LWT - Food Science and Technology* **58**, 387 – 395. DOI: http://dx.doi.org/10.1016/j.lwt.2014.03.022.

Atwell, W., Hood, L., Lineback, D., Varriano-Marston, E. & Zobel, H. (1988). The terminology and methodology associated with basic starch phenomena. *Cereal foods world.* **33**, 306.

Bahloul, N., Boudhrioua, N. & Kechaou, N. (2008). Moisture desorption–adsorption isotherms and isosteric heats of sorption of tunisian olive leaves (*Olea europaea L.*). *Industrial Crops and Products* **28**, 162 – 176. DOI: http://dx.doi.org/10.1016/j.indcrop.2008.02.003.

Bahorun, T., Luximon-Ramma, A., Crozier, A. & Aruoma, O. I. (2004). Total phenol, flavonoid, proanthocyanidin and vitamin c levels and antioxidant activities of mauritian vegetables. *Journal of the Science of Food and Agriculture* **84**, 1553–1561. DOI: http://doi.org/10.1002/jsfa.1820.

Balachandran, S., Kentish, S., Mawson, R. & Ashokkumar, M. (2006). Ultrasonic enhancement of the supercritical extraction from ginger. *Ultrasonics Sonochemistry* **13**, 471 – 479. DOI: http://dx.doi.org/10.1016/j.ultsonch.2005.11.006.

Balboa, E. M., Conde, E., Moure, A., Falqué, E. & Domínguez, H. (2013). In vitro antioxidant properties of crude extracts and compounds from brown algae. *Food Chemistry* **138**, 1764 – 1785. DOI: http://dx.doi.org/10.1016/j.foodchem.2012.11.026.

Baltsavias, A., Jurgens, A. & van Vliet, T. (1997). Rheological properties of short doughs at small deformation. *Journal of Cereal Science* **26**, 289 – 300. DOI: http://dx.doi.org/10.1006/jcrs.1997.0133.

Barbosa-Cánovas, G. V., Fontana, A. J., Schmid, S. J. & Labuza, T. P. (2007). *Water activity in fodds. Fundamentals and applications*. Iowa: Blackwell Publishing.

Barnes, H. A., Hutton, J. F. & Walters, K. (1993). *An introduction to rheology*. Amsterdam: Elsevier.

Barreira, J. C. M., Alves, R. C., Casal, S., Ferreira, I. C. F. R., Oliveira, M. B. P. P. & Pereira, J. A. (2009). Vitamin e profile as a reliable authenticity discrimination factor between chestnut (*Castanea sativa Mill.*) cultivars. *Journal of Agricultural and Food Chemistry* **57**, 5524–5528. DOI: http://doi.org/10.1021/jf900435y.

Basu, S., Shivhare, U. S. & Mujumdar, A. S. (2006). Models for sorption isotherms for foods: A review. *Drying Technology* **24**, 917–930. DOI: http://doi.org/10.1080/07373930600775979.

Baucour, P. & Daudin, J. (2000). Development of a new method for fast measurement of water sorption isotherms in the high humidity range validation on gelatine gel. *Journal of Food Engineering* **44**, 97 – 107. DOI: http://dx.doi.org/10.1016/S0260-8774(99)00171-5.

Bchir, B., Rabetafika, H. N., Paquot, M. & Blecker, C. (2014). Effect of pear, apple and date fibres from cooked fruit by-products on dough performance and bread quality. *Food and Bioprocess Technology* **7**, 1114–1127. DOI: http://doi.org/10.1007/s11947-013-1148-y.

Bell, N. L. & Labuza, N. T. (2000). *Moisture Sorption: Practical Aspects of Isotherm Measurement and Use*. St Paul, USA: Ameriacan Association of Cereal Chemists (AACC).

Benatti, P., Peluso, G., Nicolai, R. & Calvani, M. (2004). Polyunsaturated fatty acids: Biochemical, nutritional and epigenetic properties. *Journal of the American College of Nutrition* **23**, 281–302. DOI: http://doi.org/10.1080/07315724.2004.10719371.

Bertness, M., Bruno, J., Silliman, B. & Stachowicz, J. (2014). *Marine community ecology and conservation*. Sunderland, USA: Sinauer Associates Inc.

Besbes, E., Jury, V., Monteau, J.-Y. & Le Bail, A. (2014). Effect of baking conditions and storage with crust on the moisture profile, local textural properties and staling kinetics of pan bread. *LWT - Food Science and Technology* **58**, 658 – 666. DOI: http://dx.doi.org/10.1016/j.lwt.2014.02.037.

Biliaderis, C. G., Page, C. M., Maurice, T. J. & Juliano, B. O. (1986). Thermal characterization of rice starches: a polymeric approach to phase transitions of granular starch. *Journal of Agricultural and Food Chemistry* **34**, 6–14. DOI: http://doi.org/10.1021/jf00067a002.

Bird, R. B., Stewart, W. E. & Lightfoot, E. N. (2002). *Transport phenomena*. New York: John Wiley & Sons Inc., 2nd ed.

Bloksma, A. (1990). Dough structure, dough rheology, and baking quality. *Cereal Foods World* **35**(237-244).

Bogracheva, T. Y., Wang, Y. L., Wang, T. L. & Hedley, C. L. (2002). Structural studies of starches with different water contents. *Biopolymers* **64**, 268–281. DOI: http://doi.org/10.1002/bip.10190.

Bolade, M. K., Adeyemi, I. A. & Ogunsua, A. O. (2009). Influence of particle size fractions on the physicochemical properties of maize flour and textural characteristics of a maize-based nonfermented food gel. *International Journal of Food Science & Technology* **44**, 646–655. DOI: http://doi.org/10.1111/j.1365-2621.2008.01903.x.

Bonazzi, C. & Dumoulin, E. (2011). *Modern Drying Technology, Volume 3: Product Quality and Formulation*, chap. Quality Changes in Food Materials as Influenced by Drying Processes. Wiley-VCH Verlag GmbH & Co. KGaA, pp. 1–20.

Bonet, A., Blaszczak, W. & Rosell, C. M. (2006). Formation of homopolymers and heteropolymers between wheat flour and several protein sources by transglutaminase-catalyzed cross-linking. *Cereal Chemistry* **83**, 655–662. DOI: http://doi.org/10.1094/CC-83-0655.

Bonnand-Ducasse, M., Della Valle, G., Lefebvre, J. & Saulnier, L. (2010). Effect of wheat dietary fibres on bread dough development and rheological properties. *Journal of Cereal Science* **52**, 200 – 206. DOI: http://dx.doi.org/10.1016/j.jcs.2010.05.006.

Borges, O., Gonçalves, B., de Carvalho, J. L. S., Correia, P. & Silva, A. P. (2008). Nutritional quality of chestnut (*Castanea sativa Mill.*) cultivars from portugal. *Food Chemistry* **106**, 976 – 984. DOI: http://dx.doi.org/10.1016/j.foodchem.2007.07.011.

Borges, O. P., Carvalho, J. S., Correia, P. R. & Silva, A. P. (2007). Lipid and fatty acid profiles of *Castanea sativa Mill.* chestnuts of 17 native portuguese cultivars. *Journal of Food Composition and Analysis* **20**, 80 – 89. DOI: http://doi.org/10.1016/j.jfca.2006.07.008.

Borrelli, M., Maglio, M., Agnese, M., Paparo, F., Gentile, S., Colicchio, B., Tosco, A., Auricchio, R. & Troncone, R. (2010). High density of intraepithelial γ δ lymphocytes and deposits of immunoglobulin (ig)m anti-tissue transglutaminase antibodies in the jejunum of coeliac patients with iga deficiency. *Clinical & Experimental Immunology* **160**, 199–206. DOI: http://doi.org/10.1111/j.1365-2249.2009.04077.x.

Bourekoua, H., Benatallah, L., Zidoune, M. N. & Rosell, C. M. (2016). Developing gluten free bakery improvers by hydrothermal treatment of rice and corn flours. *LWT - Food Science and Technology* **73**, 342 – 350. DOI: http://dx.doi.org/10.1016/j.lwt.2016.06.032.

Bourne, M. (2002). *Food Texture and Viscosity: Concept and Measurement*. London: Academic Press.

Braga, N., Rodrigues, F. & Oliveira, M. B. P. (2015). *Castanea sativa* by-products: a review on added value and sustainable application. *Natural Product Research* **29**, 1–18. PMID: 25204784. DOI: http://doi.org/10.1080/14786419.2014.955488.

Brand-Williams, W., Cuvelier, M. & Berset, C. (1995). Use of a free radical method to evaluate antioxidant activity. *LWT - Food Science and Technology* **28**, 25 – 30. DOI: http://dx.doi.org/10.1016/S0023-6438(95)80008-5.

Brennan, J. G. (1994). *Food Dehydration: A Dictionary Guide*. Woodhead Publishing.

Brummer, Y. & Cui, S. W. (2005). *Food carbohydrates: chemistry, physical properties and applications*, chap. Understanding carbohydrate analysis. Boca Raton, USA: CRC Press, pp. 68–104.

Brunauer, S., Deming, L., Deming, W. & Teller, E. (1940). On a theory of the van der Waals adsorption of gases. *Journal of the American Chemical Society* **62**, 1723–1732. DOI: http://doi.org/10.1021/ja01269a023.

Brunauer, S., Emmett, P. H. & Teller, E. (1938). Adsorption of gases in multimolecular layers. *Journal of the American Chemical Society* **60**, 309–319. DOI: http://doi.org/10.1021/ja01269a023.

Burgers, J. M. (1935). *First report on viscosity and plasticity*. New York, USA: Nordemann Publishing Company.

Burritt, D. J., Larkindale, J. & Hurd, C. L. (2002). Antioxidant metabolism in the intertidal red seaweed *Stictosiphonia arbuscula* following desiccation. *Planta* **215**, 829–838. DOI: http://doi.org/10.1007/s00425-002-0805-6.

Bushuk, W., Hay, R. L., Larsen, N. G., Sara, R. G., Simmons, L. D. & Sutton, K. H. (1997). Effect of mechanical dough development on the extractability of wheat storage proteins from bread dough. *Cereal Chemistry* **74**, 389–395.

Campanha, R. & Franco, C. (2011). Gelatinization properties of native starches and their näegeli dextrins. *Journal of Thermal Analysis and Calorimetry,* **103**, 799–804. DOI: http://doi.org/10.1007/s10973-011-1682-7.

Capriles, V. D., dos Santos, F. G. & Arêas, J. A. G. (2016). Gluten-free breadmaking: Improving nutritional and bioactive compounds. *Journal of Cereal Science* **67**, 83 – 91. DOI: http://dx.doi.org/10.1016/j.jcs.2015.08.005.

Cavella, S., Romano, A., Giancone, T. & Masi, P. (2008). *Bubbles in Food 2: Novelty, Health and Luxury*, chap. The influence of dietary fibres on

bubble development during bread making. St Paul, EEUU: Eagan Press, pp. 311–322.

Chan, J. C.-C., Cheung, P. C.-K. & Ang, P. O. (1997). Comparative studies on the effect of three drying methods on the nutritional composition of seaweed *Sargassum hemiphyllum* (turn.) c. ag. *Journal of Agricultural and Food Chemistry* **45**, 3056–3059. DOI: http://doi.org/10.1021/jf9701749.

Chanvrier, H., Appelqvist, I. A., Li, Z., Morell, M. K. & Lillford, P. J. (2013). Processing high amylose wheat varieties with a capillary rheometer: Structure and thermomechanical properties of products. *Food Research International* **53**, 73 – 80. DOI: http://dx.doi.org/10.1016/j.foodres.2013.03.040.

Chauhan, A., Saxena, D. & Singh, S. (2015). Total dietary fibre and antioxidant activity of gluten free cookies made from raw and germinated amaranth (*Amaranthus spp.*) flour. *LWT - Food Science and Technology* **63**, 939 – 945. DOI: http://dx.doi.org/10.1016/j.lwt.2015.03.115.

Chen, F., Sun, Y., Zhao, G., Liao, X., Hu, X., Wu, J. & Wang, Z. (2007). Optimization of ultrasound-assisted extraction of anthocyanins in red raspberries and identification of anthocyanins in extract using high-performance liquid chromatography–mass spectrometry. *Ultrasonics Sonochemistry* **14**, 767 – 778. DOI: http://dx.doi.org/10.1016/j.ultsonch.2006.12.011.

Chen, X. D. & Mujumdar, A. S. (2009). *Drying Technologies in Food Processing*. Boca Raton, FL, USA: John Wiley & Sons.

Chevallier, S., Zúñiga, R. & Le-Bail, A. (2012). Assessment of bread dough expansion during fermentation. *Food and Bioprocess Technology* **5**, 609–617. DOI: http://doi.org/10.1007/s11947-009-0319-3.

Chew, Y., Lim, Y., Omar, M. & Khoo, K. (2008). Antioxidant activity of three edible seaweeds from two areas in south east asia. *LWT - Food Science and Technology* **41**, 1067 – 1072. DOI: http://dx.doi.org/10.1016/j.lwt.2007.06.013.

Collar, C., Balestra, F. & Ancarani, D. (2014). Value added of resistant starch maize-based matrices in breadmaking: Nutritional and functional assessment. *Food and Bioprocess Technology* **7**, 3579–3590. DOI: http://doi.org/10.1007/s11947-014-1371-1.

Connan, S., Deslandes, E. & Ar Gall, E. (2007). Influence of day–night and tidal cycles on phenol content and antioxidant capacity in three temperate

intertidal brown seaweeds. *Journal of Experimental Marine Biology and Ecology* **349**, 359 – 369. DOI: http://dx.doi.org/10.1016/j.jembe.2007.05.028.

Corbin, C., Fidel, T., Leclerc, E. A., Barakzoy, E., Sagot, N., Falguiéres, A., Renouard, S., Blondeau, J.-P., Ferroud, C., Doussot, J., Lainé, E. & Hano, C. (2015). Development and validation of an efficient ultrasound assisted extraction of phenolic compounds from flax (*Linum usitatissimum* l.) seeds. *Ultrasonics Sonochemistry* **26**, 176 – 185. DOI: http://dx.doi.org/10.1016/j.ultsonch.2015.02.008.

Cornish, M. L. & Garbary, D. J. (2010). Antioxidants from macroalgae: potential applications in human health and nutrition. *ALGAE* **25**, 155–171. DOI: http://doi.org/10.4490/algae.2010.25.4.155.

Correia, P. & Beirao da Costa, M. L. (1999). Potentialities of chestnut for starch production. *Acta Horticulturae* **866**, 581–586. DOI: http://doi.org/10.17660/ActaHortic.2010.866.78.

Cox, S., Abu-Ghannam, N. & Gupta, S. (2012). Effect of processing conditions on phytochemical constituents of edile seaweed *Himanthalia elongata*. *Journal of Food Processing and Preservation* **36**, 348–363. DOI: http://doi.org/10.1111/j.1745-4549.2011.00563.x.

Crank, J. (1975). *The Mathematics of Diffusion*. Oxford: Oxford University Press, 2nd ed.

Cruces, E., Rojas-Lillo, Y., Ramirez-Kushel, E., Atala, E., López-Alarcón, C., Lissi, E. & Gómez, I. (2016). Comparison of different techniques for the preservation and extraction of phlorotannins in the kelp *Lessonia spicata* (*Phaeophyceae*): assays of dpph, orac-pgr, and orac-fl as testing methods. *Journal of Applied Phycology* **28**, 573–580. DOI: http://doi.org/10.1007/s10811-015-0602-9.

Cruz, B. R., Abraão, A. S., Lemos, A. M. & Nunes, F. M. (2013). Chemical composition and functional properties of native chestnut starch (*Castanea sativa Mill.*). *Carbohydrate Polymers* **94**, 594 – 602. DOI: http://doi.org/10.1016/j.carbpol.2012.12.060.

da Silva, A. N., Coimbra, J. S. d. R., Botelho, F. M., de Moraes, M. N., de Faria, J. T., Bezerra, M. d. C. T., Martins, M. A. & Siqueira, A. M. d. O. (2013). Pear drying: Thermodynamics studies and coefficients of convective heat and mass transfer. *International Journal of Food Engineering* **9**, 365–374. DOI: http://doi.org/10.1515/ijfe-2012-0247.

Dall'Asta, C., Cirlini, M., Morini, E., Rinaldi, M., Ganino, T. & Chiavaro, E. (2013). Effect of chestnut flour supplementation on physico-chemical properties and volatiles in bread making. *LWT - Food Science and Technology* **53**(1), 233 – 239. DOI: http://dx.doi.org/10.1016/j.lwt.2013.02.025.

Darghalkar, V. & Kavlekar, D. (2004). *Seaweeds- a field manual*, vol. 1. Dona Paula, Goa, India: N.I.O. Manual.

Díaz-Rubio, M. E., Pérez-Jiménez, J. & Saura-Calixto, F. (2009). Dietary fiber and antioxidant capacity in *Fucus vesiculosus* products. *International Journal of Food Sciences and Nutrition* **60**, 23–34. DOI: http://doi.org/10.1080/09637480802189643.

De Vasconcelos, M. C., Bennett, R. N., Rosa, E. A. & Ferreira-Cardoso, J. V. (2010). Composition of european chestnut (*Castanea sativa Mill.*) and association with health effects: fresh and processed products. *Journal of the Science of Food and Agriculture* **90**, 1578–1589. DOI: http://doi.org/10.1002/jsfa.4016.

Debet, M. R. & Gidley, M. J. (2007). Why do gelatinized starch granules not dissolve completely? roles for amylose, protein, and lipid in granule "ghost" integrity. *Journal of Agricultural and Food Chemistry* **55**, 4752–4760. DOI: http://doi.org/10.1021/jf070004o.

Delgado-Vargas, F. & Paredes-Lopez, O. (2002). *Natural colorants for food and nutraceutical uses*. Boca Raton, USA: CRC Press.

Demirkesen, I. (2016). Formulation of chestnut cookies and their rheological and quality characteristics. *Journal of Food Quality* **39**, 264–273. DOI: http://doi.org/10.1111/jfq.12209.

Demirkesen, I., Campanella, O. H., Sumnu, G., Sahin, S. & Hamaker, B. R. (2014). A study on staling characteristics of gluten-free breads prepared with chestnut and rice flours. *Food and Bioprocess Technology* **7**, 806–820. DOI: http://doi.org/10.1007/s11947-013-1099-3.

Demirkesen, I., Mert, B., Sumnu, G. & Sahin, S. (2010). Utilization of chestnut flour in gluten-free bread formulations. *Journal of Food Engineering* **101**, 329 – 336. DOI: https://doi.org/10.1016/j.jfoodeng.2010.07.017.

Demirkesen, I., Sumnu, G. & Sahin, S. (2013). Image analysis of gluten-free breads prepared with chestnut and rice flour and baked in different ovens. *Food and Bioprocess Technology* **6**, 1749–1758. DOI: http://doi.org/10.1007/s11947-012-0850-5.

Demirkesen, I., Sumnu, G., Sahin, S. & Uysal, N. (2011). Optimisation of formulations and infrared–microwave combination baking conditions of chestnut–rice breads. *International Journal of Food Science & Technology* **46**, 1809–1815. DOI: http://doi.org/10.1111/j.1365-2621.2011.02682.x.

Domínguez, I. L., Azuara, E., Vernon-Carter, E. J. & Beristain, C. I. (2007). Thermodynamic analysis of the effect of water activity on the stability of macadamia nut. *Journal of Food Engineering* **81**, 566 – 571. DOI: http://dx.doi.org/10.1016/j.jfoodeng.2006.12.012.

Donovan, J. W. (1979). Phase transitions of the starch–water system. *Biopolymers* **18**, 263–275. DOI: http://doi.org/10.1002/bip.1979.360180204.

Drazkiewicz, M. & Krupa, Z. (1991). The participation of chlorophyllase in chlorophyll metabolism. *Acta Societatis Botanicorum Poloniae* **60**, 139–154. DOI: http://doi.org/10.5586/asbp.1991.012.

DuBois, M., Gilles, K. A., Hamilton, J. K., Rebers, P. A. & Smith, F. (1956). Colorimetric method for determination of sugars and related substances. *Analytical Chemistry* **28**, 350–356. DOI: http://doi.org/10.1021/ac60111a017.

EC (2015). *European Union Novel Food Catalogue*. European Commission. URL `http://ec.europa.eu/food/safety/novel_food/catalogue/index_en.htm`. Accessed 12 April 2016.

Edwards, W. P. (2007). *The Science of Bakery Products*. RSC Publishing.

Eliasson, A.-C. (1980). Effect of water content on the gelatinization of wheat starch. *Starch - Stärke* **32**, 270–272. DOI: http://doi.org/10.1002/star.19800320806.

Eliasson, A. C. (2004). *Starch in food*. CRC Press.

Şensoy, ı., Rosen, R. T., Ho, C.-T. & Karwe, M. V. (2006). Effect of processing on buckwheat phenolics and antioxidant activity. *Food Chemistry* **99**, 388 – 393. DOI: http://dx.doi.org/10.1016/j.foodchem.2005.08.007.

Erge, H. S., Karaden, Z., Koca, N. & Soyer, Y. (2008). Effect of heat treatment on chlorophyll degradation and color loss in green peas. *Gida* **33**, 225–233.

Escribano-Bailon, M. T., Santos-Buelga, C. & Rivas-Gonzalo, J. C. (2004). Anthocyanins in cereals. *Journal of Chromatography A* **1054**, 129 – 141. Food Science. DOI: http://dx.doi.org/10.1016/j.chroma.2004.08.152.

Evans, I. D. & Haisman, D. R. (1982). The effect of solutes on the gelatinization temperature range of potato starch. *Starch - Stärke* **34**, 224–231. DOI: http://doi.org/10.1002/star.19820340704.

Fan, D., Hodges, D. M., Zhang, J., Kirby, C. W., Ji, X., Locke, S. J., Critchley, A. T. & Prithiviraj, B. (2011). Commercial extract of the brown seaweed *Ascophyllum nodosum* enhances phenolic antioxidant content of spinach (*Spinacia oleracea* l.) which protects *Caenorhabditis elegans* against oxidative and thermal stress. *Food Chemistry* **124**, 195 – 202. DOI: http://dx.doi.org/10.1016/j.foodchem.2010.06.008.

FAOSTAT (2017). Statistics division of food and agriculture organization of the united nations. *Available from: http://www.fao.org/faostat* .

Fasina, O. O., Ajibola, O. & Tyler, R. (1999). Thermodynamics of moisture sorption in winged bean seed and gari. *Journal of Food Process Engineering* **22**, 405–418. DOI: http://doi.org/10.1111/j.1745-4530.1999.tb00496.x.

Feighery, C. (1999). Coeliac disease. *British Medical Journal* **319**.

Feigl, K., Kaufmann, S. F. M., Fischer, P. & Windhab, E. J. (2003). A numerical procedure for calculating droplet deformation in dispersing flows and experimental verification. *Chemical Engineering Science* **58**, 2351–2363.

Ferreira-Cardoso, J. V., Sequeira, C. A., Rodrigues, L. & Gomes, E. F. (1999). Lipid composition of *Castanea sativa Mill.* fruits of some native portuguese cultivars. *Acta Horticulturae* **494**, 133–138. DOI: http://doi.org/10.17660/ActaHortic.1999.494.19.

Ferrini, F. (1997). *Reseach on chestnut stoolbed propagation. COST G4-Workshop on Tree Physiology and Genetic Resources of Chestnut.* Torre Pellice, Italy.

Fitzgerald, M. (2004). *Rice: chemistry and technology*, chap. Starch. American Associaton of Cereal Chemists, pp. 109–141.

Flores-Silva, P. C., Berrios, J. D. J., Pan, J., Osorio-Díaz, P. & Bello-Pérez, L. A. (2014). Gluten-free spaghetti made with chickpea, unripe plantain and maize flours: functional and chemical properties and starch digestibility. *International Journal of Food Science & Technology* **49**, 1985–1991. DOI: http://doi.org/10.1111/ijfs.12529.

French, D. (1984). *Starch: Chemistry and Technology*, chap. Organization of starch granules. Orlando: Academic Press, pp. 183–256.

Fudholi, A., Ruslan, M. H., Haw, L. C., Mat, S., Othman, M. Y., Zaharim, A. & Sopian, K. (2012). Mathematical modelling of brown seaweed drying curves. In: *Proceedings of the 6th WSEAS International Conference on Computer Engineering and Applications, and Proceedings of the 2012 American Conference on Applied Mathematics*, AMERICAN-MATH'12/CEA'12. Stevens Point, Wisconsin, USA: World Scientific and Engineering Academy and Society (WSEAS).

Gallagher, E., Gormley, T. & Arendt, E. (2004). Recent advances in the formulation of gluten-free cereal-based products. *Trends in Food Science & Technology* **15**, 143 – 152. DOI: http://dx.doi.org/10.1016/j.tifs.2003.09.012.

Gallagher, E., Polenghi, O. & Gormley, T. R. (2002). Improving the quality of gluten-free breads. *Farm and Food* .

Gambus, H., Nowotna, A., Ziobro, R., Gumul, D. & Sikora, M. (2001). The effect of use of guar gum with pectin mixture in gluten-free bread. *Electronic Journal of Polish Agricultural Universities* .

Gerzhova, A., Mondor, M., Benali, M. & Aider, M. (2016). Incorporation of canola proteins extracted by electroactivated solutions in gluten-free biscuit formulation of rice–buckwheat flour blend: assessment of quality characteristics and textural properties of the product. *International Journal of Food Science & Technology* **51**, 814–827. DOI: http://doi.org/10.1111/ijfs.13034.

Ghiaus, A., Margaris, D. & Papanikas, D. (1997). Mathematical modeling of the convective drying of fruits and vegetables. *Journal of Food Science* **62**, 1154–1157. DOI: http://doi.org/10.1111/j.1365-2621.1997.tb12234.x.

Giménez-Bastida, J. A., Piskuła, M. & Zieliński, H. (2015). Recent advances in development of gluten-free buckwheat products. *Trends in Food Science & Technology* **44**, 58 – 65. DOI: http://dx.doi.org/10.1016/j.tifs.2015.02.013.

Gómez, M. & Martínez, M. M. (2016). Changing flour functionality through physical treatments for the production of gluten-free baking goods. *Journal of Cereal Science* **67**, 68 – 74. Functionality of Cereal Based Non-gluten Dough Systems. DOI: http://dx.doi.org/10.1016/j.jcs.2015.07.009.

Gómez, M., Talegón, M. & de la Hera, E. (2013). Influence of mixing on quality of gluten-free bread. *Journal of Food Quality* **36**, 139–145. DOI: http://doi.org/10.1111/jfq.12014.

Gómez-Ordóñez, E., Jiménez-Escrig, A. & Rupérez, P. (2010). Dietary fibre and physicochemical properties of several edible seaweeds from the northwestern spanish coast. *Food Research International* **43**, 2289 – 2294. DOI: http://dx.doi.org/10.1016/j.foodres.2010.08.005.

Goñi, I., Valdivieso, L. & Gudiel-Urbano, M. (2002). Capacity of edible seaweeds to modify in vitro starch digestibility of wheat bread. *Food / Nahrung* **46**, 18–20. DOI: http://doi.org/10.1002/1521-3803(20020101)46:1<18::AID-FOOD18>3.0.CO;2-C.

Greenspan, L. (1977). Humidity fixed points of binary saturated aqueous solutions. *Journal of Research of the National Bureau of Standards-A. Physics and Chemistry* **81**, 89–102.

Greer, E. N. & Stewart, B. A. (1959). The water absorption of wheat flour: Relative effects of protein and starch. *Journal of the Science of Food and Agriculture* **10**, 248–252. DOI: http://doi.org/10.1002/jsfa.2740100409.

Gularte, M. A., de la Hera, E., Gómez, M. & Rosell, C. M. (2012). Effect of different fibers on batter and gluten-free layer cake properties. *LWT - Food Science and Technology* **48**, 209 – 214. DOI: http://dx.doi.org/10.1016/j.lwt.2012.03.015.

Gupta, S., Cox, S. & Abu-Ghannam, N. (2011). Effect of different drying temperatures on the moisture and phytochemical constituents of edible irish brown seaweed. *LWT - Food Science and Technology* **44**, 1266–1272. DOI: http://doi.org/10.1016/j.lwt.2010.12.022.

Gwirtz, J. A. & Garcia-Casal, M. N. (2014). Processing maize flour and corn meal food products. *Annals of the New York Academy of Sciences* **1312**, 66–75. DOI: http://doi.org/10.1111/nyas.12299.

Hadnadev, T. D., Pajic-Lijakovic, I., Hadnadev, M., Mastilovic, J., Torbica, A. & Bugarski, B. (2013). Influence of starch sodium octenyl succinate on rheological behaviour of wheat flour dough systems. *Food Hydrocolloids* **33**, 376 – 383. DOI: http://dx.doi.org/10.1016/j.foodhyd.2013.04.008.

Hadnadev, T. D., Torbica, A. & Hadnadev, M. (2011). Rheological properties of wheat flour substitutes/alternative crops assessed by Mixolab®. *Procedia Food Science* **1**, 328 – 334. DOI: http://dx.doi.org/10.1016/j.profoo.2011.09.051.

Hahn, T., Lang, S., Ulber, R. & Muffler, K. (2012). Novel procedures for the extraction of fucoidan from brown algae. *Process Biochemistry* **47**, 1691 – 1698. DOI: http://dx.doi.org/10.1016/j.procbio.2012.06.016.

Hall, A. C., Fairclough, A. C., Mahadevan, K. & Paxman, J. R. (2012). *Ascophyllum nodosum* enriched bread reduces subsequent energy intake with no effect on post-prandial glucose and cholesterol in healthy, overweight males. a pilot study. *Appetite* **58**, 379 – 386. DOI: http://dx.doi.org/10.1016/j.appet.2011.11.002.

Halsey, G. (1948). Physical adsorption on non-uniform surfaces. *The Journal of Chemical Physics* **16**, 931–937. DOI: http://doi.org/10.1063/1.1746689.

Hamaker, B. R. (1994). *Rice science and technology*, chap. The influence of rice protins in rice quality. Marcel Dekker, pp. 177–194.

Hardman, E. W. (2002). Omega-3 fatty acids to augment cancer therapy. *Journal of Nutrition* **132**, 3508–3512.

Hardy F., G. M. (2003). *A check-list and atlas of the seaweeds of Britain and Ireland*. London, UK: British Phycological Society.

Hasjim, J., Srichuwong, S., Scott, M. P. & Jane, J.-L. (2009). Kernel composition, starch structure, and enzyme digestibility of opaque-2 maize and quality protein maize. *Journal of Agricultural and Food Chemistry* **57**, 2049–2055. DOI: http://doi.org/10.1021/jf803406y.

Heffernan, N., Smyth, T. J., FitzGerald, R. J., Soler-Vila, A. & Brunton, N. (2014). Antioxidant activity and phenolic content of pressurised liquid and solid–liquid extracts from four irish origin macroalgae. *International Journal of Food Science & Technology* **49**, 1765–1772. DOI: http://doi.org/10.1111/ijfs.12512.

Heo, S.-J., Park, E.-J., Lee, K.-W. & Jeon, Y.-J. (2005). Antioxidant activities of enzymatic extracts from brown seaweeds. *Bioresource Technology* **96**, 1613 – 1623. DOI: http://dx.doi.org/10.1016/j.biortech.2004.07.013.

Hiscock, S. (1979). *A field key to the British brown seaweeds (Heterokontophyta)*. AIDGAP.

Hoek, C., Mann, D. & Jahns, H. M. (1996). *Algae: An Introduction to Phycology*. Cambridge, UK: Cambridge University Press.

Holdt, S. L. & Kraan, S. (2011). Bioactive compounds in seaweed: functional food applications and legislation. *Journal of Applied Phycology* **23**, 543–597. DOI: http://doi.org/10.1007/s10811-010-9632-5.

Horn, S. J., Aasen, I. M. & Østgaard, K. (2000). Ethanol production from seaweed extract. *Journal of Industrial Microbiology and Biotechnology* **25**, 249–254. DOI: http://doi.org/10.1038/sj.jim.7000065.

Iglesias, H., Chirife, J. & Viollaz, P. (1976). Thermodynamics of water vapor sorption by sugar beet root. *International Journal of Food Science and Technology* **11**, 109–116. DOI: http://doi.org/10.1111/j.1365-2621.1976.tb00705.x.

Igual, M., García-Martínez, G., Camacho, M. & Martínez-Navarrete, N. (2010). Effect of thermal treatment and storage on the stability of organic acids and the functional value of grapefruit juice. *Food Chemistry* **118**, 291 – 299. DOI: http://dx.doi.org/10.1016/j.foodchem.2009.04.118.

Žilić, S., Kocadağli, T., Vančetović, J. & Gökmen, V. (2016). Effects of baking conditions and dough formulations on phenolic compound stability, antioxidant capacity and color of cookies made from anthocyanin-rich corn flour. *LWT - Food Science and Technology* **65**, 597 – 603. DOI: http://dx.doi.org/10.1016/j.lwt.2015.08.057.

Inglett, G. E., Chen, D. & Liu, S. X. (2015). Physical properties of gluten-free sugar cookies made from amaranth–oat composites. *LWT - Food Science and Technology* **63**, 214 – 220. DOI: http://dx.doi.org/10.1016/j.lwt.2015.03.056.

Inkaya, A. N., Gocmen, D., Ozturk, S. & Koksel, H. (2009). Investigation on the functional properties of chestnut flours and their potential utilization in low-fat cookies. *Food Science and Biotechnology* **14**, 1404–1410.

Jan, R., Saxena, D. & Singh, S. (2016). Physico-chemical, textural, sensory and antioxidant characteristics of gluten – free cookies made from raw and germinated chenopodium (*Chenopodium album*) flour. *LWT - Food Science and Technology* **71**, 281 – 287. DOI: http://dx.doi.org/10.1016/j.lwt.2016.04.001.

Jang, J. K. & Pyun, Y. R. (1996). Effect of moisture content on the melting of wheat starch. *Starch - Stärke* **48**, 48–51. DOI: http://doi.org/10.1002/star.19960480204.

Jayaraman, K. S., Das Gupta, D. K. & Babu Rao, N. (1990). Effect of pretreatment with salt and sucrose on the quality and stability of dehydrated

cauliflower. *International Journal of Food Science & Technology* **25**, 47–60. DOI: http://doi.org/10.1111/j.1365-2621.1990.tb01058.x.

Jefferson, D. R., Lacey, A. A. & Sadd, P. A. (2007). Crust density in bread baking: Mathematical modelling and numerical solutions. *Applied Mathematical Modelling* **31**, 209 – 225. DOI: http://dx.doi.org/10.1016/j.apm.2005.08.017.

Jiménez-Escrig, A., Jiménez-Jiménez, I., Pulido, R. & Saura-Calixto, F. (2001). Antioxidant activity of fresh and processed edible seaweeds. *Journal of the Science of Food and Agriculture* **81**, 530–534. DOI: http://doi.org/10.1002/jsfa.842.

Jiménez-Escrig, A. & Sánchez-Muniz, F. J. (2000). Dietary fibre from edible seaweeds: Chemical structure, physicochemical properties and effects on cholesterol metabolism. *Nutrition Research* **20**, 585 – 598. DOI: http://dx.doi.org/10.1016/S0271-5317(00)00149-4.

Jing, P., Bomser, J. A., Schwartz, S. J., He, J., Magnuson, B. A. & Giusti, M. M. (2008). Structure-function relationships of anthocyanins from various anthocyanin-rich extracts on the inhibition of colon cancer cell growth. *Journal of Agricultural and Food Chemistry* **56**, 9391–9398. PMID: 18800807. DOI: http://doi.org/10.1021/jf8005917.

Jovanovich, G. & Añón, M. C. (1999). Amylose–lipid complex dissociation. a study of the kinetic parameters. *Biopolymers* **49**, 81–89. DOI: http://doi.org/10.1002/(SICI)1097-0282(199901)49:1<81::AID-BIP8>3.0.CO;2-D.

Kadam, S. U., O'Donnell, C. P., Rai, D. K., Hossain, M. B., Burgess, C. M., Walsh, D., 3 & Tiwari, B. K. (2015a). Laminarin from irish brown seaweeds *Ascophyllum nodosum* and *Laminaria hyperborea*: Ultrasound assisted extraction, characterization and bioactivity. *Marine Drugs* **13**, 4270–4280. DOI: http://doi.org/10.3390/md13074270.

Kadam, S. U., Tiwari, B. K. & O'Donnell, C. P. (2013). Application of novel extraction technologies for bioactives from marine algae. *Journal of Agricultural and Food Chemistry* **61**, 4667–4675. DOI: http://doi.org/10.1021/jf400819p.

Kadam, S. U., Tiwari, B. K. & O'Donnell, C. P. (2015b). Effect of ultrasound pre-treatment on the drying kinetics of brown seaweed *Ascophyllum nodosum*. *Ultrasonics Sonochemistry* **23**, 302 – 307. DOI: http://dx.doi.org/10.1016/j.ultsonch.2014.10.001.

Kadam, S. U., Tiwari, B. K., Smyth, T. J. & O'Donnell, C. P. (2015c). Optimization of ultrasound assisted extraction of bioactive components from brown seaweed *Ascophyllum nodosum* using response surface methodology. *Ultrasonics Sonochemistry* **23**, 308 – 316. DOI: http://dx.doi.org/10.1016/j.ultsonch.2014.10.007.

Kahraman, K., Sakiyan, O., Ozturk, S., Koksel, H., Sumnu, G. & Dubat, A. (2008). Utilization of Mixolab® to predict the suitability of flours in terms of cake quality. *European Food Research and Technology* **227**, 565–570. DOI: http://doi.org/10.1007/s00217-007-0757-y.

Kaletunc, G. & Breslauer, K. J. (2003). *Characterization of Cereals and Flours: Properties, Analysis And Applications*. Marcel Dekker.

Kansou, K., Chiron, H., Della Valle, G., Ndiaye, A. & Roussel, P. (2014). Predicting the quality of wheat flour dough at mixing using an expert system. *Food Research International* **64**, 772 – 782. DOI: http://dx.doi.org/10.1016/j.foodres.2014.08.007.

Kaur, M., Sandhu, K. S., Arora, A. & Sharma, A. (2015). Gluten free biscuits prepared from buckwheat flour by incorporation of various gums: Physicochemical and sensory properties. *LWT - Food Science and Technology* **62**, 628 – 632. DOI: http://dx.doi.org/10.1016/j.lwt.2014.02.039.

Kaymak-Ertekin, F. & Gedik, A. (2005). Kinetic modelling of quality deterioration in onions during drying and storage. *Journal of Food Engineering* **68**, 443 – 453. DOI: http://dx.doi.org/10.1016/j.jfoodeng.2004.06.022.

Keetels, C., Oostergetel, G. & Vliet, T. V. (1996). Recrystallization of amylopectin in concentrated starch gels. *Carbohydrate Polymers* **30**, 61 – 64. DOI: http://dx.doi.org/10.1016/S0144-8617(96)00057-4.

Keyrouz, R., Abasq, M., Le Bourvellec, C., Blanc, N., Audibert, L., ArGall, E. & Hauchard, D. (2011). Total phenolic contents, radical scavenging and cyclic voltammetry of seaweeds from brittany. *Food Chemistry* **126**, 831 – 836. DOI: http://dx.doi.org/10.1016/j.foodchem.2010.10.061.

Khairy, H. M. & El-Sheikh, M. A. (2015). Antioxidant activity and mineral composition of three mediterranean common seaweeds from abu-qir bay, egypt. *Saudi Journal of Biological Sciences* **22**, 623 – 630. DOI: http://dx.doi.org/10.1016/j.sjbs.2015.01.010.

Khan, W., Zhai, R., Souleimanov, A., Critchley, A. T., Smith, D. L. & Prithiviraj, B. (2012). Commercial extract of ascophyllum nodosum

improves root colonization of alfalfa by its bacterial symbiont sinorhizobium meliloti. *Communications in Soil Science and Plant Analysis* **43**, 2425–2436. DOI: http://doi.org/10.1080/00103624.2012.708079.

Kieffer, R., Schurer, F., Köhler, P. & Wieser, H. (2007). Effect of hydrostatic pressure and temperature on the chemical and functional properties of wheat gluten: Studies on gluten, gliadin and glutenin. *Journal of Cereal Science* **45**, 285 – 292. DOI: http://dx.doi.org/10.1016/j.jcs.2006.09.008.

Kim, M. J., Kwak, H. S., Lee, M. J. & Kim, S. S. (2017). Quality predictive models for whole flour of immature wheat during storage and consumer acceptance on its baked product. *LWT - Food Science and Technology* **83**, 42 – 49. DOI: https://doi.org/10.1016/j.lwt.2017.04.078.

Kim, S. (ed.) (2011). *Handbook of Marine Macroalgae: Biotechnology and Applied Phycology*. New Delhi, India: John Wiley & Sons.

Kilinç, B., Cirik, S., Turan, G., Tekogul, H. & Koru, E. (2013). *Food Industry*, chap. Seaweeds for Food and Industrial Applications. InTech, pp. 735–748.

Künch, U., Scharer, H., Conedera, M., Sassella, A., Jermini, M. & Jelmini, G. (1999). Quality assesment of chestnut fruits. *Acta Horticulturae* **494**, 119–127. DOI: http://doi.org/10.17660/ActaHortic.1999.494.17.

Künsch, U., Schärer, H., Patrian, B., Höhn, E., Conedera, M., Sassella, A., Jermini, M. & Jelmini, G. (2001). Effects of roasting on chemical composition and quality of different chestnut (*Castanea sativa Mill.*) varieties. *Journal of the Science of Food and Agriculture* **81**, 1106–1112. DOI: http://doi.org/10.1002/jsfa.916.

Koivikko, R., Loponen, J., Pihlaja, K. & Jormalainen, V. (2007). High performance liquid chromatographic analysis of phlorotannins from the brown alga *Fucus vesiculosus*. *Phytochemical Analysis* **18**, 326–332. DOI: http://doi.org/10.1002/pca.986.

Korel, F. & Balaban, M. . (2009). *Tree nuts: composition, phytochemicals, and health effects*, chap. Chemical composition and health aspects of chestnut (*Castanea spp.*). CRC Press, pp. 171–181.

Krokida, M., Karathanos, V., Maroulis, Z. & Marinos-Kouris, D. (2003). Drying kinetics of some vegetables. *Journal of Food Engineering* **59**(4), 391 – 403. DOI: http://dx.doi.org/10.1016/S0260-8774(02)00498-3.

Krug, R., Hunter, W. & Grieger, R. (1976). Enthaply entropy compensation. 2. separation of the chemical from the statistical effect. *The Journal of Physical Chemistry* **80**, 2341–2351. DOI: http://doi.org/10.1021/j100562a007.

Krystyjan, M., Gumul, D., Ziobro, R. & Korus, A. (2015). The fortification of biscuits with bee pollen and its effect on physicochemical and antioxidant properties in biscuits. *LWT - Food Science and Technology* **63**(1), 640 – 646. DOI: http://dx.doi.org/10.1016/j.lwt.2015.03.075.

Kuda, T., Tsunekawa, M., Goto, H. & Araki, Y. (2005). Antioxidant properties of four edible algae harvested in the Noto Peninsula, Japan. *Journal of Food Composition and Analysis* **18**, 625 – 633. DOI: http://dx.doi.org/10.1016/j.jfca.2004.06.015.

Kuhnen, S., Menel Lemos, P. M., Campestrini, L. H., Ogliari, J. B., Dias, P. F. & Maraschin, M. (2011). Carotenoid and anthocyanin contents of grains of brazilian maize landraces. *Journal of the Science of Food and Agriculture* **91**, 1548–1553. DOI: http://doi.org/10.1002/jsfa.4346.

Kumar, A., De, A. & Mozumdar, S. (2015). Synthesis of acrylate guar-gum for delivery of bio-active molecules. *Bulletin of Materials Science* **38**(4), 1025–1032. DOI: http://doi.org/10.1007/s12034-015-0930-z.

Kyung-Tae, K. (2012). *Seasonal variation of seaweed components and novel biological function of fucoidan extracted from brown algae in Quebec*. Ph.D. thesis, Université Laval, Canada.

Labuza, T. P. (1970). Properties of water as related to the keeping quality of foods. In: *Third Annual Meeting of the International Congress of Food Scienc and Technology*. Chicago.

Labuza, T. P., Knnane, A. & Chen, J. Y. (1985). Effect of temperature on the moisture sorption isotherm and water activity shift of two dehydrated foods. *Journal of Food Science* **50**, 385–392. DOI: http://doi.org/10.1111/j.1365-2621.1985.tb13409.x.

Landrum, J. T. (2009). *Carotenoids: physical, chemical, and biological functions and properties*. Boca Raton, USA: CRC Press.

Launay, B. & Michon, C. (2008). Biaxial extension of wheat flour doughs: lubricated squeezing flow and stress relaxation properties. *Journal of Texture Studies* **39**, 496–529. DOI: http://doi.org/10.1111/j.1745-4603.2008.00156.x.

Lazaridou, A., Duta, D., Papageorgiou, M., Belc, N. & Biliaderis, C. (2007). Effects of hydrocolloids on dough rheology and bread quality parameters in gluten-free formulations. *Journal of Food Engineering* **79**, 1033 – 1047. DOI: http://dx.doi.org/10.1016/j.jfoodeng.2006.03.032.

Le Bleis, F., Chaunier, L., Chiron, H., Della Valle, G. & Saulnier, L. (2015). Rheological properties of wheat flour dough and french bread enriched with wheat bran. *Journal of Cereal Science* **65**, 167 – 174. DOI: http://dx.doi.org/10.1016/j.jcs.2015.06.014.

Le Lann, K., Jégou, C. & Stiger-Pouvreau, V. (2008). Effect of different conditioning treatments on total phenolic content and antioxidant activities in two *Sargassacean* species: Comparison of the frondose *Sargassum muticum* (yendo) fensholt and the cylindrical *Bifurcaria bifurcata* r. ross. *Phycological Research* **56**, 238–245. DOI: http://doi.org/10.1111/j.1440-1835.2008.00505.x.

Leach, H., McCowen, L. & Schoch, T. (1959). Structure of the starch granule. I. Swelling and solubility patterns of various starches. *Cereal Chemistry* **36**, 534–544.

Lee, J.-M., Kang, B.-H. & Kim, Y. K. (2010). Drying condition affects total phenol contents and antioxidant activities of *Hizikia fusiformis*. *Journal of Food Science and Nutrition* **15**, 244–247. DOI: http://doi.org/10.3746/jfn.2010.15.3.244.

Leffer, J. & Grunwald, E. (1963). *Rates and Equilibria of Organic Reactions*. New York: Wiley.

Lemus, R. A., Pérez, M., Andrés, A., Roco, T., Tello, C. M. & Vega-Gálvez, A. (2008). Kinetic study of dehydration and desorption isotherms of red alga *Gracilaria* . *LWT - Food Science and Technology* **41**, 1592 – 1599. DOI: http://dx.doi.org/10.1016/j.lwt.2007.10.011.

Li, E., Dhital, S. & Hasjim, J. (2014). Effects of grain milling on starch structures and flour/starch properties. *Starch - Stärke* **66**, 15–27. DOI: http://doi.org/10.1002/star.201200224.

Li, Y.-X., Wijesekara, I., Li, Y. & Kim, S.-K. (2011). Phlorotannins as bioactive agents from brown algae. *Process Biochemistry* **46**, 2219 – 2224. DOI: http://dx.doi.org/10.1016/j.procbio.2011.09.015.

Lianfu, Z. & Zelong, L. (2008). Optimization and comparison of ultrasound/microwave assisted extraction (umae) and ultrasonic assisted

extraction (uae) of lycopene from tomatoes. *Ultrasonics Sonochemistry* **15**, 731 – 737. DOI: http://dx.doi.org/10.1016/j.ultsonch.2007.12.001.

Lindenmeier, M. & Hofmann, T. (2004). Influence of baking conditions and precursor supplementation on the amounts of the antioxidant pronyl-l-lysine in bakery products. *Journal of Agricultural and Food Chemistry* **52**, 350–354. DOI: http://doi.org/10.1021/jf0346657.

Ling, A. L. M., Yasir, S., Matanjun, P. & Abu Bakar, M. F. (2015). Effect of different drying techniques on the phytochemical content and antioxidant activity of *Kappaphycus alvarezii*. *Journal of Applied Phycology* **27**, 1717–1723. DOI: http://doi.org/10.1007/s10811-014-0467-3.

Liu, H., Yu, L., Chen, L. & Li, L. (2007). Retrogradation of corn starch after thermal treatment at different temperatures. *Carbohydrate Polymers* **69**, 756 – 762. DOI: https://doi.org/10.1016/j.carbpol.2007.02.011.

Liu, H., Yu, L., Xie, F. & Chen, L. (2006). Gelatinization of cornstarch with different amylose/amylopectin content. *Carbohydrate Polymers* **65**, 357 – 363. DOI: http://dx.doi.org/10.1016/j.carbpol.2006.01.026.

López, A., Rico, M., Rivero, A. & Suárez de Tangil, M. (2011). The effects of solvents on the phenolic contents and antioxidant activity of *Stypocaulon scoparium* algae extracts. *Food Chemistry* **125**, 1104 – 1109. DOI: http://dx.doi.org/10.1016/j.foodchem.2010.09.101.

Létang, C., Piau, M. & Verdier, C. (1999). Characterization of wheat flour–water doughs. part i: Rheometry and microstructure. *Journal of Food Engineering* **41**, 121 – 132. DOI: http://dx.doi.org/10.1016/S0260-8774(99)00082-5.

Ma, Y.-Q., Chen, J.-C., Liu, D.-H. & Ye, X.-Q. (2009). Simultaneous extraction of phenolic compounds of citrus peel extracts: Effect of ultrasound. *Ultrasonics Sonochemistry* **16**, 57 – 62. DOI: http://dx.doi.org/10.1016/j.ultsonch.2008.04.012.

Mabeau, S. & Fleurence, J. (1993). Seaweed in food products: biochemical and nutritional aspects. *Trends in Food Science & Technology* **4**, 103 – 107. DOI: http://dx.doi.org/10.1016/0924-2244(93)90091-N.

MacGregor, W. (2005). Effects of air velocity, air temperature, and berry diameter on wild blueberry drying. *Drying Technology* **23**, 387–396. DOI: http://doi.org/10.1081/DRT-200047880.

Maeda, T., Kokawa, M., Nango, N., Miura, M., Araki, T., Yamada, M., Takeya, K. & Sagara, Y. (2015). Development of a quantification method of the gluten matrix in bread dough by fluorescence microscopy and image analysis. *Food and Bioprocess Technology* **8**, 1349–1354. DOI: http://doi.org/10.1007/s11947-015-1497-9.

Malumba, P., Boudry, C., Roiseux, O., Bindelle, J., Beckers, Y. & Béra, F. (2015). Chemical characterisation and in vitro assessment of the nutritive value of co-products yield from the corn wet-milling process. *Food Chemistry* **166**, 143 – 149. DOI: http://dx.doi.org/10.1016/j.foodchem.2014.06.001.

Mamat, H., Matanjun, P., Ibrahim, S., Md. Amin, S. F., Abdul Hamid, M. & Rameli, A. S. (2014). The effect of seaweed composite flour on the textural properties of dough and bread. *Journal of Applied Phycology* **26**, 1057–1062. DOI: http://doi.org/10.1007/s10811-013-0082-8.

Mancebo, C. M., Picón, J. & Gómez, M. (2015). Effect of flour properties on the quality characteristics of gluten free sugar-snap cookies. *LWT - Food Science and Technology* **64**, 264 – 269. DOI: http://dx.doi.org/10.1016/j.lwt.2015.05.057.

Mancebo, C. M., Rodriguez, P. & Gómez, M. (2016). Assessing rice flour-starch-protein mixtures to produce gluten free sugar-snap cookies. *LWT - Food Science and Technology* **67**, 127 – 132. DOI: http://dx.doi.org/10.1016/j.lwt.2015.11.045.

Marco, C. & Rosell, C. M. (2008). Breadmaking performance of protein enriched, gluten-free breads. *European Food Research and Technology* **227**, 1205–1213. DOI: http://doi.org/10.1007/s00217-008-0838-6.

Mason, T. J., Chemat, F. & Vinatoru, M. (2011). The extraction of natural products using ultrasound or microwaves. *Current Organic Chemistry* **15**, 237–247.

Matanjun, P., Mohamed, S., Mustapha, N. M., Muhammad, K. & Ming, C. H. (2008). Antioxidant activities and phenolics content of eight species of seaweeds from north borneo. *Journal of Applied Phycology* **20**, 367. DOI: http://doi.org/10.1007/s10811-007-9264-6.

Matos, M. E., Sanz, T. & Rosell, C. M. (2014). Establishing the function of proteins on the rheological and quality properties of rice based gluten free muffins. *Food Hydrocolloids* **35**, 150 – 158. DOI: http://dx.doi.org/10.1016/j.foodhyd.2013.05.007.

Mayor, L. & Sereno, A. M. (2004). Modelling shrinkage during convective drying of food materials: a review. *Journal of Food Engineering* **61**, 373 – 386. DOI: http://dx.doi.org/10.1016/S0260-8774(03)00144-4.

Mazza, G. & Le Magger, M. (1978). Water sorption properties of yellow globe onion (*Allium cepa L.*). *Canadian Institute of Food Science and Technology Journal* **11**, 189–193. DOI: http://doi.org/10.1016/S0315-5463(78)73269-4.

McGrance, S. J., Cornell, H. J. & Rix, C. J. (1998). A simple and rapid colorimetric method for the determination of amylose in starch products. *Starch/Staerke* **4**, 158–163. DOI: http://doi.org/10.1002/(SICI)1521-379X(199804)50:4<158::AID-STAR158>3.0.CO;2-7.

McHugh, D. J. (2003). *A guide to the seaweed industry*. FAO Fisheries Technical Paper, No. 441. Rome: Food and Agriculture Organization of the United Nations.

McMinn, W. & Magee, T. (2003). Thermodynamic properties of moisture sorption of potato. *Journal of Food Engineering* **60**, 155–157. DOI: http://doi.org/10.1016/S0260-8774(03)00036-0.

Menezes, B. S., Coelho, M. S., Meza, S. L. R., Salas-Mellado, M. & Souza, M. R. A. Z. (2015). Macroalgal biomass as an additional ingredient of bread. *International Food Research Journal* **22**, 812–817.

Mert, S., Sahin, S. & Sumnu, G. (2015). Development of gluten-free wafer sheet formulations. *LWT - Food Science and Technology* **63**, 1121 – 1127. DOI: http://dx.doi.org/10.1016/j.lwt.2015.04.035.

Miguelez, J. D. L. M., Bernardez, M. M. & Queijeiro, J. G. (2004). Composition of varieties of chestnuts from Galicia (Spain). *Food Chemistry* **84**, 401 – 404. DOI: http://dx.doi.org/10.1016/S0308-8146(03)00249-8.

Miś, A., Nawrocka, A. & Dziki, D. (2017). Behaviour of dietary fibre supplements during bread dough development evaluated using novel farinograph curve analysis. *Food and Bioprocess Technology* , 1–11DOI: http://doi.org/10.1007/s11947-017-1881-8.

Mäki, M. & Collin, P. (1997). Coeliac disease. *The Lancet* **349**, 1755–1759. DOI: http://dx.doi.org/10.1016/S0140-6736(96)70237-4.

Monaco, R. D., Miele, N. A., Cavella, S. & Masi, P. (2010). New chestnut-based chips optimization: Effects of ingredients. *LWT - Food Science and Technology* **43**, 126 – 132. DOI: http://dx.doi.org/10.1016/j.lwt.2009.07.005.

Moreira, R., Chenlo, F. & Torres, M. (2011). Rheology of commercial chestnut flour doughs incorporated with gelling agents. *Food Hydrocolloids* **25**(5), 1361 – 1371. DOI: https://doi.org/10.1016/j.foodhyd.2010.12.015.

Moreira, R., Chenlo, F. & Torres, M. (2013a). Effect of chia (*Sativa hispanica L.*) and hydrocolloids on the rheology of gluten-free doughs based on chestnut flour. *LWT - Food Science and Technology* **50**, 160 – 166. DOI: http://dx.doi.org/10.1016/j.lwt.2012.06.008.

Moreira, R., Chenlo, F., Torres, M. & Prieto, D. (2010a). Influence of the particle size on the rheological behaviour of chestnut flour doughs. *Journal of Food Engineering* **100**, 270 – 277. DOI: https://doi.org/10.1016/j.jfoodeng.2010.04.009.

Moreira, R., Chenlo, F., Torres, M. & Prieto, D. (2010b). Water adsorption and desorption isotherms of chestnut and wheat flours. *Industrial Crops and Products* **32**, 252 – 257. DOI: http://dx.doi.org/10.1016/j.indcrop.2010.04.021.

Moreira, R., Chenlo, F., Torres, M., Rama, B. & Arufe, S. (2015). Air drying of chopped chestnuts at several conditions: effect on colour and chemical characteristics of chestnut flour. *International Food Research Journal* **22**, 407–413.

Moreira, R., Chenlo, F., Torres, M. D. & Prieto, D. M. (2012). Technological assessment of chestnut flour doughs regarding to doughs from other commercial flours and formulations. *Food and Bioprocess Technology* **5**, 2301–2310. DOI: http://doi.org/10.1007/s11947-011-0524-8.

Moreira, R., Chenlo, F., Torres, M. D. & Rama, B. (2013b). Influence of the chestnuts drying temperature on the rheological properties of their doughs. *Food and Bioproducts Processing* **91**, 7 – 13. DOI: https://doi.org/10.1016/j.fbp.2012.08.004.

Moreira, R., Chenlo, F., Torres, M. D. & Vallejo, N. (2008). Thermodynamic analysis of experimental sorption isotherms of loquat and quince fruits. *Journal of Food Engineering* **88**, 514 – 521. DOI: http://dx.doi.org/10.1016/j.jfoodeng.2008.03.011.

Morrone, L., Dall'Asta, C., Silvanini, A., Cirlini, M., Beghè, D., Fabbri, A. & Ganino, T. (2015). The influence of seasonality on total fat and fatty acids profile, protein and amino acid, and antioxidant properties of traditional italian flours from different chestnut cultivars. *Scientia Horticulturae* **192**, 132 – 140. DOI: http://dx.doi.org/10.1016/j.scienta.2015.04.018.

Mujumdar, A. S. (2006). *Handbook of Industrial Drying*. Boca Raton, FL, USA: CRC Press.

Murray, J. (1999). The widening spectrum of celiac disease. *American Journal of Clinical Nutrition* **69**, 354–365.

Nagai, T. & Yukimoto, T. (2003). Preparation and functional properties of beverages made from sea algae. *Food Chemistry* **81**, 327 – 332. DOI: http://dx.doi.org/10.1016/S0308-8146(02)00426-0.

Naqash, F., Gani, A., Gani, A. & Masoodi, F. (2017). Gluten-free baking: Combating the challenges - a review. *Trends in Food Science & Technology* **66**, 98 – 107. DOI: http://dx.doi.org/10.1016/j.tifs.2017.06.004.

Neoh, Y. Y., Matanjun, P. & Lee, J. S. (2016). Comparative study of drying methods on chemical constituents of malaysian red seaweed. *Drying Technology* **34**, 1745–1751. DOI: http://doi.org/10.1080/07373937.2016.1212207.

Ngo, D.-H., Wijesekara, I., Vo, T.-S., Van Ta, Q. & Kim, S.-K. (2011). Marine food-derived functional ingredients as potential antioxidants in the food industry: An overview. *Food Research International* **44**, 523 – 529. DOI: http://dx.doi.org/10.1016/j.foodres.2010.12.030.

Noort, M. W. J., van Haaster, D., Hemery, Y., Schols, H. A. & Hamer, R. J. (2010). The effect of particle size of wheat bran fractions on bread quality – evidence for fibre–protein interactions. *Journal of Cereal Science* **52**, 59 – 64. DOI: http://dx.doi.org/10.1016/j.jcs.2010.03.003.

Norra, I., Aminah, A. & Suri, R. (2016). Effects of drying methods, solvent extraction and particle size of malaysian brown seaweed, *Sargassum sp.* on the total phenolic and free radical scavenging activity. *International Food Research Journal* **23**, 1559–1563.

Nunes, R. V. & Rotstein, E. (1991). Thermodynamics of the water-foodstuff equilibrium. *Drying Technology* **9**, 113–137. DOI: http://doi.org/10.1080/07373939108916643.

Oliver, M. J., O'Mahony, P. & Wood, A. J. (1998). "To dryness and beyond" - preparation for the dried state and rehydration in vegetative desiccation-tolerant plants. *Plant Growth Regulation* **24**, 193–201. DOI: http://doi.org/10.1023/A:1005863015130.

Orford, P. D., Ring, S. G., Carroll, V., Miles, M. J. & Morris, V. J. (1987). The effect of concentration and botanical source on the gelation and retrogradation of starch. *Journal of the Science of Food and Agriculture* **39**, 169–177. DOI: http://doi.org/10.1002/jsfa.2740390210.

Orlowska, M. & Randzio, S. L. (2010). Water content influence on thermal and volumetric properties of wheat starch gelatinization under 10 mpa. *Annals of the New York Academy of Sciences* **1189**, 43–54. DOI: http://doi.org/10.1111/j.1749-6632.2009.05205.x.

Osborne, T. B. & Vorhees, C. G. (1983). The proteins of the wheat kernel. *Journal of the American Chemical Society* **15**, 392–471.

O'Shea, N., Arendt, E. & Gallagher, E. (2014). State of the art in gluten-free research. *Journal of Food Science* **79**, R1067–R1076. DOI: http://doi.org/10.1111/1750-3841.12479.

Paciulli, M., Rinaldi, M., Cirlini, M., Scazzina, F. & Chiavaro, E. (2016). Chestnut flour addition in commercial gluten-free bread: A shelf-life study. *LWT - Food Science and Technology* **70**, 88 – 95. DOI: https://doi.org/10.1016/j.lwt.2016.02.034.

Page, G. E. (1949). *Factors influencing the maximum rates of air drying shelled corn in thin layers*. Ph.D. thesis, Purdue University.

Pádua, D., Rocha, E., Gargiulo, D. & Ramos, A. (2015). Bioactive compounds from brown seaweeds: Phloroglucinol, fucoxanthin and fucoidan as promising therapeutic agents against breast cancer. *Phytochemistry Letters* **14**, 91 – 98. DOI: http://dx.doi.org/10.1016/j.phytol.2015.09.007.

Peña, R. J. (2002). *Bread wheat improvement and production*, chap. Wheat for bread and other foods. Rome, Italy: Food and Agriculture Organization of the United Nations (FAO), pp. 483–493.

Peña-Méndez, E. M., Hernández-Suárez, M., Díaz-Romero, C. & Rodríguez-Rodríguez, E. (2008). Characterization of various chestnut cultivars by means of chemometrics approach. *Food Chemistry* **107**, 537 – 544. DOI: http://dx.doi.org/10.1016/j.foodchem.2007.08.024.

Peinado, I., Girón, J., Koutsidis, G. & Ames, J. (2014). Chemical composition, antioxidant activity and sensory evaluation of five different species of brown edible seaweeds. *Food Research International* **66**, 36 – 44. DOI: http://dx.doi.org/10.1016/j.foodres.2014.08.035.

Pejcz, E., Mularczyk, A. & Gil, Z. (2015). Technological characteristic of wheat and non-cereal flour blends and their applicability in bread making. *Journal of Food and Nutrition Research* **54**, 69–78.

Perez, E., Bahnassey, Y. A. & Breene, W. M. (1993). A simple laboratory scale method for isolation of amaranth starch. *Starch - Stärke* **45**, 211–214. DOI: https://doi.org/10.1002/star.19930450605.

Picó, Y. (2013). Ultrasound-assisted extraction for food and environmental samples. *TrAC Trends in Analytical Chemistry* **43**, 84 – 99. Highlights in Sample Preparation (for Food and Environmental Analysis). DOI: http://dx.doi.org/10.1016/j.trac.2012.12.005.

Pomeranz, Y. (1991). *Functional Properties of Food Components*. San Diego, USA: Academic Press.

Pomeranz, Y., Shogren, M. D., Finney, K. F. & Bechtel, D. B. (1977). Fiber in breadmaking effects on functional properties. *Cereal Chemistry* **54**, 25–41.

Poutanen, K., Sozer, N. & Della Valle, G. (2014). How can technology help to deliver more of grain in cereal foods for a healthy diet? *Journal of Cereal Science* **59**, 327 – 336. Cereal Science for Food Security,Nutrition and Sustainability. DOI: http://dx.doi.org/10.1016/j.jcs.2014.01.009.

Prosky, L. (2000). When is dietary fiber considered a functional food? *BioFactors* **12**, 289–297. DOI: http://doi.org/10.1002/biof.5520120143.

Pruska-Kedzior, A., Kedzior, Z., Goracy, M., Pietrowska, K., Przybylska, A. & Spychalska, K. (2008). Comparison of rheological, fermentative and baking properties of gluten-free dough formulations. *European Food Research and Technology* **227**, 1523. DOI: http://doi.org/10.1007/s00217-008-0875-1.

Ragan, M. A. & Jensen, A. (1978). Quantitative studies on brown algal phenols. ii. seasonal variation in polyphenol content of *Ascophyllum nodosum* (l.) le jol. and *Fucus vesiculosus* (l.). *Journal of Experimental Marine Biology and Ecology* **34**, 245 – 258. DOI: http://dx.doi.org/10.1016/S0022-0981(78)80006-9.

Rao, M. A. (2007). *Rheology of fluid and semisolid foods: principles and applications*. New York: Elsevier Applied Science.

Revilla, P., Landa, A., Rodríguez, V. M., Romay, M. C., Ordás, A. & Malvar, R. A. (2008). Maize for bread under organic agriculture. *Spanish Journal of Agricultural Research* **6**, 241–247.

Ribeiro, R., Pinho, M., Falcão-Cunha, L. & Freire, J. (2013). The use of chestnuts (*Castanea sativa Mill.*) as a source of resistant starch in the diet of the weaned piglet. *Animal Feed Science and Technology* **182**, 111 – 120. DOI: http://dx.doi.org/10.1016/j.anifeedsci.2013.04.009.

Rinaldi, M., Paciulli, M., Dall'Asta, C., Cirlini, M. & Chiavaro, E. (2015). Short-term storage evaluation of quality and antioxidant capacity in chestnut–wheat bread. *Journal of the Science of Food and Agriculture* **95**, 59–65. DOI: http://doi.org/10.1002/jsfa.6843.

Ring, S. G. (1985). Some studies on starch gelation. *Starch - Stärke* **37**, 80–83. DOI: http://doi.org/10.1002/star.19850370303.

Ring, S. G., Colonna, P., I'Anson, K. J., Kalichevsky, M. T., Miles, M. J., Morris, V. J. & Orford, P. D. (1987). The gelation and crystallisation of amylopectin. *Carbohydrate Research* **162**, 277 – 293. DOI: http://dx.doi.org/10.1016/0008-6215(87)80223-9.

Rioux, L.-E., Turgeon, S. & Beaulieu, M. (2007). Characterization of polysaccharides extracted from brown seaweeds. *Carbohydrate Polymers* **69**, 530 – 537. DOI: http://dx.doi.org/10.1016/j.carbpol.2007.01.009.

Rizvi, S. (1986). *Engineering properties of food*, chap. Thermodynamics of foods in dehydration. New York: Marcel Dekker, pp. 133–214.

Robertson, J. A., de Monredon, F. D., Dysseler, P., Guillon, F., Amado, R. & Thibault, J.-F. (2000). Hydration properties of dietary fibre and resistant starch: a european collaborative study. *LWT - Food Science and Technology* **33**, 72 – 79. DOI: http://dx.doi.org/10.1006/fstl.1999.0595.

Rodrigues, D., Sousa, S., Silva, A., Amorim, M., Pereira, L., Rocha-Santos, T. A. P., Gomes, A. M. P., Duarte, A. C. & Freitas, A. C. (2015). Impact of enzyme- and ultrasound-assisted extraction methods on biological properties of red, brown, and green seaweeds from the central west coast of portugal. *Journal of Agricultural and Food Chemistry* **63**, 3177–3188. PMID: 25756735. DOI: http://doi.org/10.1021/jf504220e.

Rodrigues, S., Pinto, G. A. & Fernandes, F. A. (2008). Optimization of ultrasound extraction of phenolic compounds from coconut (cocos nucifera) shell powder by response surface methodology. *Ultrasonics Sonochemistry* **15**, 95 – 100. DOI: http://dx.doi.org/10.1016/j.ultsonch.2007.01.006.

Rodríguez-Bernaldo de Quirós, A., Frecha-Ferreiro, S., Vidal-Pérez, A. M. & López-Hernández, J. (2010). Antioxidant compounds in edible brown seaweeds. *European Food Research and Technology* **231**, 495–498. DOI: http://doi.org/10.1007/s00217-010-1295-6.

Romani, S., Rocculi, P., Mendoza, F. & Rosa, M. D. (2009). Image characterization of potato chip appearance during frying. *Journal of Food*

Engineering **93**, 487 – 494. DOI: http://dx.doi.org/10.1016/j.jfoodeng.2009.02.017.

Romano, A., Toraldo, G., Cavella, S. & Masi, P. (2007). Description of leavening of bread dough with mathematical modelling. *Journal of Food Engineering* **83**, 142 – 148. DOI: http://dx.doi.org/10.1016/j.jfoodeng.2007.02.014.

Rosell, C. M., Barro, F., Sousa, C. & Mena, M. C. (2014). Cereals for developing gluten-free products and analytical tools for gluten detection. *Journal of Cereal Science* **59**, 354 – 364. Cereal Science for Food Security,Nutrition and Sustainability. DOI: http://dx.doi.org/10.1016/j.jcs.2013.10.001.

Rosell, C. M., Collar, C. & Haros, M. (2007). Assessment of hydrocolloid effects on the thermo-mechanical properties of wheat using the Mixolab®. *Food Hydrocolloids* **21**, 452 – 462. DOI: http://dx.doi.org/10.1016/j.foodhyd.2006.05.004.

Rosell, C. M., Santos, E. & Collar, C. (2010). Physical characterization of fiber-enriched bread doughs by dual mixing and temperature constraint using the Mixolab®. *European Food Research and Technology* **231**, 535–544. DOI: http://doi.org/10.1007/s00217-010-1310-y.

Rubilar, M., Pinelo, M., Ihl, M., Scheuermann, E., Sineiro, J. & Nuñez, M. J. (2006). Murta leaves (*Ugni molinae* turcz) as a source of antioxidant polyphenols. *Journal of Agricultural and Food Chemistry* **54**, 59–64. DOI: http://doi.org/10.1021/jf051571j.

Rubilar, M., Pinelo, M., Shene, C., Sineiro, J. & Nuñez, M. J. (2007). Separation and hplc-ms identification of phenolic antioxidants from agricultural residues: Almond hulls and grape pomace. *Journal of Agricultural and Food Chemistry* **55**, 10101–10109. DOI: http://doi.org/10.1021/jf0721996.

Rupérez, P. & Saura-Calixto, F. (2001). Dietary fibre and physicochemical properties of edible spanish seaweeds. *European Food Research and Technology* **212**, 349–354. DOI: http://doi.org/10.1007/s002170000264.

Russell, P. L. (1987). Gelatinisation of starches of different amylose/amylopectin content. a study by differential scanning calorimetry. *Journal of Cereal Science* **6**, 133 – 145. DOI: http://dx.doi.org/10.1016/S0733-5210(87)80050-4.

Różyło, R., Hassoon, W. H., Gawlik-Dziki, U., Siastała, M. & Dziki, D. (2017). Study on the physical and antioxidant properties of gluten-free

bread with brown algae. *CyTA - Journal of Food* **15**, 196–203. DOI: http://doi.org/10.1080/19476337.2016.1236839.

Sacchetti, G., Pinnavaia, G., Guidolin, E. & Rosa, M. (2004). Effects of extrusion temperature and feed composition on the functional, physical and sensory properties of chestnut and rice flour-based snack-like products. *Food Research International* **37**, 527 – 534. Starch Functionality. DOI: https://doi.org/10.1016/j.foodres.2003.11.009.

Sakac, M., Pestoric, M., Misan, A., Nedeljkovic, N., Jambrec, D., Jovanov, P., Banjac, V., Torbica, A. & Mandic, A. (2015). Antioxidant capacity, mineral content and sensory properties of gluten-free rice and buckwheat cookies. *Food Technology and Biotechnology* **53**, 38–47. DOI: http://doi.org/10.17113/ftb.53.01.15.3633.

Salvador, A., Sanz, T. & Fiszman, S. (2006). Dynamic rheological characteristics of wheat flour–water doughs. effect of adding NaCl, sucrose and yeast. *Food Hydrocolloids* **20**, 780 – 786. DOI: http://dx.doi.org/10.1016/j.foodhyd.2005.07.009.

Sandhu, K. S., Singh, N. & Malhi, N. S. (2007). Some properties of corn grains and their flours i: Physicochemical, functional and chapati-making properties of flours. *Food Chemistry* **101**, 938 – 946. DOI: http://dx.doi.org/10.1016/j.foodchem.2006.02.040.

Sappati, P. K., Nayak, B. & van Walsum, G. P. (2017). Effect of glass transition on the shrinkage of sugar kelp (*Saccharina latissima*) during hot air convective drying. *Journal of Food Engineering* **210**, 50 – 61. DOI: https://doi.org/10.1016/j.jfoodeng.2017.04.018.

Sarabhai, S. & Prabhasankar, P. (2015). Influence of whey protein concentrate and potato starch on rheological properties and baking performance of indian water chestnut flour based gluten free cookie dough. *LWT - Food Science and Technology* **63**, 1301 – 1308. DOI: http://dx.doi.org/10.1016/j.lwt.2015.03.111.

Sarbatly, R., Tracy, W., Bono, A. & Krishnaiah, D. (2010). Kinetic and thermodynamic characteristics of seaweed dried in the convective air drier. *International Journal of Food Engineering* **6**. DOI: http://doi.org/10.2202/1556-3758.1600.

Shahidi, F. (2009). Nutraceuticals and functional foods: Whole versus processed foods. *Trends in Food Science & Technology* **20**, 376 – 387. Natural and Safe FoodsIUFoST/Food Ingredients Asia-China Conference. DOI: http://dx.doi.org/10.1016/j.tifs.2008.08.004.

Sharma, P., Velu, V., Indrani, D. & Singh, R. (2013). Effect of dried guduchi (*Tinospora cordifolia*) leaf powder on rheological, organoleptic and nutritional characteristics of cookies. *Food Research International* **50**, 704 – 709. Stability of phytochemicals during processing. DOI: http://dx.doi.org/10.1016/j.foodres.2012.03.002.

Shehzad, A., Chiron, H., Della Valle, G., Kansou, K., Ndiaye, A. & Réguerre, A. L. (2010). Porosity and stability of bread dough during proofing determined by video image analysis for different compositions and mixing conditions. *Food Research International* **43**, 1999 – 2005. DOI: http://dx.doi.org/10.1016/j.foodres.2010.05.019.

Shenoy, A. V. (1999). *Theology of filled polymer systems*. Dordrecht: Kluwer Academic Publishers.

Shogren, R. (1992). Effect of moisture content on the melting and subsequent physical aging of cornstarch. *Carbohydrate Polymers* **19**, 83 – 90. DOI: http://dx.doi.org/10.1016/0144-8617(92)90117-9.

Silberfeld, T., Racault, M.-F. L., Fletcher, R. L., Couloux, A., Rousseau, F. & De Reviers, B. (2011). Systematics and evolutionary history of pyrenoid-bearing taxa in brown algae (*Phaeophyceae*). *European Journal of Phycology* **46**, 361–377. DOI: http://doi.org/10.1080/09670262.2011.628698.

Singh, J. & Singh, N. (2001). Studies on the morphological, thermal and rheological properties of starch separated from some indian potato cultivars. *Food Chemistry* **75**, 67–77. DOI: http://doi.org/10.1016/S0308-8146(01)00189-3.

Singleton, V. L. & Rossi, J. A. (1965). Colorimetry of total phenolics with phosphomolybdic-phosphotungstic acid reagents. *American Journal of Enology and Viticulture* **16**, 144–158.

Sivaramakrishnan, H. P., Senge, B. & Chattopadhyay, P. (2004). Rheological properties of rice dough for making rice bread. *Journal of Food Engineering* **62**, 37 – 45. DOI: http://dx.doi.org/10.1016/S0260-8774(03)00169-9.

Slade, L. & Levine, H. (1988). Non-equilibrium melting of native granular starch: Part i. temperature location of the glass transition associated with gelatinization of a-type cereal starches. *Carbohydrate Polymers* **8**, 183 – 208. DOI: http://dx.doi.org/10.1016/0144-8617(88)90002-1.

Slade, L. & Levine, H. (2004). *The food polymer science approach to understanding glass transitions in foods*. Illinois: Tanner Award Lecture.

Soria, A. C. & Villamiel, M. (2010). Effect of ultrasound on the technological properties and bioactivity of food: a review. *Trends in Food Science & Technology* **21**, 323 – 331. DOI: http://dx.doi.org/10.1016/j.tifs.2010.04.003.

Steffe, J. F. (1996). *Rheological method in food process engineering*. East Lansing, USA: Freeman Press, 2nd ed.

Stegenga, H. & Mol, I. (1983). *Flora van de Nederlandse zeewieren*. Bibliotheek van de Koninklijke Nederlandse Natuurhistorische Vereniging. Koninklijke Nederlandse Natuurhistorische Vereniging.

Stencl, J. (2004). Modelling the water sorption isotherms of yoghurt powder spray. *Mathematics and Computers in Simulation* **65**, 157 – 164. Selected papers of the IMACS/IFAC Fourth International Symposium on Mathematical Modelling and Simulation in Agricultural and Bio-Industries. DOI: http://dx.doi.org/10.1016/j.matcom.2003.09.002.

Stengel, D. B., Connan, S. & Popper, Z. A. (2011). Algal chemodiversity and bioactivity: Sources of natural variability and implications for commercial application. *Biotechnology Advances* **29**, 483 – 501. DOI: http://dx.doi.org/10.1016/j.biotechadv.2011.05.016.

Stengel, D. B. & Dring, M. J. (1998). Seasonal variation in the pigment content and photosynthesis of different thallus regions of *Ascophyllum nodosum* (*Fucales*, *Phaeophyta*) in relation to position in the canopy. *Phycologia* **37**, 259–268. DOI: http://doi.org/10.2216/i0031-8884-37-4-259.1.

Stephen, M. A., Phillips, G. O. & Williams, P. A. (2006). *Food Polysaccharides and Their Applications*. Boca Raton, FL, USA: CRC Press.

Svensson, E. & Eliasson, A.-C. (1995). Crystalline changes in native wheat and potato starches at intermediate water levels during gelatinization. *Carbohydrate Polymers* **26**, 171 – 176. DOI: http://dx.doi.org/10.1016/0144-8617(95)00007-T.

Symons, G. E. & Morey, B. (1941). The effect of drying time on the determination of solids in sewage and sewage sludges. *Sewage Works Journal* **13**, 936–939.

Tahir, R., Ellis, P. R. & Butterworth, P. J. (2010). The relation of physical properties of native starch granules to the kinetics of amylolysis catalysed by

porcine pancreatic α-amylase. *Carbohydrate Polymers* **81**, 57 – 62. DOI: http://dx.doi.org/10.1016/j.carbpol.2010.01.055.

Talmaciu, A. I., Volf, I. & Popa, V. I. (2015). A comparative analysis of the 'green' techniques applied for polyphenols extraction from bioresources. *Chemistry & Biodiversity* **12**, 1635–1651. DOI: http://doi.org/10.1002/cbdv.201400415.

Tananuwong, K. & Reid, D. S. (2004). DSC and NMR relaxation studies of starch–water interactions during gelatinization. *Carbohydrate Polymers* **58**, 345 – 358. DOI: http://dx.doi.org/10.1016/j.carbpol.2004.08.003.

Tarancón, P., Hernández, M. J., Salvador, A. & Sanz, T. (2015). Relevance of creep and oscillatory tests for understanding how cellulose emulsions function as fat replacers in biscuits. *LWT - Food Science and Technology* **62**(1, Part 2), 640 – 646. Healthy Snacks: Recent Trends and Innovative Developments to Meet Current Needs. DOI: https://doi.org/10.1016/j.lwt.2014.06.029.

Taylor, J. R., Belton, P. S., Beta, T. & Duodu, K. G. (2014). Increasing the utilisation of sorghum, millets and pseudocereals: Developments in the science of their phenolic phytochemicals, biofortification and protein functionality. *Journal of Cereal Science* **59**, 257 – 275. Cereal Science for Food Security,Nutrition and Sustainability. DOI: http://dx.doi.org/10.1016/j.jcs.2013.10.009.

Tello-Ireland, C., Lemus-Mondaca, R., Vega-Gálvez, A., López, J. & Di Scala, J. (2011). Influence of hot-air temperature on drying kinetics, functional properties, colour, phycobiliproteins, antioxidant capacity, texture and agar yield of alga *Gracilaria chilensis*. *LWT - Food Science and Technology* **44**, 2112 – 2118. DOI: http://dx.doi.org/10.1016/j.lwt.2011.06.008.

Tester, R. F. & Morrison, W. R. (1990). Swelling and gelatinization of cereal starch. i. effect of amylopectin, amylose and lipids. *Cereal Chemistry* .

Thuy, T. T. T., Ly, B. M., Van, T. T. T., Quang, N. V., Tu, H. C., Zheng, Y., Seguin-Devaux, C., Mi, B. & Ai, U. (2015). Anti-hiv activity of fucoidans from three brown seaweed species. *Carbohydrate Polymers* **115**, 122 – 128. DOI: http://dx.doi.org/10.1016/j.carbpol.2014.08.068.

Tixier, M. & Desmaison, A. M. (1980). Relation metabolique entre l'arginine et l'acide gamma-aminobutirique dans le fruit de *Castanea sativa*. *Phytochemistry* **19**, 1643–1646.

Torres, M., Moreira, R., Chenlo, F. & Morel, M. (2013). Effect of water and guar gum content on thermal properties of chestnut flour and its starch. *Food Hydrocolloids* **33**, 192 – 198. DOI: https://doi.org/10.1016/j.foodhyd.2013.03.004.

Torres, M., Raymundo, A. & Sousa, I. (2014a). Influence of Na^+, K^+ and Ca^{2+} on mechanical and structural properties of gels from chestnut and rice flours. *Carbohydrate Polymers* **102**, 30 – 37. DOI: http://dx.doi.org/10.1016/j.carbpol.2013.11.018.

Torres, M. D., Arufe, S., Chenlo, F. & Moreira, R. (2017). Coeliacs cannot live by gluten-free bread alone – every once in awhile they need antioxidants. *International Journal of Food Science & Technology* **52**(1), 81–90. DOI: http://doi.org/10.1111/ijfs.13287.

Torres, M. D., Fradinho, P., Raymundo, A. & Sousa, I. (2014b). Thermorheological and textural behaviour of gluten-free gels obtained from chestnut and rice flours. *Food and Bioprocess Technology* **7**, 1171–1182. DOI: http://doi.org/10.1007/s11947-013-1132-6.

Torres, M. D., Moreira, R., Chenlo, F., Morel, M. H. & Barron, C. (2014c). Physicochemical and structural properties of starch isolated from fresh and dried chestnuts and chestnut flour. *Food Technology and Biotechnology* **52**, 135–139.

Torres, M. D., Moreira, R., Chenlo, F. & Vázquez, M. J. (2012). Water adsorption isotherms of carboxymethyl cellulose, guar, locust bean, tragacanth and xanthan gums. *Carbohydrate Polymers* **89**, 592 – 598. DOI: http://dx.doi.org/10.1016/j.carbpol.2012.03.055.

Troller, J. A. (1977). Statistical analysis of a_w measurements obtained with the sina scope. *Journal of Food Science* **42**, 86–90. DOI: http://doi.org/10.1111/j.1365-2621.1977.tb01224.x.

Truus, K., Vaher, M. & Taure, I. (eds.) (2001). *Algal biomass from Fucus vesiculosus (Phaeophyta): investigation of the mineral and alginate components*, vol. 50 of *Proceedings of the Estonian Academy of Sciences. Chemistry.*

Tsami, E. (1991). Net isosteric heat of sorption in dried fruits. *Journal of Food Engineering* **14**, 327–335. DOI: http://doi.org/10.1016/0260-8774(91)90022-K.

Turbin-Orger, A., Shehzad, A., Chaunier, L., Chiron, H. & Della Valle, G. (2016). Elongational properties and proofing behaviour

of wheat flour dough. *Journal of Food Engineering* **168**, 129 – 136. DOI: http://dx.doi.org/10.1016/j.jfoodeng.2015.07.029.

Uribe, E., Vega-Gálvez, A., Vásquez, V., Lemus-Mondaca, R., Callejas, L. & Pastén, A. (2017). Hot-air drying characteristics and energetic requirement of the edible brown seaweed *Durvillaea antarctica*. *Journal of Food Processing and Preservation* , e13313–n/aE13313. DOI: http://doi.org/10.1111/jfpp.13313.

van den Ber, C. & Bruin, S. (1981). *Water activity and its estimation in food systems: theorycal aspects*, chap. Water activity and its estimaton in food systems: theorycal aspects. New York: Academic Press, rockland, l.b. and stewater, g.f. ed., pp. 1–61.

van Reine; Tito B. Kostermans, E. D. M. J. G. W. L. J. H. P. . W. F. P. (ed.) (2004). *A Taxonomic and Geographical Catalogue of the Seaweeds of the Western Coast of Africa and Adjacent Islands*. Stuttgart, Germany: Schweizerbart Science Publishers.

van Vliet, T. (2008). Strain hardening as an indicator of bread-making performance: A review with discussion. *Journal of Cereal Science* **48**, 1 – 9. DOI: http://dx.doi.org/10.1016/j.jcs.2007.08.010.

Vega-Gálvez, A., Ayala-Aponte, A., Notte, E., De la Fuente, L. & Lemus, R. (2008). Mathematical modeling of mass transfer during convective dehydration of brown algae *Macrocystis pyrifera*. *Drying Technology* **26**, 1610–1616. DOI: http://doi.org/10.1080/07373930802467532.

Vega-Gálvez, A., López, J., Ah-Hen, K., Torres, M. J. & Lemus-Mondaca, R. (2014). Thermodynamic properties, sorption isotherms and glass transition temperature of cape gooseberry (*Physalis peruviana L.*). *Food Technology and Biotechnology* **52**, 83–92.

Vega-Gálvez, A., Tello-Ireland, C. & Lemus, R. (2007). Mathematical simulation of drying process of chilean gracilaria (*Gracilaria chilensis*). *Ingeniare. Revista chilena de ingeniería* **15**, 55–64. DOI: http://doi.org/10.4067/S0718-33052007000100008.

Vázquez, G., Chenlo, F. & Moreira, R. (2003). Sorption isotherms of lupine at different temperatures. *Journal of Food Engineering* **60**, 449 – 452. DOI: http://dx.doi.org/10.1016/S0260-8774(03)00068-2.

Wang, T., Jónsdóttir, R., Liu, H., Gu, L., Kristinsson, H., Raghavan, S. & Olafsdóttir, G. (2012). Antioxidant capacities of phlorotannins extracted

from the brown algae *Fucus vesiculosus*. *Journal of Agriculture and Food Chemistry* **60**, 5874–5883. DOI: http://doi.org/10.1021/jf3003653.

Warren, F. J., Royall, P. G., Butterworth, P. J. & Ellis, P. R. (2012). Immersion mode material pocket dynamic mechanical analysis (imp-dma): A novel tool to study gelatinisation of purified starches and starch-containing plant materials. *Carbohydrate Polymers* **90**, 628 – 636. DOI: http://dx.doi.org/10.1016/j.carbpol.2012.05.088.

Watson, S. & Ramstad, P. E. (1987). *Corn: chemistry and technology*, chap. Structure and Composition. AACC monograph series. American Association of Cereal Chemists, pp. 53–79.

Werner, A. & Kraan, S. (2004). *Review of the potencial mechanisation of kelp harvesting in Ireland*. Marine Institute and Taighde Mara Teo.

White, G. W. (1970). Rheology in food research. *International Journal of Food Science & Technology* **5**, 1–32. DOI: http://doi.org/10.1111/j.1365-2621.1970.tb01539.x.

Wijesinghe, W. & Jeon, Y.-J. (2012). Biological activities and potential industrial applications of fucose rich sulfated polysaccharides and fucoidans isolated from brown seaweeds: A review. *Carbohydrate Polymers* **88**, 13 – 20. DOI: http://dx.doi.org/10.1016/j.carbpol.2011.12.029.

Williams, P. A. (2007). *Handbook of industrial water soluble polymers*, chap. Gelling Agents. Blackwell Publishing, pp. 73–97.

Winter, W. & Kwak, Y. (1987). Rapid-scanning raman spectroscopy: a novel approach to starch retrogradation. *Food Hydrocolloids* **1**, 461 – 463. DOI: http://dx.doi.org/10.1016/S0268-005X(87)80041-3.

Witczak, M., Ziobro, R., Juszczak, L. & Korus, J. (2016). Starch and starch derivatives in gluten-free systems – a review. *Journal of Cereal Science* **67**, 46 – 57. Functionality of Cereal Based Non-gluten Dough Systems. DOI: http://dx.doi.org/10.1016/j.jcs.2015.07.007.

Wolf, M., Walker, J. E. & Kapsalis, J. G. (1972). Water vapor sorption hysteresis in dehydrated food. *Journal of Agricultural and Food Chemistry* **20**, 1073–1077. DOI: http://doi.org/10.1021/jf60183a021.

Wolf, W., Spiess, W. E. L. & Jung, G. (1985). *Properties of water in foods: in relation to food quality and stability*, chap. Standardization of Isotherm Measurements. Dordrecht: Springer Netherlands, simatos, d. and multon, j. l. ed., pp. 661–679.

Wong, K. & Cheung, P. C. (2001). Influence of drying treatment on three *Sargassum* species. *Journal of Applied Phycology* **13**, 43–50. DOI: http://doi.org/10.1023/A:1008149215156.

Xiao, Q. & Tong, Q. (2013). Thermodynamic properties of moisture sorption in pullulan–sodium alginate based edible films. *Food Research International* **54**, 1605 – 1612. DOI: http://dx.doi.org/10.1016/j.foodres.2013.09.019.

Xie, F., Yu, L., Chen, L. & Li, L. (2008). A new study of starch gelatinization under shear stress using dynamic mechanical analysis. *Carbohydrate Polymers* **72**, 229 – 234. DOI: https://doi.org/10.1016/j.carbpol.2007.08.007.

YAN, X., CHUDA, Y., SUZUKI, M. & NAGATA, T. (1999). Fucoxanthin as the major antioxidant in hijikia fusiformis, a common edible seaweed. *Bioscience, Biotechnology, and Biochemistry* **63**, 605–607. PMID: 10227153. DOI: http://doi.org/10.1271/bbb.63.605.

Yang, Z., Han, Y., Gu, Z., Fan, G. & Chen, Z. (2008). Thermal degradation kinetics of aqueous anthocyanins and visual color of purple corn (*Zea mays L.*) cob. *Innovative Food Science & Emerging Technologies* **9**, 341 – 347. DOI: http://dx.doi.org/10.1016/j.ifset.2007.09.001.

Yeo, H. & Shibamoto, T. (1991). Effects of moisture content on the maillard browning model system upon microwave irradiation. *Journal of Agricultural and Food Chemistry* **39**, 1860–1862. DOI: http://doi.org/10.1021/jf00010a035.

Yildiz, . & Dogan, I. (2014). Optimization of gluten-free cake prepared from chestnut flour and transglutaminase: Response surface methodology approach. *International Journal of Food Engineering* **10**, 737–746. DOI: http://doi.org/10.1515/ijfe-2014-0024.

Yuan, Y. & Macquarrie, D. (2015). Microwave assisted extraction of sulfated polysaccharides (fucoidan) from *Ascophyllum nodosum* and its antioxidant activity. *Carbohydrate Polymers* **129**, 101 – 107. DOI: http://dx.doi.org/10.1016/j.carbpol.2015.04.057.

Zarzycki, P. & Sobota, A. (2015). Effect of storage temperature on falling number and apparent viscosity of gruels from wheat flours. *Journal of Food Science and Technology* **52**, 437–443. DOI: http://doi.org/10.1007/s13197-013-0975-1.

Zhu, F. (2016). Effect of processing on quality attributes of chestnut. *Food and Bioprocess Technology* **9**, 1429–1443. DOI: http://doi.org/10.1007/s11947-016-1749-3.

Zhu, F. (2017). Properties and food uses of chestnut flour and starch. *Food and Bioprocess Technology* **10**, 1173–1191. DOI: http://doi.org/10.1007/s11947-017-1909-0.

Zogzas, N. P., Maroulis, Z. B. & Marinos-Kouris, D. (1996). Moisture diffusivity data compilation in foodstuffs. *Drying Technology* **14**, 2225–2253. DOI: http://doi.org/10.1080/07373939608917205.

Appendix A

Diffusion of results

Moreira, R., Chenlo, F. & Arufe, S. (2015). Starch transitions of different gluten free flour doughs determined by dynamic thermal mechanical analysis and differential scanning calorimetry. *Carbohydrate polymers* **127**, 160-167. DOI: http://doi.org/10.1016/j.carbpol.2015.03.062. **IF**: 4.219, **Q1** Polymer Science (9/82, 2015).

Moreira, R., Chenlo, F., Arufe, S. & Rubinos, S. (2015). Physicochemical characterization of white, yellow and purple maize flours and rheological characterization of their doughs. *Journal of Food Science and Technology-Mysore* **12**, 7954–7963. DOI: http://doi.org/10.1007/s13197-015-1953-6. **IF**: 1.241, **Q3** Food Science and Technology (68/125, 2015).

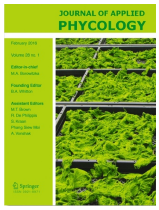

Moreira, R., Chenlo, F., Sineiro, J., Sánchez, M. & Arufe, S. (2016). Water sorption isotherms and air drying kinetics modelling of the brown seaweed *Bifurcaria bifurcata*. *Journal of Applied Phycology* **28**, 609-618. DOI: http://doi.org/10.1007/s10811-015-0553-1. **IF**: 2.616, **Q1** Marine and Freshwater Biology (18/105, 2016).

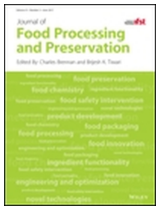

Moreira, R., Chenlo, F., Sineiro, J., Arufe, S. & Sexto, S. (2016). Water sorption isotherms and air drying kinetics of *Fucus vesiculosus* brown seaweed. *Journal of Food Processing and Preservation* IN PRESS. DOI: http://doi.org/10.1111/jfpp.12997. **IF**: 0.791, **Q3** Food Science and Technology (95/129, 2016).

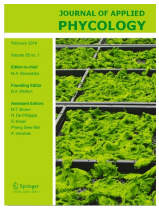

Moreira, R., Chenlo, F., Sineiro, J., Arufe, S. & Sexto, S. (2016). Drying temperature effect on powder physical properties and aqueous extract characteristics of *Fucus vesiculosus*. *Journal of Applied Phycology* **28**, 2485–2494. DOI: http://doi.org/10.1007/s10811-015-0744-9. **IF**: 2.616, **Q1** Marine and Freshwater Biology (18/105, 2016).

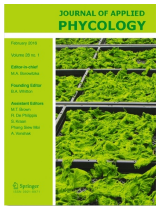

Moreira, R., Sineiro, J., Chenlo, F., Arufe, S. & Díaz, D. (2016). Aqueous extracts of *Ascophyllum nodosum* obtained by ultrasound assisted extraction: effect of drying temperature of seaweed on their properties. *Journal of Applied Phycology*. IN PRESS. DOI: http://doi.org/10.1007/s10811-017-1159-6. **IF**: 2.616, **Q1** Marine and Freshwater Biology (18/105, 2016)

Arufe, S., Della Valle, G., Chiron, H., Chenlo, F., Sineiro, J. & Moreira, R. (2017). Effect of Brown Seaweed Powder on Physical and Textural Properties of Wheat Bread. *European Food Research and Technology*. IN PRESS. DOI: http://doi.org/10.1007/s00217-017-2929-8. **IF**: 1.664, **Q2** Food Science and Technology (56/129, 2016).

Papers submitted or in writing process:

Chenlo, F., Arufe, S., Díaz, D., Torres, M. D., Sineiro, J. & Moreira, R. (2017). Air drying and rehydration characteristics of *Ascophylum nodosum* and *Undaria Pinnatifida* brown seaweeds. Submitted to: *Journal of Applied Phycology*.

Moreira, R., Chenlo, F., Sineiro, J., Torres, M. D. & Arufe, S. (2017). Mixing, rheological and thermomechanical characterization of seaweed-enriched chestnut flour doughs. To be submitted to: *Journal of Food Engineering*.

Moreira, R., Chenlo, F., Sineiro, J., Torres, M. D. & Arufe, S. (2017). Physico-Chemichal Properties of seaweed-enriched chestnut flour cookies obtained from pregelatinized doughs. To be submitted to: *Journal of Texture studies*.

Esta Tese foi escrita empregando:

LaTeX